THE DEVELOPMENT AND APPLICATION OF CHEMICAL TOOLS TO STUDY QUORUM SENSING IN *PSEUDOMONAS AERUGINOSA*

by

Michelle Elizabeth Boursier

A dissertation submitted in partial fulfillment of

the requirements for the degree of

Doctor of Philosophy

(Chemistry)

at the

UNIVERSITY OF WISCONSIN–MADISON

2017

Date of final oral examination: October 31, 2017

The dissertation is approved by the following members of the Final Oral Committee:
Helen E. Blackwell, Professor, Chemistry
Samuel H. Gellman, Professor, Chemistry and Biochemistry
David M. Lynn, Professor, Chemical & Biological Engineering and Chemistry
Sandro Mecozzi, Associate Professor, Pharmaceutical Sciences and Chemistry

THE DEVELOPMENT AND APPLICATION OF CHEMICAL TOOLS TO STUDY QUORUM SENSING IN PSEUDOMONAS AERUGINOSA

Michelle E. Boursier

Under the supervision of Professor Helen E. Blackwell

At the University of Wisconsin–Madison

ABSTRACT

Bacteria coordinate group behavior using small molecule signals in a process known as quorum sensing (QS). Gram-negative bacteria produce *N*-acyl L-homoserine lactones (AHLs) that bind to LuxR-type receptors upon reaching a threshold cell and signal density. These receptors in turn upregulate group beneficial genes. The opportunistic pathogen *Pseudomonas aeruginosa* utilizes QS to produce a host of virulence factors that contribute to its prevalence in hospital-acquired infections and its increasing antibiotic resistance. Interfering with this organism's complex QS network via non-native AHLs has shown some success in reducing virulence factor production. However, lead molecules still require further structural optimization to increase their potency, solubility, and physical stability in order to have utility as robust chemical probes. Complicating the development of improved QS modulators is the limited biochemical information about the LuxR-type receptors. It remains unclear how most small molecules are activating or inhibiting their target LuxR-type receptor. Improved chemical tools are needed to precisely modulate *P. aeruginosa*'s QS network, characterize ligand mode of action, and examine new anti-virulence approaches.

The work detailed in this dissertation describes novel chemical tools to address these three areas of QS research. In our studies performing structure-activity relationship analyses on subtle alterations to the native *P. aeruginosa* signaling molecules, we discovered key structural changes

that improve specificity and binding in all three of the *P. aeruginosa* LuxR-type receptors. These observations allowed us to develop some of the most potent and stable agonists and antagonists of the RhlR receptor known. To examine the modes by which these types of ligands act, we developed and optimized a number of biochemical assays for LuxR-type proteins, including a Förster resonance energy transfer (FRET) assay to quantify ligand binding *in vitro*. Finally, we characterized the ability of liquid crystals to behave as QS-responsive materials with a potential application for the controlled release of anti-virulence agents. We believe the advancements reported herein represent a step forward in the understanding and control of *P. aeruginosa* QS.

Helen E. Blackwell

ACKNOWLEDGEMENT

I could not have made it through graduate school without my fantastic support network. First, I would like to thank my advisor, Helen Blackwell. Through the twists and turns of my projects, I've always appreciated Helen's patience and guidance. She has pushed me to become a better communicator and a better scientist, and I'm so glad I got the opportunity to learn and grow in this lab. The last few months of research have been particularly gratifying with a number of eleventh hour findings; thanks for helping me persist through the end. I would also like to thank my committee members, Professors Dave Lynn, Sandro Mecozzi, and Sam Gellman. Their insights throughout my graduate career have helped make me a better scientist.

I sincerely appreciate my time overlapping with previous lab members J.P. Gerdt, Nora Eibergen, Joe Moore, Michael Welsh, Matt O'Reilly, Lea Koenig, and Josh Combs. J.P., Nora, Joe, and Michael shaped my early experiences in the lab, creating a fun, welcoming environment and teaching me the basics of doing research. All were incredibly generous with their time, and I have tried to emulate that as a senior student. Matt made a huge impact on my work; I don't think I could have made it through a synthesis project without him. My undergrad mentees Lea and Josh both taught me so much during my time working with them, particularly how to be a successful mentor. I wish them the best as they enter their own careers in science.

Thanks to current lab members Tian Yang, Kayleigh Nyffeler, Joseph Vasquez, Daniel Manson, Matt Styles, Korbin West, Wenqi Shen, and Betty Slinger. The lab has been a great place to work, filled with insightful discussions about research and life. I have fond memories both in and out of lab with this group. Additionally, I have greatly appreciated working with my collaborator Benjamin Ortiz. Our project was such an interesting and fulfilling interdisciplinary endeavor, even if it required some awful time points.

The friends I've made in Madison have truly enriched my time here. I'm still amazed and grateful that so many Luther College connections found the same place to start our careers. All of the runs, the grill outs, the time spent at Memorial Terrace, and the Dungeons and Dragons sessions have kept me sane. A special shout out goes to Ashley Gibson who convinced me to run not one but four marathons in graduate school. I could not ask for a better running buddy.

I am incredibly thankful for my family, particularly my Mom, my Dad, and my brother Andrew. I still remember calling home in tears after my first college chemistry quiz– thanks for believing in me as I went from general chemistry, to researching in Oklahoma and Washington State, to Madison. Your love and support means so much to me.

Finally, a big thank you goes to my husband Sam for making sure I never took myself too seriously. I'm really glad you joined me in Madison, and I'm excited for our next adventures.

TABLE OF CONTENTS

LIST OF FIGURES, TABLES, AND SCHEMES

CHAPTER 1:

Overview and Thesis Outline

1.1 Chemical Tools to Study Quorum Sensing in *Pseudomonas aeruginosa*: An Overview

1.1.1 What is quorum sensing?

Bacteria were long thought to operate as independent single celled organisms, living selfishly in all aspects of their life cycle. However, as the scientific community has learned increasingly more about the importance of inter- and intraspecies interactions, bacteria have been shown to be communal beings. For many such organisms, these interactions are not solely reactive to environmental changes. They actively coordinate the production of costly group beneficial goods based on population density in a manner critical for survival. Early studies by Nealson *et al.* showed the first instance of chemical communication the life cycle of *Vibrio fischeri*.[1] These organisms live inside of the bobtailed squid and give their host its characteristic bioluminescence. Initially this phenotype was thought to be due to population density, but it was soon discovered that bioluminescence could be induced with the addition of spent supernatant.[1] Upon isolation of an autoinducing molecule in the media, the idea of chemical communication was elucidated.[2] Subsequent explorations of bacterial communal living have found such relationships in a variety of environments ranging from beneficial soil bacteria to human pathogens.

Critical to the development of a bacterial community is their means of communication; group beneficial goods are costly to produce, so bacteria must know when they have obtained a high population density. Quorum sensing (QS) is the chemical signaling "language" that bacteria use to gauge population density and initiate group-beneficial behaviors. Signal density roughly corresponding to population density, giving bacteria an idea of their numbers.[3] Numerous QS modulators have been elucidated, ranging from small molecules to long peptides.[4] In the canonical Gram-negative QS system established in *Vibrio fischeri* (Figure 1.1), the LuxI synthase produces basal levels of easily diffusible *N*-acyl-L-homoserine lactone (AHL) signaling molecules, making the AHL concentration proportional to cell density.[3] At a high AHL concentration, the molecules bind to LuxR receptors, causing them to dimerize and bind to the promoter region of QS associated genes that then produce group beneficial traits such as

virulence or host symbiosis.[5] Additionally, the LuxR-type receptors often cause the increased production of the synthase and receptor, inducing a positive feedback loop and heightening the activity of the entire circuit.[6] Over the years, such systems have been found in a variety of organisms filling a number of environmental niches.[7] An even greater number of bacteria possess solo LuxR receptors without a cognate synthase, allowing for "evesdropping" into the surrounding microbial community.[8, 9] We are only beginning to understand the implications of such a widespread signaling system in a bacterial community.

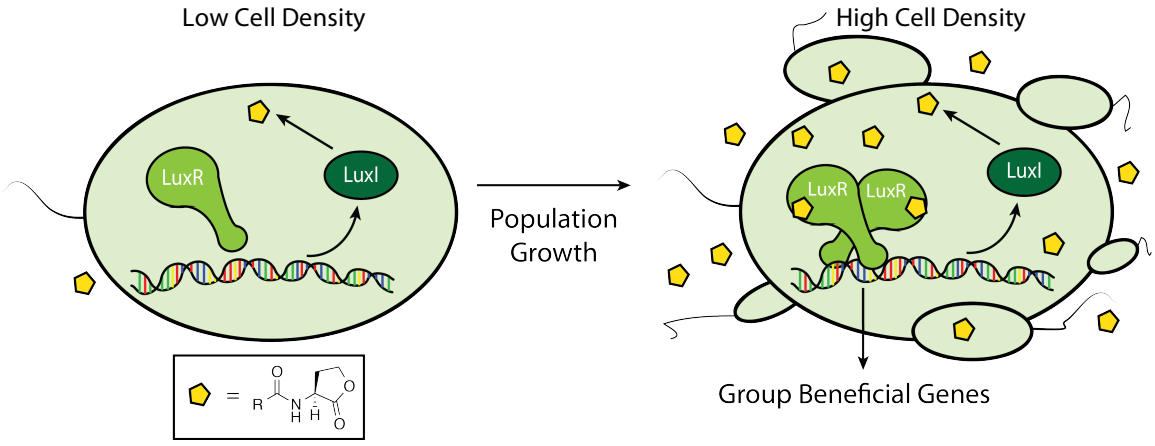

Figure 1.1. Canonical QS circuit for Gram-negative bacteria. The LuxI synthase produces AHL signals. Once the bacterial population has increased enough to produce a high concentration of AHL signals, the LuxR receptors bind to the AHL, dimerize, and bind to the DNA to induce QS phenotypes.

1.1.2 The pathogen Pseudomonas aeruginosa regulates virulence through quorum sensing

One organism of particular interest in the QS field is *Pseudomonas aeruginosa.* This bacterium is an opportunistic pathogen often associated with cystic fibrosis patients and hospital acquired infections.[10] It is particularly difficult to treat in part because of its aggressive biofilm formation, which can serve as a protective barrier against both immune response and antibiotics.[11] Finding means to combat infection and virulence is of the utmost importance for this organism as it has become increasingly antibiotic resistant.[12] Of the 51,000 cases of *P. aeruginosa* infections occurring in 2013, 6,000 or 13% were found to be multidrug resistant.[13] In fact, just in the last

year the World Health Organization has classified *P. aeruginosa* a priority pathogen, one of twelve that pose great risk to human health and requires urgent antibiotic development.[14]

Understanding *P. aeruginosa* QS is of interest for both the basic biology of cell signaling as well as antibiotic development in part because up to 10% of its genome is regulated by QS.[15] This includes many of the virulence factors that make *P. aeruginosa* such an aggressive pathogen including pyocyanin, a toxic redox active molecule; hydrogen cyanide, a volatile poison; rhamnolipid, a powerful biosurfactant; and elastase, a protein responsible for degradation of the extracellular matrix.[16] Promisingly, it has been shown that interference with QS can inhibit virulence factor production.[17, 18] QS modulation exerts limited selective pressures on bacteria, making development of resistance rather rare.[19] A broader understanding of how the QS circuit of *P. aeruginosa* can be modulated under different conditions is critical for targeting the virulence associated with this chemical communication.

1.1.3 P. aeruginosa has a complex quorum sensing circuit

Efforts to fully understand and target the QS system of *P. aeruginosa* as an antivirulence strategy have been slow due to the complexity of the circuit (Figure 1.2). Unlike the simple canonical QS system of *Vibrio fisheri*, *P. aeruginosa* has two different LuxI/LuxR-type circuits. At the perceived top of the hierarchy sits the Las system, in which the AHL *N*-(3-oxo-dodecanoyl)-L-homoserine lactone (OdDHL) is produced by the LasI synthase and binds to receptor LasR.[3] The Las pathway is named after its regulation of elastase, the primary virulence factor associated with this receptor. LasR directly upregulates the operon for the Rhl system, the second circuit in *P. aeruginosa*. Synthase RhlI produces *N*-butyryl L-homoserine (BHL), which subsequently binds to its cognate RhlR receptor.[20] RhlR is a key regulator of the rhamnolipid biosynthesis in *P. aeruginonsa* through its binding of the rhlAB operon, by which it gets its name.[21] With no ligand bound, RhlR acts as a repressor for this pathway.[22]

Adding to the complexity is an orphan LuxR-type receptor QscR, named as the Quorum-Sensing-Control Repressor. QscR has no cognate synthase and binds to OdDHL, regulating both the Las and Rhl systems.[23] The first of the three receptors to be produced during logarithmic growth, this receptor is thought to be a dampening agent for the other circuitry.[24] It is hypothesized to prevent the QS circuit from turning on at inopportune times. Specifically, it has been shown that this receptor forms inactive heterodimers with RhlR and LasR, pulling its cognate receptors away from forming their own active homodimers.[25] The Rhl and Las systems further regulate the Pseudomonas Quinolone Signaling (PQS) system, which utilizes quinolone PQS (2-heptyl-3-hydroxy-4-quinolone) as its signaling molecule. The LysR-type transcriptional regulator PqsR responds to the PQS signal, promoting further regulation primarily of pyocyanin synthetic pathway genes.[26] Additionally, RhlR activation has been shown to negatively regulate the production of pyocyanin through its repression of the pqsABCDE operon associated with the PQS pathway.[27] Such an intricate QS network is hypothesized to help *P. aeruginosa* become an effective pathogen, allowing the bacterium to finely tune its gene expression based on its surroundings.[28]

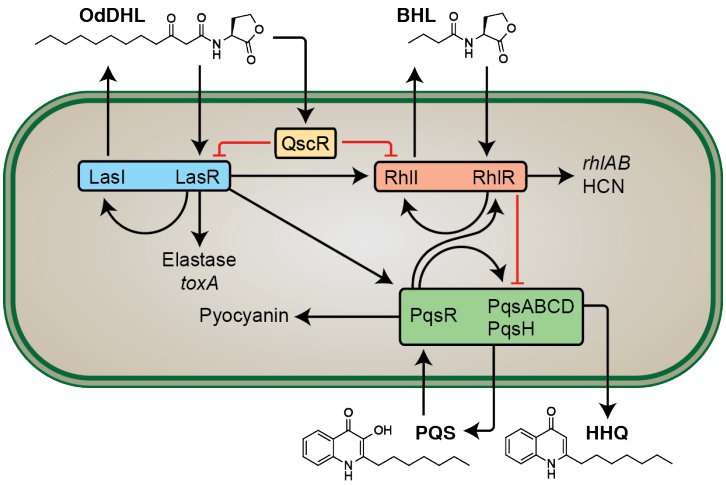

Figure 1.2: Simplified scheme of the *Pseudomonas aeruginosa* quorum sensing network. Arrows represent positive feedback (autoinducer synthesis/transcriptional regulation/receptor binding, etc.). Flat arrows represent negative regulation.

1.1.4 Efforts to understand and modulate P. aeruginosa quorum sensing receptors

Many research groups have reported non-native AHLs that modulate these QS receptors in hopes of controlling undesirable phenotypes without promoting further drug resistance.[29] A large amount of research, especially in the Blackwell group, has focused on synthesizing structural mimics of native AHLs with varying lactone head groups and acyl tails to agonize or antagonize the LuxR-type receptors and induce different QS phenotypes.[30-32] These libraries have been screened in a variety of organisms and receptors, including all three of the LuxR-type receptors in *P. aeruginosa*.

Most QS modulators are currently investigated using whole-cell assays. For *P. aeruginosa* QS receptors in particular, two reporter system types are employed. Typically, a *P. aeruginosa* reporter strain is used that has its RhlI and LasI synthases knocked out, allowing for all QS response to be attributable only to added AHLs. An added reporter plasmid with a promoter region corresponding to the LuxR-type receptor of interest allows for chemical probes to modulate the entire QS circuitry and response to be attributable to a single receptor. *E. coli* strains are used to isolate a single receptor's response to a chemical modulator. Strains heterologously express a single LuxR-type receptor of interest, which then binds to its promoter upon activation. The dual strain approach has been used extensively in the QS field due to their robust response and ease of use, providing complementary confirmation of receptor targeting for phenotypic assays as well as activity discovery in high throughput screening. Our lab has used both reporter systems extensively as complementary tools to probe modulator behavior against *P. aeruginosa*.[33]

1.1.5 Lead modulators against the P. aeruginosa quorum sensing receptors

LasR has received a significant amount of attention from a number of laboratories since it has long been considered the master regulator of *P. aeruginosa*'s QS circuit.[29] Many structures have built directly off of the OdDHL scaffold, both altering the homoserine lactone head group and adding phenyl-based tail groups rather than aliphatic tails (Figure 1.3C). Through the use of high

throughput screening campaigns, some of the most successful agonists and antagonists have moved dramatically away from the traditional homoserine lactone-based model.[34, 35] Recently, our lab undertook a systematic evaluation of various published modulators of LasR, comparing lead compounds head-to-head in order to draw direct conclusions about compound activities.[33] This analysis has prompted other endeavors in our lab to look at comparing lead modulators in a systematic fashion, consolidating the disparate results found in the literature.

RhlR had historically been less of a focus for the development of chemical modulators due to its perceived lower importance in the *P. aeruginosa* QS hierarchy. However, an increasing number of RhlR modulators have been recently elucidated (Figure 1.3D). Early studies by the Suga lab pointed towards the development of cyclopentanone and cyclohexanone derivatives of BHL.[36] Kato and coworkers showed that a cyclopentylamine-based structure also could inhibit RhlR.[37] However, recent work by the Bassler lab has shown that targeting this receptor using partial agonists result in the rescuing of a variety of organisms, including *C. elegans*, lung tissue, and mouse models.[17, 38] Work in our lab has shown that both agonizing and antagonizing this receptor can result in the inhibition of various virulence phenotypes, specifically pyocyanin and Rhamnolipid, in part through RhlR's influence on the PQS pathway.[27] When the RhlR gene is knocked out, the inverse regulation is not observed and both phenotypes are lost.[39] Only through the use of chemical modulators are these relationships perceived. These observations have bolstered efforts to generate more potent agonists and antagonists for this receptor.

QscR has not been a target for extensive small molecule modulator development, primarily due to its perceived lower importance in the QS hierarchy of *P. aeruginosa*. Efforts primarily from our lab have found a number of potent modulators for this receptor (Figure 1.3E).[40] Despite binding to the same ligand as LasR, there are some pronounced differences in AHL activities between these two receptors. Looking at the head group portion of the AHL, QscR is less tolerant of sterically large head groups. Tail groups, however, have shown to be far more varied and bulky in QscR ligands relative to LasR. One of the leading QscR activators was found to have a

branched alkyl chain at the alpha position; this ligand was more than 2000-fold less active in LasR.[40] This activity profile corresponds to the observation that QscR can be activated by a number of native AHLs. Potent antagonists of this receptor have steric bulk added alpha to the amide carbonyl, specifically in the form of an aromatic ring. Notably, these antagonists do not display unfavorable non-monotonic behavior and instead behave like true partial agonists, a relative rarity in terms of LuxR-type receptors. Compared to the studies focused on LasR and RhlR, little work has been done to probe the head group accommodations allowed by QscR.

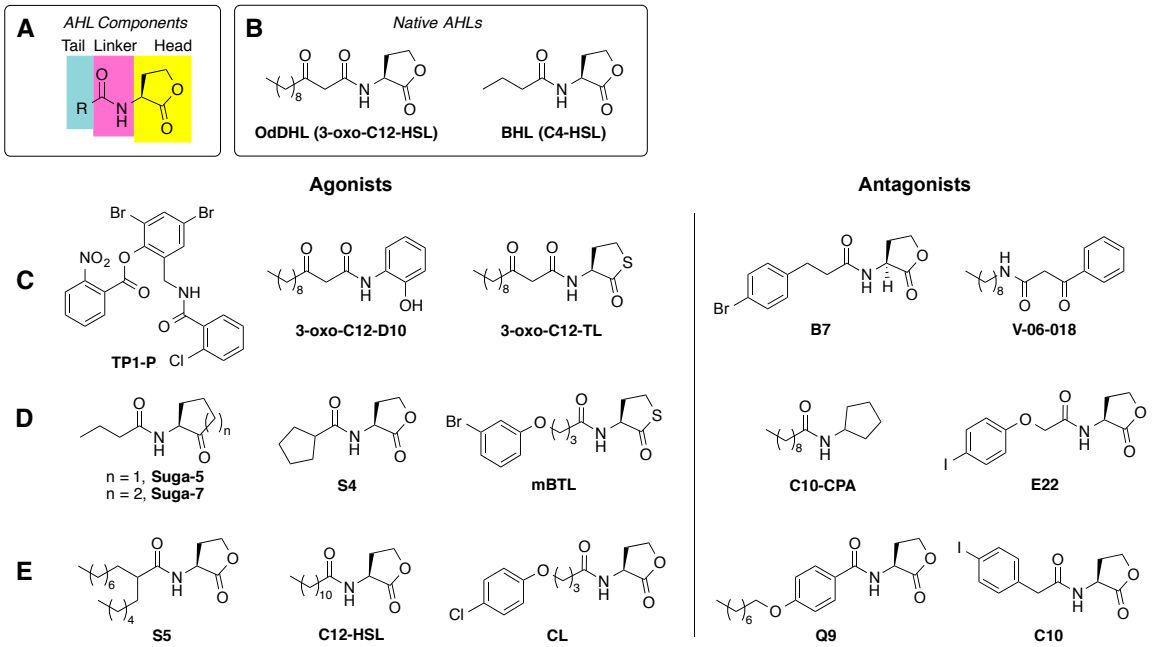

Figure 1.3. Select lead non-native agonists and antagonists of the LuxR-type receptors found in *P. aeruginosa*. A) Generic scaffold for AHLs. B) Native AHLs produced by *P. aeruginosa*. C) Lead LasR modulators. D) Lead RhlR modulators. E) Lead QscR modulators. Non-native compounds were developed in the following laboratories: **TP1-P** and **V-06-018**, Greenberg and coworkers[34, 35, 41]; **3-oxo-C12-D10**, **Suga-5**, and **Suga-7**, Suga and coworkers[36, 42]; **3-oxo-C12-TL**, Iglewski and coworkers[43]; **B7, S4**, **E22**, **S5**, **Q9**, and **C10**, Blackwell and coworkers[31, 40, 44]; **mBTL** and **CL**, Bassler and coworkers[17, 45, 46]; **C10-CPA**, Kato and coworkers.[37]

1.1.6 Limitations to data acquired by cell-based reporter assays.

While a number of the most potent known agonists and antagonists have been identified using a combinatorial approach based on the AHL scaffold, these agents require further structural

optimization to increase their potency, solubility, and physical stability. Improving these features would permit AHL usage in a broader range of biologically relevant contexts and could pave a route to novel therapeutic development. This advancement cannot be done well, however, without knowing the mode of action for current libraries versus the receptors they target. Even with the dual strain approach using *P. aeruginosa* and *E. coli* reporters, these assays are only able to provide activity data and not mechanistic information about the receptor. In other words, we have limited insight into how compounds are actually activating or inhibiting LuxR-type receptors.

Mechanistic data is in particularly dire need due to the high proportion of nonclassical partial agonists discovered via the cell-based reporters. These compounds display what our lab has termed "nonmonotonic dose response behavior".[33] Unlike compounds that are classical agonists and antagonists with well described sigmoidal effects on receptors, nonclassical partial agonists induce a pronounced decrease in receptor activity followed by a steep activation corresponding to the compound's agonism profile. The curves have a "U-shape" or "upturn". Many of these compounds are incredibly potent inhibitors, yet the inversion of activity results in a compound of decreased utility at higher concentrations. This curve profile is not an anomaly; it appears in a variety of reporter systems for a number of LuxR-type receptors with both native and non-native compounds. Nonmonotonic behavior is typically observed in toxicological studies looking at data on health-based outcomes, not in simplified receptor reporter systems.[47] Moore *et al.* investigated two possible hypotheses.[33] First, the presence of mixed heterodimers with each LuxR-type monomer bound to a different ligand. In this case, the mixed heterodimer has limited activity, but the addition of further competitor allows for a homodimer with limited activity. The second hypothesis suggested two discrete binding events occurring in the receptor dimer. Based on the analysis of dose response curves generated using varying amounts of native ligand competitor, Moore highlighted the possibility of a first binding event with competitive behavior and a second with noncompetitive behavior. To unravel these possible outcomes, biochemical studies utilizing in vitro purified LuxR-type protein is needed.

1.1.7 Protein biochemistry to understand LuxR-type receptor-ligand interactions

Unfortunately, characterizing the biochemistry of LuxR-type receptors has been challenging. There is a dearth of available structural and biochemical information. Only four full-length structures have been solved using crystallography or NMR, and these fail to provide a unifying mechanism for LuxR-type protein activity. TraR, a protein from plant pathogen *Agrobacterium tumefaciens*, was the first crystalized receptor and also the only structure solved bound to its DNA promoter.[48] SdiA, a LuxR-type receptor found in *E. coli* without a cognate synthase, is the only full-length structure to be solved both in its apo and ligand bound form.[49, 50] CviR, a receptor found in *Chromobacterium violaceum*, is crystalized bound to not an agonist, but rather a non-native antagonist.[45] This structure adopts a surprisingly stable criss-cross shape that causes the DNA binding domains to splay too far apart for productive binding. Lastly, QscR from *P. aeruginosa* has been crystalized in the presence of OdDHL.[51] A handful of additional truncated ligand binding domain structures have been solved as well, including that of LasR crystalized with both native and non-native agonists.[52] These structures have provided some insight into how non-native agonists and antagonists are interacting with these receptors, but the increasing diversity of chemical probes used versus an expanding set of LuxR-type receptors necessitates additional work to determine mode of action.

Further crystallographic analyses as well as basic biochemical experiments to probe ligand mechanism of action have been stymied by the extreme instability of these proteins without the addition of a cognate AHL agonist during isolation and purification.[3, 53] Binding between LuxR-type receptors and their native ligands was long thought to be nearly irreversible, and the ligands were assumed to be required for correct receptor folding as translated from the ribosome.[54] Such tight binding would suggest that out-competing the native ligand after the receptor:AHL complex has formed is nearly impossible, a problem for exchanging and characterizing non-native modulators. Studies looking at non-native AHL:protein interactions typically still produce and purify the protein of interest in the presence of the desired ligand rather than trying to displace it.

Fortunately, studies of binding in the *P. aeruginosa* receptors QscR and LasR have shown that these receptors can dissociate from the ligand after folding and can fold into their active forms in the absence of native ligand OdDHL[55, 56] Protein can correctly fold into a functional, albeit unstable confirmation without ligand, and binding to a native ligand allows for stabilization. Not only did this observation open up the possibility for ligand exchange during in vitro and in cell biochemical experiments, but it also allowed for a revised hypothesis on the binding of non-native and native AHLs (Figure 1.4). This model demonstrates that a non-native AHL could potentially displace a native ligand during protein folding, dimerization, or DNA binding. Antagonists in particular could be functioning through destabilization of the protein, inducing the formation of misfolded monomers that cannot dimerize, causing the formation of inactive dimers that cannot bind to DNA, or some other combination of the proposed mechanisms.

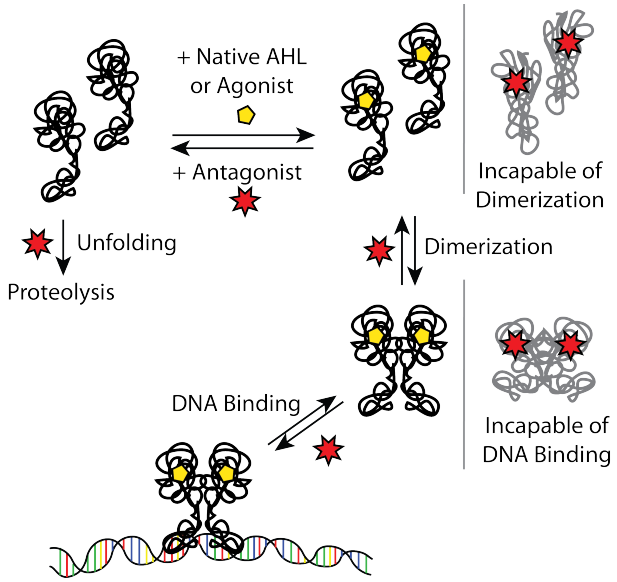

Figure 1.4. Model of LuxR-type receptor binding to AHLs. Agonists are shown in yellow and antagonists are shown in orange**.**

The QscR receptor in particular has been a boon for biochemical studies. Aside from the structural data afforded by the full length crystal structure of QscR,[51] work by Greenberg and

coworkers showed that this receptor can be purified without its native ligand; instead of OdDHL, *N*-(3-oxo-hexanoyl)-L-homoserine lactone (OHHL) is sufficient to stabilize the receptor during expression, purification, and subsequent exchange with a ligand of interest.[56] With this discovery, Greenberg *et al.* showed how varying concentrations of different native AHLs could alter the QscR dimer's binding ability.[56] We reasoned that similar experiments could easily be performed using an expanded variety of native and non-native AHLs.

1.2 Efforts to expand the chemical toolbox to investigate *P. aeruginosa* quorum sensing

1.2.1 Overview

The QS field still needs improved chemical tools to probe and understand quorum sensing, particularly in the context of *P. aeruginosa*. My work detailed herein focuses on three diverse projects that all center on expanding this toolkit. The Blackwell lab has historically come to view chemical tools as the small molecule modulators that interact directly with the receptors and induce or inhibit transcriptional response. To this end, I have developed a number of chemical libraries that have provided key insights into receptor selectivity, resulting in improved LuxR-type receptor modulation and compound stability. This work is critical as we explore the complex biology associated with these QS networks and begin to consider targeting QS as a means to reduce virulence in vivo. Importantly, I have also helped to broaden the chemical toolkit to include methods for deciphering AHL mode of action and enabling QS-associated phenotype detection.

1.2.2 Thorough SAR of AHL molecules to gain insights into receptor activation and inhibition

Combinatorial generation of small molecule libraries has been a successful means for uncovering initial hits that modulate LuxR-type receptors, but further development of AHL-based ligands requires a more thorough understanding of the molecular features critical for compound activity. Such rigorous structural analysis has been performed largely in a piecemeal fashion in

the field, with different research laboratories using highly divergent assays to monitor compound activity even for the same LuxR-type receptor. Additionally, as we strive to understand complex QS circuits both within individual bacteria and in broader interspecies context, we must have a better understanding of the key SARs driving ligand activity. Chapters 2 and 6 provide rigorous analysis of subtle structural changes to the native ligands *P. aeruginosa* uses to regulate receptors RhlR and LasR. Chapter 3 highlights a next-generation chemical library built off of the SARs developed for BHL, reporting some of the most potent and stable modulators known for this receptor.

1.2.3 Understanding AHL mode of action using both well-established and novel assay techniques for LuxR-type receptors

Foundational work with receptor QscR has shown that this protein is a candidate for biochemical studies investigating non-native AHL mode of action. Not only is there a full-length crystal structure for this receptor, but QscR also can be readily purified with an exchangeable stabilization ligand. Work performed in collaboration with the Churchill lab at CU–Denver detailed in Appendix I discusses a variety of mechanistic studies performed with some of our previously reported potent classical agonists and classical partial agonists of QscR. These observations support our current hypothesis about ligand activity in QscR and will have utility in further designing non-native AHLs for QscR modulation.

While any mechanistic info is helpful in regards to this receptor class, many of the traditional biochemical tools used to probe transcription factor activity, including those utilized in Chapter 4, are relatively low throughput. There is significant interest in developing screening methods in the QS field that move towards in vitro assays to complement cell-based reporter techniques. In vitro assays allow for a more direct quantification of protein-ligand interactions and could expedite mechanistic studies on how AHLs function. Inspired by the reliance of many high throughput screening campaigns on fluorescence-based techniques, we developed a Förster Resonance

Energy Transfer (FRET) probe for use in QscR as described in Chapter 4. This probe has allowed us to examine ligand binding and mechanism of action by competing in varying AHLs of interest and observing loss of fluorescence while moving to a higher throughput, convenient 384-well assay format.

1.2.4 Utilizing quorum sensing as a means for population-based responsive detection

Through collaboration with the Lynn lab at UW–Madison, the Blackwell lab has worked to design novel materials that release QS modulators over time with a possible utility in coatings to block bacterial communication and virulence.[57-59] This approach has been shown to inhibit QS associated phenotypes in a range of contexts.[57-59] One limitation of these materials, however, is that they are not responsive to the presence of bacteria; they consistently release material over time through diffusion or chemical degradation in an aqueous environment. This release profile means that QS control is only temporary, and the modulating signals are eventually depleted.

Liquid crystal (LC) molecules are a class of matter that can be utilized to develop materials responsive to chemical or biological particulate.[60] LCs can pack and directionally orient in a bulk solution but do not have a fixed position in space as is characteristic of a solid. Their packing and orientation can radically transition with an environmental change. LC molecules have been utilized as detectors for a number of small molecule analytes, including excreted or shed "goods" produced by bacteria and amphiphilic molecules such as lipids or surfactants.[61, 62] Additionally, LCs have served as a means of controlled release in a variety of contexts, including in drug delivery.[63] The many amphiphilic molecules produced by *P. aeruginosa,* including AHLs, toxins, and rhamnolipids, may serve as a foothold towards developing LC-based materials responsive to bacterial QS. We report in Chapter 5 the first instance of LC detection of QS-associated molecules, which may provide a new pathway for QS detection. This observation paves the way for future materials that utilize QS molecules for both sensitive bacterial detection and triggered cargo release.

1.3 Dissertation Scope

1.3.1 Chapter 2: Structure-function analyses of the N-butyryl L-homoserine lactone quorum sensing signal define features critical to activity in the P. aeruginosa RhlR receptor

Surprisingly, despite the emerging prominence of RhlR in QS pathways, there has been limited exploration of the features of the BHL scaffold that are critical to its function in *P. aeruginosa*. As detailed in Chapter 2, we sought to systematically delineate the SARs driving BHL activity for the first time. A focused library of BHL analogues was designed, synthesized, and evaluated in cell-based reporter gene assays for RhlR agonism and antagonism. These investigations allowed us to define a series of SARs for BHL-type ligands and identify structural motifs critical for both activation and inhibition of the RhlR receptor. Notably, we identified new agonists that have ~10-fold higher potencies in RhlR relative to BHL, are highly selective for RhlR over LasR, and are active in the *P. aeruginosa* background. These compounds and the SARs reported herein could provide a new pathway toward chemical strategies to study RhlR in *P. aeruginosa*.

1.3.2 Chapter 3: N-Acyl L-homocysteine thiolactones are potent and stable synthetic modulators of the RhlR quorum sensing receptor in P. aeruginosa

Non-native lactone ligands are known to modulate RhlR activity, but their utility as chemical probes is limited due to hydrolytic instability. In Chapter 3, we report our design and biological evaluation of a suite of hybrid AHL analogs with structures merging (1) features of the most promising reported RhlR ligands and (2) head groups with improved hydrolytic stabilities. The most promising compounds were *N*-acyl L-homocysteine thiolactones and showed improved hydrolytic stabilities relative to lactones. Moreover, they were highly selective for RhlR over another key QS receptor in *P. aeruginosa*, LasR. These compounds are the most potent RhlR

modulators known and represent robust, new chemical tools to dissect the complex role of RhlR in the *P. aeruginosa* QS circuitry.

1.3.3 Chapter 4: Development of a FRET assay to characterize LuxR-type receptor ligand binding

LuxR-type proteins have been found difficult to manipulate in vitro, and this problem has limited their biophysical characterization and the study of their DNA binding processes. Further, these experimental limitations have hindered the study of non-native AHL:LuxR-type protein interactions. QscR from *P. aeruginosa* has been reported to be stable in vitro and isolable in apo form. This finding prompted us to develop a new biophysical assay method to study QscR in vitro. We developed a Förster Resonance Energy Transfer (FRET) assay that utilizes a novel dansyl AHL derivative and takes advantage of endogenous tryptophans located in the ligand binding pocket as the fluorescence donor. We applied this assay both in vitro and in cellulo to probe the effects of our previously identified synthetic ligands on QscR. Binding data obtained by using the FRET assay trends well with cell-based reporter data and electrophoretic mobility shift data that report [QscR:ligand]:DNA interactions. More interestingly, these FRET data provide new insights into the mechanism of action of non-native AHLs. Notably, these data suggest that nonclassical partial agonists bind with QscR at lower affinities than expected compared to cell-based reporter data. We anticipate this approach will be useful for studying ligand binding of other LuxR-type receptors in the future.

1.3.4 Chapter 5: The application of liquid crystalline droplets as sensors for quorate populations of bacteria

Liquid crystals (LCs) have been used to detect the presence of bacteria via byproducts such as lipopolysaccharides. However, this detection approach requires membrane components that are only available upon bacterial cell lysis. We report the first instance of the use of LCs as

responsive materials for amphiphilic bacterial goods directly associated with population density. The opportunistic pathogen *P. aeruginosa* excretes long chain signaling molecule *N*-(3-oxo-dodecanoyl)-L-homoserine lactone (3-oxo-C12-HSL) to gauge population density via quorum sensing (QS). An active QS system induces the production of a range of byproducts associated with virulence, including the biosurfactant rhamnolipid. We found that both of these molecules can induce bipolar-to-radial orientation changes in LC dispersions. When LCs are added to cell culture in a permeable membrane, only cells actively producing 3-oxo-C12-HSL or rhamnolipid components can induce an LC orientation change. Additionally, we show that *N*-acyl L-homoserine lactones with acyl chains eight carbons in length or longer induce LC transitions, suggesting that this detection technique may be applicable to a variety of bacterial QS systems. These findings demonstrate that QS-responsive materials may be a means to detect bacteria and open new ways for controlling bacterial social behaviors.

1.3.5 Chapter 6: Comparative analysis of non-native N-(3-oxo-dodecanoyl)-L-homoserine lactone variants in two P. aeruginosa quorum sensing receptors (LasR and QscR) that share the same native ligand

Significant research efforts have focused on delineating the role of LasR in *P. aeruginosa* QS due to its perceived importance in the QS signaling hierarchy. QscR, a receptor that represses the effects of the LasR QS circuit, has seen far less scrutiny. Despite both receptors being activated by OdDHL, we currently have a limited understanding of the structural features of non-native ligands that engender selectivity in these two receptors. To begin to investigate such features, a small library of OdDHL analogues was synthesized with changes made to the homoserine lactone head group and screened in a cell-based reporter assays to determine activity trends in both LasR and QscR. We identified several motifs that bias ligand activation towards each of the two receptors. Many of the most potent ligands had lactone replacements that also benefit from increased hydrolytic stability relative to homoserine lactone. These findings should

be valuable for the development of more selective and stable synthetic agonists and antagonists of both LasR and QscR.

1.3.6 Appendix I: Mechanism of agonism and antagonism of the P. aeruginosa quorum sensing regulator QscR with non-native ligands

To better understand *P. aeruginosa* QS signal reception, we examined the mechanism underlying the response of QscR to synthetic agonists and antagonists using biophysical and structural approaches. The structure of QscR bound to a synthetic agonist revealed a novel mode of ligand binding supporting a general mechanism for agonist activity. In turn, antagonists of QscR with partial agonist activity were found to destabilize and greatly impair QscR dimerization and DNA binding. These results highlight the diversity of LuxR-type receptor responses to small molecule agonists and antagonists and demonstrate the potential for chemical strategies for the selective targeting of individual quorum-sensing systems.

1.4 References

1. Nealson, K. H., and Hastings, J. W. (1979) Bacterial bioluminescence: its control and ecological significance., *Microbiol. Rev. 43*, 496-518.

2. Eberhard, A., Burlingame, A. L., Eberhard, C., Kenyon, G. L., Nealson, K. H., and Oppenheimer, N. J. (1981) Structural identification of autoinducer of *Photobacterium fischeri*, *Biochem. 20*, 2444-2449.

3. Fuqua, C., and Greenberg, E. P. (2002) Listening in on bacteria: acyl-homoserine lactone signalling, *Nat. Rev. Mol. Cell Biol. 3*, 685-695.

4. Miller, M., and Bassler, B. (2001) Quorum Sensing in Bacteria, *Annu. Rev. Microbiol. 55*, 165-199.

5. Camilli, A., and Bassler, B. L. (2006) Bacterial Small-Molecule Signaling Pathways, *Science 311*, 1113-1116.

6. Engebrecht, J., Nealson, K., and Silverman, M. (1983) Bacterial bioluminescence: isolation and genetic analysis of functions from *Vibrio fischeri*, *Cell 32*, 773-781.

7. Miller, M. B., and Bassler, B. L. (2001) Quorum Sensing in Bacteria, *Annu. Rev. Microbiol. 55*, 165-199.

8. Hudaiberdiev, S., Choudhary, K. S., Vera Alvarez, R., Gelencsér, Z., Ligeti, B., Lamba, D., and Pongor, S. (2015) Census of solo LuxR genes in prokaryotic genomes, *Front. Cell. Infect. Microbiol. 5*, 1-6.

9. González, J. F., and Venturi, V. (2012) A novel widespread interkingdom signaling circuit, *Trends Plant Sci. 18*, 167-174.

10. Lyczak, J. B., Cannon, C. L., and Pier, G. B. (2000) Establishment of *Pseudomonas aeruginosa* infection: lessons from a versatile opportunist, *Microb. Infect. 2*, 1051-1060.

11. Taylor, P. K., Yeung, A. T. Y., and Hancock, R. E. W. (2014) Antibiotic resistance in *Pseudomonas aeruginosa* biofilms: Towards the development of novel anti-biofilm therapies, *J. Biotechnol. 191*, 121-130.

12. Ciofu, O., Mandsberg, L. F., Bjarnsholt, T., Wassermann, T., and Hoiby, N. (2010) Genetic adaptation of *Pseudomonas aeruginosa* during chronic lung infection of patients with cystic fibrosis: strong and weak mutators with heterogeneous genetic backgrounds emerge in mucA and/or lasR mutants, *Microbiology 156*, 1108-1119.

13. (2013) Antibiotic resistance threats in the United States, Centers for Disease Control and Prevention (CDC), Atlanta.

14. Tacconelli, E., Carmell, Y., Harbarth, S., Kahlmeter, G., Kluytmans, J., Mendelson, M., Pulcini, C., Singh, N., and Theuretzbacher, U. (2017) Global priority list of antibiotic-resistant bacteria to guide research, discovery, and development of new antibiotics, World Health Orgnaization (WHO), Geneva.

15. Whiteley, M., Lee, K., and Greenberg, E. (1999) Identification of genes controlled by quorum sensing in *Pseudomonas aeruginosa*., *Proc. Natl. Acad. Sci. USA 96*.

16. Delden, C. v. (2004) Virulence Factors in *Pseudomonas aeruginosa*, in *Virulence and Gene Regulation* (Ramos, J., Ed.), pp 3-45, Springer, Boston, MA.

17. O'Loughlin, C. T., Miller, L. C., Siryaporn, A., Drescher, K., Semmelhack, M. F., and Bassler, B. L. (2013) A quorum-sensing inhibitor blocks *Pseudomonas aeruginosa* virulence and biofilm formation, *Proc. Natl. Acad. Sci. USA 110*, 17981-17986.

18. Mattmann, M. E., and Blackwell, H. E. (2010) Small molecules that modulate quorum sensing and control virulence in *Pseudomonas aeruginosa*, *J. Org. Chem. 75*, 6737-6746.

19. Gerdt, J. P., and Blackwell, H. E. (2014) Competition Studies Confirm Two Major Barriers That Can Preclude the Spread of Resistance to Quorum-Sensing Inhibitors in Bacteria, *ACS Chem. Biol. 9*, 2291-2299.

20. Schuster, M., and Greenberg, E. P. (2006) A network of networks: quorum-sensing gene regulation in *Pseudomonas aeruginosa*., *Int. J. Med. Microbiol. 296*, 73-81.

21. Ochsner, U. A., Fiechter, A., and Reiser, J. (1994) Isolation, characterization, and expression in *Escherichia coli* of the *Pseudomonas aeruginosa* rhlAB genes encoding a rhamnosyltransferase involved in rhamnolipid biosurfactant synthesis, *J. Biol. Chem. 269*.

22. Medina, G., Jua, K., Valderrama, B., and Sobero, G. (2003) Mechanism of *Pseudomonas aeruginosa* RhlR Transcriptional Regulation of the rhlAB Promoter, *J.Bacteriol. 185*, 5976-5983.

23. Chugani, S. a., Whiteley, M., Lee, K. M., D'Argenio, D., Manoil, C., and Greenberg, E. P. (2001) QscR, a modulator of quorum-sensing signal synthesis and virulence in *Pseudomonas aeruginosa*, *Proc. Natl. Acad. Sci. USA 98*, 2752-2757.

24. Lequette, Y., Lee, J. H., Ledgham, F., Lazdunski, A., and Greenberg, E. P. (2006) A distinct QscR regulon in the *Pseudomonas aeruginosa* quorum-sensing circuit, *J. Bacteriol. 188*, 3365-3370.

25. Ledgham, F., Ventre, I., Soscia, C., Foglino, M., Sturgis, J. N., and Lazdunski, A. (2003) Interactions of the quorum sensing regulator QscR: interaction with itself and the other regulators of *Pseudomonas aeruginosa* LasR and RhlR., *Mol. Microbiol. 48*, 199-210.

26. Diggle, S. P., Cornelis, P., Williams, P., and Camara, M. (2006) 4-Quinolone signalling in *Pseudomonas aeruginosa*: Old molecules, new perspectives, *Int. J. Med. Microbiol. 296*.

27. Welsh, M. a., Eibergen, N. R., Moore, J. D., Blackwell, H. E., Welsh, M., Eibergen, N. R., Moore, J. D., and Blackwell, H. E. (2015) Small molecule disruption of quorum sensing cross-regulation in *Pseudomonas aeruginosa* causes major and unexpected alterations to virulence phenotypes, *J. Am. Chem. Soc. 137*, 1510-1519.

28. Williams, P., and Cámara, M. (2009) Quorum sensing and environmental adaptation in *Pseudomonas aeruginosa*: a tale of regulatory networks and multifunctional signal molecules, *Curr. Opin. Microbiol. 12*, 182-191.

29. Galloway, W. R. J. D., Hodgkinson, J. T., Bowden, S., Welch, M., and Spring, D. R. (2012) Applications of small molecule activators and inhibitors of quorum sensing in Gram-negative bacteria, *Trends Microbiol. 20*, 449-458.

30. Geske, G. D., Wezeman, R. J., Siegel, A. P., and Blackwell, H. E. (2005) Small molecule inhibitors of bacterial quorum sensing and biofilm formation., *J. Am. Chem. Soc. 127*, 12762-12763.

31. Geske, G. D., O'Neill, J. C., Miller, D. M., Wezeman, R. J., Mattmann, M. E., Lin, Q., and Blackwell, H. E. (2008) Comparative analyses of *N*-acylated homoserine lactones reveal unique structural features that dictate their ability to activate or inhibit quorum sensing, *ChemBioChem 9*, 389-400.

32. Mattmann, M. E., Geske, G. D., Worzalla, G. a., Chandler, J. R., Sappington, K. J., Greenberg, E. P., and Blackwell, H. E. (2008) Synthetic ligands that activate and inhibit a quorum-sensing regulator in *Pseudomonas aeruginosa*, *Bioorg. Med. Chem. Lett. 18*, 3072-3075.

33. Moore, J. D., Rossi, F. M., Welsh, M. A., Nyffeler, K. E., and Blackwell, H. E. (2015) A Comparative Analysis of Synthetic Quorum Sensing Modulators in *Pseudomonas aeruginosa*:

New Insights into Mechanism, Active Efflux Susceptibility, Phenotypic Response, and Next-Generation Ligand Design, *J. Am. Chem. Soc. 137*, 14626-14639.

34. Müh, U., Hare, B. J., Duerkop, B. a., Schuster, M., Hanzelka, B. L., Heim, R., Olson, E. R., and Greenberg, E. P. (2006) A structurally unrelated mimic of a *Pseudomonas aeruginosa* acyl-homoserine lactone quorum-sensing signal, *Proc. Natl. Acad. Sci. USA 103*, 16948-16952.

35. Müh, U., Schuster, M., Heim, R., Singh, A., Olson, E. R., and Greenberg, E. P. (2006) Novel *Pseudomonas aeruginosa* quorum-sensing inhibitors identified in an ultra-high-throughput screen, *Antimicrob. Agents Chemother. 50*, 3674-3679.

36. Smith, K. M., Bu, Y., and Suga, H. (2003) Induction and Inhibition of *Pseudomonas aeruginosa* Quorum Sensing by Synthetic Autoinducer Analogs, *Chem. Biol. 10*, 81-89.

37. Ishida, T., Ikeda, T., Takiguchi, N., Kuroda, A., Ohtake, H., and Kato, J. (2007) Inhibition of quorum sensing in *Pseudomonas aeruginosa* by *N*-acyl cyclopentylamides, *Appl. Environ. Microbiol. 73*, 3183-3188.

38. Mukherjee, S., Moustafa, D., Smith, C. D., Goldberg, J. B., and Bassler, L. (2017) The RhlR quorum-sensing receptor controls *Pseudomonas aeruginosa* pathogenesis and biofilm development independently of its canonical homoserine lactone autoinducer, *PLoS Pathog. 13*, e1006504.

39. Welsh, M. A., Eibergen, N. R., Moore, J. D., and Blackwell, H. E. (2015) Small molecule disruption of quorum sensing cross-regulation in *Pseudomonas aeruginosa* causes major and unexpected alterations to virulence phenotypes, *J. Am. Chem. Soc. 137*, 1510-1519.

40. Mattmann, M. E., Shipway, P. M., Heth, N. J., and Blackwell, H. E. (2011) Potent and Selective Synthetic Modulators of a Quorum Sensing Repressor in *Pseudomonas aeruginosa* Identified from Second-Generation Libraries of *N*-Acylated L-Homoserine Lactones, *Chembiochem 12*, 942-949.

41. Zakhari, J. S., Kinoyama, I., Struss, A. K., Pullanikat, P., Lowery, C. A., Lardy, M., and Janda, K. D. (2011) Synthesis and molecular modeling provide insight into a *Pseudomonas aeruginosa* quorum sensing conundrum, *J. Am. Chem. Soc. 133*, 3840-3842.

42. Smith, K. M., Bu, Y., and Suga, H. (2003) Library Screening for Synthetic Agonists and Antagonists of a *Pseudomonas aeruginosa* Autoinducer, *Chem. Biol. 10*, 563-571.

43. Passador, L., Tucker, K. D., Guertin, K. R., Journet, M. P., Kende, a. S., Kende, A. S., and Iglewski, B. H. (1996) Functional analysis of the *Pseudomonas aeruginosa* autoinducer PAI, *J. Bacteriol. 178*, 5995-6000.

44. Eibergen, N. R., Moore, J. D., Mattmann, M. E., and Blackwell, H. E. (2015) Potent and Selective Modulation of the RhlR Quorum Sensing Receptor by Using Non-native Ligands : An Emerging Target for Virulence Control in *Pseudomonas aeruginosa*, *ChemBioChem 16*, 2348-2356.

45. Chen, G., Swem, L. R., Swem, D. L., Stauff, D. L., O'Loughlin, C. T., Jeffrey, P. D., Bassler, B. L., and Hughson, F. M. (2011) A Strategy for Antagonizing Quorum Sensing, *Mol. Cell 42*, 199-209.

46. Swem, L. R., Swem, D. L., O'Loughlin, C. T., Gatmaitan, R., Zhao, B., Ulrich, S. M., and Bassler, B. L. (2009) A quorum-sensing antagonist targets both membrane-bound and cytoplasmic receptors and controls bacterial pathogenicity., *Mol. Cell 35*, 143-153.

47. Vandenberg, L. N., Colborn, T., Hayes, T. B., Heindel, J. J., David R. Jacobs, J., Lee, D.-H., Shioda, T., Soto, A. M., Saal, F. S. v., Welshons, W. V., Zoeller, R. T., and Myers, J. P. (2012) Hormones and Endocrine-Disrupting Chemicals: Low-Dose Effects and Nonmonotonic Dose Responses, *Endocr. Rev. 33*, 378–455.

48. Zhang, R.-g., Pappas, K. M., Brace, J. L., Miller, P. C., Oulmassov, T., Molyneaux, J. M., Anderson, J. C., Bashkin, J. K., Winans, S. C., and Joachimiak, A. (2002) Structure of a bacterial quorum-sensing transcription factor complexed with pheromone and DNA, *Nature 417*, 971-974.

49. Kim, T., Duong, T., Wu, C. A., Choi, J., Lan, N., Kang, S. W., Lokanath, N. K., Shin, D., Hwang, H. Y., and Kim, K. K. (2014) Structural insights into the molecular mechanism of *Escherichia coli* SdiA, a quorum-sensing receptor, *Acta crystallographica. Section D, Biological crystallography 70*, 694-707.

50. Nguyen, Y., Nguyen, N. X., Rogers, J. L., Liao, J., Macmillan, J. B., Jiang, Y., and Sperandio, V. (2015) Structural and Mechanistic Roles of Novel Chemical Ligands on the SdiA Quorum-Sensing Transcription Regulator, *mBio 6*, 1-10.

51. Lintz, M. J., Oinuma, K., Wysoczynski, C. L., Greenberg, E. P., and Churchill, M. E. (2011) Crystal structure of QscR, a *Pseudomonas aeruginosa* quorum sensing signal receptor, *Proc. Natl. Acad. Sci. USA 108*, 15763-15768.

52. Bottomley, M. J., Muraglia, E., Bazzo, R., and Carfì, A. (2007) Molecular insights into quorum sensing in the human pathogen *Pseudomonas aeruginosa* from the structure of the virulence regulator LasR bound to its autoinducer, *J. Biol. Chem. 282*, 13592-13600.

53. Schuster, M., and Greenberg, E. P. (2008) LuxR-Type Proteins in *Pseudomonas aeruginosa* Quorum Sensing: Distinct Mechanisms with Global Implications, in *Chemical Communication among Bacteria* (Winans S., Bassler B., Ed.), pp 133-144, ASM Press, Washington, DC.

54. Churchill, M. E., and Chen, L. (2011) Structural Basis of Acyl-homoserine Lactone-Dependent Signaling, *Chem. Rev. 111*, 68-85.

55. Sappington, K. J., Dandekar, A. A., Oinuma, K.-i., and Greenberg, E. P. (2011) Reversible Signal Binding by the *Pseudomonas aeruginosa* Quorum-Sensing Signal Receptor LasR, *mBio 2*, 1-6.

56. Oinuma, K., and Greenberg, E. P. (2011) Acyl-homoserine lactone binding to and stability of the orphan *Pseudomonas aeruginosa* quorum-sensing signal receptor QscR, *J. Bacteriol. 193*, 421-428.

57. Kratochvil, M. J., Tal-Gan, Y., Yang, T., Blackwell, H. E., and Lynn, D. M. (2015) Nanoporous Superhydrophobic Coatings That Promote the Extended Release of Water-Labile Quorum Sensing Inhibitors and Enable Long-Term Modulation of Quorum Sensing in *Staphylococcus Aureus*, *ACS Biomater. Sci. Eng. 1*, 1039-1049.

58. Kratochvil, M. J., Welsh, M. A., Manna, U., Ortiz, B. n. J., Blackwell, H. E., and Lynn, D. M. (2016) Slippery Liquid-Infused Porous Surfaces that Prevent Bacterial Surface Fouling and Inhibit Virulence Phenotypes in Surrounding Planktonic Cells, *ACS Infect. Dis. 2*, 509-517.

59. Broderick, A. H., Breitbach, A. S., Frei, R., Blackwell, H. E., and Lynn, D. M. (2013) Surface-Mediated Release of a Small-Molecule Modulator of Bacterial Biofilm Formation: A Non-Bactericidal Approach to Inhibiting Biofilm Formation in *Pseudomonas aeruginosa*, *Adv. Healthc. Mater. 7*, 993-1000.

60. Carlton, R. J., Hunter, J. T., Miller, D. S., Abbasi, R., Mushenheim, P. C., Tan, L. N., and Abbott, N. L. (2013) Chemical and biological sensing using liquid crystals, *Liq. Cryst. Rev. 1*, 29-51.

61. Lin, I.-h., Miller, D. S., Bertics, P. J., Murphy, C. J., Pablo, J. J. D., and Abbott, N. L. (2011) Endotoxin-Induced Structural Transformations in Liquid Crystalline Droplets, *Science 332*, 1297-1300.

62. Miller, D. S., and Abbott, N. L. (2013) Influence of droplet size, pH and ionic strength on endotoxin-triggered ordering transitions in liquid crystalline droplets, *Soft Matter 9*, 374-382.

63. Kim, D.-H., Jahn, A., Cho, S.-J., Kim, J. S., Ki, M.-H., and Kim, D.-D. (2015) Lyotropic liquid crystal systems in drug delivery: a review, *J. Pharm. Investig. 45*, 1-11.

CHAPTER 2:

Structure-function analyses of the *N*-butyryl L-homoserine lactone quorum sensing signal define features critical to activity in the *Pseudomonas aeruginosa* RhlR receptor

Contribution: M. E. Boursier and J. D. Moore designed experiments, synthesized non-native modulators, performed screening assays and wrote manuscript. K. N. Heitman, J. B. Combs, D. Shin, and E. C. Brown assisted with non-native modulator synthesis and characterization. S. P. Shepardson-Fungairino assisted with non-native modulator synthesis and screening assays. L. C. Koenig assisted with screening assays. R. Nagarajan contributed project planning and compound design. H. E. Blackwell guided the project and assisted manuscript preparation.

*This chapter has been prepared as a manuscript intended for publication under the same title.

2.1 Abstract

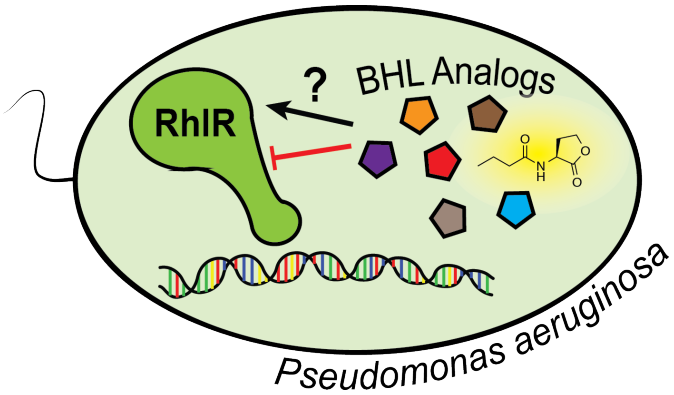

Pseudomonas aeruginosa is an opportunistic pathogen that coordinates the production of myriad virulence phenotypes at high population density via quorum sensing (QS). The LuxR-type QS receptor RhlR plays an important role in the *P. aeruginosa* infection process, and there is considerable interest in the development of chemical approaches to modulate the activity of this protein. RhlR is activated by the simple, low molecular weight *N*-acyl L-homoserine lactone signal, *N*-butyryl-L-homoserine lactone (BHL). Surprisingly, despite the emerging prominence of RhlR in QS pathways, there has been limited exploration of the features of the BHL scaffold that are critical to its function in *P. aeruginosa*. In the current study, we sought to systematically delineate the structure-activity relationships (SARs) driving BHL activity for the first time. A focused library of BHL analogues was designed, synthesized, and evaluated in cell-based reporter gene assays for RhlR agonism and antagonism. These investigations allowed us to define a series of SARs for BHL-type ligands and identify structural motifs critical for both activation and inhibition of the RhlR receptor. Notably, we identified new agonists that have ~10-fold higher potencies in RhlR relative to BHL, are highly selective for RhlR over LasR, and are active in the *P. aeruginosa* background. These compounds and the SARs reported herein should pave a route toward novel chemical strategies to study RhlR in *P. aeruginosa*.

2.2 Introduction

Certain bacteria are capable of coordinating population density with gene expression using an intercellular chemical signaling process known as quorum sensing (QS). QS allows bacteria to synchronize group-beneficial phenotypes only at high populations.[1, 2] In Gram-negative bacteria, QS is typically mediated by *N*-acyl L-homoserine lactone (AHL) signals, which are produced by LuxI-type synthases.[3] These small molecules can diffuse across the cell membrane (though in select cases, export is facilitated by efflux pumps),[4] and as population density increases, the AHLs reach an intracellular concentration at which they productively bind LuxR-type receptors. The ligand-bound LuxR-type receptors then act as transcription factors and alter gene expression levels to regulate a broad diversity of collective behaviors, including motility, biofilm formation, virulence factor production, and bioluminescence. As some of the most common agents of human infection use QS to control virulence, their QS systems have become attractive targets for infection control.[5, 6] More fundamentally, identifying chemical interventions for QS can provide novel entry into the molecular mechanisms of this important signaling pathway. Our laboratory and other have focused intently on developing such chemical strategies to attenuate QS in bacterial pathogens over the past decade.[7]

The Gram-negative bacterium *Pseudomonas aeruginosa* is the one of the most common causes of hospital-acquired bacterial infections, and uses QS to control ~10% of its genome, much of which is involved in virulence.[8-10] *P. aeruginosa* utilizes a relatively complex network of receptors and chemical signals to control QS, including multiple LuxI/LuxR pairs (Figure 2.1). The two LuxI-type synthases, LasI and RhlI, produce *N*-(3-oxododecanoyl) HL (OdDHL; Figure 2.1) and *N*-butyrl HL (BHL; Figure 2.1), respectively.[11] These two signaling molecules are recognized by their cognate LuxR-type receptors, LasR and RhlR. Both QS circuits regulate a large number of virulence factors—for example, the LasI/R system regulates the production of elastase, alkaline protease, and exotoxin A;[12] and the RhlI/R system regulates rhamnolipid production (a rhamnose-based biosurfactant) and the toxic exofactors hydrogen cyanide and

pyocyanin.[13] Interestingly, OdDHL is also recognized by the orphan LuxR-type receptor, QscR, which lacks its own associated synthase and cognate ligand. Once ligand bound, QscR has been found to both negatively regulate LasR and activate its own unique regulon of *P. aeruginosa*.[14] In addition to the Las and Rhl circuits, *P. aeruginosa* has a third circuit, Pqs, which is regulated by the lysR-type receptor PqsR (unrelated to LuxR-type receptors) and the Pseudomonas quinolone signal (PQS) and plays a role in the regulation of pyocyanin production. Adding to the complexity of QS in *P. aeruginosa* QS, each of the QS systems can positively or negatively regulate the other QS systems, and this interregulation is exquisitely sensitive to environmental factors, allowing for nimble and intricate genome regulation.[15-17]

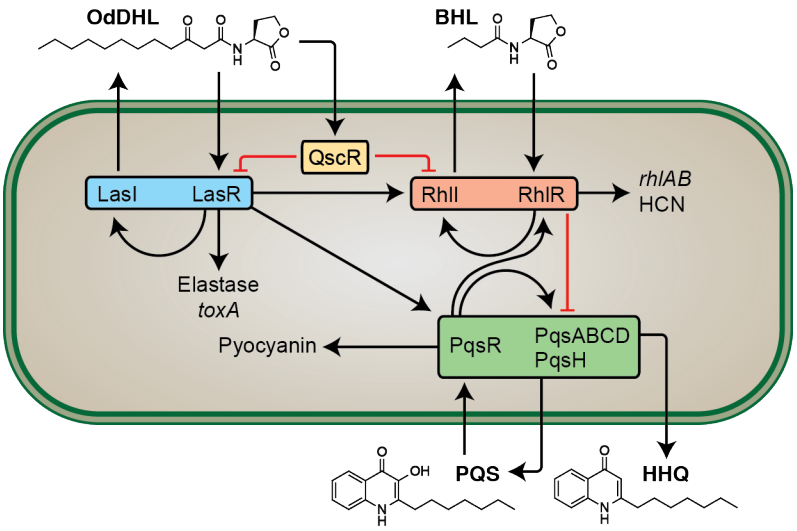

Figure 2.1: Simplified scheme of the *Pseudomonas aeruginosa* quorum sensing network. Arrows represent positive feedback (autoinducer synthesis/transcriptional regulation/receptor binding, etc.). Flat arrows represent negative regulation.

LasR is generally considered to be at the top of the *P. aeruginosa* QS receptor hierarchy, as it regulates genes associated with both the *rhl* and *pqs* circuits (Figure 2.1).[18, 19] Due to this prominent role, its not surprising that LasR has been a primary target for the design of small molecule antagonists to block QS in this pathogen.[20-22] Far fewer research efforts have been directed toward the design of non-native ligands for RhlR, likely due to its perceived secondary role in QS. However, a growing number of reports have shown that both the nutrient conditions

and stage of bacterial growth can reroute the QS regulatory circuitry so that RhlR instead is dominant, upending the traditional understanding of QS receptor regulation.[7, 9, 23-26] Experiments with small-molecule ligands have further implicated the *rhl* system in the direct regulation of virulence factors and subsequent reduction of virulence factor production using multiple animal models.[27, 28] In synergy with these reports, our laboratory has recently shown that small-molecule inhibition of pyocyanin can be achieved via agonism of RhlR.[23].

Together, these prior results highlight that the RhlR receptor presents a significantly underdeveloped opportunity for the attenuation of *P. aeruginosa* virulence. To date, only a few studies have focused on the development of synthetic modulators of RhlR.[29] In 2003, Suga and co-workers showed that BHL analogs with cyclopentanone or cyclohexanone head groups and butanoyl tails exhibit potent activity towards RhlR.[29] More recently, Bassler and co-workers reported that *meta*-bromo aryl homocysteine thiolactone AHL mimic **mBTL** strongly modulated the *rhl* system, decreasing pyocyanin production and associated virulence.[27] In 2015, we reported the screening of our in-house non-native AHL libraries for RhlR modulators and the discovery of a small collection potent RhlR modulators.[23, 30]. Perhaps not surprisingly, the compounds that were capable of potent RhlR activation (*e.g.*, **D8** and **S4**; Figure 2.2) were similar in structure to its native ligand BHL. However, to date, no systematic investigation of the structure-activity relationships (SARs) dictating BHL function have been reported. Delineation of these SARs would not only allow for a deeper fundamental understanding of the features critical to BHL activity, but also provide a framework from which to design new ligands for RhlR with improved potencies.

Herein, we report the design, synthesis, and biological characterization of a set of BHL analog libraries with the intent of discerning SAR trends important for agonism and antagonism of the RhlR receptor in *P. aeruginosa*. We tested our compounds in a series of *E. coli* reporter strains to gauge activity, potency, and receptor selectivity, and finally in *P. aeruginosa* to test for maintenance of activity in the native organism. These studies revealed the first set of detailed

SAR surrounding the BHL scaffold and some of the most potent and receptor-selective non-native RhlR agonists to be reported.

2.3 Results and Discussion

2.3.1 RhlR-targeted library design

An overview of our library design process and the structures of the BHL derived library are shown in Figure 2.2. Our library constitutes largely novel compounds; of the small subset that have been reported previously (for references, see Table 2.3), none to our knowledge have been tested for direct RhlR modulation. The library can be divided into two groups: (1) compounds with modified tails and native lactone head groups (i.e., the tail library), and (2) compounds with modified head groups and native butanoyl tails (i.e., the head library). The tail library compounds can be further divided into three subsets based on structural similarity to either BHL or our two previously reported potent RhlR activators **2** and **3**.[30] The first subset of compounds (**4**–**11**) retains the short-chain alkyl characteristics of native ligand BHL, with compounds designed to probe both tail length and alkyl substitution on the tail. We note that compound **7** (isovaleryl HL) is actually a naturally occurring AHL, first found in the symbiont *Bradyrhizobium japonicum*.[31] The second subset of tail modified compounds (**12**–**16**) expands on the structural characteristics of lead pentenyl HL **2**, probing alkene stereochemistry and position, as well as the presence of an alkene vs. an alkyne in the tail. Lastly, the third subset of tail modified compounds (**17**–**22**) explores structural features of lead cyclopentyl HL **3**, focusing on size and position of small carbocycles within the acyl tail.

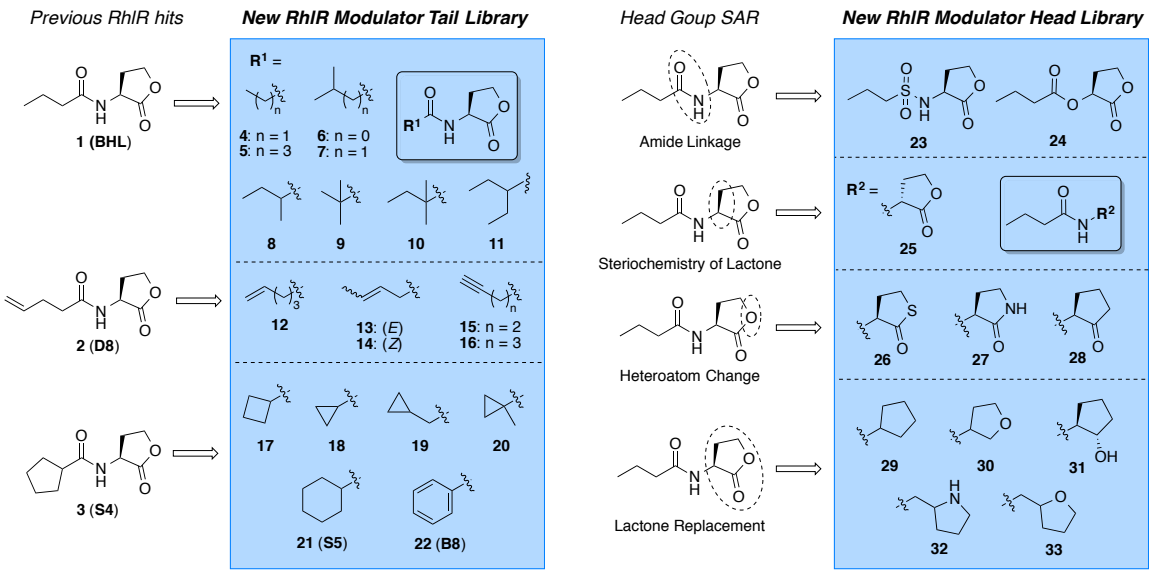

Figure 2.2: Structures of RhlR native ligand **1** (BHL), two previously reported RhlR modulators used as controls (**2**, **3**), and a focused library of compounds designed to probe SARs of RhlR (**4**–**33**). Compounds **21** and **22** were previously characterized and included for comparison in the current study.[30]

The head group library was similarly divided into four subsets of compounds (Figure 2.2). While previous studies of AHL-type ligands have explored AHL head groups expanded beyond 5-membered rings,[32, 33] we elected in the current study to focus exclusively on close mimics of the homoserine lactone to hopefully delineate more direct SAR for the BHL ligand. The first subset of head group modified compounds investigates alternate replacements for the amide linkage in the native ligand (sulfonamide **23** and ester **24**). The second, one compound "sub-set" was designed to examine the importance of native stereochemistry for BHL activity (i.e., D-BHL **25**). The third subset incorporates modifications to the lactone linkage, replacing the lactone oxygen with sulfur (**26**), nitrogen (**27**), or a methylene (**28**). The fourth subset deconstructs the five membered lactone ring even further by removing the carbonyl (**29**), replacing it with an alcohol (**31**), or drastically varying the heteroatom location in the ring (**30**, **32**, and **33**). We note that compounds **32** and **33** also contain an additional methylene between the ring and the amide bond (**32** and **33**); this feature was included simply due to ease of synthesis. We reasoned that these last two compounds could allow us to also explore the effect of increasing the distance the head group

extends into the RhlR ligand binding pocket (assuming these non-native ligands target the same site).

2.3.2 Library synthesis

AHL library compounds were synthesized using previously established solution-phase chemistry, mainly based on carbodiimide-mediated amide coupling procedures (see Methods section).[34] Yields were generally modest to good (40–80%), and all compounds were purified to >95% prior to biological testing.

2.3.3 E. coli reporter screens reveal BHL SARs and new RhlR agonists and antagonists

We first evaluated the RhlR-modulatory activity of the library compounds in an *E. coli* reporter strain (JLD271 harboring a b-galactosidase reporter for RhlR; see Methods) in order to isolate the RhlR receptor from other QS regulators in *P. aeruginosa* (most notably, LasR) and thus study its response to ligands directly. We performed initial RhlR agonism and competitive RhlR antagonism screens of the library at 10 μM. Many compounds displayed strong RhlR agonism at this concentration; however, no compounds were able to inhibit RhlR activity at 10 μM (Table 2.4). We thus submitted all compounds to a second competitive antagonism screen at 1 mM against 10 μM BHL. The results of these primary assays are listed in Table 2.1.

Table 2.1: Primary RhlR agonism and antagonism data by library members in *E. coli*.[a]

Compound	% activation[b]	% inhibition[c]	Compound	% activation[b]	% inhibition[c]
1 (BHL)	51	–	**18**	32	–
2 (D8)	54	–	**19**	70	–
3 (S4)	76	–	**20**	2	24
4	25	–	**21 (S5)**	34	–
5	25	–	**22 (B8)**[d]	1	31
6	62	–	**23**	1	55
7	86	–	**24**	0	6
8	55	–	**25**	2	11
9	1	25	**26**	71	–
10	5	7	**27**	1	35
11	28	–	**28**	35	–
12	41	–	**29**	0	45
13	21	–	**30**	0	20
14	52	–	**31**	2	12
15	45	–	**32**	0	–
16	34	–	**33**	0	57
17	79	–			

[a] Assays performed using *E. coli* JLD271 (pJN105R2/pSC11-*rhlI**); see Methods. SEM of n ≥ 3 trials did not exceed ± 10%. [b] Library compounds screened at 10 μM. RhlR activity measured relative to BHL at 1 mM. [c] Library compounds screened at 1 mM in the presence of 10 μM BHL. Values expressed relative to activation of 10 μM BHL alone. – = RhlR activation observed that was ≥10 μM BHL.

Strikingly, the primary agonism screen revealed multiple compounds with efficacies (i.e., maximal activities) greater than RhlR's native ligand BHL (**1**) at 10 mM (its EC_{50}, so ~50% activity observed; Table 2.1). The most active compounds were isovaleryl HL **7** and cyclobutyl HL **17** (86% and 79% activation, respectively), each capable of agonizing RhlR at levels equal to or greater than our previous lead RhlR agonist, **3** (**S4**). Scrutinizing the agonism data in terms of structural features critical for ligand activity, the most influential feature appeared to be substitution of the acyl tail α-carbon. Compounds with tertiary substituents at α- or β-carbons appear to be well tolerated by RhlR, yet quaternary carbons abolished agonistic activity. For example, compounds **5**–**8** show modest to strong RhlR agonism (25–86%), whereas **9** and **10** were inactive as agonists. Similarly, cyclic-tail compounds **17** and **19** (70% activation) were strong agonists, but 1-methyl-cylclopropanoyl HL **20** was inactive likely due to its quaternary α-carbon. We also observed that AHLs with 3-carbon tails (e.g., propyl derivatives **4** and **18**)

display significantly reduced abilities to activate RhlR; straight chain or cyclic AHL tails just one methylene longer (e.g., **1**, **17** and **19**) are primed for RhlR activation, however.

Amongst the set of compounds tested, the presence of an alkene or alkyne in the acyl tail had relatively little effect on RhlR agonistic activity (Table 2.1). Butenyl HL **14** and butynyl HL **15** were the most active of all compounds with unsaturated acyl tails: both displayed agonistic activities comparable BHL (**1**). Alkene isomers displayed different activity profiles; *trans* 2-butenyl derivative **13** exhibited a two-fold reduction in activity from its *cis* isomer **14**. The "kinked' *cis* alkene may enforce a tail conformation permitting **14** to bind in a manner similar to cyclopentyl HL **3**. The decrease in potency observed in the longer straight chain (6 carbon) alkenyl and alkynyl HLs **12** and **16** is consistent with the observation that AHLs with longer acyl chains are less active RhlR agonists relative to shorter chain AHLs,[29, 33]

Of the cyclic-tail AHLs tested, cyclobutanoyl HL **17** displayed the strongest RhlR-agonistic activity (79% activation; Table 2.1). While compound **18**, with a cyclopropanoyl tail alone, fails to activate RhlR strongly (32% agonism), agonism was recovered in compound **19** (70% activation) by inserting a methylene group between the cyclopropyl ring and the amide. The larger cyclohexyl tail of **21** also yielded reduced activity relative to cyclopentyl HL **3** (34% vs. 76%, respectively). Phenyl compound **22** had no agonist activity, suggesting that the tail's rigidity at the α-carbon may be detrimental to RhlR binding. In view of these data, AHLs incorporating 3–5-membered carbocylic rings in the acyl tail appear to be well suited for RhlR agonism.

AHLs **26** and **28** were the only head group modified compounds to show appreciable RhlR agonism at 10 μM (Table 2.1). Both of these compounds maintain a carbonyl in the head group, and the more active homocysteine thiolactone analog **26** (71% activation) maintains the heteroatom electron donor. Most other head group alterations shut down all agonistic activity, including replacement of the ketone in **28** to give alcohol **31**, replacing the native lactone with an amide in lactam **27**, or removing the lactone carbonyl to give cycloether **30**. Interestingly, the cyclopentyl derivative **29** does have some activity at high concentrations (Table 2.4), suggesting

that cycloether **30** makes contacts with RhlR detrimental to its activity. The D-homoserine lactone **25** showed marginal activity even at 1 mM (Table 2.4), confirming previously reported data that the stereochemistry of BHL is critical for activation.[35] The AHL amide proved to be necessary for agonistic activity, as compound **24**, the ester analog of BHL, was inactive. This result for BHL correlates with prior reports indicating that the AHL amide NH is essential for AHL:LuxR-type receptor binding, making a key hydrogen bond with a conserved aspartic acid in the ligand-binding site.[36] Compounds **32** and **33**, both extending the head group motif by an additional methylene showed no agonistic activity, suggesting a spatially restricted head group binding pocket in RhlR.

Turning next to the RhlR antagonism assay data for the tail group library (Table 2.1), only compounds **9**, **20**, and **22** were capable of inhibiting RhlR activity to a statistically significant extent (25–31%) at 1 mM. These compounds contain either a quaternary or sp^2 hybridized α-carbon in their tails, suggestive that steric bulk in close proximity to the HL engenders weak antagonistic activity for short-tail AHLs. More head group library members displayed RhlR antagonism, with compounds **23**, **27**, **29** and **33** all showing antagonism greater than 35%. Sulfonamide **23**, a 55% antagonist, has increased steric bulk adjacent to the amide NH and potentially operates through a similar mode of action as bulky tail antagonists **9** and **20**. In turn, cyclolactam **27** and cyclopentyl derivative **29** lack key hydrogen bonding contacts presented by the native lactone HL for agonism (see above), and antagonize RhlR instead. Finally, the extended, tetrahydrofurfurylamine head group of **33** caused moderate RhlR antagonism (57% at 1 mM), suggesting that this positioning of the head group enforces inhibitory interactions.

2.3.4 BHL-type analogs can antagonize, but not agonize LasR

We were also interested to examine the activity of the BHL library in LasR, as ligands selective for RhlR, or displaying opposite activities in each receptor (i.e., both a RhlR agonist and a LasR antagonist, and vice versa), would be useful as probes for teasing apart the closely

interrelated QS circuit in *P. aeruginosa* (Figure 2.1). We thus tested the library in an *E coli* LasR reporter strain (*E. coli* JLD271 harboring plasmids pJN105L and pSC11) analogous to that for RhlR above (see Methods). These LasR assays were performed in a similar fashion as those for the RhlR reporter, with compounds tested at 10 μM and 1 mM in agonism and antagonism assays.

In general, our lead RhlR agonists showed negligible LasR agonism in the *E. coli* reporter, particularly at 10 μM (Table 2.5). This result is not surprising, in view of the structural differences between the native ligands for these two receptors (short chain BHL versus long chain OdDHL). However, we found that many of the RhlR agonists, including the native ligand BHL (**1**), antagonize the LasR receptor instead at high concentrations (Table 2.5). To our knowledge, LasR antagonism by RhlR agonists (including BHL) has not been previously reported explicitly. Interestingly, the most potent RhlR agonists **7**, **17**, and **28** are also some of the most potent LasR antagonists found in the library. This activity profile for **7**, **17**, and **28** is unique, as such compounds could be utilized to suppress LasR-associated virulence factors along with those suppressed by RhlR agonism (i.e., PQS). That said, the high compound concentrations necessary for this observed activity may reduce the likelihood of implementing such dual regulation in the wild type organism.

2.3.5 Dose–response studies reveal highly potent RhlR agonists

To gauge the relative potencies of the lead RhlR agonists identified in the primary assays, we submitted these compounds to dose-response analyses using the *E. coli* RhlR reporter. All tail group compounds that showed activities comparable to or greater than that of BHL (**1**), along with two head group compounds (**26** and **28**) with promising activities, were evaluated (Table 2.2). Four of the tail library members tested were found to be significantly more potent than BHL. Cyclobutyl HL **17** rivaled in potency that of cyclopentyl HL **3**, and isovaleryl HL **7** was significantly ($p < 0.05$) more potent than **3**. Indeed, this naturally-occurring AHL was the most

potent activator of RhlR in this *E. coli* bioassay overall, with an EC_{50} almost 10-fold lower than BHL (1 mM vs. ~9 mM, respectively). Although *B. japonicum* (which utilizes **7** for QS) and *P. aeruginosa* are both found in the rhizosphere,[37] there is no direct evidence of these species sharing a niche. This result could suggest an intriguing possibility of interaction between these two species via **7**.

Of the head group library compounds tested (**26** and **28**), the homocysteine thiolactone BHL analog **26** was found to be 2-fold more potent than BHL (Table 2.2). While thiolactone analogs of other AHLs have been reported to have comparable or lower agonistic activity than their parent AHL,[38] **26** represents to our knowledge the first thiolactone analog that is more potent than the native AHL ligand. We do note that LuxR-type receptor SdiA in *Salmonella enterica* has been reported to be more strongly activated by ligands bearing thiolactone relative to lactone head groups, but this receptor is an "orphan" type LuxR receptor that lacks a native ligand for direct comparison.[39] Like SdiA (for which several structures have now been reported[40-42]), RhlR may have a larger binding pocket for the AHL head group relative to other LuxR-type receptors, allowing it to better accommodate the larger thiolactone. Indeed, RhlR shares much closer sequence identity to SdiA (45%) than to the other LuxR homologs found in *P. aeruginosa.*[43] Turning to cyclopentanone derivative **28**, this analog was found to be just under 3-fold less active than BHL, tracking with early reports by Suga and co-workers.[32] Despite its reduced potency, the ketone head group in **28** is not susceptible to hydrolysis, marking it as a potentially useful moiety for use in the design of future, hydrolytically stable AHL analogs.

Table 2.2: EC_{50} values for RhlR activation by library members in *E. coli*[a] and *P. aeruginosa*[b]

	E. coli		***P. aeruginosa***	
Compound	**EC_{50} (μM)[b]**	**95% CI (μM)**	**EC_{50} (μM)[b]**	**95% CI (μM)**
1 (BHL)	8.95	5.86 – 13.7	8.08	6.09 – 10.7
2 (D8)	7.93	6.28 – 10.02	–	–
3 (S4)	1.58	1.32 – 1.90	1.22	1.03 – 1.45
5	10.83	6.59 – 17.80	–	–
6	4.89	3.67 – 6.53	–	–
7	1.02	0.67 – 1.55	1.42	1.08 – 1.86
8	7.77	5.61 – 10.8	–	–
14	6.93	5.52 – 8.71	–	–
17	1.78	1.37 – 2.31	1.41	1.14 – 1.74
19	2.76	2.23 – 3.42	–	–
26	4.87	3.46 – 6.84	3.82	2.57 – 5.66
28	27.4	16.1 – 46.6	14.3	8.76 – 23.5

[a] Assays were performed using *E. coli* JLD271 (pJN105R2/pSC11-*rhlI**) or *P. aeruginosa* PAO-JP2 (p*rhlI*-LVA*gfp*); see Experimental Section. For both assays, EC_{50} values were determined by testing AHLs over a range of concentrations (≤ 1 mM). Assays were performed in triplicate, and 95% confidence intervals (CIs) were calculated from the SEM of n ≥ 3 trials. [b]Denotes the highest value of RhlR activation seen for each compound at any concentration within the dose–response assay. For the full agonism traces, see Figures 2.4 and 2.5 for *E. coli* and *P. aeruginosa* respectively. Complete trace characterization is shown in Table 2.6. Discussions on dose response curve shapes are in supplementary notes. [c]RhlR activity was measured relative to that of 1 mM BHL.

Library compounds capable of greater than 25% antagonistic activity against RhlR (**23**, **27**, **29**, and **33**) were also submitted to does response analysis in the *E. coli* RhlR reporter strain versus 10 μM BHL. Overall, this set of compounds showed limited potencies (IC_{50} > 60 mM, dose response curves shown in Figure 2.6); only the dose-response curve for cyclopentyl head group derivative **29** yielded a calculable IC_{50} value (52.2 μM). As this library was designed to very closely mimic the BHL scaffold, it is not surprising that we mostly identified agonists as opposed to antagonists. However, uniting of the head group components of these RhlR antagonists with other lead tail groups may allow for activity improvement; such studies are ongoing in our laboratories.

2.3.6 Lead RhlR agonists maintain their potencies in P. aeruginosa background

We next performed dose response analyses on the lead RhlR agonists in *P. aeruginosa* to determine if they maintained their potencies in the native organism. For these experiments, we used the *P. aeruginosa* double synthase mutant PAO-JP2 (Δ*lasIrhlI*) harboring the RhlR reporter plasmid p*rhlI*-LVA*gfp* (see Methods). Because the production of RhlR is dependent on LasR in *P. aeruginosa* (in LB medium[7]), all assays were performed in the presence of 100 nM OdDHL. Our assay data is listed in Table 2.2, with full dose response curves shown in Figure 2.5.

We were pleased to observe that all of the lead RhlR agonists retained similar potencies in the *P. aeruginosa* background relative to the *E. coli* RhlR reporter. Notably, isovaleryl HL **7** and cyclobutyl HL **17** (alongside compound **3**) represent, to our knowledge, the most potent non-native agonists of RhlR in *P. aeruginosa* known. While AHLs are believed to, at least in part, exit and enter the cell via passive diffusion mechanisms, short-chain AHLs such as BHL diffuse across the *P. aeruginosa* cell membrane at a much higher rate than longer chain AHLs such as OdDHL,[4] and are not processed by AHL acylases. Because all of the compounds tested herein contain short (≤ 6 carbon) acyl tails, it is not surprising that compound potencies between the *E. coli* and *P. aeruginosa* reporter strains match so well. Furthermore, as the lead RhlR agonists only display appreciable LasR antagonism at mid-micromolar concentrations (Table 2.5), the observed RhlR activities of lead compounds are likely not a result of indirect modulation of RhlR with LasR, but rather are due to direct interaction with RhlR.

2.4 Summary

The goal of this study was to delineate key SARs dictating the activity of the natural *P. aeruginosa* QS signal, BHL, in the RhlR receptor. We addressed this goal via the design, synthesis, and biological characterization of a focused library of non-native AHL analogs closely based on the BHL scaffold. The library contained a series of analogs with small perturbations to the BHL head group and acyl tails, examining molecular features that have been yet to explored

in the context of BHL-mediated RhlR activity. These studies revealed the following SARs critical to BHL activity (Figure 2.3): first, the head group should maintain (*S*) stereochemistry as well as a carbonyl adjacent to the stereocenter, and there should be an amide linkage between the head and tail groups. The AHL head group carbonyl and amide are well documented to make hydrogen-bonding contacts in LuxR receptors with well conserved tryptophan and asparagine residues, respectively. Second, the head group can accommodate multiple heteroatom changes alpha to the head group carbonyl, but proton donors such as an amide are not tolerated. Third, looking at the AHL tail, the tail must be four carbons in length; longer or shorter tails result in reduced agonism. The tail also must have a secondary or tertiary carbon alpha to amide linker. Carbons with sp^2 or quaternary character at this position do not agonize RhlR . We also found changes resulting in agonists with improved agonism activity over BHL. These agonists were shown to have added bulk, specifically homocysteine thiolactone head groups and cyclobutyl, cyclopentyl, or isovaleryl moieties for tail groups. Notably, removing or altering many of the critical components for RhlR activation resulted in antagonists. Only the removal of the amide nitrogen resulted in compounds that had no RhlR activity. Future antagonist libraries may benefit from the removal of activating components determined in this study.

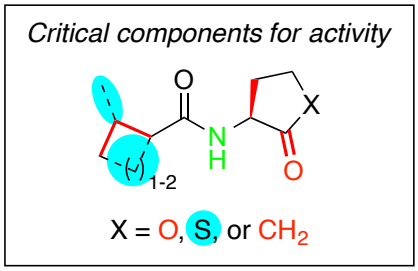

Figure 2.3. Summary of key SAR trends for RhlR activators as revealed in this study. Red moieties are vital for activation. Blue moieties improve agonism beyond levels achieved by the native ligand BHL. The amide shown in green is critical for both activation and inhibition.

In the course of these experiments, we identified several compounds capable of fully agonizing RhlR with higher potencies than the native ligand BHL, both with and without

modified head groups. Notably, isovaleryl HL **7** and cyclobutyl HL **17** are almost 10-fold more potent than BHL as RhlR agonists, active in *P. aeruginosa*, and selective for RhlR. Agonism (or partial agonism) of the RhlR system has already been implicated as a promising antivirulence strategy.[23, 44] As such, the structural insights and new RhlR ligands reported here will be useful to advance new chemical probe development and for further study of this important QS receptor.

2.5 Methods

2.5.1 General

All reagents and solvents were purchased from commercial sources (Alfa-Aesar, Sigma-Aldrich, and Acros Organics) and used without purification, except for dichloromethane (DCM), which was distilled prior to use. The native AHLs, BHL and OdDHL, were purchased from Cayman Chemical and Sigma-Aldrich, respectively. The substrates for Miller absorbance (i.e., β-galactosidase) assays, chlorophenol red-β-D-galactopyranoside (CPRG) and ortho-nitrophenyl-β-galactoside (ONPG), were purchased from Roche and Sigma-Aldrich, respectively. Media and reagents for bacterial culture were purchased from commercial sources and used according to package instructions. See SI for a description of instruments and analytical methods.

2.5.2 Chemistry

Most compounds were synthesized using previously established solution-phase, EDC-mediated amide coupling procedures,[34] with the following modifications: all AHL-type compounds were prepared from L-homoserine lactone and carboxylic acids in ≥ 50 mg quantities. The primary base used was triethylamine (two equivalents per one equivalent of carboxylic acid). The reaction was catalyzed with 10 mol % 4-dimethylaminopyridine (DMAP). Following washing with aqueous 10% HCl, crude products were additionally washed with aqueous saturated $NaHCO_3$ and brine. Variations on this protocol were required for compounds **30**, **32** and **33,** as detailed in the SI. Compound **27** head group (*S*)-3-amino-2-pyrrolidinone was synthesized as

previously described,[45] and then coupled to butyryl chloride. Compounds **23**,[46] **28**, and **31**[32] were synthesized using established protocols. See SI for full characterization data for new compounds.

2.5.3 General bacterial growth conditions and assay methods

Bacteria were cultured in Luria−Bertani broth (LB) at 37 °C with shaking at 200 rpm. Compound stock solutions (100 mM) were prepared in DMSO and stored at -20 °C. Absorbance measurements were performed in 96-well microtiter plates and pathlength-corrected using a Biotek Synergy 2 plate reader and Gen 5 software (version 1.05). Bacterial growth was quantified according to absorbance at 600 nm (OD_{600}). All biological assay data were processed using Microsoft Excel and GraphPad Prism 6.

2.5.4 Bacterial strains

The following reporter strains were used: (i) *E. coli* strain JLD271 (Δ*sdiA*) harboring the RhlR expression plasmid pJN105R2 and the *rhlI-lacZ* transcriptional fusion reporter pSC11-rhlI*, (ii) *E. coli* strain JLD271 (Δ*sdiA*) harboring the LasR expression plasmid pJN105L and the *lasI-lacZ* transcriptional fusion reporter pSC11, and (iii) the *P. aeruginosa* strain PAO-JP2 (Δ*lasIrhlI*) harboring the *rhlI-gfp* transcriptional fusion reporter p*rhlI*-LVA*gfp*. Reporter strains JLD271/pJN105R2/pSC11-rhlI* and JLD271/pJN105L/pSC11 were grown in LB containing 100 μg/mL ampicillin and 10 μg/mL gentamicin.

2.5.5 E. coli RhlR and LasR reporter assay protocols

The *E. coli* reporters JLD271/pJN105R2/pSC11-*rhlI** and JLD271/pJN105L/pSC11 were used as previously described to assay compound activities and potencies,[30] with the following modifications: in the RhlR agonism reporter assay performed with substrate CPRG, non-native compounds (10 μM or 1 mM) were compared to 1 mM BHL as the positive control; LasR assays

were processed using our protocol for the substrate ONPG;[47] and LasR antagonism assays were performed versus the EC_{50} for OdDHL (2 nM).

2.5.6 P. aeruginosa RhlR reporter assay protocol

To evaluate the RhlR-modulatory activities of selected compounds in *P. aeruginosa*, the PAO-JP2 strain harboring p*rhlI*-LVA*gfp* was used as previously reported,[23] with the following modifications: in the RhlR agonism assay, non-native compounds were compared to 1 mM BHL as a positive control; and RhlR antagonism assays were performed versus the EC_{50} for BHL (10 μM).

2.6 Supplemental information

2.6.1 Instrumentation and analytical methods

NMR spectra were recorded in deuterated NMR solvents at 300 MHz on a Varian MercuryPlus 300 spectrometer, at 400 MHz on a Bruker Avance-400 spectrometer with SmartProbe and SampleJet, at 500 MHz on a Bruker Avance-500 spectrometer with DCH cryoprobe and SampleXpress, or at 600 MHz on a Bruker Avance III 600 spectrometer. Chemical shifts are reported in parts per million (ppm, δ) using corresponding solvents or tetramethylsilane (TMS) as a reference. Couplings are reported in hertz (Hz). Electrospray ionization MS measurements were performed on a Waters LCT. Samples were dissolved in acetonitrile and sprayed with a sample cone voltage of 20. For exact mass measurements (EMM), an aliquot of a known compound (lock mass) is added to the sample and resprayed. FT-IR spectra were recorded with a Bruker Tensor 27 IR spectrometer, outfitted with a single reflection MIRacle Horizontal attenuated total reflectance (ATR) unit from Pike Technologies. A ZnSe crystal with spectral range 20,000 to 650 cm-1 was used for ATR-IR measurements.

2.6.2 Compound characterization data and synthetic methods

^{1}H and ^{13}C NMR, ESI MS, and IR data are reported below for all new compounds and select intermediates. Characterization data for compounds **4**-**7**, **9, 10**, **16**, **17**, **23**-**26**, and **29** are also included as they have not been fully characterized in past studies reporting their structures. See Table 2.3 for complete references. Details of synthetic methods to generate these compounds are either included in the main text or alongside characterization data below (i.e., for compounds **27**, **30**, **32**, and **33**).

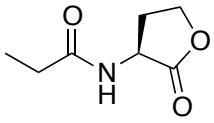

4: ^{1}H NMR: (400 MHz, $CDCl_3$) δ 6.30 (d, *J* = 6.5 Hz, 1H), 4.61 (ddd, *J* = 11.6, 8.6, 6.2 Hz, 1H), 4.47 (td, *J* = 9.0, 1.3 Hz, 1H), 4.29 (ddd, *J* = 11.3, 9.3, 5.9 Hz, 1H), 2.82 (dddd, *J* = 12.6, 8.7, 5.9, 1.3 Hz, 1H), 2.30 (qd, *J* = 7.7, 1.1 Hz, 2H), 2.16 (dtd, *J* = 12.4, 11.4, 8.8 Hz, 1H), 1.17 (t, *J* = 7.6 Hz, 3H); ^{13}C NMR (101 MHz, $CDCl_3$) δ 175.78, 174.39, 66.13, 49.14, 30.44, 29.16, 9.47; ESI MS: Expected $[M+H]^+$: 158.0812, observed: 158.0810; IR (cm^{-1}): 3311, 2980, 2939, 1792, 1641, 1535, 1170, 1028.

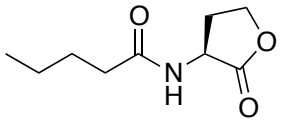

5: ^{1}H NMR (400 MHz, $CDCl_3$) δ 6.09 (s, 1H), 4.56 (ddd, *J* = 11.6, 8.6, 5.9 Hz, 1H), 4.47 (td, *J* = 9.0, 1.2 Hz, 1H), 4.29 (ddd, *J* = 11.3, 9.3, 5.8 Hz, 1H), 2.86 (dddd, *J* = 12.6, 8.6, 5.9, 1.2 Hz, 1H), 2.26 (dd (apparent t), *J* = 8.3, 7.0 Hz, 2H), 2.13 (dtd, *J* = 12.4, 11.4, 8.8 Hz, 1H), 1.64 (p, *J* = 8.2, 7.6 Hz, 2H), 1.36 (h, *J* = 7.3 Hz, 2H), 0.92 (t, *J* = 7.3 Hz, 3H); ^{13}C NMR (101 MHz, $CDCl_3$) δ 175.60, 173.75, 66.13, 49.25, 35.91, 30.65, 27.51, 22.33, 13.78; ESI MS: Expected $[M+H]^+$: 186.1125, observed: 186.1123; IR (cm^{-1}): 3309, 3078, 2950, 1774, 1649, 1545, 1169, 933.

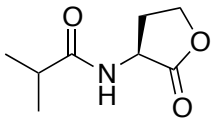

6: ^{1}H NMR (400 MHz, $CDCl_3$) δ 6.05 (s, 1H), 4.53 (ddd, *J* = 11.7, 8.7, 5.8 Hz, 1H), 4.48 (td, *J* = 9.2, 0.8 Hz, 1H), 4.29 (ddd, *J* = 11.4, 9.3, 5.9 Hz, 1H), 2.87 (dddd, *J* = 12.6, 8.6, 5.8, 1.2 Hz, 1H), 2.45 (hept, *J* = 6.9 Hz, 1H), 2.12 (dtd, *J* = 12.6, 11.5, 8.8 Hz, 1H), 1.19 (CH_3, dd, *J* = 6.9 Hz, 3H), 1.18 (d, J = 6.9 Hz, 3H); ^{13}C NMR (101 MHz, $CDCl_3$) δ 177.58, 175.61, 66.13, 49.23, 35.22, 30.72, 19.50, 19.37; ESI MS: Expected $[M+H]^+$: 172.0969, observed: 172.0963; IR (cm^{-1}): 3305, 2968, 2930, 1178, 1655, 1550, 1170, 1015.

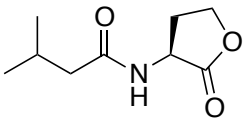

7: ^{1}H NMR (400 MHz, $CDCl_3$) δ 5.96 (s, 1H), 4.54 (ddd, *J* = 11.6, 8.6, 5.7 Hz, 1H), 4.48 (td, *J* = 9.1, 1.2 Hz, 1H), 4.29 (ddd, *J* = 11.3, 9.3, 5.9 Hz, 1H), 2.88 (dddd, *J* = 12.9, 8.6, 6.1, 1.2 Hz, 1H), 2.21 – 2.02 (m, 4H), 1.02 – 0.93 (m, 6H); ^{13}C NMR (101 MHz, $CDCl_3$) δ 175.44, 173.06, 66.11, 49.29, 45.44, 30.71, 26.14, 22.46, 22.38; ESI MS: Expected $[M+H]^+$: 186.1125, observed: 186.1118; IR (cm^{-1}): 3308, 2956, 2869, 1774, 1642, 1546, 1169, 1014.

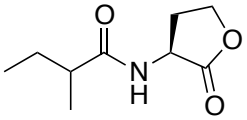

8: *2 diastereomers – analogous overlapping signals are reported together.* ^{1}H NMR (400 MHz, $CDCl_3$) δ 6.01 (diastereomers overlapping, s, 1H), 4.54 (diastereomers 0.008 ppm apart, ddd, *J* = 11.0, 8.0, 5.4 Hz, 1H), 4.48 (diastereomers 0.005 ppm apart, td, *J* = 9.0, 1.2 Hz, 1H), 4.29 (diastereomers 0.002 ppm apart, ddd, *J* = 11.4, 9.4, 6.0 Hz, 1H), 2.88 (diastereomers 0.015 ppm apart), ddd, *J* = 13.0, 8.7, 5.9, 1.3 Hz, 1H), 2.26 – 2.06 (diastereomers overlapping, m, 2H), 1.75 – 1.62 (diastereomers overlapping, m, 1H), 1.54 – 1.41 (tail CH_2, diastereomers overlapping, m, 1H), 1.17 (diastereomers 0.003 ppm apart, d, *J* = 6.9 Hz, 3H), 0.93 (diastereomers 0.02 ppm

apart, t, J = 7.4 Hz, 3H); ^{13}C NMR (101 MHz, $CDCl_3$) δ 177.13, 177.07, 175.55, 175.50, 66.13, 66.10, 49.26, 49.19, 42.64 (2C), 30.77, 30.70, 27.35, 27.20, 17.28, 17.21, 11.81 (2C); ESI MS: Expected $[M+H]^+$: 186.1125, observed: 186.1119; IR (cm^{-1}): 3306, 2967, 2926, 1776, 1645, 1545, 1174, 1016.

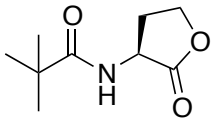

9: ^{1}H NMR (400 MHz, $CDCl_3$) δ 6.18 (s, 1H), 4.53 – 4.43 (m, 2H), 4.30 (ddd, J = 11.1, 9.3, 5.9 Hz, 1H), 2.87 (ladddd, J = 12.6, 8.6, 6.0, 1.3 Hz, 1H), 2.12 (dtd, J = 12.5, 11.3, 8.9 Hz, 1H), 1.23 (s, 9H); ^{13}C NMR (101 MHz, $CDCl_3$) δ 179.19, 175.66, 66.13, 49.37, 38.71, 30.62, 27.44; ESI MS: Expected $[M+H]^+$: 186.1125, observed: 186.1123; IR (cm^{-1}): 3324, 2963, 1779, 1643, 1525, 1165, 1013.

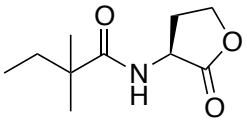

10: ^{1}H NMR (400 MHz, $CDCl_3$) δ 6.16 (s, 1H), 4.54 – 4.43 (m, 2H), 4.29 (ddd, J = 11.1, 9.3, 6.0 Hz, 1H), 2.86 (dddd, J = 13.0, 8.6, 6.0, 1.3 Hz, 1H), 2.12 (dtd, J = 12.4, 11.2, 8.9 Hz, 1H), 1.65 – 1.50 (ABX_3 qq, J_{AB} = 13.5 Hz, J_{AX} = ~7 Hz, J_{BX} = ~7 Hz, 2H), 1.19 (s, 3H), 1.19 (s, 4H), 0.86 (t, J = 7.5 Hz, 3H); ^{13}C NMR (101 MHz, $CDCl_3$) δ 178.50, 175.64, 66.12, 49.36, 42.42, 33.89, 30.58, 24.84, 24.77, 9.13; ESI MS: Expected $[M+H]^+$: 200.1282, observed: 200.1273; IR (cm^{-1}): 3312, 2967, 2914, 1770, 1632, 1530, 1170, 1028.

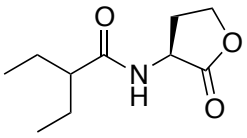

11: ^{1}H NMR (400 MHz, $CDCl_3$) δ 6.00 (s, 1H), 4.54 (ddd, J = 11.5, 8.6, 5.6 Hz, 1H), 4.48 (td, J = 9.0, 1.3 Hz, 1H), 4.29 (ddd, J = 11.2, 9.3, 5.9 Hz, 1H), 2.94 – 2.83 (m, 1H), 2.13 (dtd, J = 12.7, 11.4, 8.8 Hz, 1H), 1.97 (tt, J = 9.0, 5.3 Hz, 1H), 1.71 – 1.44 (m, 4H), 0.92 (t, J = 7.4 Hz, 3H),

0.90 (t, J = 7.4 Hz, 3H); ^{13}C NMR (101 MHz, $CDCl_3$) δ 176.47, 175.44, 66.12, 50.81, 49.25, 30.71, 25.70, 25.63, 12.03, 12.00; ESI MS: Expected $[M+H]^+$: 200.1282, observed: 200.1280; IR (cm^{-1}): 3300, 2969, 2923, 1777, 1645, 1543, 1169, 1020.

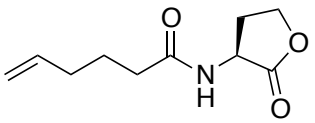

12: ^{1}H NMR (300 MHz, $CDCl_3$) δ 6.18 (d, J = 6.3 Hz, 1H), 5.78 (ddt, J = 16.9, 10.2, 6.7 Hz, 1H), 5.04 (dq, J = 16.5, 1.6 Hz, 1H), 4.99 (dq, J = 9.4, 1.0 Hz, 1H), 4.58 (ddd, J = 11.6, 8.6, 6.1 Hz, 1H), 4.47 (td, J = 9.1, 1.3 Hz, 1H), 4.29 (ddd, J = 11.2, 9.3, 5.9 Hz, 1H), 2.83 (dddd, J = 12.5, 8.6, 5.9, 1.3 Hz, 1H), 2.27 (dd (apparent t), 2H), 2.25 – 2.03 (m, 3H), 1.76 (p, J = 7.5 Hz, 2H); ^{13}C NMR (75 MHz, $CDCl_3$) δ 175.80, 173.66, 137.86, 115.72, 66.31, 49.40, 35.47, 33.23, 30.72, 24.62; ESI MS: Expected $[M+H]^+$: 198.1125, observed: 198.1119; IR (cm^{-1}): 3312, 3077, 2935, 1774, 1643, 1544, 1169, 1013.

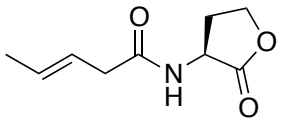

13: ^{1}H NMR (400 MHz, $CDCl_3$) δ 6.16 (d, J = 5.7 Hz, 1H), 5.68 (dqt, J = 14.6, 6.3, 1.2 Hz, 1H), 5.55 (dtq, J = 14.5, 7.2, 1.6 Hz, 1H), 4.54 (ddd, J = 11.6, 8.6, 5.9 Hz, 1H), 4.47 (td, J = 9.0, 1.1 Hz, 1H), 4.28 (ddd, J = 11.3, 9.3, 5.9 Hz, 1H), 3.00 (dt, J = 7.0, 1.3 Hz, 2H), 2.85 (dddd, J = 12.5, 8.9, 5.8, 1.2 Hz, 1H), 2.14 (qd, J = 11.7, 8.8 Hz, 1H), 1.74 (dd, J = 6.5, 1.6 Hz, 3H); ^{13}C NMR (101 MHz, $CDCl_3$) δ 175.33, 171.98, 131.77, 122.84, 66.07, 49.29, 40.03, 30.56, 18.08; ESI MS: Expected $[M+H]^+$: 184.0969, observed: 184.0964; IR (cm^{-1}): 3326, 3292, 2946, 1773, 1644, 1166, 1015, 962.

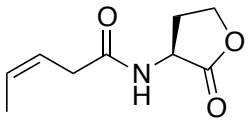

14: ^{1}H NMR (400 MHz, $CDCl_3$) δ 6.16 (s, 1H), 5.81 (dqt, J = 11.0, 6.9, 1.4 Hz, 1H), 5.59 (dtq, J

= 11.1, 7.5, 1.8 Hz, 1H), 4.54 (ddd, *J* = 11.7, 8.5, 5.8 Hz, 1H), 4.47 (td, *J* = 9.0, 1.2 Hz, 1H), 4.28 (ddd, *J* = 11.4, 9.3, 5.8 Hz, 1H), 3.09 (d, *J* = 7.5 Hz, 2H), 2.86 (dddd, *J* = 12.6, 8.6, 5.9, 1.2 Hz, 1H), 2.12 (dtd, *J* = 12.5, 11.5, 8.8 Hz, 1H), 1.68 (ddt, *J* = 7.0, 1.9, 0.9 Hz, 3H); ^{13}C NMR (101 MHz, $CDCl_3$) δ 175.35, 171.58, 129.89, 121.89, 66.06, 49.25, 34.43, 30.50, 12.99; ESI MS: Expected $[M+H]^+$: 184.0974, observed: 184.0978; IR (cm^{-1}) 3305, 2943, 1773, 1647, 1542, 1165, 999, 944.

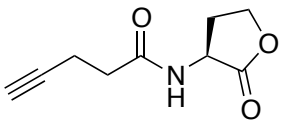

15: ^{1}H NMR (400 MHz, $CDCl_3$) δ 6.23 (d, *J* = 5.7 Hz, 1H), 4.57 (ddd, *J* = 11.6, 8.5, 5.7 Hz, 1H), 4.48 (td, *J* = 9.1, 1.2 Hz, 1H), 4.30 (ddd, *J* = 11.4, 9.3, 5.8 Hz, 1H), 2.88 (dddd, *J* = 12.7, 8.6, 5.8, 1.2 Hz, 1H), 2.59 – 2.52 (m, 2H), 2.52 – 2.42 (m, 2H), 2.16 (dtd, *J* = 12.5, 11.4, 8.8 Hz, 1H), 2.03 (t, *J* = 2.5 Hz, 1H); ^{13}C NMR (101 MHz, $CDCl_3$) δ 175.28, 171.55, 82.51, 69.68, 66.15, 49.43, 34.84, 30.64, 14.67; ESI MS: Expected $[M+H]^+$: 182.0812, observed: 182.0817; IR (cm^{-1}): 3339, 3254, 2921, 1783, 1648, 1540, 1178, 1020, 709.

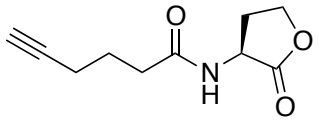

16: ^{1}H NMR (300 MHz, $CDCl_3$) δ 6.32 (s, 1H), 4.59 (ddd, *J* = 11.6, 8.7, 6.3 Hz, 1H), 4.47 (td, *J* = 9.1, 1.3 Hz, 1H), 4.29 (ddd, *J* = 11.1, 9.3, 5.9 Hz, 1H), 2.81 (dddd, *J* = 12.5, 8.7, 5.9, 1.3 Hz, 1H), 2.41 (t, *J* = 7.5 Hz, 2H), 2.28 (td, *J* = 6.9, 2.6 Hz, 2H), 2.17 (dtd, *J* = 12.6, 11.4, 8.9 Hz, 1H), 1.99 (t, *J* = 2.6 Hz, 1H), 1.88 (p, *J* = 7.1 Hz, 2H); ^{13}C NMR (75 MHz, $CDCl_3$) δ 175.75, 173.09, 83.51, 77.68, 77.25, 76.83, 69.58, 66.30, 49.40, 34.66, 30.54, 24.10, 18.01; ESI MS: Expected $[M+H]^+$: 196.0969, observed: 196.0966; IR (cm^{-1}): 3325, 3279, 2946, 1772, 1646, 1543, 1166, 1013.

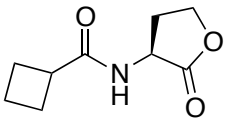

17: ^{1}H NMR (400 MHz, $CDCl_3$) δ 5.97 (s, 1H), 4.55 (ddd, *J* = 11.6, 8.6, 5.9 Hz, 1H), 4.47 (td, *J* = 9.1, 1.2 Hz, 1H), 4.29 (ddd, *J* = 11.3, 9.3, 5.9 Hz, 1H), 3.07 (pd, *J* = 8.5, 1.0 Hz, 1H), 2.86 (dddd, *J* = 12.9, 8.6, 5.8, 1.3 Hz, 1H), 2.38 – 2.06 (m, 5H), 2.06 – 1.83 (m, 2H); ^{13}C NMR (101 MHz, $CDCl_3$) δ 175.63, 175.57, 66.12, 49.17, 39.39, 30.68, 25.27, 25.23, 18.15; ESI MS: Expected $[M+H]^+$: 184.0969, observed: 184.0972; IR (cm^{-1}): 3307, 2980, 2943, 1777, 1643, 1550, 1172, 1014.

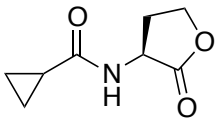

18: ^{1}H NMR (400 MHz, $CDCl_3$) δ 6.32 (s, 1H), 4.60 (ddd, J = 11.6, 8.6, 5.9 Hz, 1H), 4.52 – 4.42 (m, 1H), 4.29 (ddd, J = 11.3, 9.3, 5.8 Hz, 1H), 2.84 (dddd, J = 12.6, 8.6, 5.9, 1.2 Hz, 1H), 2.16 (dtd, J = 12.5, 11.5, 8.8 Hz, 1H), 1.46 (tt, J = 7.9, 4.6 Hz, 1H), 1.07 – 0.94 (m, 2H), 0.88 – 0.74 (m, 2H); ^{13}C NMR (101 MHz, $CDCl_3$) δ 175.74, 174.28, 66.13, 49.43, 30.72, 14.46, 7.85 (2C); ESI MS: Expected $[M+H]^+$: 170.0812, observed: 170.0806; IR (cm^{-1}): 3317, 3084, 3012, 2945, 1778, 1641, 1556, 1169.

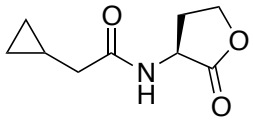

19: ^{1}H NMR (400 MHz, $CDCl_3$) δ 6.52 (d, J = 6.1 Hz, 1H), 4.58 (ddd, J = 11.6, 8.6, 6.0 Hz, 1H), 4.46 (td, J = 9.1, 1.2 Hz, 1H), 4.28 (ddd, J = 11.2, 9.3, 5.9 Hz, 1H), 2.84 (dddd, *J* = 12.8, 8.4, 5.9, 1.3 Hz, 1H), 2.27 – 2.08 (m, 3H), 1.06 – 0.91 (m, 1H), 0.69 – 0.54 (m, 2H), 0.29 – 0.13 (m, 2H); ^{13}C NMR (101 MHz, $CDCl_3$) δ 175.69, 173.23, 66.22, 49.28, 41.14, 30.65, 7.06, 4.80, 4.75; ESI MS: Expected $[M+H]^+$: 184.0969, observed: 184.0962; IR (cm^{-1}): 3315, 2951, 1774, 1648, 1543, 1171, 1015, 999.

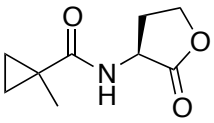

20: ^{1}H NMR (400 MHz, $CDCl_3$) δ 6.31 (s, 1H), 4.53 (ddd, *J* = 11.6, 8.7, 5.7 Hz, 1H), 4.47 (td, *J* = 9.2, 1.3 Hz, 1H), 4.28 (ddd, *J* = 11.2, 9.3, 5.9 Hz, 1H), 2.83 (dddd, *J* = 12.9, 8.6, 6.1, 1.3 Hz, 1H), 2.14 (dtd, *J* = 12.5, 11.4, 8.8 Hz, 1H), 1.36 (s, 3H), 1.29 – 1.15 (m, 2H), 0.69 – 0.59 (m, 2H); ^{13}C NMR (101 MHz, $CDCl_3$) δ 175.79, 175.73, 66.13, 49.61, 30.64, 19.38, 18.98, 16.69, 16.64; ESI MS: Expected $[M+H]^+$: 184.0969, observed: 184.0967; IR (cm^{-1}): 3299, 2918, 1764, 1636, 1524, 1170, 1022, 938.

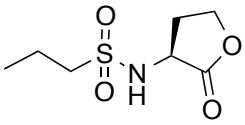

23: ^{1}H NMR (300 MHz, $CDCl_3$) δ 5.16 (d, *J* = 7.0 Hz, 1H), 4.43 (t, *J* = 9.0 Hz, 1H), 4.38 – 4.18 (m, 2H), 3.16 (dd, *J* = 9.1, 6.6 Hz, 2H), 2.82 – 2.61 (m, 1H), 2.28 (qd, *J* = 11.9, 9.1 Hz, 1H), 1.88 (dtt, *J* = 14.1, 6.7, 3.3 Hz, 2H), 1.06 (t, *J* = 7.4 Hz, 3H); ^{13}C NMR (126 MHz, $CDCl_3$) δ 174.6, 65.8, 56.2, 52.3, 31.6, 17.5, 13.0; Expected $[M+H]^+$: 225.0904, observed: 225.0901; IR (cm^{-1}): 3248, 2970, 1767, 1318, 1187, 1139, 999, 767.

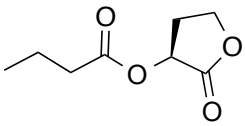

24: ^{1}H NMR (400 MHz, $CDCl_3$) δ 5.44 (dd, *J* = 9.5, 8.8 Hz, 1H), 4.48 (td, *J* = 9.1, 2.5 Hz, 1H), 4.32 (td, *J* = 9.6, 6.5 Hz, 1H), 2.72 (dddd, *J* = 12.9, 8.8, 6.5, 2.5 Hz, 1H), 2.47 – 2.24 (m, 3H), 1.69 (h, *J* = 7.4 Hz, 2H), 0.98 (t, *J* = 7.4 Hz, 3H); ^{13}C NMR (126 MHz, $CDCl_3$) δ 172.9, 172.7, 67.5, 65.1, 35.8, 29.1, 18.4, 13.7; Expected $[M+H]^+$: 173.0808, observed: 173.0808; IR (cm^{-1}): 2967, 1786, 1740, 1381, 1161, 1102, 1011.

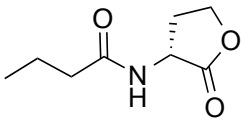

25: ^{1}H NMR (400 MHz, $CDCl_3$) δ 5.93 (s, 1H), 4.54 (ddd, *J* = 11.7, 8.6, 5.7 Hz, 1H), 4.47 (t, *J* = 8.9 Hz, 1H), 4.29 (ddd, *J* = 11.3, 9.3, 5.8 Hz, 1H), 2.99 – 2.78 (m, 1H), 2.24 (td, *J* = 7.3, 1.3 Hz, 2H), 2.20 – 2.03 (m, 1H), 1.69 (h, *J* = 7.4 Hz, 2H), 0.97 (t, *J* = 7.4 Hz, 3H); ^{13}C NMR (126 MHz, $CDCl_3$) δ 175.6, 173.7, 66.3, 49.5, 38.2, 30.9, 19.0, 13.8; ESI MS: Expected $[M+H]^+$: 172.0968, observed: 172.0967; IR (cm^{-1}): 3308, 2958, 1775, 1643, 1546, 1365, 1170, 1007, 649.

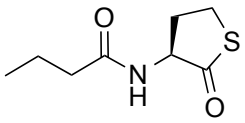

26: ^{1}H NMR (300 MHz, $CDCl_3$) δ 6.10 (s, 1H), 4.53 (dt, *J* = 13.0, 6.6 Hz, 1H), 3.49 – 3.14 (m, 2H), 2.89 (dt, *J* = 12.1, 5.9 Hz, 1H), 2.20 (t, *J* = 7.5 Hz, 2H), 2.04 – 1.78 (m, 1H), 1.65 (h, *J* = 7.5 Hz, 2H), 0.93 (t, *J* = 7.4 Hz, 3H); ^{13}C NMR (126 MHz, $CDCl_3$) δ 205.8, 194.6, 173.6, 173.60, 59.7, 38.44, 32.4, 27.78, 19.1, 13.8; Expected $[M+H]^+$: 188.0740, observed: 188.0739; IR (cm^{-1}): 3264, 2963, 1693, 1641, 1543, 1442, 981, 692.

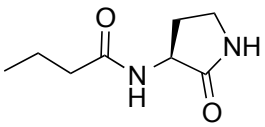

27: To a solution of (3*S*)-3-amino-2-pyrrolidinone (50 mg, 0.50 mmol, 1 eq) and triethylamine (168 µL, 1 mmol, 2 eq) in acetonitrile (5 mL), butyryl chloride (78 µL, 0.75 mmol, 1.5 eq) was added at room temperature. The solution was allowed to stir for 1 h at room temperature, after which the solvent was removed under reduced pressure. The remaining solid was purified using flash column chromatography (90/10 DCM/MeOH) to afford product (55.3 mg, 65% yield). ^{1}H NMR (400 MHz, $CDCl_3$) δ 6.96 (s, 1H), 6.76 – 6.33 (m, 1H), 4.37 (ddd, *J* = 10.6, 8.3, 6.1 Hz, 1H), 3.46 – 3.22 (m, 2H), 2.82 – 2.58 (m, 1H), 2.26 – 2.08 (m, 2H), 2.01 – 1.77 (m, 1H), 1.63 (h, *J* = 7.4 Hz, 2H), 0.91 (t, *J* = 7.4 Hz, 3H); ^{13}C NMR (126 MHz, $CDCl_3$) δ 175.5, 173.9, 50.8, 39.3,

38.4, 30.6, 19.1, 13.9; Expected $[M+H]^+$: 171.1128, observed: 171.1127; IR (cm^{-1}): 3273, 2961, 2874, 1687, 1638, 1540, 1291.

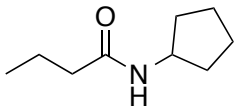

29: ^1H NMR (400 MHz, $CDCl_3$) δ 5.34 (s, 1H), 4.21 (h, *J* = 7.1 Hz, 1H), 2.11 (t, *J* = 7.5 Hz, 2H), 1.99 (dq, *J* = 12.0, 6.5, 6.0 Hz, 2H), 1.70 – 1.56 (m, 6H), 1.35 (dq, *J* = 13.0, 6.3 Hz, 2H), 0.94 (t, *J* = 7.4 Hz, 3H); ^{13}C NMR (126 MHz, $CDCl_3$) δ 172.6, 51.2, 39.1, 33.4, 23.9, 19.4, 13.9; ESI MS: Expected $[M+H]^+$: 156.1383, observed: 156.1382; IR (cm^{-1}): 3295, 2956, 2869, 1636, 1542, 1453, 1218, 695.

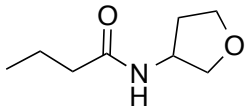

30: To a solution of butyric acid (253 mg, 2.9 mmol) dissolved in 15 mL of water at room temperature, was added *N*-hydroxysuccinimide (330 mg, 2.9 mmol) followed by EDC•HCl (550 mg, 2.9 mmol). The reaction was stirred for 30 min before 3-aminotetrahydrofuran (250 mg, 2.9 mmol) was added. After 24 h, the solution was extracted with chloroform (3 x 5 mL). The combined chloroform layers were washed with a saturated aqueous solution of sodium bicarbonate (2 x 5 mL), dried with $MgSO_4$, and filtered. The solvent was then removed under reduced pressure to afford **22** as a clear oil (82.3 mg, 18% yield). ^1H NMR (600 MHz, $CDCl_3$): δ 5.81 (s, 1H), 4.52-4.46 (m, 1H), 3.88 (ddd, 1H, J=8.0 Hz), 3.77 (dd, 1H, J= 5.4, 9.4 Hz), 3.76-3.72 (m, 1H), 3.61 (dd, 1H, J=2.5, 9.4 Hz), 2.26-2.18 (m, 1H), 2.10 (t, 2H, J= 7.4 Hz), 1.79-1.71 (m, 1H), 1.61 (sex, 2H, J=7.4 Hz), 0.90 (t, 3H, J=7.4 Hz); ^{13}C NMR (150 MHz, $CDCl_3$): δ 172.7, 73.6, 66.8, 50.1, 38.6, 33.2, 19.1, 13.7; ESI MS: Expected $[M+H]^+$: 158.1176, observed: 158.1175; IR (cm^{-1}): 3282, 3068, 2963, 2935, 2873, 1740, 1639, 1540, 1450, 1379, 1286, 1213, 1143, 1063, 908, 802.

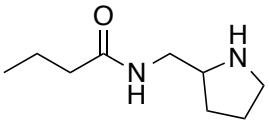

32: To a solution of butyric acid (82 mg, 0.9 mmol) dissolved in 10 mL of water at room temperature, was added *N*-hydroxysuccinimide (106 mg, 0.9 mmol) followed by EDC•HCl (177 mg, 0.9 mmol). The reaction was stirred for 15 min before 1-Boc-2-(aminomethyl)pyrrolidine (185 mg, 0.9 mmol) was added. After 24 h, the solution was then extracted with chloroform (3 x 5 mL). The combined chloroform layers were washed with a saturated aqueous solution of sodium bicarbonate (3 x 5 mL), dried with $MgSO_4$, and filtered. The solvent was removed to afford the Boc-protected product (an oil). The following Boc-deprotection procedure used was adapted from the protocol of Romo *et al*.[48] The oil was dissolved in DCM (5 mL) and Amberlyst 15 resin (0.625 g) was added. The mixture was stirred for 24 h and filtered. The resin was then washed with hexane (5 mL), THF (5 mL) and MeOH (2 x 5 mL). The resin was placed in a 4 M ammonia methanolic solution (5 mL) and stirred for 2 h. DCM (5 mL) was added to the mixture, which was stirred for an additional 20 h. The resin was then filtered and the solution evaporated under reduced pressure to yield a brown oil. The oil was dissolved in DCM (5 mL) and colored impurities removed using activated charcoal. Filtration and removal of the solvent afforded **32** as a yellow oil (56.9 mg, 36% yield).^{1}H NMR (600 MHz, $CDCl_3$): δ 6.49 (s, 1H), 3.56 (s, 1H), 3.38-3.33 (m, 1H), 3.28-3.22 (m, 1H), 3.08-3.01 (m, 1H), 2.88 (t, 2H), 2.10 (t, 2H), 1.86-1.79 (m, 1H), 1.78-1.71 (m, 1H), 1.70-1.63 (m, 1H), 1.59 (sex, 2H), 1.39-1.31 (m, 1H), 0.87 (t, 3H); ^{13}C NMR (150 MHz, $CDCl_3$): δ 173.5, 58.1, 46.3, 43.1, 38.6, 28.9, 25.6, 19.2, 13.8; ESI MS: Expected $[M+H]^+$: 171.1492, observed: 171.1490; IR (cm^{-1}): 3296, 3077, 2961, 2872, 1642, 1548, 1458, 1429, 1363, 1284, 1250, 1209, 1119, 1039, 999, 892.

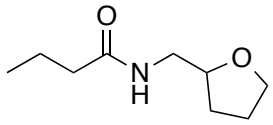

33: To a solution of butyric acid (218 mg, 2.5 mmol) dissolved in 15 mL of water at room temperature, was added *N*-hydroxysuccinimide (285 mg, 2.5 mmol) followed by EDC•HCl (474 mg, 2.5 mmol). The reaction was stirred for 30 min before 2-(aminomethyl)tetrahydrofuran (250 mg, 2.5 mmol) was added. After 48 h, the aqueous solution was extracted with chloroform (4 x 5 mL). The combined chloroform layers were washed with a saturated aqueous solution of sodium bicarbonate (3 x 5 mL), dried with $MgSO_4$, and filtered. The solvent was removed under reduced pressure to afford **33** as an oil (210.4 mg, 50% yield). ^{1}H NMR (600 MHz, $CDCl_3$): δ 5.92 (s, 1H), 3.92-3.86 (m, 1H), 3.82-3.76 (m, 1H), 3.72-3.66 (m, 1H), 3.55-3.49 (m, 1H), 3.10-3.03 (m, 1H), 2.10 (t, 2H, J=7.4 Hz), 1.95-1.87 (m, 1H), 1.86-1.80 (m, 2H), 1.60 (sex, 2H, J=7.4 Hz), 1.52-1.43 (m, 1H), 0.88 (t, 3H, J=7.4 Hz); ^{13}C NMR (150 MHz, $CDCl_3$): δ 173.1, 77.8, 68.0, 43.0, 38.6, 28.6, 25.8, 19.1, 13.7; ESI MS: Expected $[M+H]^+$: 172.1332, observed: 172.1331; IR (cm^{-1}): 3297, 2963, 2933, 2873, 1643, 1545, 1459, 1378, 1284, 1252, 1210, 1073, 1026, 922, 821.

Table 2.3. Literature sources for previously synthesized compounds.

Compound	Comments	Sources
4	Synthesized as a series of AHLs with viariable tail length for pH-dependent ring-opening experiments,	[32, 49]
5	Example AHL in synthesis methods paper	[32]
6	NMR characterization of common AHL molecules	[50]
7	Identification of Isovaleryl-homoserine lactone, a branched-chain quorum-sensing signal from the soybean symbiont *Bradyrhizobium japonicum*	[31]
9	Isomer of Isovaleryl-homoserine lactone synthesized for AHL identification in culture	[31]
10	Synthesized as part of a library testing for antagonism of *Agrobacterium tumefaciens* QS	[51]
16	Synthetic intermediate for triazole-based AHLs	[52]
17	Synthesized as part of a library testing for antagonism of *Agrobacterium tumefaciens* QS	[53]
23	Identified in a patent as a bacterial virulence factor inhibitor in a library of sulfonamides	[46]
24	Produced in a patent to show a novel method of hydroxy-γ-butyrolactone synthesis	[54]
25	Synthesized to determine the absolute configuration of natural autoinducers	[35]
26	Synthesized to probe violacein production in *Chromobacterium violaceum*	[55]
28	Used to probe the optimal steriochemistry for non-native AHL binding	[32]
29	Screened in a cyclopentylamine library as an inhibitor of *Pseudomonas aeruginosa* quorum sensing	[56]
31	Used to probe the optimal steriochemistry for non-native AHL binding	[32]

Table 2.4. Complete primary RhlR agonism and antagonism data by library members.[a]

Compound	% activation (10μM)[b]	% activation (1 mM)[c]	% inhibition (10 μM)[d]	% inhibition (1 mM)[e]
1 (BHL)	51	100	–	–
2 (D8)	54	92	-21	-88
3 (S4)	76	94	-52	-95
4	25	82	-5	-66
5	25	82	-18	-91
6	62	89	-30	-112
7	86	99	-62	-123
8	55	91	-24	-101
9	1	11	0	25
10	5	34	3	7
11	28	77	2	-66
12	41	88	-4	-69
13	21	77	9	-47
14	52	101	-12	-74
15	45	97	-7	-83
16	34	86	-2	-76
17	79	95	-66	-110
18	32	83	-2	-69
19	70	107	-47	-108
20	2	9	2	24
21 (S5)	34	84	2	-43
22 (B8)[f]	1	2	8	31
23	1	8	8	55
24	0	0	4	6
25	2	24	1	11
26	71	92	-8	-75
27	1	5	-1	35
28	35	85	-37	-82
29	0	18	9	45
30	0	0	-5	20
31	2	32	4	12
32	0	1	-3	-1
33	0	3	1	57

[a] Assays were performed using the heterologous RhlR reporter strain JLD271/pJN105R2/pSC11-*rhlI**. SEM of n ≥ 3 trials did not exceed ± 10%. [b] Library compounds were screened at 10 μM. RhlR activity was measured relative to that of 1 mM BHL. [b] Library compounds were screened at 1 mM. RhlR activity was measured relative to that of 1 mM BHL. [d] Library compounds were screened at 10 μM in the presence of 10 μM BHL. Negative numbers indicate agonism stronger than that of 10 μM BHL alone. [e] Library compounds were screened at 1 mM in the presence of 10 μM BHL. Negative numbers indicate agonism stronger than that of 10 μM BHL alone. [f] Screened at a maximal concentration of 200 μM due to solubility concerns at higher concentrations. [g] Screened at a maximal concentration of 100 μM due to solubility concerns at higher concentrations.

Table 2.5. Complete primary LasR agonism and antagonism data by library members.[a]

Compound	% activation (10μM)[b]	% activation (1 mM)[c]	% inhibition (10 μM)[d]	% inhibition (1 mM)[e]
1 (BHL)	1	6	-2	35
2 (D8)	0	25	9	56
3 (S4)	6	21	19	32
4	0	6	2	49
5	0	10	-16	54
6	0	10	13	59
7	0	0	10	74
8	1	19	24	65
9	0	38	6	-70
10	0	6	4	-24
11	1	4	15	71
12	0	9	22	73
13	4	2	15	72
14	0	0	4	-25
15	1	78	-5	-128
16	0	2	15	77
17	0	2	8	73
18	0	11	7	46
19	1	22	6	42
20	0	30	-1	-35
21 (S5)	0	18	27	47
22 (B8)[f]	1	2	-13	-7
23	0	51	0	-72
24	0	13	14	-21
25	0	18	5	-18
26	4	21	2	36
27	0	13	8	3
28	0	8	18	72
29	11	10	-1	1
30	4	86	-14	-125
31	0	72	1	-103
32	0	0	11	6
33	25	104	3	-66
OdDHL[f]	100	100	–	–

[a] Assays were performed using the heterologous LasR reporter strain JLD271/pJN105L/pSC11. SEM of n ≥ 3 trials did not exceed ± 10%. [b] Library compounds were screened at 10 μM. LasR activity was measured relative to that of 100 μM OdDHL. [b] Library compounds were screened at 1 mM. LasR activity was measured relative to that of 100 μM OdDHL. [d] Library compounds were screened at 10 μM in the presence of 2 nM OdDHL. Negative numbers indicate agonism stronger than that of 2 nM OdDHL alone. [e] Library compounds were screened at 1 mM in the presence of 2 nM OdDHL. Negative numbers indicate agonism stronger than that of 2 nM OdDHL alone. [f] Screened at a maximal concentration of 200 μM due to solubility concerns at higher concentrations. [g] Screened at a maximal concentration of 100 μM due to solubility concerns at higher concentrations.

Table 2.6: Complete RhlR agonism curve data from *E. coli*[a] and *P. aeruginosa*[b] reporters

	E. coli			*P. aeruginosa*		
Compound	**EC_{50} (μM)[b]**	**95% CI (μM)**	**Maximum activation (%)[c]**	**EC_{50} (μM)[b]**	**95% CI (μM)**	**Maximum activation (%)[c]**
1 (BHL)	8.95	5.86 – 13.7	100	8.08	6.09 – 10.7	100
2 (D8)	7.93	6.28 – 10.02	94	–	–	–
3 (S4)	1.58	1.32 – 1.90	100	1.22	1.03 – 1.45	106
5	10.83	6.59 – 17.80	96	–	–	–
6	4.89	3.67 – 6.53	95	–	–	–
7	1.02	0.67 – 1.55	105	1.42	1.08 – 1.86	94
8	7.77	5.61 – 10.8	95	–	–	–
14	6.93	5.52 – 8.71	87	–	–	–
17	1.78	1.37 – 2.31	100	1.41	1.14 – 1.74	96
19	2.76	2.23 – 3.42	95	–	–	–
26	4.87	3.46 – 6.84	102	3.82	2.57 – 5.66	95
28	27.4	16.1 – 46.6	92	14.3	8.76 – 23.5	94

[a] Assays were performed using *E. coli* JLD271 (pJN105R2/pSC11-*rhlI**) or *P. aeruginosa* PAO-JP2 (p*rhlI*-LVA*gfp*); see Experimental Section. For both assays, EC_{50} values were determined by testing AHLs over a range of concentrations (≤ 1 mM). Assays were performed in triplicate, and 95% confidence intervals (CIs) were calculated from the SEM of n ≥ 3 trials. [b]Denotes the highest value of RhlR activation seen for each compound at any concentration within the dose–response assay. [c]RhlR activity was measured relative to that of 1 mM BHL.

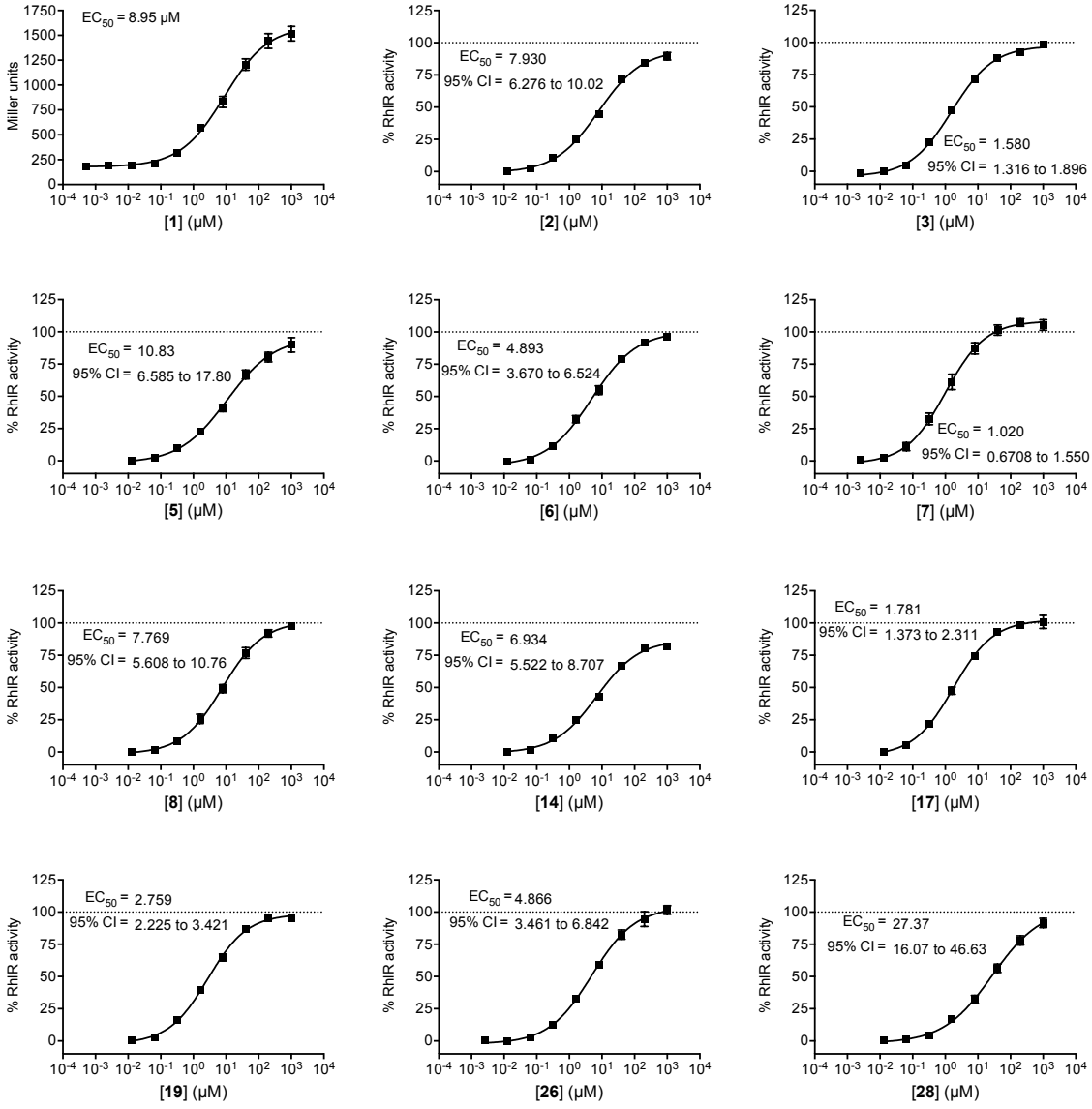

Figure 2.4. Dose–response curves for RhlR agonism in *E. coli* by BHL and lead agonist AHLs
Assay performed using the E. coli JLD271/pJN105R2/pSC11-rhlI* reporter strain. % Activity is defined as the activity of the synthetic AHL relative to maximum possible RhlR activity (i.e., activity effected by BHL at 1 mM). EC_{50} values and 95% Confidence Intervals (CI; shown on each plot) calculated using GraphPad Prism. Error bars, SEM of $n \geq 3$ trials.

Note: Comments on Hill slopes for RhlR agonist dose response curves in *E. coli* and *P. aeruginosa.*

The dose-response curve of BHL is shallower (Hill slope = 0.7) in the *E. coli* RhlR reporter strain (Hill slope = ~1.0) than curves for other AHL ligands in related LuxR-type receptor report strains. This characteristic was conserved across all of the agonists in Table 2.2. Shallow dose–response curves are often indicative of negative cooperativity of the small molecule binding to multiple sites on the receptor.[57] Since RhlR functions as a dimer, this negative cooperativity scenario is feasible if binding of an agonist to RhlR reduces binding affinity of the second dimer site for the agonist. Reporter systems are complex, however, and this apparent negative cooperativity could be related to DNA binding or transcriptional machinery recruitment rather than simply ligand–receptor binding. Nevertheless, since the Hill slopes of all compound dose–response curves were consistently around 0.7, the single-concentration efficacy determined in initial screens and overall compound potency tracked each other quite closely for each compound. All dose–response curves in the *P. aeruginosa* background had Hill slopes much closer to 1.0 (Figure 2.5), suggesting that the shallow dose–response relationships common in the *E. coli* reporter may simply be artifacts of heterologous expression.

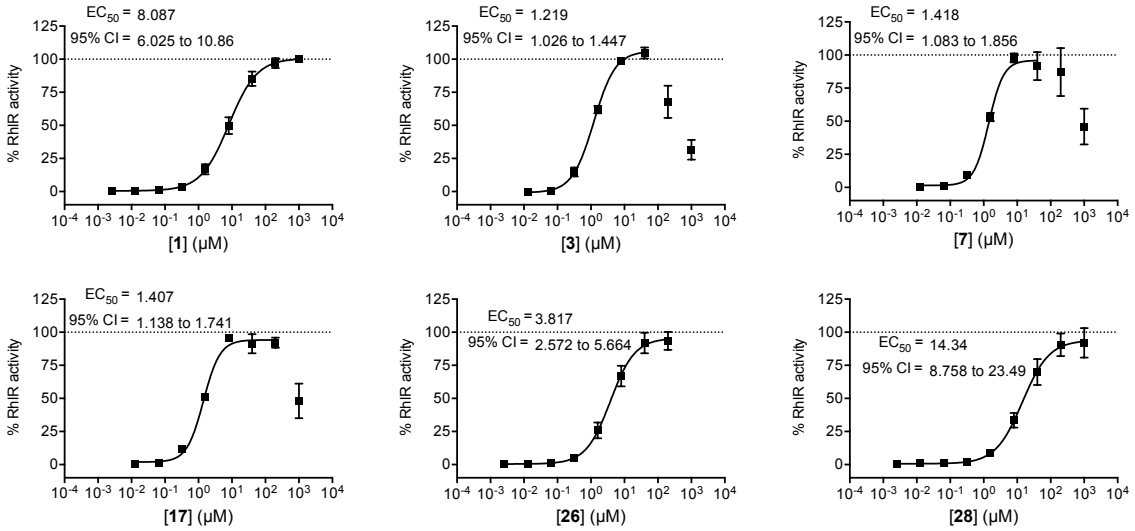

Figure 2.5. Dose–response curves for RhlR agonism in *P. aeruginosa* by BHL and best agonist AHLs. Assays performed using the *P. aeruginosa* PAO-JP2/p*rhlI*-LVA*gfp* reporter strain. % Activity is defined as the activity of the synthetic AHL relative to maximum possible RhlR activity (i.e., activity effected by BHL at 1 mM). The EC_{50} values for the synthetic compounds were calculated from the region of the dose–response curve that indicated RhlR agonism. EC_{50} values and associated 95% Confidence Intervals (CI; shown on each plot) calculated using GraphPad Prism. Error bars, SEM of $n \geq 3$ trials.

Note: Comments on non-monotonic dose response curves for RhlR agonists in *P. aeruginosa*

We note that compounds **3**, **7** and **17** displayed non-monotonic dose curves in the *P. aeruginosa* reporter (*e.g.*, curves that increase in activity at low concentrations, followed by a decrease at high concentrations—often referred to as an "inverted U-shape" curve). Surprisingly, compounds **26** and **28** with modified head groups did not display any non-monotonic character. It is possible the decreased potency of these compounds relative to the modified tail compounds may have hidden this curve characteristic; native ligand BHL also does not show an "inverted U" shape and is 6-fold less potent than compounds **3**, **7**, and **17**.

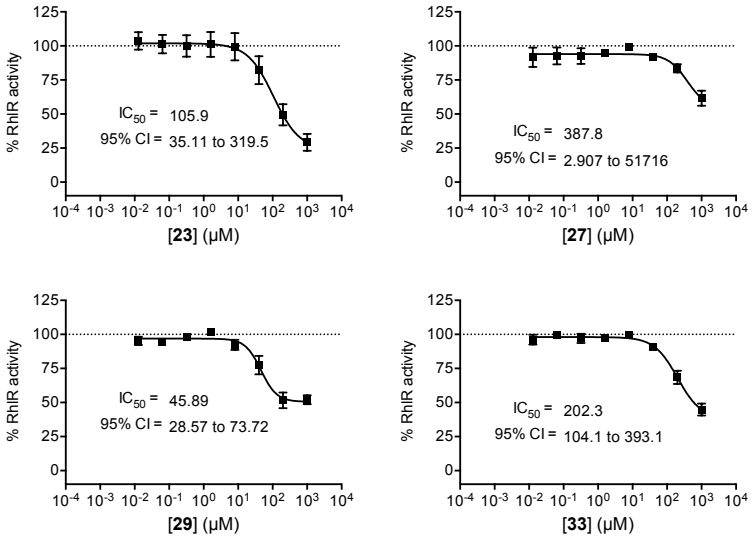

Figure 2.6. Dose–response curves for RhlR antagonism in *E. coli* by lead antagonist AHLs.
Assay performed using the E. coli JLD271/pJN105R2/pSC11-rhlI* reporter strain with the addition of 10 μM BHL. % Activity is defined as the activity of the synthetic AHL relative to half maximal RhlR activity (i.e., activity effected by BHL at 10 μM). IC_{50} values and 95% Confidence Intervals (CI; shown on each plot) calculated using GraphPad Prism. Error bars, SEM of n ≥ 3 trials.

2.7 ^{1}H- and ^{13}C-NMR spectra for compounds synthesized in this study

D1406161618_c3AHL_H.10.fid — Group Blackwell — PROTON CDCl3 /home/jmoore/av400 jmoore 78

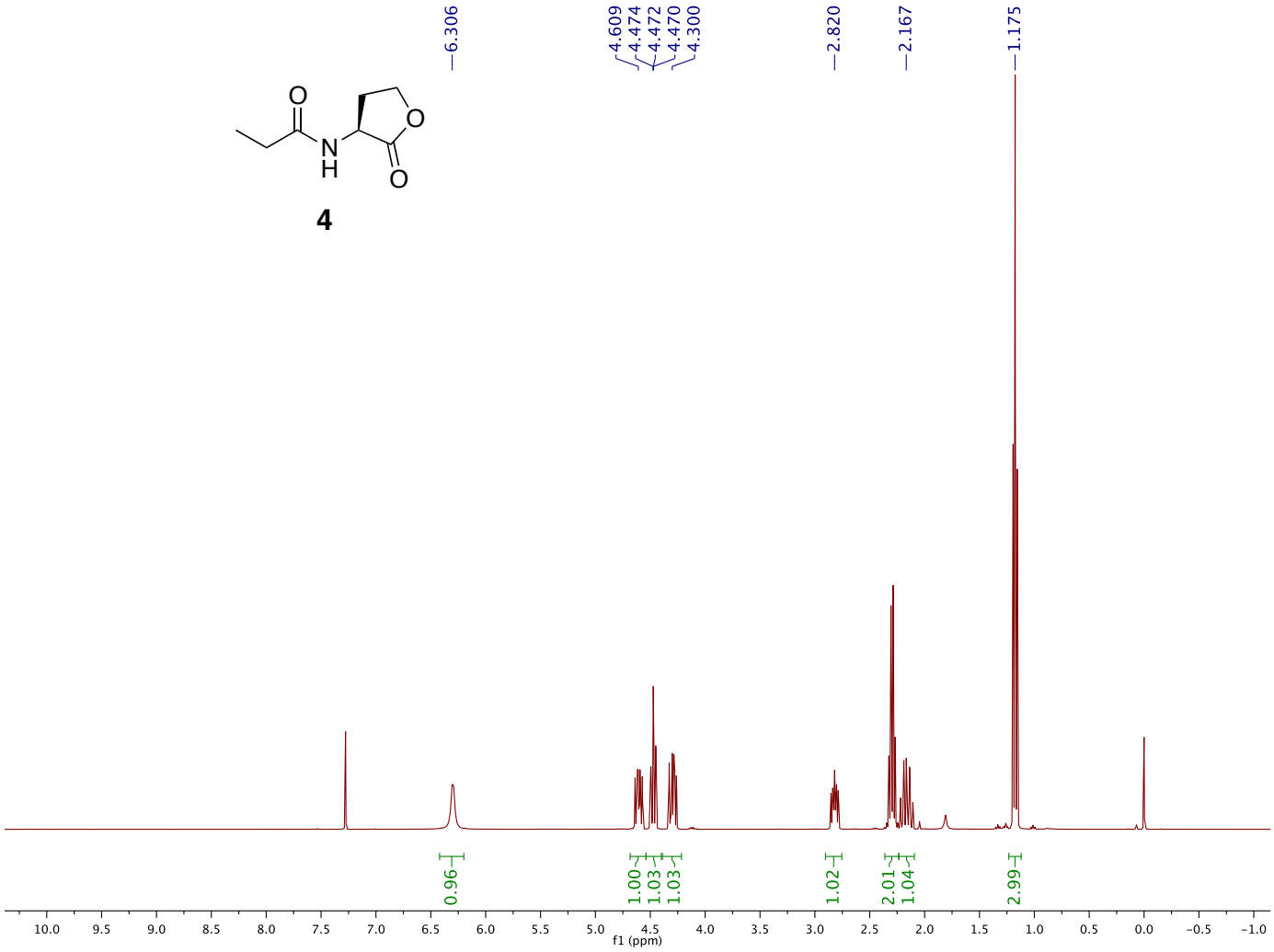

D1406161618_c3AHL_C.10.fid
Group Blackwell
C13CPD32 CDCl3 /home/jmoore/av400 jmoore 78

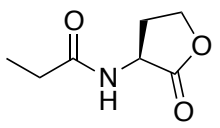

4

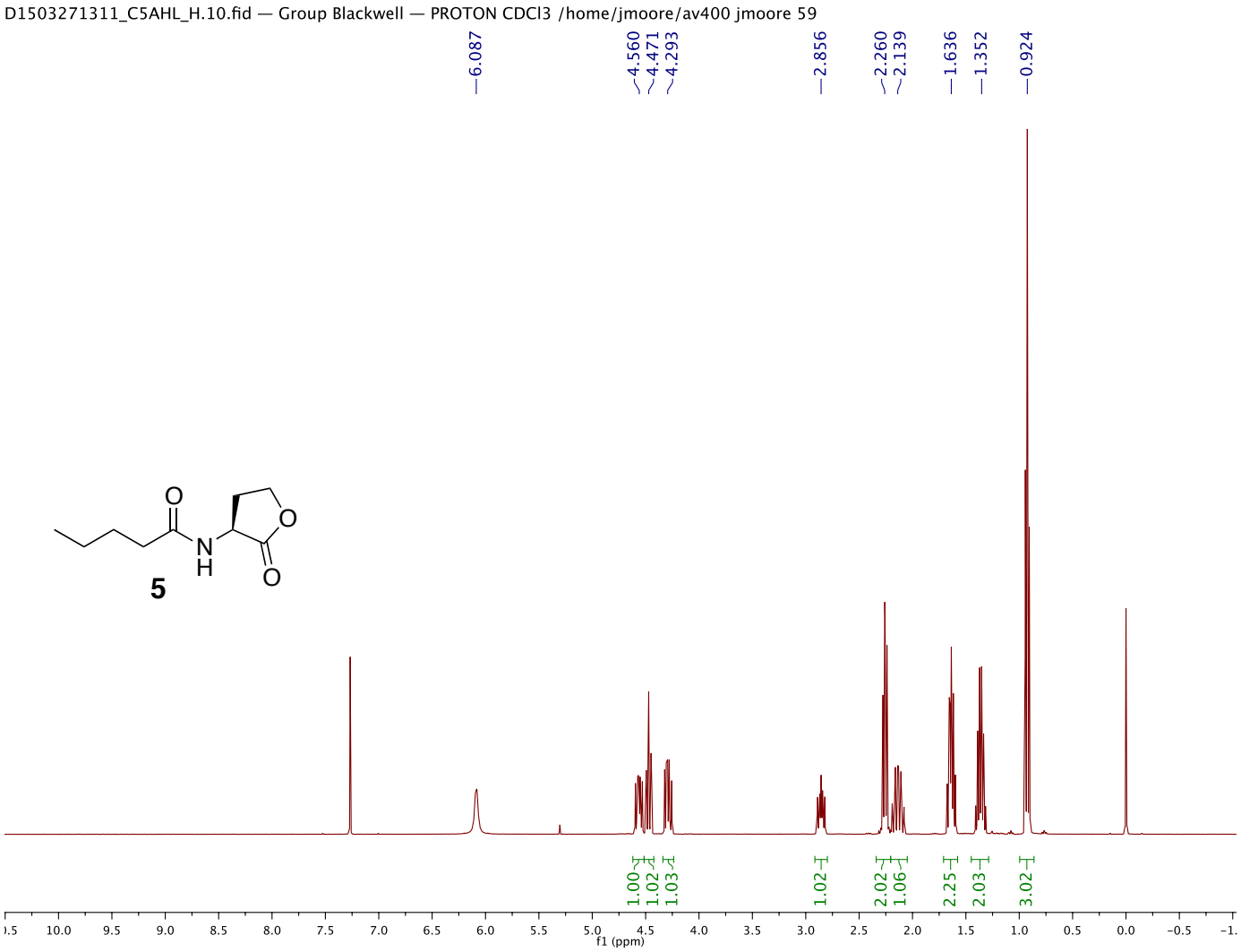
D1503271311_C5AHL_H.10.fid — Group Blackwell — PROTON CDCl3 /home/jmoore/av400 jmoore 59
6.087
4.560
4.471
4.293
2.856
2.260
2.139
1.636
1.352
0.924
O
N
H
O
O
5
1.00
1.02
1.03
1.02
2.02
1.06
2.25
2.03
3.02
f1 (ppm)

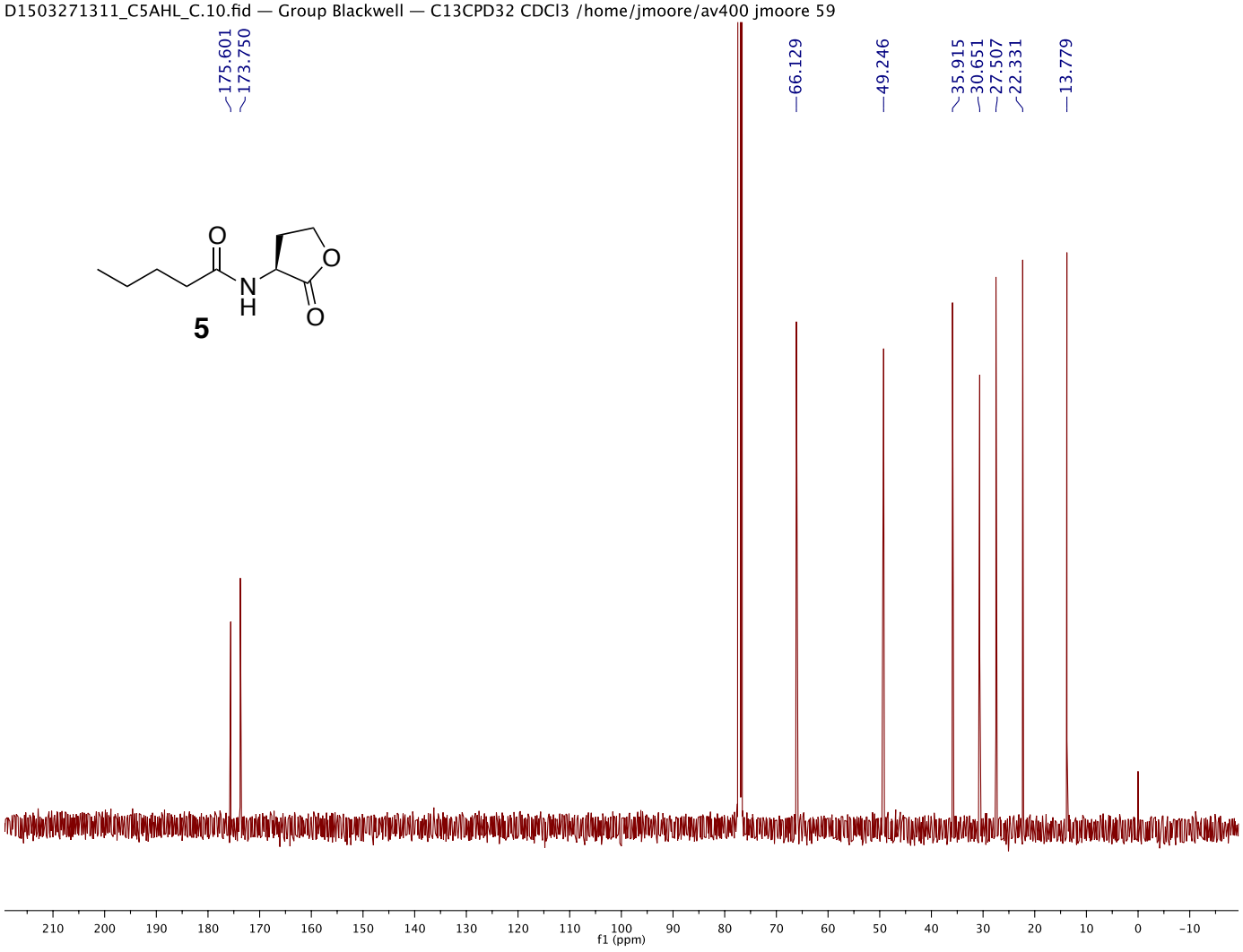
D1503271311_C5AHL_C.10.fid — Group Blackwell — C13CPD32 CDCl3 /home/jmoore/av400 jmoore 59
175.601
173.750
66.129
49.246
35.915
30.651
27.507
22.331
13.779
O
N
H
O
O
5
210 200 190 180 170 160 150 140 130 120 110 100 90 80 70 60 50 40 30 20 10 0 -10
f1 (ppm)

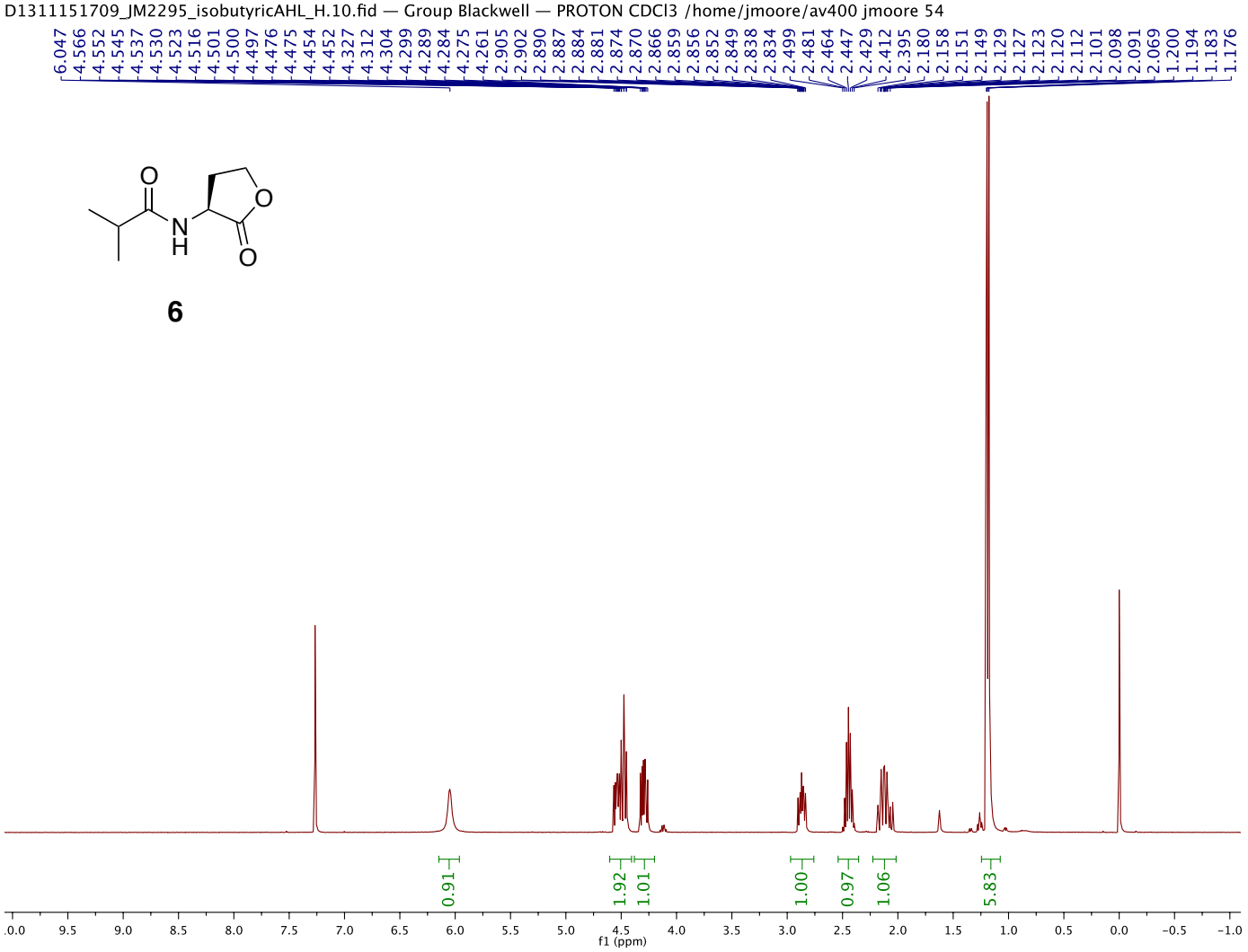
D1311151709_JM2295_isobutyricAHL_H.10.fid — Group Blackwell — PROTON CDCl3 /home/jmoore/av400 jmoore 54
6.047
4.566
4.552
4.545
4.537
4.530
4.523
4.516
4.501
4.500
4.497
4.476
4.475
4.454
4.452
4.327
4.312
4.304
4.299
4.289
4.284
4.275
4.261
2.905
2.902
2.890
2.887
2.884
2.881
2.874
2.870
2.866
2.859
2.856
2.852
2.849
2.838
2.834
2.499
2.481
2.464
2.447
2.429
2.412
2.395
2.180
2.158
2.151
2.149
2.129
2.127
2.123
2.120
2.112
2.101
2.098
2.091
2.069
1.200
1.194
1.183
1.176
O
N
H
O
O
6
0.91
1.92
1.01
1.00
0.97
1.06
5.83
f1 (ppm)

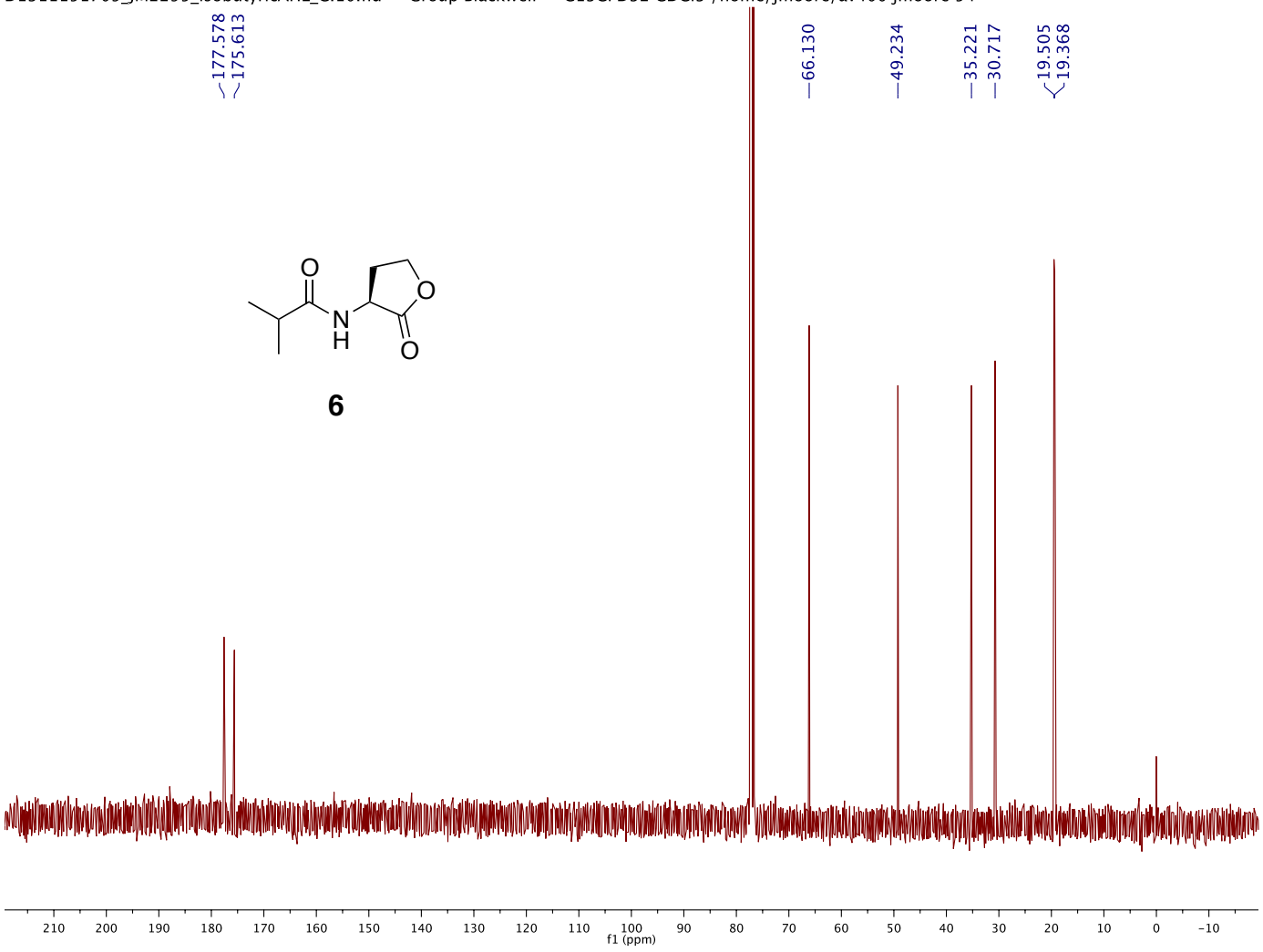
D1311151709_JM2295_isobutyricAHL_C.10.fid — Group Blackwell — C13CPD32 CDCl3 /home/jmoore/av400 jmoore 54
177.578
175.613
66.130
49.234
35.221
30.717
19.505
19.368
O
N
H
O
O
6
210 200 190 180 170 160 150 140 130 120 110 100 90 80 70 60 50 40 30 20 10 0 -10
f1 (ppm)

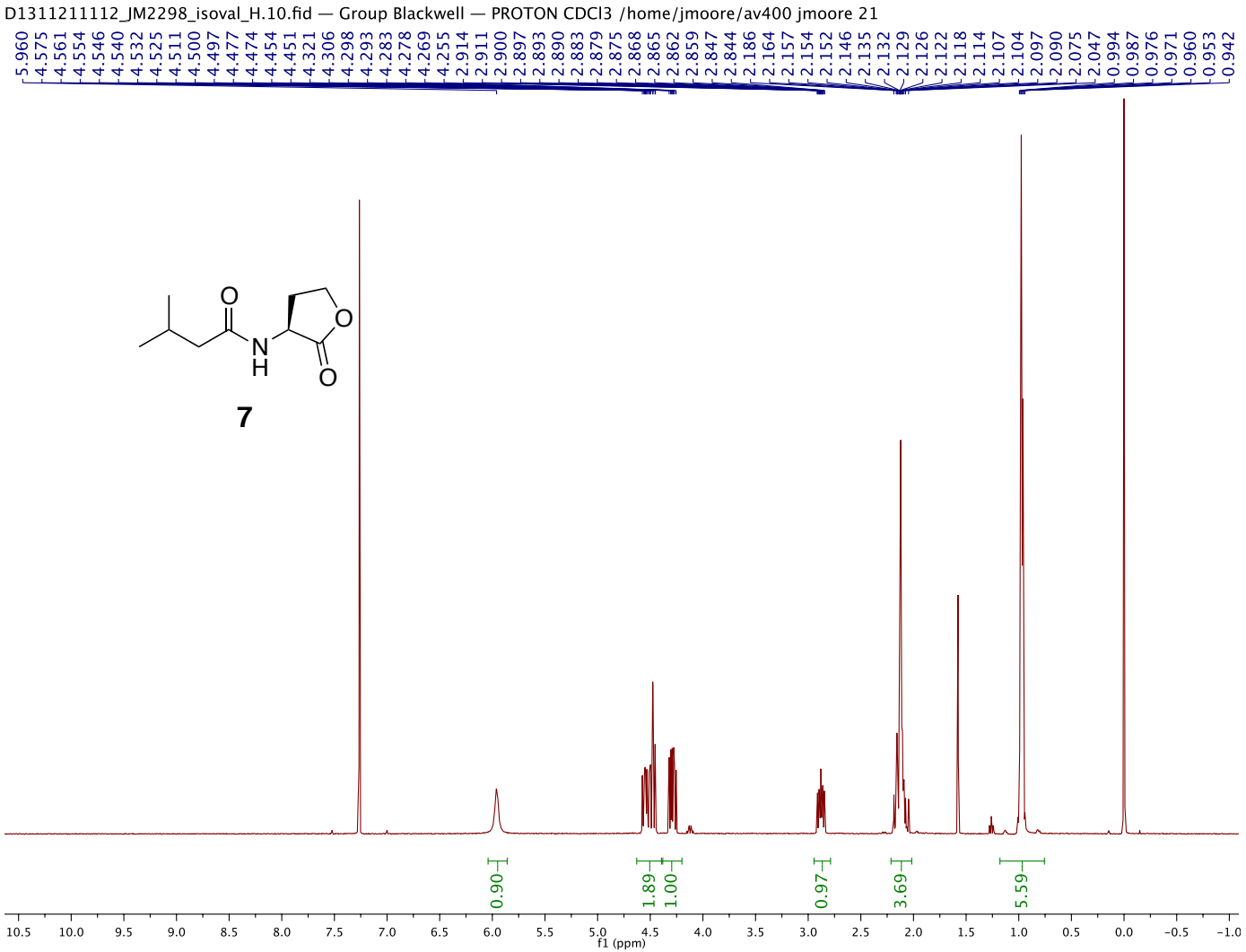
D1311211112_JM2298_isoval_H.10.fid — Group Blackwell — PROTON CDCl3 /home/jmoore/av400 jmoore 21
5.960
4.575
4.561
4.554
4.546
4.540
4.532
4.525
4.511
4.500
4.497
4.477
4.474
4.454
4.451
4.321
4.306
4.298
4.293
4.283
4.278
4.269
4.255
2.914
2.911
2.900
2.897
2.893
2.890
2.883
2.879
2.875
2.868
2.865
2.862
2.859
2.847
2.844
2.186
2.164
2.157
2.154
2.152
2.146
2.135
2.132
2.129
2.126
2.122
2.118
2.114
2.107
2.104
2.097
2.090
2.075
2.047
0.994
0.987
0.976
0.971
0.960
0.953
0.942
O
O
N
H
O
O
7
0.90
1.89
1.00
0.97
3.69
5.59
10.5
10.0
9.5
9.0
8.5
8.0
7.5
7.0
6.5
6.0
5.5
5.0
4.5
4.0
3.5
3.0
2.5
2.0
1.5
1.0
0.5
0.0
-0.5
-1.0
f1 (ppm)

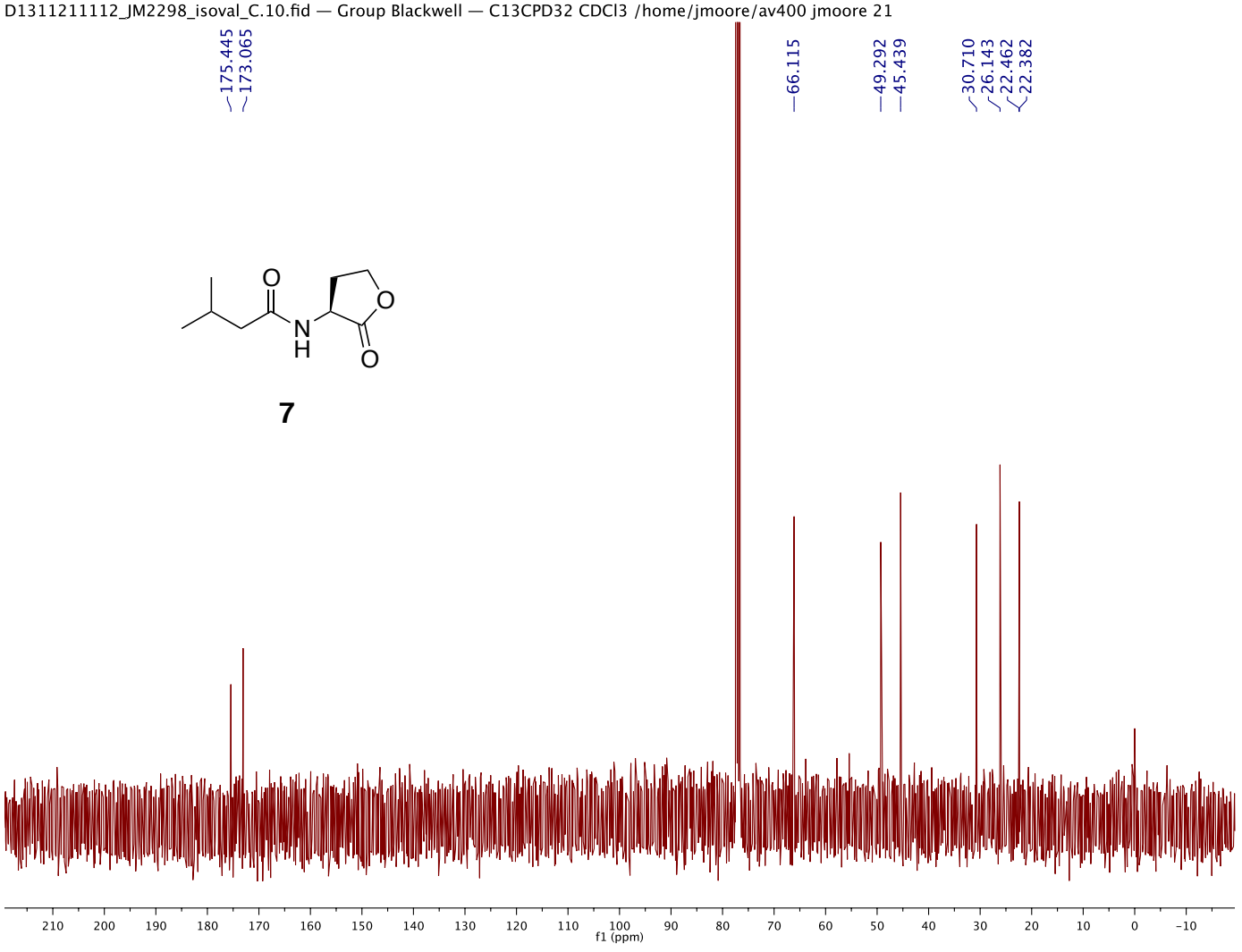
D1311211112_JM2298_isoval_C.10.fid — Group Blackwell — C13CPD32 CDCl3 /home/jmoore/av400 jmoore 21
175.445
173.065
66.115
49.292
45.439
30.710
26.143
22.462
22.382
O
N
H
O
O
7
210
200
190
180
170
160
150
140
130
120
110
100
90
80
70
60
50
40
30
20
10
0
-10
f1 (ppm)

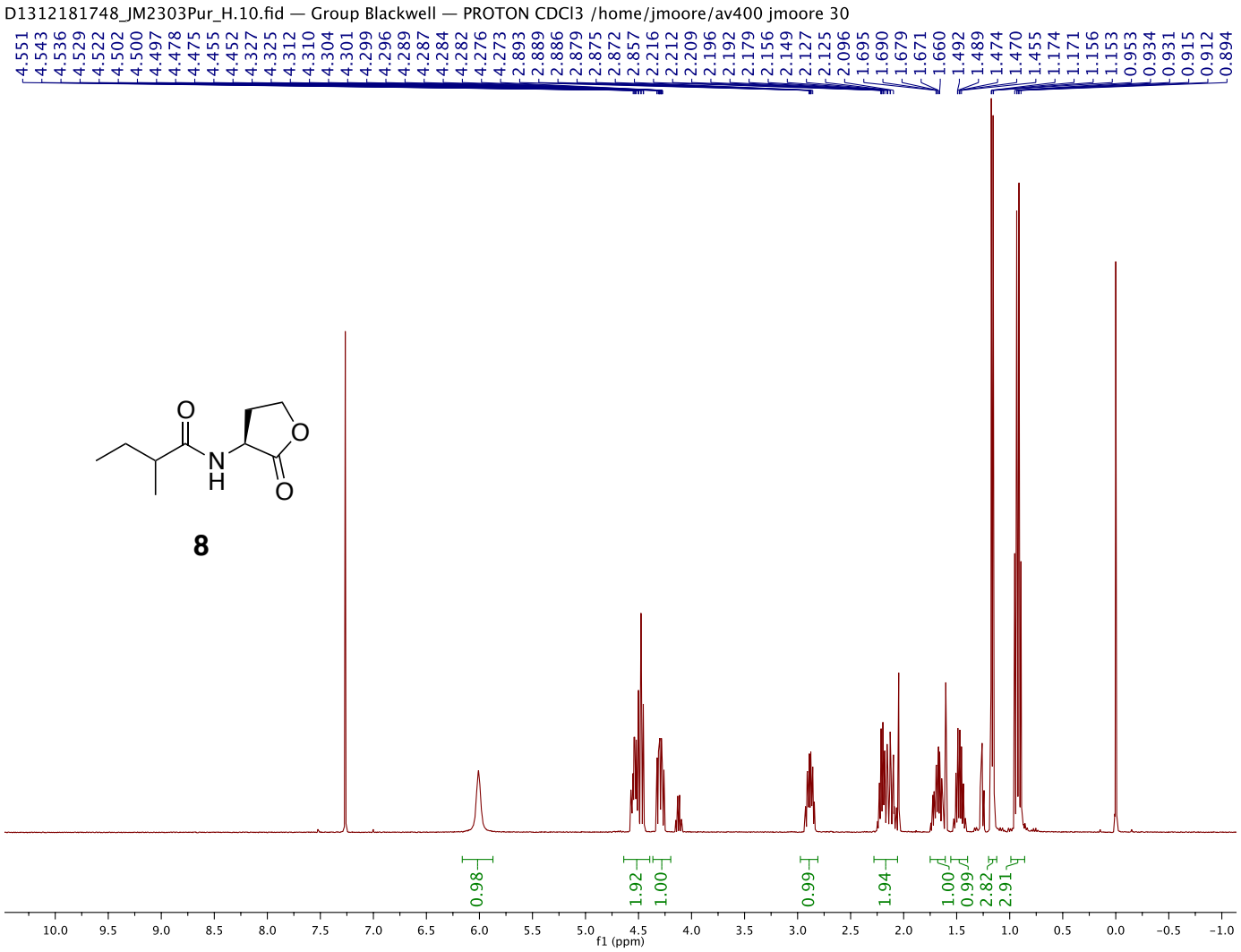
D1312181748_JM2303Pur_H.10.fid — Group Blackwell — PROTON CDCl3 /home/jmoore/av400 jmoore 30
4.551
4.543
4.536
4.529
4.522
4.502
4.500
4.497
4.478
4.475
4.455
4.452
4.327
4.325
4.312
4.310
4.304
4.301
4.299
4.296
4.289
4.287
4.284
4.282
4.276
4.273
2.893
2.889
2.886
2.879
2.875
2.872
2.857
2.216
2.212
2.209
2.196
2.192
2.179
2.156
2.149
2.127
2.125
2.096
1.695
1.690
1.679
1.671
1.660
1.492
1.489
1.474
1.470
1.455
1.174
1.171
1.156
1.153
0.953
0.934
0.931
0.915
0.912
0.894
O
N
H
O
O
8
0.98
1.92
1.00
0.99
1.94
1.00
0.99
2.82
2.91
10.0
9.5
9.0
8.5
8.0
7.5
7.0
6.5
6.0
5.5
5.0
4.5
4.0
3.5
3.0
2.5
2.0
1.5
1.0
0.5
0.0
-0.5
-1.0
f1 (ppm)

D1312181748_JM2303Pur_C.10.fid — Group Blackwell — C13CPD32 CDCl3 /home/jmoore/av400 jmoore 30

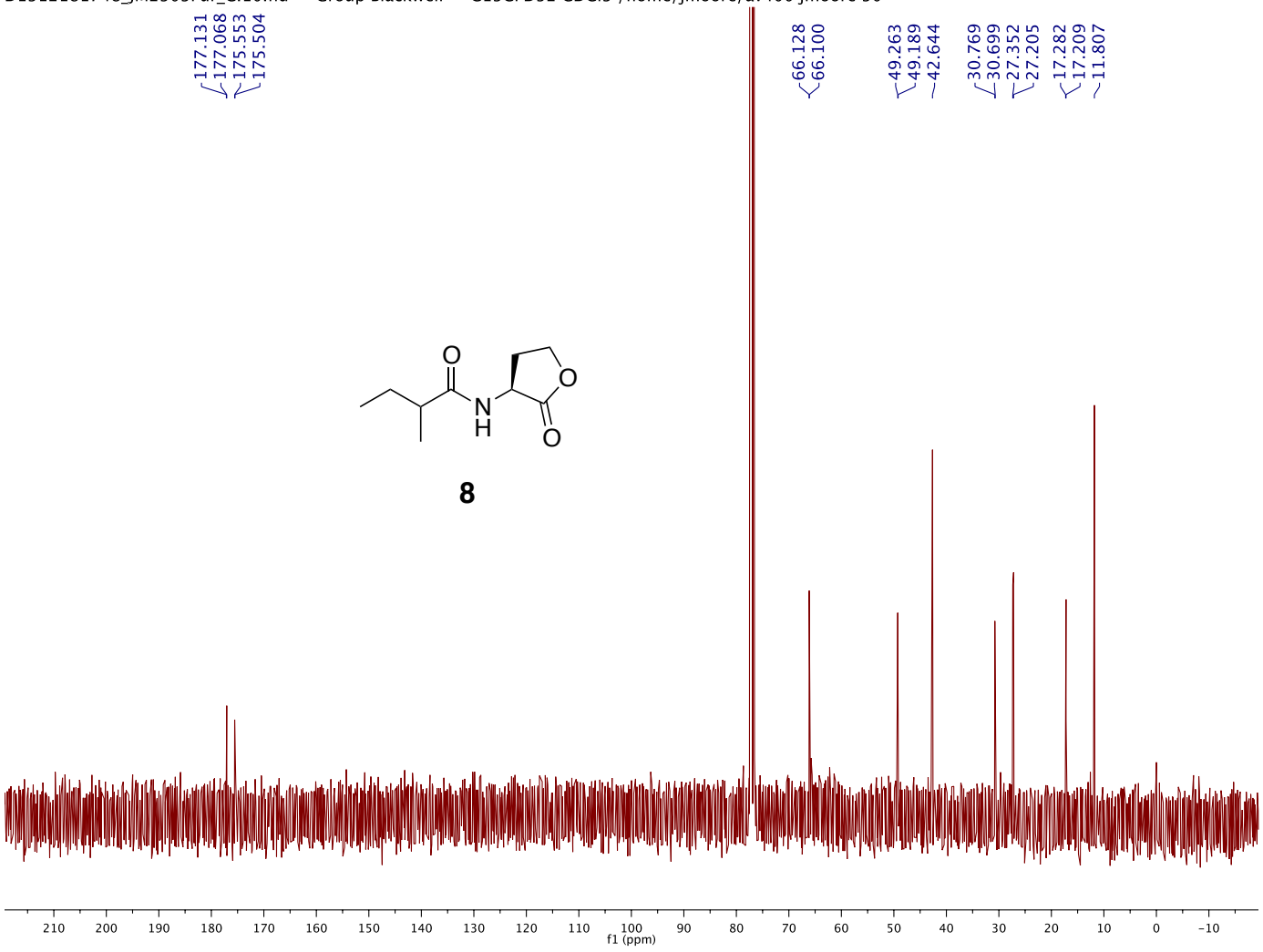

8

D1407041444_SPS24_tBuAHL_H.10.fid — Group Blackwell — PROTON CDCl3 /home/jmoore/av400 jmoore 32

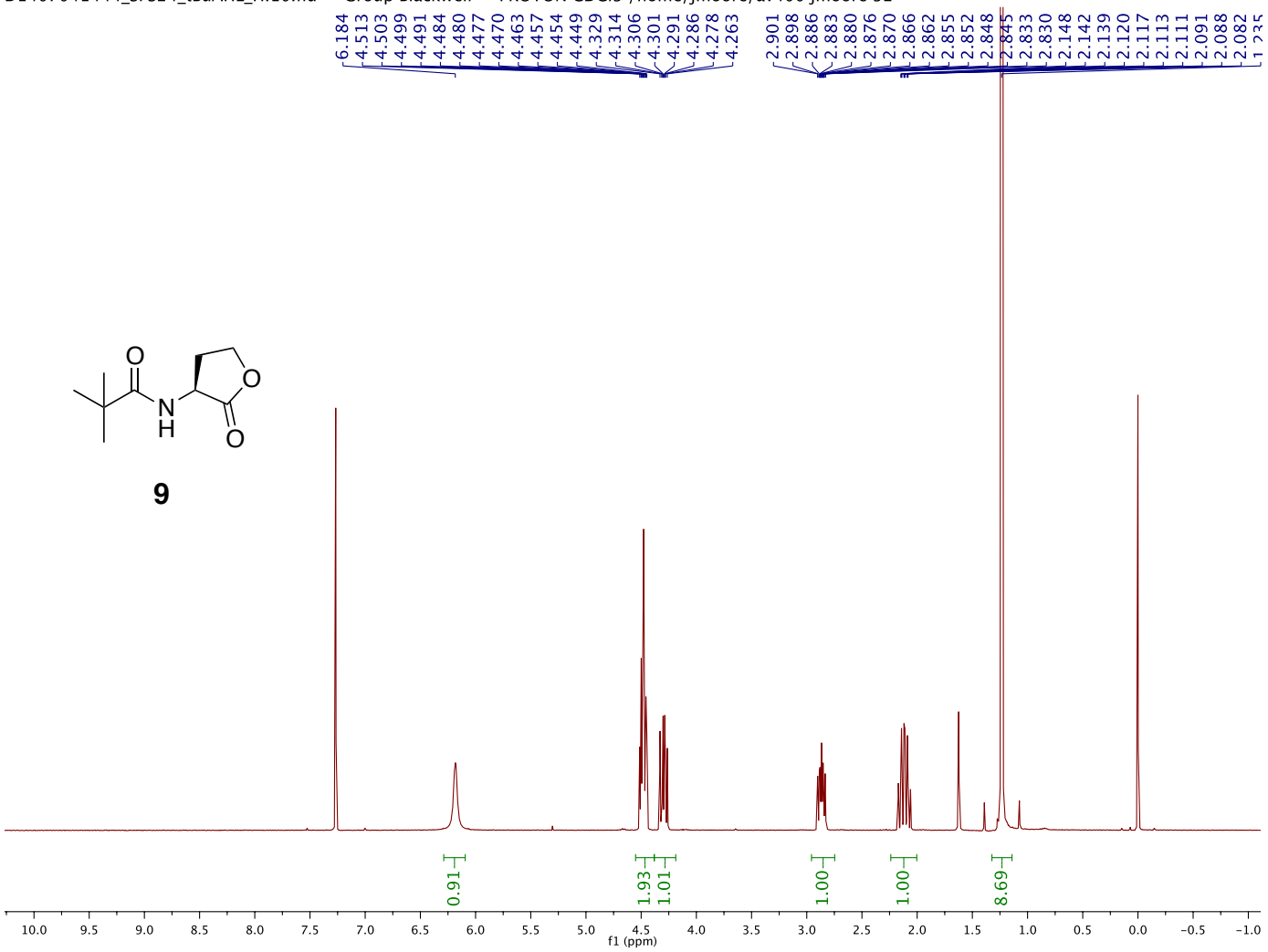

9

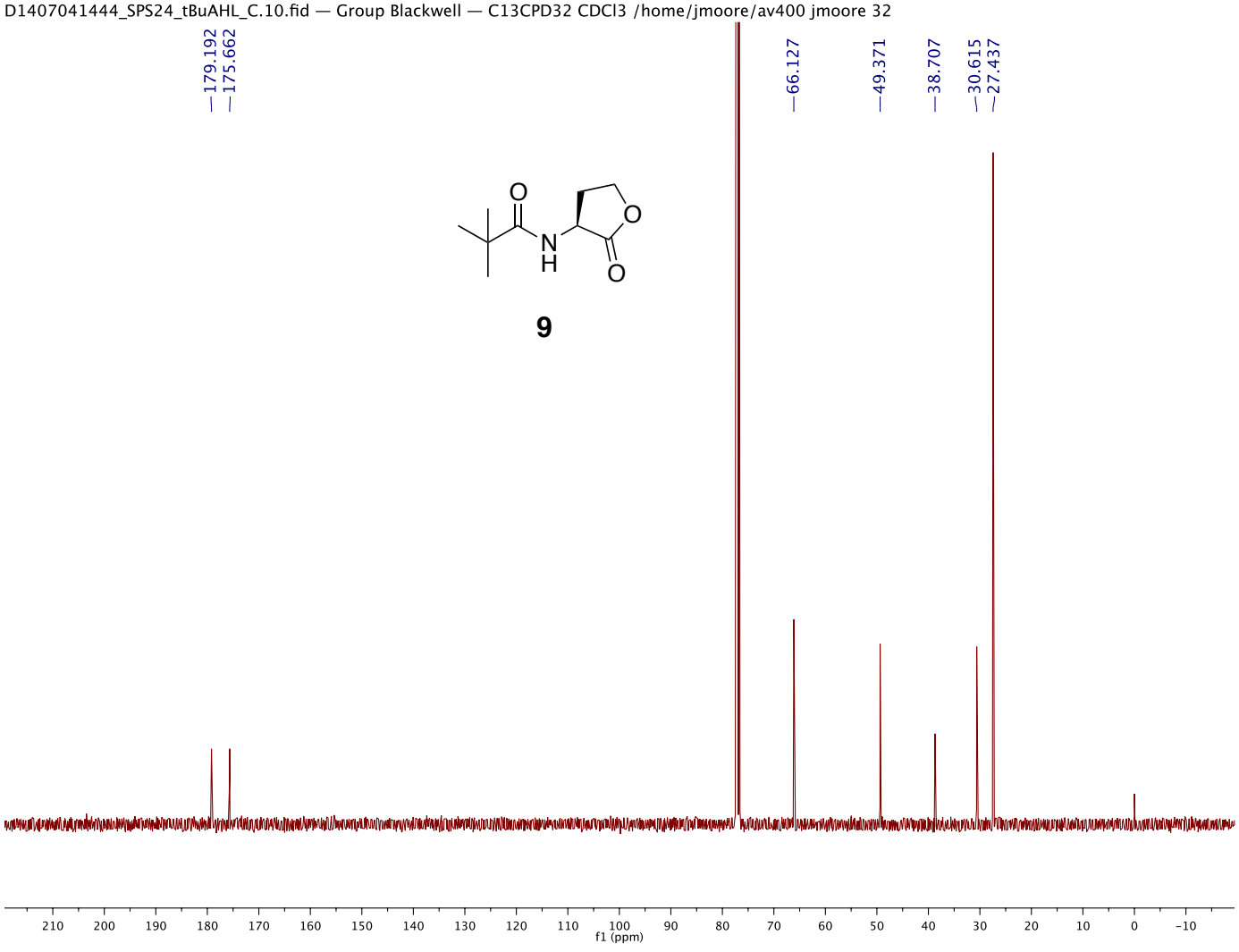
D1407041444_SPS24_tBuAHL_C.10.fid — Group Blackwell — C13CPD32 CDCl3 /home/jmoore/av400 jmoore 32
179.192
175.662
66.127
49.371
38.707
30.615
27.437
O
N
H
O
O
9
210 200 190 180 170 160 150 140 130 120 110 100 90 80 70 60 50 40 30 20 10 0 -10
f1 (ppm)

D1407041444_SPS26_diMeButAHL_H.10.fid — Group Blackwell — PROTON CDCl3 /home/jmoore/av400 jmoore 33

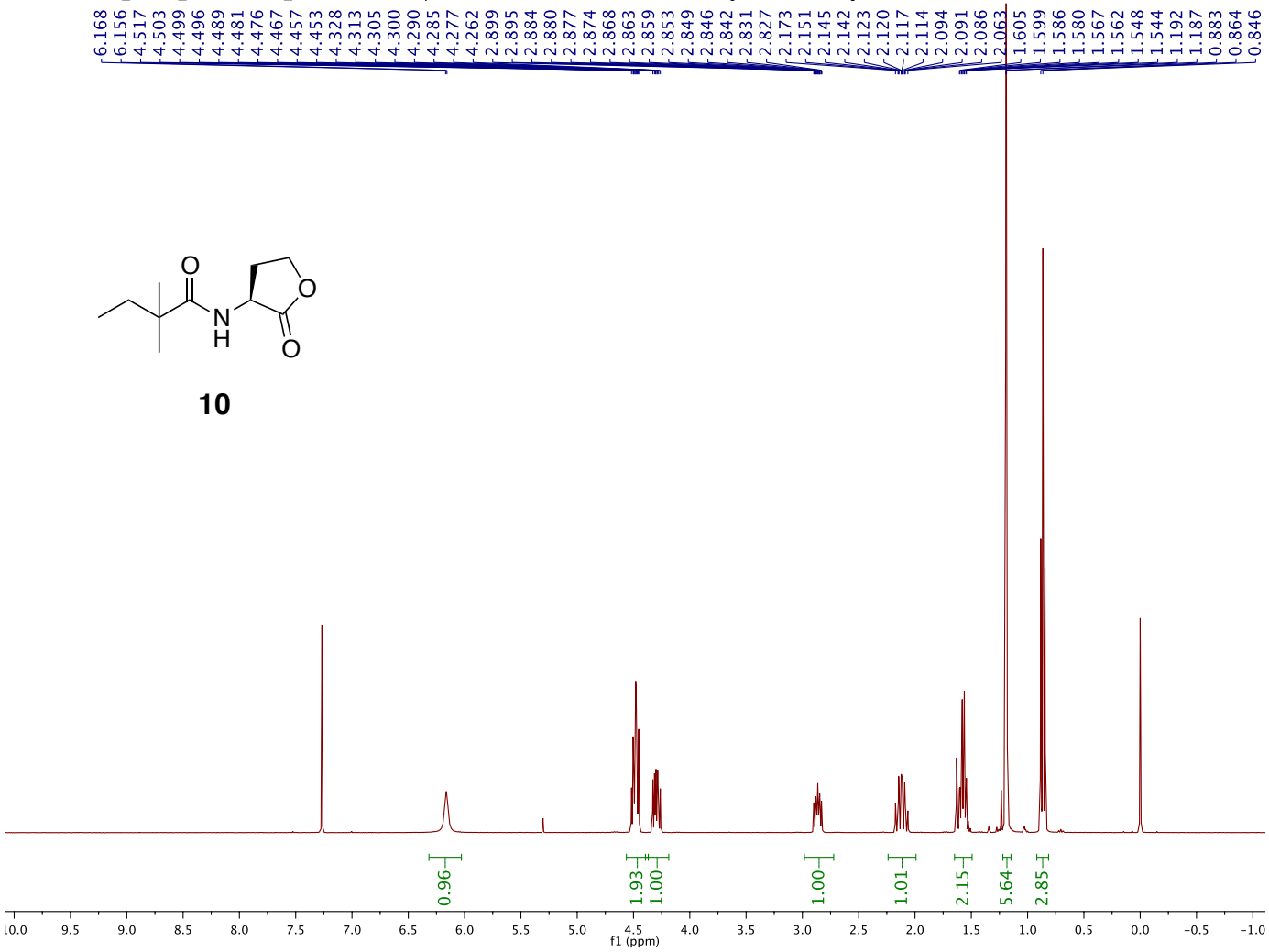

10

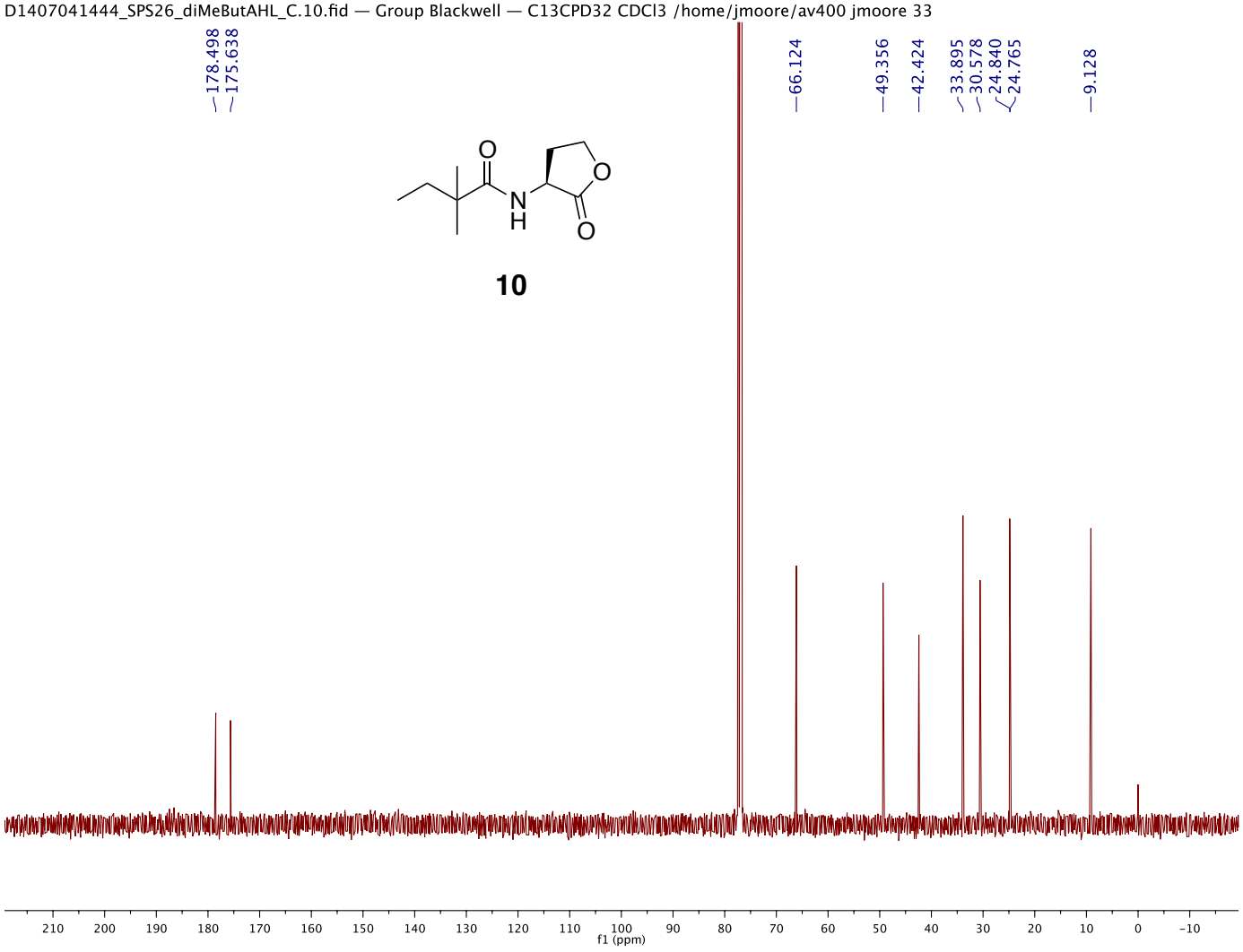
D1407041444_SPS26_diMeButAHL_C.10.fid — Group Blackwell — C13CPD32 CDCl3 /home/jmoore/av400 jmoore 33
178.498
175.638
66.124
49.356
42.424
33.895
30.578
24.840
24.765
9.128
O
N
H
O
O
10
210 200 190 180 170 160 150 140 130 120 110 100 90 80 70 60 50 40 30 20 10 0 -10
f1 (ppm)

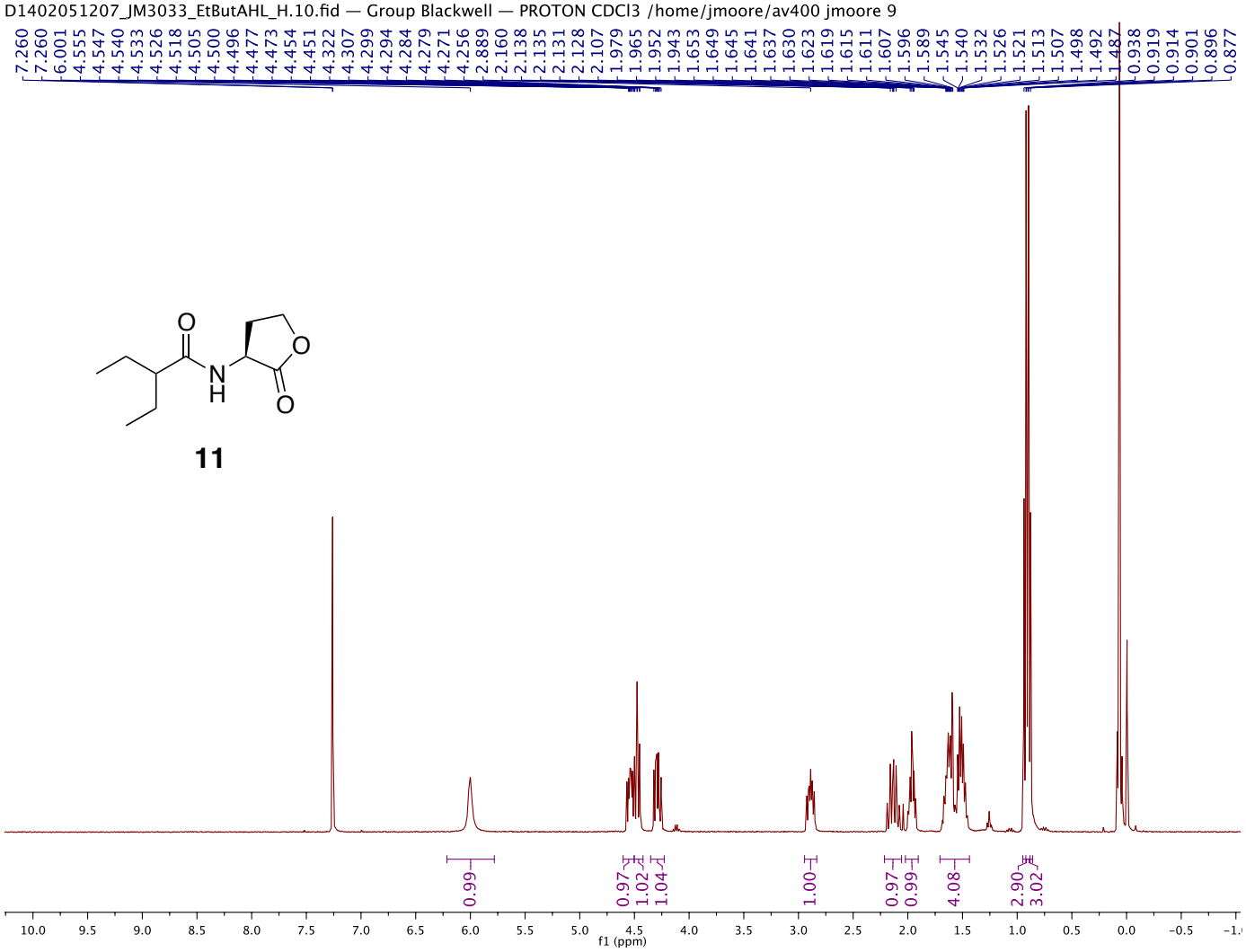
D1402051207_JM3033_EtButAHL_H.10.fid — Group Blackwell — PROTON CDCl3 /home/jmoore/av400 jmoore 9
7.260
7.260
6.001
4.555
4.547
4.540
4.533
4.526
4.518
4.505
4.500
4.496
4.477
4.473
4.454
4.451
4.322
4.307
4.299
4.294
4.284
4.279
4.271
4.256
2.889
2.160
2.138
2.135
2.131
2.128
2.107
1.979
1.965
1.952
1.943
1.653
1.649
1.645
1.641
1.637
1.630
1.623
1.619
1.615
1.611
1.607
1.596
1.589
1.545
1.540
1.532
1.526
1.521
1.513
1.507
1.498
1.492
1.487
0.938
0.919
0.914
0.901
0.896
0.877
O
N
H
O
O
11
0.99
0.97
1.02
1.04
1.00
0.97
0.99
4.08
2.90
3.02
10.0
9.5
9.0
8.5
8.0
7.5
7.0
6.5
6.0
5.5
5.0
4.5
4.0
3.5
3.0
2.5
2.0
1.5
1.0
0.5
0.0
-0.5
f1 (ppm)

D1402051207_JM3033_EtButAHL_C.10.fid — Group Blackwell — C13CPD32 CDCl3 /home/jmoore/av400 jmoore 9

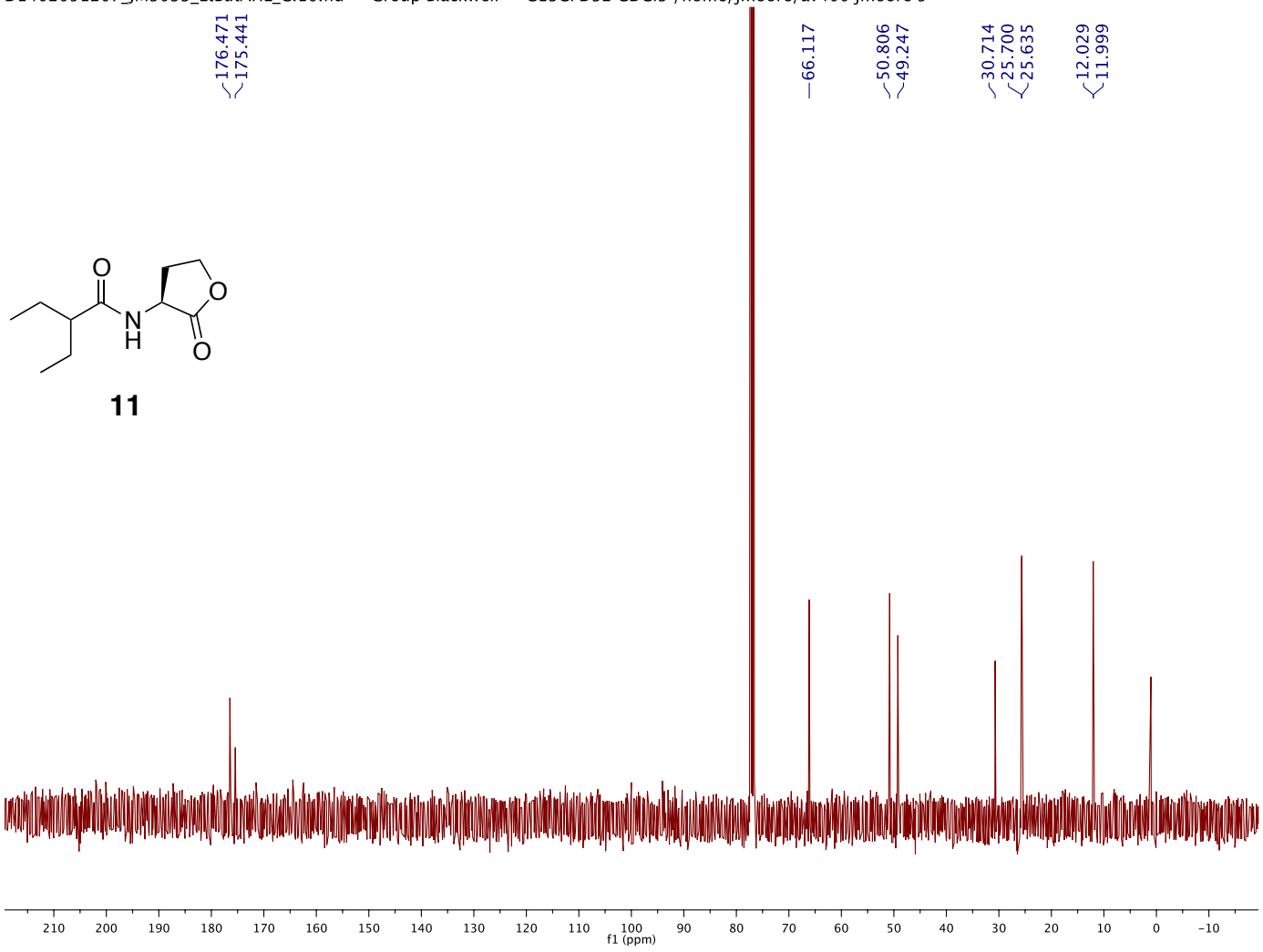

11

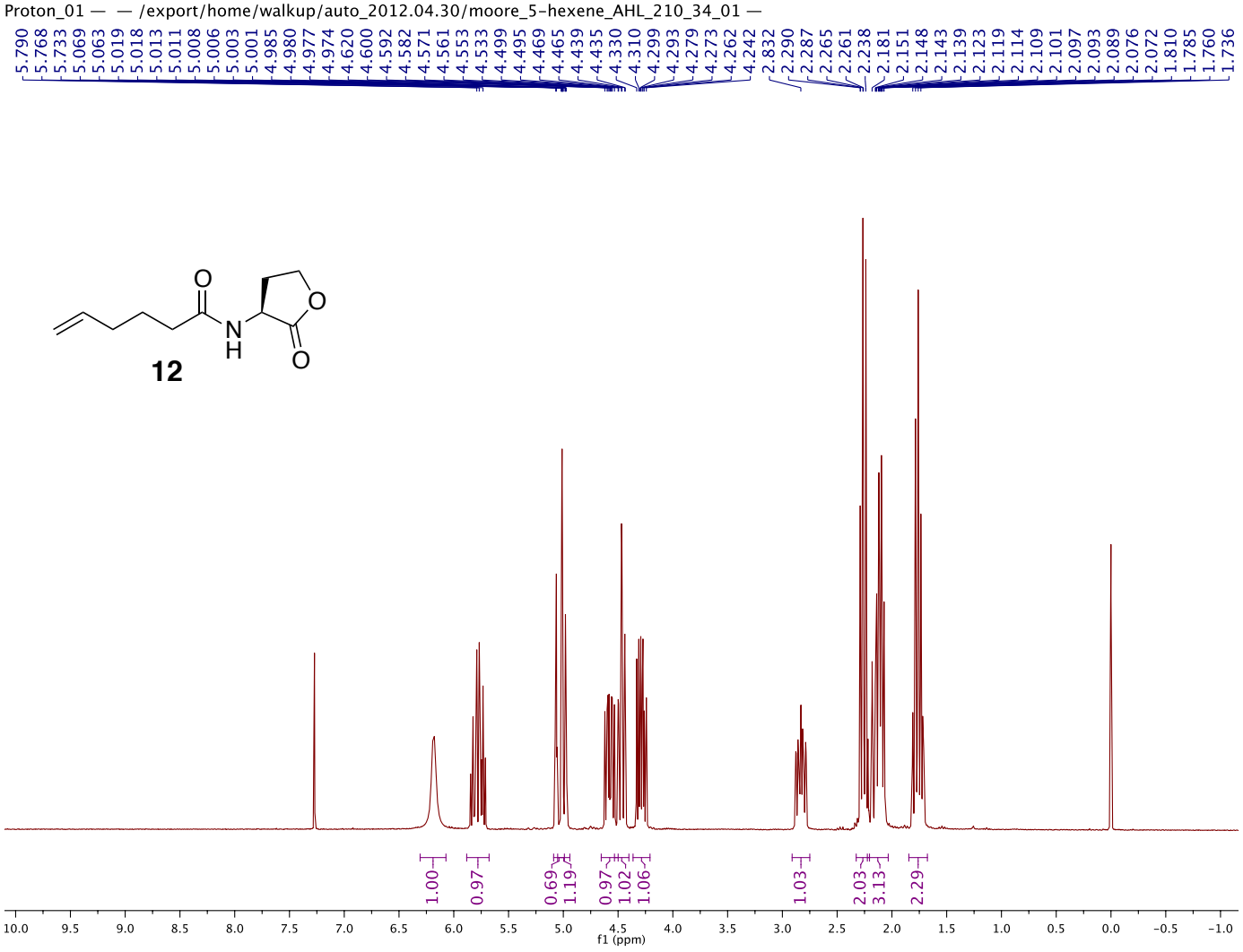
Proton_01 — — /export/home/walkup/auto_2012.04.30/moore_5-hexene_AHL_210_34_01 —
5.790 5.768 5.733 5.069 5.063 5.019 5.018 5.013 5.011 5.008 5.006 5.003 5.001 4.985 4.980 4.977 4.974 4.620 4.600 4.592 4.582 4.571 4.561 4.553 4.533 4.499 4.495 4.469 4.465 4.439 4.435 4.330 4.310 4.299 4.293 4.279 4.273 4.262 4.242 2.832 2.290 2.287 2.265 2.261 2.238 2.181 2.151 2.148 2.143 2.139 2.123 2.119 2.114 2.109 2.101 2.097 2.093 2.089 2.076 2.072 1.810 1.785 1.760 1.736
O
N
H
O
O
12
1.00 0.97 0.69 1.19 0.97 1.02 1.06 1.03 2.03 3.13 2.29
10.0 9.5 9.0 8.5 8.0 7.5 7.0 6.5 6.0 5.5 5.0 4.5 4.0 3.5 3.0 2.5 2.0 1.5 1.0 0.5 0.0 -0.5 -1.0
f1 (ppm)

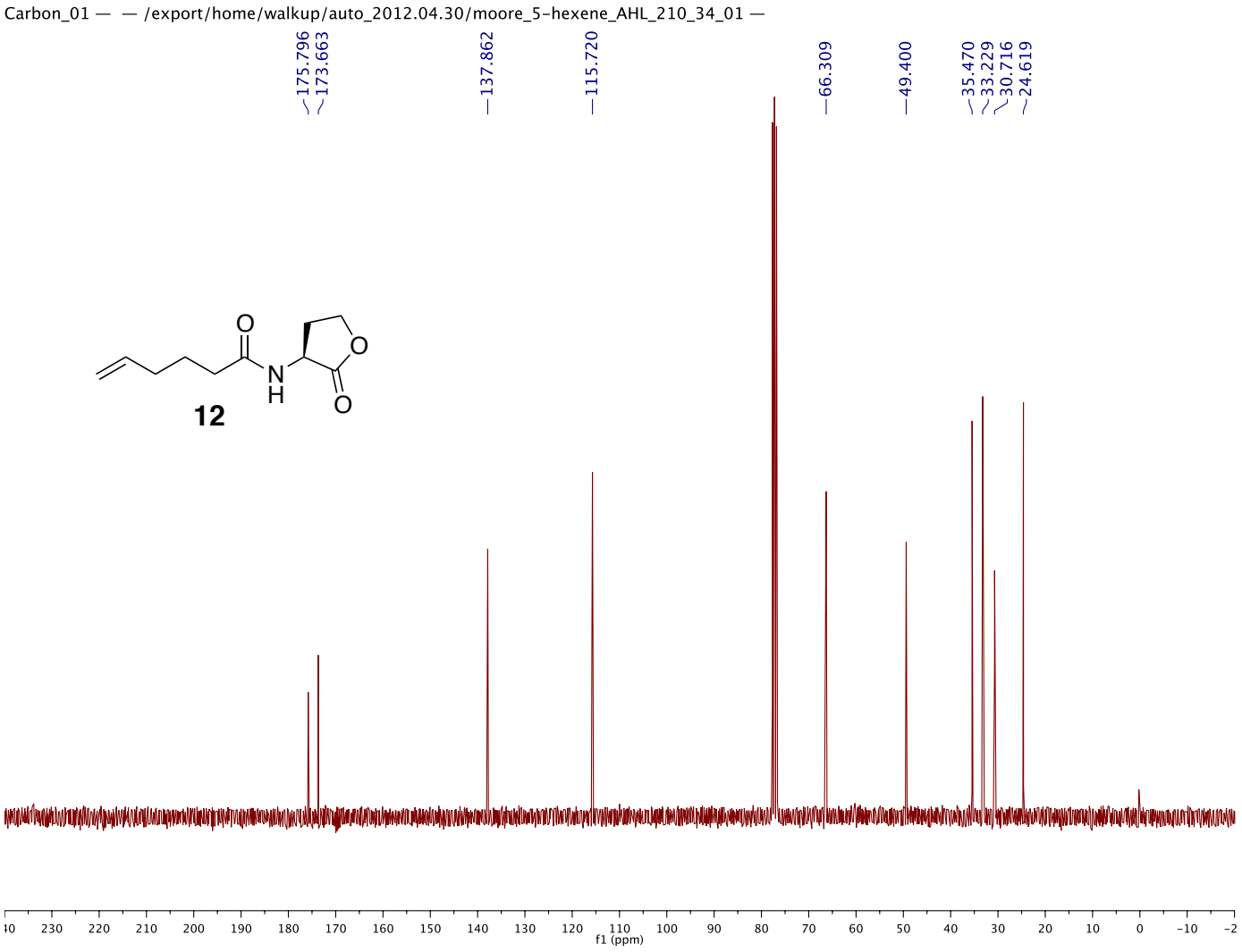
Carbon_01 — — /export/home/walkup/auto_2012.04.30/moore_5-hexene_AHL_210_34_01 —
175.796
173.663
137.862
115.720
66.309
49.400
35.470
33.229
30.716
24.619
O
N
H
O
O
12
f1 (ppm)

D1504101529_J4.10.fid — Group Blackwell — PROTON CDCl3 /home/dzzz/av400 blacku 23

6.164 6.150 5.710 5.693 5.676 5.671 5.659 5.655 5.568 5.564 5.560 5.546 5.542 5.526 5.522 4.573 4.558 4.552 4.544 4.537 4.529 4.522 4.508 4.495 4.493 4.473 4.470 4.450 4.447 4.317 4.302 4.294 4.289 4.279 4.274 4.265 4.251 3.016 3.012 3.009 2.999 2.994 2.991 2.870 2.867 2.863 2.860 2.853 2.849 2.845 2.839 2.836 2.831 2.828 2.817 2.814 2.165 2.143 2.135 2.113 1.746 1.742 1.730 1.726

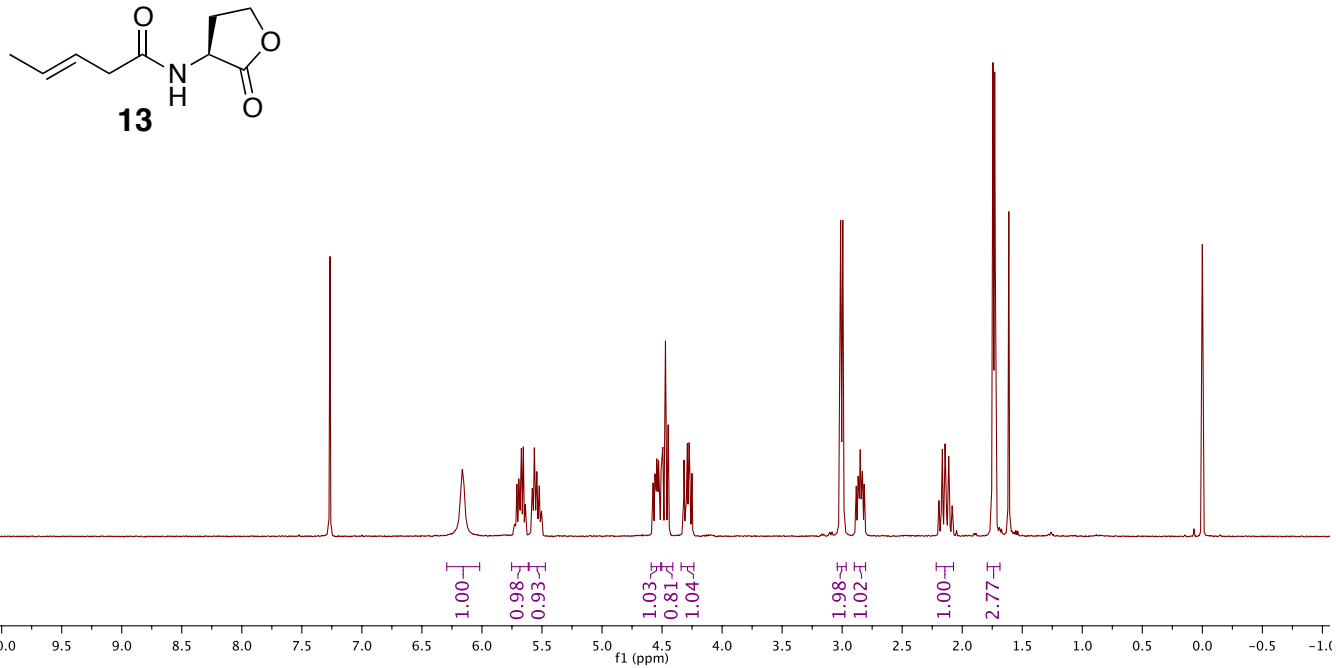

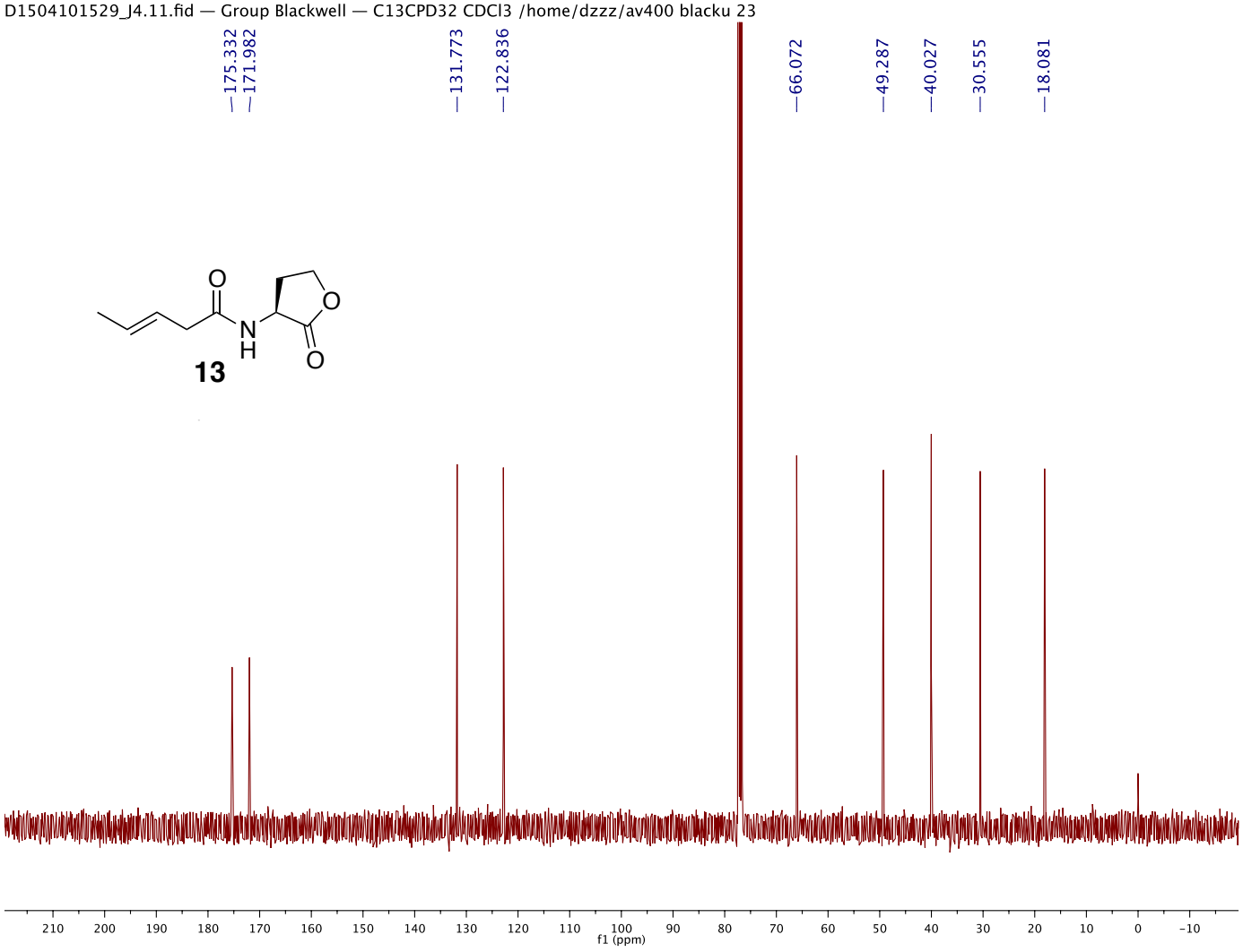
D1504101529_J4.11.fid — Group Blackwell — C13CPD32 CDCl3 /home/dzzz/av400 blacku 23
175.332
171.982
131.773
122.836
66.072
49.287
40.027
30.555
18.081
O
N
H
O
O
13
210 200 190 180 170 160 150 140 130 120 110 100 90 80 70 60 50 40 30 20 10 0 -10
f1 (ppm)

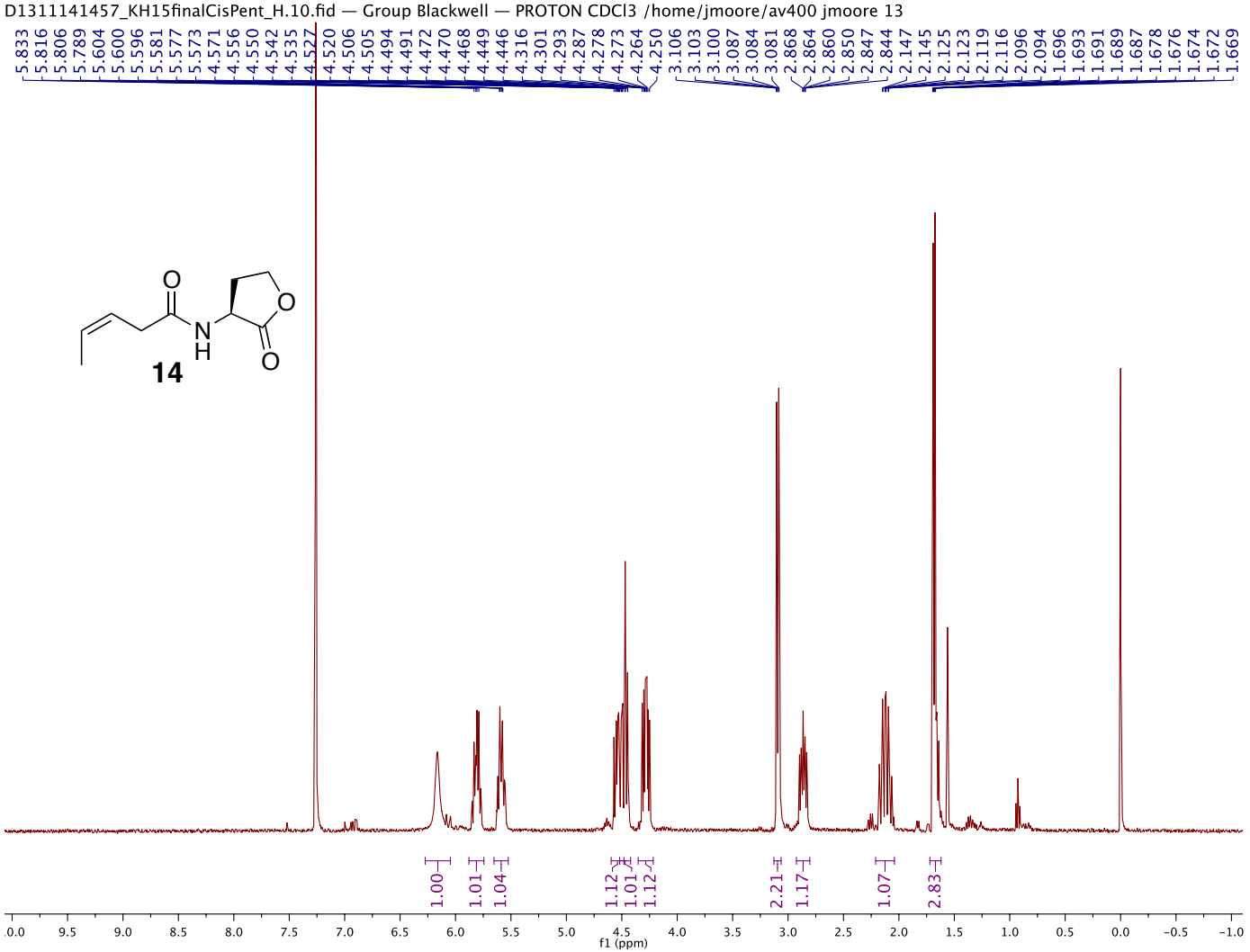
D1311141457_KH15finalCisPent_H.10.fid — Group Blackwell — PROTON CDCl3 /home/jmoore/av400 jmoore 13
5.833 5.816 5.806 5.789 5.604 5.600 5.596 5.581 5.577 5.573 5.571 4.556 4.550 4.542 4.535 4.527 4.520 4.506 4.505 4.494 4.491 4.472 4.470 4.468 4.449 4.446 4.316 4.301 4.293 4.287 4.278 4.273 4.264 4.250 3.106 3.103 3.100 3.087 3.084 3.081 2.868 2.864 2.860 2.850 2.847 2.844 2.147 2.145 2.125 2.123 2.119 2.116 2.096 2.094 1.696 1.693 1.691 1.689 1.687 1.678 1.676 1.674 1.672 1.669
O
N
H
O
O
14
1.00 1.01 1.04 1.12 1.01 1.12 2.21 1.17 1.07 2.83
f1 (ppm)

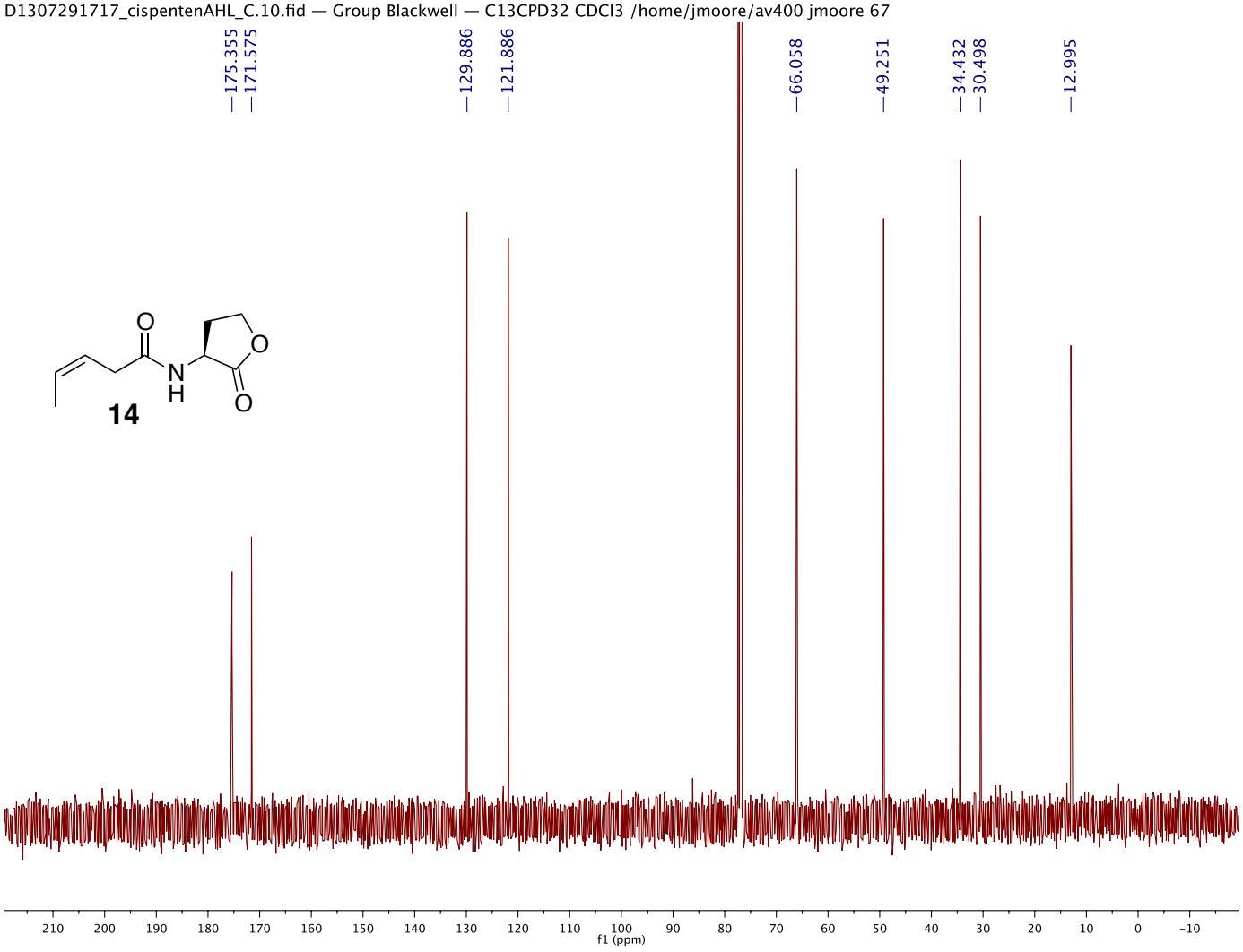
D1307291717_cispentenAHL_C.10.fid — Group Blackwell — C13CPD32 CDCl3 /home/jmoore/av400 jmoore 67
175.355
171.575
129.886
121.886
66.058
49.251
34.432
30.498
12.995
O
N
H
O
O
14
210 200 190 180 170 160 150 140 130 120 110 100 90 80 70 60 50 40 30 20 10 0 -10
f1 (ppm)

D1311081121_JM2013_H.10.fid — Group Blackwell — PROTON CDCl3 /home/jmoore/av400 jmoore 24

6.230 4.600 4.586 4.579 4.571 4.565 4.557 4.550 4.536 4.506 4.503 4.483 4.480 4.460 4.457 4.329 4.314 4.306 4.301 4.291 4.286 4.277 4.263 2.901 2.898 2.894 2.891 2.885 2.881 2.877 2.870 2.867 2.863 2.860 2.848 2.572 2.566 2.562 2.557 2.554 2.551 2.546 2.543 2.540 2.536 2.516 2.511 2.503 2.497 2.494 2.489 2.480 2.467 2.183 2.180 2.161 2.158 2.154 2.152 2.132 2.129 2.035 2.028 2.023

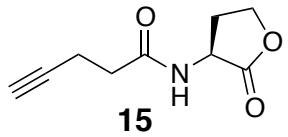

15

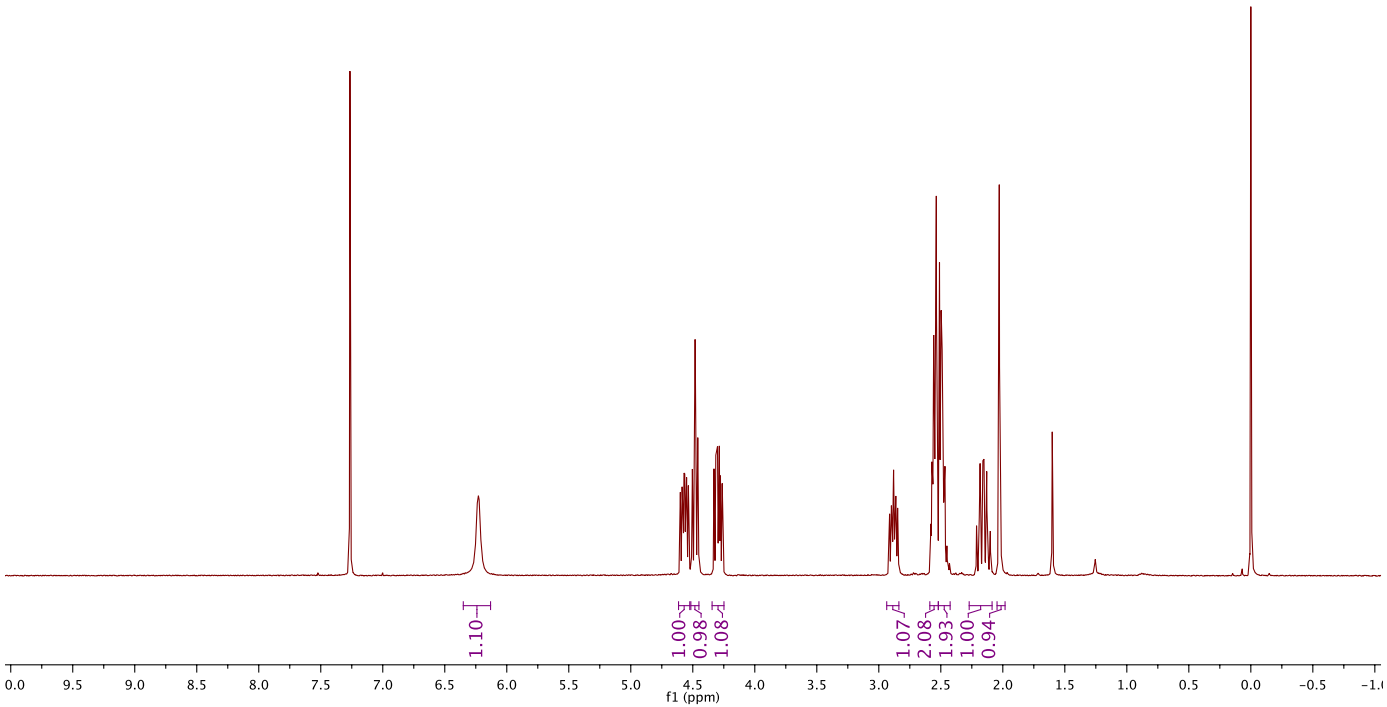

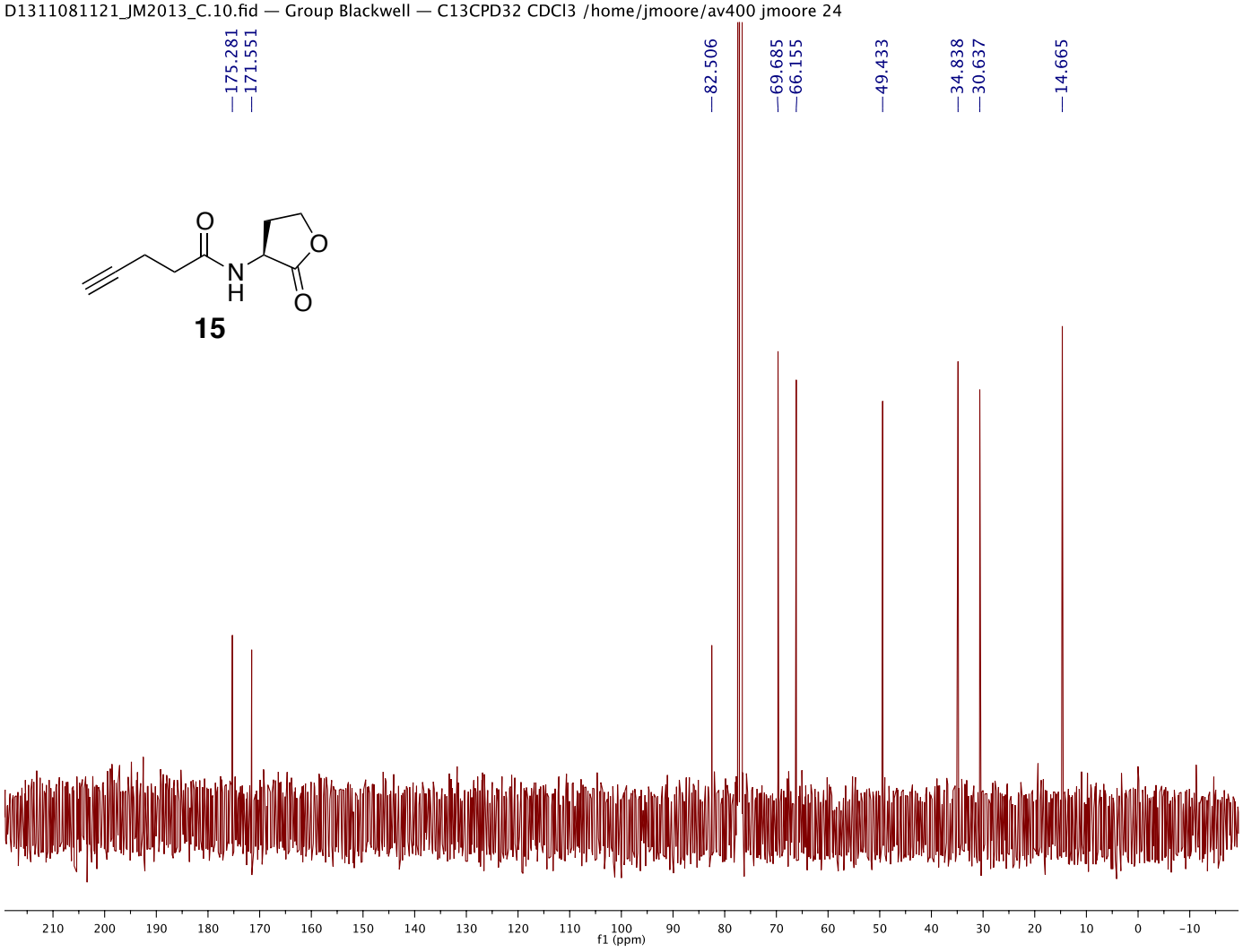
D1311081121_JM2013_C.10.fid — Group Blackwell — C13CPD32 CDCl3 /home/jmoore/av400 jmoore 24
175.281
171.551
82.506
69.685
66.155
49.433
34.838
30.637
14.665
O
N
H
O
O
15
210 200 190 180 170 160 150 140 130 120 110 100 90 80 70 60 50 40 30 20 10 0 -10
f1 (ppm)

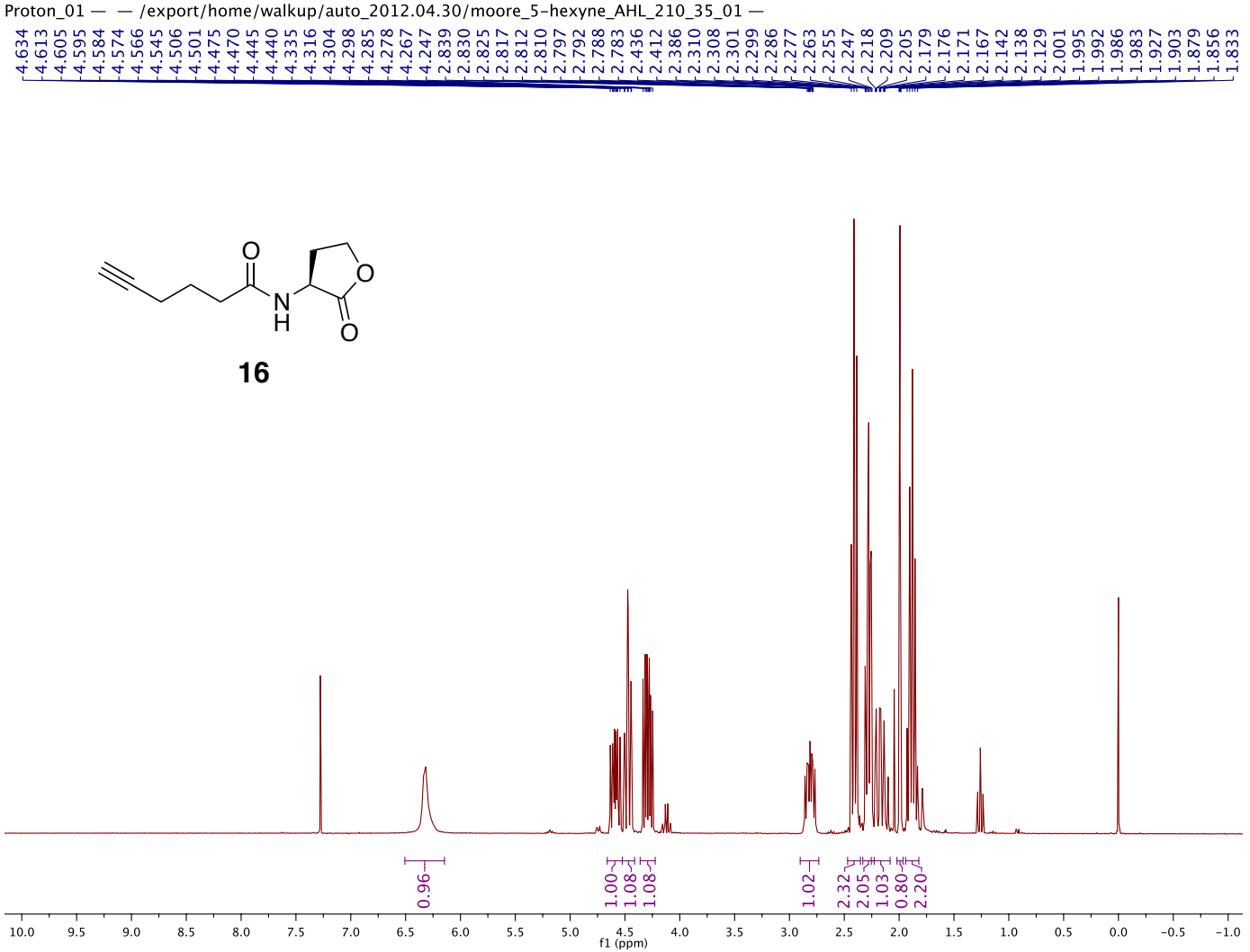
Proton_01 — — /export/home/walkup/auto_2012.04.30/moore_5-hexyne_AHL_210_35_01 —
4.634 4.613 4.605 4.595 4.584 4.574 4.566 4.545 4.506 4.501 4.475 4.470 4.445 4.440 4.335 4.316 4.304 4.298 4.285 4.278 4.267 4.247 2.839 2.830 2.825 2.817 2.812 2.810 2.797 2.792 2.788 2.783 2.436 2.412 2.386 2.310 2.308 2.301 2.299 2.286 2.277 2.263 2.255 2.247 2.218 2.209 2.205 2.179 2.176 2.171 2.167 2.142 2.138 2.129 2.001 1.995 1.992 1.986 1.983 1.927 1.903 1.879 1.856 1.833
O
O
N
H
O
16
0.96
1.00
1.08
1.08
1.02
2.32
2.05
1.03
0.80
2.20
10.0 9.5 9.0 8.5 8.0 7.5 7.0 6.5 6.0 5.5 5.0 4.5 4.0 3.5 3.0 2.5 2.0 1.5 1.0 0.5 0.0 -0.5 -1.0
f1 (ppm)

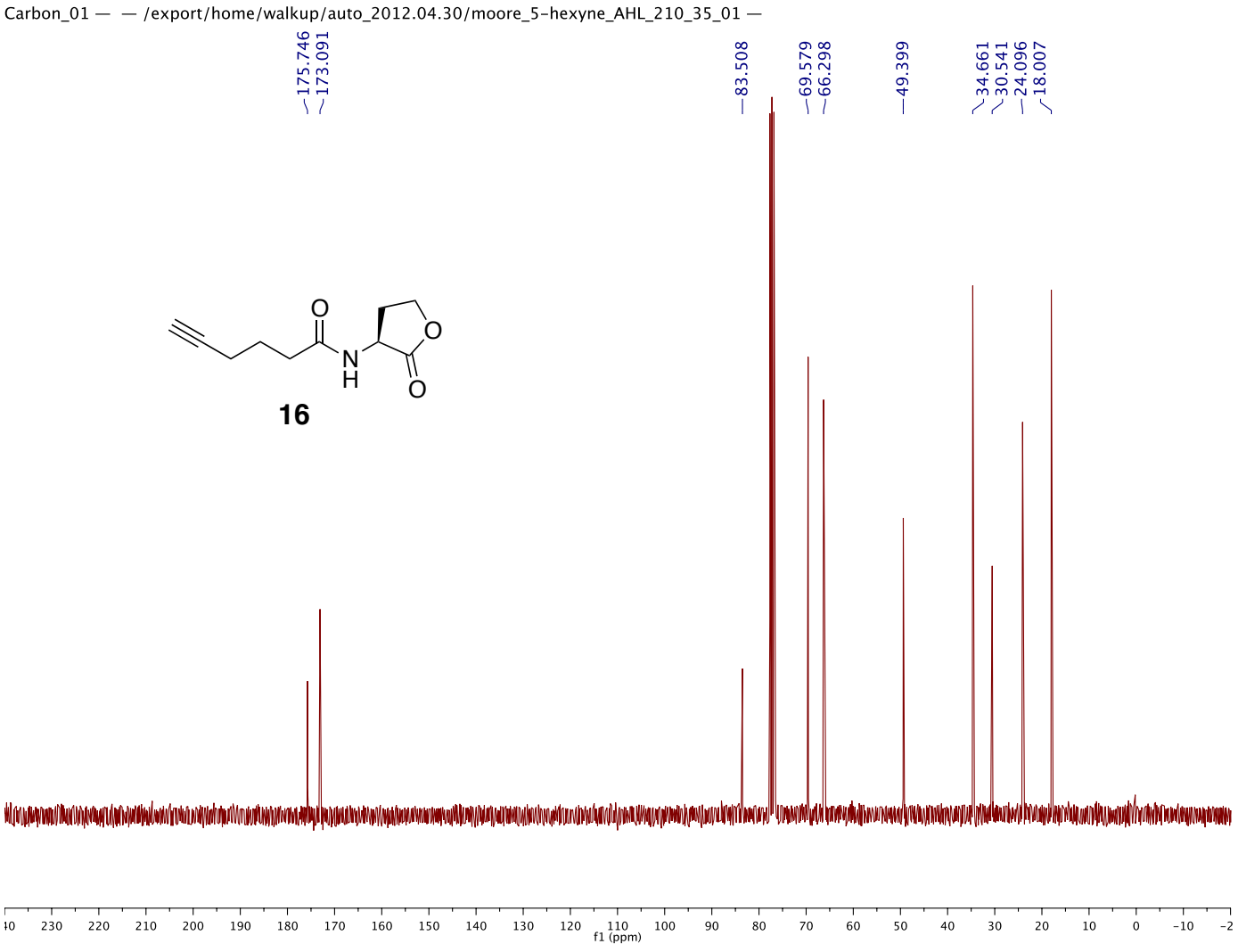
Carbon_01 — — /export/home/walkup/auto_2012.04.30/moore_5-hexyne_AHL_210_35_01 —
175.746
173.091
83.508
69.579
66.298
49.399
34.661
30.541
24.096
18.007
O
N
H
O
O
16
f1 (ppm)

D1504101529_J24.10.fid — Group Blackwell — PROTON CDCl3 /home/dzzz/av400 blacku 24

4.585 4.570 4.564 4.556 4.549 4.541 4.535 4.520 4.497 4.494 4.474 4.471 4.452 4.448 4.325 4.310 4.302 4.297 4.287 4.282 4.273 4.259 3.095 3.093 3.074 3.071 3.053 3.050 2.862 2.858 2.845 2.841 2.336 2.318 2.314 2.310 2.306 2.296 2.288 2.283 2.266 2.206 2.198 2.195 2.190 2.186 2.177 2.168 2.164 2.158 2.155 2.136 2.133 2.129 2.127 2.107 2.105 2.020 1.999 1.993 1.971 1.949 1.899 1.896

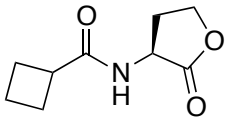

17

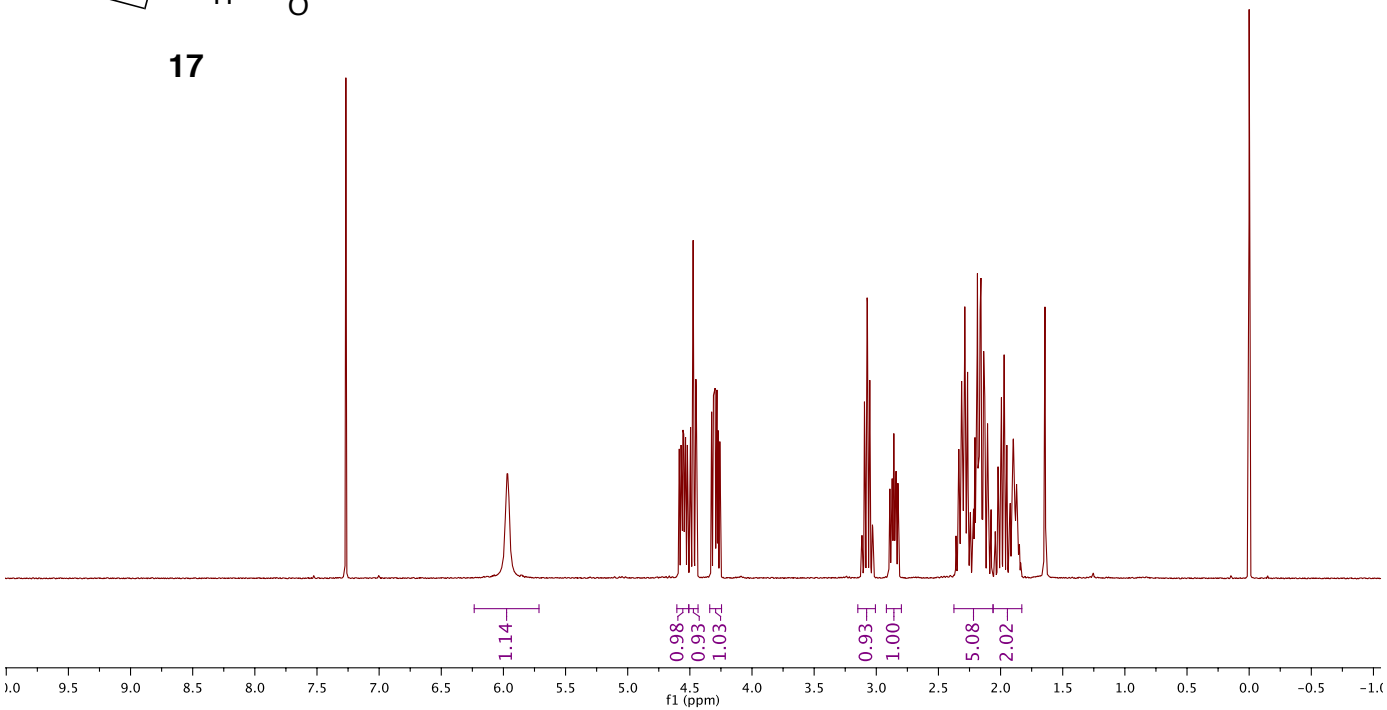

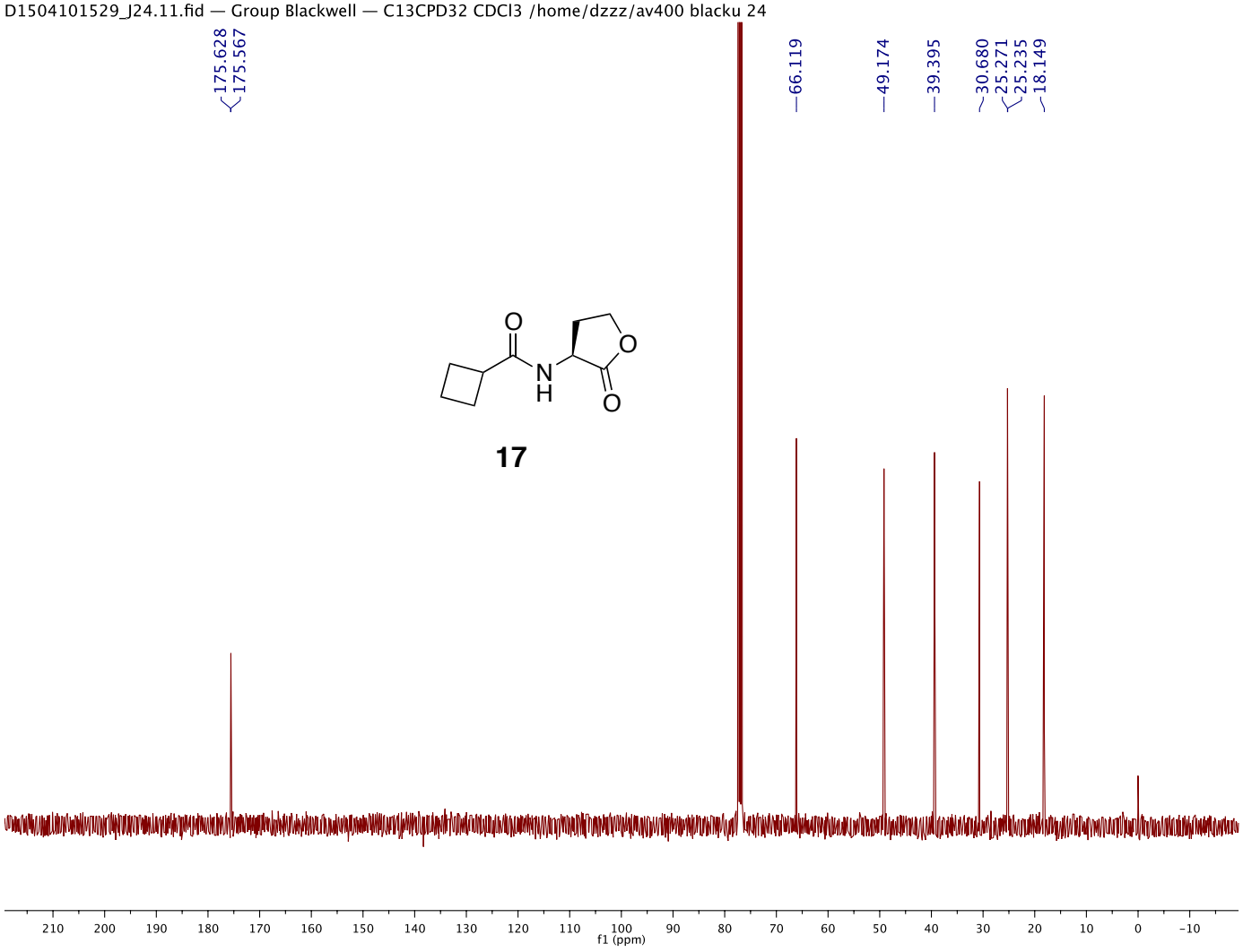
D1504101529_J24.11.fid — Group Blackwell — C13CPD32 CDCl3 /home/dzzz/av400 blacku 24
175.628
175.567
66.119
49.174
39.395
30.680
25.271
25.235
18.149
O
N
H
O
O
17
210
200
190
180
170
160
150
140
130
120
110
100
90
80
70
60
50
40
30
20
10
0
-10
f1 (ppm)

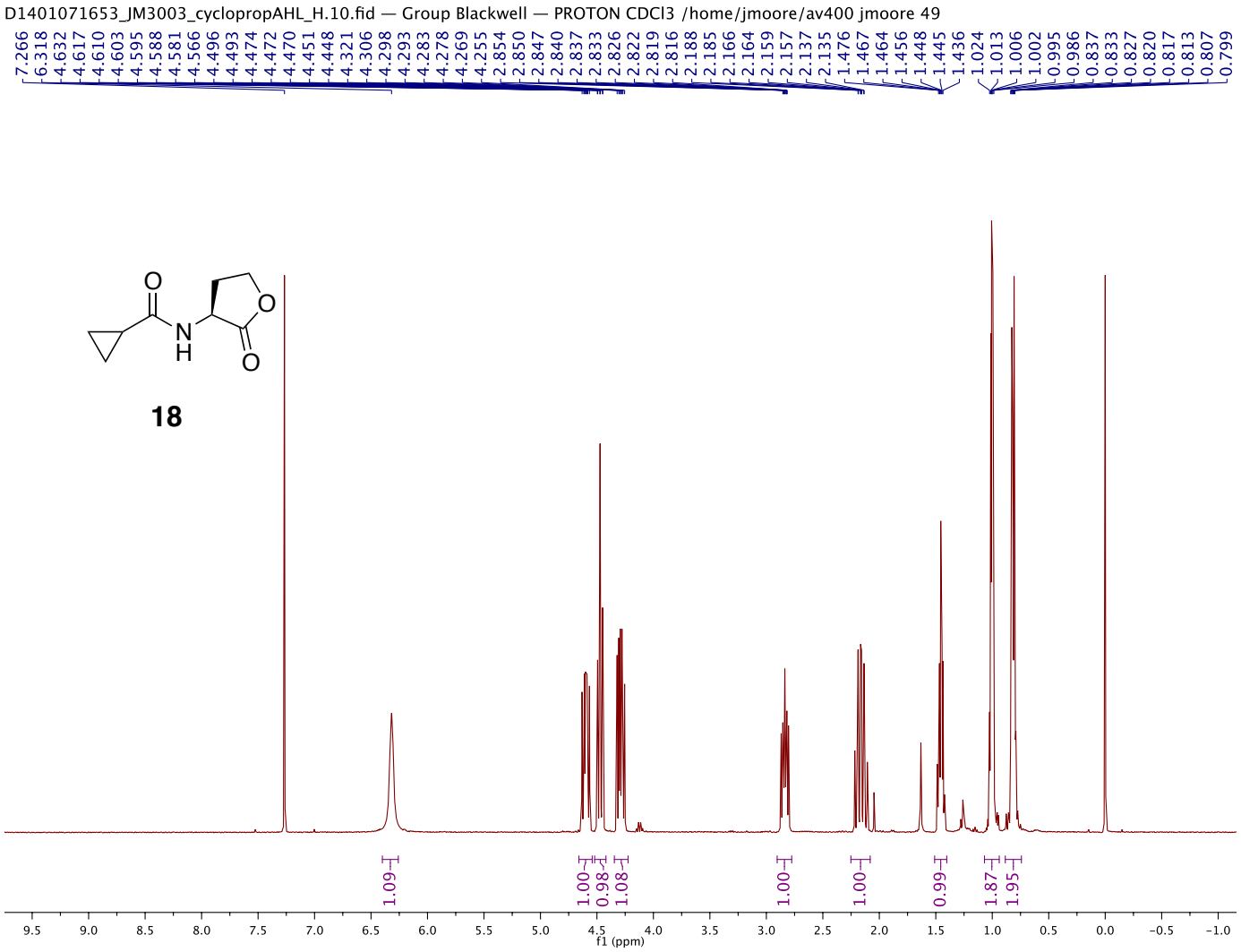
D1401071653_JM3003_cyclopropAHL_H.10.fid — Group Blackwell — PROTON CDCl3 /home/jmoore/av400 jmoore 49
7.266
6.318
4.632
4.617
4.610
4.603
4.595
4.588
4.581
4.566
4.496
4.493
4.474
4.472
4.470
4.451
4.448
4.321
4.306
4.298
4.293
4.283
4.278
4.269
4.255
2.854
2.850
2.847
2.840
2.837
2.833
2.826
2.822
2.819
2.816
2.188
2.185
2.166
2.164
2.159
2.157
2.137
2.135
1.476
1.467
1.464
1.456
1.448
1.445
1.436
1.024
1.013
1.006
1.002
0.995
0.986
0.837
0.833
0.827
0.820
0.817
0.813
0.807
0.799
O
N
H
O
O
18
1.09
1.00
0.98
1.08
1.00
1.00
0.99
1.87
1.95
9.5
9.0
8.5
8.0
7.5
7.0
6.5
6.0
5.5
5.0
4.5
4.0
3.5
3.0
2.5
2.0
1.5
1.0
0.5
0.0
-0.5
-1.0
f1 (ppm)

D1401071653_JM3003_cyclopropAHL_C.10.fid — Group Blackwell — C13CPD32 CDCl3 /home/jmoore/av400 jmoore 49

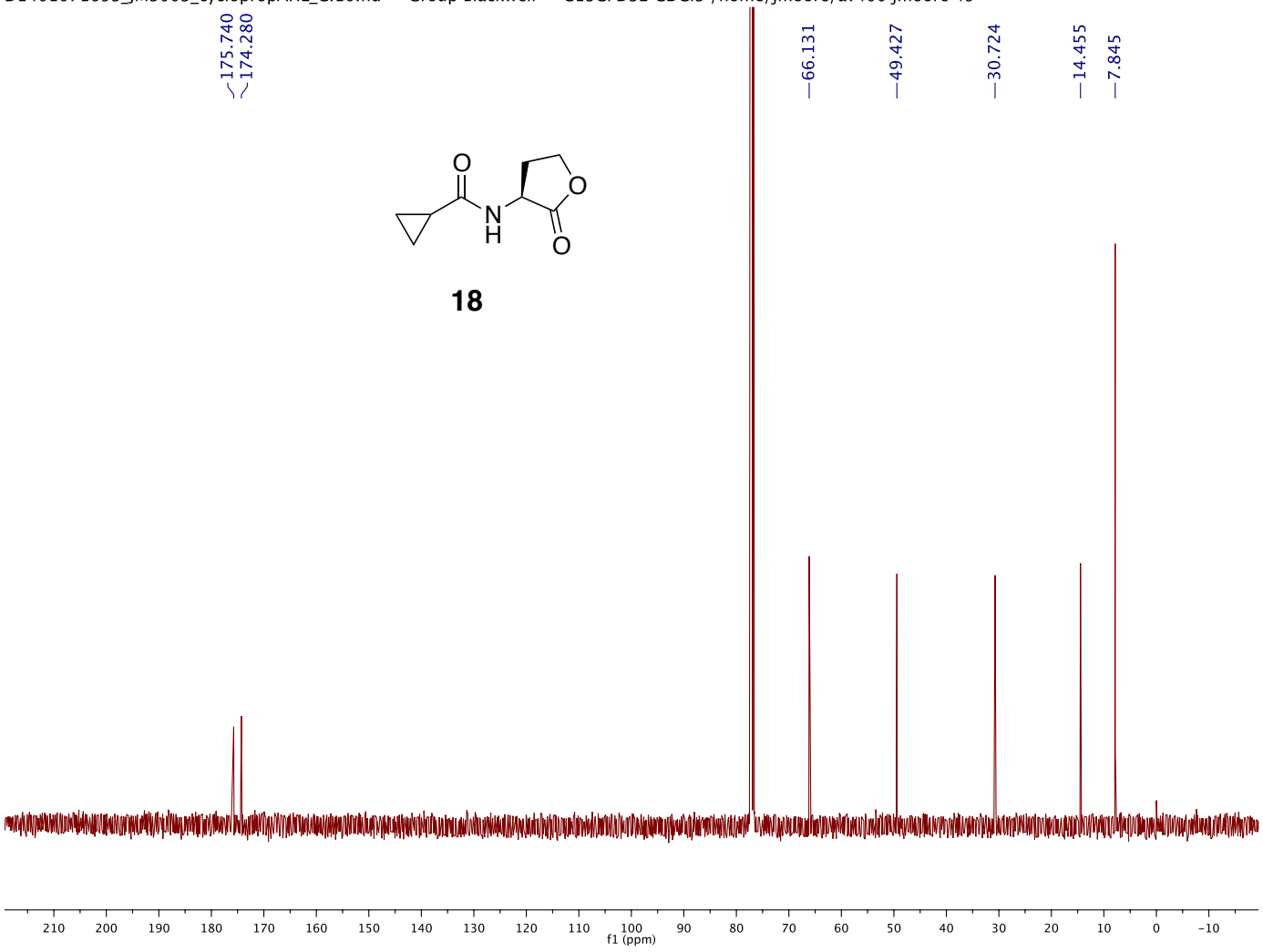

18

D1504151357_KH55_F13-14_H.10.fid — Group Blackwell — PROTON CDCl3 /home/jmoore/av400 jmoore 59

6.525 6.510 4.612 4.597 4.591 4.583 4.576 4.568 4.562 4.547 4.488 4.485 4.466 4.463 4.443 4.440 4.316 4.301 4.293 4.288 4.278 4.273 4.264 4.250 2.856 2.852 2.843 2.839 2.834 2.828 2.825 2.821 2.818 2.217 2.210 2.199 2.191 2.184 2.181 2.162 2.159 2.156 2.153 2.134 2.131 1.006 0.987 0.974 0.967 0.638 0.630 0.627 0.619 0.615 0.610 0.606 0.599 0.228 0.221 0.217 0.211 0.205 0.200 0.193

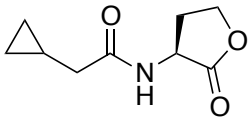

19

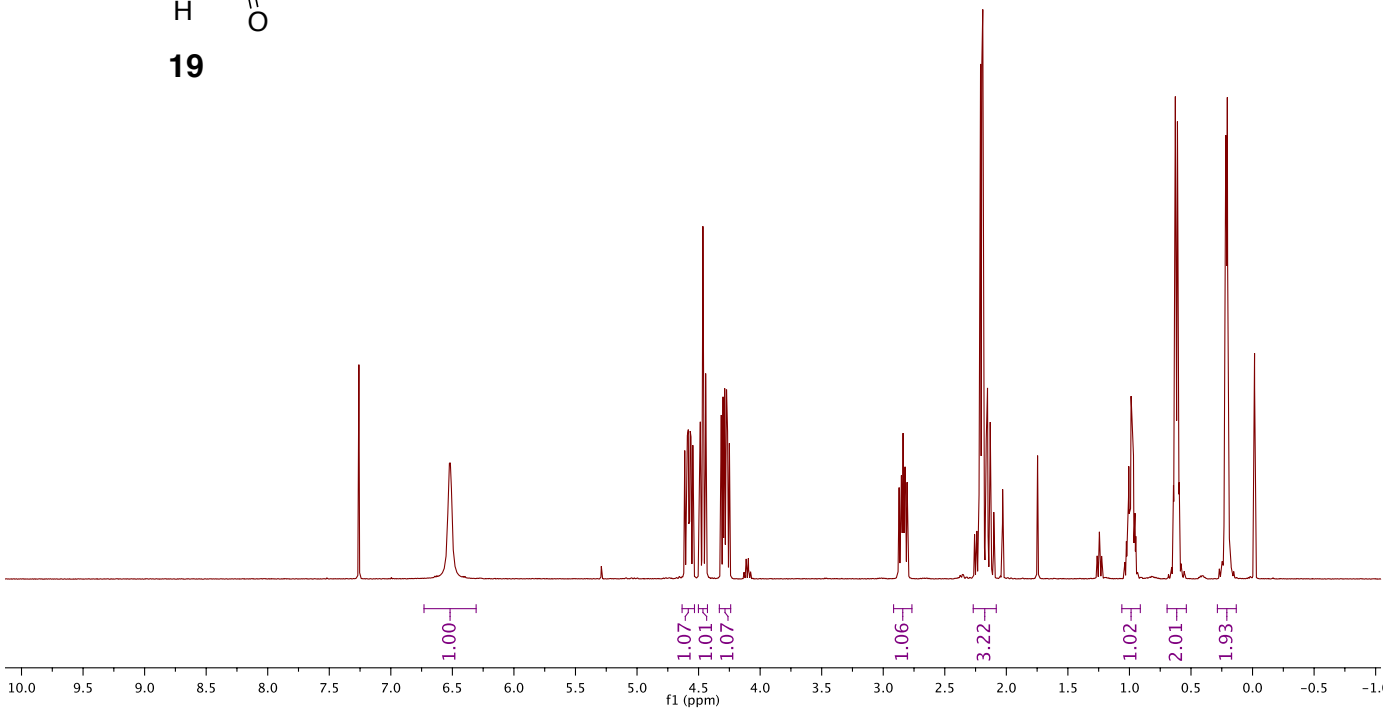

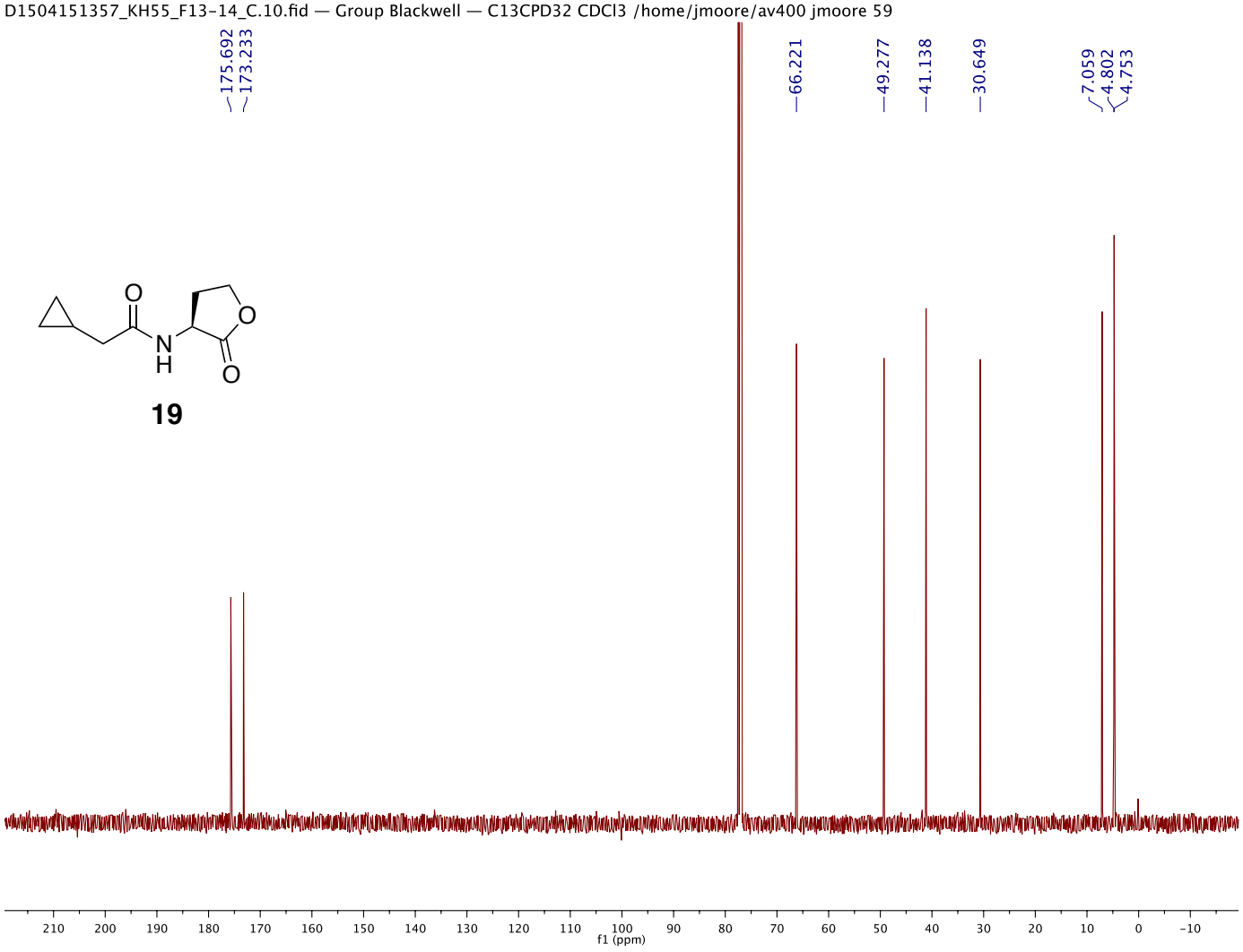
D1504151357_KH55_F13-14_C.10.fid — Group Blackwell — C13CPD32 CDCl3 /home/jmoore/av400 jmoore 59
175.692
173.233
66.221
49.277
41.138
30.649
7.059
4.802
4.753
O
N
H
O
O
19
210 200 190 180 170 160 150 140 130 120 110 100 90 80 70 60 50 40 30 20 10 0 -10
f1 (ppm)

D1407101148_SPS28_1-Me-cylcoprop-AHL_H.10.fid — Group Blackwell — PROTON CDCl3 /home/jmoore/av400 jmoore 41

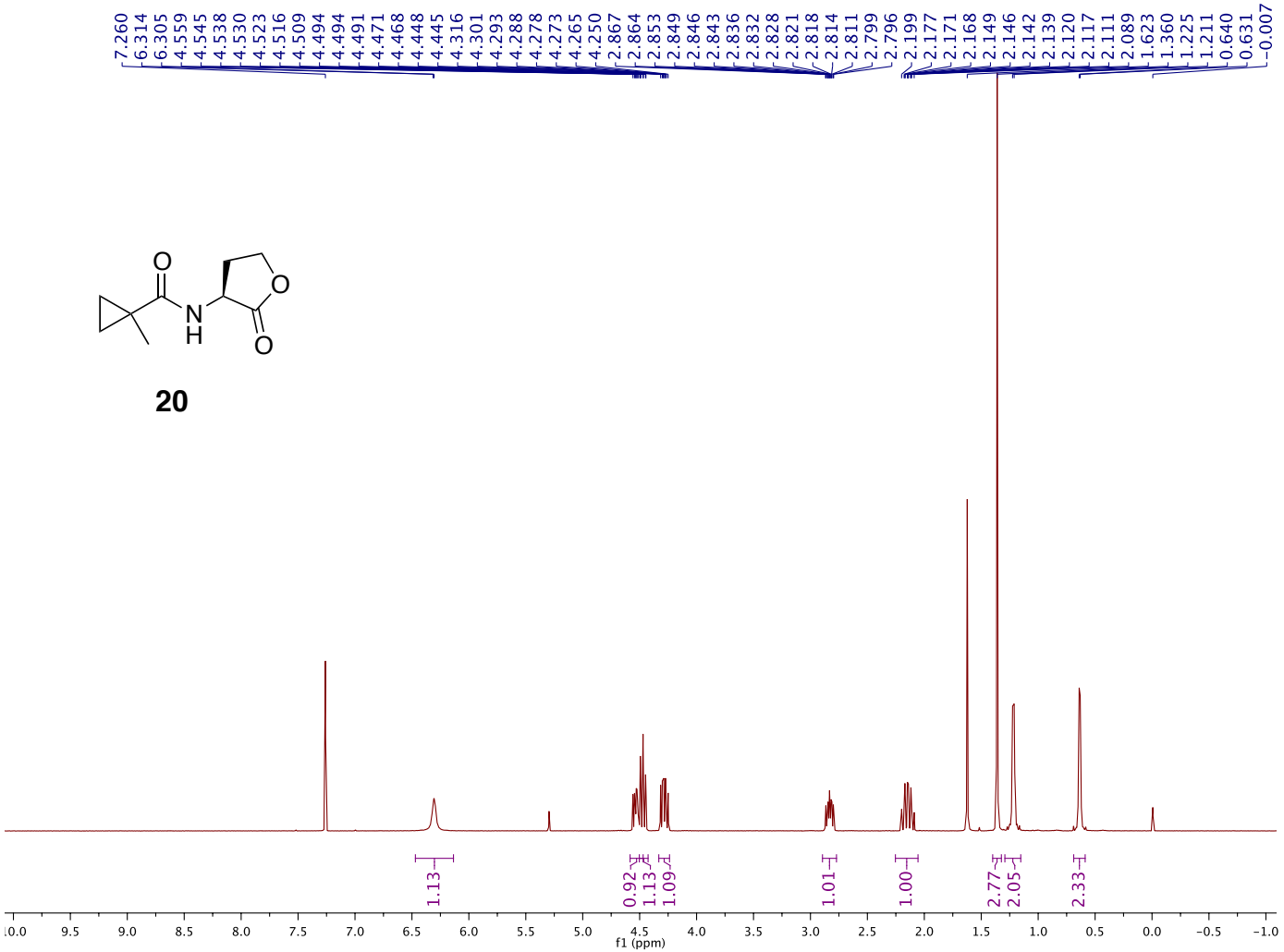

20

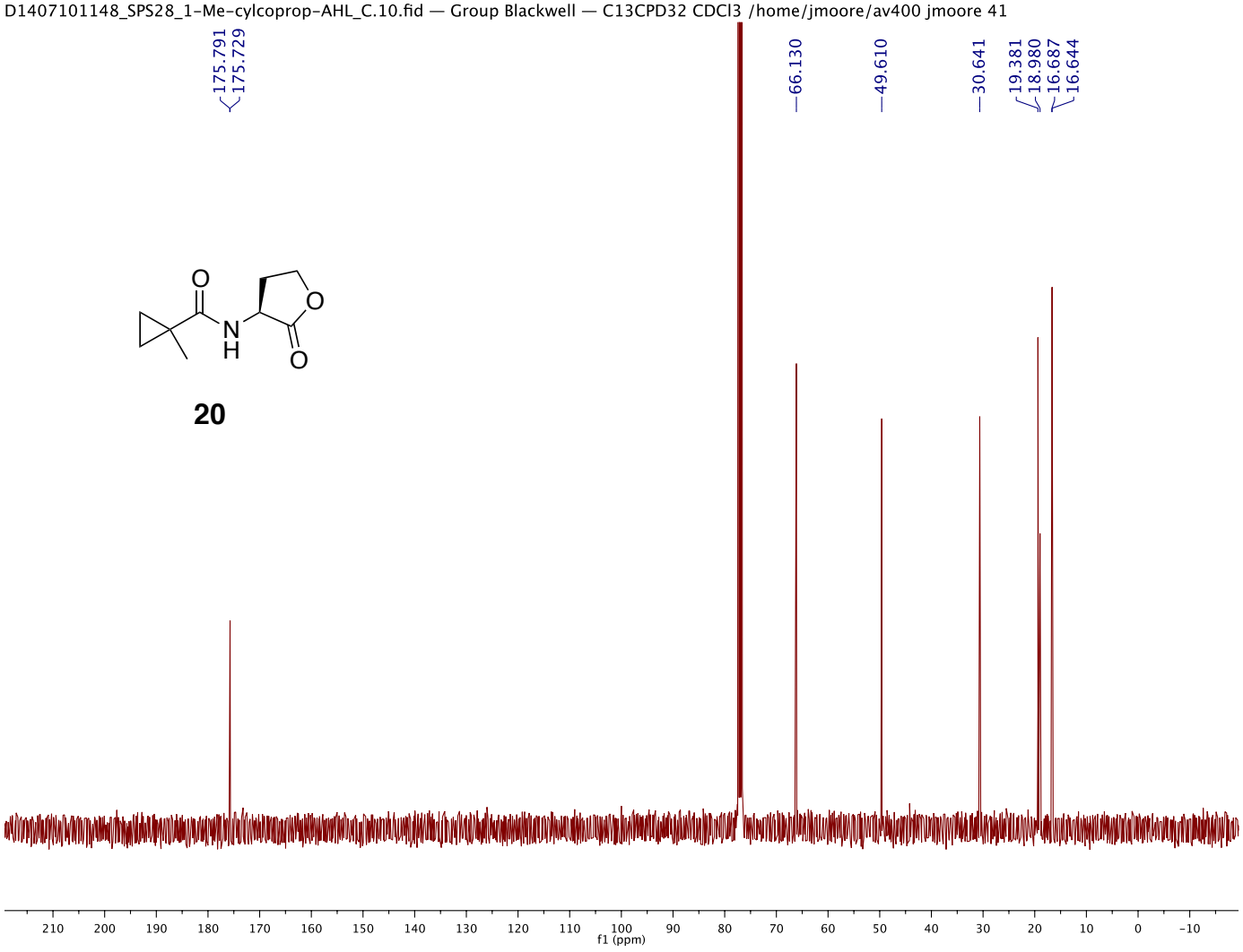
D1407101148_SPS28_1-Me-cylcoprop-AHL_C.10.fid — Group Blackwell — C13CPD32 CDCl3 /home/jmoore/av400 jmoore 41
175.791
175.729
66.130
49.610
30.641
19.381
18.980
16.687
16.644
O
N
H
O
O
20
210
200
190
180
170
160
150
140
130
120
110
100
90
80
70
60
50
40
30
20
10
0
-10
f1 (ppm)

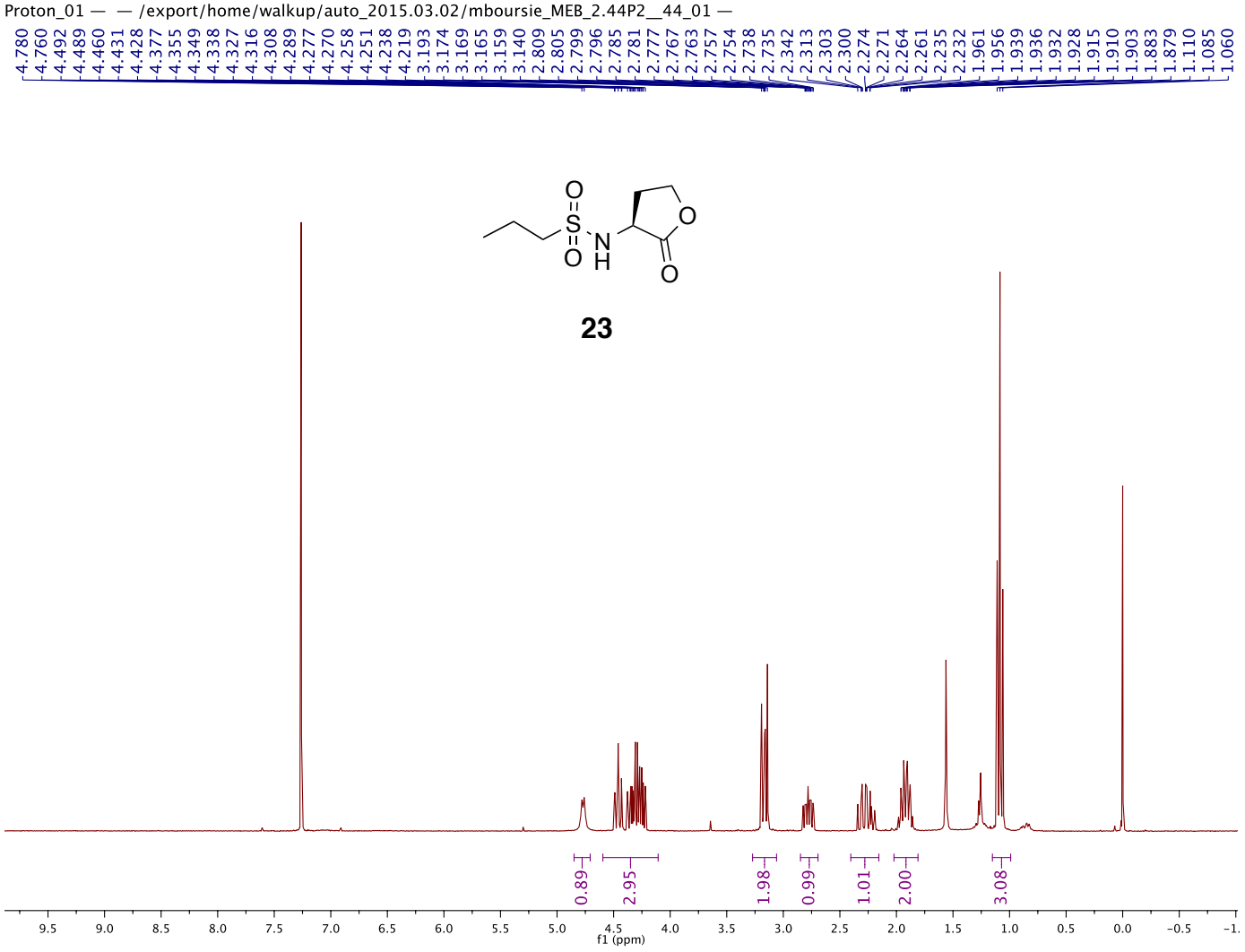
Proton_01 — — /export/home/walkup/auto_2015.03.02/mboursie_MEB_2.44P2__44_01 —
4.780 4.760 4.492 4.489 4.460 4.431 4.428 4.377 4.355 4.349 4.338 4.327 4.316 4.308 4.289 4.277 4.270 4.258 4.251 4.238 4.219 3.193 3.174 3.169 3.165 3.159 3.140 2.809 2.805 2.799 2.796 2.785 2.781 2.777 2.767 2.763 2.757 2.754 2.738 2.735 2.342 2.313 2.303 2.300 2.274 2.271 2.264 2.261 2.235 2.232 1.961 1.956 1.939 1.936 1.932 1.928 1.915 1.910 1.903 1.883 1.879 1.110 1.085 1.060
O
S
O
N
H
O
O
23
0.89
2.95
1.98
0.99
1.01
2.00
3.08
9.5 9.0 8.5 8.0 7.5 7.0 6.5 6.0 5.5 5.0 4.5 4.0 3.5 3.0 2.5 2.0 1.5 1.0 0.5 0.0 -0.5
f1 (ppm)

C1508101720_MEB_RN6.11.fid — Group Blackwell — C13CPD32 CDCl3 /home/mboursier/callisto mboursier 49

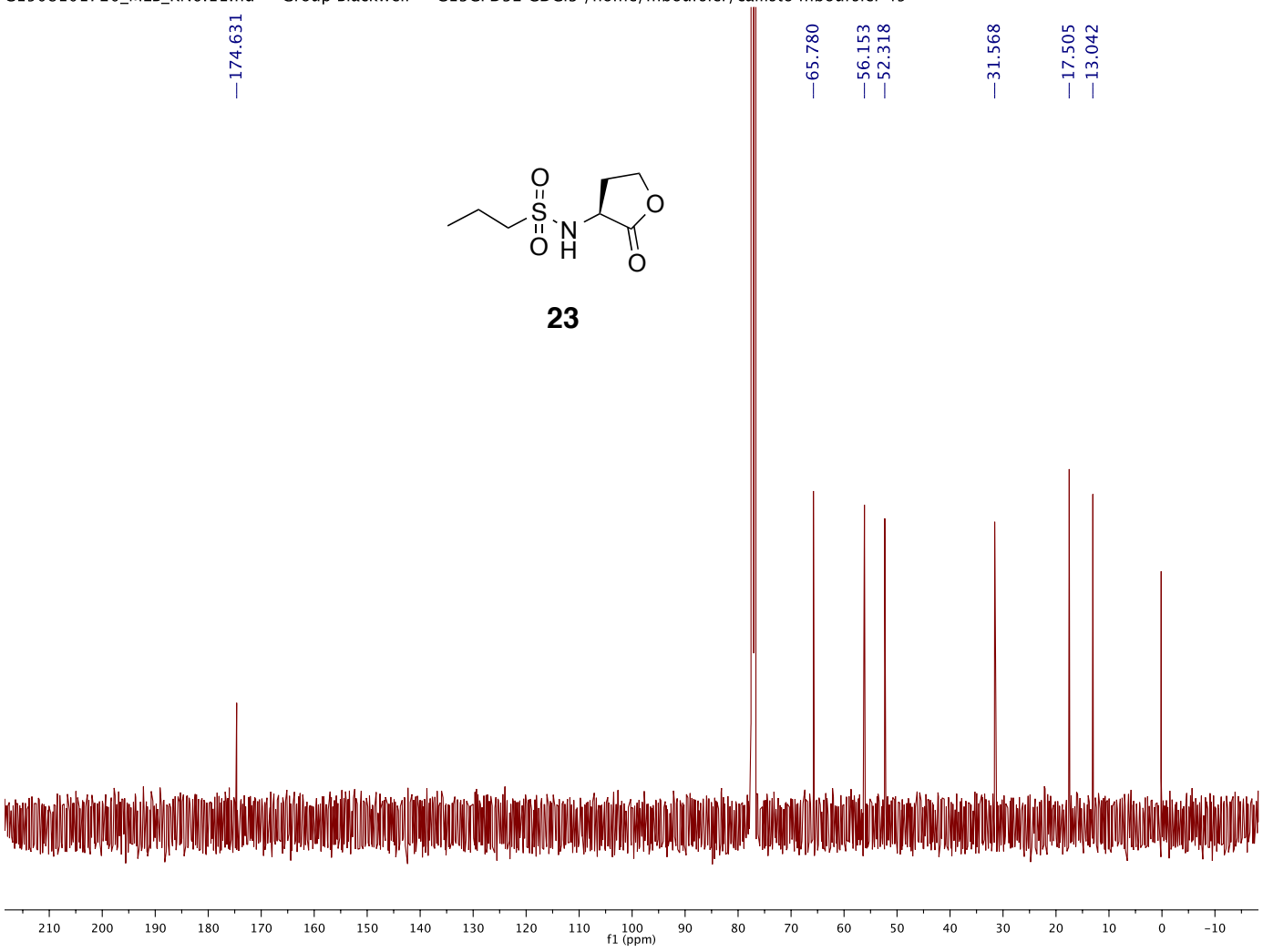

23

D1502161001_MEB_2.39P.10.fid — Group Blackwell — PROTON CDCl3 /home/mboursier/av400 mboursier 10

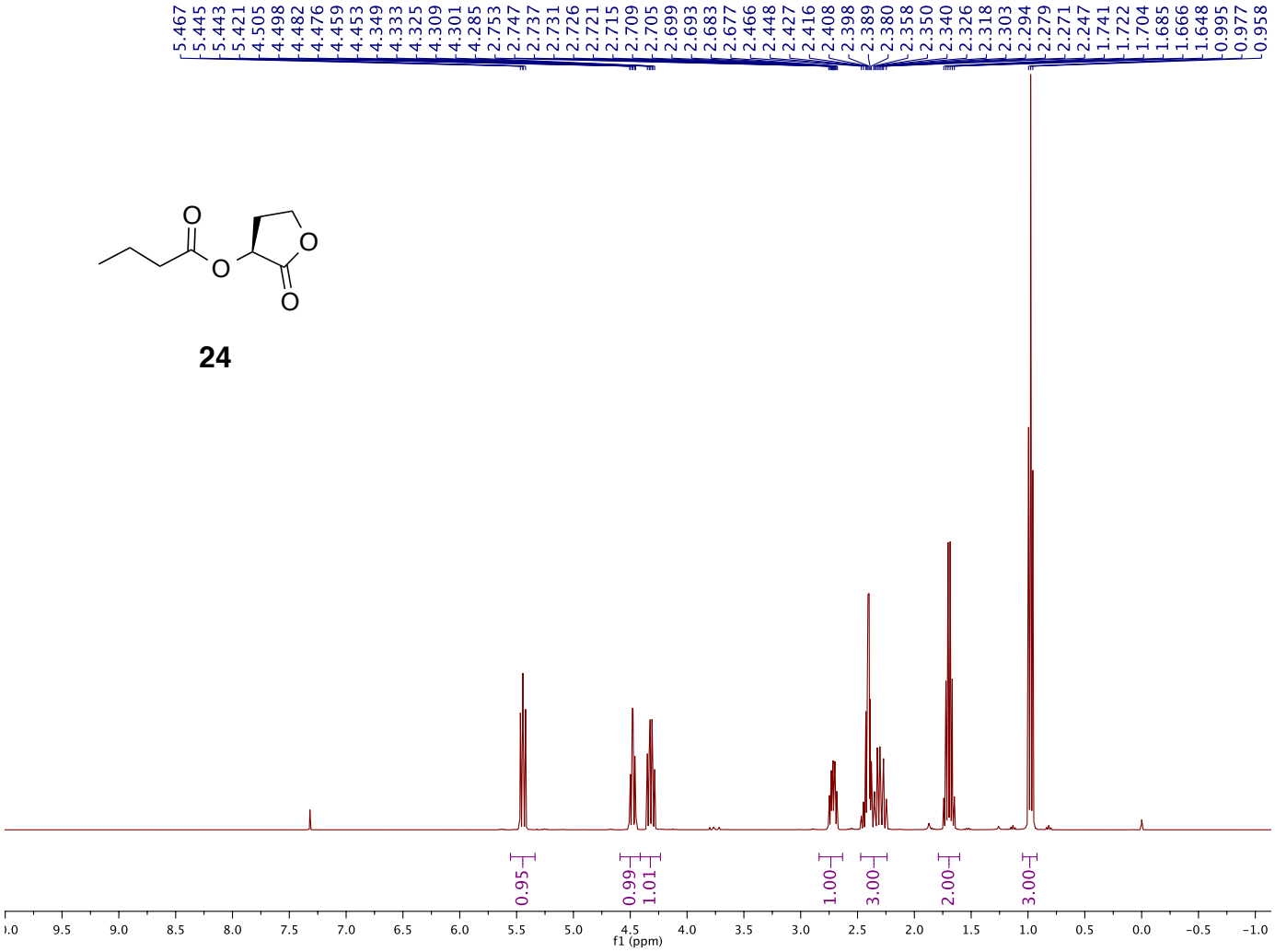

24

C1508041419_MEB_RN7_2.39.10.fid — Group Blackwell — C13CPD32 CDCl3 /home/mboursier/callisto mboursier 27

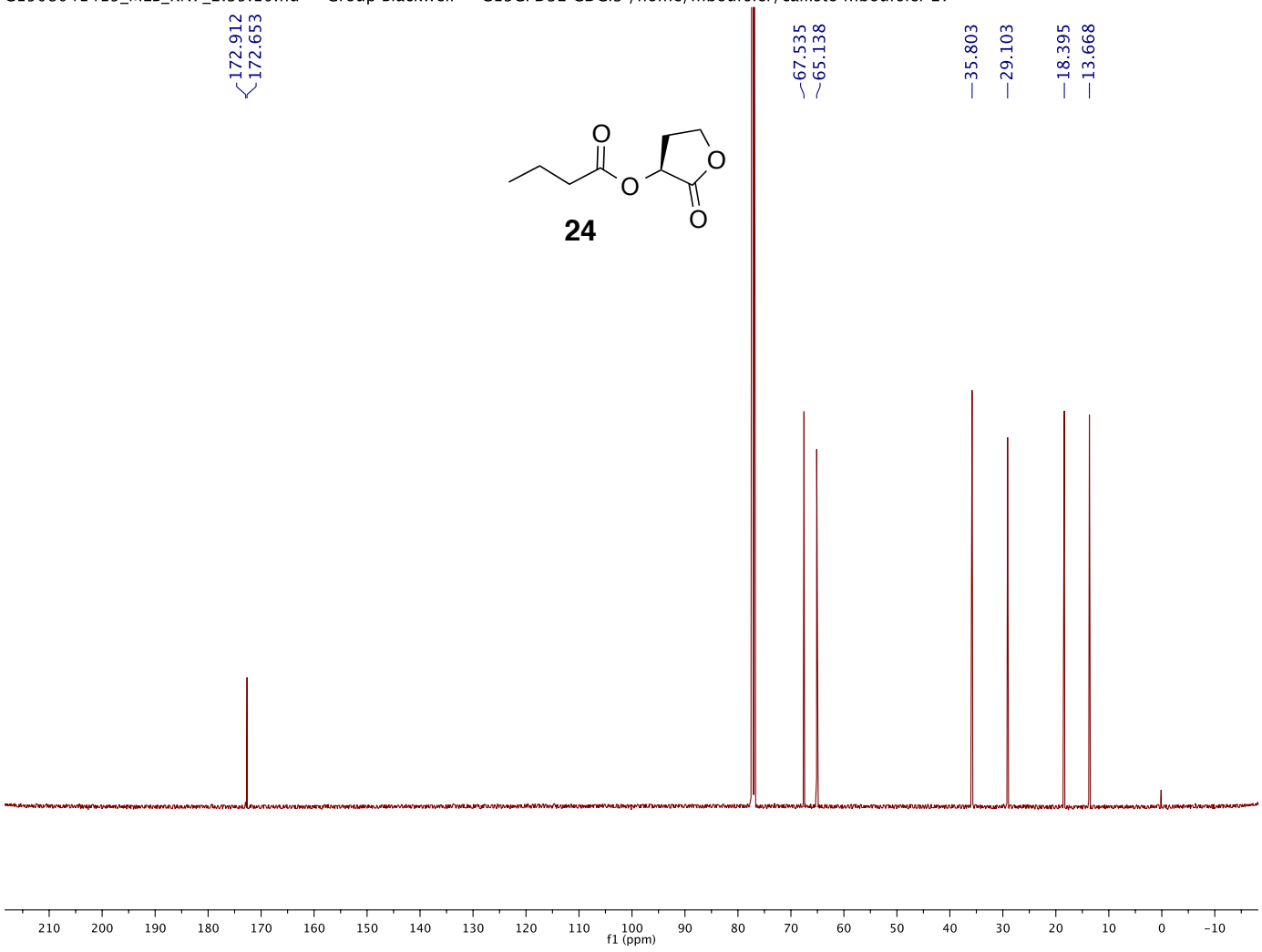

D1501191059_MEB_2.29-3.10.fid — Group Blackwell — PROTON CDCl3 /home/mboursier/av400 mboursier 39

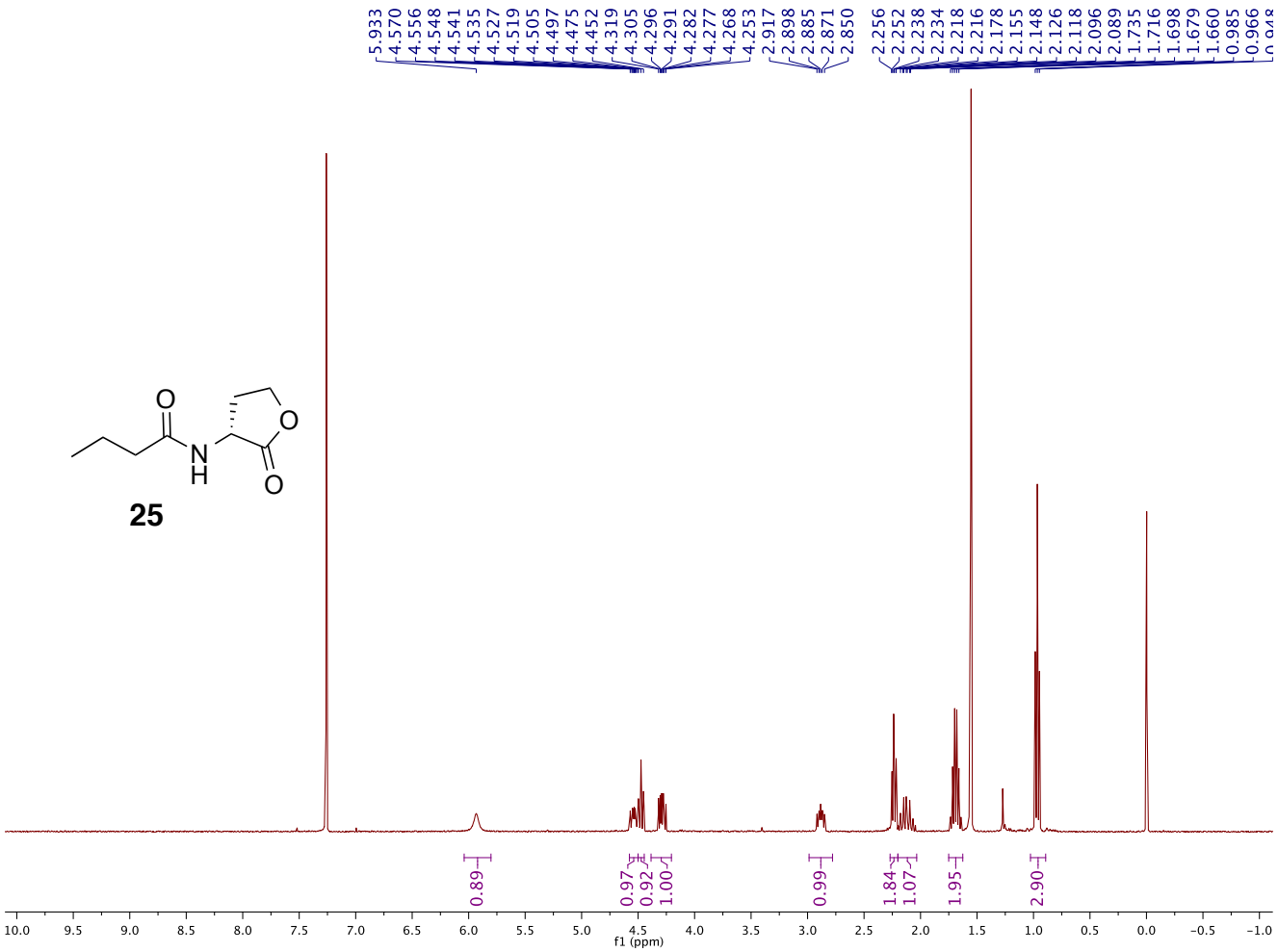

C1508101719_MEB_RN5.11.fid — Group Blackwell — C13CPD32 CDCl3 /home/mboursier/callisto mboursier 45

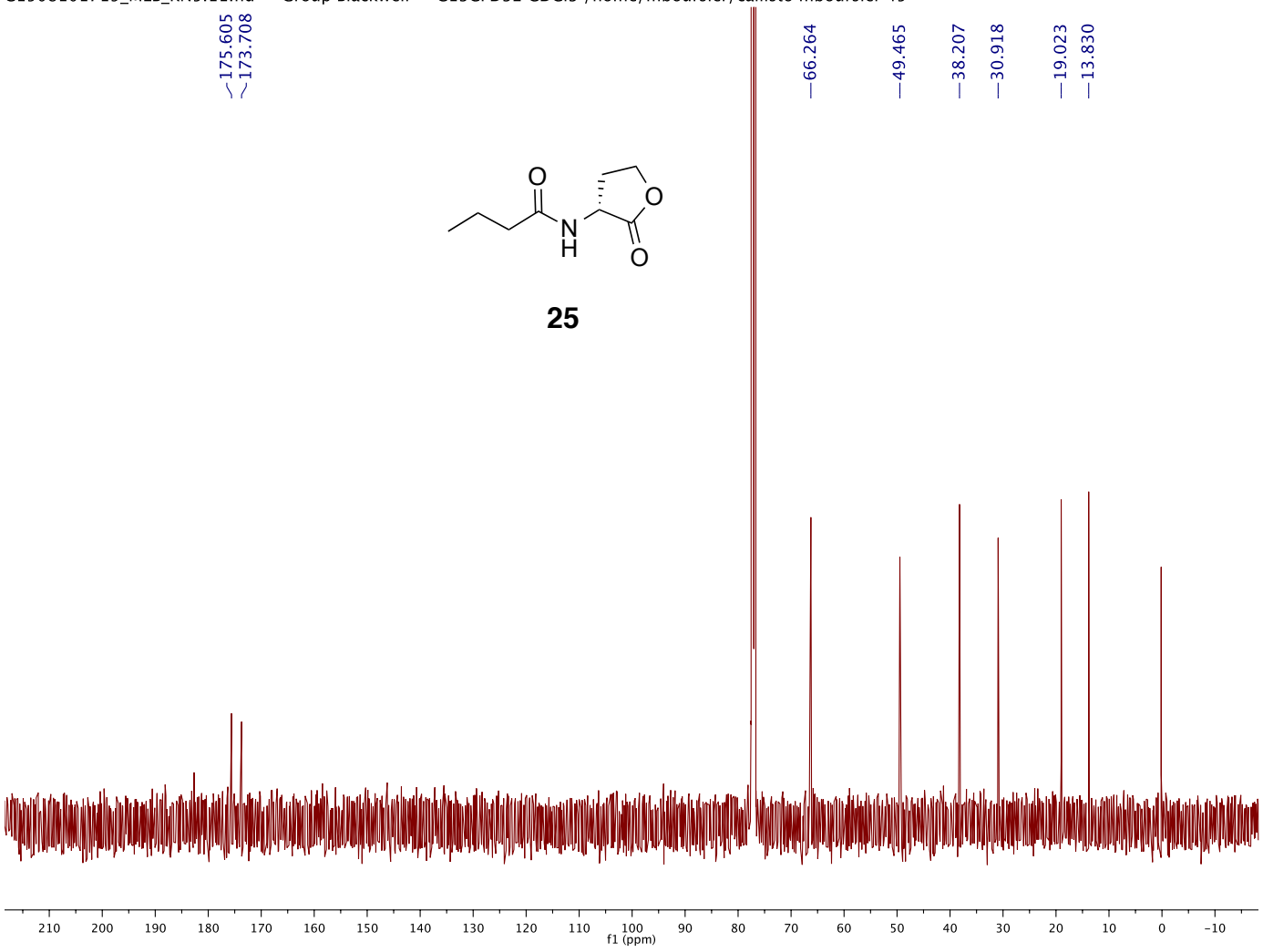

25

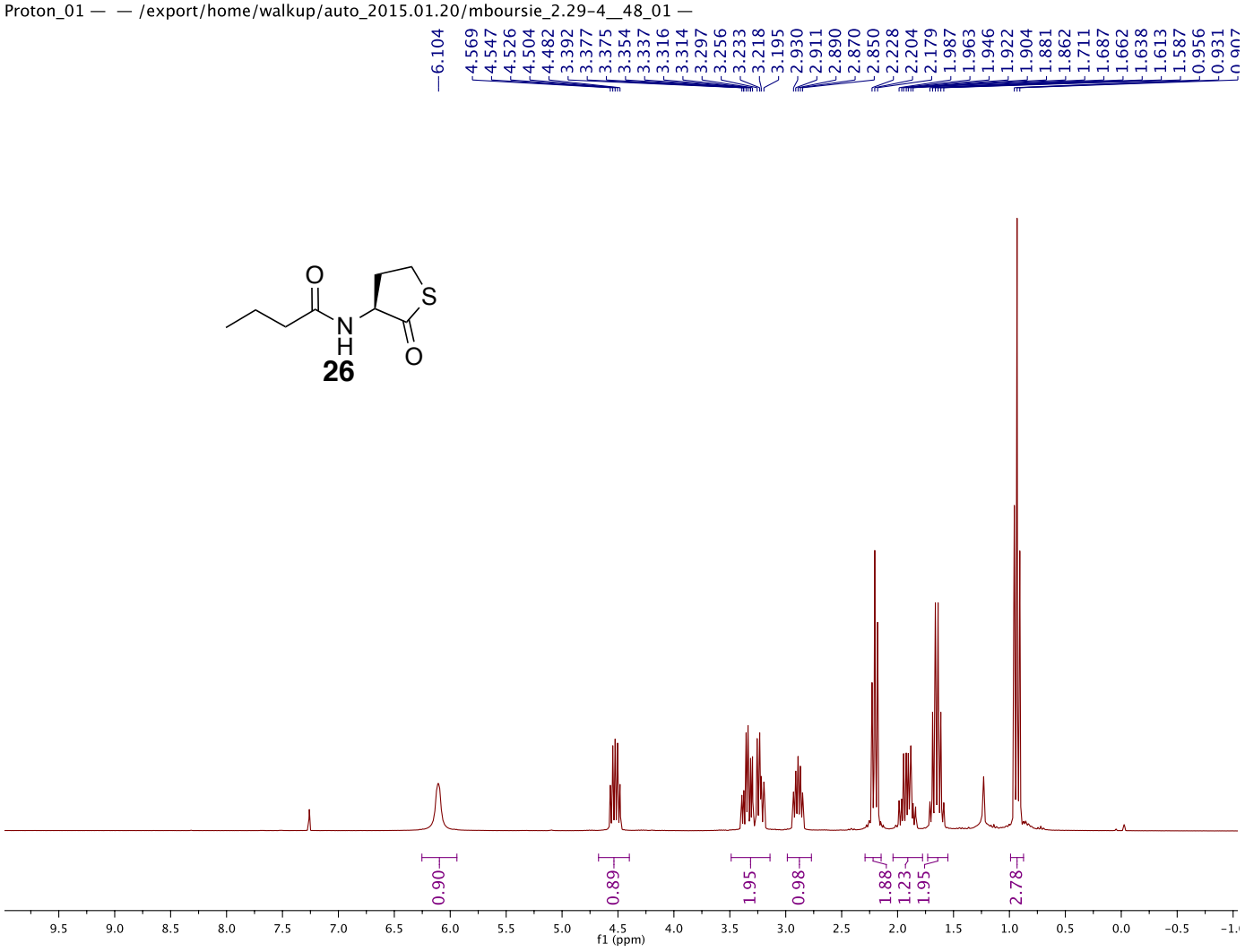
Proton_01 — — /export/home/walkup/auto_2015.01.20/mboursie_2.29-4__48_01 —
6.104
4.569
4.547
4.526
4.504
4.482
3.392
3.377
3.375
3.354
3.337
3.316
3.314
3.297
3.256
3.233
3.218
3.195
2.930
2.911
2.890
2.870
2.850
2.228
2.204
2.179
1.987
1.963
1.946
1.922
1.904
1.881
1.862
1.711
1.687
1.662
1.638
1.613
1.587
0.956
0.931
O
N
H
S
O
26
0.90
0.89
1.95
0.98
1.88
1.23
1.95
2.78
9.5
9.0
8.5
8.0
7.5
7.0
6.5
6.0
5.5
5.0
4.5
4.0
3.5
3.0
2.5
2.0
1.5
1.0
0.5
0.0
-0.5
f1 (ppm)

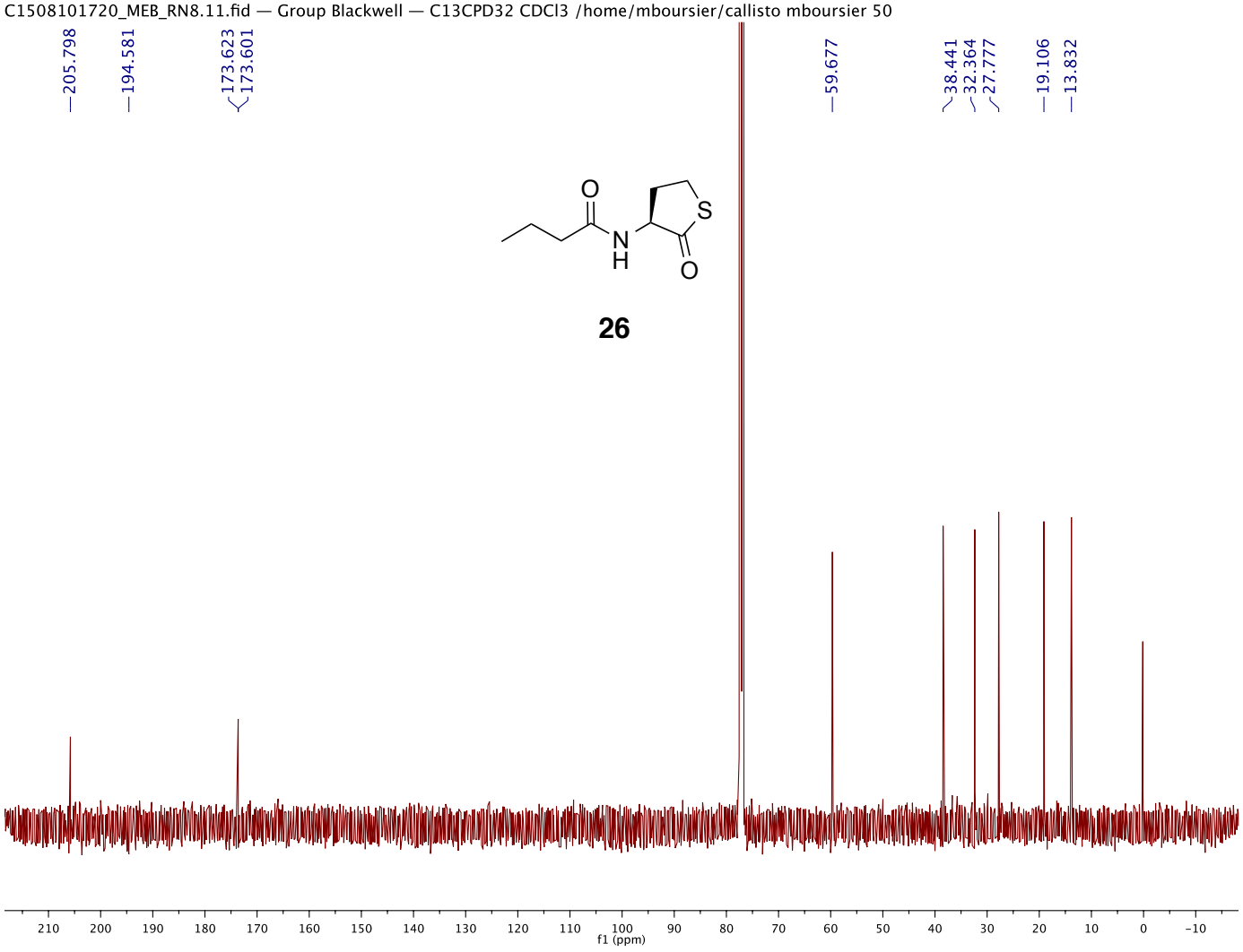
C1508101720_MEB_RN8.11.fid — Group Blackwell — C13CPD32 CDCl3 /home/mboursier/callisto mboursier 50
205.798
194.581
173.623
173.601
59.677
38.441
32.364
27.777
19.106
13.832
O
N
H
S
O
26
210 200 190 180 170 160 150 140 130 120 110 100 90 80 70 60 50 40 30 20 10 0 -10
f1 (ppm)

D1504131131_MEB_2.84P.11.fid — Group Blackwell — PROTON CDCl3 /home/mboursier/av400 mboursier 40

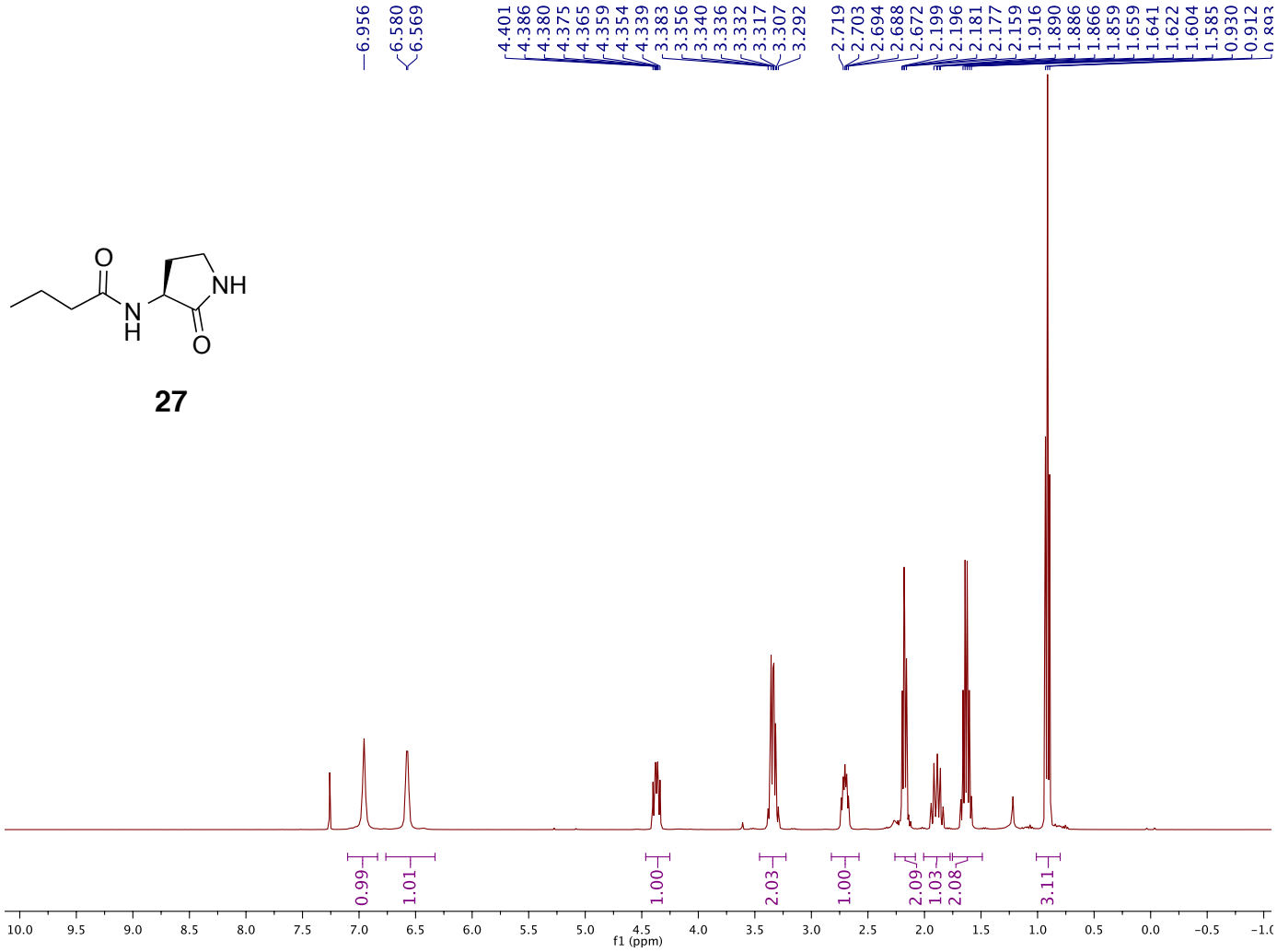

27

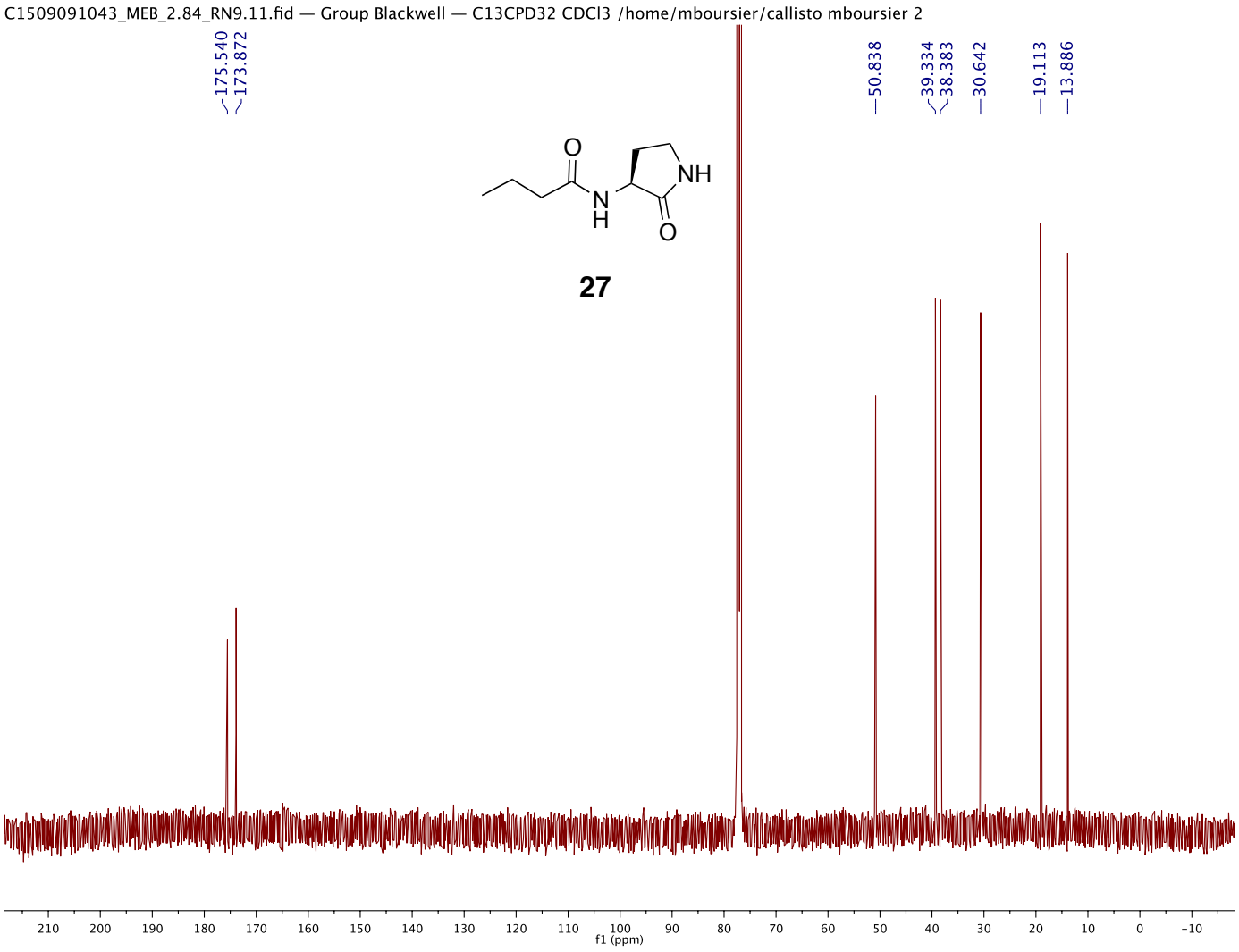
C1509091043_MEB_2.84_RN9.11.fid — Group Blackwell — C13CPD32 CDCl3 /home/mboursier/callisto mboursier 2
175.540
173.872
50.838
39.334
38.383
30.642
19.113
13.886
O
N
H
NH
O
27
210 200 190 180 170 160 150 140 130 120 110 100 90 80 70 60 50 40 30 20 10 0 -10
f1 (ppm)

D1501161006_MEB-2.28_1-7.10.fid — Group Blackwell — PROTON CDCl3 /home/mboursier/av400 mboursier 62

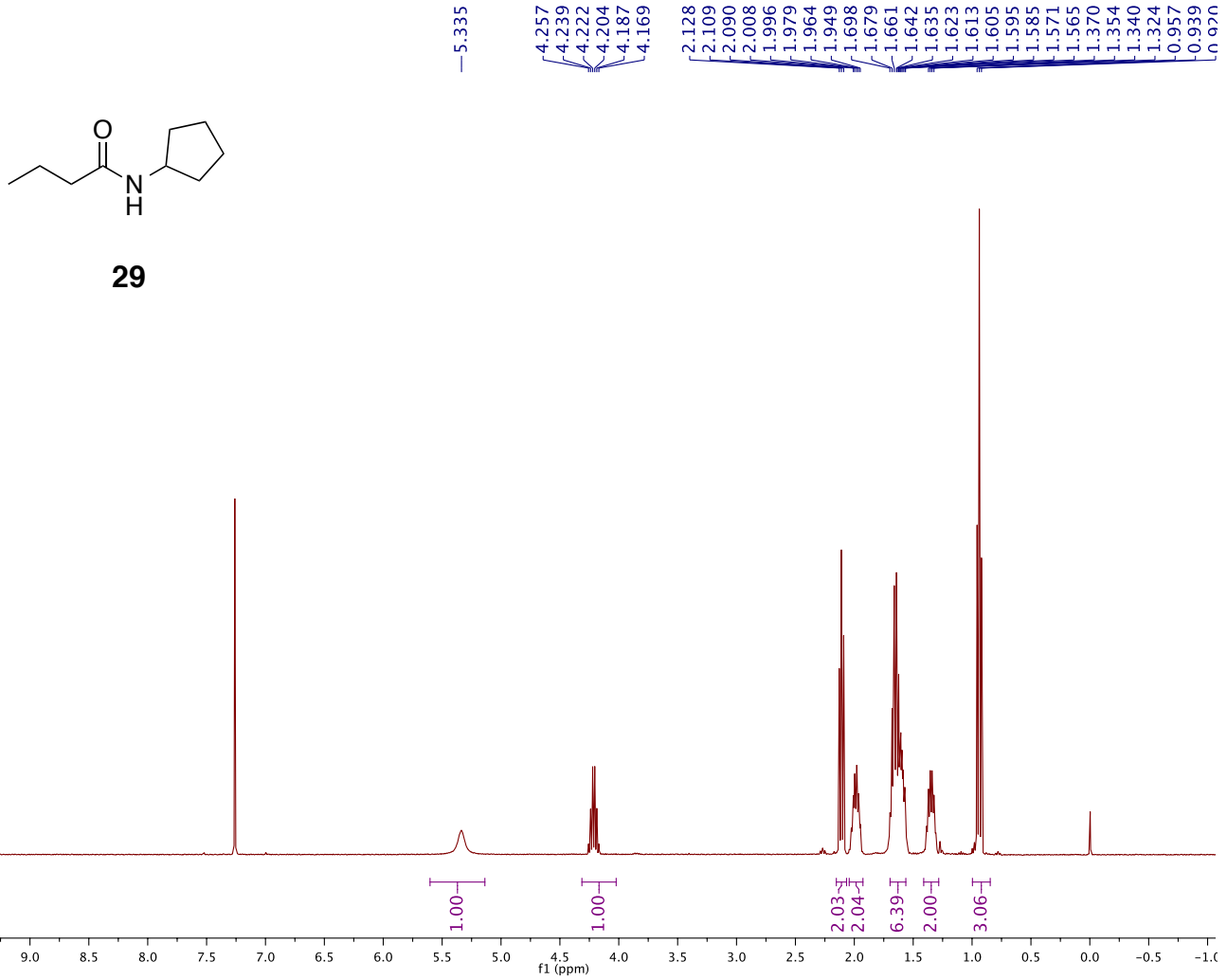

29

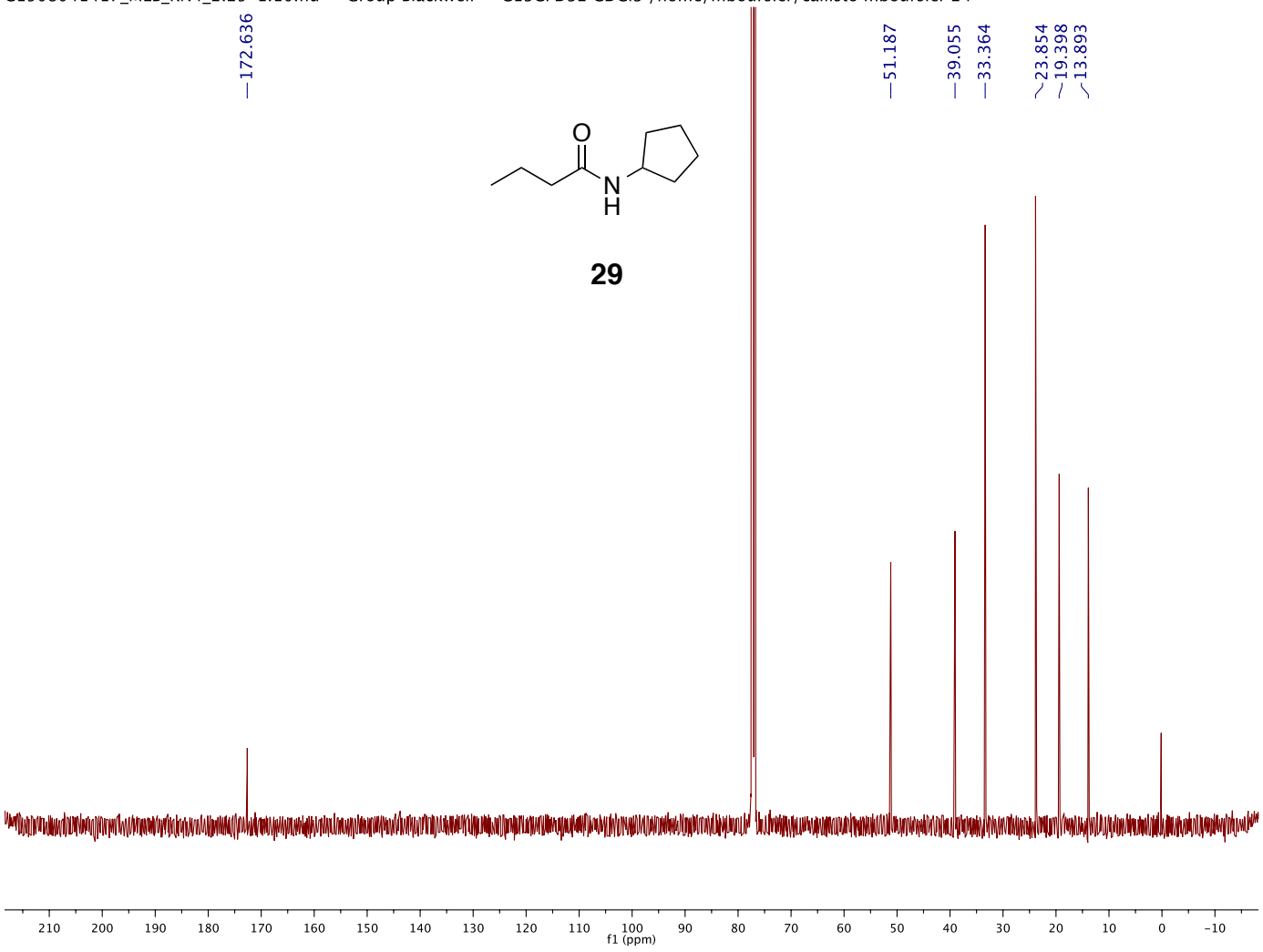
C1508041417_MEB_RN4_2.29-1.10.fid — Group Blackwell — C13CPD32 CDCl3 /home/mboursier/callisto mboursier 24
172.636
51.187
39.055
33.364
23.854
19.398
13.893
O
N
H
29
210 200 190 180 170 160 150 140 130 120 110 100 90 80 70 60 50 40 30 20 10 0 -10
f1 (ppm)

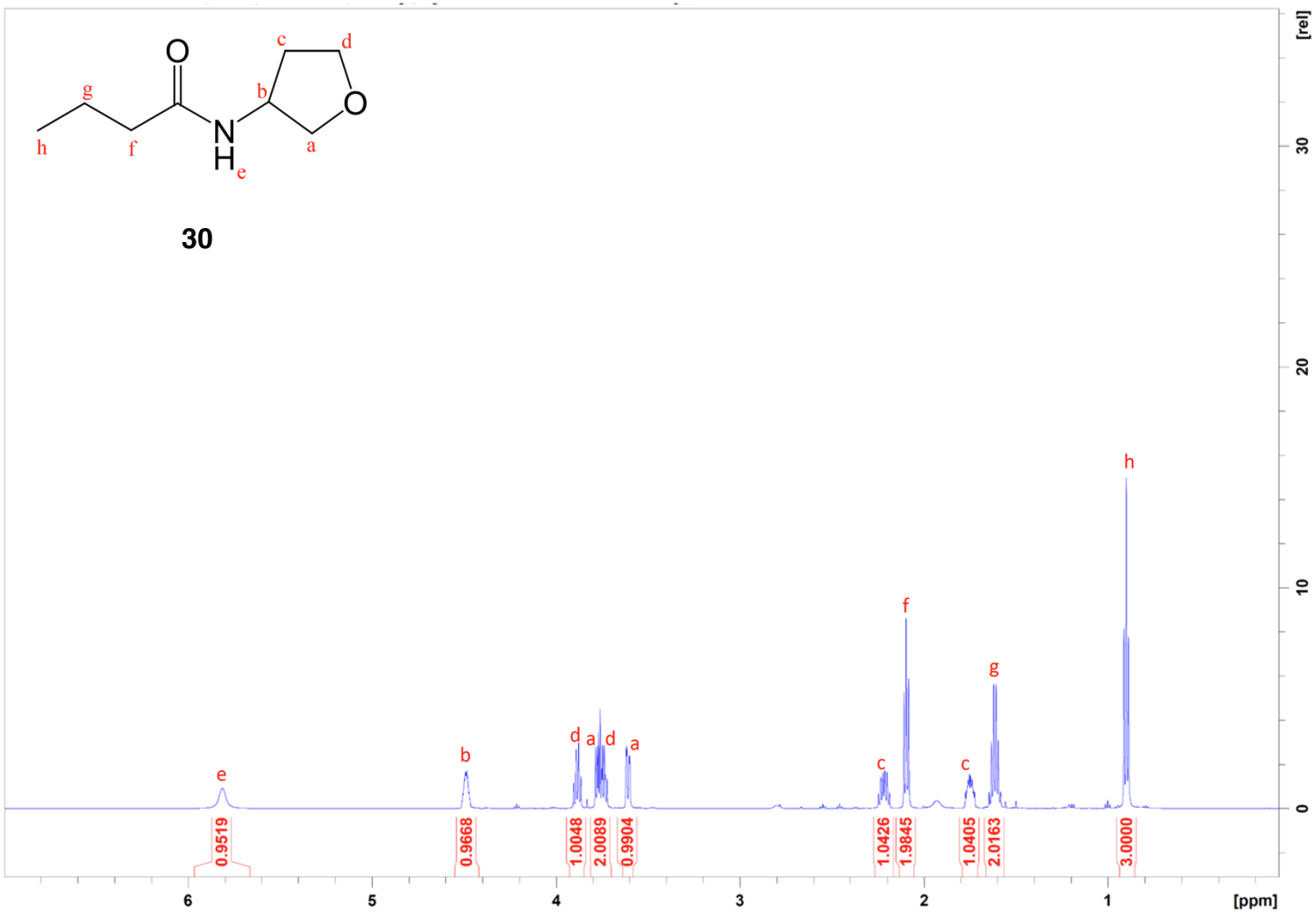
O
c
d
g
b
O
h
f
N
H
e
a
30
[rel]
30
20
10
0
h
f
g
e
b
d
a
d
a
c
c
0.9519
0.9668
1.0048
2.0089
0.9904
1.0426
1.9845
1.0405
2.0163
3.0000
6
5
4
3
2
1
[ppm]

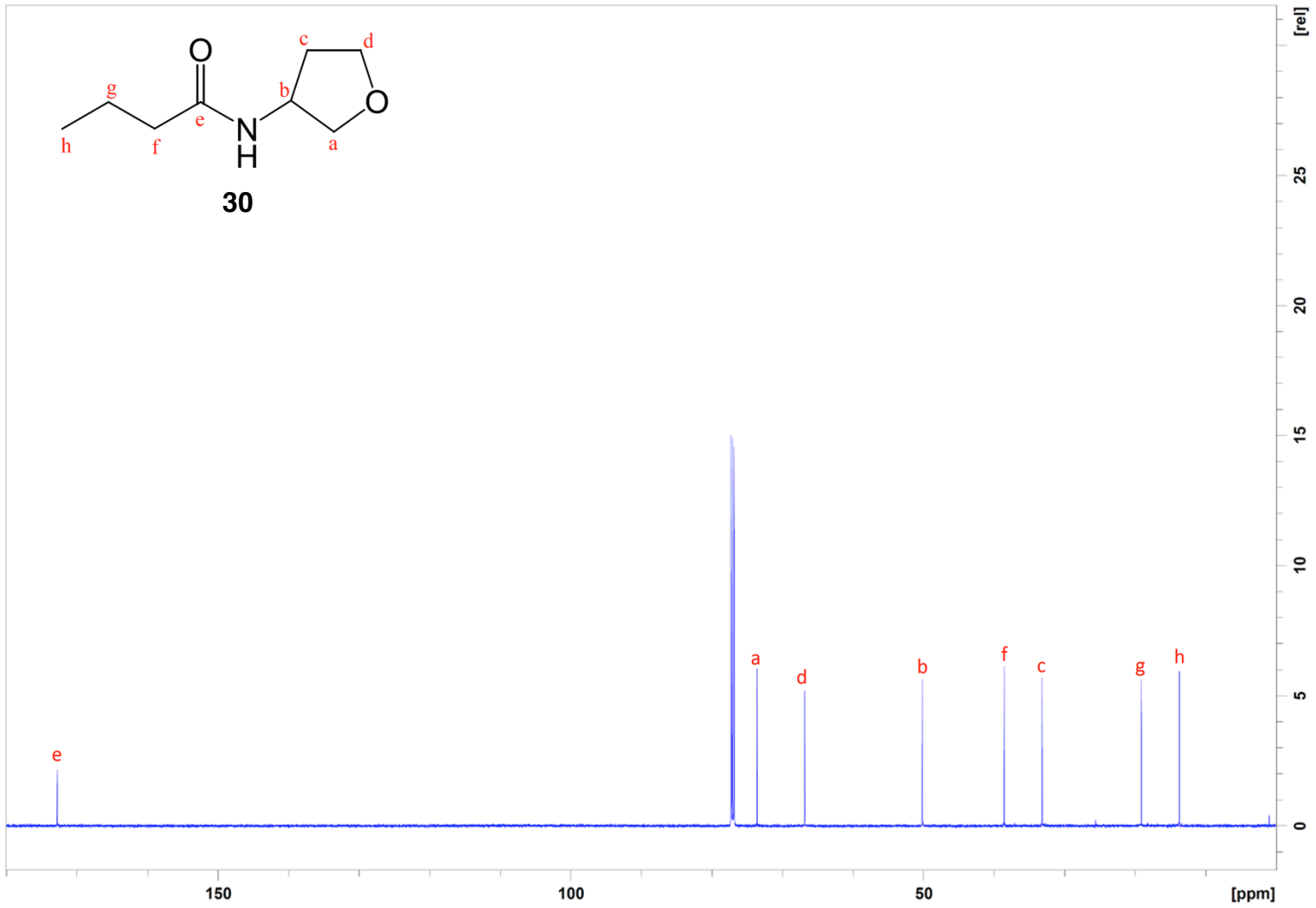
O
c
d
g
b
O
e
N
H
h
f
a
30
[rel]
25
20
15
10
5
0
a
d
b
f
c
g
h
e
150
100
50
[ppm]

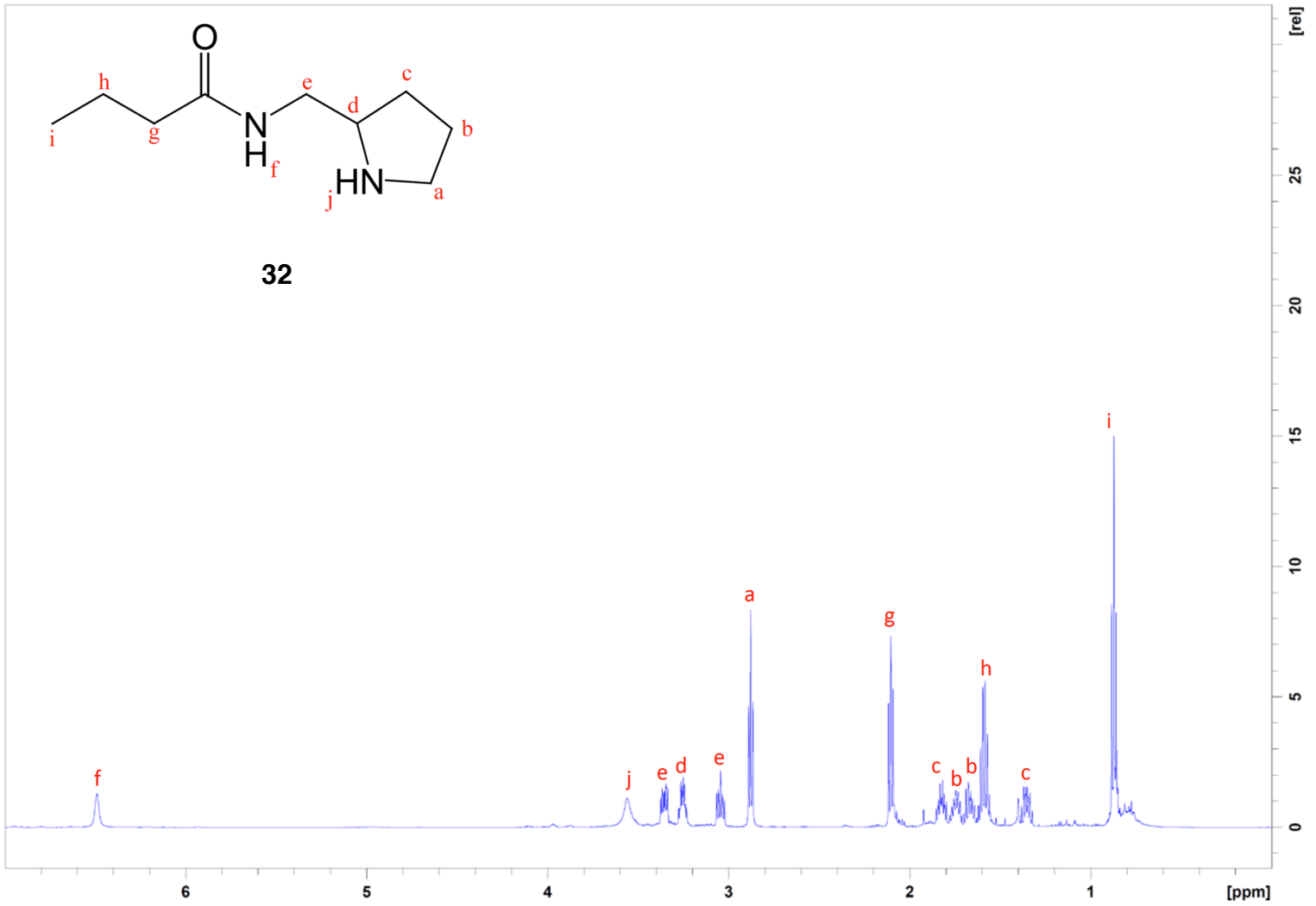
O
h
i
g
N
H
f
e
d
c
b
HN
j
a
[rel]
25
20
15
10
5
0
i
a
g
h
f
j
e
d
e
c
b
b
c
6
5
4
3
2
1
[ppm]

32

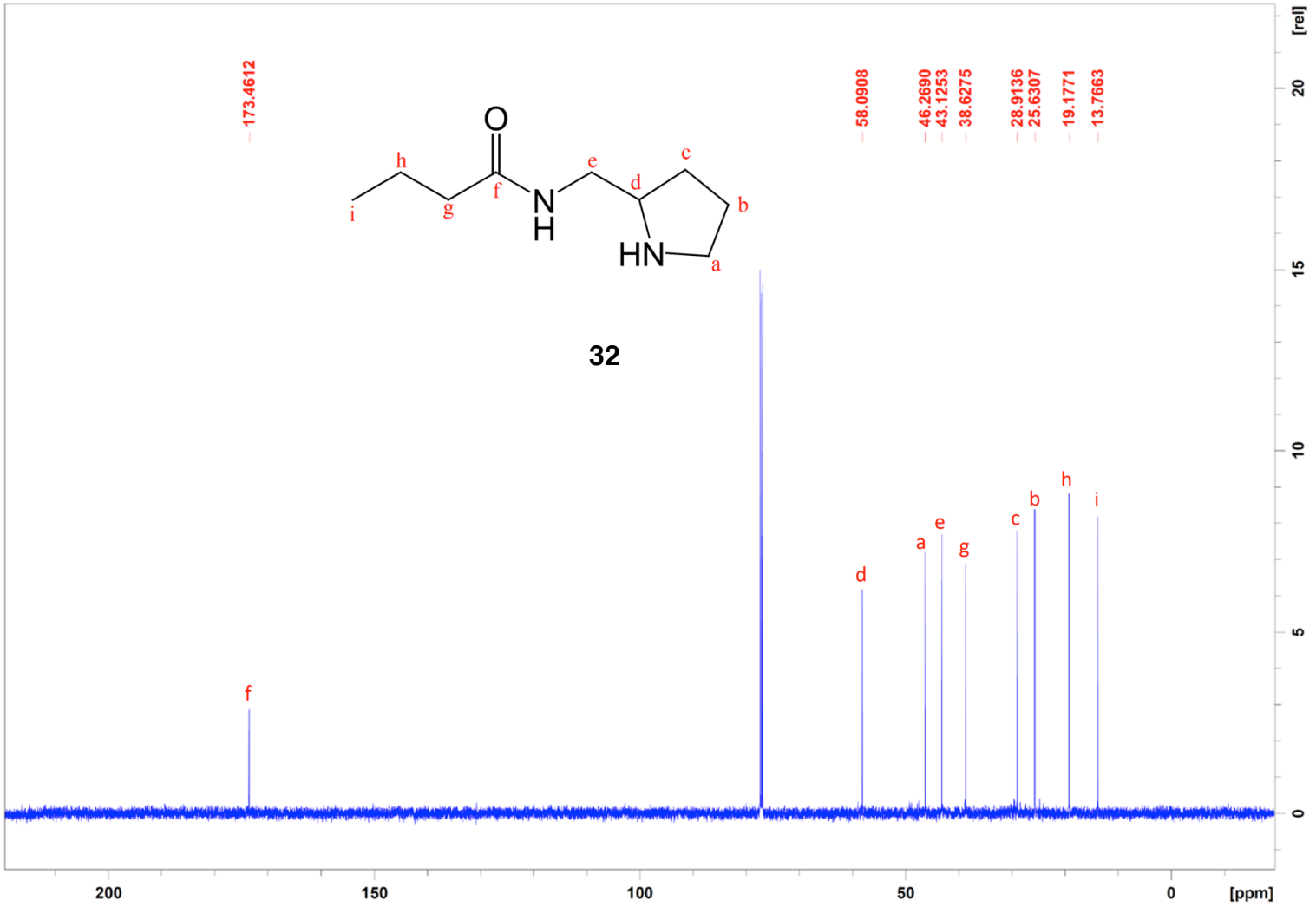
173.4612
58.0908
46.2690
43.1253
38.6275
28.9136
25.6307
19.1771
13.7663
O
N
H
HN
a
b
c
d
e
f
g
h
i
32
[rel]
20
15
10
5
0
200
150
100
50
0
[ppm]

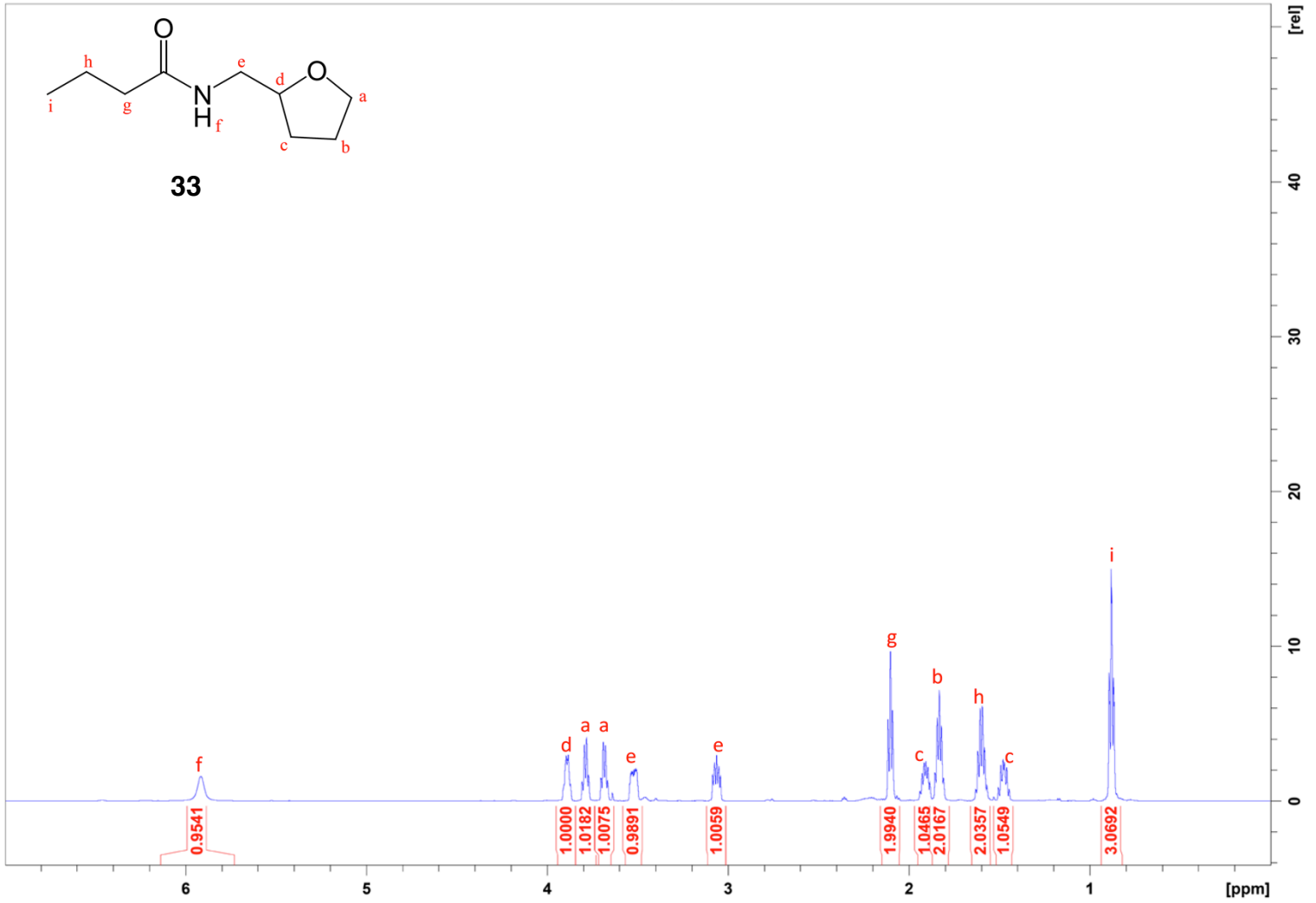
O
h
e
d
O
a
i
g
N
H
f
c
b
33
[rel]
40
30
20
10
0
f
d
a
a
e
e
g
b
h
c
c
i
0.9541
1.0000
1.0182
1.0075
0.9891
1.0059
1.9940
1.0465
2.0167
2.0357
1.0549
3.0692
6
5
4
3
2
1
[ppm]

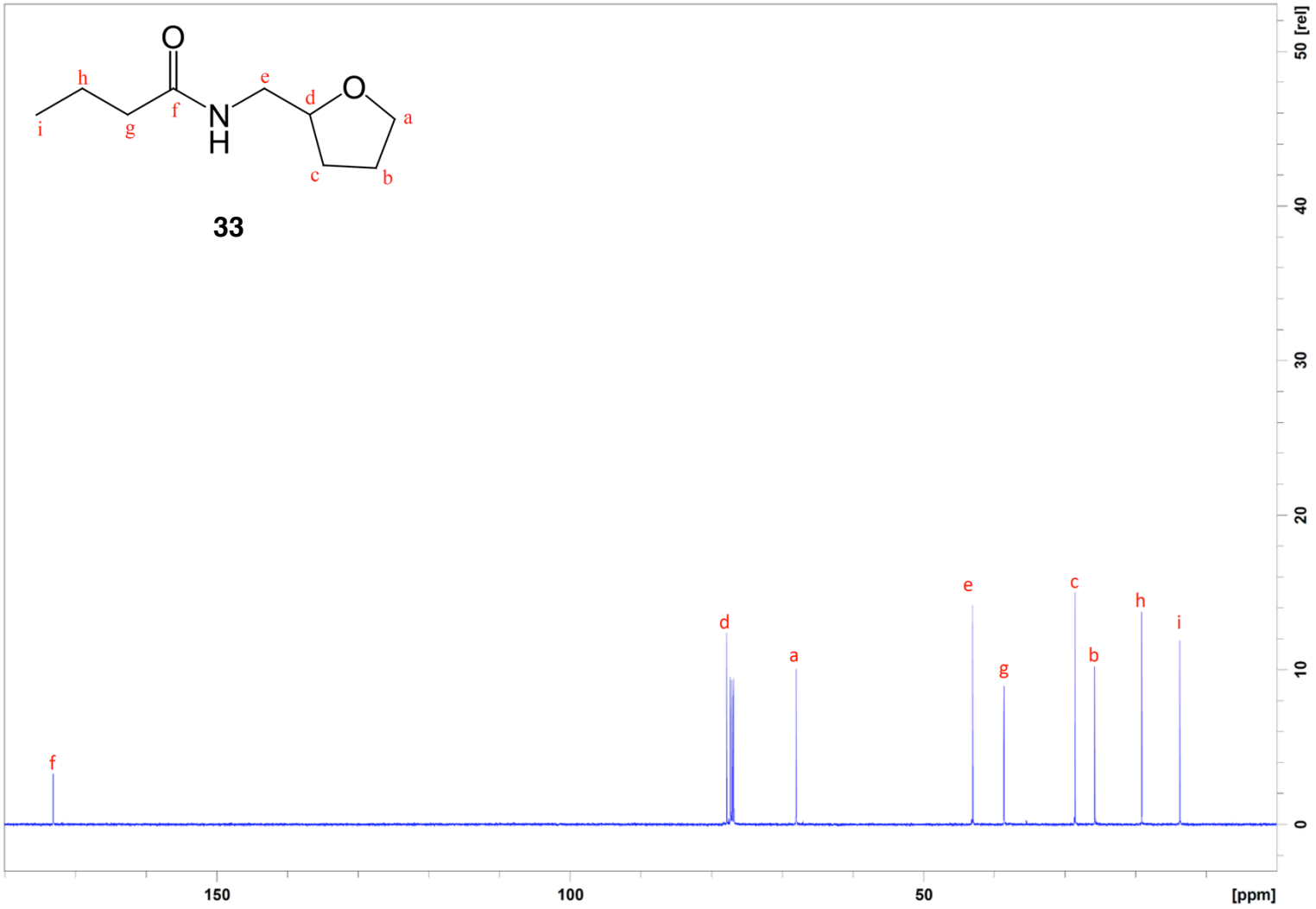
O
h
e
d
O
a
i
g
f
N
H
c
b
33
50 [rel]
40
30
20
10
0
d
a
e
g
c
b
h
i
f
150
100
50
[ppm]

2.8 References

1. Camilli, A., and Bassler, B. L. (2006) Bacterial Small-Molecule Signaling Pathways, *Science 311*, 1113-1116.

2. Williams, P., Winzer, K., Chan, W. C., and Cámara, M. (2007) Look who's talking: communication and quorum sensing in the bacterial world, *Philos. Trans. R. Soc. Lond. Series B, Biol. Sci. 362*, 1119-1134.

3. Fuqua, C., and Greenberg, E. P. (2002) Listening in on bacteria: acyl-homoserine lactone signalling, *Nat. Rev. Mol. Cell Biol. 3*, 685-695.

4. Pearson, J. P., Van Delden, C., and Iglewski, B. H. (1999) Active Efflux and Diffusion Are Involved in Transport of *Pseudomonas aeruginosa* Cell-to-Cell Signals, *J. Bacteriol. 181*, 1203-1210.

5. O'Connell, K. M., Hodgkinson, J. T., Sore, H. F., Welch, M., Salmond, G. P., and Spring, D. R. (2013) Combating Multidrug-Resistant Bacteria: Current Strategies for the Discovery of Novel Antibacterials, *Angew. Chem. Int. Ed. 52*, 10706-10733.

6. Clatworthy, A. E., Pierson, E., and Hung, D. T. (2007) Targeting virulence: a new paradigm for antimicrobial therapy, *Nat. Chem. Biol. 3*, 541-548.

7. Welsh, Michael A., and Blackwell, Helen E. (2016) Chemical Genetics Reveals Environment-Specific Roles for Quorum Sensing Circuits in Pseudomonas aeruginosa, *Cell Chem Biol.*, 1-9.

8. Kerr, K. G., and Snelling, A. M. (2009) *Pseudomonas aeruginosa*: a formidable and ever-present adversary, *J. Hosp. Infect. 73*, 338-344.

9. Folkesson, A., Jelsbak, L., Yang, L., Johansen, H. K., Ciofu, O., Høiby, N., and Molin, S. (2012) Adaptation of *Pseudomonas aeruginosa* to the cystic fibrosis airway: an evolutionary perspective, *Nat. Rev. Microbiol. 10*, 841-851.

10. Mesaros, N., Nordmann, P., Plésiat, P., Roussel-Delvallez, M., Van Eldere, J., Glupczynski, Y., Van Laethem, Y., Jacobs, F., Lebecque, P., Malfroot, A., Tulkens, P. M., and Van Bambeke, F. (2007) *Pseudomonas aeruginosa*: resistance and therapeutic options at the turn of the new millennium, *Clin. Microbiol. Infect. 13*, 560-578.

11. Schuster, M., and Greenberg, E. P. (2006) A network of networks: quorum-sensing gene regulation in *Pseudomonas aeruginosa*, *Int. J. Med. Microbiol. 296*, 73-81.

12. Gambello, M. J., Kaye, S., and Iglewski, B. H. (1993) LasR of *Pseudomonas aeruginosa* is a transcriptional activator of the alkaline protease gene (*apr*) and an enhancer of exotoxin A expression, *Infect. Immun. 61*, 1180-1184.

13. Brint, J. M., and Ohman, D. E. (1995) Synthesis of multiple exoproducts in *Pseudomonas aeruginosa* is under the control of RhlR-RhlI, another set of regulators in strain PAO1 with homology to the autoinducer-responsive LuxR-LuxI family, *J. Bacteriol. 177*, 7155-7163.

14. Chugani, S. a., Whiteley, M., Lee, K. M., D'Argenio, D., Manoil, C., and Greenberg, E. P. (2001) QscR, a modulator of quorum-sensing signal synthesis and virulence in Pseudomonas aeruginosa., *Proc. Natl. Acad. Sci. USA 98*, 2752-2757.

15. Venturi, V. (2006) Regulation of quorum sensing in *Pseudomonas*, *FEMS Microbiol. Rev. 30*, 274-291.

16. Smith, R. (2003) *P. aeruginosa* quorum-sensing systems and virulence, *Curr. Opin. Microbiol. 6*, 56-60.

17. Welsh, M. A., and Blackwell, H. E. (2016) Chemical probes of quorum sensing: from compound development to biological discovery, *FEMS Microbiol. Rev. 40*, 774-794.

18. Schuster, M., Lostroh, C. P., Ogi, T., and Greenberg, E. P. (2003) Identification, Timing, and Signal Specificity of *Pseudomonas aeruginosa* Quorum-Controlled Genes: a Transcriptome Analysis, *J. Bacteriol. 185*, 2066-2079.

19. Wagner, V. E., Bushnell, D., Passador, L., Brooks, A. I., and Iglewski, B. H. (2003) Microarray Analysis of *Pseudomonas aeruginosa* Quorum-Sensing Regulons: Effects of Growth Phase and Environment, *J. Bacteriol. 185*, 2080-2095.

20. Geske, G. D., O'Neill, J. C., and Blackwell, H. E. (2008) Expanding dialogues: from natural autoinducers to non-natural analogues that modulate quorum sensing in Gram-negative bacteria, *Chem. Soc. Rev. 37*, 1432-1447.

21. Galloway, W., Hodgkinson, J. T., Bowden, S. D., Welch, M., and Spring, D. R. (2011) Quorum Sensing in Gram-Negative Bacteria: Small-Molecule Modulation of AHL and Al-2 Quorum Sensing Pathways, *Chem. Rev. 111*, 28-67.

22. Moore, J. D., Rossi, F. M., Welsh, M. A., Nyffeler, K. E., and Blackwell, H. E. (2015) A Comparative Analysis of Synthetic Quorum Sensing Modulators in *Pseudomonas aeruginosa*: New Insights into Mechanism, Active Efflux Susceptibility, Phenotypic Response, and Next-Generation Ligand Design, *J. Am. Chem. Soc. 137*, 14626-14639.

23. Welsh, M. A., Eibergen, N. R., Moore, J. D., and Blackwell, H. E. (2015) Small Molecule Disruption of Quorum Sensing Cross-Regulation in *Pseudomonas aeruginosa* Causes Major and Unexpected Alterations to Virulence Phenotypes, *J. Am. Chem. Soc. 137*, 1510-1519.

24. Van Delden, C., Pesci, E. C., Pearson, J. P., and Iglewski, B. H. (1998) Starvation Selection Restores Elastase and Rhamnolipid Production in a *Pseudomonas aeruginosa* Quorum-Sensing Mutant, *Infect. Immun. 66*, 4499-4502.

25. Dekimpe, V., and Déziel, E. (2009) Revisiting the quorum-sensing hierarchy in *Pseudomonas aeruginosa*: the transcriptional regulator RhlR regulates LasR-specific factors, *Microbiology 155*, 712-723.

26. Bjarnsholt, T., Jensen, P. O., Jakobsen, T. H., Phipps, R., Nielsen, A. K., Rybtke, M. T., Tolker-Nielsen, T., Givskov, M., Hoiby, N., and Ciofu, O. (2010) Quorum sensing and virulence of *Pseudomonas aeruginosa* during lung infection of cystic fibrosis patients, *PLoS ONE 5*, e10115.

27. O'Loughlin, C. T., Miller, L. C., Siryaporn, A., Drescher, K., Semmelhack, M. F., and Bassler, B. L. (2013) A quorum-sensing inhibitor blocks *Pseudomonas aeruginosa* virulence and biofilm formation, *Proc. Natl. Acad. Sci. USA 110*, 17981-17986.

28. Mukherjee, S., Moustafa, D., Smith, C. D., Goldberg, J. B., and Bassler, B. L. (2017) The RhlR quorum-sensing receptor controls *Pseudomonas aeruginosa* pathogenesis and biofilm development independently of its canonical homoserine lactone autoinducer, *PLoS Path. 13*, e1006504.

29. Smith, K. M., Bu, Y., and Suga, H. (2003) Induction and Inhibition of *Pseudomonas aeruginosa* Quorum Sensing by Synthetic Autoinducer Analogs, *Chem. Biol. 10*, 81-89.

30. Eibergen, N. R., Moore, J. D., Mattmann, M. E., and Blackwell, H. E. (2015) Potent and Selective Modulation of the RhlR Quorum Sensing Receptor by Using Non-native Ligands : An Emerging Target for Virulence Control in *Pseudomonas aeruginosa*, *ChemBioChem 16*, 2348-2356.

31. Lindemann, A., Pessi, G., Schaefer, A. L., Mattmann, M. E., Christensen, Q. H., Kessler, A., Hennecke, H., Blackwell, H. E., Greenberg, E. P., and Harwood, C. S. (2011) Isovaleryl-homoserine lactone, an unusual branched-chain quorum-sensing signal from the soybean symbiont *Bradyrhizobium japonicum*, *Proc. Natl. Acad. Sci. USA 108*, 16765-16770.

32. Jog, G. J., Igarashi, J., and Suga, H. (2006) Stereoisomers of *P. aeruginosa* autoinducer analog to probe the regulator binding site, *Chem. Biol. 13*, 123-128.

33. Smith, K. M., Bu, Y., and Suga, H. (2003) Library Screening for Synthetic Agonists and Antagonists of a *Pseudomonas aeruginosa* Autoinducer, *Chem. Biol. 10*, 563-571.

34. Morkunas, B., Galloway, W. R., Wright, M., Ibbeson, B. M., Hodgkinson, J. T., O'Connell, K. M., Bartolucci, N., Della Valle, M., Welch, M., and Spring, D. R. (2012) Inhibition of the production of the *Pseudomonas aeruginosa* virulence factor pyocyanin in wild-type cells by quorum sensing autoinducer-mimics, *Org. Biomol. Chem. 10*, 8452-8464.

35. Ikeda, T., Kajiyama, K., Kita, T., Takiguchi, N., Kuroda, A., Kato, J., and Ohtake, H. (2001) The Synthesis of Optically Pure Enantiomers of *N*-Acyl-homoserine Lactone Autoinducers and Their Analogues., *Chem. Lett.*, 314-315.

36. Gerdt, Joseph P., McInnis, Christine E., Schell, Trevor L., Rossi, Francis M., and Blackwell, Helen E. (2014) Mutational Analysis of the Quorum-Sensing Receptor LasR Reveals Interactions that Govern Activation and Inhibition by Nonlactone Ligands, *Chem. Biol. 21*, 1361-1369.

37. Kent, A. D., and Triplett, E. W. (2002) Microbial communities and their interactions in soil and rhizosphere ecosystems, *Annu. Rev. Microbiol. 56*, 211-236.

38. McInnis, C. E., and Blackwell, H. E. (2011) Thiolactone modulators of quorum sensing revealed through library design and screening, *Biorg. Med. Chem. 19*, 4820-4828.

39. Janssens, J. C. A., Metzger, K., Daniels, R., Ptacek, D., Verhoeven, T., Habel, L. W., Vanderleyden, J., De Vos, D. E., and De Keersmaecker, S. C. J. (2007) Synthesis of *N*-Acyl Homoserine Lactone Analogues Reveals Strong Activators of SdiA, the *Salmonella enterica* Serovar Typhimurium LuxR Homologue, *Appl. Environ. Microbiol. 73*, 535-544.

40. Kim, T., Duong, T., Wu, C. A., Choi, J., Lan, N., Kang, S. W., Lokanath, N. K., Shin, D., Hwang, H. Y., and Kim, K. K. (2014) Structural insights into the molecular mechanism of *Escherichia coli* SdiA, a quorum-sensing receptor., *Acta Crystallogr. D Biol. Crystallogr. 70*, 694-707.

41. Wu, C., Lokanath, N. K., Kim, D. Y., Nguyen, L. D. N., and Kim, K. K. (2008) Crystallization and preliminary X-ray studies of SdiA from *Escherichia coli*, *Acta Crystallogr. Sect. F Struct. Bio.l Cryst. Commun. 64*, 19-21.

42. Yao, Y., Martinez-Yamout, M. a., Dickerson, T. J., Brogan, A. P., Wright, P. E., and Dyson, H. J. (2006) Structure of the *Escherichia coli* quorum sensing protein SdiA: activation of the folding switch by acyl homoserine lactones, *J. Mol. Biol. 355*, 262-273.

43. Li, W., Cowley, A., Uludag, M., Gur, T., McWilliam, H., Squizzato, S., Park, Y. M. i., Buso, N., and Lopez, R. (2015) The EMBL-EBI bioinformatics web and programmatic tools framework, *Nucleic Acids Res. 43*, W580-W584.

44. Chen, G., Swem, L. R., Swem, D. L., Stauff, D. L., O'Loughlin, C. T., Jeffrey, P. D., Bassler, B. L., and Hughson, F. M. (2011) A strategy for antagonizing quorum sensing, *Mol. Cell 42*, 199-209.

45. Skowronek, P., and Gawronski, J. (1999) Absolute configuration of α-phthalimido carboxylic acid derivatives from circular dichroism spectra, *Tetrahedron: Asymmetry 10*, 4585-4590.

46. Nielsen, J., and Givskov, M. (2003) Preparation of N-sulfonyl homoserine lactones for controlling bacterial virulence, WO2003106445.

47. O'Reilly, M. C., and Blackwell, H. E. (2016) Structure-Based Design and Biological Evaluation of Triphenyl Scaffold-Based Hybrid Compounds as Hydrolytically Stable Modulators of a LuxR-Type Quorum Sensing Receptor, *ACS Infect. Dis. 2*, 32-38.

48. Liu, Y.-s., Zhao, C., Bergbreiter, D. E., and Romo, D. (1998) Simultaneous Deprotection and Purification of BOC-amines Based on Ionic Resin Capture, *The Journal of Organic Chemistry 63*, 3471-3473.

49. Yates, E. A., Philipp, B., Buckley, C., Atkinson, S., Chhabra, S. R., Sockett, R. E., Goldner, M., Dessaux, Y., Cámara, M., Smith, H., and Williams, P. (2002) N-acylhomoserine lactones undergo lactonolysis in a pH-, temperature-, and acyl chain length-dependent manner during growth of *Yersinia pseudotuberculosis* and *Pseudomonas aeruginosa*, *Infect. Immun. 70*, 5635-5646.

50. Lao, W., Kjelleberg, S., Kumar, N., Read, R. W., and Steinberg, P. (1999) ^{13}C NMR study of *N*-acyl-*S*-homoserine lactone derivatives, *Magn. Reson. Chem.3 37*, 157-158.

51. Kim, C., Kim, J., Park, H. Y., McLean, R. J., Kim, C. K., Jeon, J., Yi, S. S., Kim, Y. G., Lee, Y. S., and Yoon, J. (2007) Molecular modeling, synthesis, and screening of new bacterial quorum-sensing antagonists, *J. Microbiol. Biotechnol. 17*, 1598-1606.

52. Stacy, D. M., Quement, T. L., Hansen, C. L., Clausen, J. W., Tolker-nielsen, T., Brummond, J. W., Givskov, M., Nielsen, E., and Blackwell, H. E. (2013) Synthesis and biological evaluation

of triazole-containing *N*-acyl homoserine lactones as quorum sensing modulators, *Org. Biomol. Chem. 11*, 938-954.

53. Zhu, J., Beaber, J. W., Moré, M. I., Fuqua, C., Eberhard, A., and Winans, S. C. (1998) Analogs of the autoinducer 3-oxooctanoyl-homoserine lactone strongly inhibit activity of the TraR protein of *Agrobacterium tumefaciens*, *J. Bacteriol. 180*, 5398-5405.

54. Petersen, M., and Kalbermatten, G. (2001) Method for producing (R) or (S)-hydroxy-γ-butyrolactone, WO 2001018231.

55. Mcclean, K. H., Winson, M. K., Fish, L., Taylor, A., Chhabra, S. R., Camara, M., Daykin, M., John, H., Swift, S., Bycroft, B. W., Stewart, G. S. a. B., and Williams, P. (1997) Quorum sensing and *Chrornobacteriurn violaceum*: exploitation of violacein production and inhibition for the detection of *N*-acyl homoserine lactones, *Microbiology 143*, 3703-3711.

56. Ishida, T., Ikeda, T., Takiguchi, N., Kuroda, A., Ohtake, H., and Kato, J. (2007) Inhibition of quorum sensing in *Pseudomonas aeruginosa* by *N*-acyl cyclopentylamides, *Appl. Environ. Microbiol. 73*, 3183-3188.

57. Prinz, H. (2010) Hill coefficients, dose-response curves and allosteric mechanisms, *J. Chem. Biol. 3*, 37-44.

CHAPTER 3:

N-Acyl L-homocysteine thiolactones are potent and stable synthetic modulators of the RhlR quorum sensing receptor in *Pseudomonas aeruginosa*

M. E. Boursier designed experiments, synthesized non-native modulators, performed screening assays, and gauged compound stabilities. J. B. Combs assisted with non-native modulator synthesis and characterization. H. E. Blackwell assisted in writing the manuscript.

*This chapter has been prepared as a manuscript intended for publication under the same title.

3.1 Abstract

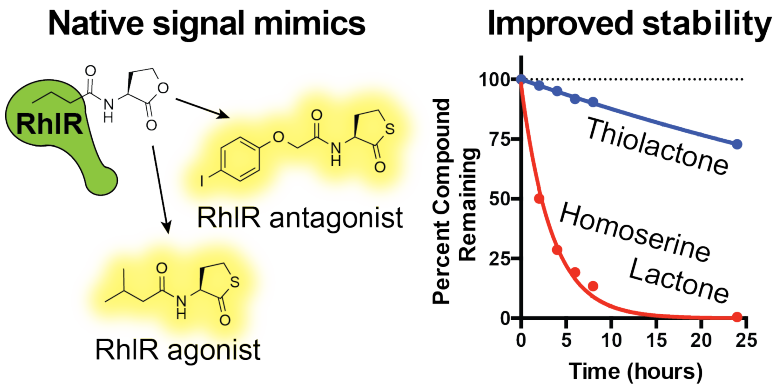

The RhlR quorum sensing (QS) receptor in the pathogen *Pseudomonas aeruginosa* plays a prominent role in infection, and both antagonism and agonism of RhlR have been shown to negatively regulate important virulence phenotypes. Non-native lactone ligands are known to modulate RhlR activity, but their utility as chemical probes is limited due to hydrolytic instability. Herein, we report our design and biological evaluation of a suite of hybrid AHL analogs with structures merging (1) features of the most promising reported RhlR ligands and (2) head groups with improved hydrolytic stabilities. The most promising compounds were *N*-acyl L-homocysteine thiolactones and showed improved hydrolytic stabilities relative to lactones. Moreover, they were highly selective for RhlR over another key QS receptor in *P. aeruginosa*, LasR. These compounds are the most potent RhlR modulators known and represent robust, new chemical tools to dissect the complex role of RhlR in the *P. aeruginosa* QS circuitry.

3.2 Introduction

Quorum sensing (QS) is a chemical signaling mechanism that certain bacteria use to assess their local population densities and coordinate group behavior once a threshold cell number is achieved. Gram-negative bacteria typically use *N*-acyl L-homoserine lactones (AHLs) as their QS signals, which are produced by LuxI-type synthases and sensed by cytoplasmic LuxR-type transcription factors. Upon ligand binding, LuxR-type receptors most commonly dimerize, bind to DNA, and regulate QS-associated genes. The opportunistic pathogen *Pseudomonas aeruginosa* utilizes a relatively complex QS system to regulate a host of virulence factors at high cell density. Two LuxI-type synthases, LasI and RhlI, produce *N*-(3-oxododecanoyl) HL (OdDHL) and *N*-butyryl HL (BHL), respectively (Figure 3.1A).[1] These two signaling molecules are recognized by their cognate LuxR-type receptors, LasR and RhlR. OdDHL is also recognized by a third LuxR-type receptor, QscR, which has been found to both negatively regulate LasR and activate its own unique regulon of *P. aeruginosa*.[2] LasR is generally considered to be at the top of the *P. aeruginosa* QS receptor hierarchy, as it regulates genes associated with other QS circuits.[3, 4] Due to this prominent role, LasR has been a primary target over the past ~15 years for the design of small molecule antagonists to block QS and reduce virulence in *P. aeruginosa*.[5-9]

However, there is increasing evidence that targeting RhlR with small molecule tools could be advantageous. Our laboratory has recently shown that small-molecule activation and inhibition of RhlR can alter the expression levels of several different and important virulence factors; for example, when RhlR is activated, pyocyanin production is reduced. In turn, when RhlR is inhibited, rhamnolipid production drops.[10] Bassler and co-workers have also shown that partial agonism of RhlR could reduce *P. aeruginosa* virulence in a *C. elegans* infection model.[11] To date, the most potent reported synthetic RhlR modulators contain homoserine lactone headgroups (**S4** and **E22**, Figure 3.1A).[12] We identified these two ligands (an agonist and antagonist, respectively) in a comprehensive analysis of our non-native AHL libraries for RhlR modulators.[12] However, the hydrolytic instability of these ligands' lactone head groups is a significant liability (half-lives

of ~4-6 h in buffered media), especially as *P. aeruginosa* culture media is observed to become more alkaline over time.[13] Synthetic RhlR ligands with enhanced stability over **S4** and **E22**, whilst maintaining their potencies, would be of significant utility to study QS pathways in *P. aeruginosa.*

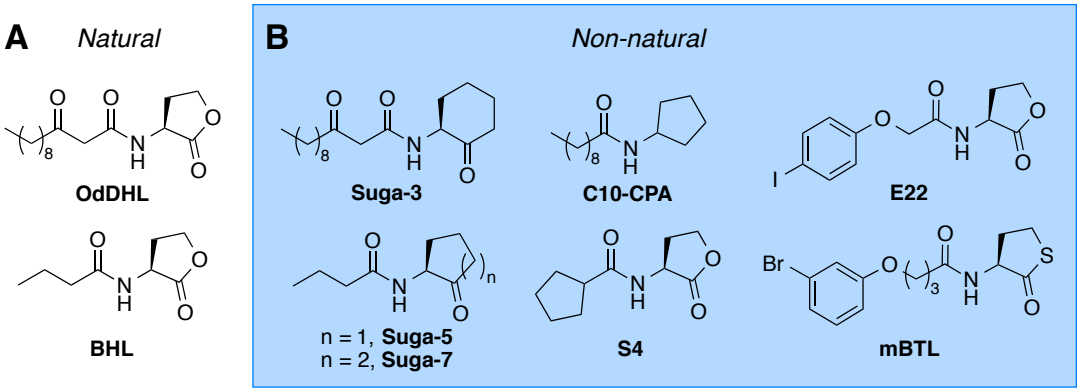

Figure 3.1: Selected natural AHLs (A) and lead non-natural modulators (B) of the *P. aeruginosa* RhlR receptor [**Suga-3**, **Suga-5**, and **Suga-7**, Suga and coworkers;[14] **C10-CPA**, Kato and coworkers;[15] **S4** and **E22**, Blackwell and coworkers;[12] **mBTL**, Bassler and coworkers[11]].

In general, RhlR has seen far less scrutiny as a target for non-native ligand design relative to LasR in *P. aeruginosa*.[5, 16] Interestingly, beyond our recent forays into the development of RhlR modulators,[12, 17] most prior studies on synthetic RhlR ligands have actually involved examination of AHL analogues with non-lactone headgroups. In 2003, Suga and co-workers investigated both BHL and OdDHL analogs that contained heterocyclic replacements for the lactone head group yet retained the native tail groups. The authors found that BHL variants with cyclopentanone and cyclohexanone head groups showed agonistic activity towards RhlR (**Suga-5, Suga-7**; Figure 3.1B).[14] A 12-carbon OdDHL mimic with a cyclohexanone head group proved surprisingly to be the most potent RhlR antagonist in this study, suggesting the utility of larger tail groups in inhibiting this receptor (**Suga-3**; Figure 3.1B). Later, Kato and co-workers found that *N*-decanoyl cyclopentylamide inhibits *P. aeruginosa* QS through the antagonism of both LasR and RhlR (**C10-CPA**, Figure 3.1B).[15] More recently, Bassler and co-workers reported that a *meta*-bromo

aryl homocysteine thiolactone (i.e., **mBTL**; Figure 3.1B) was a RhlR partial agonist.[11] Homocysteine thiolactones have been examined in AHL analogs previously, but, except for **mBTL**, have not been explored in RhlR.[11, 18-21] Together, these prior studies indicated that RhlR can accommodate non-lactone head groups (assuming these AHL mimetics target the BHL-binding site) and that further research into such compound scaffolds could be fruitful for new ligand design.

Herein, we report our design and biological evaluation of a suite of hybrid AHL analogs with structures merging (1) features of the most promising reported RhlR ligands and (2) head groups with improved hydrolytic stabilities. These studies revealed the most potent non-native RhlR agonist known, along with a highly potent new RhlR antagonist. Notably, these two compounds are both homocysteine thiolactones, show improved hydrolytic stabilities relative to prior AHL-type ligands, and are selective for RhlR over the other key LuxR-type receptor in *P. aeruginosa*, LasR.

3.3 Results And Discussion

Active compounds uncovered in our recent BHL structure-activity relationship (SAR) study[17] and previously published RhlR leads (Figure 3.1B), as well as scaffolds with enhanced hydrolytic stability, motivated our selection of head and tail groups for new ligand design. Our SAR studies suggested that both cyclopentanone and homocysteine thiolactone BHL analogs were capable of RhlR agonism, consistent with the work of the Suga and Bassler labs, respectively.[11, 14] In addition, we found that RhlR well tolerates additional bulk in the alpha-position of the acyl tail, as exemplified by **S4**, resulting in agonists exceeding the potency of BHL. We reasoned that combining these structural features could yield new RhlR agonists, and tested this hypothesis by uniting the cyclopentanone and homocysteine thiolactone head groups with the isovaleryl or cyclobutanoyl tails in compounds **34**–**37** (Figure 3.2A). Building on the prior work of Kato[15] and with an eye toward the development of new RhlR antagonists, we coupled the cyclopentylamine

head group with the isovaleryl or cyclobutanoyl tails to yield derivatives **38** and **39** (Figure 3.2B). Also with a view toward RhlR antagonism, we united the cyclopentylamine, tetrahydrofurfurylamine, and homocysteine thiolactone head groups with the tails from our potent and selective RhlR antagonist **E22** (Figure 1B) to give compounds **40**–**42**.[10, 12] These hybrid compounds were synthesized using standard amide coupling chemistry in modest to good yields (40–80%) and purified to >95% prior to biological testing (see Methods).

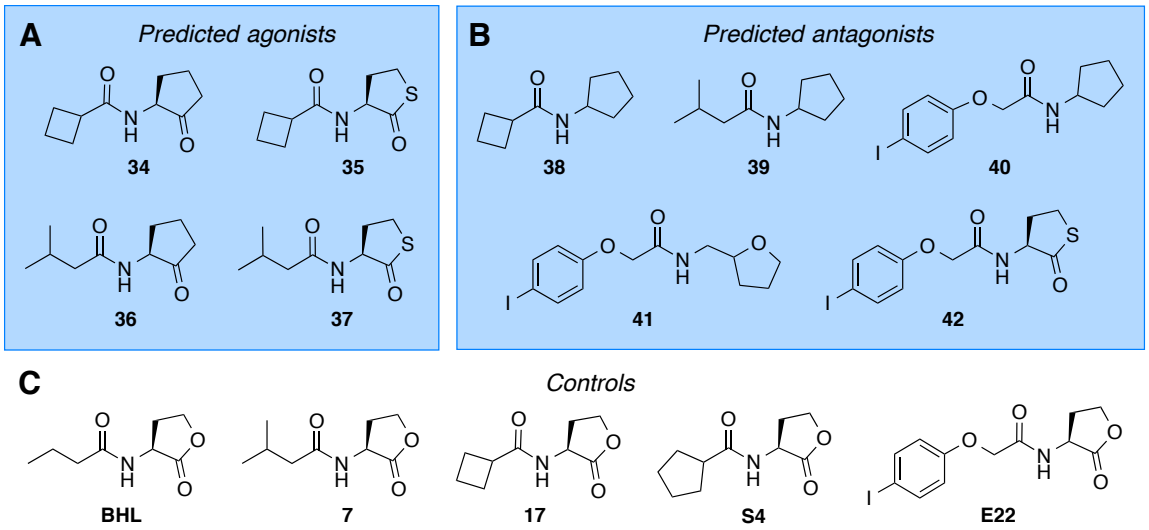

Figure 3.2. New structures reported herein blending (A) agonist head and tail groups for predicted RhlR agonist generation or blending (B) agonist and antagonist heads and tail groups for predicted RhlR antagonist generation. C) Control compounds for comparison to new ligands.

To start, the compounds were evaluated for their ability to either agonize or antagonize RhlR using an *Escherichia coli* strain harboring a RhlR expression plasmid and a reporter plasmid that allowed straightforward read-out of RhlR activity (Table 3.3; see Methods). We simultaneously also screened the compounds in an analogous *E. coli* reporter system for LasR to assay for selectivity for RhlR over LasR (Table 3.4). In the RhlR agonism screen, compounds **34**–**37** proved highly active at 10 μM and 1 mM, displaying greater than 50% activity at 10 μM. In the RhlR antagonism screen, compounds **38** and **41** were modest antagonists, while compound **42** was found to inhibit RhlR more than any other compound in this study at both 10 μM (28%

inhibition) and 1 mM (74% inhibition). Notably, all of the compounds showed generally limited activity in LasR assays as either agonists or antagonists, highlighting the selectivity of these hybrid ligand classes for RhlR modulation over LasR. The four lead hybrid agonists (**34**–**37**) and three lead hybrid antagonists (**38**, **41**, and **42**) were next submitted to dose response screening in the RhlR *E. coli* reporter to determine their potencies. BHL along with four parent compounds from our previous studies (**7**, **17**, **S4**, and **E22**) were included as controls to better assess relative compound potency and efficacy (Figure 3.2C). The resulting EC_{50} and IC_{50} values for the compounds are listed in Table 1.

Table 3.1: EC_{50} and IC_{50} values for RhlR activation by AHL analogs in *E. coli* or *P. aeruginosa*.[a] Control compounds shaded in grey.

	E. coli			***P. aeruginosa***		
Compound	EC_{50} (μM)	95% CI (μM)[b]	Maximum Activation (%)	EC_{50} (μM)	95% CI (μM)[b]	Maximum Activation (%)
34	5.94	4.19 – 8.41	93	7.35	5.26 – 10.3	96
35	1.72	1.34 – 2.21	106	1.65	1.24 – 2.21	90
36	7.58	5.80 – 9.90	101	11.24	7.41 – 17.1	96
37	0.463	0.336 – 0.640	93	2.58	1.86 – 3.56	91
BHL	8.95	5.86 – 13.7	100	8.08	6.09 – 10.7	100
7	1.02	0.67 – 1.55	105	1.42	1.08 – 1.86	94
17	1.78	1.37 – 2.31	100	1.41	1.14 – 1.74	96
S4	1.58	1.32 – 1.90	100	1.22	1.03 – 1.45	106
	IC_{50} (μM)	95% CI (μM)[b]	Maximum Inhibition (%)	IC_{50} (μM)	95% CI (μM)[b]	Maximum Inhibition (%)
38	26.7	10.1 – 71.0	32	–	–	–
41	>100	–	56	–	–	–
42	19.6	14.3 – 26.9	81	31.4	19.6 – 50.4	85
E22	17.3	12.1 – 24.6	74	23.9	16.6 – 31.6	96

[a] See Methods for assay details. For the full dose response curves, see Figures 3.4–3.7. [b] CI = confidence interval.

Hybrid compounds **34**–**37** proved either equipotent (**34** and **36**) or more potent (**35** and **37**) agonists than the native RhlR ligand, BHL (Table 3.1). The homocysteine thiolactone derivatives were the most potent overall, with cyclobutanoyl derivative **35** equipotent to its parent lactone

compound **17**, and more notably, isovaryl homocysteine thiolactone **37** displaying two-fold greater potency over its lactone variant **7** and previous our lead agonist **S4**. Compound **37,** with an EC_{50} of 463 nM in the *E. coli* reporter, represented the most potent RhlR agonist identified in this study.

In terms of RhlR antagonism, a homocysteine thiolactone derivative (**42**) again was the most potent, with analog **42** showing potency comparable to its parent lactone **E22** (Table 3.2). This result is interesting, as a previous study with a pair of aryl homoserine lactone and homocysteine thiolactone analogs in LasR were found to display opposite, i.e., antagonist and agonist activities, respectively. Mutagenesis and computational studies in LasR implicated a hydrogen bond between the homoserine lactone (or homocysteine thiolactone) carbonyl and a Trp residue in the LasR ligand-binding site to be important for tuning compound activity.[22] Our results showing that both homocysteine thiolactone **42** and its lactone analog **E22** are strong RhlR antagonists indicate that this hypothesis may not be accurate for RhlR, at least with this aryl ligand scaffold. Of the other two antagonists submitted to dose response analyses, cyclopentylamine **38** proved the next most active, with a potency only slightly lower than thiolactone **42**, albeit with a significantly lower efficacy (32% vs. 81%, Table 3.1).

We next sought to determine if the activity profiles for the most potent compounds in the *E. coli* reporter would be maintained in RhlR's native background, *P. aeruginosa.* Active efflux, along with the presence of acylases and reduced overall permeability, have been shown to decrease the activity of AHLs in *P. aeruginosa* relative to *E. coli.*[23-25] Agonists **34**–**37** and antagonist **42** were submitted to an analogous dose-response RhlR reporter assays in a *P. aeruginosa* (Table 3.1; see Methods). Compounds **34**–**36** maintained their strong potency profiles between the two different reporters, whilst compound **37** demonstrated a ~5-fold lower potency in *P. aeruginosa* relative to *E. coli*. Still, the homocysteine lactone analogs **35** and **37** were the most potent in *P. aeruginosa* (EC_{50} values of 1.65 and 2.58 mM, respectively), further underscoring the utility of this head group for potent RhlR agonism. This trend was continued for RhlR

antagonism, with homocysteine lactone **42** maintaining its strong potency and efficacy in *P. aeruginosa* (with 85% maximum inhibition, Table 3.1) and marking it as one of the most potent antagonists of RhlR reported to date.

We were intrigued that our lead RhlR agonist (**35**) and RhlR antagonist (**42**) in *P. aeruginosa* were homocysteine thiolactone derivatives, results that corroborated the work of Bassler with the agonist **mBTL** in RhlR.[11] We reasoned that these alternate headgroups could alter the hydrolytic stabilities of these derivative and play a role in tuning the activity of these compounds over time. Indeed, in an earlier study we had shown that certain homocysteine thiolactone derivatives have increased hydrolytic stability relative to AHLs in Luria-Bertani medium as monitored via a biosensor assay.[21] To evaluate their stability in a more direct and quantitative assay, we elected to monitor the stability of homocysteine thiolactone **42** relative to its homoserine lactone homolog **E22** over time and at varying pH values using HPLC and MS (see Methods). Interestingly, the homocysteine thiolactone displayed remarkable stability in this assay, with half lives ranging from approximately 6 to 23 times longer than the half lives of the homoserine lactone headgroup at varying pH values (Figure 3.3).

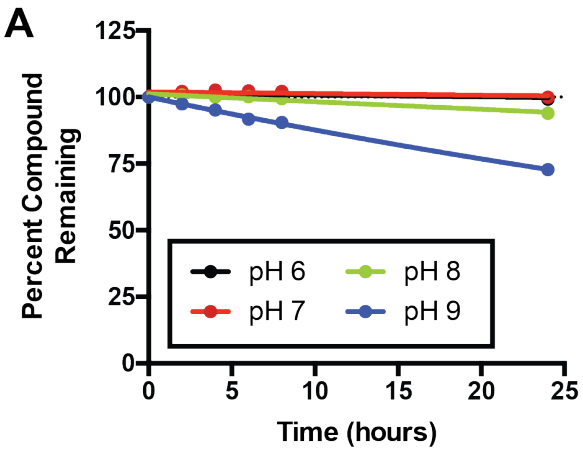

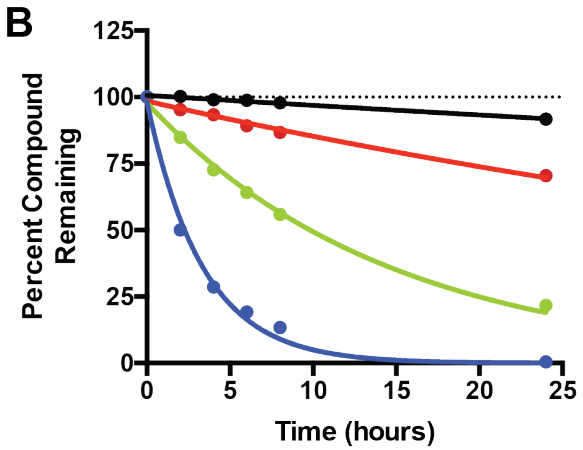

C

	Half Life (hours)			
Compound	**pH 6**	**pH 7**	**pH 8**	**pH 9**
42	1100	1100	240	52
E22	180	48	10	2.3

Figure 3.3. Compound degradation at varying pH values over time for (A) homocysteine thiolactone **42** and (B) homoserine lactone **E22** and resulting half lives (C) as reported via HPLC. MS data is reported in Table 3.5.

The results of these stability studies for **42** and **E22** contradict data supporting the thermodynamic favorability of alkyl thioester hydrolysis.[26] However, thioesters are known to have slow rates of hydrolysis, and published rate constants have typically been for electronically activated thioesters (e.g., trifluorothioacetate).[27] In the compounds tested here, homocysteine thiolactone ring size may also play a crucial role in the observed stability. Previous studies comparing homocysteine thiolactones and homoserine lactones in aqueous acetone solutions

showed that homoserine lactones hydrolyze at a two-fold faster rate.[28] The resulting γ-mercapto acids from homocysteine thiolactone hydrolysis also readily recyclize upon acid exposure; thiolactones with larger ring sizes are far less likely to recyclize.[29] The stability results for **42** and **E22** (Figure 3.3) thus support these past reports on the kinetics of homocysteine thiolactone hydrolysis. As previous studies have also highlighted the stability of homocysteine thiolactones over homoserine lactones in the presence of bacterial lactonases,[18] we believe that our homocysteine thiolactone compounds (i.e., **35**, **37**, and **42**) constitute physically robust probes for the study of *P. aeruginosa* QS in a variety of environments.

3.4 Summary

This study was motivated by our interest in the RhlR QS receptor in the pathogen *P. aeruginosa*. This LuxR-type receptor plays a prominent role in the infection process, and both antagonism and agonism of RhlR have been shown to negatively regulate important virulence phenotypes. While prior chemical efforts have delivered synthetic ligands for RhlR, the most potent of these compounds are all lactone based and suffer from low hydrolytic stability. We designed a suite of new compounds that integrated the structures of these lead compounds with alternate head groups, and evaluated them in cell-based reporter assays for RhlR activity. The most promising compounds identified contain homocysteine thiolactones (**35**, **37**, and **42**) and showed improved hydrolytic stabilities relative to lactone analogs. Moreover, they were highly selective for RhlR over another key QS receptor in *P. aeruginosa*, LasR, and are active in the *P. aeruginosa* background. Homocysteine thiolactones (**35**, **37**, and **42**) represent the most potent RhlR modulators known and new tools to investigate the role of RhlR in QS regulation. Moreover, they underscore the utility of the thiolactone motif for LuxR-type receptor ligand design.

3.5 Methods

3.5.1 Chemistry

AHL library compounds were synthesized and purified using our previously reported procedures.[17, 30]

3.5.2 Bacteriology methods

Bacteria were cultured in Luria−Bertani medium (LB) at 37 °C. Absorbance measurements were performed in 96-well microtiter plates and pathlength-corrected using a Biotek Synergy 2 plate reader running Gen 5 software (version 1.05). Bacterial growth was assessed by measuring absorbance at 600 nm (OD_{600}).

3.5.3 Bacterial strains and assay protocols

The bacterial reporter strains used for this study were (i) *E. coli* strain JLD271 (Δ*sdiA*) harboring the RhlR expression plasmid pJN105R2 and the *rhlI-lacZ* transcriptional fusion reporter pSC11-rhlI*, (ii) *E. coli* strain JLD271 (Δ*sdiA*) harboring the LasR expression plasmid pJN105L and the *lasI-lacZ* transcriptional fusion reporter pSC11, and (iii) the *P. aeruginosa* strain PAO-JP2 (Δ*lasIrhlI*) harboring the *rhlI-gfp* transcriptional fusion reporter p*rhlI*-LVA*gfp*. Miller assays and GFP fluorescence assays were performed in these *E. coli* and *P. aeruginosa* reporters as previously described.[17, 31]

3.5.4 Homocysteine thiolactone/homoserine lactone stability studies

Homocysteine thiolactone and homoserine lactone stability studies were performed as reported previously,[31] with the following modifications: compounds (50 μM) were dissolved in either 1 mM 2-(N-morpholino)ethanesulfonic acid (MES) buffer at pH 6, or 1 mM tris(hydroxymethyl)aminomethane (TRIS) buffer at pH 7, 8, or 9. Solutions were stored at room temperature, and 150 μL aliquots were taken out every 2 h for 8 h, then again at 24 h. Samples

were immediately analyzed via HPLC, and the area under the curve (AUC) at 220 nm was calculated and compared to the area at t = 0. Caffeine (50 μM) was added as an internal standard and maintained the same AUC throughout the assay (error ≤ 1-5%). Degradation of both compounds to the hydrolysis product was confirmed via mass spectrometry (MS) of the resulting byproduct peak.

3.6 Supplemental Information

3.6.1 General chemical information

All chemical reagents and solvents were purchased from commercial sources and used without further purification, except for dichloromethane (DCM), which was distilled and dried over activated molecular sieves. Water (18 MΩ) was purified using a Thermo Scientific Barnstead Nanopure system. Chlorophenol red-β-D-galactopyranoside (CPRG) was purchased from Roche. Ortho-nitrophenyl-β-galactoside (ONPG) was purchased from Sigma Aldrich. All media and reagents for bacterial culture were purchased from commercial sources.

3.6.2 Instrumentation and analytical methods

NMR spectra were recorded in deuterated NMR solvents at 300 MHz on a Varian MercuryPlus 300 spectrometer, at 400 MHz on a Bruker Avance-400 spectrometer with SmartProbe and SampleJet, or at 500 MHz on a Bruker Avance-500 spectrometer with DCH cryoprobe and SampleXpress. Chemical shifts are reported in parts per million (ppm, δ) using corresponding solvents or tetramethylsilane (TMS) as a reference. Couplings are reported in hertz (Hz). Electrospray ionization MS measurements were performed on a Waters LCT. Samples were dissolved in acetonitrile and sprayed with a sample cone voltage of 20. For exact mass measurements (EMM), an aliquot of a known compound (lock mass) was added to the sample and resprayed.

Reversed-phase high performance liquid chromatography (RP-HPLC) was performed using a Shimadzu system equipped with a SCL-10Avp controller, a LC-20AT pump, a SIL-10AF autosampler, a CTO-20A oven, and a SPD-M20A UV/vis diode array detector. A Phenomenex Gemini C18 column (5 μm, 4.6 mm x 250 mm) was used for all analytical RP-HPLC work. Standard RP-HPLC conditions were as follows: flow rates were 1 mL min^{-1} for analytical separations; mobile phase A = 18 MΩ water + 0.1% TFA; mobile phase B = acetonitrile + 0.1% TFA. Purities were determined by integration of peaks with UV detection at 220 nm. For all compounds and stability studies, the method was as follows: (i) start with isocratic 10% B (3 min), (ii) followed by a linear gradient from 10% to 95% B (27 min), and (iii) end with isocratic 95% B (2 min). Curves generated for stability studies were analyzed using a one phase decay curve fit.

FT-IR spectra were recorded with a Bruker Tensor 27 IR spectrometer outfitted with a single reflection MIRacle Horizontal attenuated total reflectance (ATR) unit from Pike Technologies. A ZnSe crystal with spectral range 20,000 to 650 cm^{-1} was used for ATR-IR measurements.

3.6.3 Compound characterization data

^{1}H and ^{13}C NMR, ESI MS, and IR data are reported below for all new compounds and select intermediates. Characterization data for compound **38** is included as it has not been fully characterized in past studies reporting this structure.[32]

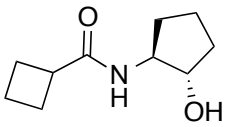

Alcohol precursor to **34**: ^{1}H NMR (400 MHz, $CDCl_3$) δ 5.71 (s, 1H), 4.80 (s, 1H), 3.91 (q, *J* = 6.7 Hz, 1H), 3.78 (ddt, *J* = 14.3, 8.8, 5.3 Hz, 1H), 3.00 (p, *J* = 8.5 Hz, 1H), 2.26 – 1.61 (m, 11H), 1.40 (dq, *J* = 12.8, 8.3 Hz, 1H); ^{13}C NMR (126 MHz, $CDCl_3$) δ 177.4, 80.0, 61.1, 39.7, 32.8, 30.7, 25.6, 25.5, 21.5, 18.2; Expected $[M+H]^+$: 184.1332, observed: 184.1331; IR (cm^{-1}): 3275, 2941, 2866, 1635, 1548, 1258, 685.

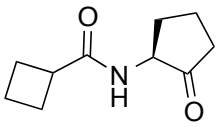

34: ^{1}H NMR (300 MHz, $CDCl_3$) δ 5.79 (s, 1H), 4.22 – 3.96 (m, 1H), 3.15 – 2.90 (m, 1H), 2.76 – 2.55 (m, 1H), 2.47 – 1.76 (m, 11H), 1.57 (qd, *J* = 12.3, 6.9 Hz, 1H); ^{13}C NMR (101 MHz, $CDCl_3$) δ 215.6, 175.5, 58.2, 39.7, 35.1, 30.4, 25.5, 25.4, 18.3, 18.2; Expected $[M+H]^+$: 182.1176, observed: 182.1176; IR (cm^{-1}): 3250, 2923, 2859, 1742, 1635, 1548, 1270.

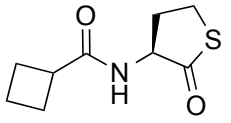

35: ^{1}H NMR (400 MHz, $CDCl_3$) δ 6.08 (d, 1H), 4.51 (dt, *J* = 13.1, 6.7 Hz, 1H), 3.33 (td, *J* = 11.8, 5.2 Hz, 1H), 3.21 (dd, *J* = 11.1, 6.7 Hz, 1H), 3.04 (p, *J* = 8.5 Hz, 1H), 2.92 – 2.78 (m, 1H), 2.34 – 2.06 (m, 4H), 2.00 – 1.76 (m, 3H); ^{13}C NMR (126 MHz, $CDCl_3$) δ 205.8, 175.6, 59.6, 39.8, 32.4, 27.8, 25.5, 25.5,18.3; Expected $[M+H]^+$: 200.0740, observed: 200.0739; IR (cm^{-1}): 3250, 2975, 2933, 1686, 1637, 1552, 1257, 913.

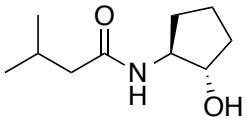

Alcohol precursor to **36**: ^{1}H NMR (500 MHz, $CDCl_3$) δ 5.56 (s, 1H), 4.60 (s, 1H), 3.95 (q, *J* = 6.4 Hz, 1H), 3.89 – 3.73 (m, 1H), 2.19 – 1.97 (m, 5H), 1.80 (dtdd, *J* = 12.5, 9.2, 6.4, 2.7 Hz, 1H), 1.75 – 1.62 (m, 2H), 1.41 (dq, *J* = 12.8, 8.3 Hz, 1H), 0.97 (dd, *J* = 6.3, 1.0 Hz, 6H); ^{13}C NMR (126 MHz, $CDCl_3$) δ 175.0, 80.1, 61.2, 45.8, 32.8, 30.8, 26.4, 22.6, 22.5, 21.6; Expected $[M+H]^+$: 186,1489, observed: 186.1487; IR (cm^{-1}): 3286, 3088, 2953, 2925, 2867, 1636, 1551, 1049.

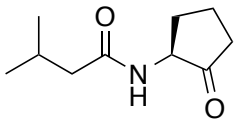

36: ^{1}H NMR (300 MHz, $CDCl_3$) δ 5.84 (s, 1H), 4.24 – 3.98 (m, 1H), 2.66 (dddd, *J* = 14.0, 7.9, 3.7, 1.6 Hz, 1H), 2.49 – 2.34 (m, 1H), 2.27 – 1.99 (m, 5H), 1.86 (tddd, *J* = 13.0, 10.7, 8.9, 6.1 Hz, 1H), 1.58 (qd, *J* = 12.3, 6.9 Hz, 1H), 0.95 (dd, *J* = 6.5, 3.2 Hz, 5H); ^{13}C NMR (126 MHz, $CDCl_3$) δ 215.4, 173.0, 58.3, 45.8, 35.0, 30.3, 26.3, 22.6, 22.5, 18.2; Expected $[M+H]^+$: 184.1332, observed: 184.1331; IR (cm^{-1}): 3256, 3073, 2958, 2869, 1748, 1637, 1550, 1372.

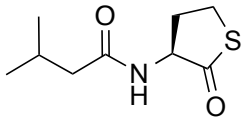

37: ^{1}H NMR (300 MHz, $CDCl_3$) δ 6.04 (s, 1H), 4.53 (dt, *J* = 12.9, 6.5 Hz, 1H), 3.35 (td, *J* = 11.7, 5.1 Hz, 1H), 3.29 – 3.16 (m, 1H), 2.99 – 2.83 (m, 1H), 2.08 (d, *J* = 6.5 Hz, 3H), 1.91 (qd, *J* = 12.4, 7.0 Hz, 1H), 1.00 – 0.88 (m, 6H); ^{13}C NMR (126 MHz, $CDCl_3$) δ 205.8, 173.1, 59.5, 45.8, 32.2, 27.7, 26.3, 22.6, 22.5; Expected $[M+H]^+$: 202.0896, observed: 202.0893; IR (cm^{-1}): 3267, 3071, 2952, 2924, 2866, 1690, 1638, 1548, 917.

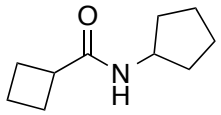

38: ^{1}H NMR (400 MHz, $CDCl_3$) δ 5.81 (d, 1H), 4.09 (h, *J* = 7.1 Hz, 1H), 2.91 (p, *J* = 8.4 Hz, 1H), 2.18 (pd, *J* = 9.2, 2.3 Hz, 2H), 2.07 – 1.95 (m, 2H), 1.94 – 1.68 (m, 4H), 1.66 – 1.40 (m, 4H), 1.28 (dq, *J* = 14.1, 7.5, 7.0 Hz, 2H); ^{13}C NMR (126 MHz, $CDCl_3$) δ 174.6, 51.1, 40.2, 33.4, 25.5, 23.9, 18.2; Expected $[M+H]^+$: 168.1383, observed: 168.1381; IR (cm^{-1}): 3290, 2946, 2865, 1636, 1545,1257, 678.

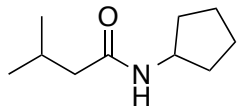

39: ^{1}H NMR (500 MHz, $CDCl_3$) δ 5.31 (d, *J* = 10.9 Hz, 1H), 4.22 (h, *J* = 7.0 Hz, 1H), 2.10 (dp, *J* = 13.2, 6.6 Hz, 1H), 2.03 – 1.94 (m, 4H), 1.71 – 1.54 (m, 4H), 1.42 – 1.28 (m, 2H), 0.94 (d, *J* = 6.6 Hz, 6H); ^{13}C NMR (126 MHz, $CDCl_3$) δ 172.1, 51.2, 46.5, 33.4, 26.4, 23.8, 22.6; Expected $[M+H]^+$: 170.1539, observed: 170.1537; IR (cm^{-1}): 297, 3073, 2954, 2868, 1633, 1541.

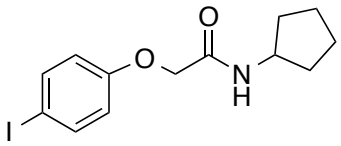

40: ^{1}H NMR (400 MHz, $CDCl_3$) δ 7.59 (d, *J* = 8.7 Hz, 2H), 6.70 (d, *J* = 8.7 Hz, 2H), 6.39 (s, 1H), 4.42 (s, 2H), 4.29 (h, *J* = 7.0 Hz, 1H), 2.01 (dd, *J* = 12.4, 5.7 Hz, 2H), 1.66 (dt, *J* = 19.4, 7.9 Hz, 4H), 1.41 (dd, *J* = 12.6, 6.3 Hz, 2H); ^{13}C NMR (101 MHz, $CDCl_3$) δ 167.2, 157.2, 138.7, 117.1, 84.6, 67.6, 50.9, 33.1, 23.8; Expected $[M+H]^+$: 346.0299, observed: 346.0290; IR (cm^{-1}): 3271, 2925, 2865, 1647, 1553, 1482, 1453, 1234, 843.

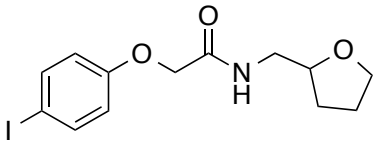

41: ^{1}H NMR (500 MHz, $CDCl_3$) δ 7.60 – 7.53 (m, 2H), 6.88 – 6.77 (m, 1H), 6.75 – 6.66 (m, 2H), 4.46 (s, 2H), 3.98 (qd, *J* = 7.1, 3.4 Hz, 1H), 3.86 – 3.69 (m, 2H), 3.61 (ddd, *J* = 13.8, 6.4, 3.4 Hz,

1H), 3.32 – 3.21 (m, 1H), 2.01 – 1.90 (m, 1H), 1.86 (dq, *J* = 14.0, 6.9, 6.4 Hz, 2H), 1.51 (dq, *J* = 12.1, 7.6 Hz, 1H); ^{13}C NMR (126 MHz, $CDCl_3$) δ 167.9, 157.2, 138.7, 117.1, 84.5, 77.6, 68.4, 67.5, 42.7, 28.7, 26.0; Expected $[M+H]^+$: 362.0248, 362.0241; IR (cm^{-1}): 3277, 2969, 2924, 2864, 1655, 1547, 1481, 1240, 1058

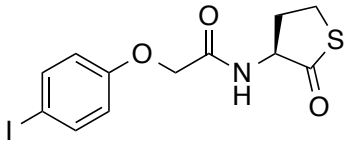

42: ^{1}H NMR (500 MHz, $CDCl_3$) δ 7.70 – 7.48 (m, 2H), 6.94 (d, *J* = 7.6 Hz, 1H), 6.77 – 6.68 (m, 2H), 4.61 (dt, *J* = 13.2, 6.7 Hz, 1H), 4.50 (d, *J* = 2.6 Hz, 2H), 3.39 (td, *J* = 11.8, 5.1 Hz, 1H), 3.32 – 3.27 (m, 1H), 3.02 – 2.88 (m, 1H), 2.01 (qd, *J* = 12.4, 7.0 Hz, 1H); ^{13}C NMR (126 MHz, $CDCl_3$) δ 204.7, 168.4, 157.0, 138.8, 117.2, 84.9, 67.4, 59.1, 31.8, 27.7; Expected $[M+H]^+$: 377.9655, observed: 377.9650; IR (cm^{-1}): 3282, 2974, 2926, 2858, 1696, 1655, 1536, 1233

Table 3.3. Complete primary RhlR agonism and antagonism data for BHL and AHL analogs in this study.[a]

Compound	% activation (10 μM)[b]	% activation (1 mM)[c]	% inhibition (10 μM)[d]	% inhibition (1 mM)[e]
BHL	51	100	–	–
S4	76	94	-52	-95
34	56	101	-39	-98
35	88	103	-85	-114
36	42	84	-35	-122
37	85	92	-59	-81
38	0	34	24	25
39	0	20	11	31
40[g]	1	1	6	24
41	0	0	6	61
42	1	7	28	74

[a]Assays performed using the *E. coli* RhlR reporter strain JLD271/pJN105R2/pSC11-*rhlI**. SEM of n ≥ 3 trials did not exceed ± 10%. [b]Library compounds were screened at 10 μM. RhlR activity was measured relative to that of 1 mM BHL. [c]Library compounds were screened at 1 mM. RhlR activity was measured relative to that of 1 mM BHL. [d]Library compounds were screened at 10 μM in the presence of 10 μM BHL. Negative numbers indicate agonism stronger than that of 10 μM BHL alone. [e]Library compounds were screened at 1 mM in the presence of 10 μM BHL. Negative numbers indicate agonism stronger than that of 10 μM BHL alone. [f]Screened at a maximal concentration of 200 μM due to solubility concerns at higher concentrations. [g]Screened at a maximal concentration of 100 μM due to solubility concerns at higher concentrations.

Table 3.4. Complete primary LasR agonism and antagonism data for BHL, OdDHL, and AHL analogs in this study.[a]

Compound	% activation (10μM)[b]	% activation (1 mM)[c]	% inhibition (10 μM)[d]	% inhibition (1 mM)[e]
BHL	1	6	-2	35
OdDHL[f]	100	100	–	–
S4	6	21	19	32
34	0	15	16	60
35	0	10	18	63
36	0	0	-7	53
37	0	7	25	63
38	0	0	-2	22
39	1	1	-2	13
40[g]	3	1	11	2
41	11	0	-16	58
42	35	53	18	-14

[a]Assays performed using the *E. coli* LasR reporter strain JLD271/pJN105L/pSC11. SEM of n ≥ 3 trials did not exceed ± 10%. [b]Library compounds were screened at 10 μM. LasR activity was measured relative to that of 100 μM OdDHL. [c]Library compounds were screened at 1 mM. LasR activity was measured relative to that of 100 μM OdDHL. [d]Library compounds were screened at 10 μM in the presence of 2 nM OdDHL. Negative numbers indicate agonism stronger than that of 2 nM OdDHL alone. [e]Library compounds were screened at 1 mM in the presence of 2 nM OdDHL. Negative numbers indicate agonism stronger than that of 2 nM OdDHL alone. [f]Screened at a maximal concentration of 200 μM due to solubility concerns at higher concentrations. [g]Screened at a maximal concentration of 100 μM due to solubility concerns at higher concentrations.

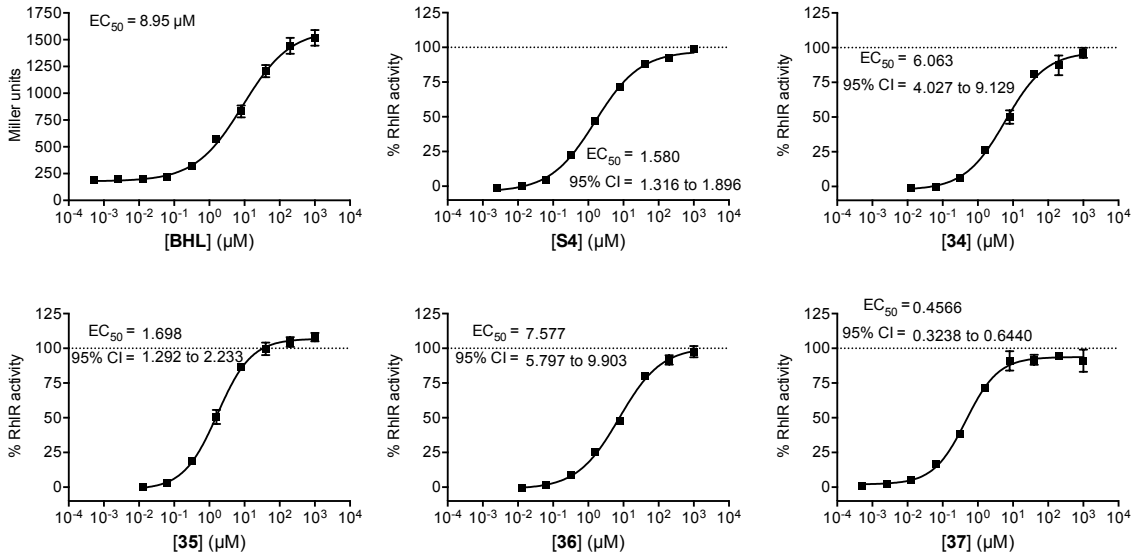

Figure 3.4. Dose–response curves for RhlR agonism in E. coli by BHL and lead agonist AHLs.

Assay performed using the *E. coli* JLD271/pJN105R2/pSC11-rhlI* reporter strain. % Activity is defined as the activity of the synthetic AHL relative to maximum possible RhlR activity (i.e., activity effected by BHL at 1 mM). EC_{50} values and 95% Confidence Intervals (CI; shown on each plot) calculated using GraphPad Prism. Error bars, SEM of $n \geq 3$ trials.

Note: Comments on Hill slopes for RhlR agonist dose response curves in *E. coli* and *P. aeruginosa.*

The dose-response curves of **BHL** and **S4** are shallower (Hill slope = 0.7) in the *E. coli* RhlR reporter strain (Hill slope = ~1.0) than curves for other AHL ligands in related LuxR-type receptor report strains. Shallow dose–response curves are often indicative of negative cooperativity of the small molecule binding to multiple sites on the receptor.[33] Since RhlR functions as a dimer, this negative cooperativity scenario is feasible if binding of an agonist to RhlR reduces binding affinity of the second dimer site for the agonist.

For lead hybrid agonists **34** and **36** the Hill slope in the dose response curves remained similar to previous agonists (~0.7). However, compounds **35** and **37** displayed slopes much closer to ~1.0. As this slope is more typical for LuxR-type receptor-ligand binding, it is plausible the thiolactone hybrids are not reducing the binding affinity of the second AHL upon binding. Further kinetic studies are required to determine whether this change in Hill slope is representative of a unique mechanism of action. Additionally, all dose–response curves in the *P. aeruginosa* background had Hill slopes much closer to 1.0 (Figure 3.5), suggesting that the shallow dose–response relationships common in the *E. coli* reporter may simply be artifacts of heterologous expression.

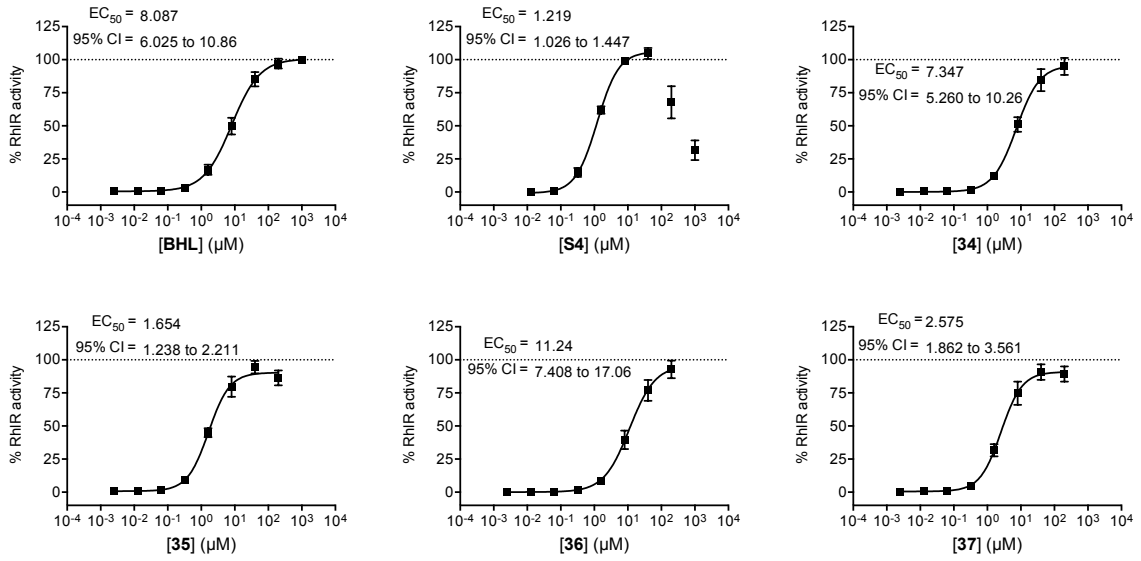

Figure 3.5. Dose–response curves for RhlR agonism in P. aeruginosa by BHL and lead agonist AHLs.
Assays performed using the *P. aeruginosa* PAO-JP2/p*rhlI*-LVA*gfp* reporter strain. % Activity is defined as the activity of the synthetic AHL relative to maximum possible RhlR activity (i.e., activity effected by BHL at 1 mM). The EC_{50} values for the synthetic compounds were calculated from the region of the dose–response curve that indicated RhlR agonism. EC_{50} values and associated 95% Confidence Intervals (CI; shown on each plot) calculated using GraphPad Prism. Error bars, SEM of $n \geq 3$ trials.

Note: Comments on non-monotonic dose response curves for RhlR agonists in *P. aeruginosa*

We note that compounds **S4** displays non-monotonic dose behavior in the *P. aeruginosa* reporter (*e.g.*, curves that increase in activity at low concentrations, followed by a decrease at high concentrations—often referred to as an "inverted U-shape" curve). Hybrid compounds **34**–**37** do not have non-monotonic dose curves, suggesting that the modified head group may contribute to this alternate behavior.

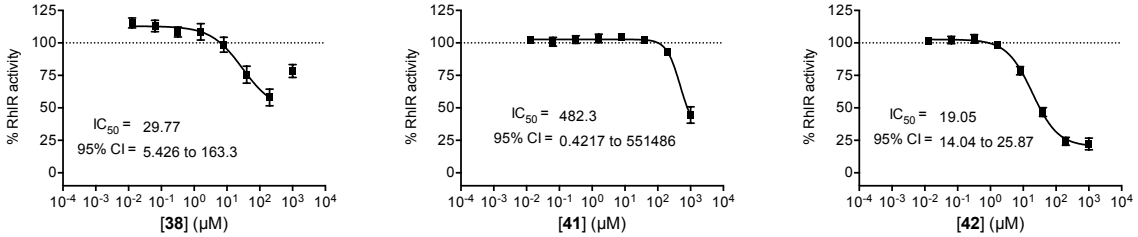

Figure 3.6. Dose–response curves for RhlR antagonism in E. coli by lead antagonist AHLs.
Assay performed using the *E. coli* JLD271/pJN105R2/pSC11-rhlI* reporter strain with the addition of 10 μM BHL. % Activity is defined as the activity of the synthetic AHL relative to half maximal RhlR activity (i.e., activity effected by BHL at 10 μM). IC_{50} values and 95% Confidence Intervals (CI; shown on each plot) calculated using GraphPad Prism. Error bars, SEM of $n \geq 3$ trials.

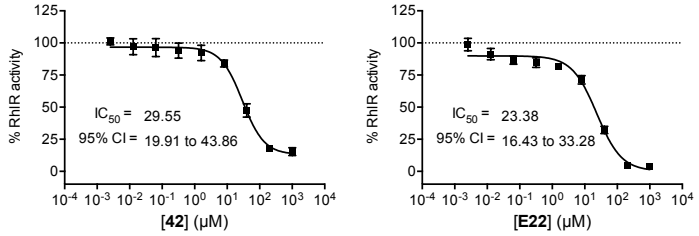

Figure 3.7. Dose–response curves for RhlR antagonism in P. aeruginosa by antagonist AHLs.
Assays performed using the *P. aeruginosa* PAO-JP2/p*rhlI*-LVA*gfp* reporter strain with the addition of 10 μM BHL. % Activity is defined as the activity of the synthetic AHL relative to half maximal RhlR activity (i.e., activity effected by BHL at 10 μM). The IC_{50} values for the synthetic compounds were calculated from the region of the dose–response curve that indicated RhlR agonism. IC_{50} values and associated 95% Confidence Intervals (CI; shown on each plot) calculated using GraphPad Prism. Error bars, SEM of $n \geq 3$ trials.

Table 3.5. Mass spectroscopy data for degradation peak collected via HPLC

Compound	Expected $[M-H]^-$	Observed
42	377.9844	377.9845
E22	393.9615	393.9613

3.6.4 HPLC traces indicating compound stability.

Compound **E22** at pH 6.

Caffeine retention time (t_R): 12.1 min; **E22** t_R: 22.5 min; hydrolysis product t_R: 19.6 min

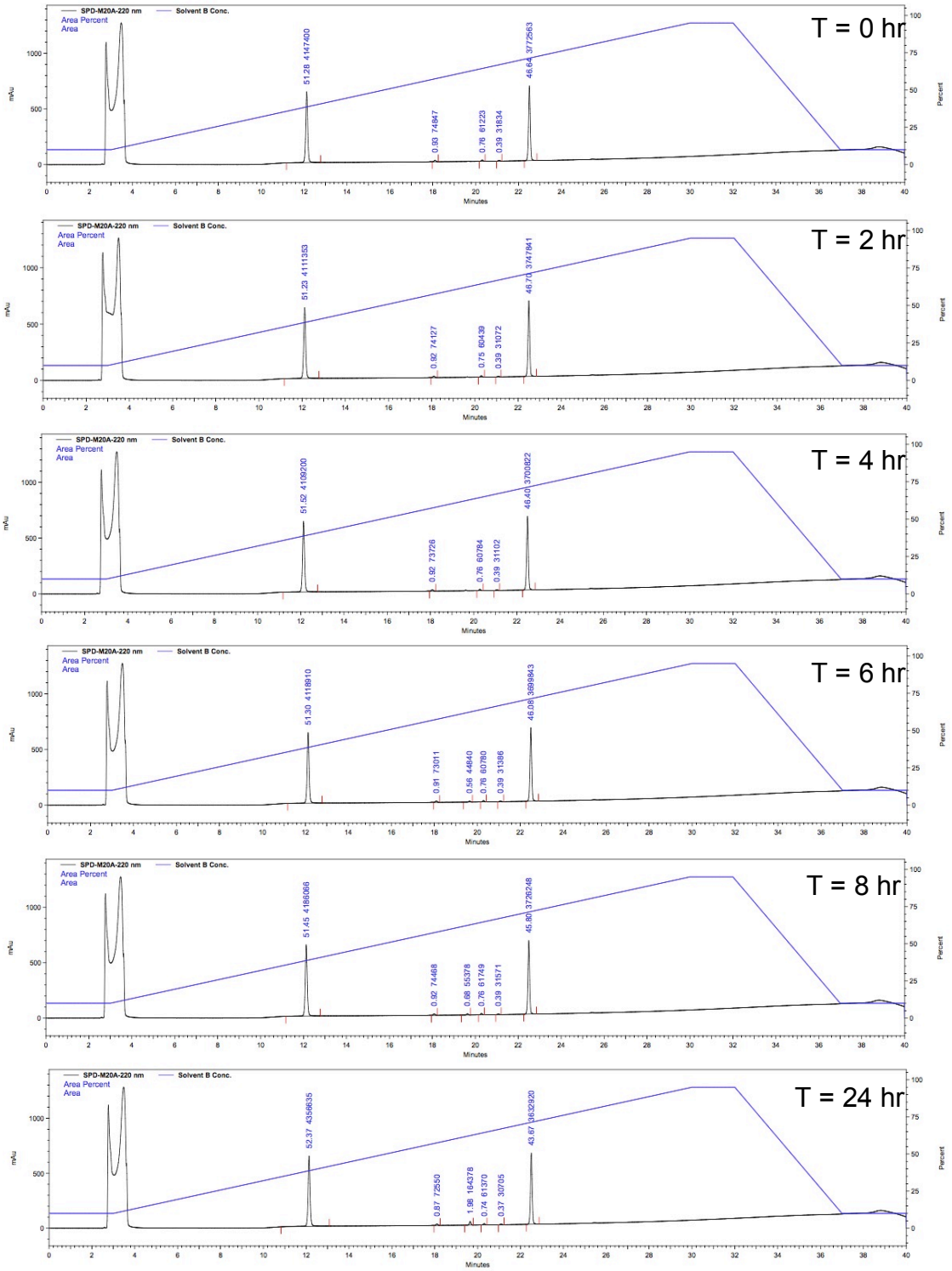

Time	0 Hours	2 Hours	4 Hours	6 Hours	8 Hours	24 Hours
% Remaining	100	100	99	99	98	92

Compound **42** at pH 6.

Caffeine t_R: 12.1 min; **42** t_R: 24.7 min; hydrolysis product t_R: 23.5 min

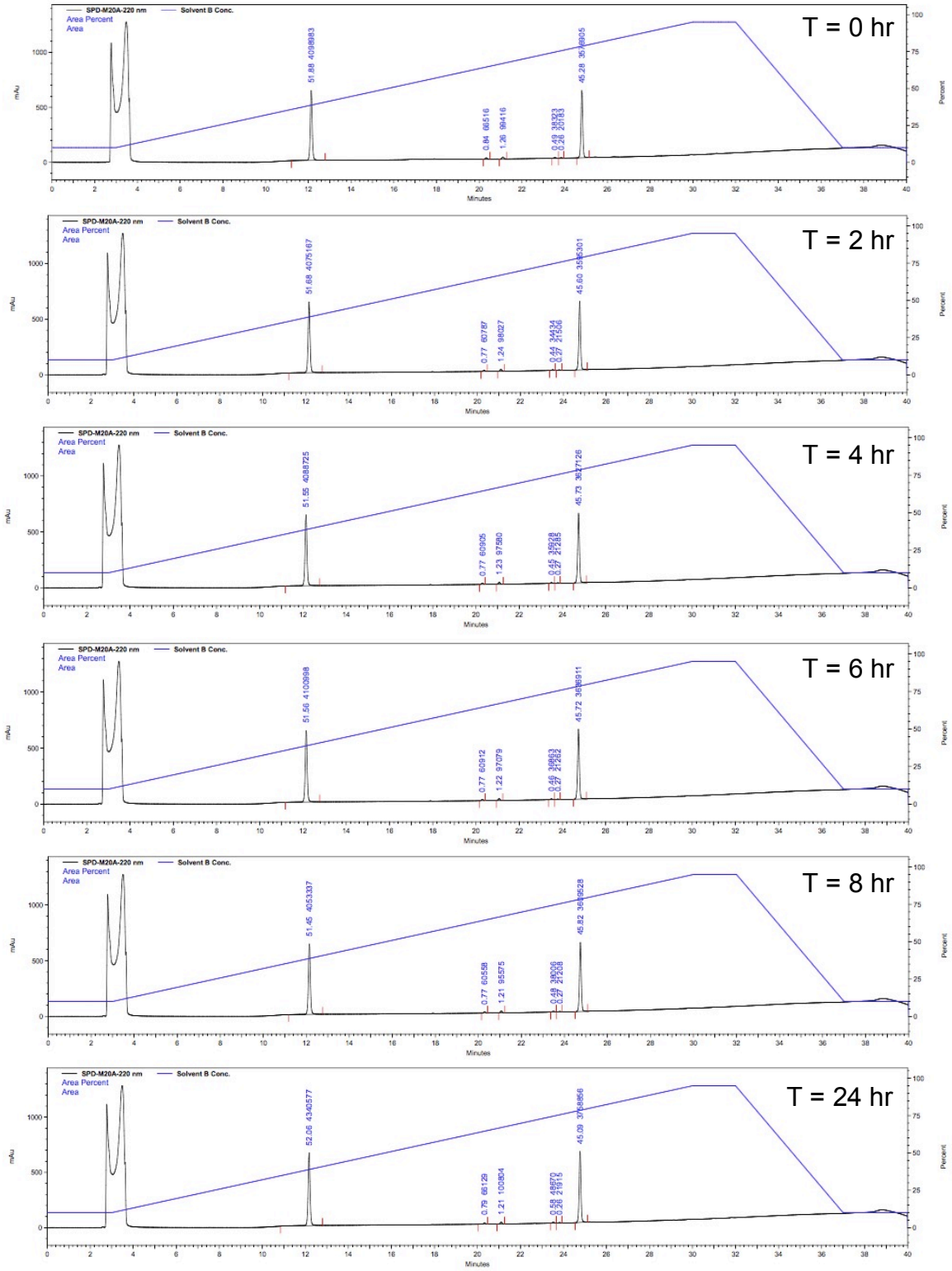

Time	0 Hours	2 Hours	4 Hours	6 Hours	8 Hours	24 Hours
% Remaining	100	100	100	100	100	99

Compound **E22** at pH 7.

Caffeine t_R: 12.1 min; **E22** t_R: 22.5 min; hydrolysis product t_R: 19.6 min

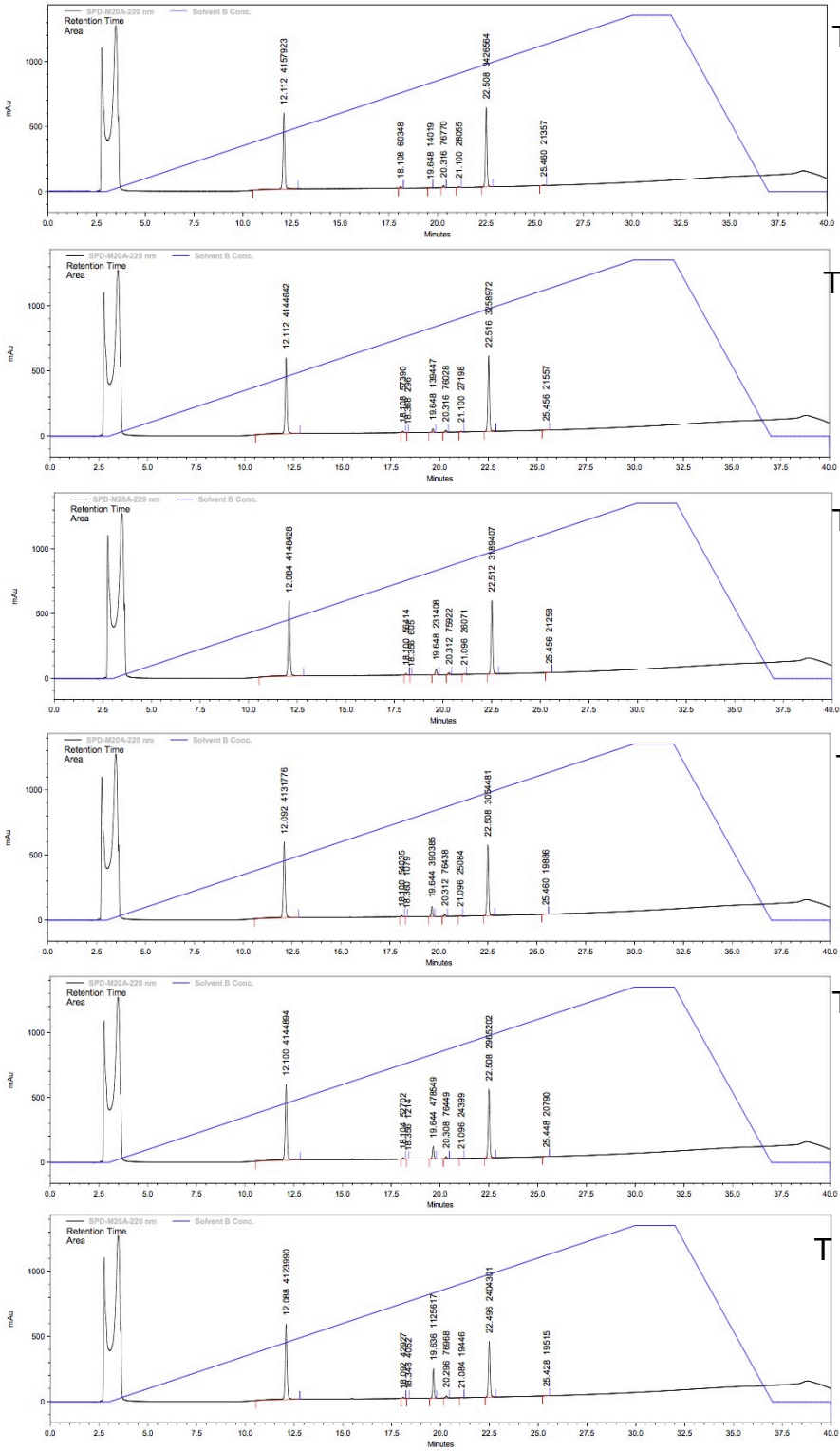

Time	0 Hours	2 Hours	4 Hours	6 Hours	8 Hours	24 Hours
% Remaining	100	95	93	89	87	70

Compound **42** at pH 7.

Caffeine t_R: 12.1 min; **42** t_R: 24.7 min; hydrolysis product t_R: 23.5 min

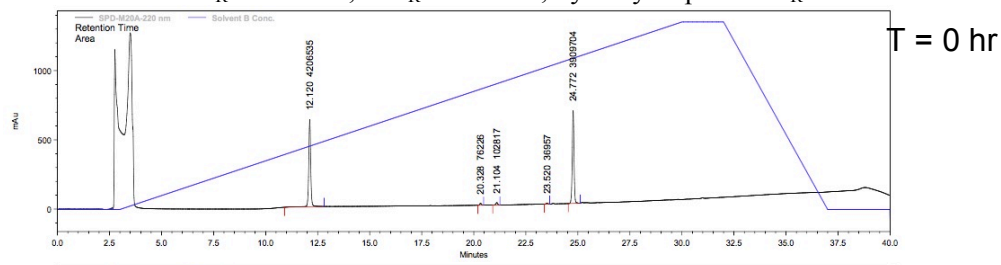

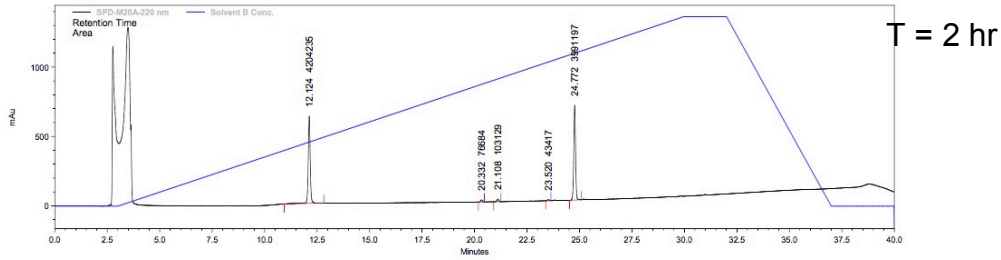

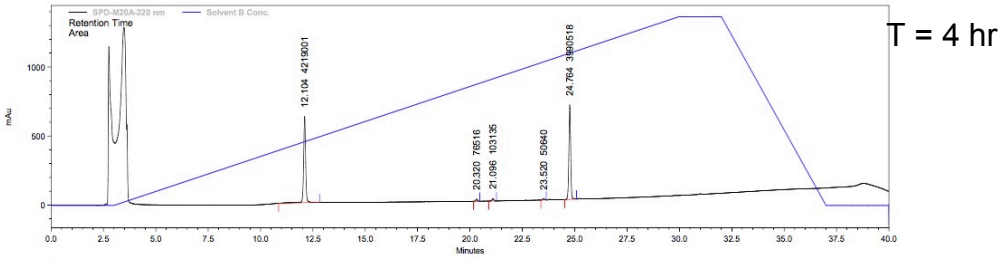

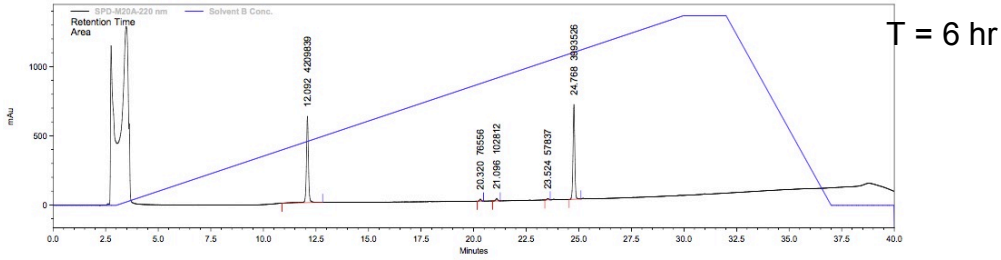

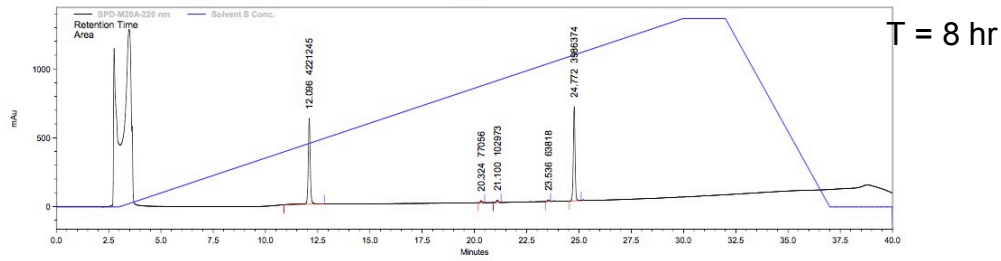

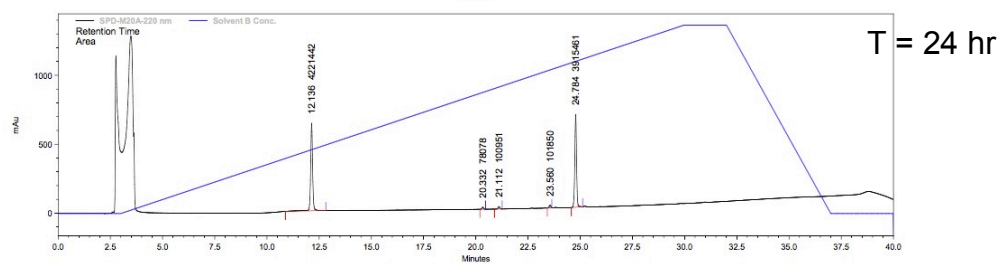

Time	0 Hours	2 Hours	4 Hours	6 Hours	8 Hours	24 Hours
% Remaining	100	100	100	100	100	100

Compound **E22** at pH 8.

Caffeine t_R: 12.1 min; **E22** t_R: 22.5 min; hydrolysis product t_R: 19.6 min

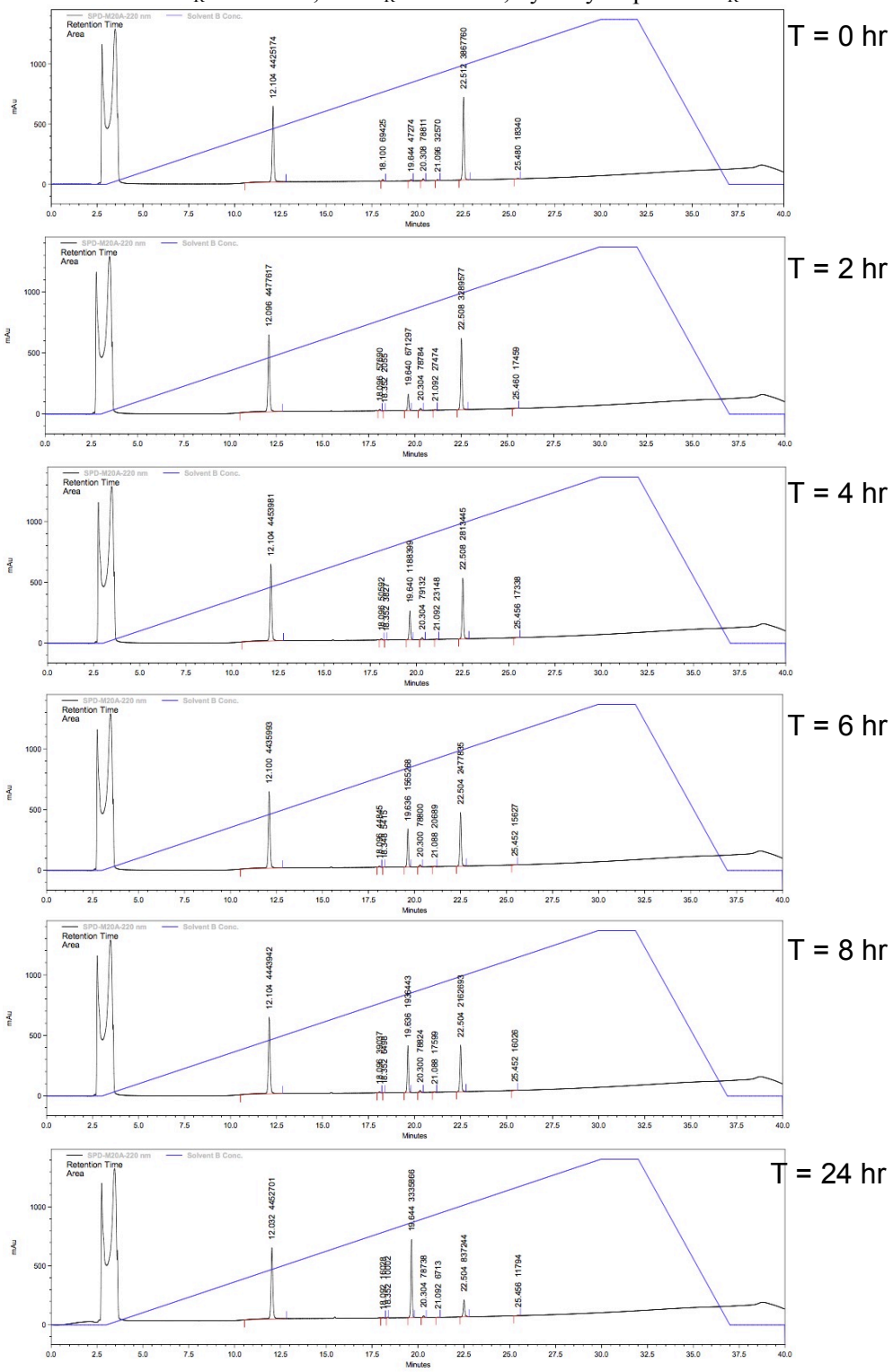

Time	0 Hours	2 Hours	4 Hours	6 Hours	8 Hours	24 Hours
% Remaining	100	85	73	64	56	22

Compound **42** at pH 8.

Caffeine t_R: 12.1 min; **42** t_R: 24.7 min; hydrolysis product t_R: 23.5 min

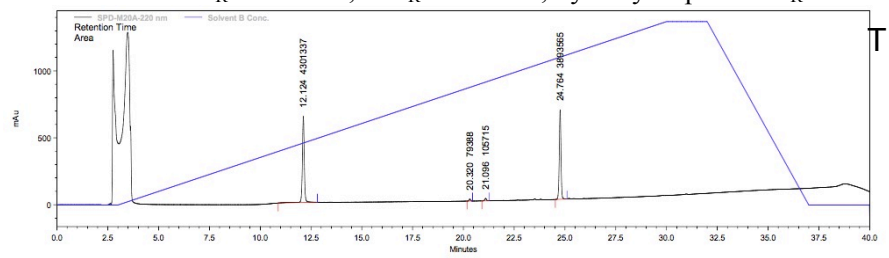

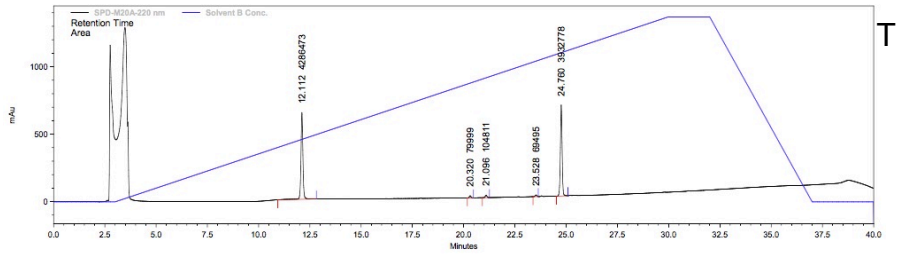

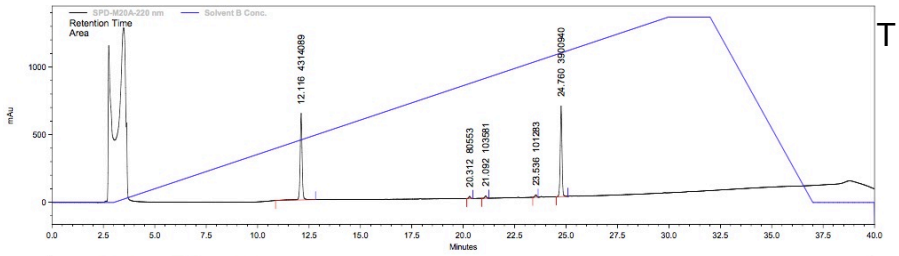

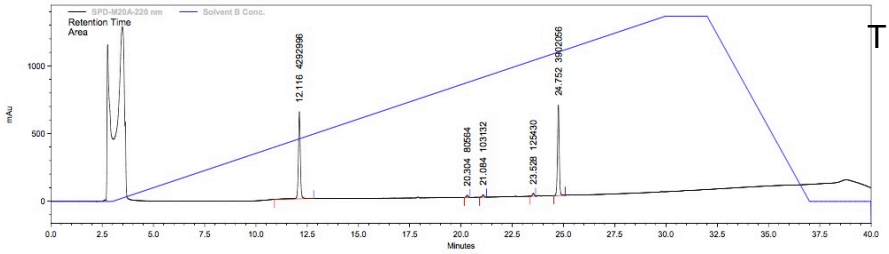

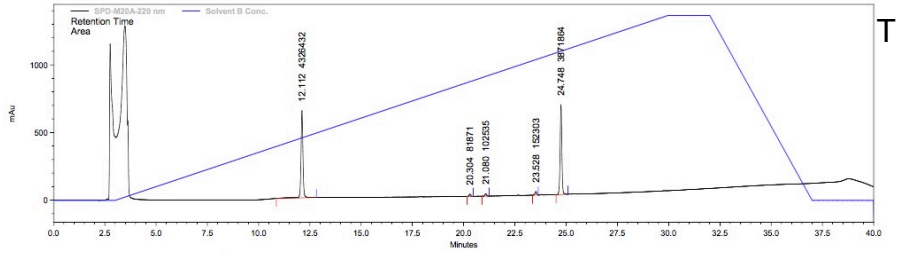

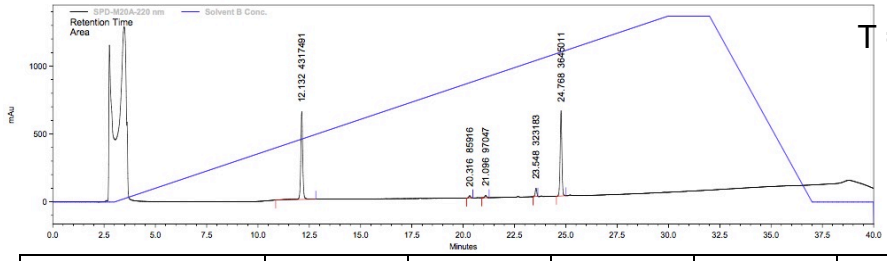

Time	0 Hours	2 Hours	4 Hours	6 Hours	8 Hours	24 Hours
% Remaining	100	100	100	100	99	94

Compound **E22** at pH 9.

Caffeine t_R: 12.1 min; **E22** t_R: 22.5 min; hydrolysis product t_R: 19.6 min

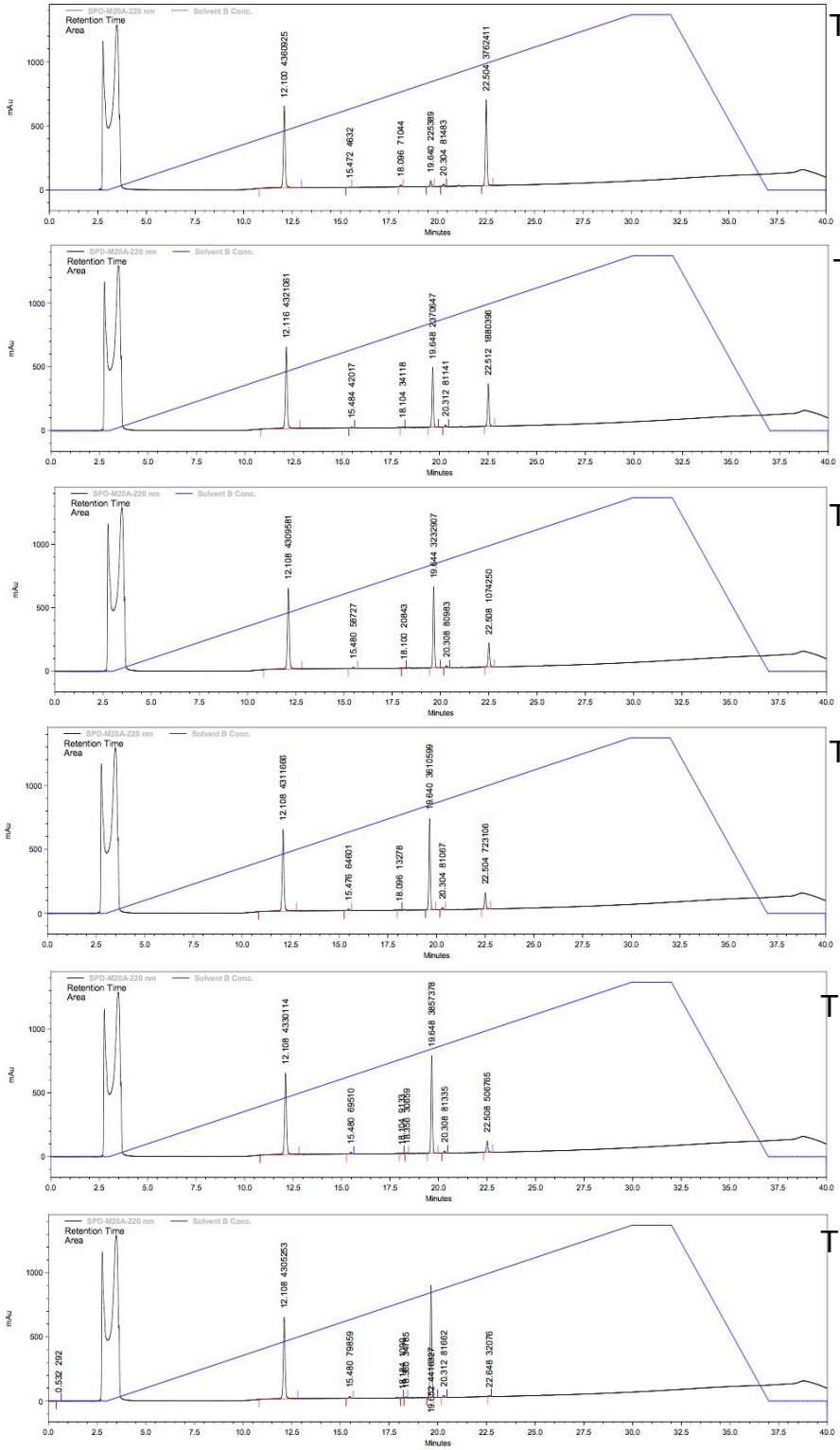

Time	0 Hours	2 Hours	4 Hours	6 Hours	8 Hours	24 Hours
% Remaining	100	50	29	19	13	0

Compound **42** at pH 9.

Caffeine t_R: 12.1 min; **42** t_R: 24.7 min; hydrolysis product t_R: 23.5 min

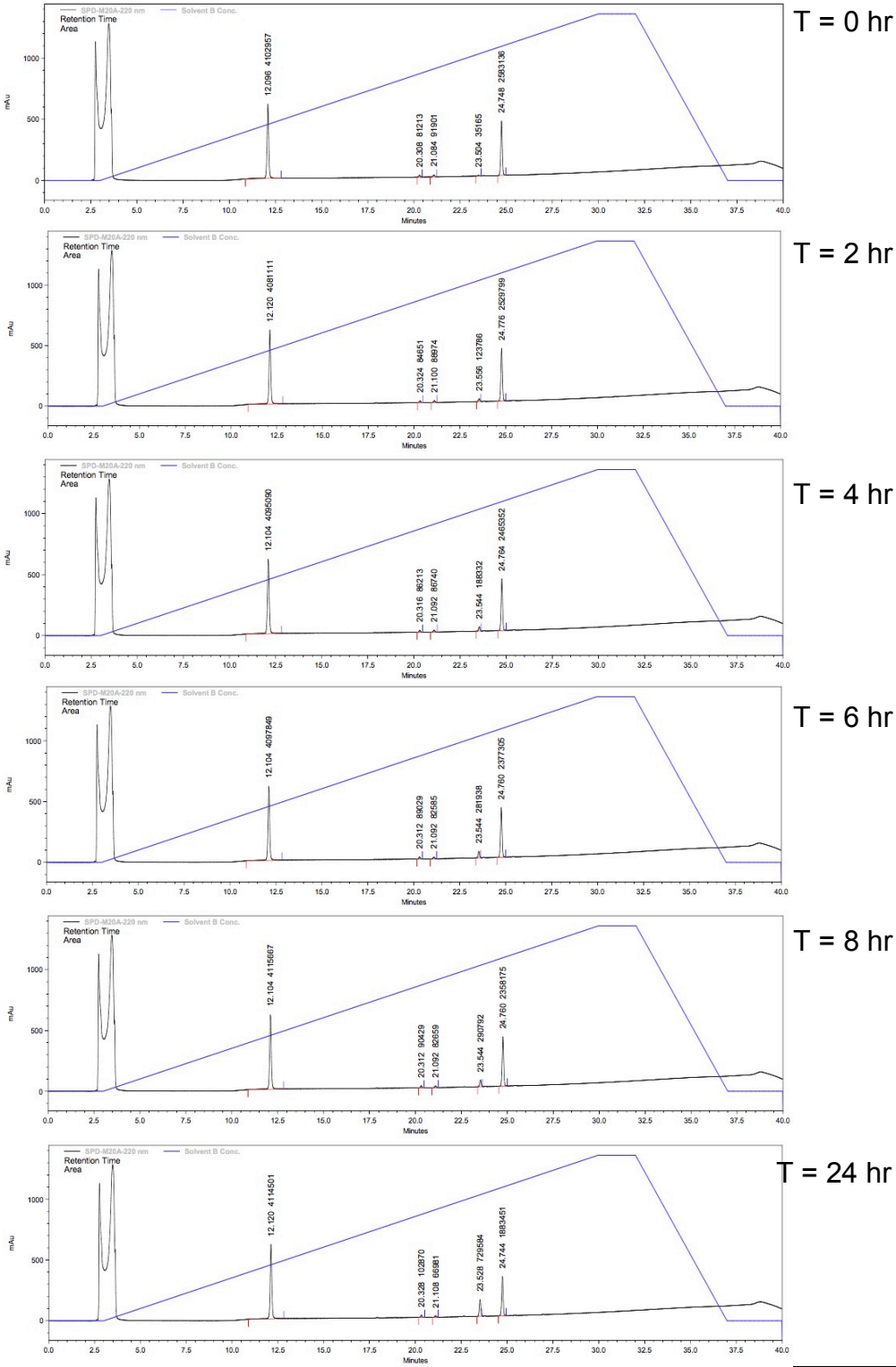

Time	0 Hours	2 Hours	4 Hours	6 Hours	8 Hours	24 Hours
% Remaining	100	97	95	92	91	73

3.7 ^{1}H- and ^{13}C-NMR spectra

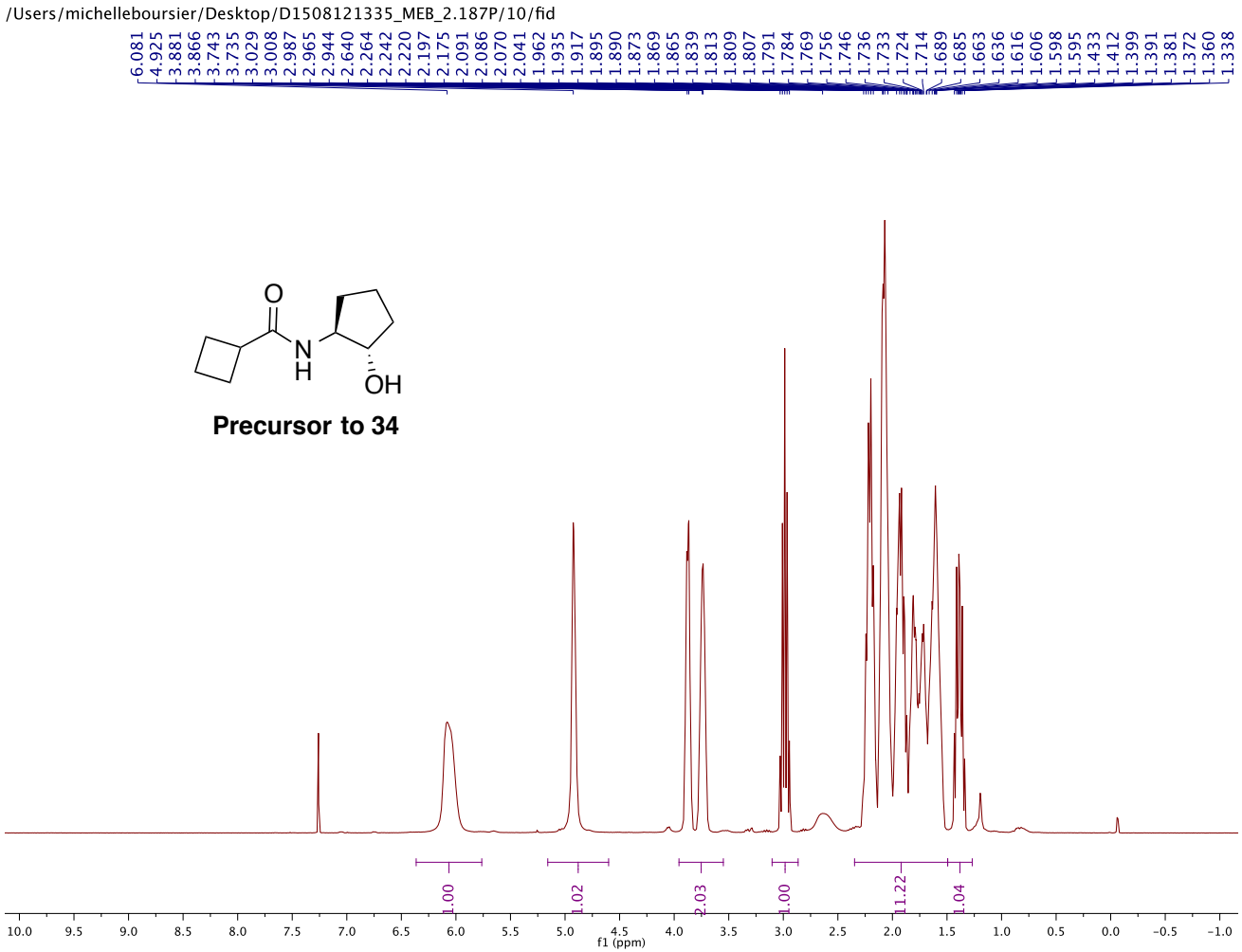

C1509091044_MEB_RN12OH.11.fid — Group Blackwell — C13CPD32 CDCl3 /home/mboursier/callisto mboursier 3

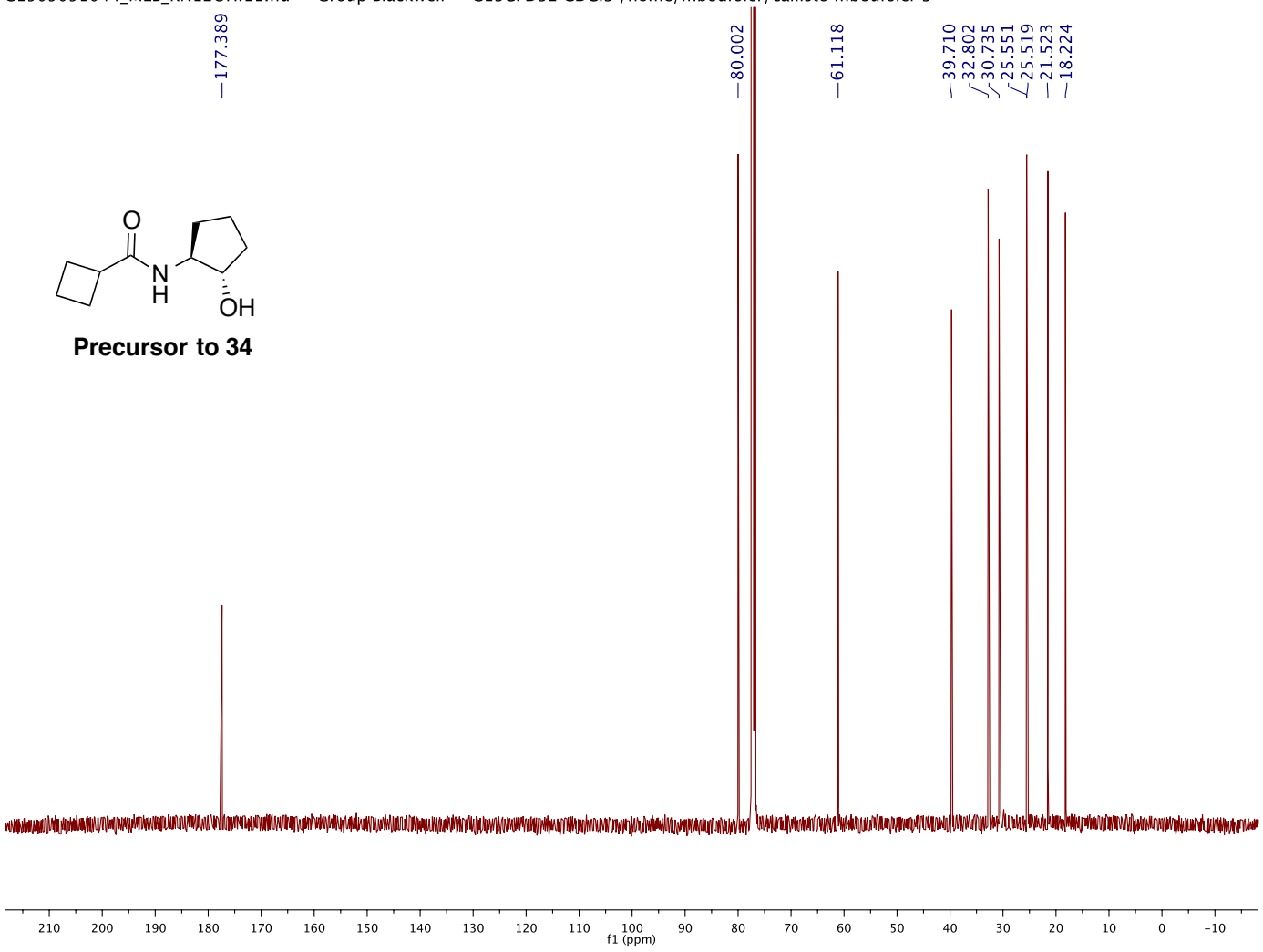

Precursor to 34

D1509080935_MEB_2.201_12-17.10.fid — Group Blackwell — PROTON CDCl3 /home/mboursier/av400 mboursier 51

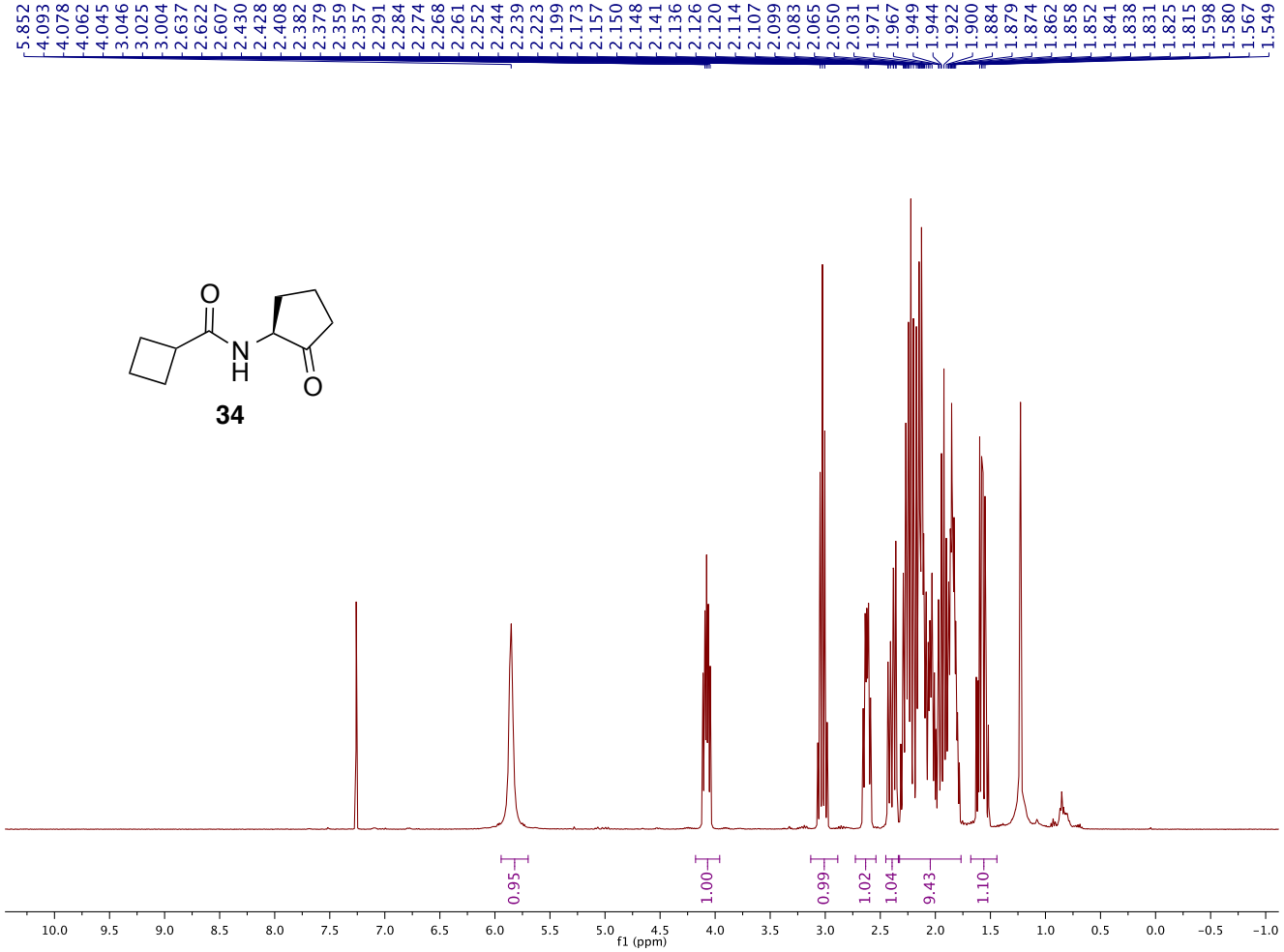

D1509080935_MEB_2.201_12-17.11.fid — Group Blackwell — C13CPD32 CDCl3 /home/mboursier/av400 mboursier 51

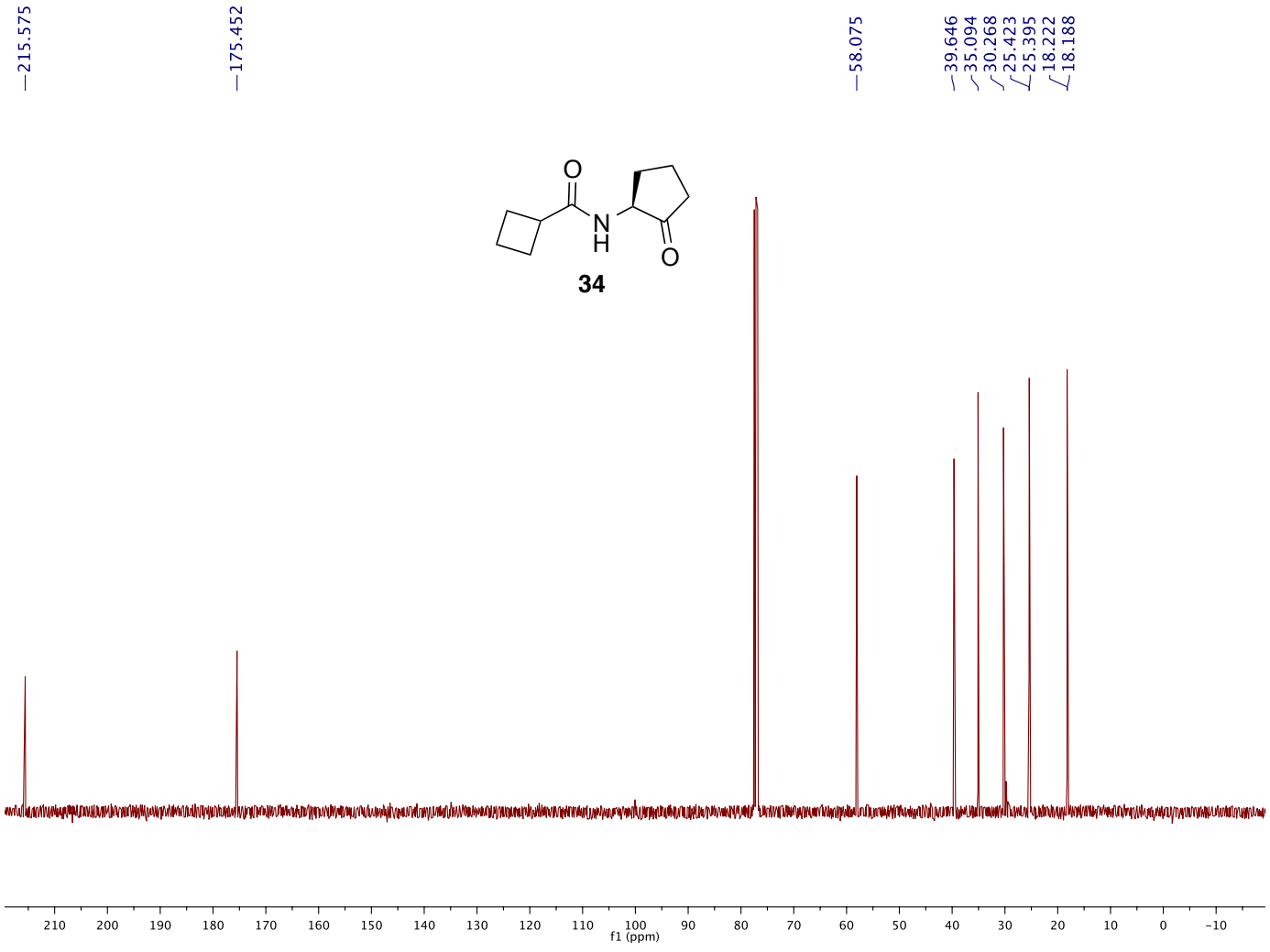

2.139 Pure — 400MHz, chloroform-d — 061815

6.081 6.069 4.539 4.523 4.507 4.490 4.474 3.369 3.356 3.340 3.327 3.310 3.297 3.234 3.218 3.207 3.190 3.082 3.061 3.040 3.019 2.997 2.878 2.876 2.862 2.848 2.846 2.831 2.817 2.308 2.285 2.278 2.262 2.256 2.233 2.210 2.187 2.160 2.151 2.139 2.130 2.120 2.110 2.102 2.090 2.081 1.987 1.966 1.960 1.949 1.936 1.917 1.904 1.894 1.887 1.873 1.866 1.855 1.842 1.841 1.834 1.831 1.827 1.816

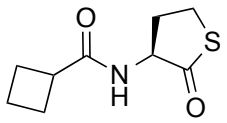

35

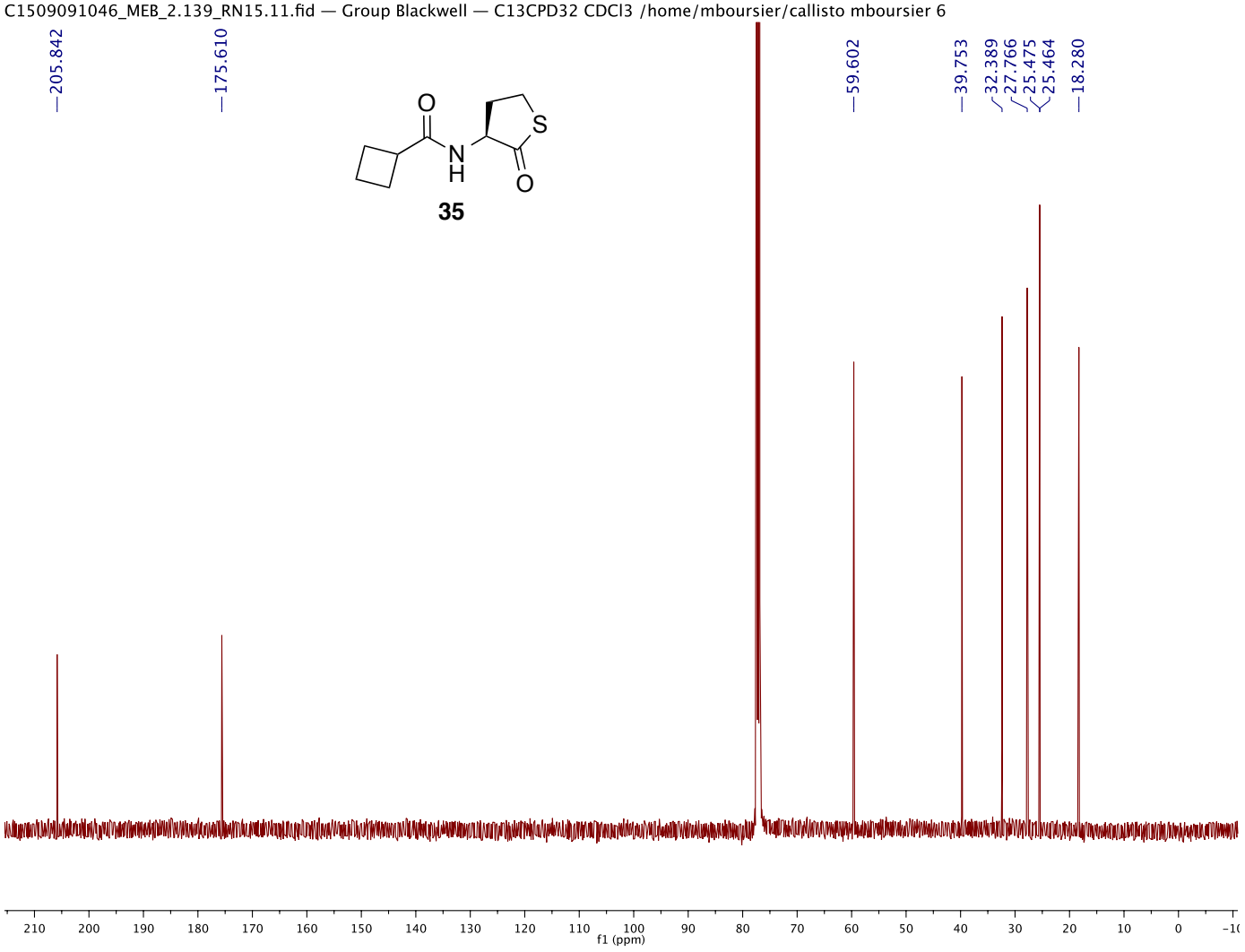
C1509091046_MEB_2.139_RN15.11.fid — Group Blackwell — C13CPD32 CDCl3 /home/mboursier/callisto mboursier 6
205.842
175.610
59.602
39.753
32.389
27.766
25.475
25.464
18.280
O
N
H
S
O
35
210 200 190 180 170 160 150 140 130 120 110 100 90 80 70 60 50 40 30 20 10 0
f1 (ppm)

C1606281816_RN19OH.10.fid — Group Blackwell — H1_standard.UW CDCl3 /home/mboursier/callisto mboursier 37

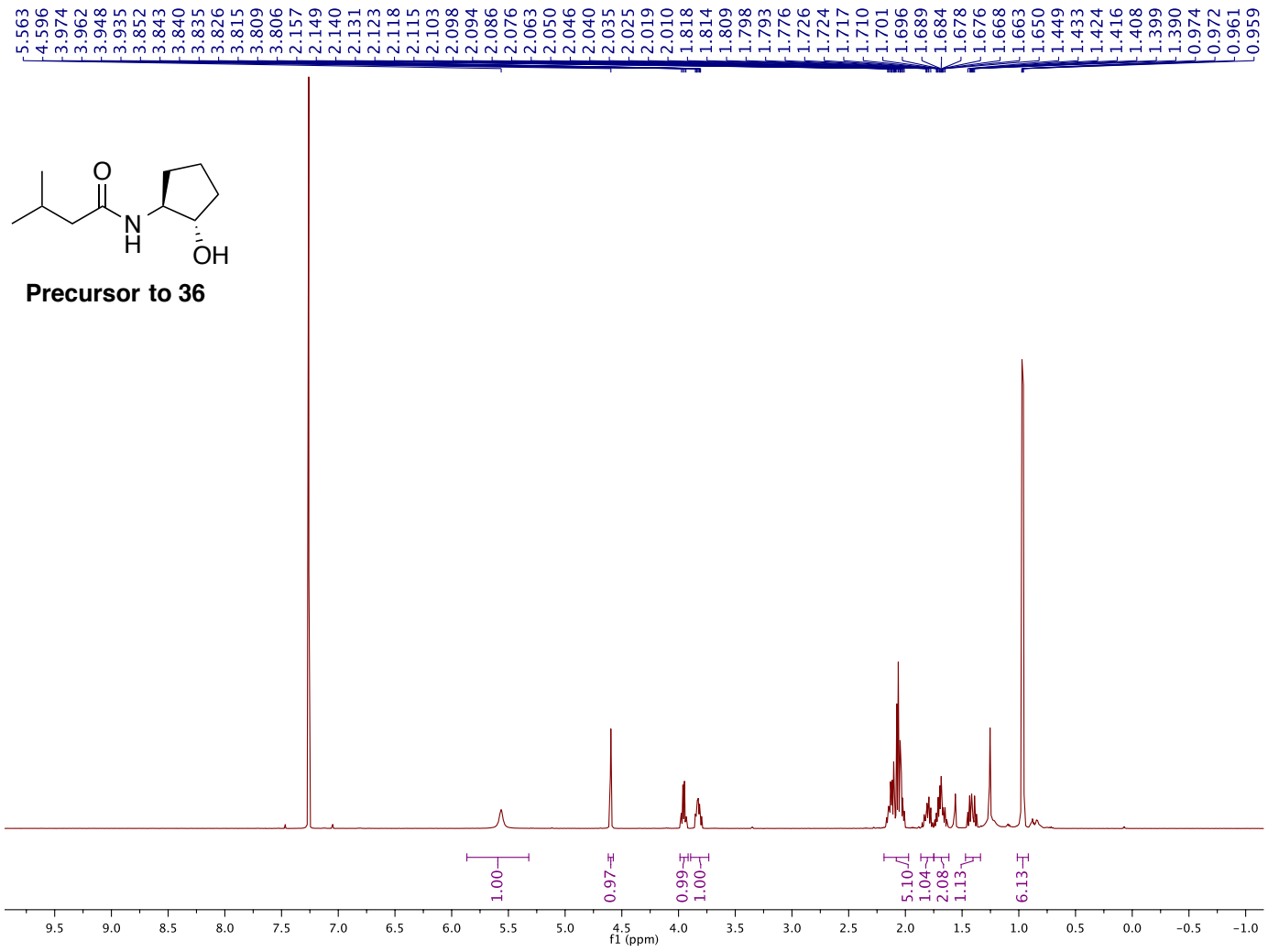

Precursor to 36

C1606281816_RN19OH.11.fid — Group Blackwell — C13_H1dec.UW CDCl3 /home/mboursier/callisto mboursier 37

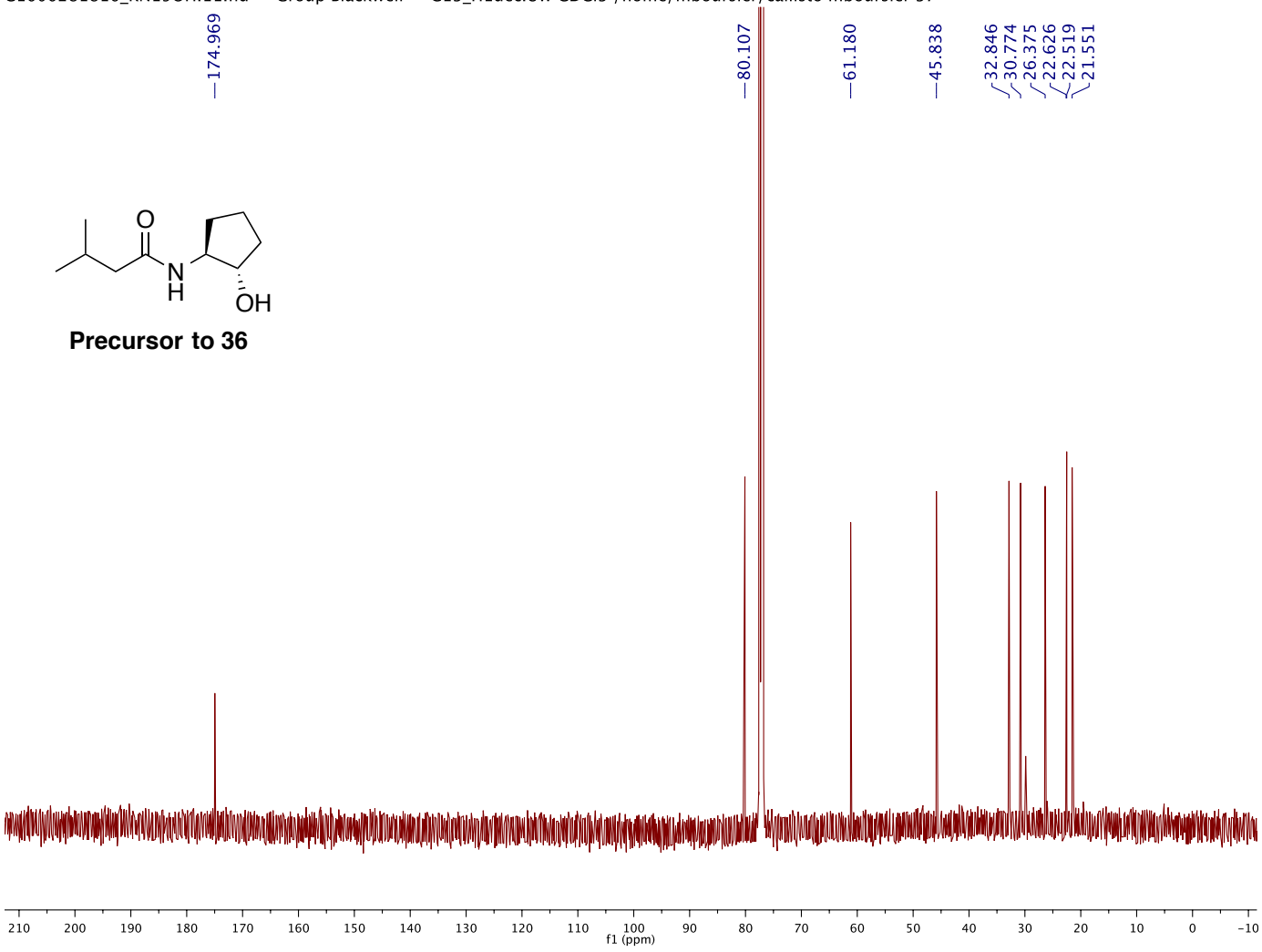

Precursor to 36

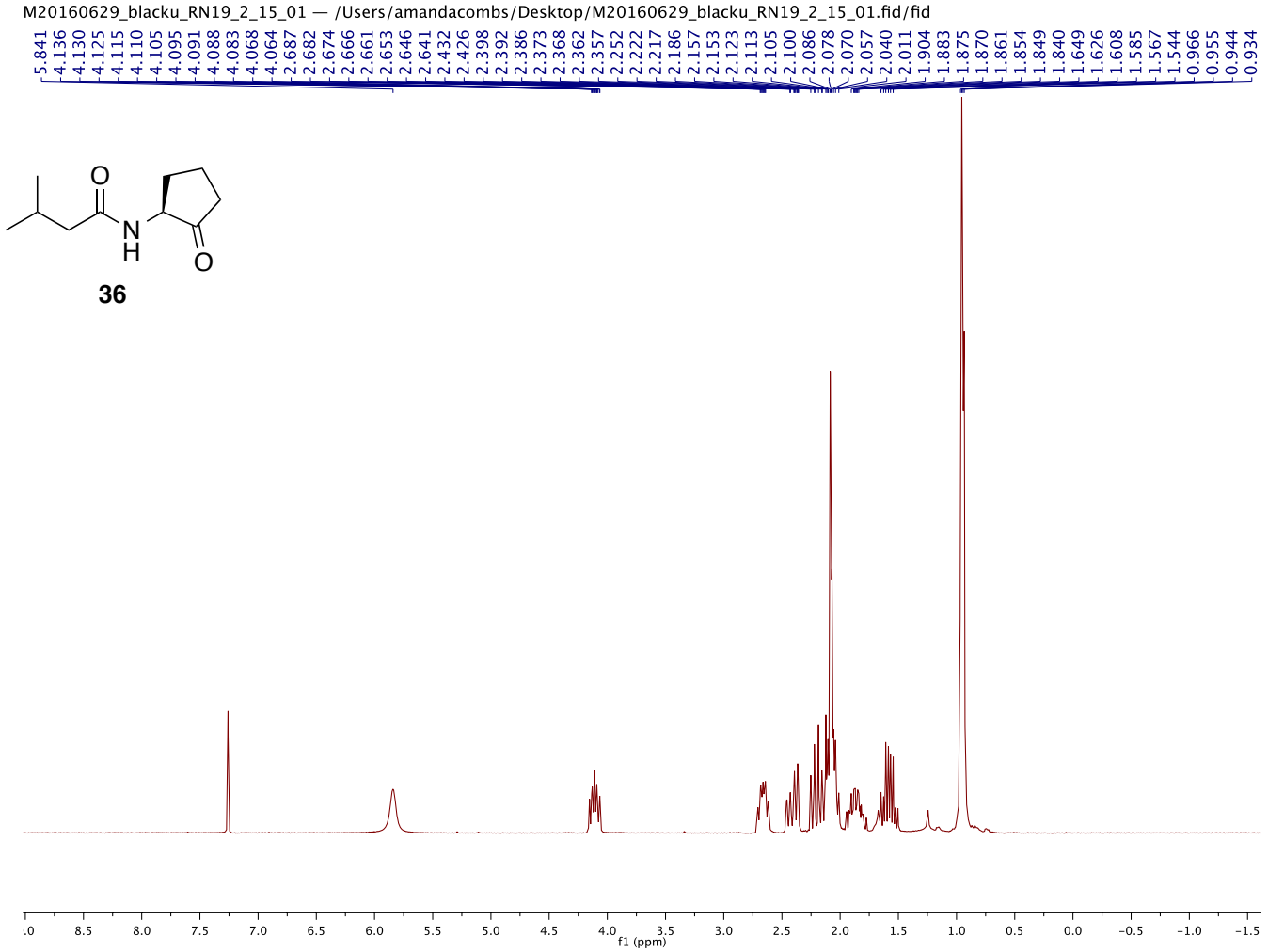
M20160629_blacku_RN19_2_15_01 — /Users/amandacombs/Desktop/M20160629_blacku_RN19_2_15_01.fid/fid
5.841
4.136
4.130
4.125
4.115
4.110
4.105
4.095
4.091
4.088
4.083
4.068
4.064
2.687
2.682
2.674
2.666
2.661
2.653
2.646
2.641
2.432
2.426
2.398
2.392
2.386
2.373
2.368
2.362
2.357
2.252
2.222
2.217
2.186
2.157
2.153
2.123
2.113
2.105
2.100
2.086
2.078
2.070
2.057
2.040
2.011
1.904
1.883
1.875
1.870
1.861
1.854
1.849
1.840
1.649
1.626
1.608
1.585
1.567
1.544
0.966
0.955
0.944
0.934
O
N
H
O
36
.0
8.5
8.0
7.5
7.0
6.5
6.0
5.5
5.0
4.5
4.0
3.5
3.0
2.5
2.0
1.5
1.0
0.5
0.0
-0.5
-1.0
-1.5
f1 (ppm)

C1606281816_RN19.12.fidGroup Blackwell — C13_H1dec.UW CDCl3 /home/mboursier/callisto mboursier 36

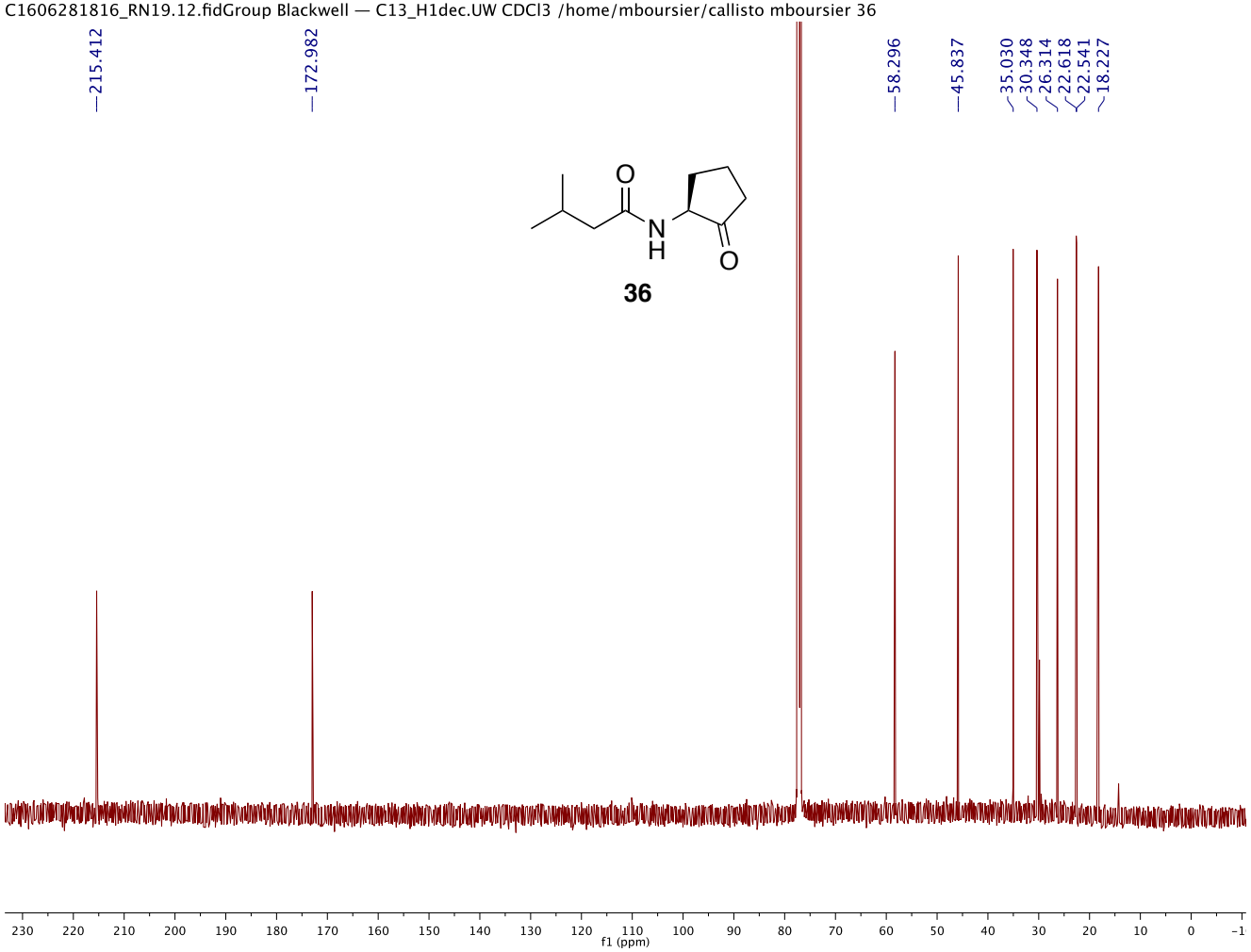

M20160413_mboursier_MEB_3_45_5-8_20_01

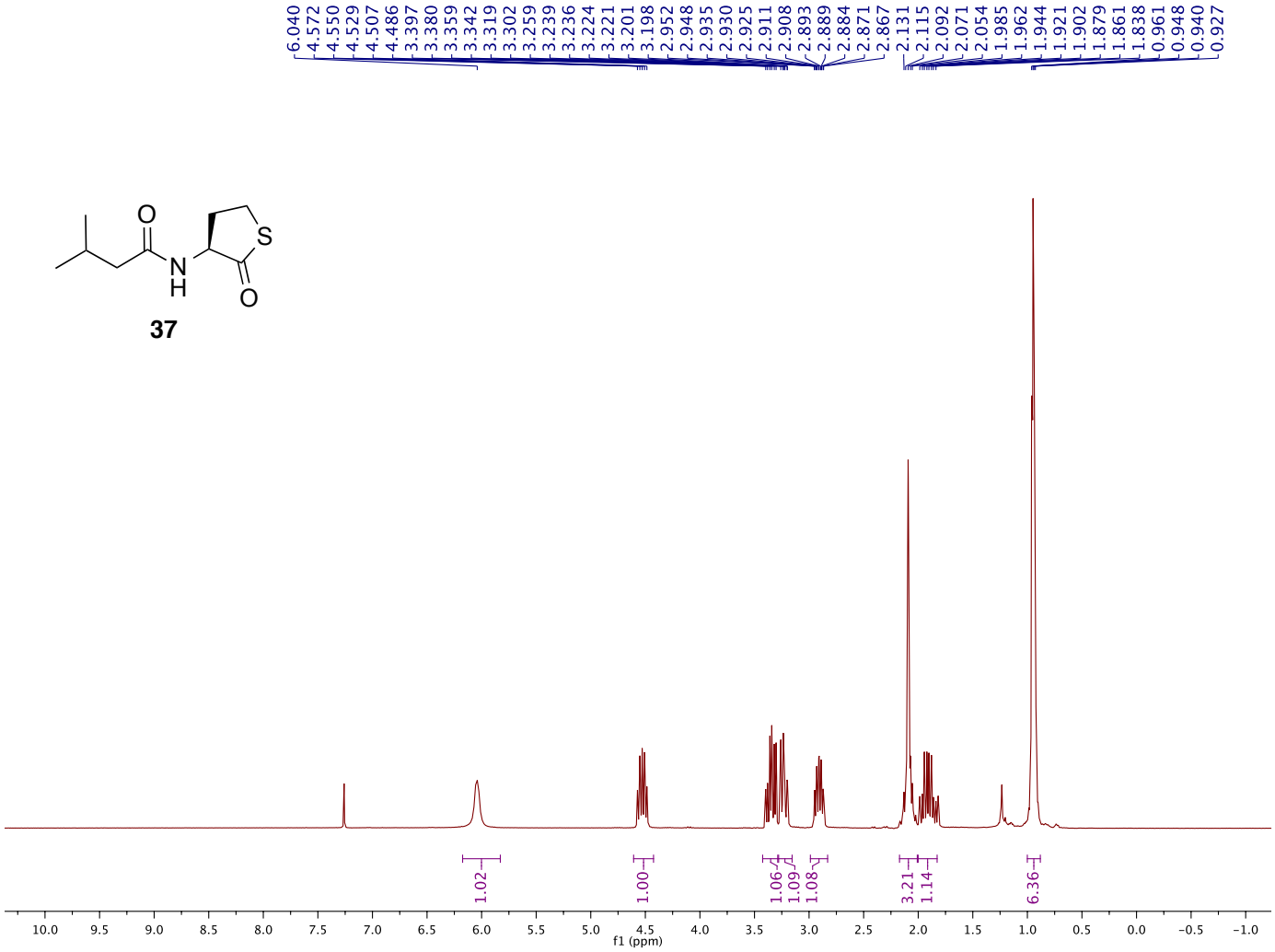

M20160413_mboursier_MEB_3_45_5-8carbon_20_01 — /Users/michelleboursier/Desktop/M20160413_mboursier_MEB_3_45_5-8carbon_20_01.fid/fid —

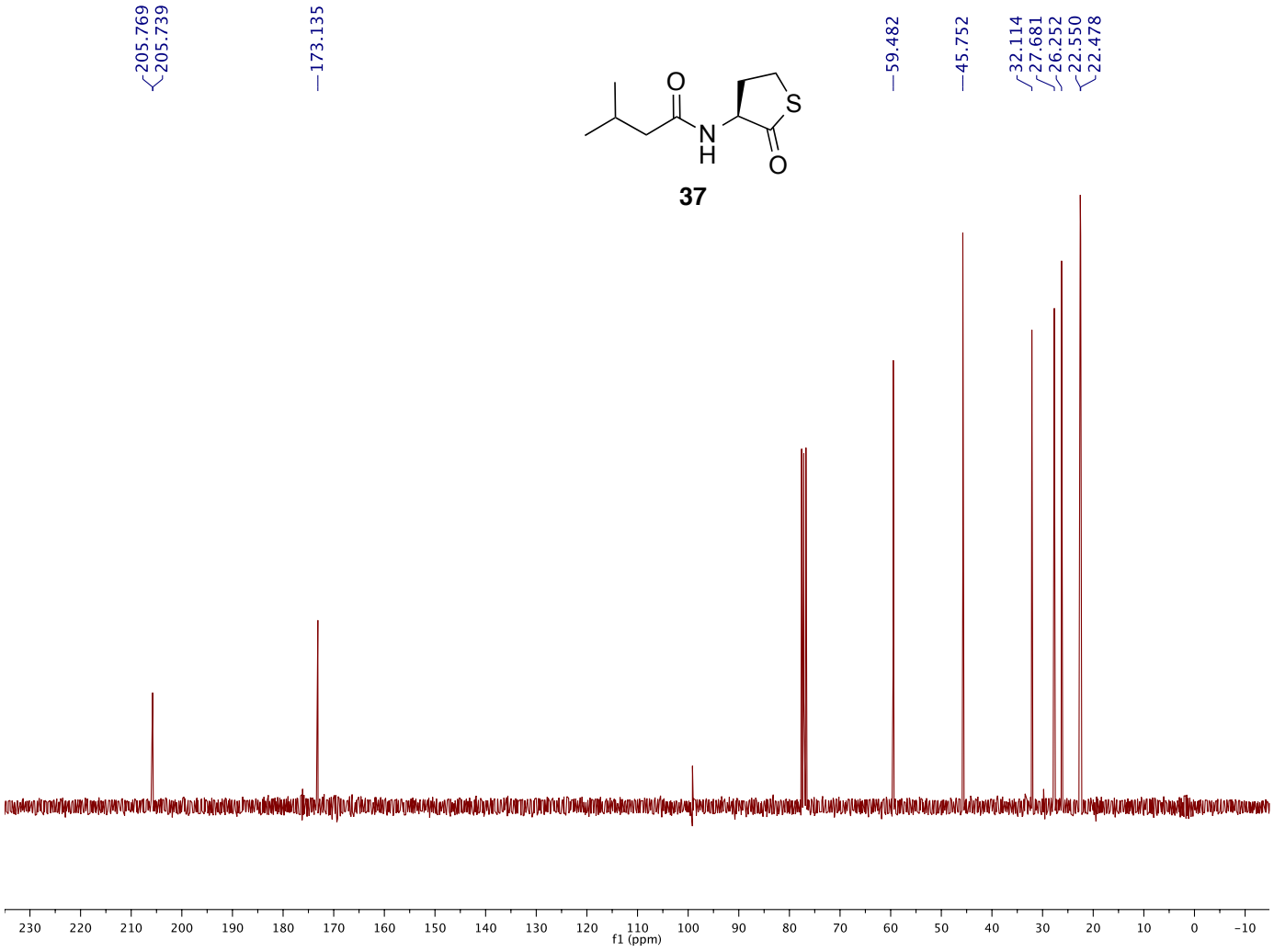

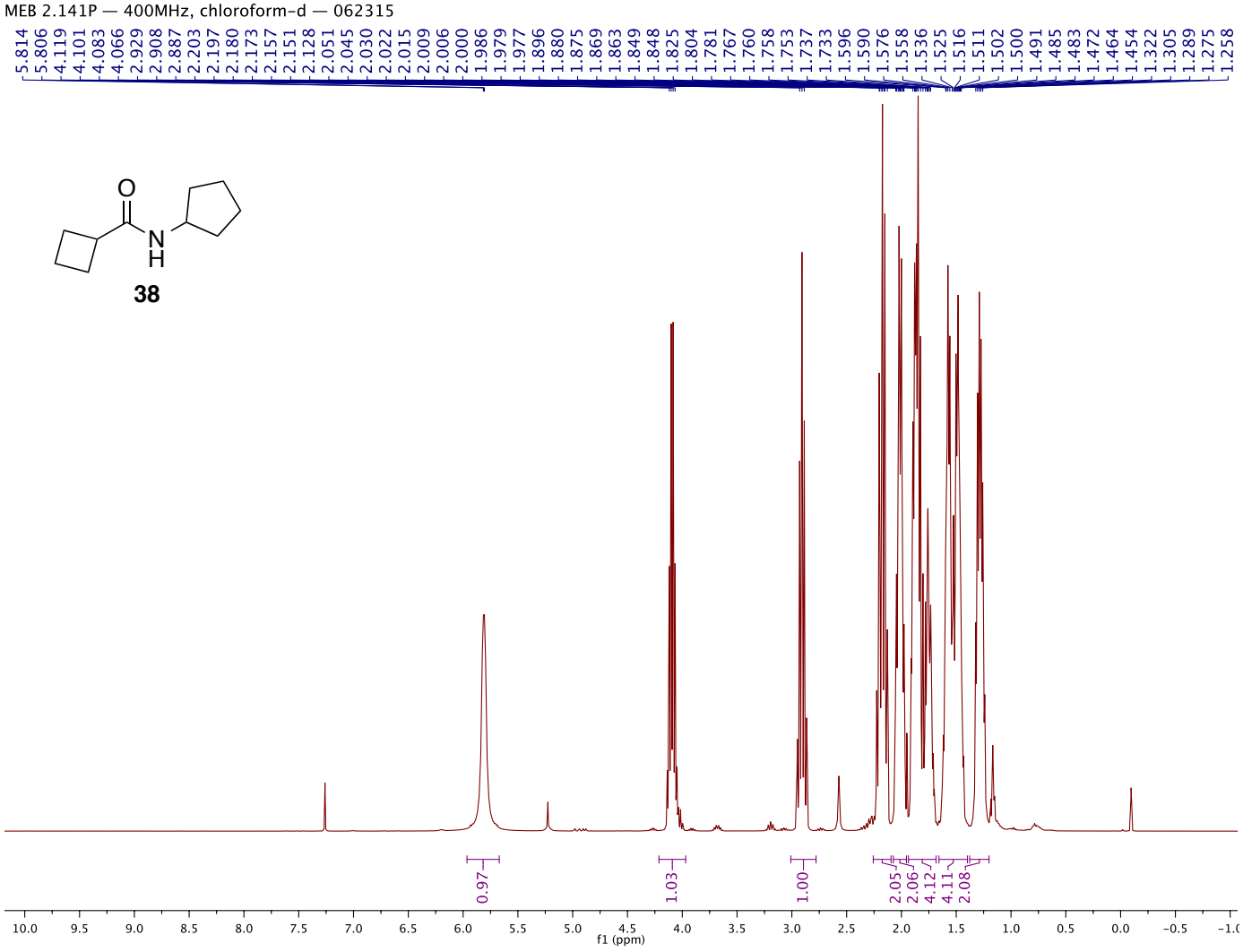
MEB 2.141P — 400MHz, chloroform-d — 062315
5.814 5.806 4.119 4.101 4.083 4.066 2.929 2.908 2.887 2.203 2.197 2.180 2.173 2.157 2.151 2.128 2.051 2.045 2.030 2.022 2.015 2.009 2.006 2.000 1.986 1.979 1.977 1.896 1.880 1.875 1.869 1.863 1.849 1.848 1.825 1.804 1.781 1.767 1.760 1.758 1.753 1.737 1.733 1.596 1.590 1.576 1.558 1.536 1.525 1.516 1.511 1.502 1.500 1.491 1.485 1.483 1.472 1.464 1.454 1.322 1.305 1.289 1.275 1.258
O
N
H
38
0.97
1.03
1.00
2.05
2.06
4.12
4.11
2.08
10.0 9.5 9.0 8.5 8.0 7.5 7.0 6.5 6.0 5.5 5.0 4.5 4.0 3.5 3.0 2.5 2.0 1.5 1.0 0.5 0.0 -0.5
f1 (ppm)

C1509091045_MEB_2.141_RN13.11.fid — Group Blackwell — C13CPD32 CDCl3 /home/mboursier/callisto mboursier 4

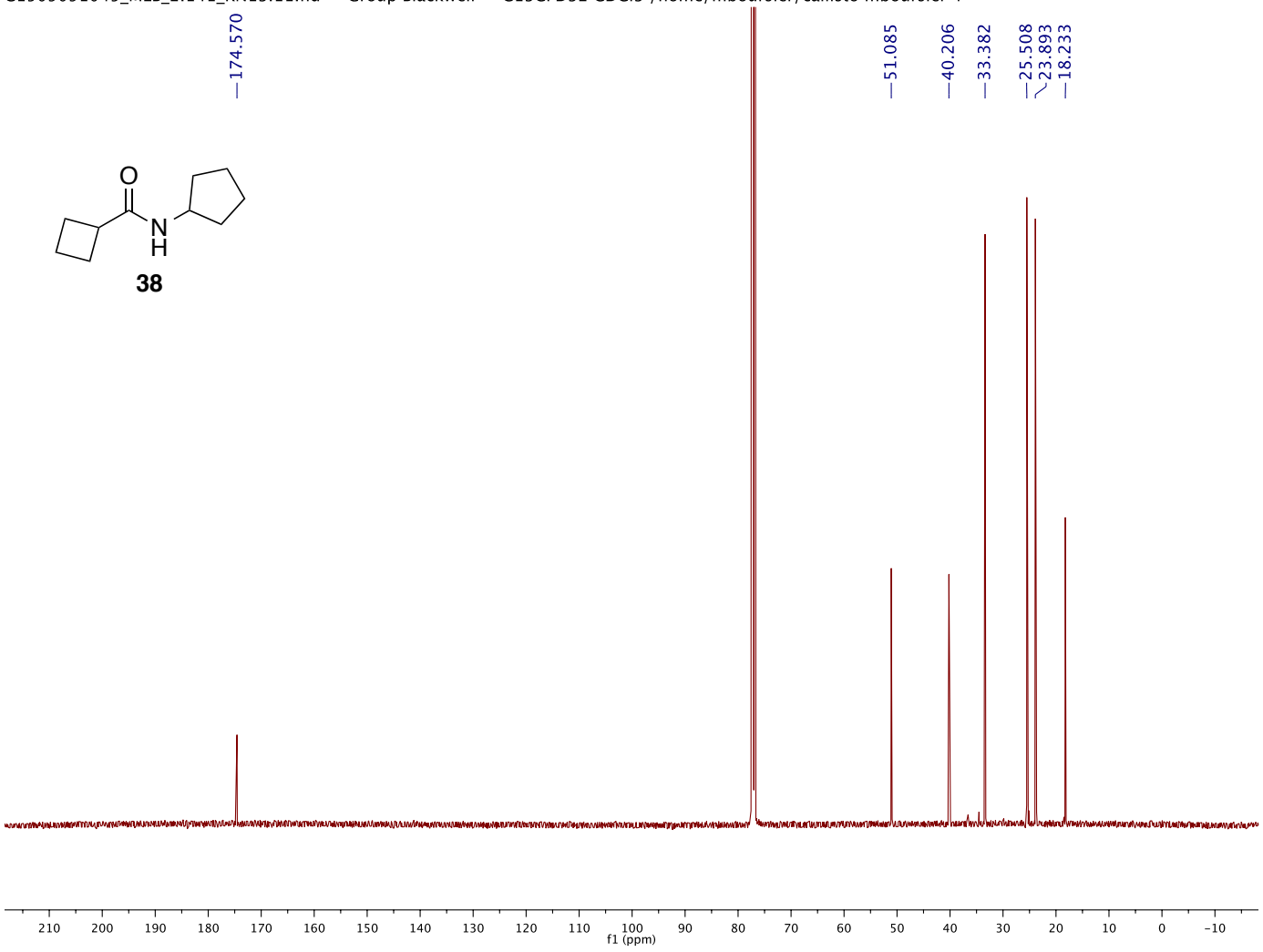

C1606281816_RN20.10.fid — Group Blackwell — H1_standard.UW CDCl3 /home/mboursier/callisto mboursier 38

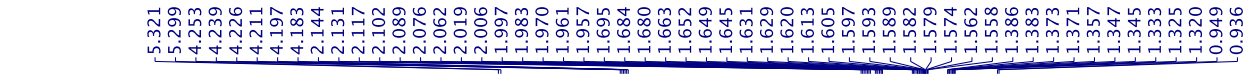

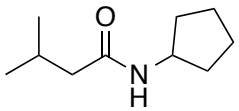

39

C1606281816_RN20.11.fid — Group Blackwell — C13_H1dec.UW CDCl3 /home/mboursier/callisto mboursier 38

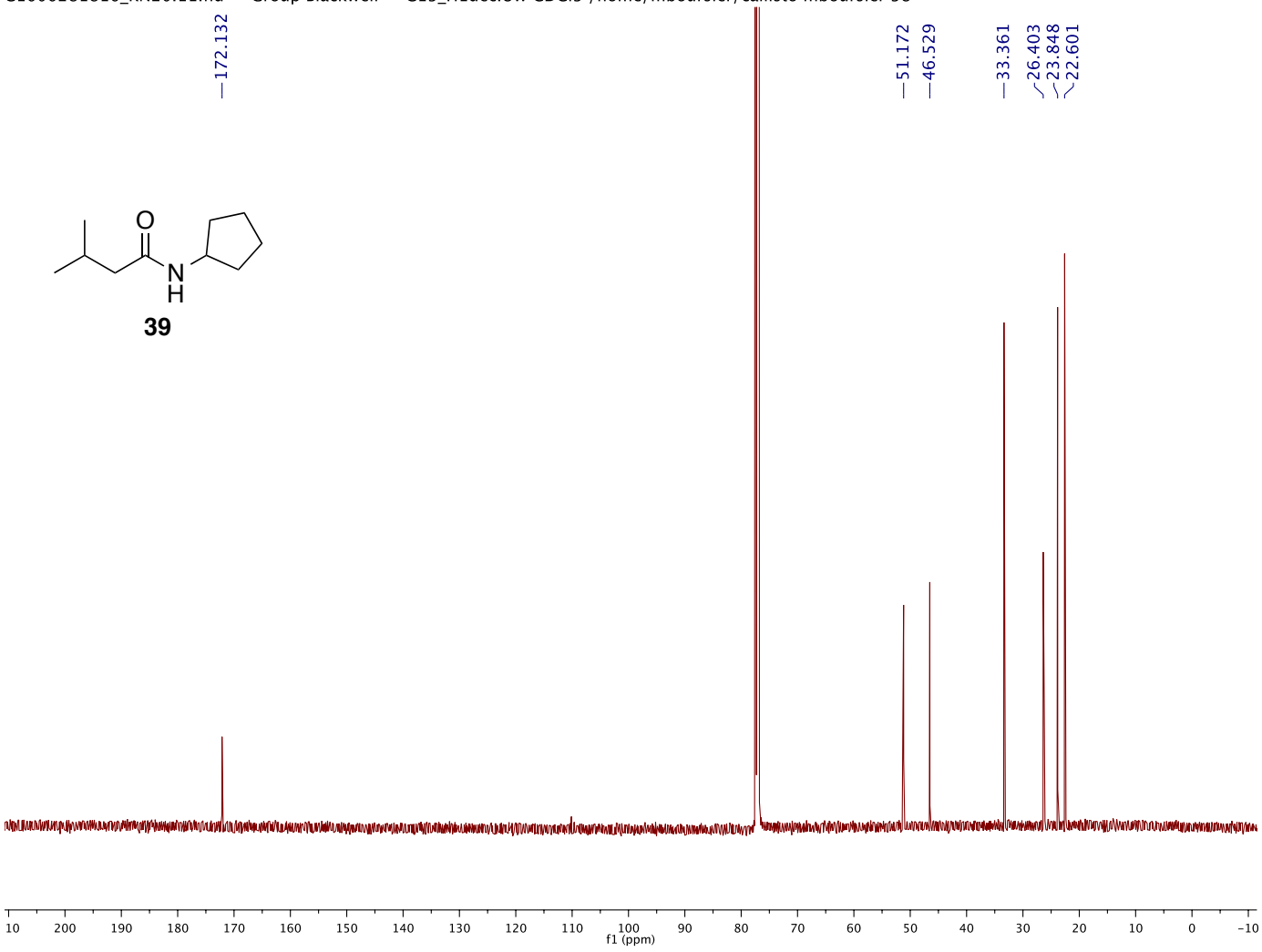

D1604141010_MEB_3.40RC.10.fid — Group Blackwell — H1_standard.UW CDCl3 /home/mboursier/av400 mboursier 70

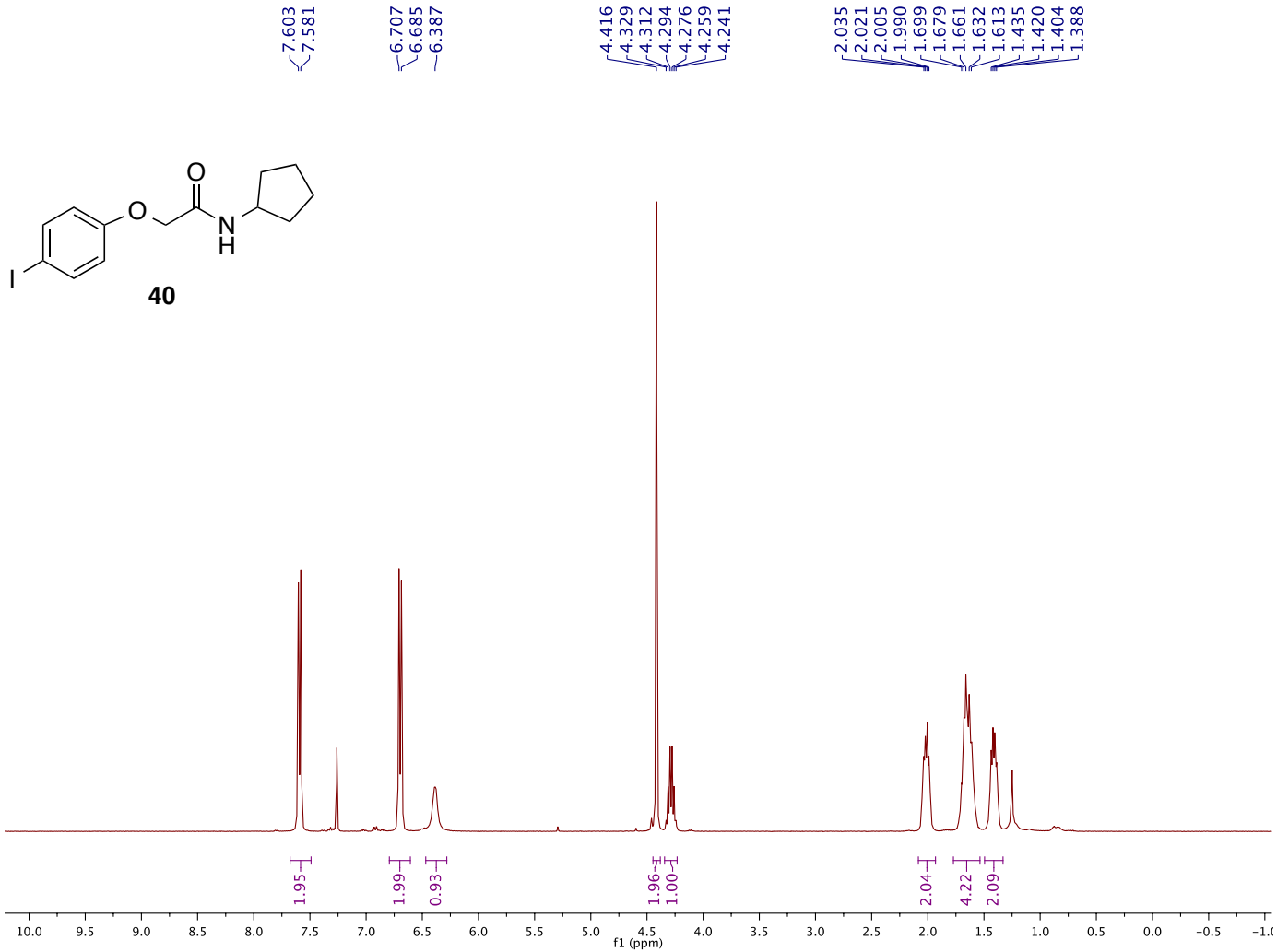

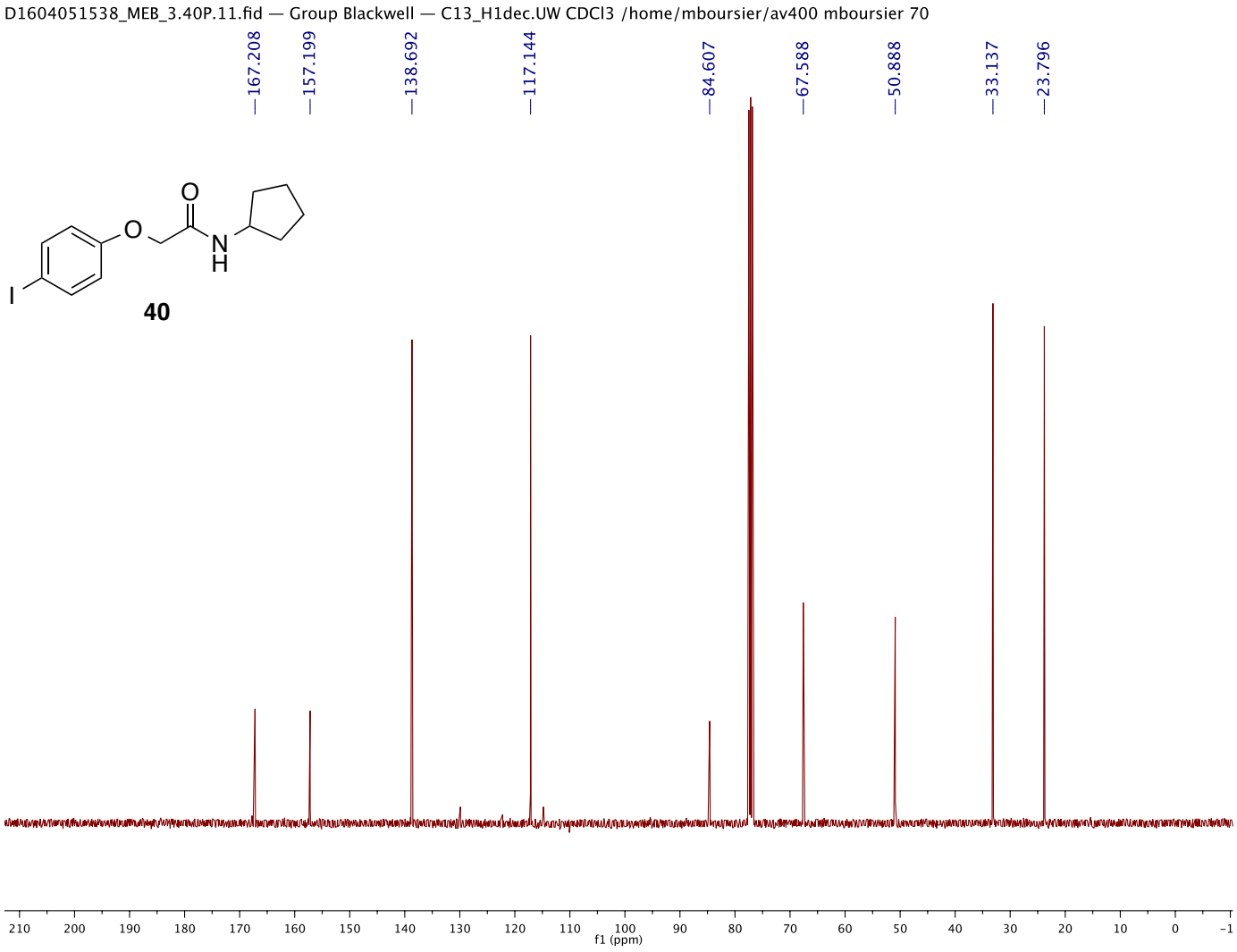
D1604051538_MEB_3.40P.11.fid — Group Blackwell — C13_H1dec.UW CDCl3 /home/mboursier/av400 mboursier 70
167.208
157.199
138.692
117.144
84.607
67.588
50.888
33.137
23.796
O
O
N
H
I
40
210 200 190 180 170 160 150 140 130 120 110 100 90 80 70 60 50 40 30 20 10 0 −1
f1 (ppm)

C1606281816_RN21.10.fid — Group Blackwell — H1_standard.UW CDCl3 /home/mboursier/callisto mboursier 39

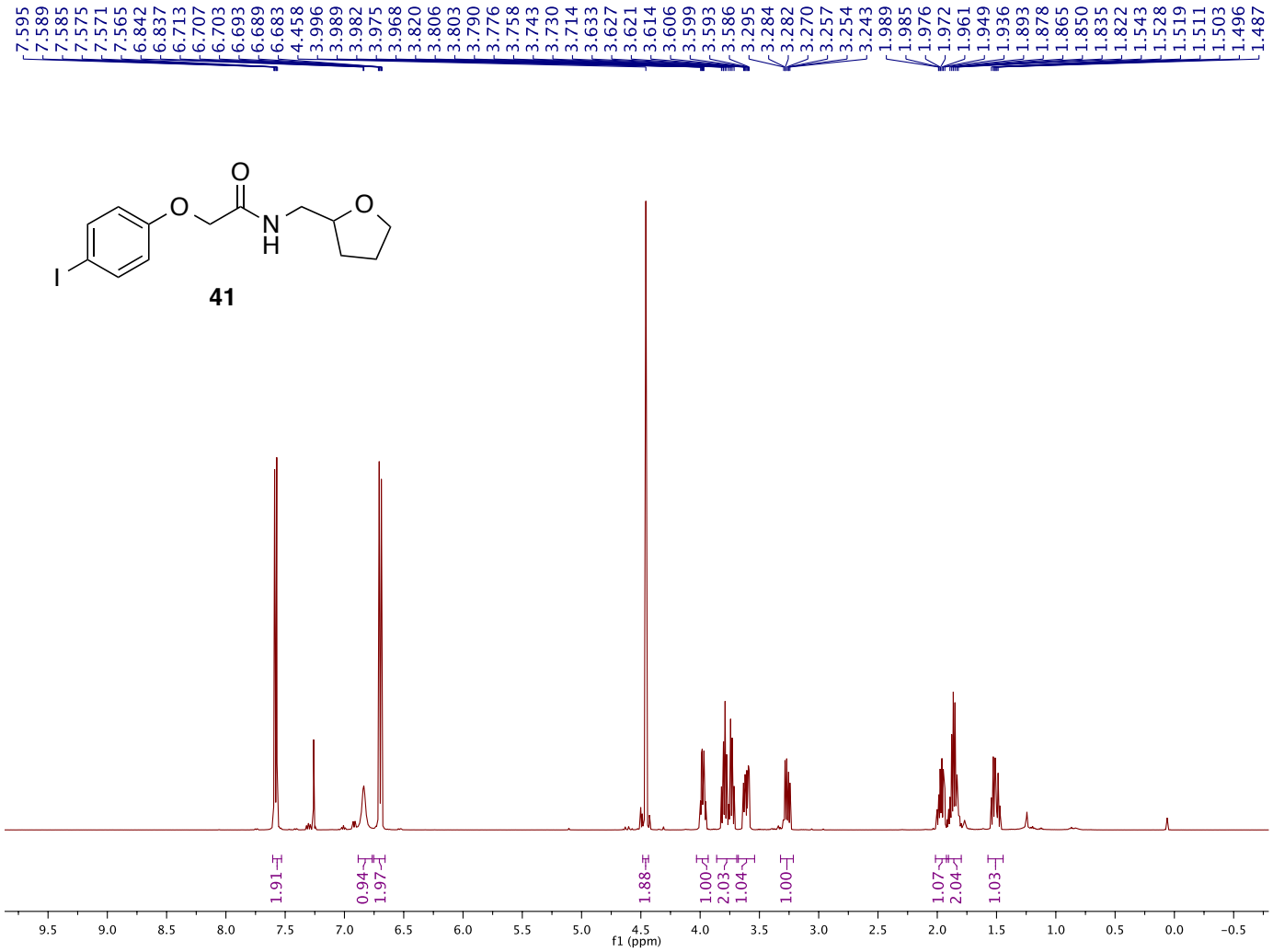

C1606281816_RN21.11.fid — Group Blackwell — C13_H1dec.UW CDCl3 /home/mboursier/callisto mboursier 39

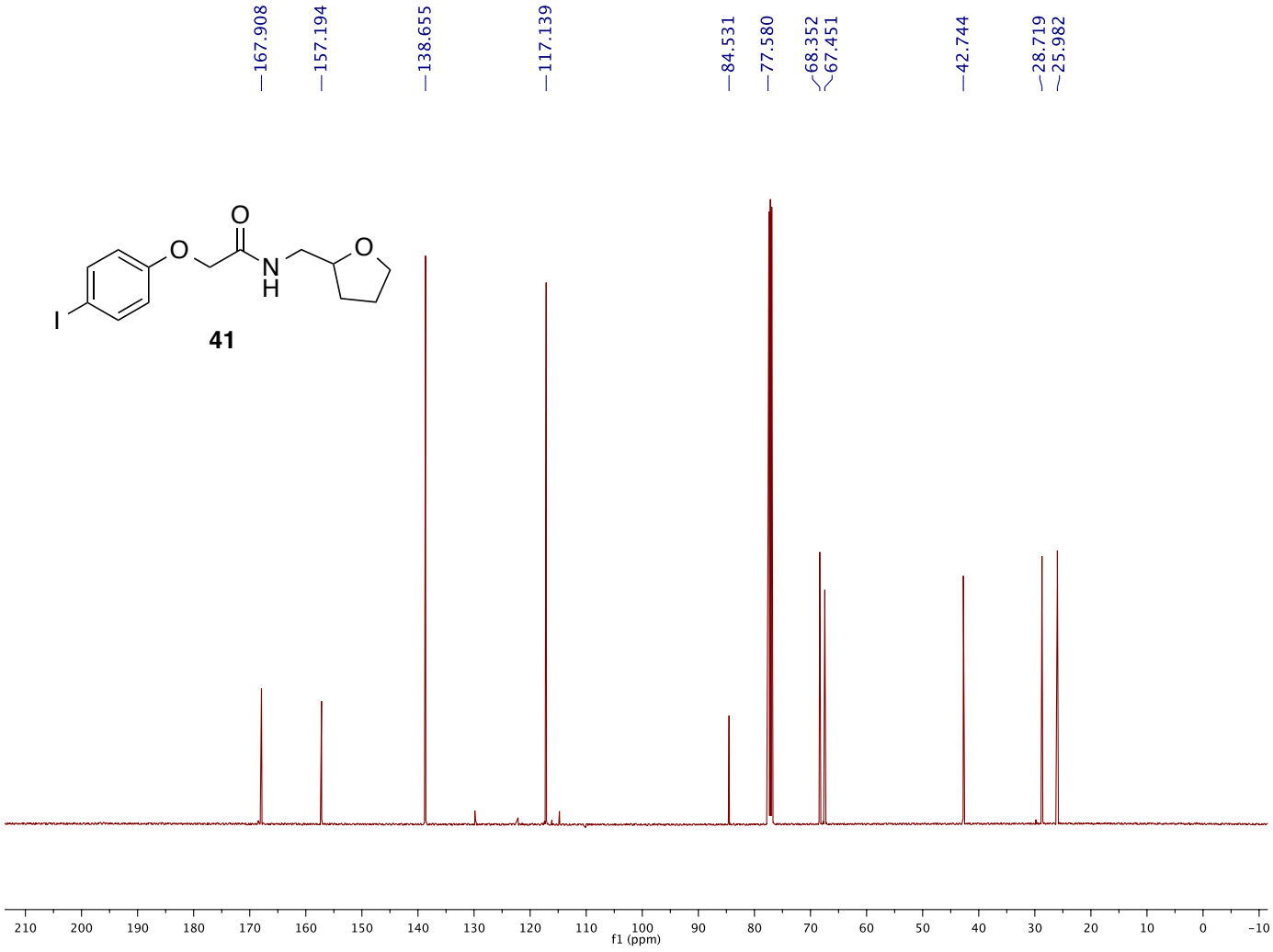

C1606281816_RN22.10.fid — Group Blackwell — H1_standard.UW CDCl3 /home/mboursier/callisto mboursier 40

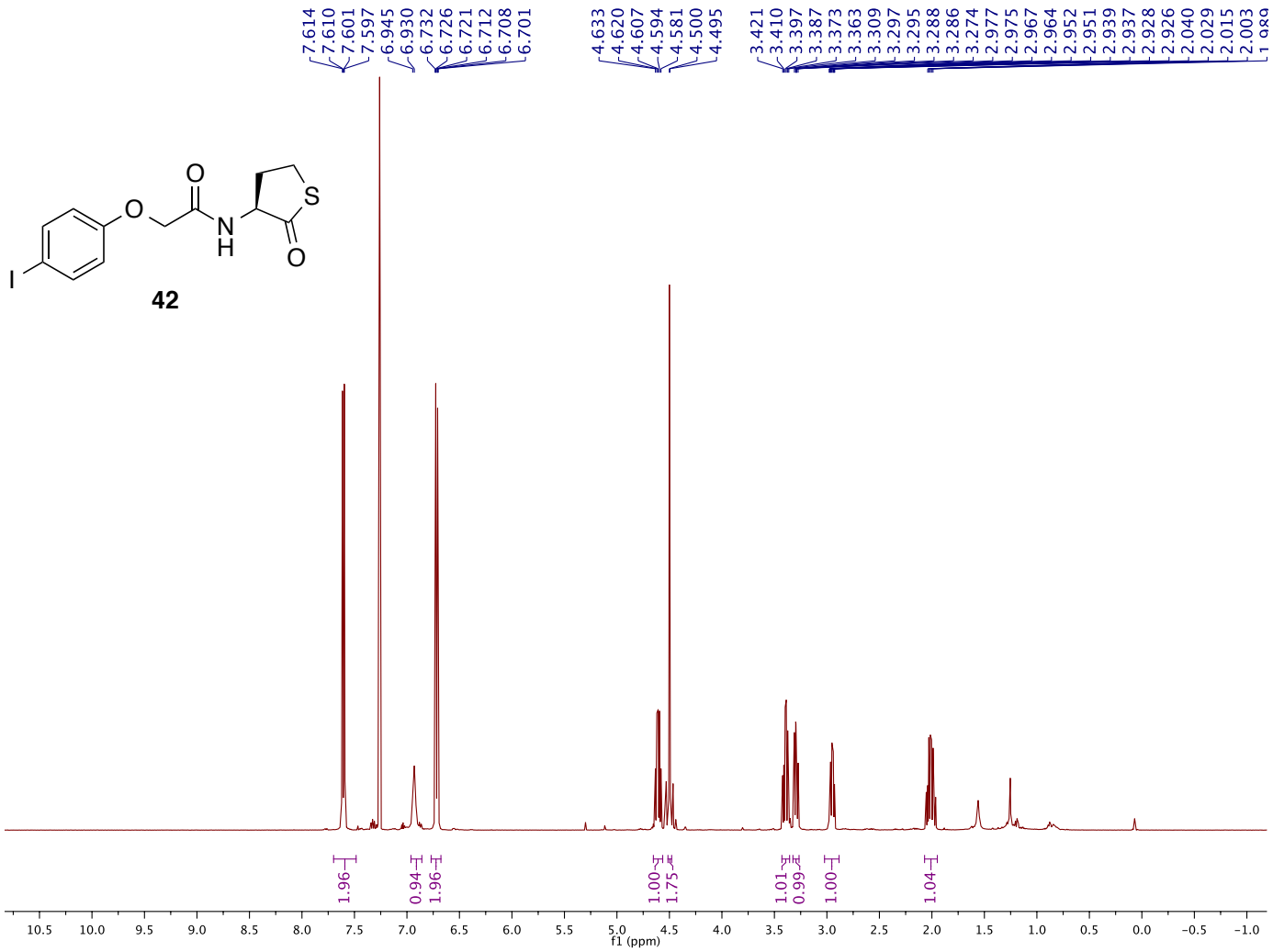

C1606281816_RN22.11.fid — Group Blackwell — C13_H1dec.UW CDCl3 /home/mboursier/callisto mboursier 40

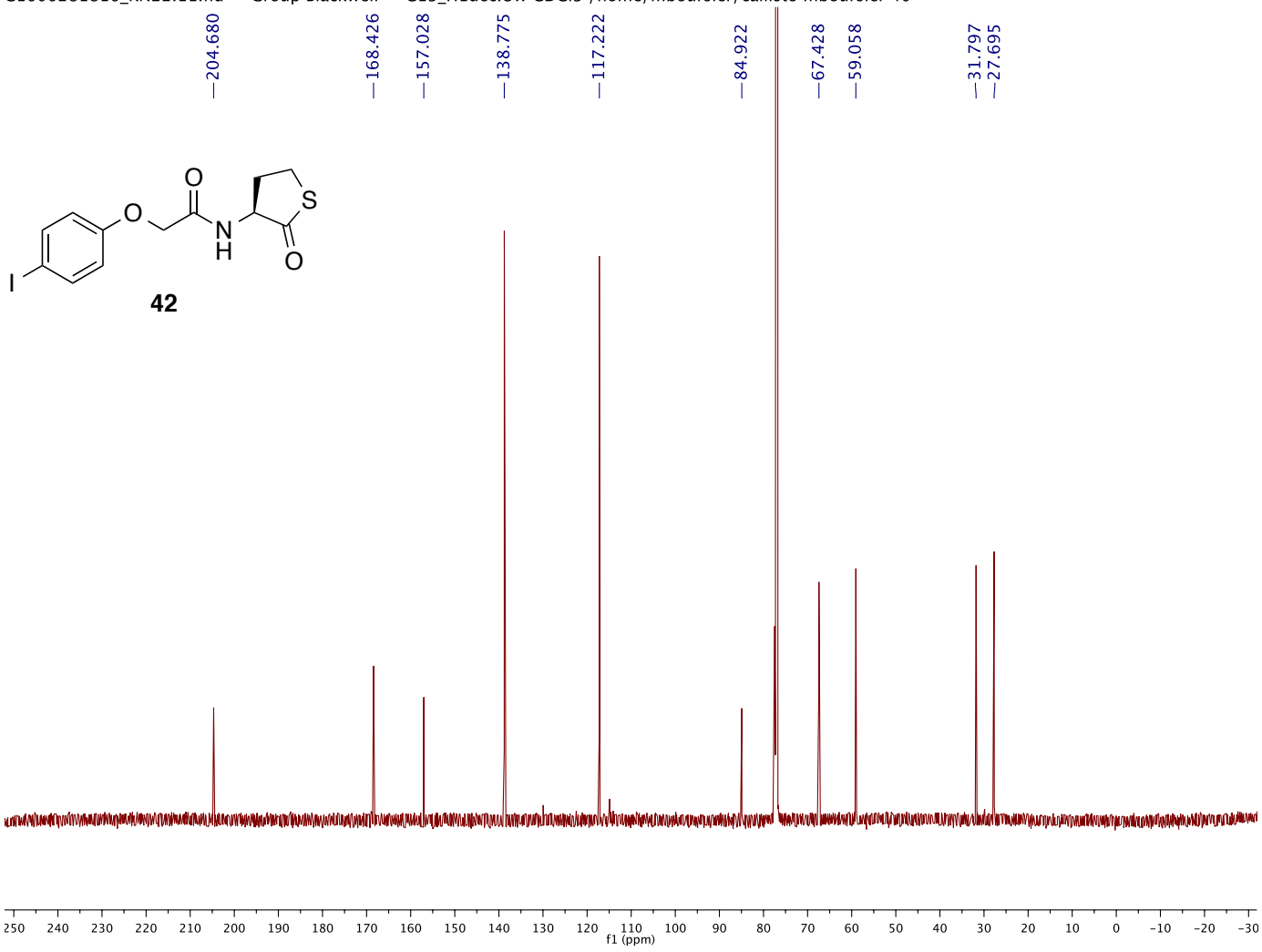

3.8 References

1. Schuster, M., and Greenberg, E. P. (2006) A network of networks: quorum-sensing gene regulation in *Pseudomonas aeruginosa*, *Int. J. Med. Microbiol. 296*, 73-81.

2. Chugani, S. a., Whiteley, M., Lee, K. M., D'Argenio, D., Manoil, C., and Greenberg, E. P. (2001) QscR, a modulator of quorum-sensing signal synthesis and virulence in *Pseudomonas aeruginosa*, *Proc. Natl. Acad. Sci. USA 98*, 2752-2757.

3. Schuster, M., Lostroh, C. P., Ogi, T., and Greenberg, E. P. (2003) Identification, Timing, and Signal Specificity of *Pseudomonas aeruginosa* Quorum-Controlled Genes: a Transcriptome Analysis, *J. Bacteriol. 185*, 2066-2079.

4. Wagner, V. E., Bushnell, D., Passador, L., Brooks, A. I., and Iglewski, B. H. (2003) Microarray Analysis of *Pseudomonas aeruginosa* Quorum-Sensing Regulons: Effects of Growth Phase and Environment, *J. Bacteriol. 185*, 2080-2095.

5. Galloway, W. R. J. D., Hodgkinson, J. T., Bowden, S. D., Welch, M., and Spring, D. R. (2011) Quorum sensing in Gram-negative bacteria: small-molecule modulation of AHL and AI-2 quorum sensing pathways, *Chem. Rev. 111*, 28-67.

6. Amara, N., Gregor, R., Rayo, J., Dandela, R., Daniel, E., Liubin, N., Willems, H. M. E., Ben-Zvi, A., Krom, B. P., and Meijler, M. M. (2016) Fine-Tuning Covalent Inhibition of Bacterial Quorum Sensing, *ChemBioChem 17*, 825-835.

7. Amara, N., Mashiach, R., Amar, D., Krief, P., Spieser, S. a. H., Bottomley, M. J., Aharoni, A., and Meijler, M. M. (2009) Covalent inhibition of bacterial quorum sensing, *J. Am. Chem. Soc. 131*, 10610-10619.

8. Moore, J. D., Rossi, F. M., Welsh, M. A., Nyffeler, K. E., and Blackwell, H. E. (2015) A Comparative Analysis of Synthetic Quorum Sensing Modulators in *Pseudomonas aeruginosa*: New Insights into Mechanism, Active Efflux Susceptibility, Phenotypic Response, and Next-Generation Ligand Design, *J. Am. Chem. Soc. 137*, 14626-14639.

9. Galloway, W. R. J. D., Hodgkinson, J. T., Bowden, S., Welch, M., and Spring, D. R. (2012) Applications of small molecule activators and inhibitors of quorum sensing in Gram-negative bacteria, *Trends in microbiology 20*, 449-458.

10. Welsh, M. A., Eibergen, N. R., Moore, J. D., and Blackwell, H. E. (2015) Small Molecule Disruption of Quorum Sensing Cross-Regulation in *Pseudomonas aeruginosa* Causes Major and Unexpected Alterations to Virulence Phenotypes, *J. Am. Chem. Soc. 137*, 1510-1519.

11. O'Loughlin, C. T., Miller, L. C., Siryaporn, A., Drescher, K., Semmelhack, M. F., and Bassler, B. L. (2013) A quorum-sensing inhibitor blocks *Pseudomonas aeruginosa* virulence and biofilm formation, *Proc. Natl. Acad. Sci. USA 110*, 17981-17986.

12. Eibergen, N. R., Moore, J. D., Mattmann, M. E., and Blackwell, H. E. (2015) Potent and Selective Modulation of the RhlR Quorum Sensing Receptor by Using Non-native Ligands : An Emerging Target for Virulence Control in *Pseudomonas aeruginosa*, *ChemBioChem 16*, 2348-2356.

13. Yates, E. A., Philipp, B., Buckley, C., Atkinson, S., Chhabra, S. R., Sockett, R. E., Goldner, M., Dessaux, Y., Cámara, M., Smith, H., and Williams, P. (2002) *N*-acylhomoserine lactones undergo lactonolysis in a pH-, temperature-, and acyl chain length-dependent manner during growth of Yersinia pseudotuberculosis and *Pseudomonas aeruginosa*, *Infect. Immun. 70*, 5635-5646.

14. Smith, K. M., Bu, Y., and Suga, H. (2003) Induction and Inhibition of *Pseudomonas aeruginosa* Quorum Sensing by Synthetic Autoinducer Analogs, *Chem. Biol. 10*, 81-89.

15. Ishida, T., Ikeda, T., Takiguchi, N., Kuroda, A., Ohtake, H., and Kato, J. (2007) Inhibition of quorum sensing in *Pseudomonas aeruginosa* by *N*-acyl cyclopentylamides, *Appl. Environ. Microbiol. 73*, 3183-3188.

16. Welsh, M. A., and Blackwell, H. E. (2016) Chemical probes of quorum sensing: from compound development to biological discovery, *FEMS Microbiol. Rev. 40*, 774-794.

17. Boursier, M. E., Moore, J. D., Heitman, K. N., Fungairino, S. P. S.-., Combs, J. B., Koenig, L. C., Shin, D., Brown, E. C., Nagarajan, R., and Blackwell, H. E. Structure-function analyses of the N-butyryl L-homoserine lactone quorum sensing signal define features critical to activity in the *Pseudomonas aeruginosa* RhlR receptor, *In preparation*.

18. Janssens, J. C. A., Metzger, K., Daniels, R., Ptacek, D., Verhoeven, T., Habel, L. W., Vanderleyden, J., De Vos, D. E., and De Keersmaecker, S. C. J. (2007) Synthesis of N-Acyl Homoserine Lactone Analogues Reveals Strong Activators of SdiA, the *Salmonella enterica* Serovar Typhimurium LuxR Homologue, *Appl. Environ. Microbiol. 73*, 535-544.

19. Schaefer, A. L., Hanzelka, B. L., Eberhard, A., and Greenberg, E. P. (1996) Quorum sensing in Vibrio fischeri: Probing autoinducer-LuxR interactions with autoinducer analogs, *J. Bacteriol. 178*, 2897-2901.

20. Chhabra, S. R., Stead, P., Bainton, N. J., Salmond, G. P. C., Stewart, G. S. A. B., Williams, P., and Bycroft, B. W. (1993) Autoregulation of carbapenem biosynthesis in Erwinia carotovora by analogues of N-(3-oxohexanoyl)-L-homoserine lactone, *J. Antibiot. 46*, 441-454.

21. McInnis, C. E., and Blackwell, H. E. (2011) Thiolactone modulators of quorum sensing revealed through library design and screening, *Bioorg. Med. Chem. Lett. 19*, 4820-4828.

22. Gerdt, Joseph P., McInnis, Christine E., Schell, Trevor L., Rossi, Francis M., and Blackwell, Helen E. (2014) Mutational Analysis of the Quorum-Sensing Receptor LasR Reveals Interactions that Govern Activation and Inhibition by Nonlactone Ligands, *Chem. Biol.*, 1-9.

23. Moore, J. D., Gerdt, J. P., Eibergen, N. R., and Blackwell, H. E. (2014) Active Efflux Influences the Potency of Quorum Sensing Inhibitors in *Pseudomonas aeruginosa*, *ChemBioChem 15*, 435-442.

24. Sio, C. F., Otten, L. G., Cool, R. H., Diggle, S. P., Braun, P. G., Bos, R., Daykin, M., Cámara, M., Williams, P., and Quax, W. J. (2006) Quorum Quenching by an N -Acyl-Homoserine Lactone Acylase from *Pseudomonas aeruginosa* PAO1, *Infect. Immun. 74*, 1673-1682.

25. Pearson, J. P., van Delden, C., and Iglewski, B. H. (1999) Active Efflux and Diffusion Are Involved in Transport of *Pseudomonas aeruginosa* Cell-to-Cell Signals, *J. Bacteriol. 181*, 1203-1210.

26. Jencks, W. P., Cordes, S., and Carriuolo, J. (1960) The Free Energy of Thiol Ester Hydrolysis, *J. Biol. Chem. 235*, 3608-3614.

27. Barnett, R., and Jencks, W. P. (1969) The Rates of Hydrolysis of Two Thiol Esters in Water, *J. Org. Chem. 34*, 38-40.

28. Stevens, C. M., and Tarbell, D. S. (1954) The Kinetics Of Basic Hydrolysis Of Some γ-Lactones And γ-Thiolactones In Aqueous Acetone, *J. Org. Chem. 19*, 1996-2003.

29. Lin'kova, M. G., Kuleshova, N. D., and Knunyants, I. L. (1964) Thiolactones, *Russ. Chem. Rev. 33*, 493-507.

30. Morkunas, B., Galloway, W. R., Wright, M., Ibbeson, B. M., Hodgkinson, J. T., O'Connell, K. M., Bartolucci, N., Della Valle, M., Welch, M., and Spring, D. R. (2012) Inhibition of the production of the *Pseudomonas aeruginosa* virulence factor pyocyanin in wild-type cells by quorum sensing autoinducer-mimics, *Org. Biomol. Chem. 10*, 8452-8464.

31. O'Reilly, M. C., and Blackwell, H. E. (2016) Structure-Based Design and Biological Evaluation of Triphenyl Scaffold-Based Hybrid Compounds as Hydrolytically Stable Modulators of a LuxR-Type Quorum Sensing Receptor, *ACS Infect. Dis. 2*, 32-38.

32. Zirvi, K. A., and Jarboe, C. H. (1971) Infrared Spectral Characteristics of the Cyclobutane Ring System, *J. Chem. Soc. B*, 1603-1606.

33. Prinz, H. (2010) Hill coefficients, dose-response curves and allosteric mechanisms, *J. Chem. Biol. 3*, 37-44.

CHAPTER 4:

Development of a FRET assay to characterize LuxR-type receptor ligand binding

Contributions: M. E. Boursier conceptualized project, performed FRET assays, and prepared manuscript. M. J. Styles performed NMR and photophysical measurements. Margrith E. Mattmann designed initial probe and performed preliminary screening. N. R Eibergen and K. E. Nyffeler performed cell-based reporter screening for unlabeled AHLs. H. E. Blackwell guided research and assisted in writing.

4.1 Abstract

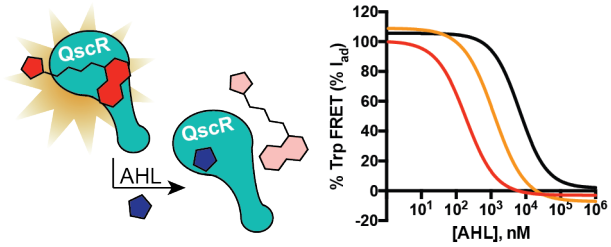

Gram-negative bacteria utilize a discrete set of small molecules (*N*-acyl L-homoserine lactones, or AHLs) and their cognate receptors (LuxR-type proteins) to control quorum sensing (QS). Upon binding to LuxR-type proteins, AHLs activate a series of macromolecular interactions that lead to the expression of QS genes. To date, full-length LuxR-type proteins have proved challenging to manipulate in vitro, and this problem has limited their biophysical characterization and the study of their DNA binding processes. Further, these experimental limitations have hindered the study of AHL:protein, and non-native ligand:protein, interactions. One LuxR-type protein, the QS control repressor (QscR) from *Pseudomonas aeruginosa* has been reported to be relatively stable in vitro. This finding prompted us to develop a new biophysical assay method to study ligand:QscR interactions in vitro. We developed a Förster Resonance Energy Transfer (FRET) assay that utilizes a novel dansyl AHL derivative and takes advantage of endogenous tryptophans located in the ligand binding pocket as the fluorescence donor. We applied this assay both in vitro and in cellulo to probe the effects of our previously identified synthetic ligands on QscR. Binding data obtained by using the FRET assay trends well with cell-based reporter data and electrophoretic mobility shift data that report [QscR:ligand]:DNA interactions. More interestingly, these FRET data provide new insights into the mechanism of action of non-native AHLs. Notably, these data suggest that nonclassical partial agonists bind with QscR at lower affinities than expected compared to cell-based reporter data. We anticipate this approach will be useful for studying ligand binding of other LuxR-type receptors in the future.

4.2 Introduction

Quorum sensing (QS) is a bacterial "language" composed of low molecular weight chemical signals and their corresponding receptors.[1] In Gram-negative bacteria, diffusible *N*-acyl L-homoserine lactones (AHLs) target their cognate cytoplasmic LuxR-type receptor proteins.[2] As the bacterial population increases, the AHL signals also increase in concentration. At a threshold cell density, these signals bind to their cognate receptors that then dimerize and interact with target DNA sequences, upregulating transcription of QS genes. Virulence factor production is often under the control of QS in numerous common pathogenic bacteria.[3, 4] Accordingly, QS has attracted significant recent attention due to its connection to serious human infection, and a number of chemical biological approaches have been aimed towards disrupting this communication process in order to attenuate virulence.[5]

Upon binding to their native AHL signal, LuxR-type proteins adopt an alternate confirmation that displays markedly enhanced stability relative to the apo-form.[6-8] This binding event is essential for QS. Considerable QS research, therefore, has focused on interrupting the binding of the native AHL signal to its cognate receptor protein.[5] Rational design, structural modeling, and high-throughput screening (HTS) using cell-based reporter assays have provided potent modulators of LuxR-type proteins.[9] However, further ligand development has been slowed by the limited mechanistic information on how lead compounds interact with receptor proteins. It is hypothesized that compounds bind in the ligand binding pocket, causing destabilization, misfolded monomers that cannot dimerize, or dimers that cannot bind to DNA (Figure 4.1). Especially powerful would be the ability to directly scrutinize protein:ligand binding events in vitro and compare the results to those obtained from reporter gene assays performed in whole cells that serve only as indirect readouts of ligand activity.

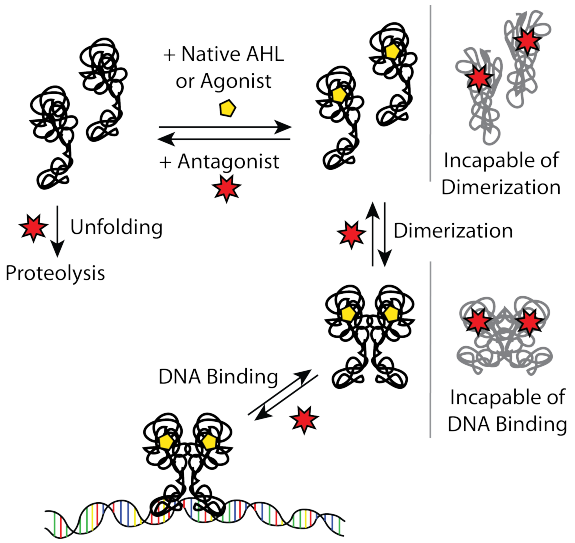

Figure 4.1. Proposed mechanism of action for agonists or antagonists versus LuxR-type receptors.

The empirical difficulties of handling these proteins, both in the presence and absence of ligand, has limited our understanding of the mechanism by which non-native ligands interact with LuxR-type receptors. Only four full-length crystal structures have been solved, including just one structure bound to an antagonist.[10-14] Much of the biochemical efforts to understand mode of action have focused on native AHLs.[10, 15, 16] Our recent collaboration with the Churchill lab has provided some insight into how both non-native agonists and antagonists are interacting with *Pseudomonas aeruginosa* receptor QscR.[17] Still, more work is needed to explore varying structural and functional classes of modulators. These efforts could be expedited with the development of a robust, high throughout biochemical assay to measure LuxR-type protein:ligand interactions.

Fluorescence based techniques are commonly developed as some of the most sensitive, robust, and widely used assays for the study of protein interactions. There has been limited success, however, incorporating these techniques into the study of LuxR-type receptors. Previously, AHL binding to LuxR-type receptors has been quantified using tryptophan fluorescence changes.[16, 18] Tryptophan is extremely sensitive to the chemical characteristics of the bound ligand, and subtle changes in compound structures can result in either enhancement or

quenching.[16] Changes in tryptophan fluorescence can also result in protein conformation changes or unfolding,[19] complicating studies examining ligand binding. Alternatively, fluorescence polarization (FP) has been used to quantify LuxR-type protein binding to fluorophore labeled DNA with the introduction of varying ligands.[13] These efforts yielded limited and indirect mechanistic data for ligand binding. Additionally, FP assays are limited by probe size or buffer viscosity, reducing the utility of this technique to look at other aspects of LuxR-type receptor mechanism of action.[20] Förster Resonance Energy Transfer (FRET), however, does not have the same limitations as FP and tryptophan fluorescence. FRET involves the excitation of a donor molecule followed by the transfer of energy to a nearby acceptor molecule, which in turn fluoresces and emits at a different wavelength.[21] Successful energy transfer requires donor and acceptor fluorophores to be 10 to 100 Å apart, limiting the likelihood of detecting nonspecific interactions.[21] Past studies examining LuxR-type protein dimerization and ligand binding have utilized FRET based techniques, generating fusion proteins with GFP and related fluorescent proteins.[22, 23] These studies did not report the activity of the wild-type protein or its interactions with non-native ligands, however.

An alternative means of utilizing FRET harnesses the useful fluorescent properties of intrinsic tryptophan rather than relying on tagged proteins. Tryptophan can be excited at 280 nm and emits at around 330 nm, which can readily excite fluorophores such as dansyl and cumarin.[24, 25] Additionally, this amino acid is relatively rare and is frequently found near protein binding pockets, often prompting the selection of tryptophans as donors in such FRET experiments.[26, 27] Lee and Peterson recently described the use of intrinsic tryptophan fluorescence in streptavidin in conjunction with a corresponding biotin FRET probe as a means to gather competitive inhibition constants (K_i) for a variety of unlabeled ligands.[28] They noted that the binding information gathered through their analysis was more precise than fluorescence quenching, fluorescence enhancement, or fluorescence polarization (FP) measurements. Fluorescence quenching and

enhancement is extremely sensitive to environmental conditions and aggregation, whereas FP data is limited by the fluorescence lifetime of the probe fluorophore.

Because 95% of known LuxR-type receptors have a conserved tryptophan in their AHL binding site that is believed to make a critical hydrogen binding contact with the homoserine lactone carbonyl (Figure 4.2A),[12, 29] we reasoned that we could apply the concepts of intrinsic FRET to the design of a new biophysical assay to measure LuxR-type protein: ligand interactions. To test this hypothesis, we focused on QscR from *P. aeruginosa*. From our prior experiments and those of other labs, we knew that QscR can be purified in good yield in the presence of readily displaceable *N*-3-oxo-hexanoyl-L-homoserine lactone (OHHL) rather than its preferred native ligand, OdDHL.[15] We developed a novel fluorescent AHL probe that could displace OHHL from QscR, By exciting the tryptophans found around the ligand binding pocket, we discovered that we could perform FRET with the fluorescent AHL. The displacement of this ligand resulted in a loss of FRET and the ability to monitor ligand binding (figure 4.2B). We utilized the FRET probe to develop both an in vitro and in cellulo assay, allowing for flexibility in use. Using this new assay, we have gathered some of the first known quantitative binding data for non-native AHLs with a LuxR-type protein. Moreover, these experiments afforded new insights into the mechanism of action for LuxR-type proteins and our non-native AHLs.

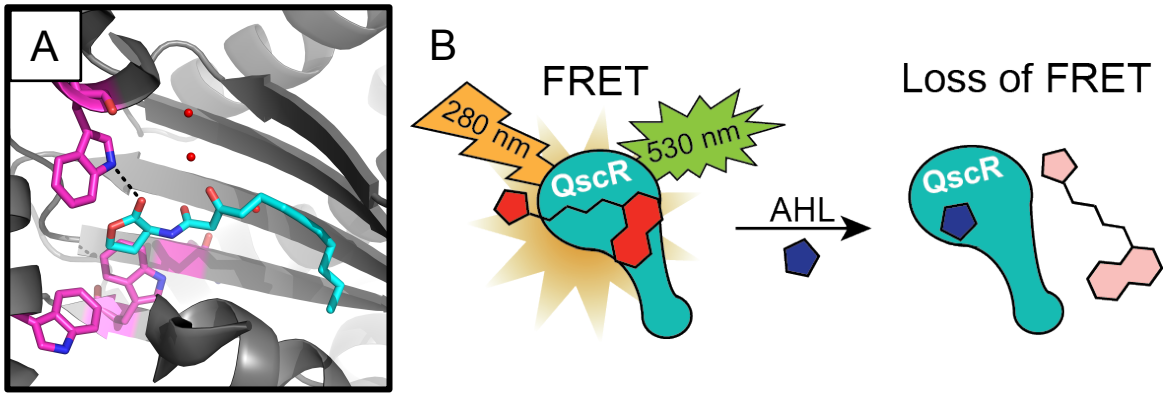

Figure 4.2. A) Image of the ligand binding pocket of QscR (list PDB code). OdDHL is shown in cyan. Tryptophan residues are highlighted in pink.[30] The highly conserved tryptophan residue (Trp62) is shown making hydrogen binding contact with homoserine lactone carbonyl of OdDHL. B) Cartoon depicting our competitive FRET method in QscR.

4.3 Results and discussion

4.3.1 Development of a QscR FRET probe

To develop a probe for competitive displacement experiments, we sought a moderately potent QscR agonist. Such an activity profile would allow for protein binding and activation, but still permit competitive displacement with other ligands of interest (either agonists or antagonists). We also had to consider the technical requirement that QscR is purified with OHHL as a stabilizing agent,[15] so any potential FRET ligand had to be sufficiently potent to displace this AHL. Since the homoserine lactone head group is known to be important component for potent LuxR-type receptor modulator development, we sought to develop a fluorescent probe that maintained this moiety. We reasoned that the fluorophore then could be installed on the acyl tail, and we selected a dansyl group in our initial probe design as this fluorophore has a steric profile similar to aryl groups found in our previously reported synthetic AHLs that are active in QscR.[31, 32] We produced a small suite of dansyl AHLs, with varying aliphatic linkers between the homoserine lactone and the dansyl group, via standard amide coupling chemistry. These compounds were tested for QscR agonism using an established reporter assay in *E. coli* (data not shown),[33] and a lead compound (**MMF5**, Figure 4.3) displaying modest agonistic activity was selected for further study (Table 4.1). In comparison with QscR's preferred native ligand OdDHL, **MMF5** was approximately 30-fold less potent. Critically, however, **MMF5** was more than 20-fold more potent than OHHL, making it an excellent mid-range agonist for further study.

Table 4.1. Activity data for OdDHL, **MMF5**, and OHHL in an *E. coli* reporter assay.[a]

	EC_{50} (μM)	95% CI (μM)	Activation (%)[b]
OdDHL	0.015	0.013 – 0.019	100
MMF5	0.47	0.37 – 0.60	84
OHHL	13	7.7 – 24	61

[a]Assays were performed using *E. coli* JLD271 (pJN105Q/pSC11-Q); see Experimental Section. EC_{50} values were determined by testing AHLs over a range of concentrations (≤ 100μM). Assays were performed in triplicate, and 95% confidence intervals (CIs) were calculated from the SEM of n ≥ 3 trials. [b]Denotes the highest value of LasR or QscR activation seen for each compound at any concentration within the dose–response assay. For the full agonism traces, see Figures S1. QscR activity was measured relative to that of 100 μM OdDHL.

We next sought to evaluate the excitation and emission spectra of QscR and **MMF5**. The respective emission and excitation spectra showed areas of distinct overlap, suggesting compatibility for FRET pairing (Figure 4.4A). QscR excitation at 280 nm did show some overlap with the excitation of **MMF5**, but this amount of overlap was not deemed prohibitive for FRET due to its relative size. Encouraged by this observation, we next worked to both miniaturize the assay into a 384 well format and show that FRET occurred with the incubation of **MMF5** and protein. Plate-based assays allow for increased screening efficiency and are critical for the development for higher-throughput assays. We incubated **MMF5** with a five-fold higher concentration of QscR, minimizing the amount of free ligand present. The resulting emission spectra of **MMF5** and QscR showed a FRET peak corresponding to 512 nm. Notably, 1 μM of **MMF5** did not produce a fluorescence peak at this concentration, likely due to the low quantum yield of this fluorophore in polar media.[24] Dansyl has a larger quantum yield in nonpolar solvents,[34] and the hydrophobic pocket found in QscR may similarly improve fluorescence output.

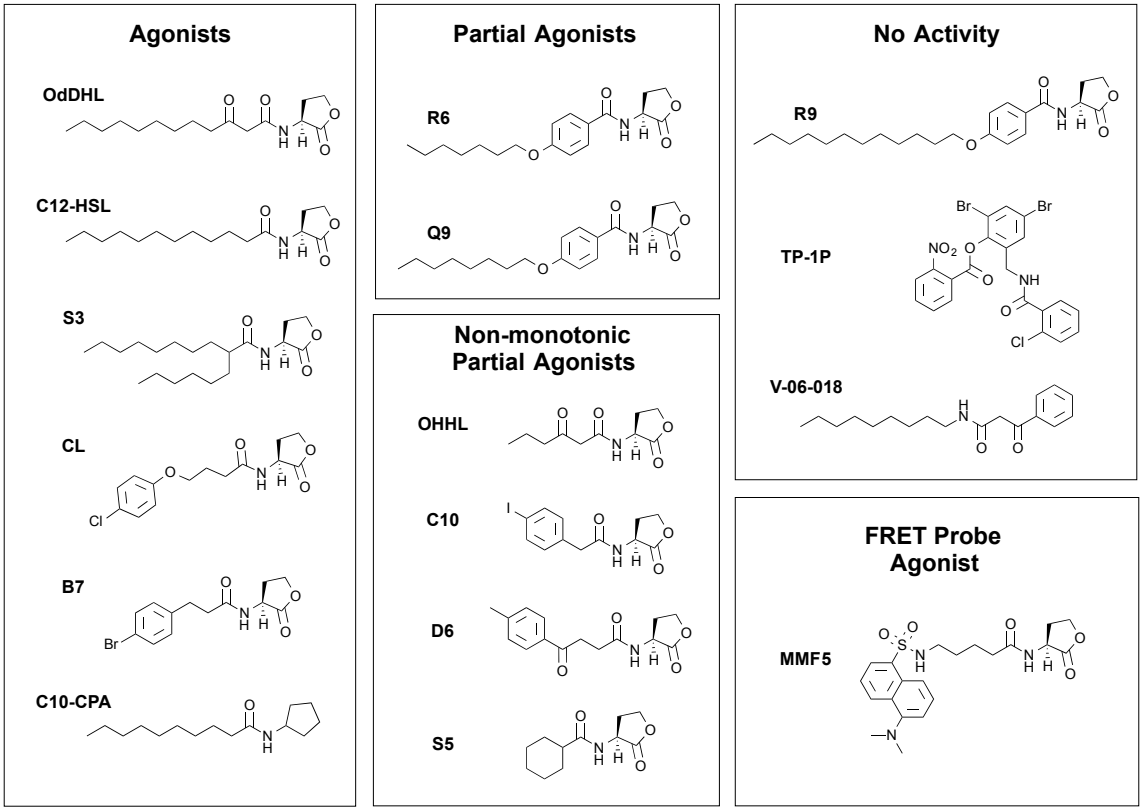

Figure 4.3. Structures of AHLs and AHL analogs tested in this study. Compounds were developed by the following labs: **CL**, Bassler and coworkers[35]; **C10-CPA**, Kato and coworkers[36]; **TP-1P** and **V-06-018**, Greenberg and coworkers[37-39]; all remaining non-native AHLs, Blackwell and coworkers.[32, 40]

To show that this interaction between **MMF5** and QscR was specific and not due to another interaction, we added 100 μM OdDHL to the solution. This addition resulted in a 70% reduction in FRET. The remaining fluorescence potentially suggests another interaction between QscR and **MMF5** that is nonspecific. We note that QscR has six total tryptophan and 10 tyrosine residues that could be engaging in FRET interactions with **MMF5**, and these may be the origin of the residual fluorescence. However, the observed difference in **MMF5** bound and unbound was deemed adequate to investigate further binding studies. To further ensure that this FRET interaction was specific for our probe, we performed an analogous fluorescence experiment using free dansylamine in the presence of QscR. No FRET was observed using the same concentrations of ligand and protein (data not shown).

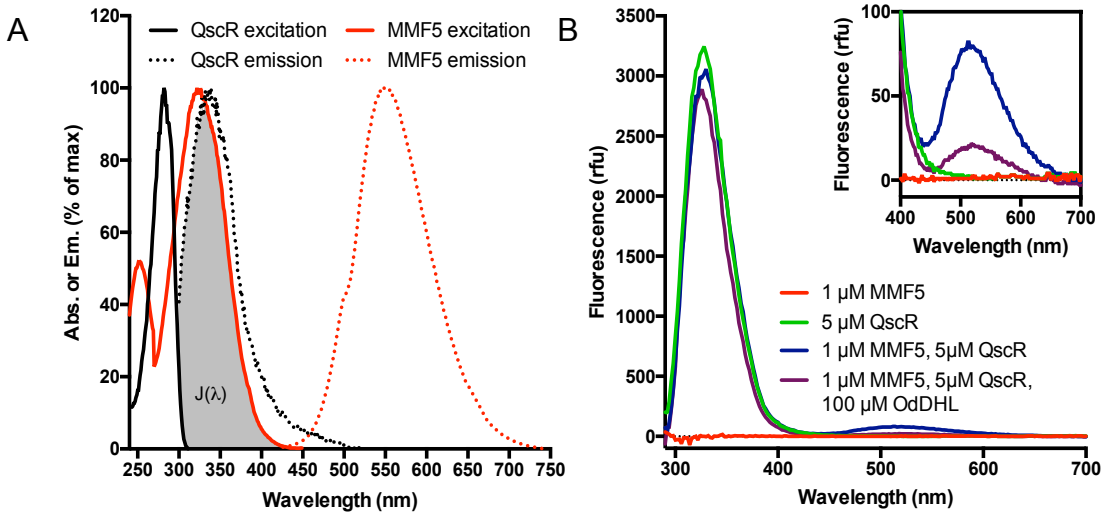

Figure 4.4. Spectral information for QscR and **MMF5**. A) Normalized excitation and emission spectra for QscR (ex: 280 nm) and **MMF5** (ex: 330 nm). J(λ) indicates the spectral overlap critical for FRET. B) FRET emission spectra (ex: 280 nm) upon binding of QscR and **MMF5**.

In order compare the binding profiles of other ligands to **MMF5** with QscR, we sought to calculate the K_d of binding between **MMF5** and QscR. To this end, we added increasing concentrations of protein to 50 nM of probe, a concentration expected to be well below its K_d value (Figure 4.5). We calculated a K_d of 1.01 ± 0.19 μM, approximately in the same regime as the EC_{50} in the cell-based reporter assay. QscR is expected to be a monomer at concentrations below 1 μM,[15] suggesting the ability of this assay to look solely at ligand-protein interactions without the complexity of dimerization. This K_d value was also in a regime comparable to other K_d values calculated for LuxR-type protein:AHL binding obtained using isothermal titration calorimetry (ITC) and intrinsic protein fluorescence quenching.[10, 16] Notably, intrinsic FRET required much less protein as compared to ITC and did not show the unpredictable changes in fluorescence observed with observing tryptophan alone. We decided to move forward in developing competition assays using a variety of unlabeled AHLs versus **MMF5** in QscR.

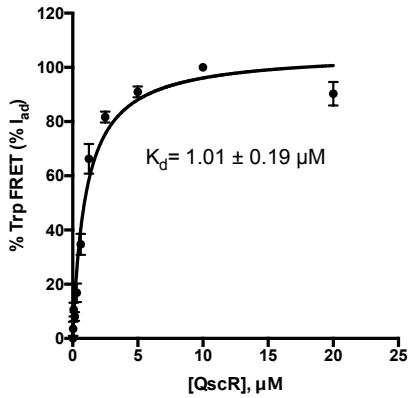

Figure 4.5. Direct binding curve for **MMF5** to calculate K_d of binding. Samples were excited at 280 nm and emission measured at 530 nm. Concentration is based on monomeric QscR. Curve is a compilation of n = 3 trials. Error bars show SEM.

4.3.2 Compound selection for competitive FRET screening

In selecting our compounds for testing in the FRET assay, we focused on compounds displaying a range of activities and activity profiles in QscR, favoring compounds reported in our recent in vitro biochemical studies in collaboration with the Churchill lab (Figure 4.3, see Table 4.4 in Supplemental Information for screening data).[17] The selected agonists were some of the most potent compounds identified in QscR, including C12-AHL, which actually equally as potent as OdDHL based on EC_{50} and % agonism, compound **CL**, and **S3**. **B7** was selected since it is a potent agonist of QscR, but also displays strong agonism and antagonism profiles in a number of LuxR-type receptors.[31, 40] The similar EC_{50} values in our QscR reporter assay for these potent agonists were intriguing due to the varied structures of these compounds. Finally, **C10-CPA** was found to agonize QscR with similar activity to **MMF5**, and thus would serve as a comparable control.

We also chose a range of partial QscR agonists for study in the FRET assay (Figure 4.3). Partial agonist compounds show agonism in the QscR reporter, yet also cause a decrease in QscR activity when competing against native ligand OdDHL. The agonism and antagonism profiles then converge at the compound's overall maximal agonism activity. We selected partial agonist compounds with two different activity profiles in the QscR cell-based reporter assays, i.e.,

classical and nonclassical partial agonists. Examples of these partial agonist profiles are shown in Figure 4.6.

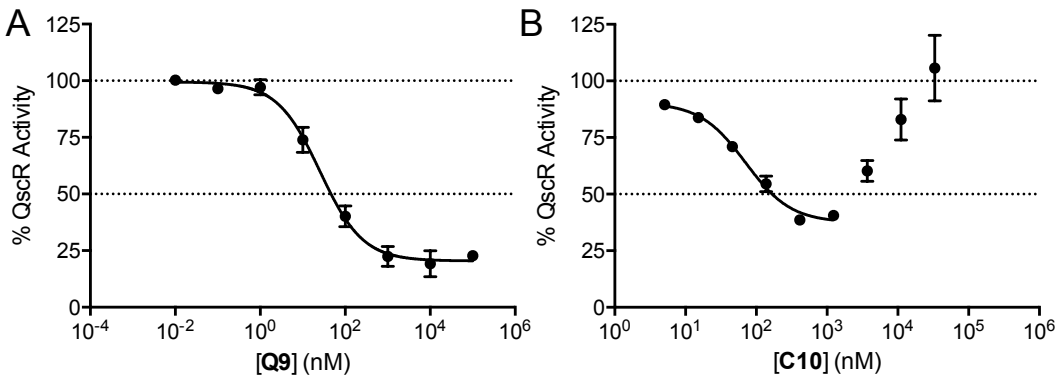

Figure 4.6. Representative antagonism curves for (A) classical partial agonist **Q9** and (B) nonclassical partial agonist **C10**. Complete screening data for all compounds tested is shown in Table 4.4.

Compounds **R6** and **Q9** are the most potent known classical partial agonists of QscR. Their respective EC_{50} and IC_{50} values, all in the mid-nanomolar range, are comparable to each other. These compounds are hypothesized to operate by shifting the protein equilibrium towards its monomeric form, leaving the protein more unstable and susceptible to proteolysis.[17] Any dimer that is formed is not in its most stable confirmation as when bound to OdDHL.[17] We also selected nonclassical partial agonists displaying what we have termed "nonmonotonic" behavior.[41] In an inhibition assay, these compounds cause an activity decrease like a typical partial agonist, but this is abruptly followed by a steep increase or "upturn" in activity that corresponds to the agonism profile of the compound. Such behavior is hypothesized to be related to protein:ligand interactions, as the nonmonotonic curve is still observed when cell-based antagonism assays are performed with various surfactants at concentrations known to break up compound aggregation (Figure 4.13, Supplemental Information). The origin of this nonmonotonic activity is currently unknown, and developing an understanding of it was one motivation for these in vitro studies. **C10** is the most potent nonclassical partial agonist, whereas **S5** has the greatest percent

antagonism of QscR's total activity. **D6** was selected since it is one of the strongest agonists that also displays nonmonotonic character, activating QscR 68% at 100 μM. We also included OHHL in this group. Interestingly, this ligand stabilizes QscR during protein purification, yet displays nonclassical partial agonist character in cell-based reporter assays.

Lastly, we selected three additional compounds to serve as negative controls that displayed limited or no activity in QscR reporter assays (Figure 4.3). **R9** has a similar structure to partial agonists **R6** and **Q9**, but shows no activity in either agonism or antagonism assays. We hypothesize that this compound is likely too long to fit in the QscR binding pocket. **TP-1P** and **V-06-018** are two of the most potent known LasR agonists and antagonists, respectively, yet both show limited activity in QscR. Interestingly, while LasR and QscR both bind to the same native ligand OdDHL and have a fair amount of structural homology, QscR is far less accommodating of ligands with head groups larger than the homoserine lactone.

4.3.3 Competitive FRET experiments correlate with cell-based screening data

We proceeded to test the selected compounds for QscR binding in the competitive FRET assay. Compounds were evaluated at a variety of concentrations to obtain dose-response profiles. In each well, the QscR concentration was maintained at 50 nM, again well below the calculated K_d for **MMF5**. This protein concentration keeps the bulk of the FRET probe unbound by QscR, simplifying experimental setup and data analysis.[42] Protein was preincubated with 1.25 μM **MMF5**, a concentration selected to be just above the K_d value. Compound was then added and plates incubated. After reading both FRET and **MMF5** fluorescence, curves were generated plotting the normalized loss of fluorescence versus compound concentration and correcting for fluorescence quenching (Figure 4.7). IC_{50} values generated from these plots were converted to K_i values using the Cheng-Prusoff equation (Table 4.2).

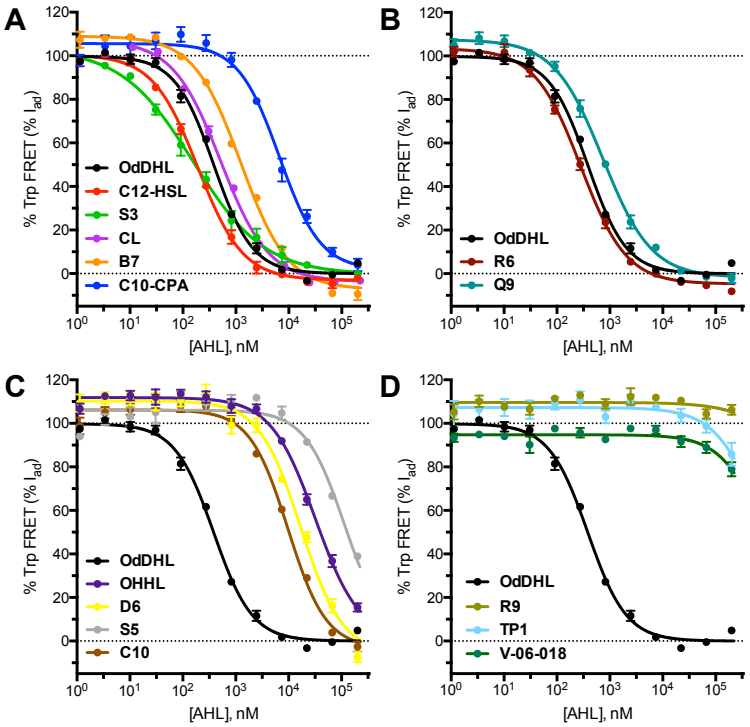

Figure 4.7. Competitive binding curves for QscR agonists (A), classical partial agonists (B), nonclassical partial agonists (C), and limited activity compounds (D) competed against QscR bound to **MMF5**. The binding curve for native ligand OdDHL is included on each plot. Tryptophan residues were excited at 280 nM, and FRET was measured at 530 nm. Values have been corrected for fluorescence quenching and normalized to OdDHL. Curves are a compilation of n = 3 trials.

The classical QscR agonists were found to have larger differences in apparent binding affinities as determined via the FRET assay than anticipated, despite having comparable EC_{50} values in cell-based reporter assays. For instance, compounds C12-HSL and **S3** displayed two-fold greater K_i values than native ligand OdDHL. These trends for C12-HSL and **S3** appeared to correlate, at least in part, with the calculated logP of the compound (Table 4.5, Supplemental Information); C12-HSL and **S3** are much more hydrophobic by this measure than other tested AHLs with comparable reporter EC_{50} values, and we speculate that they less able to dissociate from the greasy binding pocket. However, this logP trend did not hold for other compounds tested in this study. We note crystal structures acquired with C12-HSL or **S3** and QscR showed that the protein forms slightly altered structures relative to OdDHL-bound QscR.[17] These changes in structure may also have an influence on binding. Compounds **B7** and **CL** were not as potent as

OdDHL, with **B7** proving to be two-fold less potent than **CL**. This difference could be attributable to ligand size since **CL** is longer than **B7**, but further comparative analyses are required to determine whether this is a trend for other non-native ligands with comparable cell-based reporter activities. **C10-CPA** has a K_i that is in the same low micromolar regime as FRET probe **MMF5**, an expected trend based on the cell-based reporter data.

Table 4.2. Competition IC_{50} values[a] and calculated K_i values[b] and corresponding *E. coli* reporter assay data.[c]

	In-vitro FRET				Cell-based Reporter	
Compound	**IC_{50} (μM)**	**95% CI (μM)**	**Average K_i (μM)**	**SEM (μM)**	**EC_{50} (μM)**	**IC_{50} (μM)**
OdDHL	0.38	0.34 – 0.43	0.170	0.010	0.015	–
C12-HSL	0.19	0.17 – 0.22	0.0865	0.0087	0.015	–
S3	0.16	0.12 – 0.21	0.0768	0.0188	0.036	–
CL	0.52	0.45 – 0.59	0.232	0.019	0.016	–
B7	1.2	1.1 – 1.4	0.553	0.019	0.015	–
C10-CPA	6.6	5.3 – 8.3	2.98	0.33	0.62	–
R6	0.28	0.24 – 0.32	0.126	0.008	0.074	0.042
Q9	0.74	0.64 – 0.85	0.330	0.020	0.12	0.026
OHHL	32	28 – 37	14.3	0.7	13	0.16
D6	17	14 – 21	7.55	0.07	2.9	0.18
S5	110	90 – 150	51.1	3.0	–	0.74
C10	9.7	8.3 – 11	4.32	0.05	0.66	0.070
TP-1P	–	–	–	–	–	–
R9	–	–	–	–	–	–
V-06-018	–	–	–	–	–	–

[a]Calculated from three experimental replicates over a range of concentrations (≤ 200μM). [b]Values were calculated by averaging the K_i values associated with the IC_{50} of three independent replicates. [c]Assays were performed using *E. coli* JLD271 (pJN105Q/pSC11-Q); see Experimental Section. EC_{50} values were determined by testing AHLs over a range of concentrations (≤ 100μM). Assays were performed in triplicate. See Table 4.4 for complete reporter data.

Classical partial agonists **Q9** and **R6** proved to be potent binders to QscR in the FRET assay, yielding binding constants at concentrations comparable to OdDHL. These profiles are similar to those in cell-based reporter assays, where the EC_{50} for OdDHL, as well as the EC_{50}/IC_{50} values for **Q9** and **R6,** are in the mid-nanomolar range. Since the mechanism of action proposed for **Q9**

and **R6** suggests that these ligands are inhibiting dimer formation,[17] it is not surprising that in an assay with monomer protein we observe no drastic changes in binding ability. Interestingly, in the cell-based assay **R6** is a more potent agonist and less potent inhibitor based on percent activity as compared to **Q9**, and **R6** displays a lower K_i value. This result suggests that a compound's percent activity in the cell-based reporter may correlate in part with K_i data calculated via the in vitro FRET assay.

The nonclassical partial agonist compounds proved to be far less active in the FRET assay as compared to the classical agonists and the classical partial agonists. Their K_i values tracked closely with their cell-based reporter assay EC_{50} values in the low- to mid-micromolar range. This trend was somewhat unexpected, as these compounds also show inhibitory activity in the nanomolar range in the cell-based reporter assay. We hypothesize that the inhibition observed in cell-based assays is not related solely to ligand binding and instead relates to the QscR dimerization and DNA binding. Since we are evaluating protein monomers in the FRET assay, any effects that these compounds have on the protein dimer should not be observable. Further studies are ongoing to investigate this hypothesis.

As expected, compounds that showed limited or no activity in the QscR reporter strain also showed comparable activity in the FRET assay. The assay setup was able to detect the marginal activity associated with compounds **V-06-018** as well as **TP-1P** and no activity with compound **R9**. These data, along with that for all of the compound classes described above, gave us confidence in the broad applicability of this FRET based assay for small molecule screening in QscR.

4.3.4 Confirmation of agonist activity with electrophoretic mobility shift assays

We next sought to verify the observed trends in the competitive QscR FRET assay by utilizing electrophoretic mobility shift assays (EMSAs). Such experiments allow for DNA binding to be quantified in a more direct manner than in a cell-based reporter assay. Varying

concentrations of AHLs were incubated with QscR and a fluorescein-labeled DNA sequence containing QscR's primary promoter region. We selected only a subset of compounds for this analysis (native ligand OdDHL, FRET probe **MMF5**, **CL**, **R6** and **C10**), which represented some of the most potent compounds in each compound class (Figure 4.8A). We were particularly interested in further delineating differences between our classical and nonclassical partial QscR agonists in the presence of DNA. Gel shift assays were quantified by comparing free DNA band intensities between QscR-treated samples both with and without ligand, and then calculating the fraction of DNA in a bound complex; this accounts for any DNA bound complexes that do not clearly appear on the native gel (Figure 4.8B). Concentrations of AHL at which QscR is half saturated with DNA ($K_{0.5}$) can be calculated from these binding curves (Figure 4.8C). We note the occasional presence of shifted band in samples without added ligand. This shift is likely due to the residual amount of OHHL, an agonist, present in the QscR samples (an artifact of the protein purification strategy). To reduce the effect of these slight shifts on quantification, lanes with QscR added but without ligand served as the negative controls (Lane 2, Figure 4.8A).

The agonist compounds behaved largely as expected in the EMSA assays, causing almost complete DNA shifts at high AHL concentrations. Native ligand OdDHL resulted in the greatest DNA shift at lower concentrations of ligand. **CL** caused a substantial shift as well, albeit the calculated $K_{0.5}$ was at a 10-fold higher concentration than that of OdDHL. This result was unexpected as **CL** had comparable activity to OdDHL in both the cell-based reporter data and the FRET binding assay. As QscR must productively dimerize and bind to DNA in this assay in order for a DNA shift to occur, it is possible that the **CL**-QscR dimer is not as stable as one with OdDHL in absence of cellular machinery (i.e., in vitro). Another possibility is that the gel shift is in part correlated with maximal receptor activation in the cell-based reporter assay. Despite having a more than ten-fold higher EC_{50} in a reporter, **MMF5** caused only two-fold less gel shift than **CL** based on $K_{0.5}$. Both agonize QscR to about 85% of the activity achieved by OdDHL in the QscR reporter (Table 4.4). The difference in $K_{0.5}$ between OdDHL and **MMF5** was about 18-

fold, a comparable difference to EC_{50} values observed in the cell-based reporter assay data. Further work is needed to explore the relationship between gel shift and reporter activity data for classical agonists, particularly to determine variations in agonist mechanism of action.

Drastically different binding profiles were observed with the two partial agonist compounds. The EMSA data for nonclassical partial agonist **C10** roughly correlated with its agonism profile in the report assay, with both EMSA and reporter data suggesting that there is no DNA binding at lower ligand concentrations associated with the non-monotonic dose response behavior. Notably, while **MMF5** and **C10** have relatively comparable EC_{50} values in the cell-based reporter, **C10** has a $K_{0.5}$ that is five-fold higher than **MMF5**. This difference is roughly comparable with the difference between the K_d of **MMF5** and the K_i of **C10** calculated via in vitro FRET, and may be related in part to the percent activation observed in the reporter assay. Despite these compounds having similar potencies based on EC_{50} values, they are not equally efficacious at agonizing the receptor. **C10** agonizes QscR to 36% activity in reporter assay, whereas **MMF5** agonizes to 84%. Classical partial agonist **R6** shows no appreciable shift at any ligand concentration tested. Not only is **R6** a fairly poor agonist based on percent activation of QscR in a reporter (Table 4.4), but we have also shown **R6** to induce a gel shift only with high concentrations of both ligand and QscR.[17] This ligand is shown to alter the protein dimer-monomer equilibrium towards the monomeric state,[17] so in these studies there is likely not sufficient dimer formed to show a sizable DNA gel shift. These data further supports different mechanisms of action between these two classes of partial agonists, potentially relating to alternative effects on receptor dimerization.

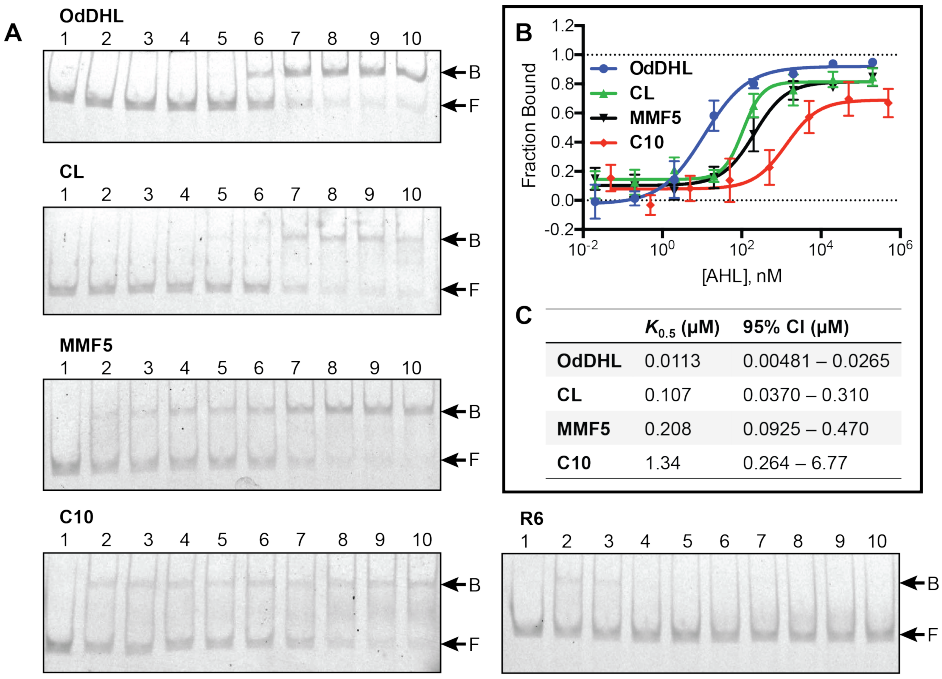

Figure 4.8. A) Electrophoretic mobility shift assays for compounds OdDHL, **CL**, **MMF5**, **C10**, and **R6**. Lane 1, 250 pM fluorescently labeled DNA with no QscR added. Lane 2, 5 nM QscR added, no ligand added. Lanes 3 through 10 include AHL in concentrations ranging from 20 pM to 200 μM for all compounds besides **C10**, which ranges 50 pM to 500 μM. QscR-free target DNA (F), and QscR-bound DNA (B) are indicated by the arrows to the right of the gel. B) Comparison of fraction bound for OdDHL, **CL**, **MMF5**, and **C10** made by quantifying the free DNA band at each compound concentration. Values are an average of n = 3 replicates. C) The concentrations of AHLs at which QscR is half saturated.

4.3.5 FRET approach is amenable to whole cell assays

We next investigated whether our FRET technique could be performed in cells. This ability would circumvent the relatively time consuming protein purification steps required for in vitro QscR studies and, with further development, could provide a pathway towards monitoring LuxR-type receptor locations and quantities in cell. Native and non-native AHLs are generally thought to be freely permeable across the cell membrane. Dye molecules have also been shown to pass through the bacterial membrane as well. Lending further support to our direct approach in cells, Meijler and coworkers showed in 2011 that the covalent capture of an AHL bound to LasR with a BODIPY probe could be performed in *P. aeruginosa*.[43] For our proof of concept studies, we

selected the same *E. coli* QscR overexpression strain used for generating purified QscR, as QscR is produced at very low levels in *P. aeruginosa*.[15] Following overnight protein expression in the presence of OHHL for protein stabilization, we found that doping in increasing amounts of **MMF5** to the cells and measuring fluorescence emission resulted in a dose response curve, with saturating amounts of FRET observed around 30 μM **MMF5** (Figure 4.14, Supplemental Information). To perform competitive FRET in cell, we selected a probe concentration of 5 μM, a concentration at which we observed greater than 50% of the FRET signal occur. Cells were washed to remove residual OHHL, and then incubated with the FRET probe for 30 minutes at room temperature. Cells were then added to culture plates with varying concentrations of AHLs. The same suite of AHLs was tested in cells that were used in the in vitro setup. We were delighted to see a significant decrease in FRET upon the addition various active ligands (Figure 4.9). Despite being limited to calculating only IC_{50} values (and no K_i values, since exact protein concentration could not determined), similar inhibition trends to the in vitro assay were observed for most AHLs (Table 4.3). Figure 4.10 compares the IC_{50} values for compounds tested in both assays, with compounds grouped as either classical or nonclassical modulators.

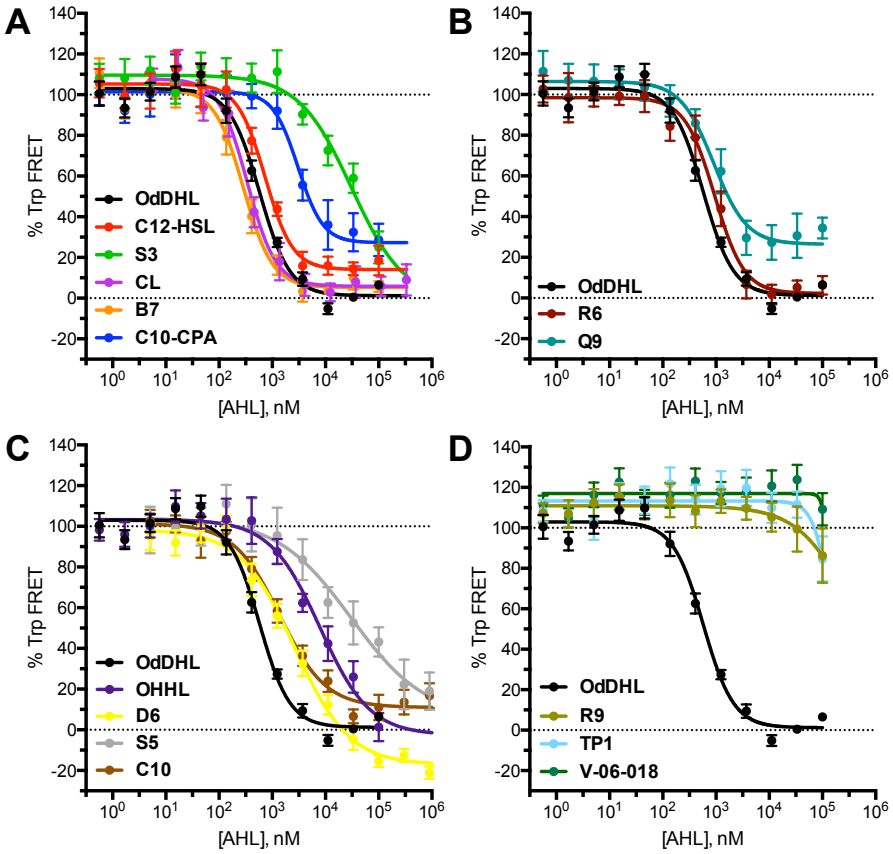

Figure 4.9. Competitive binding curves for QscR agonists (A), classical partial agonists (B), nonclassical partial agonists (C), and limited activity compounds (D) competed against a QscR overexpression strain incubated with **MMF5**. The binding curve for native ligand OdDHL is included on each plot. Tryptophan residues were excited at 280 nM, and FRET was measured at 530 nm. Values have been background corrected and normalized to OdDHL. Curves are a compilation of n = 3 trials.

The differences in classical agonist and classical partial agonist activity were not as striking with in cell FRET versus in vitro FRET. OdDHL, C12-HSL, **B7**, and **CL** show comparable IC_{50} values, with 95% confidence intervals that greatly overlap. **C10-CPA** maintained fairly comparable binding ability, with an IC_{50} value remaining in the low micromolar range. Surprisingly, **B7** had the largest change from in vitro to in cell FRET, going from one of the weaker classical agonist binders to one of the most potent. Additional work is required to determine if this difference is related to a different mechanism of action. Because these four compounds had similar EC_{50} values in the cell-based reporter assay and the in cell FRET assay, we suggest that this in cell FRET assay could be a means to obtain binding data in a similar

cellular environment. Classical partial agonists displayed IC_{50} values comparable to OdDHL, tracking closely with data both in vitro and in the reporter assay. The difference in activity between **R6** and **Q9** based on IC_{50} virtually disappears, although we note that the maximal loss of FRET is not the same between the two compounds in this assay. Limited activity compounds **R9**, **V-06-018**, and **TP-1P** showed marginal activity once again, in analogy to the in vitro protocol.

Table 4.3. In-cell competitive FRET IC_{50} data[a] and corresponding in vitro competitive FRET IC_{50} data.[b]

	In-cell FRET		In vitro FRET	
Compound	**IC_{50} (μM)**	**95% CI (μM)**	**IC_{50} (μM)**	**95% CI (μM)**
OdDHL	0.58	0.46 – 0.73	0.38	0.34 – 0.43
C12-HSL	0.73	0.52 – 1.0	0.19	0.17 – 0.22
S3	31	14 – 68	0.16	0.12 – 0.21
CL	0.34	0.24 – 0.48	0.52	0.45 – 0.59
B7	0.29	0.21 – 0.39	1.2	1.1 – 1.4
C10-CPA	3.1	1.8 – 5.1	6.6	5.3 – 8.3
R6	0.94	0.66 – 1.3	0.28	0.24 – 0.32
Q9	0.90	0.52 – 1.6	0.74	0.64 – 0.85
OHHL	7.9	4.0 – 15	32	28 – 37
D6	2.6	1.8 – 3.9	17	14 – 21
S5	31	8.7 – 110	110	90 – 150
C10	1.4	0.91 – 2.1	9.7	8.3 – 11
TP-1P	–	–	–	–
R9	–	–	–	–
V-06-018	–	–	–	–

[a]Calculated from three experimental replicates over a range of concentrations (≤ 100μM). [b]Calculated from three experimental replicates over a range of concentrations (≤ 200μM).

Nonclassical partial agonists had a fairly dramatic decrease in IC_{50} values, showing an increase in potency. Strikingly, this shift was remarkably consistent for all compounds. The resulting trend line generated for nonclassical partial agonists in Figure 4.10 is far more robust than that generated for classical modulators. In the cellular context, these compounds have an improved ability to displace **MMF5** versus in vitro studies. We also note that the associated Hill slopes for these compounds are shallower than both the classical agonists in this assay and all

compounds in vitro (data not shown). This difference may again be due to an influence of the associated cellular machinery or architecture; confined proteins may be more likely to dimerize due to increased local concentrations, influencing ligand-binding ability. Further study is required to determine the mechanistic implications for this IC_{50} change.

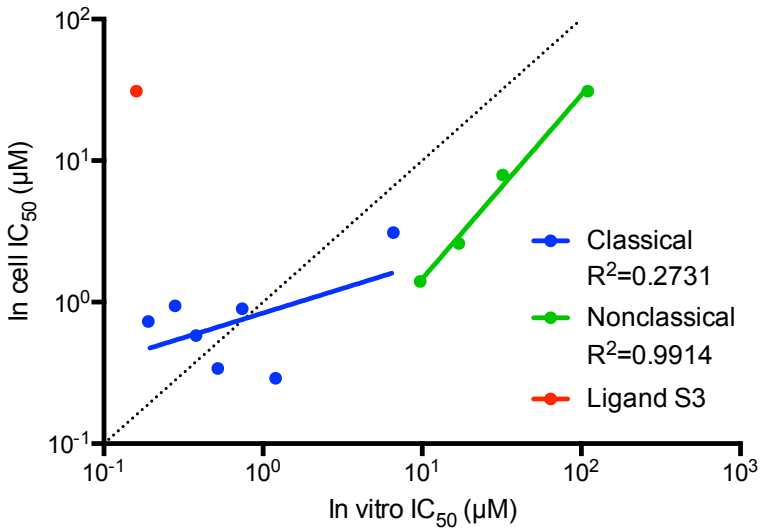

Figure 4.10. Comparison of IC_{50} values for classical (blue) and nonclassical (green) compounds in vitro and in cell. Dotted diagonal line designates an equal relationship between IC_{50} values in the two assays. Classical agonist S3 (red) deviates dramatically from other compounds tested.

We note several aspects of this assay that are in need of further exploration. Notably, ligand **S3** had greatly reduced activity in this in cell FRET system (Figure 4.10). Due to this compound's structural similarity to phospholipids with its branched tail, we hypothesize that it may be associating with the cell membrane and reducing intracellular interactions with QscR. As this compound is highly potent in our cell-based reporter assays (also in *E. coli*), the shorter time course and lower temperature of our assay may be limiting diffusion of this AHL through the membrane. This assay also does not introduce AHLs of interest during protein production and folding; it is possible that **S3** binds and stabilizes the protein in the initial stages of biosynthesis in cell. LuxR-type receptors bind their ligands reversibly, but this binding is extremely tight (as underscored in our studies here) and helps stabilize active protein.[44] Additionally, compound **D6**

proved to consistently reduce FRET fluorescence over 20% below the baseline achieved by OdDHL. This compound could be interfering with specific or nonspecific **MMF5**-QscR interactions. Alternatively, this compound could serve as a fluorescence quencher, reducing the amount of light emitted in the presence of the cell mixture. These observations suggest assay limitations for certain classes of ligand. We are actively investigating these phenomena further to improve this assay.

4.4 Summary

The development of chemical probes for LuxR-type proteins is hampered by the lack of mechanistic information on the modes by which native and non-native ligands interact with these receptors and modulate their function. The QS field would greatly benefit from techniques allowing for the rapid analysis of direct receptor:ligand binding for the screening of compounds. To this end, we have developed a FRET-based technique that utilizes the intrinsic tryptophan residues characteristic of most LuxR-type proteins. This technique has allowed us to characterize the binding of a series of non-native AHLs to the QscR receptor from *P. aeruginosa* for the first time. We have also successfully transferred this technique into a cell-based setup, potentially eliminating the labor-intensive protein purification for preliminary binding screens.

Our competitive FRET assay with QscR showed binding trends that are similar to observed reporter assay data. There were several interesting activity trends, however, when data from the QscR FRET, reporter, and EMSA assays were examined together. For example, classical agonist compounds that have nearly identical activity profiles in the cell-based reporter assay can have subtle differences in vitro and in EMSAs, suggesting slight differences in agonist mode of action. Classical partial agonists bind QscR with low K_d values, yet promote very little DNA binding. This corroborates prior studies indicating that this ligand class interferes with dimer formation. Nonclassical partial agonist binding in vitro does not occur at concentrations associated with the antagonism regime of the nonmonotonic activity curve. This disconnect indicates that the

observed inhibition is likely due to alterations in protein dimerization or DNA binding, or another downstream effect, not direct ligand:protein binding. Notably, these trends remained relatively consistent upon moving to an in-cell FRET setup, although subtle changes in some activity profiles indicate that the cellular environment may influence compound binding. Additional efforts will explore variations in these assay setups to further understand their scope and limitations. More broadly, we anticipate that this FRET assay protocol and **MMF5** (or analogs thereof) will be exportable to other LuxR-type proteins. The ability to reliably study the interactions of these receptors with ligands in vitro will significantly expand the understanding of this important QS receptor class.

4.5 Materials and Methods

4.5.1 Compound handling and reagents

The AHLs used in the DNA binding studies were described and completely characterized elsewhere.[32, 40, 41] Stock solutions of synthetic compounds (10 mM) were prepared in DMSO and stored at -20 °C in sealed vials. Solvent resistant polypropylene 96-well plates (Corning Costar cat. no. 3790), polystyrene 96-well plates (Corning Costar cat. no. 3997), 384-Well optical bottom polystyrene plates (Nunc cat. no. 142761), or polypropylene 384- well plates (Corning Costar cat. no. 3575) were used when appropriate. All biological reagents were purchased from Sigma Aldrich and used according to enclosed instructions. Buffers and solutions for Miller absorbance assays were prepared as described. HPLC-purified DNA was purchased from IDT.

4.5.2 Instrumentation

FRET assay results were obtained using a PerkinElmer Wallac 2100 EnVision multilabel plate reader using Wallac Manager v1.03 software. A filter of 600 nm was used for reading bacterial cell density. Filters of 280 nm and 530 nm were used to read fluorescence excitation and emission, respectively, for the 384-well FRET assays; filters of 355 nm and 530 nm were used for

dansyl fluorescence excitation and emission. Excitation and emission spectra of QscR and **MMF5** as well as quantum yield determination were recorded using an ISS PC1 steady state fluorimeter (500 nM slit widths) using an ultra-micro cuvette (Hellma 105.252). FRET spectra in the 384-well format were obtained using a Tecan Infinite M1000 Pro. EMSA images were captured using a GE Typhoon FLA 9500 imager.

4.5.3 Bacterial strains, plasmids, and culture conditions

E. coli strain JLD271 containing the QscR expression vector pJN105Q and the PA1897-*lacZ* vector psc11-Q was used for the agonism and antagonism cell-based reporter assays and cultured as previously reported.[33] *E. coli* strain JLD271 containing the LasR expression vector pJN105L and the lasI'-*gfp*[LVA] transcriptional fusion vector pPROBE-KL was used in assays testing for surfactant effects on nonmonotonic dose response behavior.[45] GFP assays were performed as previously described,[45] but with some modifications. DMSO stocks containing AHLs of interest were added to a 96 well plate, and cells were diluted 1:10 in LB before adding to the plate as well. Cells were grown for 6 hours at 37 °C shaking at 200 RPMs, after which GFP was quantified and normalized as previously documented. For strains screened with added surfactant, overnight cultures of *E. coli* were diluted 1:10 in LB containing Tween 20, Tween 80, or Triton X-100, respectively, at a final concentration of 0.025%. BL21 DE3 pLysS containing pET3a-qscR was used for the production of native QscR and for use in the cell-based FRET experiments.

4.5.4 Protein production and handling

Native QscR was expressed and purified bound to OHHL as previously described.[15] When needed, protein samples were concentrated using a stirred cell (Amicon). Protein concentrations were determined using a BCA protein assay (Peirce). Aliquots were flash frozen and stored at -80 °C.

4.5.5 Chemical characterization

^{1}H NMR spectra were recorded on a Bruker AC-300 spectrometer in deuterated solvents at 300 MHz. Chemical shifts are reported in parts per million (ppm, δ) using the solvent peak as an internal reference. Couplings are reported in hertz. Electrospray ionization (ESI) MS were obtained using a Shimadzu LCMS-2010 system (Columbia, MD) equipped with two pumps (LC-10ADvp), controller (S**CL**-10Avp), autoinjector (SIL-10ADvp), UV diode array detector (SPD-M10Avp), and single quadrupole analyzer. Compound logP values were calculated using ChemDraw 14.0.

*4.5.6 QscR and **MMF5** spectra collection*

QscR was thawed and diluted to 18 μM in low salt purification buffer, final DMSO concentration 2%. **MMF5** was added to low salt buffer to a final concentration of 100 μM, 2% DMSO. Spectra were obtained on a steady state fluorimeter at room temperature. To observe FRET spectra, QscR was thawed and diluted to 5 μM. **MMF5** (1μM) was added and incubated for 1 hour on ice. 100 μM OdDHL was added and the QscR was allowed to equilibrate at room temperature for 30 minutes. All samples maintained a DMSO concentration of 2%.

*4.5.7 K_d determination for **MMF5***

Protein was thawed and diluted to a range of concentrations (20 μM – 20 nM). 24.5 μL of each dilution was added to a 384 well plate containing 0.5 μL 2.5 μM **MMF5** in DMSO (50 nM final concentration, 2% DMSO). Plates were allowed to incubate for 30 minutes at room temperature, shaking. FRET and fluorescence were read at this time. Data was processed as previously described.[28]

4.5.8 Competitive FRET in-vitro assay setup

Protein was thawed and diluted to 50 nM concentration in low salt QscR purification buffer. Protein for competition studies was incubated for 1 hour on ice in the presence of 1.25 μM **MMF5**, a concentration just above the Kd. In 384 well plate, 0.6 μL DMSO stocks of varying compound concentrations were added. 29.4 μL protein solution was added to each well (2% DMSO final volume) Control wells with compound of interest at varying concentrations were included to account for ligand fluorescence. Plates were incubated for 30 minutes, shaking, at room temperature. FRET and fluorescence were read at this time. Data was processed as previously described, with background ligand fluorescence subtracted from FRET and fluorescence measurements.[28]

4.5.9 FRET in cellulo assay setup

QscR expression *E. coli* strain was grown as previously described. Cultures were pelleted (10 min at 3500xg) and washed 2 times in LB. Upon resuspension, 5 μM **MMF5** was added to a portion of the cells. Cells were incubated for 30 min, shaking, at room temperature. In a 394 well plate, 59.4 μL of cells were added to wells containing 0.6 μL DMSO stock (1% DMSO final volume) and plates were incubated at room temperature, shaking for 30 minutes. FRET, fluorescence, and OD_{600} were read at this time. Data was processed using a simple FRET background correction as previously described.[28] No effects on OD_{600} were observed during the time course of this assay.

4.5.10 Electrophoretic mobility shift assays

EMSAs were performed as previously described,[17] with the following modifications. Experiments utilized a fluorescein containing palindromic 50 base-pair DNA dimer [15] of sequence: 5' 6FAM- CT CTC CGC AGA TAC CTG CCC GGA AGG GCA GGT TGT CCC TGC CGG GCT GTG- 3'. Single strands were HPLC purified by IDT, resuspended in duplex

buffer and mixed in equimolar amount. DNA was then warmed to 95 °C in a water bath for 5 minutes and allowed to cool slowly overnight to form a duplex. In a 20 µL total reaction volume, 5 nM QscR was added to 250 pM DNA in LS buffer along with increasing concentrations of AHL of interest and 50 ng/mL poly(dI-dC). After incubation for 20 minutes at room temperature, 1 µL of loading dye was added (0.1% xylene cyanol in 50% glycerol). The samples were electrophoresed for 45 min at 4°C using an 8% non-denaturing TBE polyacrylamide gel (37.5:1 acrylamide:bis-acrylamide ratio) in 0.5 X TBE. Gels were imaged using the Typhoon PhosphorImager (488 nm excitation, 526 BP filter) and quantified using ImageQuant software.

4.6 Supplemental Information

4.6.1 Compound characterization data

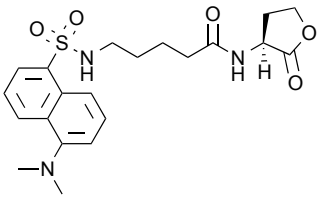

MMF5: 6-(5-Dimethylaminonaphthalene-1-sulfonylamino)-pentanoic acid was synthesized as previously described.[46] The acid (81.5 mg, 0.23 mmol, 1 eq) was then dissolved in DMF (4 mL). Triethylamine (64 µL, 0.46 mmol, 2 eq), HBr homoserine lactone (51 mg, 0.28 mmol, 1.2 eq), and HATU (131 mg, 0.35 mmol, 1.5 eq) was added at room temperature. The solution was allowed to stir overnight at room temperature, after which 20 mL EtOAc was added. The solution was washed with 1M citric acid (20 mL) and brine (20 mL), then dried using MgSO4. Remaining solvent was removed under reduced pressure. The resulting solid was purified using flash column chromatography (100% EtOAc) to afford product (76.8 mg, 77% yield). ^{1}H NMR: (299.7 MHz, CDC3N) δ 8.55 (Ar-H, t, J = 8.53 Hz, 1H), 8.26 (Ar-H, t, J = 9.0 Hz, 1H), 8.17 (Ar-H, dd, J = 7.4, 1.1 Hz, 1H), 7.60 (Ar-H, m, 2H), 7.27 (Ar-H, dd, J = 7.1, 4.7, 1H), 6.65 (NH, app s, 1H), 5.88 (NH, app s, 1H), 4.42 (CH-lac, ddd, J = 11.3, 8.8, 8.0 Hz, 1H), 4.35 (CH-lac, td, J = 9.3, 2.2 Hz,

1H), 4.19 (CH-lac, ddd, J = 10.7, 8.8, 6.3 Hz, 1H), 4.02 (CH-lac, dddd, J = 11.4, 9.6, 6.5 Hz, 1H), 2.87 (CH3, s, 6H), 2.82 (CH2, q, J = 6.4 Hz, 2H), 2.43 (CH-lac, ddd, J = 9.6, 6.7, 2.1 Hz, 1H), 2.02 (CH2, t, J = 7.8 Hz, 2H), 1.40 (CH2, m, 4H); Exp [M+] = 433.52; obs [M+] = 433, [M+Na+] = 456.2.

Table 4.4. Complete cell-based reporter assay data for compounds screened in this study.[a]

Compound	EC_{50} (μM)	95 % CI (μM)	Max Activation[b]	IC_{50} (μM)	95 % CI (μM)	Max Inhibition[c]
MMF5	0.47	0.37 – 0.60	84%	–	–	–
OdDHL	0.015	0.012 – 0.018	100%	–	–	–
C12-HSL[d]	0.015	0.011 – 0.020	110%	–	–	–
S3[d]	0.036	0.021 – 0.060	88%	–	–	–
CL[d]	0.016	0.010 – 0.027	86%	–	–	–
B7	0.015	0.0059 – 0.040	91%	–	–	–
C10-CPA	0.62	0.35 – 1.1	91%	–	–	–
R6	0.074	0.025 – 0.22	23%	0.042	0.017 – 0.10	58%
Q9	0.12	0.0037 – 3.6	11%	0.026	0.015 – 0.042	80%
OHHL	13	7.6 – 24	61%	0.16	0.0077 – 3.2	34%
D6	2.9	1.2 – 6.9	68%	0.18	0.0061 – 5.6	43%
S5	–	–	24%	0.74	0.49 – 1.1	92%
C10	0.66	0.21 – 2.1	36%	0.070	0.051 – 0.097	61%
TP-1P	–	–	–	–	–	26%
R9	–	–	–	–	–	–
V-06-018	–	–	22%	–	–	–

[a]Assays were performed using *E. coli* JLD271 (pJN105Q/pSC11-Q); see Experimental Section. For both agonism and antagonism assays, EC_{50} values were determined by testing AHLs over a range of concentrations (≤ 100μM). Assays were performed in triplicate, and 95% confidence intervals (CIs) were calculated from the SEM of $n \geq 3$ trials. [b]Denotes the highest value of QscR activation seen for each compound at any concentration within the dose–response assay. [c]Denotes the lowest value of QscR inhibition seen for each compound at any concentration within the dose–response assay. For the full agonism and antagonism traces, see Figures 4.10 and 4.11. QscR activity was measured relative to that of 100 μM OdDHL for agonism, 15 nM for antagonism. [d]Data is previously reported elsewhere.[17] Full dose response curves are shown in Figures 4.10 and 4.11.

Table 4.5. logP values calculated for the AHLs screened in this study.[a]

Compound	logP
MMF5	2.76
OdDHL	1.97
C12-HSL	3.23
S3	5.05
CL	1.43
B7	1.91
C10-CPA	3.98
R6	3.09
Q9	3.51
OHHL	-0.53
D6	2.02
S5	0.63
C10	0.8
TP1P	5.62
R9	5.17
V-06-018	3.98

[a]Calculated using ChemDraw 14.0.

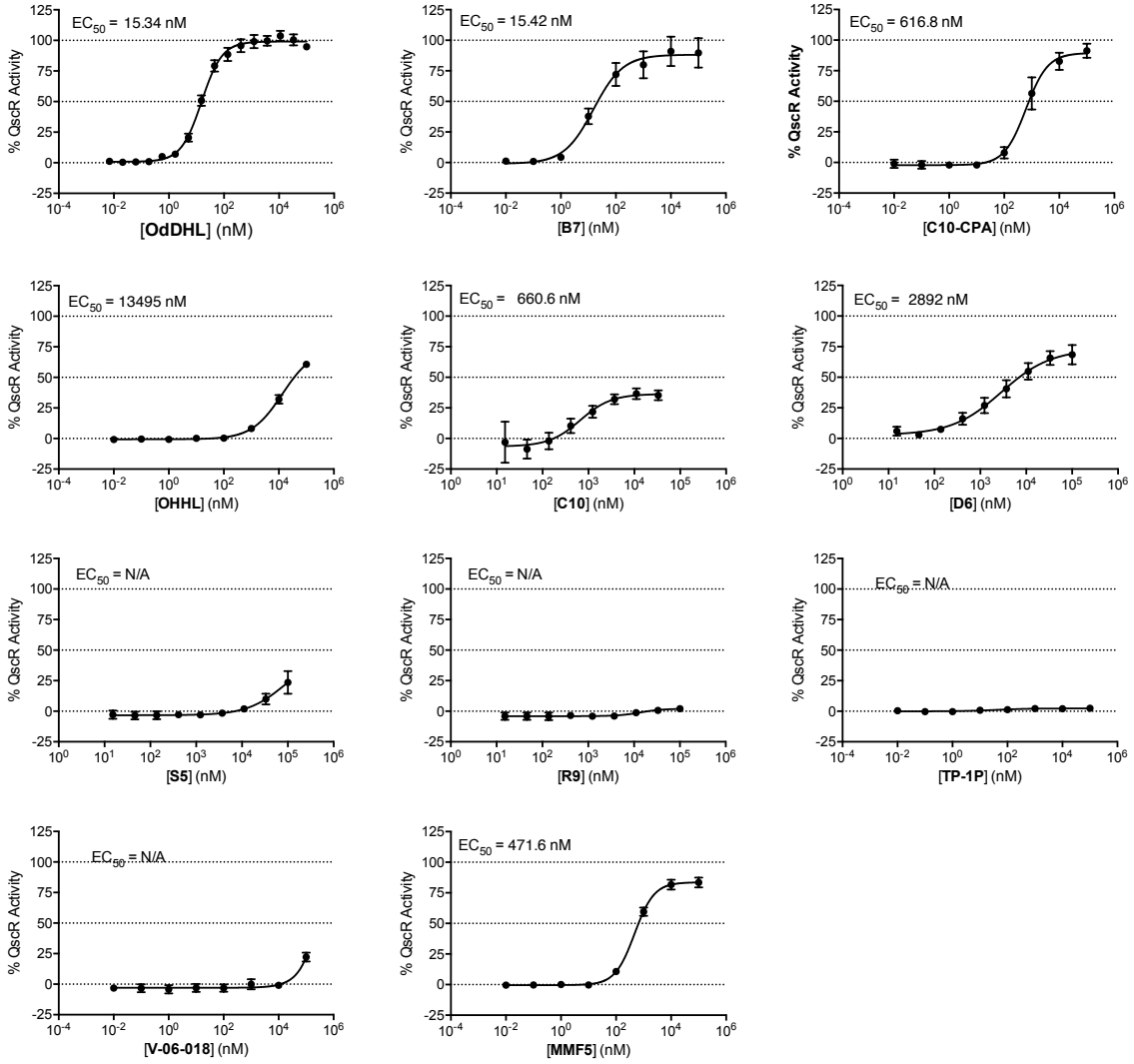

Figure 4.11. Dose–response curves for QscR agonism in *E. coli* by compounds tested in this study and not previously screened using the *E. coli* JLD271/pJN105Q/pSC11-Q reporter strain. % Activity is defined as the activity of the synthetic AHL relative to maximum possible OdDHL activity (i.e., activity effected by OdDHL at 100 μM). EC_{50} values and 95% Confidence Intervals (CI; shown in Table 4.4) calculated using GraphPad Prism. Error bars, SEM of $n \geq 3$ trials.

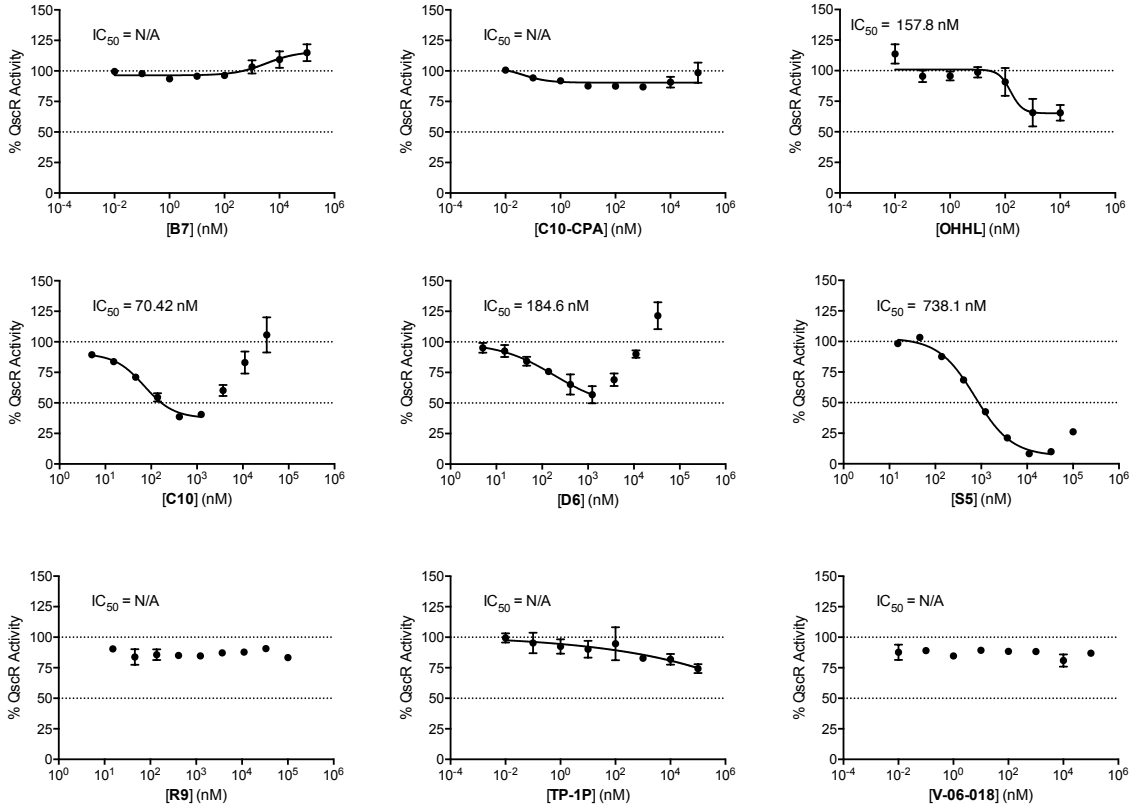

Figure 4.12. Dose–response curves for QscR antagonism in *E. coli* by compounds tested in this study and not previously screened using the *E. coli* JLD271/pJN105Q/pSC11-Q reporter strain. Assay performed with the addition of 15 nM OdDHL. % Activity is defined as the activity of the synthetic AHL relative to half maximal QscR activity (i.e., activity effected by OdDHL at 15 nM). IC_{50} values and 95% Confidence Intervals (CI; shown in Table 4.4) calculated using GraphPad Prism. Error bars, SEM of $n \geq 3$ trials.

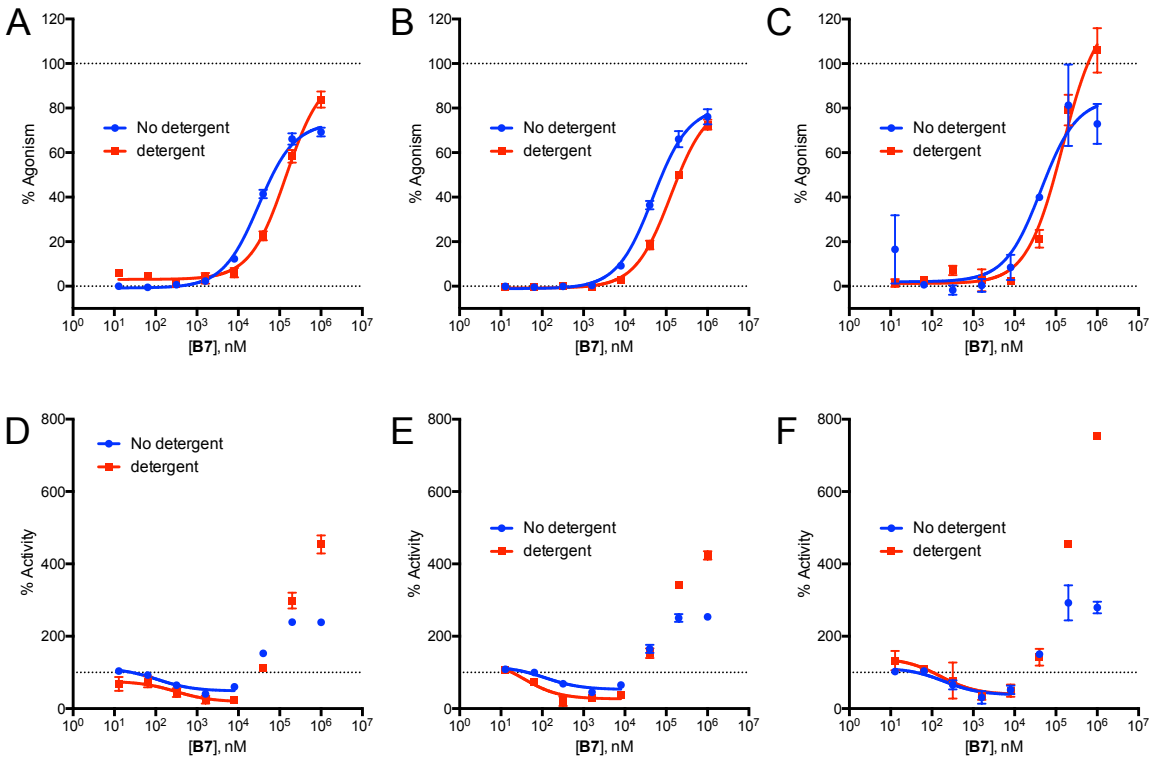

Figure 4.13. Dose–response curves for LasR agonism (A-C) and antagonism (D-F) of **B7** with and without detergent using the *E. coli* JLD271/pJN105L/pPROBE-KL reporter strain. Surfactant does not eliminate the nonmonotonic dose response character in the antagonism assay. Screens were performed using Tween 20 (A and D), Tween 80 (B and E), or Triton X-100 (C and F). Antagonism assay performed with the addition of 2 nM OdDHL, the EC_{50} for this receptor. % Activity in agonism assays is defined as the activity of the synthetic AHL relative to maximum possible OdDHL activity (i.e., activity effected by OdDHL at 100 µM). % Activity in antagonism assays is defined as the activity of the synthetic AHL relative to half maximal LasR activity (i.e., activity effected by OdDHL at 2 nM). Error bars, SEM of n =1 trial.

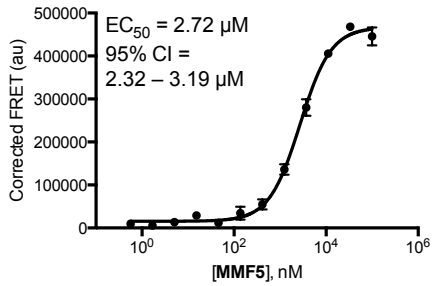

Figure 4.14. FRET observed at increasing concentrations of **MMF5** in QscR *E. coli* overexpression strain BL21 DE3 pLysS/pET3a-qscR.

4.7 References

1. Fuqua, W. C., Winans, S. C., and Greenberg, E. P. (1994) Quorum sensing in bacteria: the LuxR-LuxI family of cell density-responsive transcriptional regulators, *J. Bacteriol. 176*, 269-275.

2. Ni, N., Li, M., Wang, J., and Wang, B. (2009) Inhibitors and antagonists of bacterial quorum sensing, *Med. Res. Rev. 29*, 65-124.

3. Willcox, M. D. P., Zhu, H., Conibear, T. C. R., Hume, E. B. H., Givskov, M., Kjelleberg, S., and Rice, S. A. (2008) Role of quorum sensing by *Pseudomonas aeruginosa* in microbial keratitis and cystic fibrosis, *Microbiology (Reading, Engl) 154 (Pt 8)*, 2184-2194.

4. Wagner, V. E., and Iglewski, B. H. (2008) *P. aeruginosa* Biofilms in CF Infection, *Clinic. Rev. Allerg. Immunol. 35*, 124-134.

5. Geske, G. D., O'Neill, J. C., and Blackwell, H. E. (2008) Expanding dialogues: from natural autoinducers to non-natural analogues that modulate quorum sensing in Gram-negative bacteria, *Chem. Soc. Rev, 37*, 1432-1447.

6. Lee, J.-H., Lequette, Y., and Greenberg, E. P. (2006) Activity of purified QscR, a *Pseudomonas aeruginosa* orphan quorum-sensing transcription factor, *Mol. Microbiol. 59*, 602-609.

7. Kiratisin, P., Tucker, K. D., and Passador, L. (2002) LasR, a Transcriptional Activator of *Pseudomonas aeruginosa* Virulence Genes, Functions as a Multimer, *J. Bacteriol. 184*, 4912-4919.

8. Qin, Y., Luo, Z.-Q., Smyth, A. J., Gao, P., von Bodman, S. B., and Farrand, S. K. (2000) Quorum-sensing signal binding results in dimerization of TraR and its release from membranes into the cytoplasm, *EMBO J. 19*, 5212-5221.

9. Mattmann, M. E., and Blackwell, H. E. (2010) Small molecules that modulate quorum sensing and control virulence in *Pseudomonas aeruginosa*, *J. Org. Chem. 75*, 6737-6746.

10. Nguyen, Y., Nguyen, N. X., Rogers, J. L., Liao, J., Macmillan, J. B., Jiang, Y., and Sperandio, V. (2015) Structural and Mechanistic Roles of Novel Chemical Ligands on the SdiA Quorum-Sensing Transcription Regulator, *mBio 6*, 1-10.

11. Kim, T., Duong, T., Wu, C. A., Choi, J., Lan, N., Kang, S. W., Lokanath, N. K., Shin, D., Hwang, H. Y., and Kim, K. K. (2014) Structural insights into the molecular mechanism of *Escherichia coli* SdiA, a quorum-sensing receptor, *Acta Crystallogr. D Biol. Crystallogr. 70*, 694-707.

12. Zhang, R.-g., Pappas, K. M., Brace, J. L., Miller, P. C., Oulmassov, T., Molyneaux, J. M., Anderson, J. C., Bashkin, J. K., Winans, S. C., and Joachimiak, A. (2002) Structure of a bacterial quorum-sensing transcription factor complexed with pheromone and DNA, *Nature 417*, 971-974.

13. Chen, G., Swem, L. R., Swem, D. L., Stauff, D. L., O'Loughlin, C. T., Jeffrey, P. D., Bassler, B. L., and Hughson, F. M. (2011) A Strategy for Antagonizing Quorum Sensing, *Mol. Cell 42*, 199-209.

14. Lintz, M. J., Oinuma, K.-I., Wysoczynski, C. L., Greenberg, E. P., and Churchill, M. E. a. (2011) Crystal structure of QscR, a *Pseudomonas aeruginosa* quorum sensing signal receptor, *Proc. Natl. Acad. Sci. USA 108*, 15763-15768.

15. Oinuma, K.-I., and Greenberg, E. P. (2011) Acyl-homoserine lactone binding to and stability of the orphan *Pseudomonas aeruginosa* quorum-sensing signal receptor QscR., *J. Bacteriol. 193*, 421-428.

16. Welch, M., Todd, D. E., Whitehead, N. a., McGowan, S. J., Bycroft, B. W., and Salmond, G. P. (2000) N-acyl homoserine lactone binding to the CarR receptor determines quorum-sensing specificity in Erwinia., *EMBO J. 19*, 631-641.

17. Wysoczynski-Horita, C. L., Boursier, M. E., Hill, R., Hansen, K., Blackwell, H. E., and Churchill, M. E. A. Mechanism of agonism and antagonism of the *Pseudomonas aeruginosa* quorum sensing regulator QscR with non-native ligands, *In preparation*.

18. Minogue, T. D., Wehland-Von Trebra, M., Bernhard, F., and Von Bodman, S. B. (2002) The autoregulatory role of EsaR, a quorum-sensing regulator in *Pantoea stewartii* ssp. stewartii: Evidence for a repressor function, *Mol. Microbiol. 44*, 1625-1635.

19. Eftink, M. R. (1994) The use of fluorescence methods to monitor unfolding transitions in proteins, *Biophys. J. 66*, 482-501.

20. Jameson, D. M., and Ross, J. A. (2010) Fluorescence polarization/anisotropy in diagnostics and imaging, *Chem. Rev. 110*, 2685-2708.

21. Wu, P. G., and Brand, L. (1994) Resonance Energy Transfer: Methods and Applications, *Analytical Biochem. 218*, 1-13.

22. Zhang, C., and Ye, B. C. (2014) Real-time measurement of quorum-sensing signal autoinducer 3OC6HSL by a FRET-based nanosensor, *Bioprocess Biosys. Eng. 37*, 849-855.

23. Ventre, I., Ledgham, F., Prima, V., Lazdunski, A., Foglino, M., and Sturgis, J. N. (2003) Dimerization of the quorum sensing regulator RhlR: development of a method using EGFP fluorescence anisotropy, *Mol. Microbiol. 48*, 187-198.

24. Zhang, Y., Yang, X., Liu, L., Huang, Z., Pu, J., Long, G., Zhang, L., Liu, D., Xu, B., Liao, J., and Liao, F. (2013) Comparison of Förster-resonance-energy-transfer acceptors for tryptophan and tyrosine residues in native proteins as donors, *J. Fluoresc. 23*, 147-157.

25. Kim, J. H., Sumranjit, J., Kang, H. J., and Chung, S. J. (2014) Discovery of coumarin derivatives as fluorescence acceptors for intrinsic fluorescence resonance energy transfer of proteins, *Mol. BioSys. 10*, 30-33.

26. Bogan, A. A., and Thorn, K. S. (1998) Anatomy of hot spots in protein interfaces, *Journal of Mol. Biol. 280*, 1-9.

27. Khazanov, N. A., and Carlson, H. A. (2013) Exploring the Composition of Protein-Ligand Binding Sites on a Large Scale, *PLoS Comp. Biol. 9*, e1003321.

.

28. Lee, M. M., and Peterson, B. R. (2016) Quantification of Small Molecule–Protein Interactions using FRET between Tryptophan and the Pacific Blue Fluorophore, *ACS Omega 1*, 1266-1276.

29. Whitehead, N. A., Barnard, A. M. L., Slater, H., Simpson, N. J. L., and Salmond, G. P. C. (2001) Quorum-sensing in Gram-negative bacteria, *FEMS Microbiol. Rev. 25*, 365-404.

30. Churchill, M. E. a., and Chen, L. (2011) Structural basis of acyl-homoserine lactone-dependent signaling, *Chem. Rev. 111*, 68-85.

31. Mattmann, M. E., Geske, G. D., Worzalla, G. a., Chandler, J. R., Sappington, K. J., Greenberg, E. P., and Blackwell, H. E. (2008) Synthetic ligands that activate and inhibit a quorum-sensing regulator in *Pseudomonas aeruginosa*., *Bioorg. Med. Chem. Lett. 18*, 3072-3075.

32. Mattmann, M. E., Shipway, P. M., Heth, N. J., and Blackwell, H. E. (2011) Potent and Selective Synthetic Modulators of a Quorum Sensing Repressor in *Pseudomonas aeruginosa* Identified from Second-Generation Libraries of *N*-Acylated L-Homoserine Lactones, *Chembiochem 12*, 942-949.

33. Eibergen, N. R., Moore, J. D., Mattmann, M. E., and Blackwell, H. E. (2015) Potent and Selective Modulation of the RhlR Quorum Sensing Receptor by Using Non-native Ligands : An Emerging Target for Virulence Control in *Pseudomonas aeruginosa*, *ChemBioChem 16*, 2348-2356.

34. Li, Y.-H., Chan, L.-M., Tyer, L., Moody, R. T., Himel, C. M., and Hercules, D. M. (1975) Solvent effects on the fluorescence of 1-(dimethylamino)-5-naphthalenesulfonic acid and related compounds, *J. Am. Chem. Soc 97*, 3118-3126.

35. Swem, L. R., Swem, D. L., O'Loughlin, C. T., Gatmaitan, R., Zhao, B., Ulrich, S. M., and Bassler, B. L. (2009) A quorum-sensing antagonist targets both membrane-bound and cytoplasmic receptors and controls bacterial pathogenicity, *Mol. cell 35*, 143-153.

36. Ishida, T., Ikeda, T., Takiguchi, N., Kuroda, A., Ohtake, H., and Kato, J. (2007) Inhibition of quorum sensing in *Pseudomonas aeruginosa* by *N*-acyl cyclopentylamides, *Appl. Environ. Microbiol. 73*, 3183-3188.

37. Müh, U., Hare, B. J., Duerkop, B. a., Schuster, M., Hanzelka, B. L., Heim, R., Olson, E. R., and Greenberg, E. P. (2006) A structurally unrelated mimic of a *Pseudomonas aeruginosa* acyl-homoserine lactone quorum-sensing signal, *Proc. Natl. Acad. Sci. USA 103*, 16948-16952.

38. Müh, U., Schuster, M., Heim, R., Singh, A., Olson, E. R., and Greenberg, E. P. (2006) Novel *Pseudomonas aeruginosa* quorum-sensing inhibitors identified in an ultra-high-throughput screen, *Antimicrob. Agents Chemother. 50*, 3674-3679.

39. Zakhari, J. S., Kinoyama, I., Struss, A. K., Pullanikat, P., Lowery, C. A., Lardy, M., and Janda, K. D. (2011) Synthesis and molecular modeling provide insight into a *Pseudomonas aeruginosa* quorum sensing conundrum, *J. Am. Chem. Soc. 133*, 3840-3842.

40. Geske, G. D., O'Neill, J. C., Miller, D. M., Wezeman, R. J., Mattmann, M. E., Lin, Q., and Blackwell, H. E. (2008) Comparative analyses of *N*-acylated homoserine lactones reveal unique structural features that dictate their ability to activate or inhibit quorum sensing, *ChemBioChem 9*, 389-400.

41. Moore, J. D., Rossi, F. M., Welsh, M. A., Nyffeler, K. E., and Blackwell, H. E. (2015) A Comparative Analysis of Synthetic Quorum Sensing Modulators in *Pseudomonas aeruginosa*: New Insights into Mechanism, Active Efflux Susceptibility, Phenotypic Response, and Next-Generation Ligand Design, *J. Am. Chem. Soc. 137*, 14626-14639.

42. Pollard, T. D. (2010) A guide to simple and informative binding assays, *Mol. Biol. Cell 21*, 4061-4067.

43. Rayo, J., Amara, N., Krief, P., and Meijler, M. M. (2011) Live cell labeling of native intracellular bacterial receptors using aniline-catalyzed oxime ligation, *J. Am. Chem. Soc. 133*, 7469-7475.

44. Sappington, K. J., Dandekar, A. A., Oinuma, K.-i., Binding, R. S., Lasr, Q.-s. S. R., Feeds, R. S. S., and Journal, A. S. M. (2011) Reversible Signal Binding by the *Pseudomonas aeruginosa* Quorum-Sensing Signal Receptor LasR, *mBio 2*, e00011-11.

45. Moore, J. D., Gerdt, J. P., Eibergen, N. R., and Blackwell, H. E. (2014) Active Efflux Influences the Potency of Quorum Sensing Inhibitors in *Pseudomonas aeruginosa*, *Chembiochem 15*, 435-442.

46. Kong, Y., Jung, M., Wang, K., Grindrod, S., Velena, A., Lee, S. a., Dakshanamurthy, S., Yang, Y., Miessau, M., Zheng, C., Dritschilo, A., and Brown, M. L. (2011) Histone deacetylase cytoplasmic trapping by a novel fluorescent HDAC inhibitor, *Mol. Cancer Ther. 10*, 1591-1599.

CHAPTER 5:

The application of liquid crystalline droplets as sensors for quorate populations of bacteria

Contributions: B. J. Ortiz and M. E. Boursier designed experiments, performed LC dialysis cassette incubations, and composed chapter. B. J. Ortiz performed characterizations of LC-amphiphile interactions. M. E. Boursier quantified rhamnolipids and performed live-dead assays. M. E. Boursier and K. Veldkamp performed AHL quantification. D. Amador-Noguez provided experimental guidance. H. E. Blackwell and D. M. Lynn directed the project.

5.1 Abstract

Liquid crystals (LCs) have been used to detect the presence of bacteria via byproducts such as lipopolysaccharides. However, this detection approach requires membrane components that are only available upon bacterial cell lysis. We report the first instance of the use of LCs as responsive materials for amphiphilic bacterial goods directly associated with population density. The opportunistic pathogen *P. aeruginosa* excretes long chain signaling molecule *N*-(3-oxo-dodecanoyl)-L-homoserine lactone (3-oxo-C12-HSL) to gauge population density via quorum sensing (QS). An active QS system induces the production of a range of byproducts associated with virulence, including the biosurfactant rhamnolipid. We found that both of these molecules can induce bipolar-to-radial orientation changes in LC dispersions. When LCs are added to cell culture in a permeable membrane, only cells actively producing 3-oxo-C12-HSL or rhamnolipid components can induce an LC orientation change. Additionally, we show that *N*-acyl L-homoserine lactones with acyl chains eight carbons in length or longer induce LC transitions, suggesting that this detection technique may be applicable to a variety of bacterial QS systems. These findings demonstrate that QS-responsive materials may be a means to detect bacteria and open new ways for controlling bacterial social behaviors.

5.2 Introduction

Bacteria have evolved in a number of ways to sense and adapt to changing environments as a group. To achieve this, numerous species of bacteria coordinate ensemble behaviors in a process termed quorum sensing (QS). This cell-cell communication process includes the production, release, and detection of extracellular molecules known as autoinducers. The concentration of autoinducers increases proportionally to bacterial population.[1, 2] Through the activation of QS receptors at a threshold cell and signal density, bacteria are able to control gene expression initiating the production of group beneficial goods. This includes multiple virulence factors, which result in distinguishable changes in their environment. These factors include biofilm formation and the production of other virulence factors such as rhamnolipids, toxins, and redox-active pigments.[3, 4] The excreted goods that result from the upregulation of QS modulated genes could serve as analytes for stimuli-responsive materials, allowing for the detection of virulent bacteria at quorate populations.

An emerging paradigm for the suppression of bacterial infections involves the interception of innate cell-cell communication pathways by the release of QS-inhibitors from judicially designed polymeric coatings. These approaches conventionally entail the release of enzymes that degrade bacterial signaling molecules or antagonists that bind to QS cognate receptors, quenching gene expression and abating subsequent virulence factor production. Our groups[5-8] and others[9-14] have demonstrated that QS inhibitors can be immobilized on or incorporated into a range of surfaces and materials, including the commonly employed in medical devices.[15] Approaches such as these have some inherent limitations; since there is a finite amount of QS modulator housed in the materials, the control over QS is essentially temporary. Additionally, the release is irrespective of the environmental conditions (i.e., not dependent on the presence of bacteria or their population density).

To circumvent these disadvantages, synthetic soft materials with elements able to recognize and respond to prokaryotic cells, chemical signals, or QS-related virulence factors may prove

useful in controlling bacterial collective behaviors only on demand. Micrometer-sized thermotropic liquid crystals (LCs) droplets dispersed in aqueous media represent an attractive platform for the design of such stimuli-responsive soft materials. In this context, the ordering of nematic LC phases confined to spherical shapes have been explored for reporting on molecular interactions occurring at the interface of LC and aqueous phases. This ordering is possible due to the control of the surface energetics over the orientation of the mesogen molecules, which can propagate up to the bulk of the LC and lead to changes in the optical appearance of the LCs. This phenomenon has been used as the basis for the reporting of assemblies of several adsorbates, ranging from simple synthetic surfactants to protein-receptor complexes.[16-20] The transitions observed depend on the density of surfactant at the interface, as this influences the tilted angles of the interpenetrated tails.[13, 21, 22] Notably, transitions have been observed with endotoxin associated with the cell membrane of *E. coli*, suggesting the utility of LCs in detecting bacterial biproducts.[23, 24] Many bacteria produce other amphiphilic goods that are excreted without cell lysis; LCs thus could serve as a reactive detection tool for a variety of clinically relevant organisms.

The opportunistic pathogen *P. aeruginosa* produces numerous amphiphiles through its QS circuitry, including two distinct *N*-acyl-L-homoserine lactone (AHL) signaling molecules (Table 5.1). Long chain AHLs in particular can aggregate like surfactants due to their long acyl tail and polar lactone head group.[25] In the *P. aeruginosa* QS system, *N*-3-oxo-dodecanoyl-L-homoserine lactone (3-oxo-C12-HSL) is produced by the LasI synthase and binds to the LasR receptor. LasR upregulates the Rhl system in which *N*-butanoyl-L-homoserine lactone (C4-HSL) is produced by RhlI and binds to RhlR (Figure 5.1).[26] Receptor QscR also binds to 3-oxo-C12-HSL and serves as a repressor for the Las and Rhl systems when activated.[27] Besides producing amphiphilic AHLs, *P. aeruginosa* is one of the primary bacterial species that produces rhamnolipid biosurfactants.[28] As illustrated in Figure 5.1, rhamnolipid synthesis is directly controlled by the Las and Rhl QS systems.[29] Both receptors LasR and RhlR bind to their cognate AHL and upregulate the

production of the *rhlAB* operon. RhlA condenses two β-hydroxyacyl-acyl carrier proteins to 3-(3-hydroxyalkanoyloxy)alkanoic acid (HAA), and rhamnosyltransferase RhlB adds a rhamnose sugar to HAAs.[30] RhlC then adds a second rhamnose sugar.[31] As a QS associated virulence factor, rhamnolipids act as immune modulators and are involved in surface motility as well as bacterial biofilm development.[32]

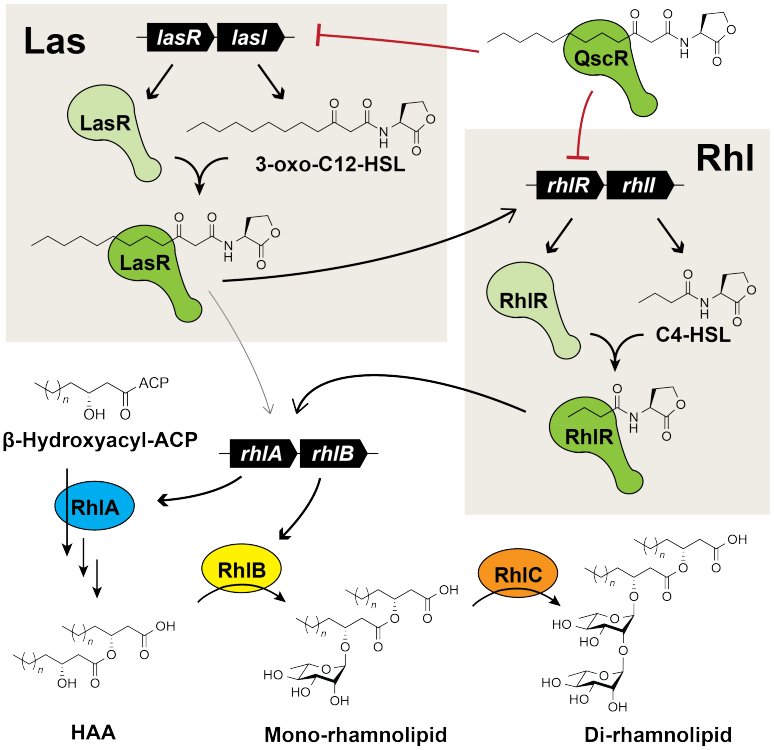

Figure 5.1: Regulatory QS pathways, Las and Rhl, used by *P. aeruginosa* to control rhamnolipid synthesis. QscR serves as a repressor for the Las and Rhl systems, and Las upregulates the Rhl system. Both receptors upregulate the production of the *rhlAB* operon. RhlA helps to convert β-hydroxyacyl-acyl carrier proteins to 3-(3- hydroxyalkanoyloxy)alkanoic acids (HAAs). RhlB and RhlC sequentially add rhamnose sugars to HAAs. Solid arrowheads indicate positive regulation, while flat, red arrowheads indicate negative regulation. Lighter arrow colors indicate minor regulatory pathways.

In this study, we invetigated whether *P. aeruginosa*'s QS-regulated amphiphilic molecules could interact with LCs and alter their configuration. We demonstrated that LC droplets are responsive to a variety of native AHLs as well as rhamnolipids. We also determined that LCs encapsulated in a permeable dialysis membrane are sensitive to surfactants produced by cultures

of *P. aeruginosa* at quorate densities. The system introduced here, as a proof of concept, can open new possibilities for the sensing and control of bacterial behaviors. Moreover, we foresee that sophisticated designs based on this approach can be useful in a biomedical context, for example, as biosensors, actuators or as advanced drug delivery structures.

5.3 Results and Discussion

5.3.1 LC induced ordering transitions by AHLs and rhamnolipid biosurfactants

We first sought to understand whether factors involved in the QS of *P. aeruginosa* could induce an orientational transformation in LC emulsions. A set of amphiphiles (Table 5.1) was compiled for testing that included 3-oxo-C12-HSL, C4-HSL, and rhamnolipid produced natively by *P. aeruginosa*. To fully explore differences in LC transitions based on AHL tail length, we also selected AHLs that included acyl chains ranging from 4 to 12 carbons. In addition, to probe how differences in the 3-oxo-C12-HSL structure change LC interactions, a hydrolyzed homoserine lactone "head group" and analogs with different oxidation states (hydroxyl, oxo, or methylene?) at the third carbon of the acyl chain were also included. All AHLs tested are natively involved in the QS of multiple Gram-negative bacteria species.[33]

Table 5.1. Structure of native AHLs involved in the QS of several Gram-negative bacteria species and biosurfactant rhamnolipids used in this study.

Ligand	Structure
3-oxo-C12-HSL*	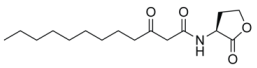
3-oxo-C12-HS*	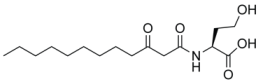
3-OH-C12-HSL	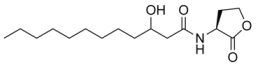
C10-HSL	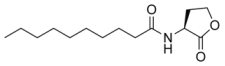
C8-HSL	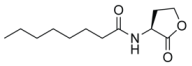
C6-HSL	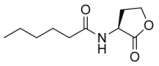
C4-HSL*	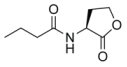
Rhamnolipid*	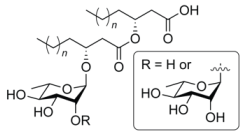

*produced natively by the human pathogen *P. aeruginosa*. Rhamnolipid acyl chain length, n = 3-11.[47]

With an amphiphile library in hand, we next tested the compounds' influence on the anchoring of 4'-pentyl-4-cyanobiphenyl (5CB, a nematic LC at room temperature) emulsions in aqueous buffer. These experiments were performed by evaluating the ordering transitions in micrometer-scaled 5CB droplets dispersed in a phosphate buffer saline (PBS) solution using polarized light microscopy and flow cytometry, according to our previously reported protocol.[34, 35] This analytical approach exploits the differences in the light scattering of bipolar and radial droplets to quantify the number of droplets with a radial configuration within a sample consisting of a mixture of the two. The bipolar state consists on the tangential alignment of the mesogen molecules to droplet surface, resulting in two topological defects at the pole of the droplet, shown in Figure 5.2A. This state is the preferred orientation for LCs at aqueous interfaces, but the adsorption of amphiphiles, such as sodium dodecyl sulfate (SDS),[24, 36, 37] can cause the

reorientation of the LCs to the radial state with a perpendicular alignment of LCs with respect to the droplet surface. The radial state is characterized by a single geometric point defect at its center (Figure 5.2A). These two LC configurations (bipolar and radial) translate to two distinct scatterings easily observed when plotting side-scattering (SSC) as a function of forward scattering (FSC) obtained from flow cytometry measurements (Figure 5.2B). Furthermore, the FSC histogram of the analyzed sample can be used to quantify the amount of droplets with a radial configuration based on the scattering differences using protocols previously reported.[35] This analysis technique allows for the efficient characterization of a large population of LC droplets.

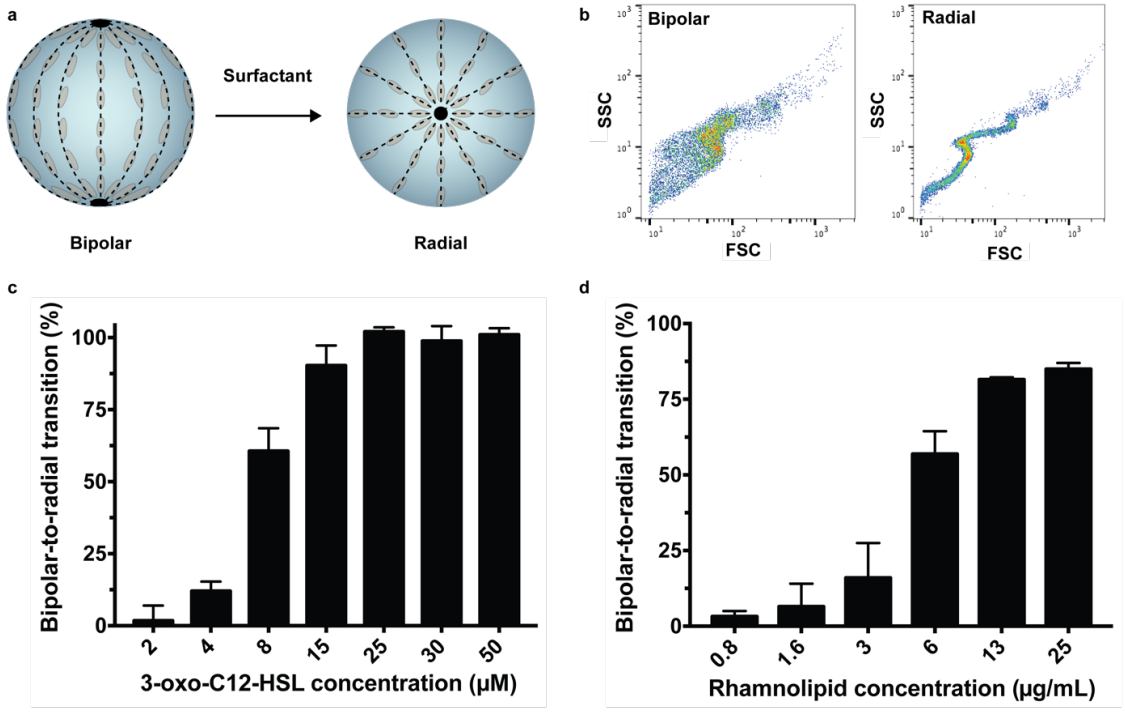

Figure 5.2. (a) Representation of LC droplets showing the director profiles in the bipolar and radial states. (b) Representative scatter plots obtained from the flowing of 5CB droplets before (bipolar) and after (radial) adding 3-oxo-C12-HSL through the flow cytometer. (c) Percentage of droplets transformed from bipolar-to-radial as a function of the concentration of 3-oxo-C12-HSL in PBS with 10 μM SDS and 1% DMSO. (d) Percentage of droplets transformed from bipolar-to-radial as a function of the concentration of a rhamnolipid mixture in PBS. Plots are representative of three independent experiments.

We first characterized and quantified the changes in the ordering of LC droplets upon exposure to 3-oxo-C12-HSL at biologically relevant concentrations (ranging from 2-50 μM (>50 μM have been reported in bacterial biofilms))[38] and to rhamnolipids at biologically relevant concentrations (ranging from 0.8 to 25 μg/mL). We predicted that these molecules would have robust affects on LCs. A sample of 5CB emulsion prepared using 10 μM SDS solutions in PBS was added to solutions of either 3-oxo-C12-HSL or rhamnolipids to achieve the desired final concentrations and a dispersion of ~ 10,000 droplets/μL. LC droplets scattering plots for 3-oxo-C12-HSL and rhamnolipids at the upper limit concentration used in this study, 50 μM and 25 μg/mL exhibit the characteristic "S-shape" of radial droplets (Figure 5.5, Supplemental Information). Further analysis revealed a concentration dependence in the ordering of LC droplets in the presence of 3-oxo-C12-HSL or rhamnolipid.

We quantified the LC response by calculating the proportion of droplets with a radial configuration relative to all droplets characterized (Table 5.2). For 3-oxo-C12-HSL, more than 50% of the total droplets in the sample exhibited a radial configuration at 8 μM concentrations compared to a predominantly bipolar sample at 2 μM concentration. For rhamnolipid, the concentration required to transformed more than 50 % of the droplets to the radial state was 6 μg/mL. Together, these results suggest the ability of 3-oxo-C12-HSL and rhamnolipids to induce changes in the anchoring energy of 5CB droplets, resulting in the transformation of droplet configuration. Previous studies using conventional single tail and two-tailed amphiphiles have found that the concentrations required to induced ordering transitions of droplets is around 10 μg/mL and require nearly saturated monolayer coverage;[23] the same order of magnitude is observed in the present study.

We next explored the remaining AHLs with various alkyl chain differences and structural changes from 3-oxo-C12-HSL (Table 5.1). Past studies using synthetic surfactants with distinct tail architectures indicate that the length or branching of the aliphatic tails are crucial factors for the orientation of LCs at the water-LC interface.[39-41] These studies also concluded that the effects

of the head group of the surfactants were imperceptible beyond adsorption isotherms.[39, 41] LC analysis was performed at a range of bulk AHL concentrations in order to determine the minimum concentration of each AHL necessary to induce a change in the ordering state. Figure 5.6 A-F shows the percentage of 5CB droplets dispersed in solutions of C4 to C10-HSL, 3-oxo-C12-HS and 3-OH-C12-HSL with a radial configuration as a function of the concentration of each AHL (Supplemental information). We documented the concentration at which each AHL induced at least a 50% LC transition (Table 5.2).

Table 5.2. Concentration of each AHL and rhamnolipid required to induce a bipolar-to-radial transformation to at least 50% of the 5CB droplet population in the sample. The change in configuration was determined in solutions containing 10 μM SDS in PBS at pH 7.4 containing 1 % v/v of DMSO of 10^4 5CB droplets analyzed.

Ligand	Concentration required to induce radial configuration (μM)
3-oxo-C12-HSL	8
3-oxo-C12-HS	25
3-OH-C12-HSL	25
C10-HSL	100
C8-HSL	400
C6-HSL	–
C4-HSL	–
Rhamnolipid	13[a]

[a] indicates units of μg/mL

The longer tail AHLs, namely 3-oxo-C12-HSL, 3-oxo-C12-HS and 3-OH-C12-HSL, had the ability to readily change the orientation of at least 50% of the LC droplets analyzed at concentrations of 8, 25, and 25 μM, respectively (Table 5.2). These small differences between the concentrations of 3-oxo-C12-HSL and the two AHLs with a 12 carbon tail length required to induce a transition could well arise from differences in the interfacial density between each AHL.[41] In contrast, decreasing the tail length by 2 carbons increases the concentration required to induce ordering transitions by 4 fold, from 25 μM for 3-oxo-C12-HS and 3-OH-C12-HSL to 100 μM for C10-HSL (Figure 5.6 and Table 5.2). This pattern was also observed between C10-HSL and C8-HSL. However, bipolar-to-radial ordering transitions for solutions of C8-HSL at higher

concentrations did not fully trigger a bipolar-to-radial change for the droplet population (Figure 5.6 and Table 5.2). For AHLs with acyl chains containing 6 or less carbons, namely C6-HSL and C4-HSL, no bipolar-to-radial transitions were observed even at considerable high concentrations of 1 mM. These results are congruent with past studies, which suggest that areal density of surfactant and the extension of aliphatic chain are crucial for changes in the LC anchoring.[41]

5.3.2 LC transitions in P. aeruginosa cell culture

Motivated by the robust transitions observed using both long chain AHLs and rhamnolipids, we next sought to test the ability of amphiphiles in cell culture to induce an LC transition. We selected the standard wild type laboratory strain *P. aeruginosa* PAO1 for these studies. We devised an experimental setup in which LC droplets were encased in a dialysis cassette and placed in a cell culture flask (Figure 5.3A). This allowed for small molecule surfactants produced by the bacteria to pass freely across the dialysis membrane from bulk culture. Cultures were grown to varying time points before incubation with the LC dialysis cassette in order to observe LC response changes over time. The cultures were cooled to room temperature before adding LCs to prevent 5CB from transitioning into an isotropic state. LC dialysis cassettes were incubated at 20 °C for 90 minutes, a time shown to be adequate for small molecule diffusion across the dialysis membrane (data not shown). Cassettes were then removed and the LCs analyzed via flow cytometry. Concurrently, we also tested the lethality of 5CB emulsions versus PAO1 by incubating culture in the presence of LCs. Varying concentrations of LCs up to 10,000 counts per μL were added to saturated cell culture, and cells were incubated for 90 minutes at 20 °C or 37 °C. These temperatures configure the LCs into nematic and isotropic states, respectively. Live cells were quantified using a live-dead assay after this time.

Wild type PAO1 cultures were shown to induce increasing amounts of LC transitions at 6, 12, and 24 hours (Figure 5.3B). Nearly full transition was observed with 24 hour cultures. Very little transition was observed with the negative control, LB medium, confirming a component in the

wild type culture caused a robust LC transition over time. Critically, we did not observe substantial killing in the live-dead assay, supporting the use of 5CB particles in cell culture (Figure 5.7, Supplemental Information). To determine whether this LC transition was due to AHL and rhamnolipid concentrations, we next performed the same experiment with genetic knockout strains eliminating genes critical to either QS or rhamnolipid biosynthesis (Strains listed in Table 5.3, Supplemental Information). PAO1 Δ*lasI*, Δ*rhlI* is unable to produce either 3-oxo-C12-HSL or C4-HSL, respectively. This strain cannot produce QS-associated virulence factors, including the biosurfactant rhamnolipid. Strain PAO1 Δ*rhlB* lacks the rhamnosyltransferase required to produce mono-rhamnolipids, and PAO1 Δ*rhlA* removes the ability for P. aeruginosa to produce rhamnolipid precursor HAA and all downstream rhamnolipids. Finally, to test the ability of rhamnolipids to produce a transition without the presence of long chain AHLs, we tested PAO1 Δ*lasI*, Δ*rhlI* with 200 μM C4-HSL added. Previous studies have shown that adding C4-HSL to an AHL synthase knockout results in rhamnolipid production.[29] While both the Las and Rhl systems regulate rhamnolipid production, RhlR is the primary regulator for this system.[42] These strains were tested in a comparable setup to wild type *P. aeruginosa* (Figure 5.3B).

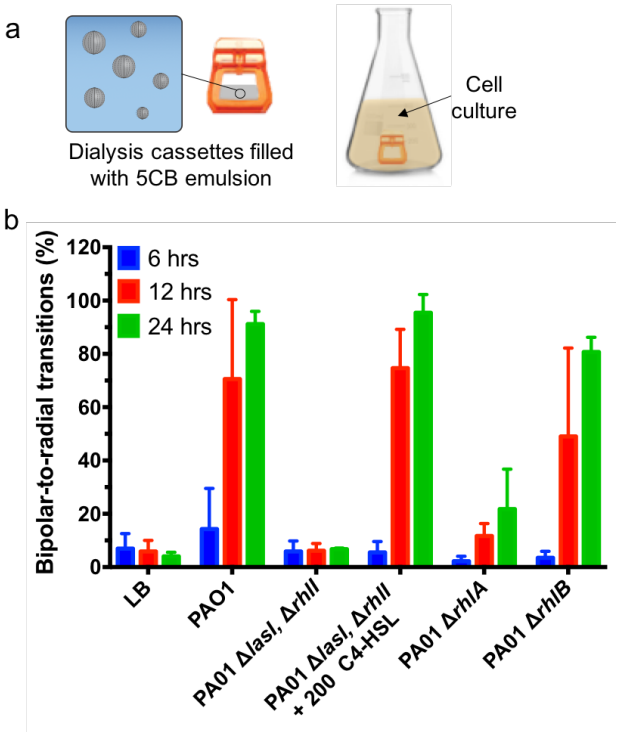

Figure 5.3. (a) Schematic illustration of the experimental set up for the incubation of LC-aqueous emulsions with *P. aeruginosa* cultures using dialysis cassettes filled with 5CB droplets. (b) Percentage of 5CB droplets that were transformed from their bipolar state to the radial state after incubation of cassettes filled with LC emulsions for 90 min at 20 °C with *P. aeruginosa* cultures grown for 6 hours, 12 hours, and 24 hours. Plots are representative of three independent experiments.

We were encouraged to find that strain PAO1 Δ*lasI*, Δ*rhlI* resulted in no LC transitions; data was comparable to the LB control even at 24 hours. Any cellular debris and metabolites associated with growth do not interfere with LCs in this experimental setup, strongly implicating a QS signal or factor as cause for the transition. The addition of C4-HSL to the synthase knockout strain allows for a full recovery of LC transition. This result suggested that rhamnolipid is likely a primary inducer of the change. Strain PAO1 Δ*rhlB* induced slightly less transition than the wild type strain, and PAO1 Δ*rhlA* caused even less transition. We hypothesized that the transitions associated with PAO1 Δ*rhlA* were due to the hydrolyzed and unhydrolized forms of 3-oxo-C12-HSL produced by this strain. The transitions in Δ*rhlB* were likely due to both 3-oxo-C12-HSL and HAA. This rhamnolipid precursor has been shown to behave as a surfactant important for cell

motility.[43] Our results suggest that 3-oxo-C12-HSL appears to play some role in LC transition, but more can be ascribed to rhamnolipid and precursor HAA. We note that cell densities were virtually identical at all time points tested, indicating that the observed transitions are due to the excreted goods associated with QS rather than the metabolites associated with cell growth (Figure 5.8, Supplemental Information).

5.3.3 Quantitation of AHLs and rhamnolipid in P. aeruginosa cell culture

To further verify the cellular goods causing LC transitions, we sought to quantify the amounts of AHLs and rhamnolipids produced by the various strains of interest. Aliquots of cell supernatant were taken in the dialysis experiments prior to LC incubation for further analysis. Hydrolyzed and unhydrolyzed 3-oxo-C12-HSL was quantified using an established MS technique specific for AHLs (Figure 5.4A).[44] C4-HSL was also quantified; the quantities observed did not appear to affect LC transition (Figure 5.9, Supplemental Information). Rhamnolipids were measured via an established orcinol-based colorimetric assay (Figure 5.4B).[45] This technique measures the rhamnose sugars associated with rhamnolipids.

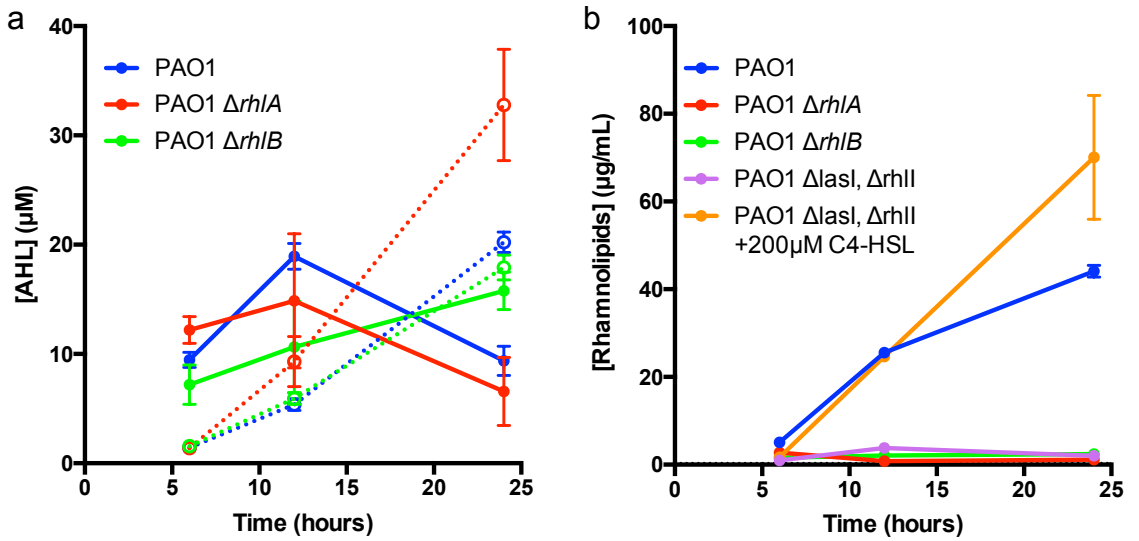

Figure 5.4. (a) 3-oxo-C12-HSL (closed circles) and 3-oxo-C12-HS bulk concentrations (open circles) measured in the supernatant of wild type, Δ*rhlA*, and Δ*rhlB P. aeruginosa* cultures grown for 6, 12 and 24 hours. Total OdDHL and BHL concentrations are shown in Figures 5.9 and 5.10, supplemental information. (b) Bulk concentrations of a mixture of rhamnolipids measured in the supernatant of wild type, Δ*rhlA*, and Δ*rhlB P. aeruginosa* cultures grown for 6, 12, and 24 hours.

As expected, 3-oxo-C12-HSL was only present in strains containing the RhlI and LasI synthases. These strains had relatively similar 3-oxo-C12-HSL concentration patterns over time. At the 6 hour time point, concentrations ranged from 7 to 12 μM, followed by an increase to the 12 hour time point with a range from 12 to 19 μM. The 24 hour time point saw a slight decrease in 3-oxo-C12-HSL, with concentrations ranging from 6 μM to 15 μM amongst the three strains. There was a much greater increase over time when the amount of hydrolyzed 3-oxo-C12-HSL was also monitored. Concentrations increase linearly from 1 μM to more than 20 μM for all three strains. *P. aeruginosa* media grows increasingly alkaline over time, contributing to this growing amount of hydrolyzed 3-oxo-C12-HSL.[46] These data roughly correlate with the amount of 3-oxo-C12-HSL observed in previously published studies.[47]

Turning next to rhamnolipid concentrations, we only found this biosurfactant present in the wild type PAO1 and C4-HSL-added synthase knockout strain, as expected (Figure 5.4B).

Concentrations of rhamnolipids increased linearly over time for both strains, with the C4-HSL added strain exceeding the concentration of rhamnolipid observed in wild type PAO1 by 50% at 24 hours. While previous studies have suggested that rhamnolipid levels cannot be recovered to wild type levels without an activated Las system, these data suggest that sufficiently high C4-HSL concentration can actually prompt heightened production.[29] The concentrations observed in the wild type strain are consistent with literature values.[48]

Overall, quantities of 3-oxo-C12-HSL and rhamnolipids correspond with the LC transition trends observed in the dialysis cassette experiments. AHL 3-oxo-C12-HSL is responsible for a portion of the LC changes, but rhamnolipid and its HAA precursor play a larger role in this interaction. We note that the concentrations of 3-oxo-C12-HSL and rhamnolipid were higher than expected based on the observed LC response in the dialysis cassette experiments. LC experiments with isolated AHL and rhamnolipid showed 50% LC transitions at 8 μM and 13 μg/mL, respectively. However, more than double these concentrations appear to be necessary in order to observe an LC response. We hypothesize that this is due in part to adsorption of these amphiphiles to various cellular components. AHLs have shown little adsorption to cells,[49] but they do adsorb to other materials.[50] Rhamnolipids have been shown to adsorb to a number of materials and surfaces, including cell membranes.[51] Our lab is actively investigating cellular adsorption of AHLs and rhamnolipids to determine the exact amounts of these molecules adsorbing at these various time points.

5.4 Summary

In summary, we have demonstrated the feasibility of using LCs as a material responsive to QS associated goods. This discovery was made by exploiting the interactions between LCs, amphiphilic QS signaling molecules, and the biosurfactant rhamnolipid produced under the QS regulation of *P. aeruginosa*. By protecting the LC dispersions from the bulk culture and using a permeable dialysis membrane, we demonstrated that the observations in simplified conditions can

be translated to physiologically relevant conditions. Specifically, we found that LCs display a material response stimulated predominantly by rhamnolipids for a bacterial strain that had achieved a quorate population.

To the best of our knowledge, these LC soft materials are the first example of a stimuli-responsive system that specifically reacts towards QS goods. Because QS signals are also produced at lower population densities (albeit at much lower, basal levels), future optimization of LC systems could result in materials tuned to varying stages of population growth and development. LC materials are also poised for responsive release of QS modulators; various LCs are already being tested in drug delivery systems.[52] We foresee QS responsive materials impacting our understanding of bacteria regulatory networks and providing a fertile avenue towards the control of bacterial social behaviors.

5.5 Materials and Methods

5.5.1 Reagents

Nematic liquid crystal (LC) 4'-pentyl-cyanobiphenyl (5CB) was purchased from EMD chemicals. Disposable culture tubes (12 x 75 mm) were purchased from VWR (West Chester, PA). Phosphate buffered saline concentrate (137 mM NaCl; 2.7 mM KCl; 10 mM phosphate) was obtained from Omnipur (EM Science, Gibbstown, NJ). Sodium dodecyl sulfate (SDS) electrophoresis-grade was purchased from Fisher Scientific (Pittsburgh, PA). Rhamnolipids were purchased from AGAE Technologies. Dialysis cassettes (10k MWCO, gamma irradiated, 0.5 mL) were purchased from ThermoFisher Scientific. Luria−Bertani medium, Lennox forumlation (LB) was purchased from EMD Millipore. The native AHLs, BHL and OdDHL, were purchased from Cayman Chemical and Sigma-Aldrich, respectively.

5.5.2 General Experimental Information

All absorbance measurements were made in 200 µL of solution in a clear 96-well microtiter plate (Costar 3370) using a Biotek Synergy 2 plate reader running Gen 5 software (version 1.05). Bacterial growth was measured through monitoring culture density via absorbance at 600 nm (OD_{600}). All flow cytometry data measurements were performed at room temperature using a BD FACSCalibur™. Assay data were analyzed using Microsoft Excel for Mac 2011, cytometry data was analyzed using FlowJo™ (v10), and graphs were created using GraphPad Prism 6 (version 6.0h). HPLC-MS/MS data analysis was performed using the MAVEN software[53] and Thermo Xcalibur software (Thermo scientific).

5.5.3 Preparation and configuration characterization of LC emulsions

Emulsions of LC-in-water were prepared by adding 6 µL of 5CB to glass test tubes and 3 mL of a 10 µM SDS solution in PBS. The mixture was vortexed for 30 s at ~3000 rpm to yield a milky white emulsion and allowed to settle for 1 hour. The emulsion was divided in aliquots of 50 µL and diluted into 500 µL of aqueous solutions at each AHL or rhamnolipid concentration to obtain a droplet density of ~10800 ± 900 droplets/µL. This mixture was allowed to sit for at least 1 hour before characterizing droplets light scattering by flow cytometry. Forward light scattering (FSC) was measured at a detection angle of 0° ± 15°, and data collected consisted on the measurement of 10,000 droplets pumped through the flow cytometer at a flow rate of 12 µL/min. Quantitative analysis of scattering plots for determining the percentage of droplets with a radial configuration for each sample was quantified using a previously reported procedure.[34, 35]

5.5.4 Bacterial strains and growth conditions

The bacterial strains used in this study are listed in Table 5.3. Bacteria were cultured in Luria–Bertani broth (LB) at 37 °C with shaking at 200 RPM unless otherwise noted. Freezer stocks for the bacterial strains were stored at -80 °C in LB with 25% glycerol. Spent media was

collected at varying time points by centrifugation (3500 x*g*, 15 minutes) and stored at -80 °C until use.

5.5.5 Incubation of bacteria with 5CB droplets

A 2 mL overnight culture of each *P. aeruginosa* PAO1 strain was grown for 20 hours in a sterile borosilicate glass test tube. A subculture was prepared by directly diluting overnight culture 1:100 in 75 mL fresh LB medium. For the induction of rhamnolipid production in PAO-SC4 (Δ*rhlI* Δ*lasI)*, 150 µL of 100 mM BHL stock solution was added for a final concentration of 200 µM. To all other strains 150 µL of DMSO vehicle was added (0.2% DMSO). Subcultures were grown for 6, 12 or 24 hours. Cultures were then briefly chilled on ice. Dialysis cassettes were equilibrated in LB according to manufacturer's instructions. 600 µL of LC suspension was added to the cassette, and the cassette was added to the chilled culture. Cultures were incubated at 20 °C with shaking for 1.5 hours. Cassettes were removed from culture, and the LCs were collected for analysis by light scattering through flow cytometry.

5.5.6 Rhamnolipid quantification assay protocol

Rhamnolipid was quantified using the method described by Welsh *et al.* with the following modifications.[45] From the 75 mL subculture at timepoints of interest, 2 mL of culture was removed and the cells pelleted at 3500 x*g* for 15 minutes. 1 mL of supernatant was removed, extracted, and submitted to an orcinol assay previously described. The remaining supernatant was saved for AHL quantification as discussed below. Samples were background corrected using an LB negative control. Rhamnolipids were quantified using a rhamnose standard curve multiplied 2.5, a relationship described by Pearson *et al.*[29]

5.5.7 Cell viability assay

LC-in-water stock emulsions were prepared as described above. Droplet density was estimated based on a calibration curve obtained from correlations between event counts/μL detected using a BD Accuri C6 flow cytometer and dilutions from a stock LC-in-water emulsions of at least three different dilutions. A solution with a droplet density of 20,000 events/ μL was prepared from stock LC emulsion based on the estimated dilution from calibration curve. Serial dilutions were performed from this LC emulsion. A 2 mL overnight culture of wild type *P. aeruginosa* PAO1 was grown for 20 hours and plated in a 1:1 dilution with varying dilutions of LC droplets in a 96 well microtiter plate. Plates were incubated static for 1.5 hours at either 37 °C or room temperature. Cell viability was quantified using BacTiter-Glo™ Microbial Cell Viability Assay (Promega Corporation) and normalized using a no-LC control.

5.5.8 HPLC-MS/MS supernatant analysis for AHLs quantification

Cell free supernatant was collected from each sample at 6, 12, and 24 hours prior to addition of the dialysis cassette and treated as previously mentioned. After thawing, the samples were diluted 1:10 in 10:90 methanol:water with 5 mM ammonium formate and 0.1% formic acid (any samples doped with BHL, including BHL standards, were diluted 1:100 in the same solvent). AHL concentrations were obtained using external calibration curves. Ring opened AHL standards were incubated in 1M NaOH for 12 hours at room temperature. In-tact AHL standards were prepared in PBS immediately before use.

The method for HPLC-MS/MS analysis was adapted from Patel et al.[44] Aliquots totaling 2.5 μL of diluted supernatant samples were subjected to HPLC-MS/MS analysis. HPLC was performed on a Vanquish™ uHPLC system (Thermo Scientific) using a C18 reverse-phase column (1.7 um particle size, 2.1x50 mm; Acquity UPLC BEH). Solvent A consisted of 10:90 methanol:water with 5 mM ammonium formate and 0.1% formic acid, and solvent B was 100% methanol. The gradient profile for chromatography was as follows: 100% solvent A for 1 min,

linear increase in solvent B to 90% over 4 min, isocratic 90% solvent B for 5.5 min, and then equilibration with 100% solvent A for 2 min. The flow rate was constant at 0.2 ml/min.

Compounds separated by HPLC were detected by heated electrospray ionization coupled to high-resolution mass spectroscopy (HESI-MS) (QExactive; Thermo scientific). Analysis was performed under positive ionization mode. Settings for the ion source were: 10 aux gas flow rate, 35 sheath gas flow rate, 1 sweep gas flow rate, 4 μA spray current, 4 kV spray voltage, 320°C capillary temperature, 300°C heater temperature, and 50 S-lens RF level. Nitrogen was used as nebulizing gas by the ion trap source. The MS/MS method was designed to perform an MS1 full-scan (100 to 510 m/z, no fragmentation) together with a series of MS/MS scans (all-ion fragmentation) that divided the m/z range into partially overlapping windows of 40 m/z each. The MS1 full-scan provides data on $[M + H]^+$ pseudo-molecular ions, while the MS/MS scans provide corresponding (matched by retention time) fragmentation spectra, all obtained within a single chromatographic run. MS/MS scans (all-ion fragmentation) were centered at 160, 210, 245, 280, 315, 350, 385, 420, 455, 490 m/z using an isolation width of 40.0 m/z. Fragmentations were performed at 17.5, 35, and 52.5 NCE (normalized-collision energy). Mass resolution was set at 35000, AGC target was 1E6, and injection time was 40 ms.

5.6 Supplemental Information

Table 5.3. *P. aeruginosa* strains used in this study

Strain	Description*	Reference
PAO1	Wild-type, isolated by B. Holloway from human wound.	[54]
PW6886 (Δ*rhlA*)	PAO1 rhlA-E08::ISphoA/hah, Tc^R	[55]
PAO1 Δ*rhlB*	PAO1 containing an unmarked, in-frame *rhlB* deletion	[56]
PAO-SC4 (Δ*lasI*, Δ*rhlI*)	PAO1 containing unmarked, in-frame *rhlI* and *lasI* deletions	A generous gift from E. P. Greenberg

* Abbreviations: Tc^R, tetracycline resistance

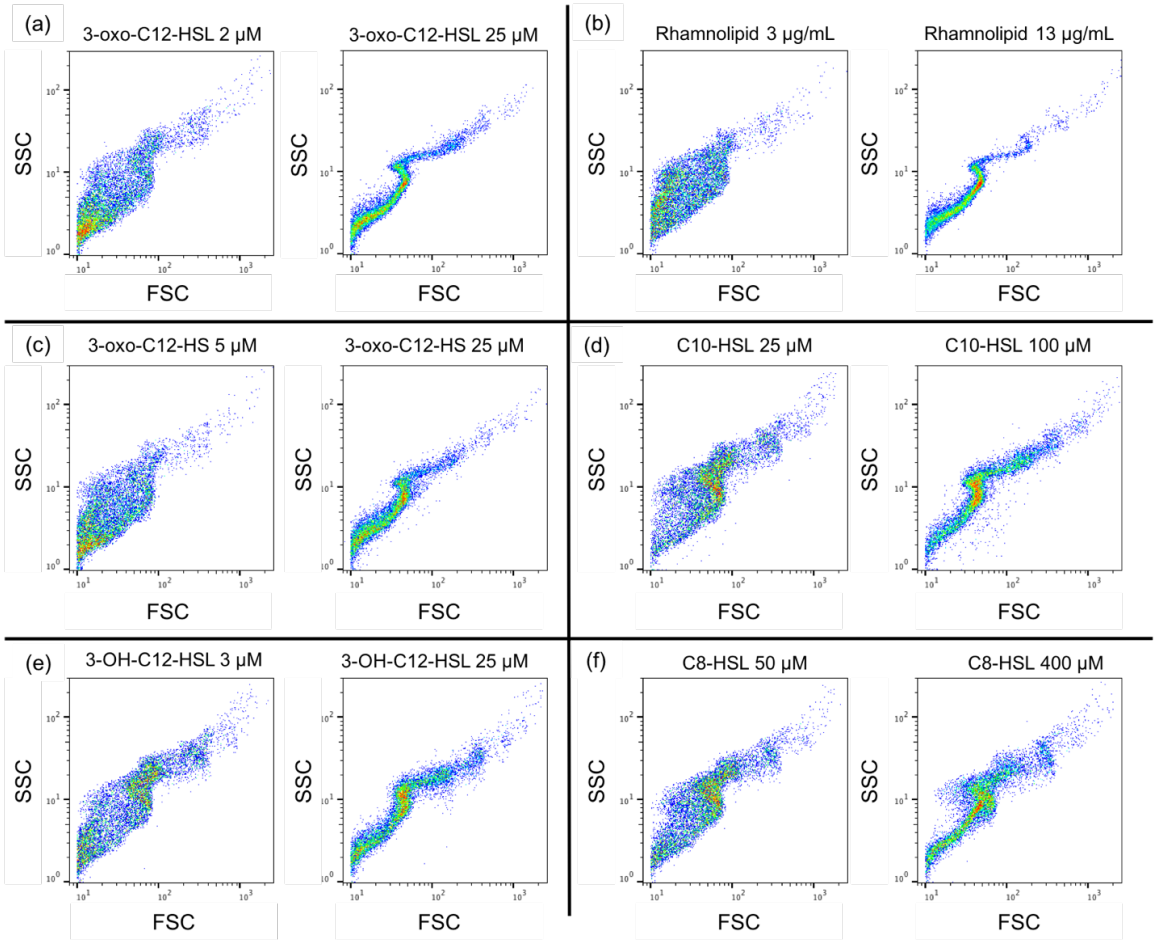

Figure 5.5. Representative scatter plots obtained from the flowing of 5CB droplets before (bipolar) and after (radial) transition occur at given concentrations of (a) 3-oxo-C12-HSL, (b) rhamnolipid, (c) 3-oxo-C12-HS, (d) C10-HSL, (e) 3-OH-C12-HSL, (f) C8-HSL through the flow cytometer.

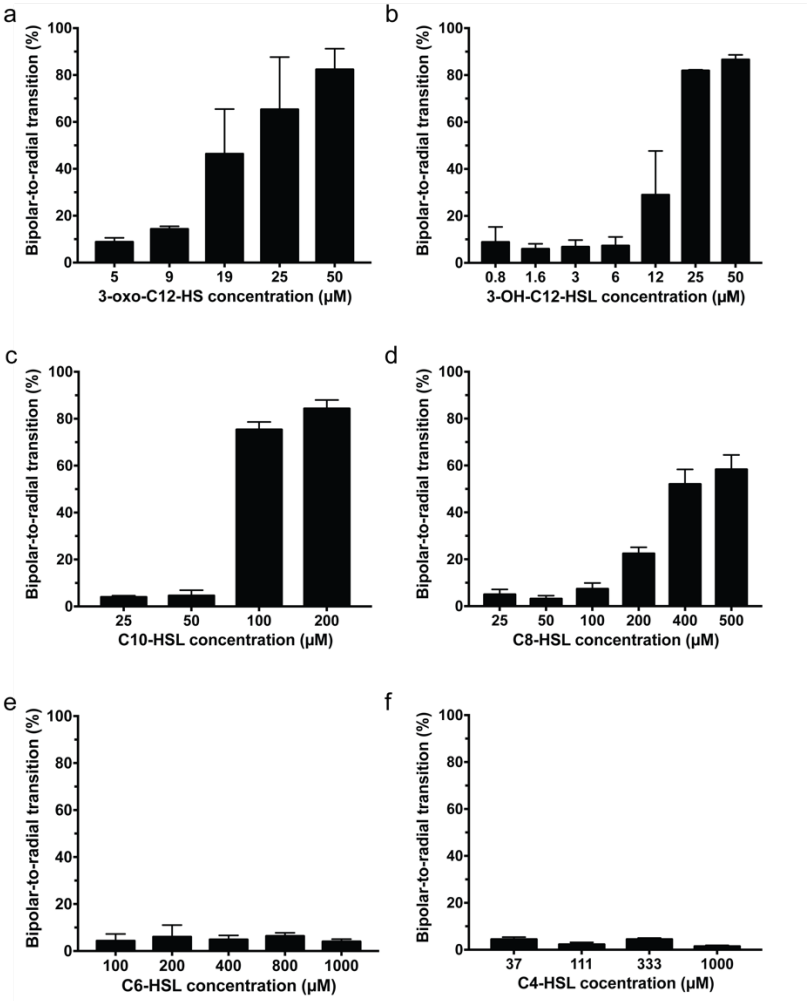

Figure 5.6. Percentage of droplets transformed from bipolar-to-radial as a function of the concentration of (a) 3-oxo-C12-HS, (b) 3-OH-C12-HSL, (c) C10-HSL, (d) C8-HSL, (e) C6-HSL, (f) C4-HSL in PBS with 10 μM SDS and 1% DMSO. Plots are representative of three independent experiments.

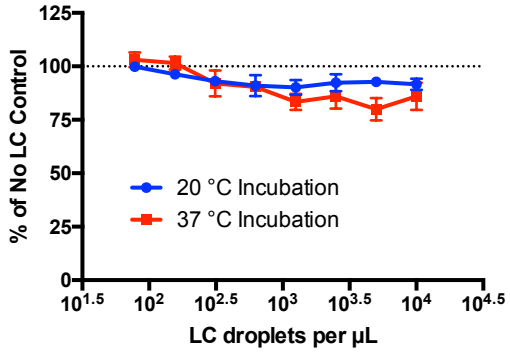

Figure 5.7. *P. aeruginosa* PAO1 viability upon incubation with varying concentrations of 5CB LC droplets. Cells were grown statically in 1:1 PBS:LB for 90 minutes.

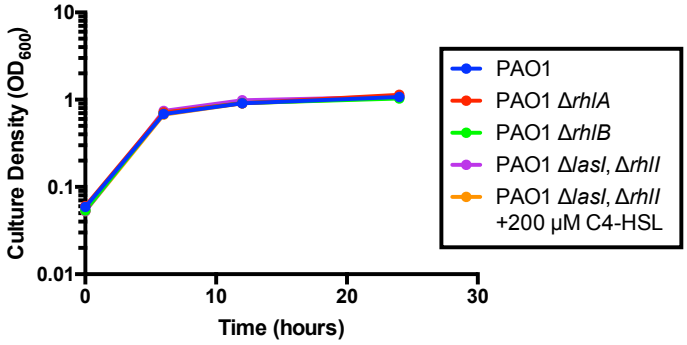

Figure 5.8. Optical density at 0, 6, 12, and 24 hours measured via absorbance at 600 nm. Comparable growth was observed for all strains.

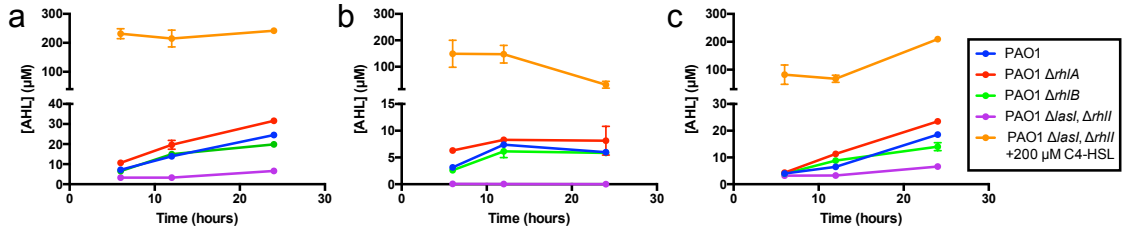

Figure 5.9. Concentrations of (a) total hydrolyzed and unhydrolyzed C4-HSL (b) unhydrolyzed C4-HSL and (c) C4-HS in various *P. aeruginosa* strains grown for 6, 12 and 24 hours.

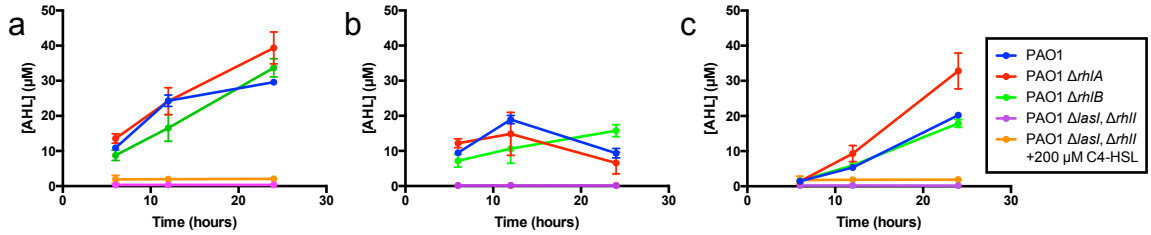

Figure 5.10. Concentrations of (a) total hydrolyzed and unhydrolyzed 3-oxo-C12 (b) unhydrolyzed 3-oxo-C12-HSL and (c) 3-oxo-C12-HS in various *P. aeruginosa* strains grown for 6, 12 and 24 hours.

5.7 References

1. Camilli, A., and Bassler, B. L. (2006) Bacterial small-molecule signaling pathways, *Science 311*, 1113-1116.

2. Williams, P. (2007) Quorum sensing, communication and cross-kingdom signalling in the bacterial world, *Microbiology 153*, 3923-3938.

3. Rutherford, S. T., and Bassler, B. L. (2012) Bacterial Quorum Sensing: Its Role in Virulence and Possibilities for Its Control, *Cold Spring Harb. Perspect. Med. 2*, a012427.

4. Miller, M., and Bassler, B. (2001) Quorum Sensing in Bacteria, *Annu. Rev. Microbiol. 55*, 165-199.

5. Breitbach, A. S., Broderick, A. H., Jewell, C. M., Gunasekaran, S., Lin, Q., Lynn, D. M., and Blackwell, H. E. (2011) Surface-mediated release of a synthetic small-molecule modulator of bacterial quorum sensing: gradual release enhances activity, *Chem. Commun. (Camb) 47*, 370-372.

6. Broderick, A. H., Breitbach, A. S., Frei, R., Blackwell, H. E., and Lynn, D. M. (2013) Surface-Mediated Release of a Small-Molecule Modulator of Bacterial Biofilm Formation: A Non-Bactericidal Approach to Inhibiting Biofilm Formation in *Pseudomonas aeruginosa*, *Adv. Healthc. Mater. 2*, 993-1000.

7. Kratochvil, M. J., Tal-Gan, Y., Yang, T., Blackwell, H. E., and Lynn, D. M. (2015) Nanoporous Superhydrophobic Coatings That Promote the Extended Release of Water-Labile Quorum Sensing Inhibitors and Enable Long-Term Modulation of Quorum Sensing in *Staphylococcus Aureus*, *ACS Biomater. Sci. Eng. 1*, 1039-1049.

8. Melamed Yerushalmi, S., Buck, M. E., Lynn, D. M., Lemcoff, N. G., and Meijler, M. M. (2013) Multivalent Alteration of Quorum Sensing in *Staphylococcus Aureus*, *Chem. Commun. 49*, 5177-5179.

9. Gomes, J., Grunau, A., Lawrence, A. K., Eberl, L., and Gademann, K. (2013) Bioinspired, releasable quorum sensing modulators., *Chem. Commun. 49*, 155-157.

10. Hume, E. B. H., Baveja, J., Muir, B., Schubert, T. L., Kumar, N., Kjelleberg, S., Griesser, H. J., Thissen, H., Read, R., Poole-Warren, L. A., Schindhelm, K., and Willcox, M. D. P. (2004) The control of *Staphylococcus epidermidis* biofilm formation and in vivo infection rates by covalently bound furanones, *Biomaterials 25*, 5023-5030.

11. Nafee, N., Husari, A., Maurer, C. K., Lu, C., de Rossi, C., Steinbach, A., Hartmann, R. W., Lehr, C.-M., and Schneider, M. (2014) Antibiotic-free nanotherapeutics: Ultra-small, mucus-penetrating solid lipid nanoparticles enhance the pulmonary delivery and anti-virulence efficacy of novel quorum sensing inhibitors, *J. Control. Release 192C*, 131-140.

12. Shenderovich, J., Feldman, M., Kirmayer, D., Al-Quntar, A., Steinberg, D., Lavy, E., and Friedman, M. (2015) Local sustained-release delivery systems of the antibiofilm agent thiazolidinedione-8 for prevention of catheter-associated urinary tract infections, *Int. J. Pharm. 485*, 164-170.

13. Lu, H. D., Spiegel, A. C., Hurley, A., Perez, L. J., Maisel, K., Ensign, L. M., Hanes, J., Bassler, B. L., Semmelhack, M. F., and Prud'Homme, R. K. (2015) Modulating *Vibrio cholerae* Quorum-Sensing-Controlled Communication Using Autoinducer-Loaded Nanoparticles, *Nano Lett. 15*, 2235-2241.

14. Ho, K. K. K., Chen, R., Willcox, M. D. P., Rice, S. A., Cole, N., Iskander, G., and Kumar, N. (2014) Quorum sensing inhibitory activities of surface immobilized antibacterial dihydropyrrolones via click chemistry, *Biomaterials 35*, 2336-2345.

15. Baveja, J. K., Willcox, M. D. P., Hume, E. B. H., Kumar, N., Odell, R., and Poole-Warren, L. A. (2004) Furanones as potential anti-bacterial coatings on biomaterials, *Biomaterials 25*, 5003-5012.

16. McUmber, A. C., Noonan, P. S., and Schwartz, D. K. (2012) Surfactant–DNA interactions at the liquid crystal–aqueous interface, *Soft Matter 8*, 4335.

17. Kim, J., Khan, M., and Park, S. Y. (2013) Glucose sensor using liquid-crystal droplets made by microfluidics, *ACS Appl. Mater. Interfaces 5*, 13135-13139.

18. Brake, J. M., Daschner, M. K., Luk, Y.-y., and Abbott, N. L. (2003) Biomolecular Interactions at Phospholipid-Decorated Surfaces of Liquid Crystals, *Science 302*, 2094-2097.

19. Price, A. D., and Schwartz, D. K. (2008) DNA hybridization-induced reorientation of liquid crystal anchoring at the nematic liquid crystal/aqueous interface, *J. Am. Chem. Soc. 130*, 8188-8194.

20. Aliño, V. J., Pang, J., and Yang, K. L. (2011) Liquid crystal droplets as a hosting and sensing platform for developing immunoassays, *Langmuir 27*, 11784-11789.

21. Poulin, P., Stark, H., Lubensky, T. C., and Weitz, D. A. (1997) Novel Colloidal Interactions in Anisotropic Fluids, *Science 275*, 1770-1773.

22. Poulin, P., and Weitz, D. A. (1998) Inverted and Multiple Nematic Emulsions, *Phys. Rev. E 57*, 626-637.

23. Lin, I.-h., Miller, D. S., Bertics, P. J., Murphy, C. J., Pablo, J. J. D., and Abbott, N. L. (2011) Endotoxin-Induced Structural Transformations in Liquid Crystalline Droplets, *Science 332*, 1297-1300.

24. Miller, D. S., and Abbott, N. L. (2013) Influence of droplet size, pH and ionic strength on endotoxin-triggered ordering transitions in liquid crystalline droplets, *Soft Matter 9*, 374-382.

25. Davis, B. M., Richens, J. L., and O'Shea, P. (2011) Label-free critical micelle concentration determination of bacterial quorum sensing molecules, *Biophys. J. 101*, 245-254.

26. Schuster, M., and Greenberg, E. P. (2006) A network of networks: Quorum-sensing gene regulation in *Pseudomonas aeruginosa*, *Int. J. Med. Microbiol. 296*, 73-81.

27. Ledgham, F., Ventre, I., Soscia, C., Foglino, M., Sturgis, J. N., and Lazdunski, A. (2003) Interactions of the quorum sensing regulator QscR: interaction with itself and the other regulators of *Pseudomonas aeruginosa* LasR and RhlR, *Mol Microbiol. 48*, 199-210.

28. Mohammad, A., Abdel-Mawgoud, Lépine, F., and Déziel, E. (2010) Rhamnolipids: Diversity of structures, microbial origins and roles, *Appl. Microbiol. Biotechnol. 86*, 1323-1336.

29. Pearson, J. P., Pesci, E. C., and Iglewski, B. H. (1997) Roles of *Pseudomonas aeruginosa* las and rhl quorum-sensing systems in control of elastase and rhamnolipid biosynthesis genes, *J. Bacteriol. 179*, 5756-5767.

30. Ochsner, U. A., Fiechter, A., and Reiser, J. (1994) Isolation, characterization, and expression in *Escherichia coli* of the *Pseudomonas aeruginosa* rhlAB genes encoding a rhamnosyltransferase involved in rhamnolipid biosurfactant synthesis, *J. Biol. Chem. 269*, 19787-19795.

31. Rahim, R., Ochsner, U. A., Olvera, C., Graninger, M., Messner, P., Lam, J. S., and Soberón-Chávez, G. (2001) Cloning and functional characterization of the *Pseudomonas aeruginosa* rhlC gene that encodes rhamno- syltransferase 2, an enzyme responsible for di-rhamnolipid biosynthesis, *Mol. Microbiol. 40*, 708-718.

32. Abdel-Mawgoud, A. M., Lépine, F., and Déziel, E. (2010) Rhamnolipids: Diversity of structures, microbial origins and roles, *Appl. Microbiol. Biotechnol. 86*, 1323-1336.

33. Churchill, M. E., and Chen, L. (2011) Structural Basis of Acyl-homoserine Lactone-Dependent Signaling, *Chem. Rev. 111*, 68-85.

34. Carter, M. C. D., Miller, D. S., Jennings, J., Wang, X., Mahanthappa, M. K., Abbott, N. L., and Lynn, D. M. (2015) Synthetic Mimics of Bacterial Lipid A Trigger Optical Transitions in Liquid Crystal Microdroplets at Ultralow Picogram-per-Milliliter Concentrations, *Langmuir 31*, 12850-12855.

35. Miller, D. S., Wang, X., Buchen, J., Lavrentovich, O. D., and Abbott, N. L. (2013) Analysis of the internal configurations of droplets of liquid crystal using flow cytometry, *Anal. Chem. 85*, 10296-10303.

36. Lowe, A. M., and Abbott, N. L. (2012) Liquid crystalline materials for biological applications, *Chem. Mater. 24*, 746-758.

37. Gupta, J. K., Zimmerman, J. S., De Pablo, J. J., Caruso, F., and Abbott, N. L. (2009) Characterization of adsorbate-induced ordering transitions of liquid crystals within monodisperse droplets, *Langmuir 25*, 9016-9024.

38. Charlton, T. S., de Nys, R., Netting, a., Kumar, N., Hentzer, M., Givskov, M., and Kjelleberg, S. (2000) A novel and sensitive method for the quantification of N-3-oxoacyl homoserine lactones using gas chromatography-mass spectrometry: application to a model bacterial biofilm, *Environ. microbiol. 2*, 530-541.

39. Lockwood, N. A., de Pablo, J. J., and Abbott, N. L. (2005) Influence of Surfactant Tail Branching and Organization on the Orientation of Liquid Crystals at Aqueous-Liquid Crystal Interfaces, *Langmuir 21*, 6805-6814.

40. Brake, J. M., and Abbott, N. L. (2002) An Experimental System for Imaging the Reversible Adsorption of Amphiphiles at Aqueous-Liquid Crystal Interfaces, *Langmuir 18*, 6101-6109.

41. Brake, J. M., Mezera, A. D., and Abbott, N. L. (2003) Effect of Surfactant Structure on the Orientation of Liquid Crystals at Aqueous−Liquid Crystal Interfaces, *Langmuir 19*, 6436-6442.

42. Schuster, M., Lostroh, C. P., Ogi, T., and Greenberg, E. P. (2003) Identification, Timing, and Signal Specificity of *Pseudomonas aeruginosa* Quorum-Controlled Genes: a Transcriptome Analysis, *J. Bacteriol. 185*, 2066-2079.

43. Déziel, E., Lépine, F., Milot, S., and Villemur, R. (2003) rhlA is required for the production of a novel biosurfactant promoting swarming motility in *Pseudomonas aeruginosa*: 3-(3-hydroxyalkanoyloxy)alkanoic acids (HAAs), the precursors of rhamnolipids, *Microbiology 149*, 2005-2013.

44. Patel, N. M., Moore, J. D., Blackwell, H. E., and Amador-Noguez, D. (2016) Identification of Unanticipated and Novel N -Acyl L-Homoserine Lactones (AHLs) Using a Sensitive Non-Targeted LC-MS/MS Method, *PLoS ONE 11*, e0163469.

45. Welsh, M. A., Eibergen, N. R., Moore, J. D., and Blackwell, H. E. (2015) Small molecule disruption of quorum sensing cross-regulation in *Pseudomonas aeruginosa* causes major and unexpected alterations to virulence phenotypes, *J. Am. Chem. Soc. 137*, 1510-1519.

46. Yates, E. A., Philipp, B., Buckley, C., Atkinson, S., Chhabra, S. R., Sockett, R. E., Goldner, M., Dessaux, Y., Cámara, M., Smith, H., and Williams, P. (2002) *N*-acylhomoserine lactones undergo lactonolysis in a pH-, temperature-, and acyl chain length-dependent manner during growth of *Yersinia pseudotuberculosis* and *Pseudomonas aeruginosa*, *Infect. Immun. 70*, 5635-5646.

47. Davenport, P., Griffin, J. L., and Welch, M. (2015) Quorum sensing is accompanied by global metabolic changes in the opportunistic human pathogen, *Pseudomonas aeruginosa*, *J. Bacteriol. 197*, 2072-2082.

48. Read, R. C., Roberts, P., Munro, N., Rutman, A., Hastie, A., Shryock, T., Hall, R., McDonald-Gibson, W., Lund, V., Taylor, G., and et, a. (1992) Effect of *Pseudomonas aeruginosa* rhamnolipids on mucociliary transport and ciliary beating, *Journal of Applied Physiology 72*, 2271-2277.

49. Fekete, A., Kuttler, C., Rothballer, M., Hense, B. A., Fischer, D., Buddrus-Schiemann, K., Lucio, M., Müller, J., Schmitt-Kopplin, P., and Hartmann, A. (2010) Dynamic regulation of *N*-acyl-homoserine lactone production and degradation in *Pseudomonas putida* IsoF, *FEMS Microbiol. Ecol. 72*, 22-34.

50. Liu, P., Chen, X., and Chen, W. (2015) Adsorption of *N*-acyl-Homoserine Lactone onto Colloidal Minerals Presents Potential Challenges for Quorum Sensing in the Soil Environment, *Geomicrobiol. J. 32*, 602-608.

51. Zhong , H., Zeng, G., Yuan, X., Fu, H., Huang, G., and Ren, F. (2007) Adsorption of dirhamnolipid on four microorganisms and the effect on cell surface hydrophobicity, *Appl. Microbiol. Biotechnol. 77*, 447-455.

52. Kim, D.-H., Jahn, A., Cho, S.-J., Kim, J. S., Ki, M.-H., and Kim, D.-D. (2015) Lyotropic liquid crystal systems in drug delivery: a review, *J. Pharm. Investig. 45*, 1-11.

53. Clasquin, M. F., Melamud, E., and Rabinowitz, J. D. (2002) LC-MS Data Processing with MAVEN: A Metabolomic Analysis and Visualization Engine, in *Current Protocols in Bioinformatics*, John Wiley & Sons, Inc, Hoboken, NJ.

54. Holloway, B. W. (1955) Genetic recombination in *Pseudomonas aeruginosa*, *J. Gen. Microbiol. 13*, 572-581.

55. Jacobs, M. A., Alwood, A., Thaipisuttikul, I., Spencer, D., Haugen, E., Ernst, S., Will, O., Kaul, R., Raymond, C., Levy, R., Chun-Rong, L., Guenthner, D., Bovee, D., Olson, M. V., and Manoil, C. (2003) Comprehensive transposon mutant library of *Pseudomonas aeruginosa*, *Proc. Natl. Acad. Sci. USA 100*, 14339-14344.

56. Smalley, N. E., An, D., Parsek, M. R., Chandler, J. R., and Dandekar, A. A. (2015) Quorum sensing protects *Pseudomonas aeruginosa* against cheating by other species in a laboratory coculture model, *J. Bacteriol. 197*, 3154-3159.

CHAPTER 6:

Comparative analysis of non-native *N*-(3-oxo-dodecanoyl)-L-homoserine lactone variants in two *Pseudomonas aeruginosa* quorum sensing receptors (LasR and QscR) that share the same native ligand

Contributions: J. B. Combs planned experiments, synthesized compounds, performed screening assays, and prepared portions of initial chapter draft. M. E. Boursier planned experiments, directed the project, and prepared the final chapter. H. E. Blackwell guided research and assisted in writing.

*This chapter has been prepared as a manuscript intended for publication under the same title.

6.1 Abstract

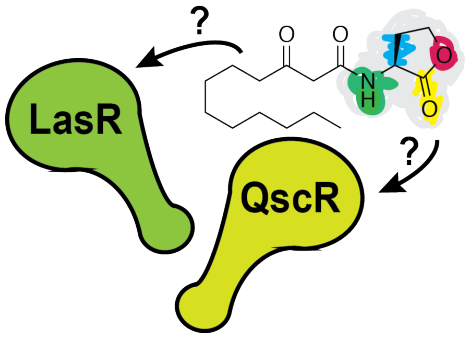

Many common bacteria use cell-cell signaling to coordinate group behaviors in a phenomenon known as quorum sensing (QS). The opportunistic pathogen *Pseudomonas aeruginosa* has a relatively complex quorum sensing circuit, including two LuxR-type receptors LasR and QscR that bind to the same small molecule signal, *N*-3-(oxododecanoyl)-L-homoserine lactone (OdDHL). Significant research efforts have focused on delineating the role of LasR in QS, as LasR regulation has higher perceived importance in the QS signaling hierarchy. QscR, a receptor that represses the effects of the LasR QS circuit, has seen far less scrutiny. We currently have a limited understanding of the structural features of non-native ligands that engender selectivity in these two receptors. To start to investigate such features, a small library of OdDHL analogues was synthesized with changes made to the homoserine lactone head group and screened in a cell-based reporter assays to determine activity trends in both LasR and QscR. We identified several motifs that bias ligand activation towards each of the two receptors. Many of the most potent ligands with lactone replacements also benefit from increased hydrolytic stability relative to homoserine lactone. These findings should be valuable for the development of more selective and stable synthetic agonists and antagonists of both LasR and QscR.

6.2 Introduction

Bacteria are able communicate with chemical signals in a process called quorum sensing (QS). In the canonical LuxI/R systems found in Gram-negative bacteria, autoinducers called *N*-acyl-L-homoserine lactones (AHLs) are produced by LuxI-type synthases at a basal level.[1] At a sufficiently high enough cell and signal density, LuxR-type receptors bind to the autoinducer, dimerize, and alter the expression of group beneficial genes. The production of LuxI/R is also upregulated, resulting in a positive feedback loop that is a hallmark of QS systems.[1]

One organism of particular interest in the QS field is *Pseudomonas aeruginosa*, an increasingly antibiotic resistant bacterium that infects immunocompromized individuals, most notably cystic fibrosis patients.[2-4] Many of its virulence factors are regulated via QS, making modulation of the QS circuit an attractive target for anti-virulence efforts. However, the development of ligands that modulate QS in *P. aeruginosa* is challenging due to its complex QS circuit with two distinct LuxI/R systems working in tandem, along with the (non-LuxI/R) Pseudomonas Quinolone System (PQS).[5] The LuxR-type receptor LasR, considered at the top of the QS hierarchy, is activated by autoinducer, *N*-3-(oxododecanoyl)-L-homoserine lactone (OdDHL) produced by the synthase LasI. This receptor regulates the rhl system, in which the RhlR receptor is activated by *N*-butryl- L homoserine lactone (BHL), produced by RhlI. Both of these systems are regulated by an orphan receptor LuxR-type receptor, QscR, which does not have its own corresponding synthase and also binds to OdDHL.[5] Interestingly, QscR serves as a repressor of LasR and RhlR activity, at least in part through the formation of inactive heterodimers.[6]

Approximately 10% of the *P. aeruginosa* genome is regulated through QS, and a significant portion of these genes are modulated directly by the three LuxR-type receptors.[7] There is a significant amount of overlap in the receptor regulons, suggesting some redundancies in modulation.[8-10] Even so, LasR is known to be the primary inducer of virulence factors elastase, endotoxin A, and alkaline protease,[11] whereas RhlR primarily regulates the biosurfactant

rhamnolipid.[12] QscR has been shown to regulate a number of genes, but their functions are not currently known.[8] Significant effort in the Blackwell laboratory[13-15] and others[16] has been to develop synthetic ligands targeting specific LuxR-type receptors in this circuit and to selectively reduce virulence factor production in the wild type organism. These chemical probes have been useful to understand *P. aeruginosa* QS interregulation that cannot be observed using standard genetic knockouts.[17] Selective modulators for RhlR have been recently established,[18] but far less is known about the molecular features that drive the selectivity of non-native ligands for LasR and QscR. Compounds that capable of selective QscR agonism, for instance, could provide a pathway to inhibition of both the las and rhl circuits. Indeed, initial studies have shown that QscR activators can reduce virulence factor production in *P. aeruginosa*.[19]

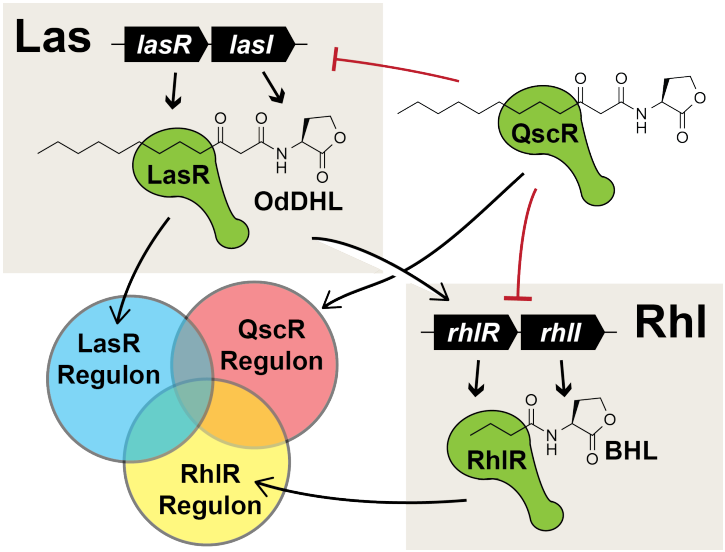

Figure 6.1. Simplified QS circuit of LuxR-type receptors in *P. aeruginosa*. Receptors directly regulate the other circuits and also have overlapping regulons that regulate group beneficial genes.

` Despite binding to the same native ligand, QscR and LasR have several key distinctions in terms of their structures. While both possess the nine well-conserved amino acids found in the (known and predicted) primarily around the ligand-binding site of most LuxR-type receptors,[20] these two receptors have only a 16% sequence similarity.[21] Several of the hydrogen binding

contacts with OdDHL in the two receptors utilize different amino acids (Figure 6.2). QscR is shown to be more amenable to ligand exchange in vitro relative to LasR, allowing for its biochemical manipulation with a variety of AHLs.[22] Additionally, QscR is able to bind to a wider assortment of native AHLs than LasR[23] as well as non-native AHLs with added acyl chain bulk.[14] This more relaxed binding ability may be due to amount of order found in the water molecules bonding to OdDHL's 3-oxo position, specifically (Figure 6.2).[24] QscR has a less structured water molecule network than LasR.

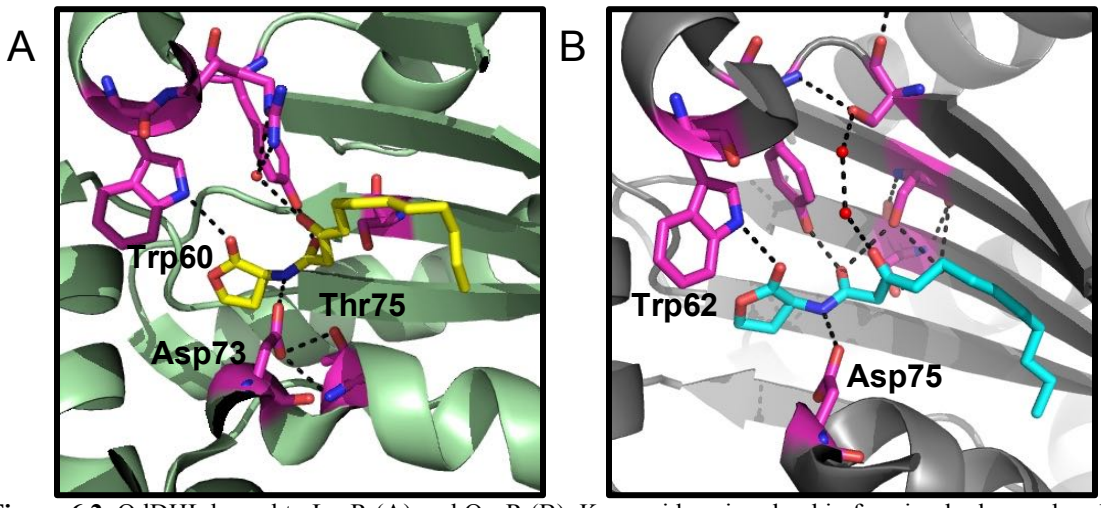

Figure 6.2. OdDHL bound to LasR (A) and QscR (B). Key residues involved in forming hydrogen bonding to the homoserine lactone or amide hydrogen are labeled. PDB IDs 3IX3, 3SZT.[24, 25]

Much less is known about the differences in how LasR and QscR bind to AHLs with variations in the homoserine lactone "head group". Development of QS modulators in *P. aeruginosa* has often focused on widely varying the acyl chain, leaving the homoserine lactone head group in tact.[26] Maintaining this moiety has been necessary in part due to the key hydrogen binding contacts the lactone makes with LuxR-type receptors.[27] Crystal structure data of both LasR and QscR highlight critical bond between the ester carbonyl and a conserved tryptophan residue (Figure 6.2).[24, 25] The amide proton linking the homoserine lactone to the acyl chain forms a hydrogen bonding contact as well. However, a problem for the use of AHL analogs as chemical probes is that the homoserine lactone moiety is hydrolytically unstable, with half lives of ~4-24

hours.[28, 29] For these reason, several compounds have been developed for the LasR receptor that replace this moiety entirely, with some levels of success.[30-32] Still, homoserine lactone-based analogs remain some of the most potent modulators of LasR (and other related receptors).[33] Further analysis of subtle changes, particularly in the head group, could result in compounds with improved stability, activity, and selectivity profiles.

Recent studies in our lab investigating BHL analogs with subtly modified lactone head groups resulted in compounds with enhanced stability and potency in RhlR.[28] We sought to apply a similar structure-activity relationship (SAR) study with OdDHL, making subtle changes in the homoserine lactone head group and quantifying agonistic activity in both LasR and QscR using cell-based reporter strains. Herein, we report the findings of these studies on a small focused library of OdDHL analogs. Overall, we found a series of head groups that resulted in improved selectivity for either receptor. Some of the most potent homoserine lactone analogs should have significantly improved compound stability. These observations will allow for the future development of selective and robust chemical probes to modulate the complex *P. aeruginosa* QS circuit.

6.3 Results and Discussion

6.3.1 Library design, historical background, and synthesis

Our library was designed using inspiration from the literature and our previous work developing BHL analogs as previously discussed (Figure 6.3). We note that many of the proposed compounds have been previously described in the QS literature and screened against LasR. In 1996, Iglewski and coworkers compiled an expansive lactone mimic library, including homocysteine thiolactone **3** and γ-lactam **4** analogs.[34] The thiolactone was found to agonize LasR comparably to OdDHL, whereas the lactam was about 100-fold less potent based on EC_{50}. The Suga lab later looked at non-hydrolyzable cyclopentanone **5** and cyclopentanol **8**.[35] With the carbonyl maintained on the cyclopentanone, **5** was active in LasR but not nearly as potent as the

native ligand. Compound **8** induced some LasR activity only at 400 μM. Further testing of thiolactone **3** and introduction of cyclopentylamine **6** against LasR were performed in our lab, again confirming the potency of the thiolactone moiety.[36, 37] Compound **6** showed some agonism compared to LasR, but an EC_{50} value was not calculated. Sulfonamide variant **10** was the only compounds to be tested in both LasR and QscR, again by the Blackwell lab.[13, 26, 38] This compound was found to have no agonism profile in LasR, and mild agonism in QscR. Ester linkage compound **11** and D-homoserine lactone **2** were synthesized in 2004 and 2006 respectively, but there is no available reporter data against *P. aeruginosa* receptors, likely due to their predicted inactivity.[39, 40] Tetrahydrofuran derivatives **7** and **9** have not previously been synthesized to our knowledge. These compounds allow for the maintenance of the oxygen in the heterocycle and also a lengthening of the head group in the binding pocket.

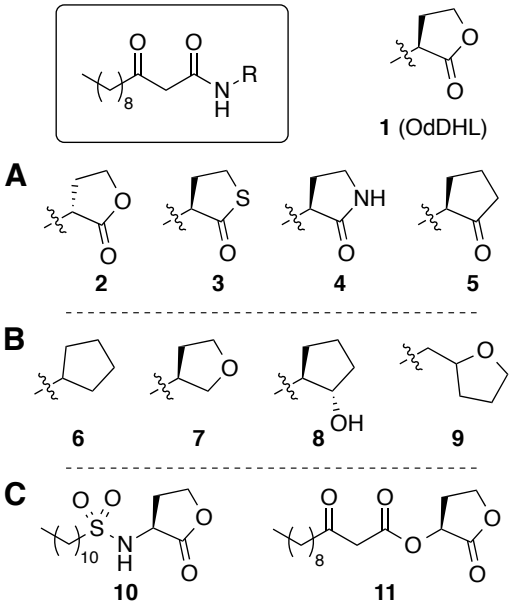

Figure 6.3. Compound library with head group changes derived from OdDHL (**1**). Structures are grouped based on lactone variations (A), lactone replacements (B), and amide linker modifications. Compounds were developed in the following laboratories: **2**, Ishiguro and coworkers[40]; **3** and **4**, Iglewski and coworkers[34]; **5**, **8** and **11**, Suga and coworkers[35, 39]; **6** and **10**, Blackwell and coworkers.[36, 37]

We organized the structures in the library into three groups. Group 1 (Figure 6.3A) consists of lactone variants, changing the stereochemistry of the ring with compound **2**, and changing the heteroatom in the ring from oxygen to a sulfur, nitrogen, or methylene with compounds **3**, **4**, and **5**, respectively. The different atoms influence the ring size as well as the hydrogen bonding ability of the carbonyl and ring atoms. Group 2 (Figure 6.3B) contains compounds possess lactone replacements, specifically removing the carbonyl. Compound **6** maintains the ring structure without any hydrogen bond acceptors, whereas the oxygen in the 5-membered ring remains in compound **7**. Alcohol **8** converts the carbonyl into a proton donor. Finally, compound **9** adds a methylene to the tetrahydrofuran derivative and extends the head group. Compounds in Group 3 (Figure 6.3C) change the amide linker between the head group and alkyl chain to either a sulfonamide with compound **10** or an ester with compound **11**. The latter compound removes a hydrogen bond donor. All compound groups maintained an alkyl tail of equivalent structure to that in OdDHL (3-oxododecanoyl). Compounds were synthesized in moderate to good yield using previously described methods.[41-43]

6.3.2 Biological assays in LasR and QscR

In examining these previous studies we identified disparate screening setups, making compound activities very hard to compare. Reporters in *P. aeruginosa* have the entire QS circuit in tact as well as an arsenal of quorum quenching pumps and acylases, making the activity profile convoluted. The various studies also don't use similar promoter regions for LasR; LasR binds to several known promoter regions with varying affinities that may skew the screening results.[44] Additionally, few of the noted studies performed dose-response experiments to get an EC_{50} value as a measure of potency. This is the best measure to compare compound activities. We also identify the lack of screening information against QscR as a large gap in our understanding of *P. aeruginosa* QS. Without exploring compound activity in both of these receptors, it is difficult to say how exactly OdDHL analogs influence the QS circuit.

To remedy some of the complexities associated with the *P. aeruginosa* QS circuit, the Blackwell lab has recently developed robust *E. coli* reporter strains for all three of the luxR-type receptors.[17, 18] This advancement has allowed us to more rigorously compare compound activity between receptors as well as compare compounds screened initially in different screening conditions. Aside from standardizing the receptor expression and reporter plasmids, these reporter constructs eliminate *E. coli*'s LuxR-type receptor SdiA, removing a possible AHL "sink" that would alter activity profiles. These assays have allowed us to discover selective RhlR modulators[18] and also perform comprehensive analysis of the best lead LasR modulators in the QS field.[33] In this study, compounds were submitted to dose response screening in the LasR and QscR *E. coli* reporters using our previously described methods (See Methods).[18, 30] Screening data was analyzed by examining both maximum activity and EC_{50} values (Table 6.1). Additionally, the fold-change in compound EC_{50} values from native ligand OdDHL were determined (Table 6.2).

Table 6.1. Compound activity in the LasR and QscR reporter strains.[a]

	LasR			QscR		
Compound	**EC_{50} (μM)**	**95% CI (μM)**	**Activation (%)[b]**	**EC_{50} (μM)**	**95% CI (μM)**	**Activation (%)[b]**
1 (OdDHL)	0.00151	0.000908 – 0.00250	100	0.0147	0.00675 – 0.0322	100
2	0.110	0.0814 – 0.149	99	1.38	0.437 – 4.33	108
3	0.00153	0.000713 – 0.00329	104	0.0805	0.0422 – 0.154	110
4	0.0297	0.0112– 0.0787	110	3.32	1.58 – 6.96	56
5	0.0149	0.00771 – 0.0288	110	0.834	0.454 – 1.53	77
6	0.162	0.0733 – 0.359	88	0.359	0.233 – 0.554	103
7	0.906	0.758 – 1.08	81	0.815	0.529 – 1.26	74
8	1.88	1.44 – 2.46	96	3.46	1.74 – 6.87	107
9	0.256	0.131 – 0.498	96	–	–	3.2
10	–	–	6.4	1.59	1.00 – 2.53	72
11	–	–	27	–	–	37

[a]Assays were performed using E. coli JLD271 (pJN105L/pSC11) or JLD271 (pJN105Q/pSC11-Q); see Experimental Section. For both assays, EC_{50} values were determined by testing AHLs over a range of concentrations (≤ 100μM). Assays were performed in triplicate, and 95% confidence intervals (CIs) were calculated from the SEM of n ≥ 3 trials. [b]Denotes the highest value of LasR or QscR activation seen for each compound at any concentration within the dose–response assay. For the full agonism traces, see Figures S1. LasR or QscR activity was measured relative to that of 100 μM OdDHL.

Looking first at Group 1 compounds maintaining lactone structure, all compounds in this class activated LasR to nearly 100% with EC_{50} values in the nanomolar range. D-homoserine lactone **2** was the poorest activator, which was unsurprising based on previous reports of the critical importance of stereochemistry for LasR activation by OdDHL.[42] Lactam and cyclopentanone variants **4** and **5** were about 10-fold less active than the native ligand, suggesting that these changes are moderately well tolerated. Thiolactone **3** was found to be the most potent agonist of LasR and had a comparable EC_{50} to OdDHL, corroborating previous reports.[34, 36]

These trends were not totally mirrored in QscR. Compound **2** also showed a nearly 100-fold reduction in activity, suggesting that the two receptors have similar intolerances for the inverted stereochemistry. However much larger differences were observed in varying the heteroatom in the lactone ring. Unlike in LasR, homocysteine thiolactone **3** was five-fold less potent than the native ligand in QscR. Previous studies have suggested thiolactones to have a stabilizing effect on LasR due to their larger size and capability for hydrogen-bonding,[45] so it is possible that QscR does not accommodate larger ring sizes well. This observation is corroborated by the reporter assay data for compound **4**, a lactam. The lactam amine is closer in size to a sulfur atom than oxygen based on covalent radii,[46] and will also interact with the ligand binding pocket differently because of the added hydrogen bond donor. These differences contributed to a >200-fold reduction in potency for lactam **4** relative to OdDHL. This trend is observed for cyclopentaone **5** as well; the subtly larger size of the cyclopentanone versus the homoserine lactone results in a 57-fold difference overall. LasR could much better tolerate this head group.

In the Group 2 set of OdDHL analogs, LasR activity was significantly reduced in compounds lacking a carbonyl. Cyclopentylamine **6** was the most potent compound, with a 100-fold loss of activity relative to OdDHL. Compound **7** maintains an oxygen in the 5 membered ring at a position comparable to the in-tact homoserine lactone, unlike compound **6**, but has a higher EC_{50}. The presence of this oxygen could possibly result in a disfavored hydrogen bonding interaction. Interestingly, a similar loss in potency is not observed in extended tetrahydrofuran compound **9**.

The added methylene linker is enough to place the head group in a more favorable position for ligand binding. Alcohol compound **8** changes the hydrogen bonding character of the oxygen entirely and resulted in the lowest potency of the group, with the compound proving to be more than 1000-fold less potent. As a hydrogen bonding donor, we hypothesize that this molecule makes drastically changed and/or unfavorable hydrogen binding contacts in the pocket that alter the LasR protein configuration.

QscR was much better able to accommodate Group 2 ligands without the lactone carbonyl relative to its native ligand, with an order of magnitude less change in activity from OdDHL relative to the changes observed in LasR (Table 6.2). Cyclopentylamine **6** was still the most potent of the group in QscR, suffering only a 24-fold reduction in potency relative to OdDHL. Tetrahydrofuran variant **7** was slightly less potent than cyclopentylamine **6**, possibly suggesting that this ligand is making an undesirable contact in QscR as well as in LasR. Alcohol **8** had an EC_{50} value in the micromolar range in QscR, its hydrogen bond donor again reducing potency as observed in LasR?. Compound **9**, however, showed negligible activity in QscR. The extended head group was not tolerated, further suggesting that QscR cannot accommodate bulky head groups. Notably, both LasR and QscR had similar EC_{50} values for this series of compounds. This suggests that the added affinity LasR has for OdDHL variants is due in part to the orientation the molecule creates when locked in place with the Trp60-carbonyl hydrogen bonding interaction (Figure 6.2).

Compounds in Group 3 with deviations from the amide linker show limited activity in both receptors. Sulfonamide **10** shows activity only in QscR, corroborating previously published studies on this receptor.[38] Since some of the most potent previously reported agonists and antagonists of QscR have added bulk alpha to the amide linker,[14] it is not surprising that the sulfonamide can be tolerated with modest activity. Ester linker **11** lacks the ability to be a hydrogen bond donor, and loses all potency in LasR and QscR. This loss of activity is supported by a mutagenesis study showing that when LasR Asp73 is mutated to a leucine, OdDHL loses all

potency in that receptor.[45] This would suggest that the hydrogen bonding roles of Asp73 and Thr75 in LasR and Asp75 in QscR observed in the respective crystal structures play vital roles in allowing the proteins to become functional when binding AHLs (Figure 6.2).[24, 25]

Table 6.2. Fold differences in compound EC_{50} values from OdDHL EC_{50} values in LasR and QscR.[a]

	Fold Difference from OdDHL EC_{50}	
Compound	**LasR**	**QscR**
2	73	94
3	1	5
4	20	226
5	10	57
6	107	24
7	600	55
8	1245	235
9	170	–
10	–	108
11	–	–

[a] Calculated by dividing compound EC_{50} by OdDHL EC_{50} in each receptor.

6.4 Summary

In revisiting a set of OdDHL analogs using a standardized set of reporter experiments for comparative analysis, we have uncovered a clearer understanding of how compounds with modest head group changes modulate LasR and QscR. Using this method, we identified a relationship between the size of the lactone group, and receptor specific activity. LasR activity is more greatly affected by the removal of the homoserine lactone carbonyl. Additionally, this receptor cannot tolerate bulk at the carbonyl of the amide. QscR is less amenable to added ring bulk, including subtle changes in the heteroatom. Extended head groups show no activity. Both receptors are about equally affected by changes in ring stereochemistry, suggesting a comparable pocket shape. Finally, both receptors require a proton donor at the amide linker in order to be active. These overall all SARs are shown schematically in Figure 6.4.

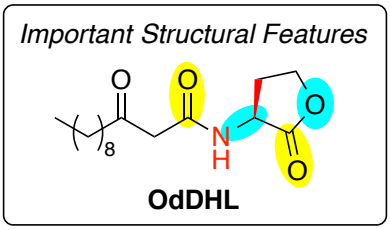

Figure 6.4. Structural features important for the activation of LasR and QscR receptors. Features more important for LasR activation are shown in yellow (i.e. removal of the lactone carbonyl, added bulk around amide carbonyl). Features more important for QscR activation are shown in cyan (i.e. increased linker length, heteroatom change). Changes equally detrimental for activation of both receptors are shown in red.

Looking to the future, these studies have revealed a number of head groups as potential leads for generating probe compounds with improved stability over time. Thiolactone, lactam, and cyclopentanone compounds **3**, **4**, and **5** all are more stable than homoserine lactone and maintain potencies in LasR in the mid-nanomolar range. These compounds have increased selectivity for LasR, making them excellent leads for future libraries targeting this receptor. While changes in the homoserine lactone heteroatom generally result in reduced activity in both LuxR-type receptors, these activity differences may not be as critical if the compounds have longer half-lives, allowing them to remain active over prolonged period in a range of biologically relevant environments. Homocysteine thiolactones are particularly interesting as we have shown them to remain intact significantly longer than the native lactone head group.[28, 36] These head groups will expand the utility of the modulators in assays versus wild type *P. aeruginosa*. Alternatively, QscR selective compounds may benefit from the incorporation of a sulfonamide linker or from the removal of the homoserine lactone carbonyl. Both changes resulted in mild QscR agonists with limited to no activity versus LasR.

Future research will focus on testing the poor agonists in this study in antagonism assays; it is not uncommon for compounds to show activity in either agonism or antagonism assays. Compounds with no activity may still be binding either LasR or QscR, but the receptors may be adopting an inactive conformation when bound. Such studies, along with the further development of the lead agonists reported here, are ongoing in our lab and will be reported in due course.

6.5 Methods

6.5.1 Chemistry

The synthesis for sulfonamide **10** was performed as previously described.[41] For all other compounds the alkyl tail group was made by producing 2-(2-nonyl-1,3-dioxolan-2-yl) acetic acid as developed by Spring and coworkers.[43] This acid was coupled to each head group using standard amide coupling detailed elsewhere,[47] and the product was deprotected to produce the final compound.[43] Compound **4** head group (*S*)-3-amino-2-pyrrolidinone was prepared as previously described.[48] Compounds **5** and **8** required a coupling variation and subsequent oxidation as previously described.[42]

6.5.2 Bacteriology methods

Bacteria were cultured in Luria−Bertani medium (LB) at 37 °C. Absorbance measurements were performed in 96-well microtiter plates and pathlength-corrected using a Biotek Synergy 2 plate reader running Gen 5 software (version 1.05). Bacterial growth was assessed by measuring absorbance at 600 nm (OD_{600}).

6.5.3 Bacterial strains and assay protocols

The bacterial reporter strains used for this study were (i) *E. coli* strain JLD271 (Δ*sdiA*) harboring the QscR expression plasmid pJN105Q and the *rhlI-lacZ* transcriptional fusion reporter pSC11-Q, and (ii) *E. coli* strain JLD271 (Δ*sdiA*) harboring the LasR expression plasmid pJN105L and the *lasI-lacZ* transcriptional fusion reporter pSC11. Miller assays were performed in these *E. coli* and *P. aeruginosa* reporters as previously described.[47, 49]

6.6 Supplemental Information

6.6.1 General chemical information

All chemical reagents and solvents were purchased from commercial sources and used without further purification, except for dichloromethane (DCM), which was distilled and dried over activated molecular sieves. Water (18 MΩ) was purified using a Thermo Scientific Barnstead Nanopure system. Chlorophenol red-β-D-galactopyranoside (CPRG) was purchased from Roche. Ortho-nitrophenyl-β-galactoside (ONPG) was purchased from Sigma Aldrich. All media and reagents for bacterial culture were purchased from commercial sources.

6.6.2 Instrumentation and analytical methods

NMR spectra were recorded in deuterated NMR solvents at 500 MHz on a Bruker Avance-500 spectrometer with DCH cryoprobe and SampleXpress. Chemical shifts are reported in parts per million (ppm, δ) using corresponding solvents or tetramethylsilane (TMS) as a reference. Couplings are reported in hertz (Hz). Electrospray ionization MS measurements were performed on a Waters LCT. Samples were dissolved in acetonitrile and sprayed with a sample cone voltage of 20. For exact mass measurements (EMM), an aliquot of a known compound (lock mass) is added to the sample and resprayed.

6.6.3 Compound characterization data

^{1}H and ^{13}C NMR, and ESI MS data are reported below for all newly synthesized non-native QS modulators. Characterization data for compounds **4** and **11** are also included as they have not been fully characterized in past studies reporting their structures.[34, 50] We note that small amounts of enol tautomer appear in all spectra.

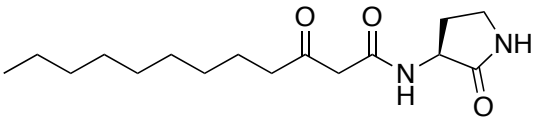

4: ^{1}H NMR (500 MHz, $CDCl_3$) δ 7.56 (s, 1H), 6.38 (d, *J* = 32.2 Hz, 1H), 4.44 (ddd, *J* = 11.0, 8.4, 6.3 Hz, 1H), 3.50 – 3.32 (m, 4H), 2.83 – 2.62 (m, 1H), 2.53 (t, *J* = 7.4 Hz, 2H), 1.98 (dq, *J* = 12.3, 9.8 Hz, 1H), 1.68 – 1.48 (m, 2H), 1.26 (d, *J* = 7.0 Hz, 15H), 0.87 (t, *J* = 6.8 Hz, 3H); ^{13}C NMR (126 MHz, $CDCl_3$) δ 206.57, 166.60, 50.76, 48.98, 43.92, 39.35, 31.99, 29.85, 29.78, 29.54, 29.50, 29.39, 29.15, 23.52, 22.80, 14.25; ESI MS: Expected $[M+H]^+$: 297.2173, observed: 297.2169.

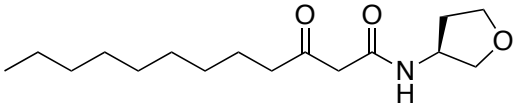

7: ^{1}H NMR (500 MHz, $CDCl_3$) δ 4.50 (dtd, *J* = 7.0, 3.7, 1.9 Hz, 1H), 3.93 (dt, *J* = 8.6, 7.3 Hz, 1H), 3.89 – 3.76 (m, 2H), 3.65 (dd, *J* = 9.4, 3.1 Hz, 1H), 3.37 (d, *J* = 1.7 Hz, 2H), 2.50 (t, *J* = 7.3 Hz, 2H), 2.35 – 2.19 (m, 1H), 1.81 (dddd, *J* = 13.1, 7.5, 5.6, 3.4 Hz, 1H), 1.56 (dd, *J* = 13.5, 6.8 Hz, 3H), 1.40 – 1.16 (m, 14H), 0.87 (t, *J* = 6.9 Hz, 3H); ^{13}C NMR (126 MHz, $CDCl_3$) δ 207.35, 165.51, 73.49, 67.04, 50.39, 48.58, 44.17, 33.17, 31.98, 29.51, 29.47, 29.37, 29.13, 23.49, 22.79, 14.24; ESI MS: Expected $[M+H]^+$: 284.2220, observed: 284.2215.

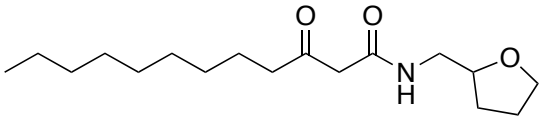

9: ^{1}H NMR (500 MHz, Chloroform-*d*) δ 7.11 (s, 1H), 3.98 (qd, *J* = 7.0, 3.6 Hz, 1H), 3.88 (dt, *J* = 8.3, 6.6 Hz, 1H), 3.80 – 3.71 (m, 1H), 3.54 (ddd, *J* = 13.7, 6.2, 3.6 Hz, 1H), 3.39 (d, *J* = 2.6 Hz, 2H), 3.22 (ddd, *J* = 13.6, 7.1, 5.2 Hz, 1H), 2.52 (t, *J* = 7.4 Hz, 2H), 2.06 – 1.81 (m, 3H), 1.76 – 1.46 (m, 3H), 1.26 (d, *J* = 6.7 Hz, 12H), 0.87 (t, *J* = 6.9 Hz, 3H); ^{13}C NMR (126 MHz, CDCl3) δ 206.85, 165.88, 77.58, 68.35, 49.17, 44.05, 43.39, 32.00, 29.53, 29.49, 29.39, 29.15, 28.80, 26.02, 23.54, 22.80, 14.25; ESI MS: Expected $[M+H]^+$: 298.2377, observed: 298.2372.

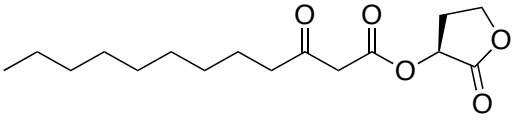

11: ^{1}H NMR (500 MHz, $CDCl_3$) 5.44 (t, *J* = 8.9 Hz, 1H), 4.48 (td, *J* = 9.1, 2.7 Hz, 1H), 4.36 – 4.25 (m, 1H), 3.69 – 3.40 (m, 2H), 2.74 (dddd, *J* = 13.1, 9.0, 6.5, 2.7 Hz, 1H), 2.54 (t, *J* = 7.3 Hz, 2H), 2.36 (dq, *J* = 12.9, 9.4 Hz, 1H), 1.58 (h, *J* = 8.3, 7.8 Hz, 2H), 1.27 (dd, *J* = 11.5, 6.2 Hz, 14H), 0.97 – 0.71 (m, 3H); ^{13}C NMR (126 MHz, $CDCl_3$) δ 202.24, 172.28, 166.22, 68.37, 65.18, 48.62, 43.18, 31.85, 29.38, 29.34, 29.24, 28.97, 28.77, 23.43, 22.66, 14.11; ESI MS: Expected $[M+H]^+$: 316.2119, observed: 316.2114

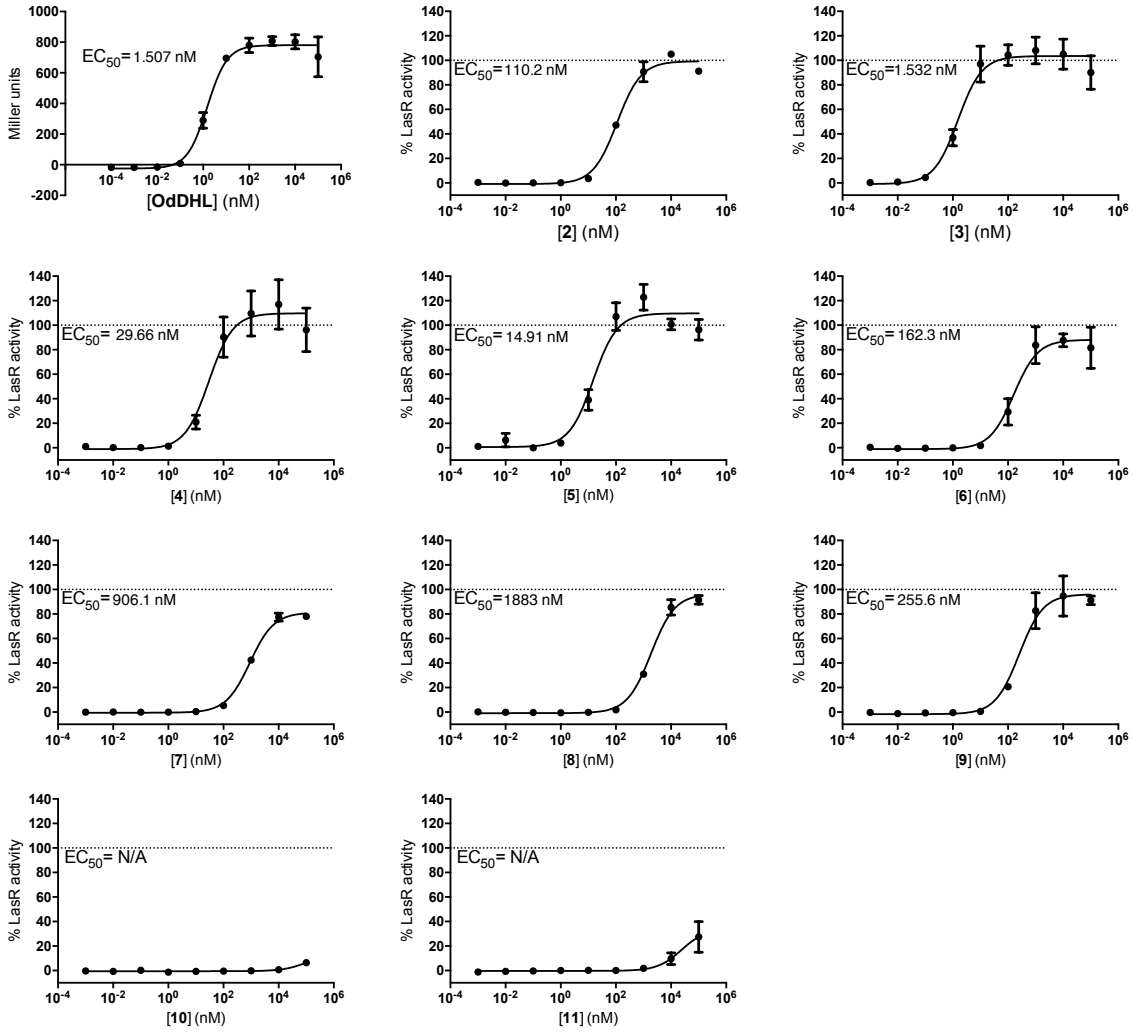

Figure 7.5 Dose–response curves for LasR agonism in *E. coli* by all compounds.
Assay performed using the E. coli JLD271/pJN105L/pSC11 reporter strain. % Activity is defined as the activity of the synthetic AHL relative to maximum possible LasR activity (i.e., activity effected by OdDHL at 100 μM). EC_{50} values and 95% Confidence Intervals (CI; shown in Table 7.1) calculated using GraphPad Prism. Error bars, SEM of $n \geq 3$ trials.

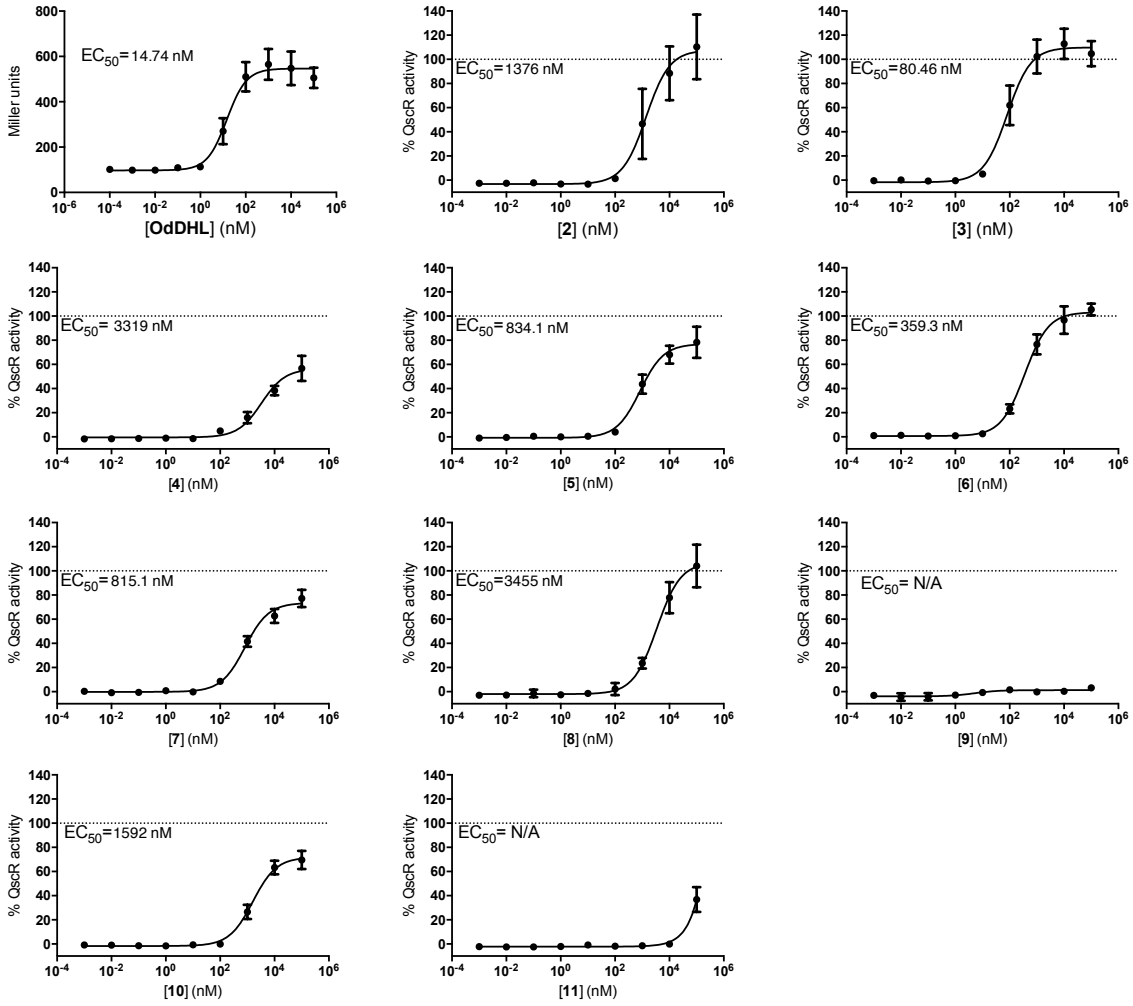

Figure 7.6 Dose–response curves for QscR agonism in *E. coli* by all compounds.
Assay performed using the E. coli JLD271/pJN105Q/pSC11-Q reporter strain. % Activity is defined as the activity of the synthetic AHL relative to maximum possible QscR activity (i.e., activity effected by OdDHL at 100 μM). EC_{50} values and 95% Confidence Intervals (CI; shown in Table 7.1) calculated using GraphPad Prism. Error bars, SEM of $n \geq 3$ trials.

6.7 ^{1}H- and ^{13}C-NMR spectra for compounds novel or undercharacterized compounds in this study

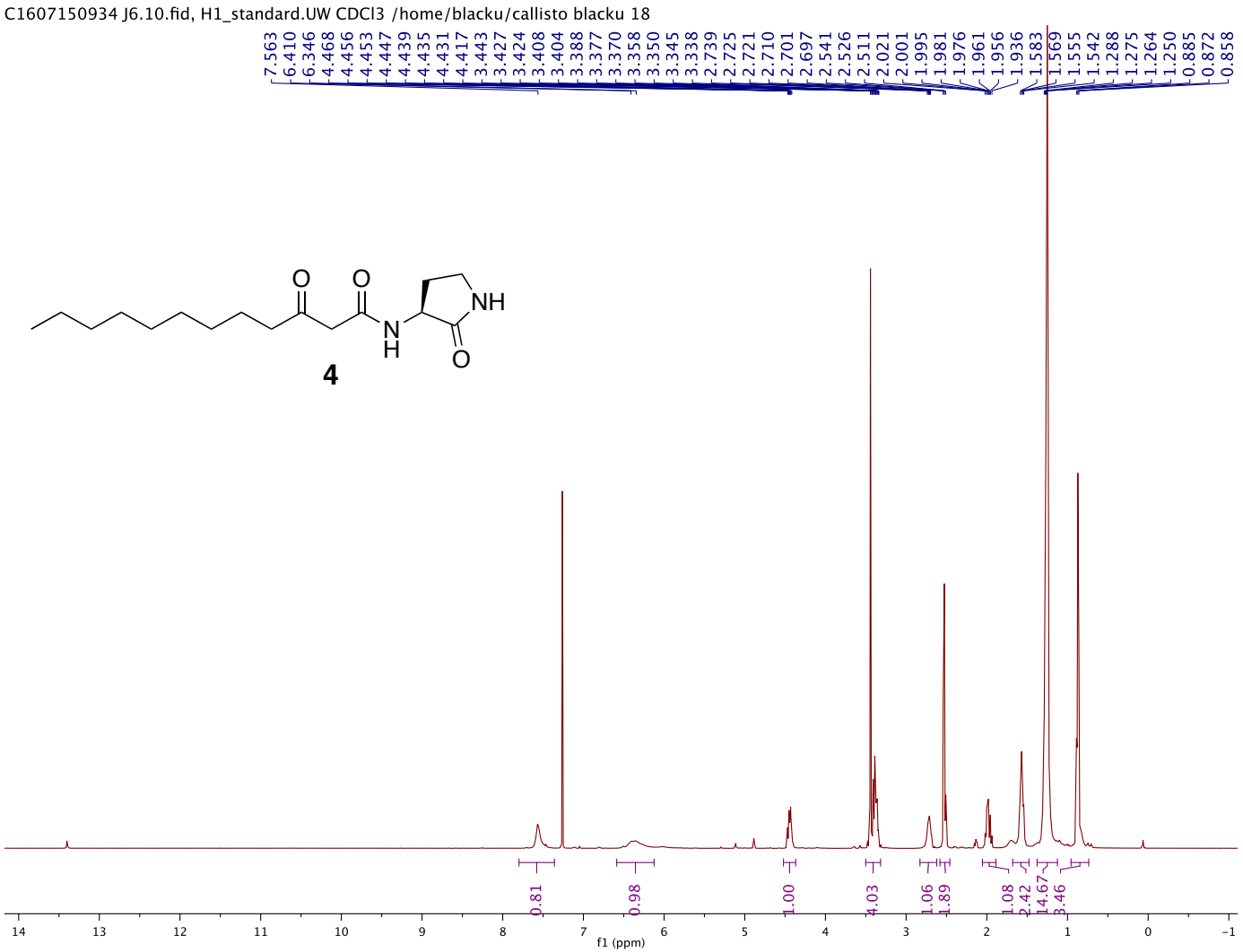

C1607150934 J6.11.fid, C13_H1dec.UW CDCl3 /home/blacku/callisto blacku 18

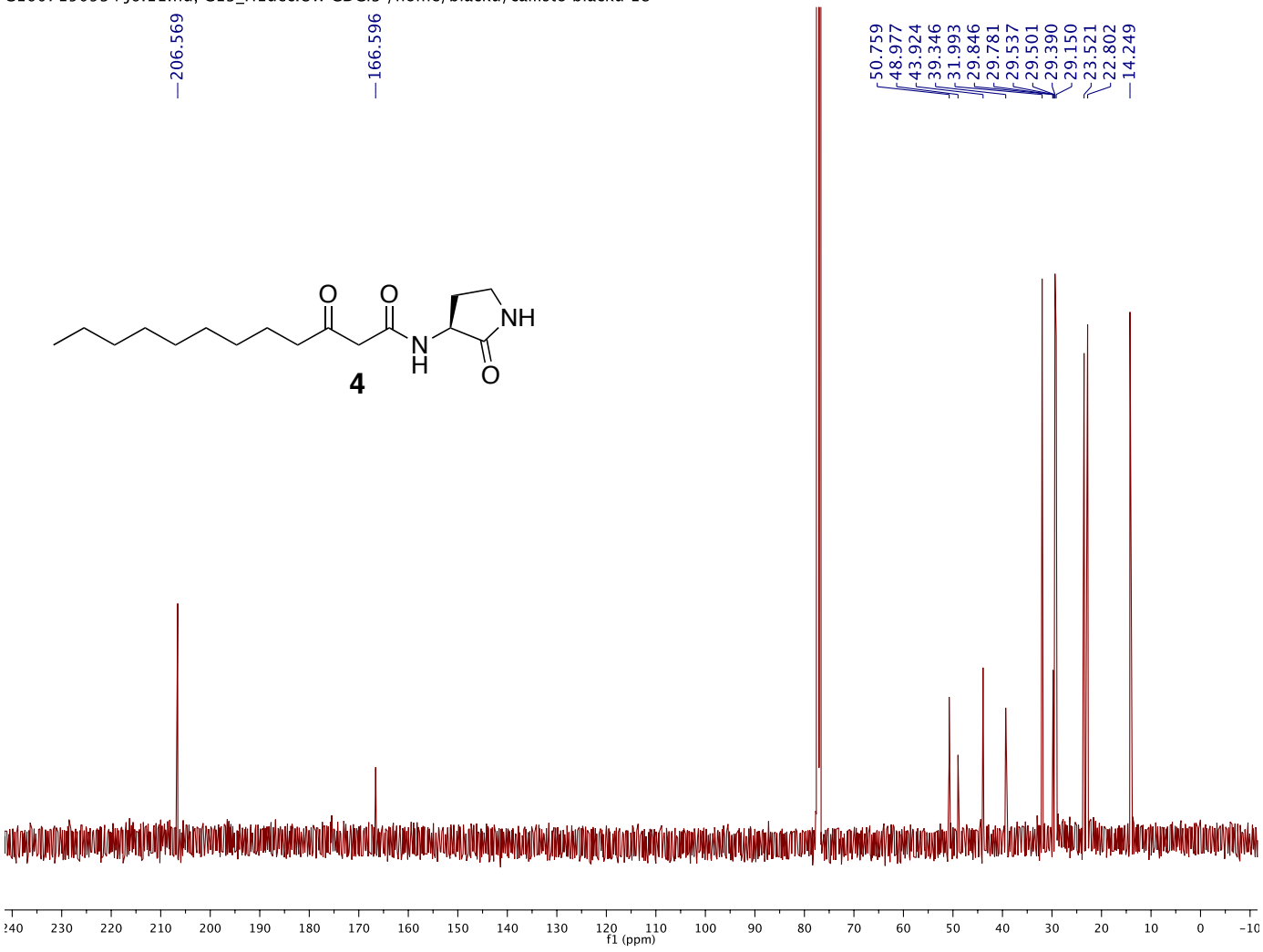

C1607150934 J1.10.fid, H1_standard.UW CDCl3 /home/blacku/callisto blacku 12

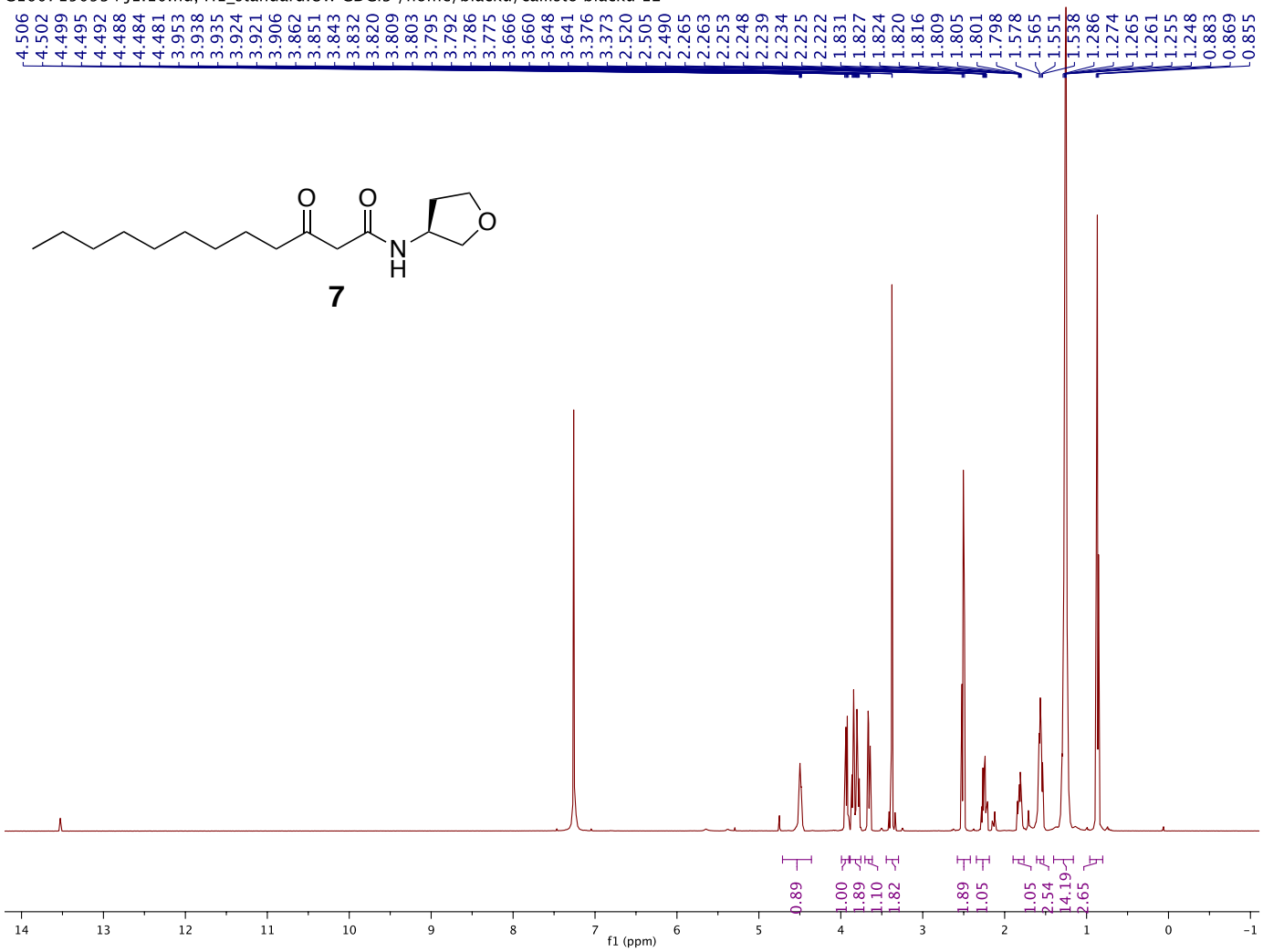

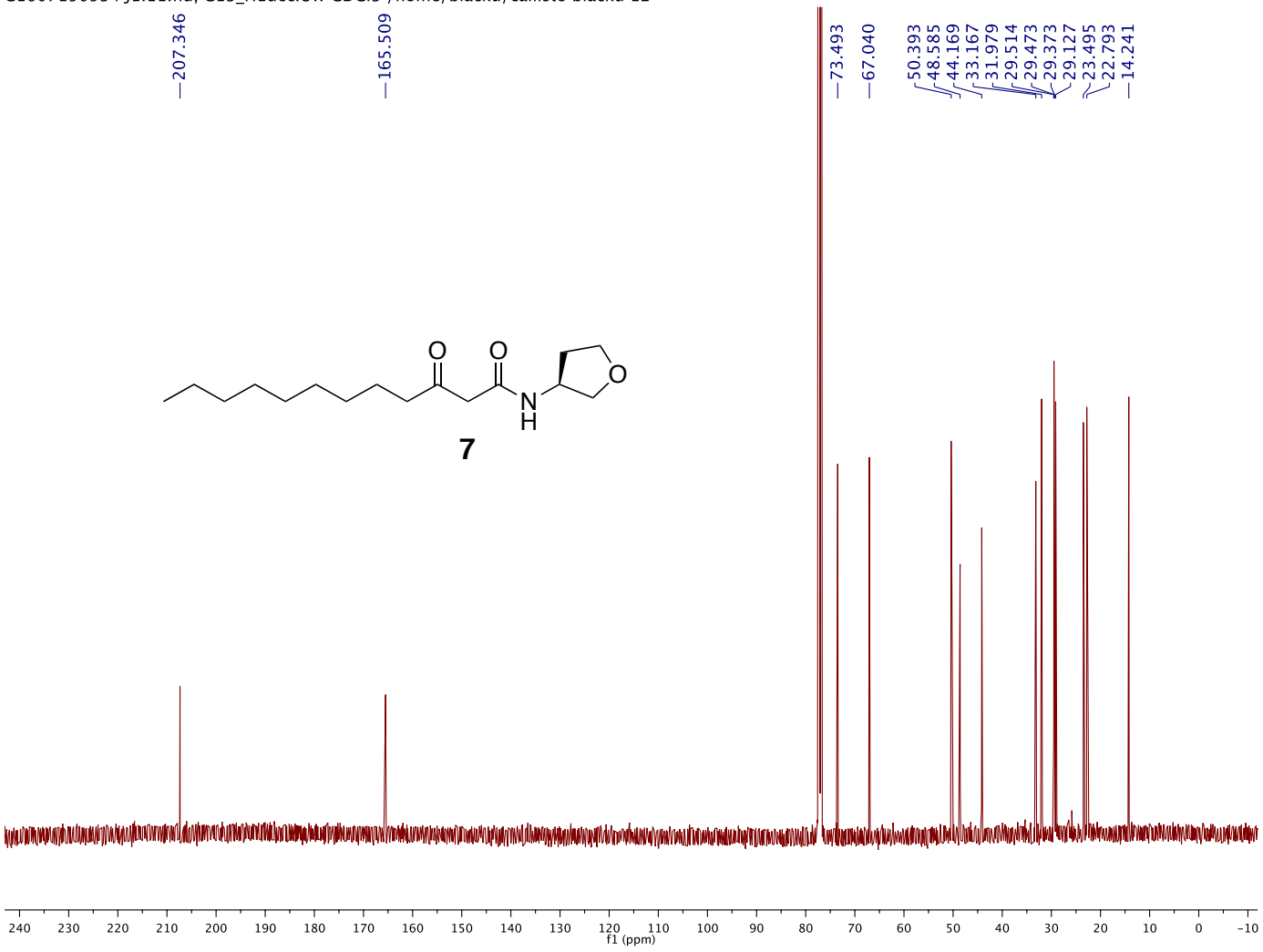
C1607150934 J1.11.fid, C13_H1dec.UW CDCl3 /home/blacku/callisto blacku 12
207.346
165.509
73.493
67.040
50.393
48.585
44.169
33.167
31.979
29.514
29.473
29.373
29.127
23.495
22.793
14.241
O
O
N
H
O
7
240 230 220 210 200 190 180 170 160 150 140 130 120 110 100 90 80 70 60 50 40 30 20 10 0 -10
f1 (ppm)

C1607150934 J7.10.fid, H1_standard.UW CDCl3 /home/blacku/callisto blacku 19

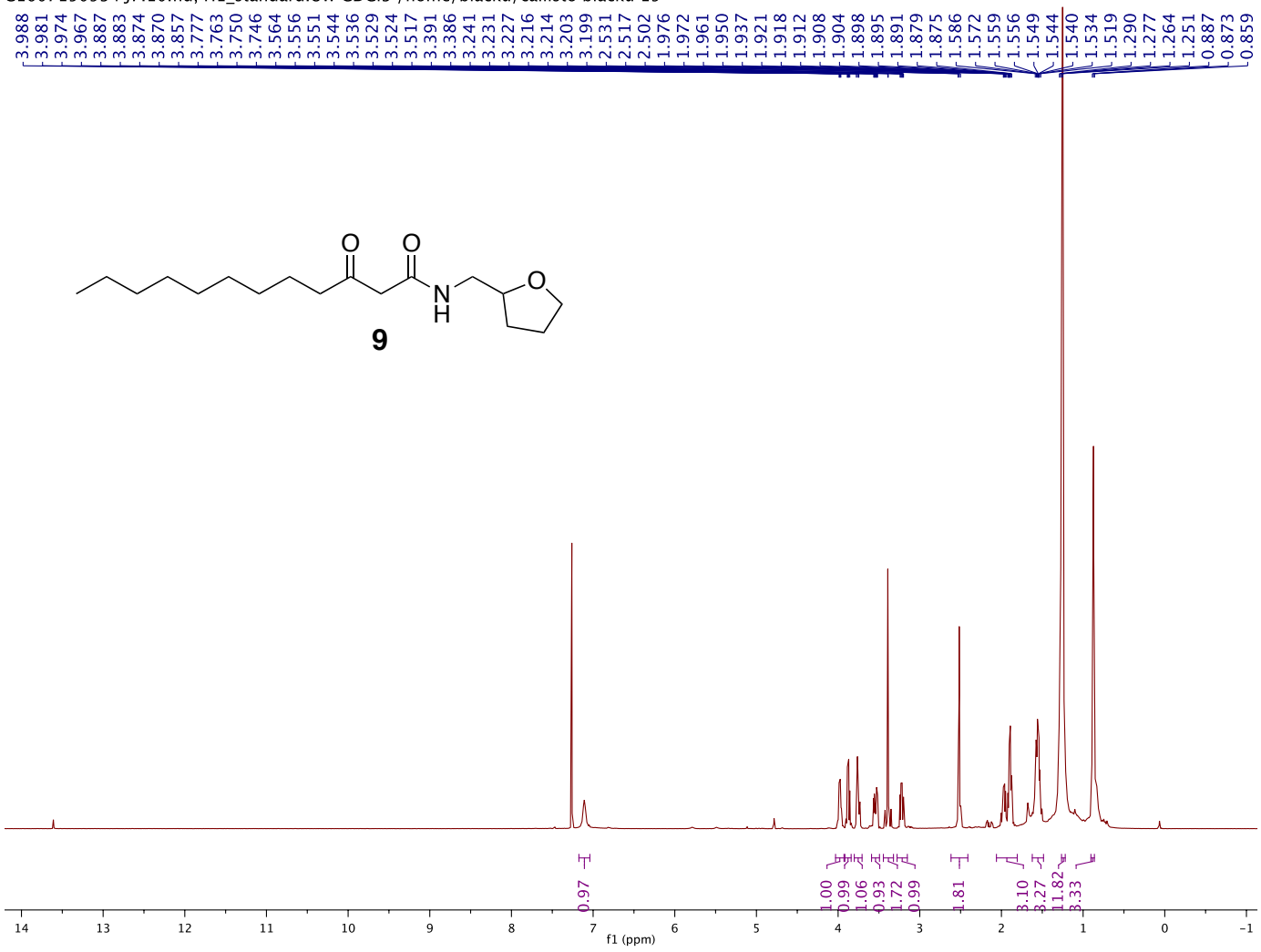

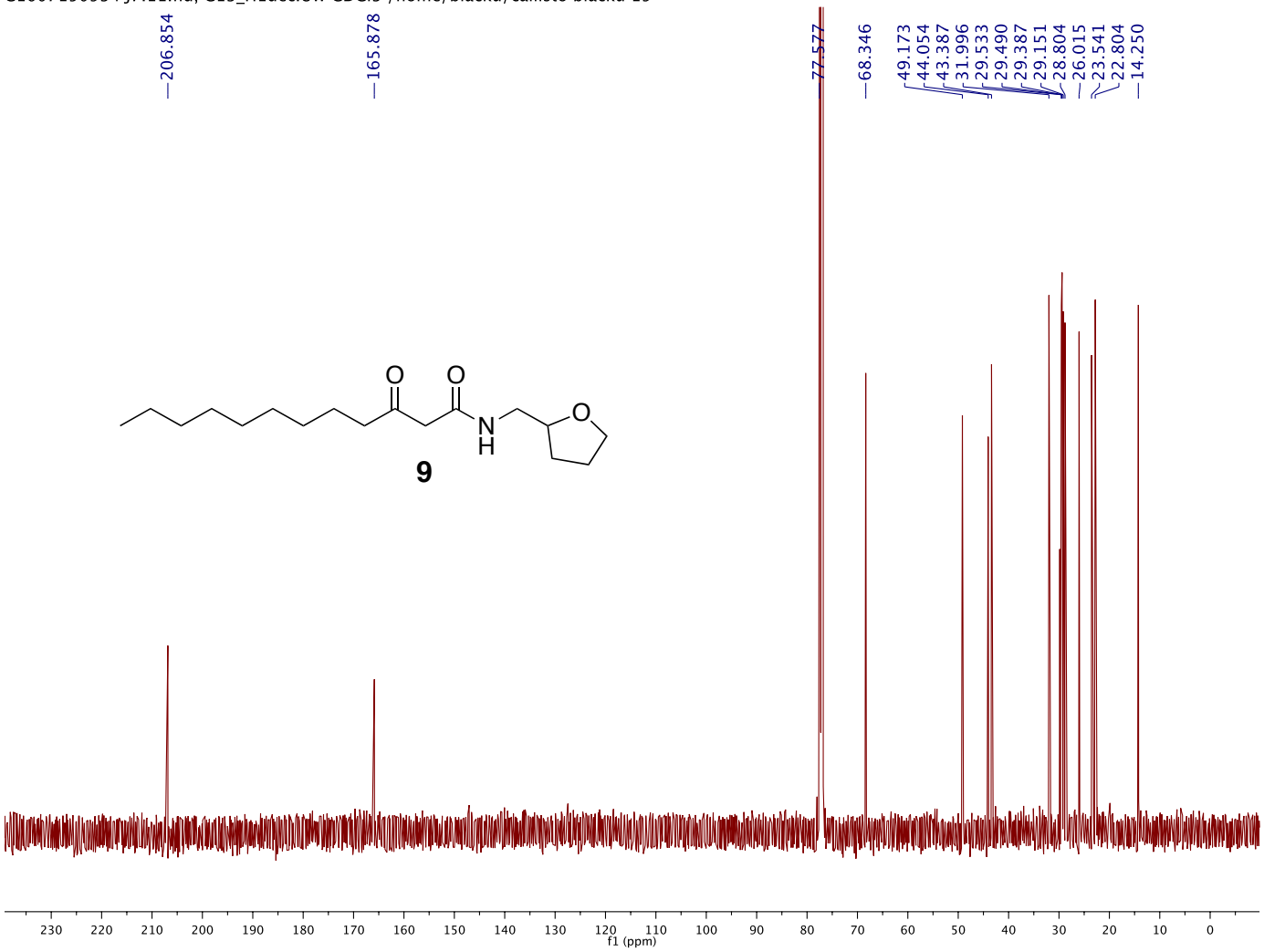
C1607150934 J7.11.fid, C13_H1dec.UW CDCl3 /home/blacku/callisto blacku 19
206.854
165.878
77.577
68.346
49.173
44.054
43.387
31.996
29.533
29.490
29.387
29.151
28.804
26.015
23.541
22.804
14.250
O
O
N
H
O
9
230 220 210 200 190 180 170 160 150 140 130 120 110 100 90 80 70 60 50 40 30 20 10 0
f1 (ppm)

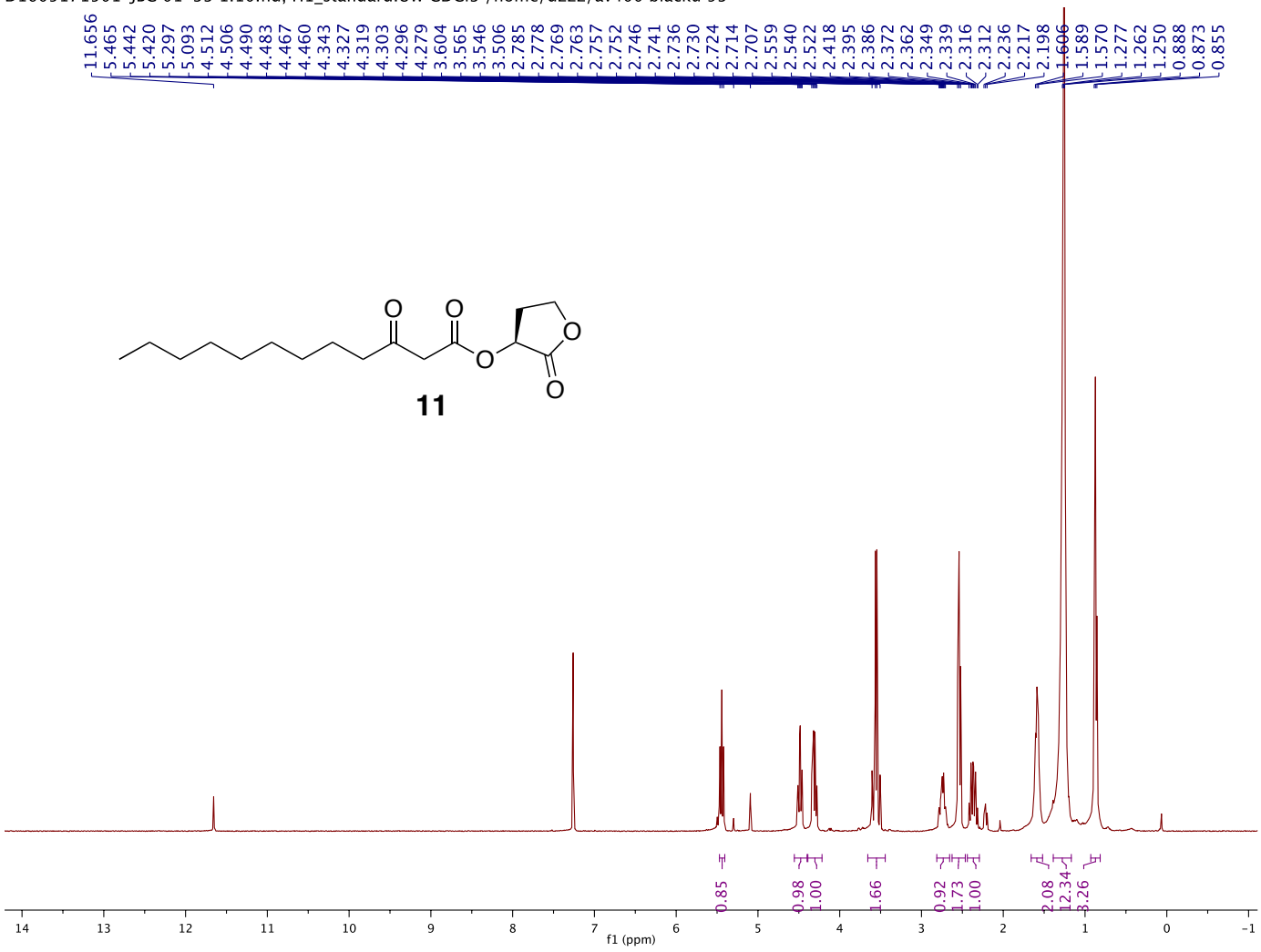
D1605171501-JBC 01-33 1.10.fid, H1_standard.UW CDCl3 /home/dzzz/av400 blacku 93
11.656
5.465
5.442
5.420
5.297
5.093
4.512
4.506
4.490
4.483
4.467
4.460
4.343
4.327
4.319
4.303
4.296
4.279
3.604
3.565
3.546
3.506
2.785
2.778
2.769
2.763
2.757
2.752
2.746
2.741
2.736
2.730
2.724
2.714
2.707
2.559
2.540
2.522
2.418
2.395
2.386
2.372
2.362
2.349
2.339
2.316
2.312
2.236
2.217
2.198
1.606
1.589
1.570
1.277
1.262
1.250
0.888
0.873
0.855
O
O
O
O
O
11
0.85
0.98
1.00
1.66
0.92
1.73
1.00
2.08
12.34
3.26
14
13
12
11
10
9
8
7
6
5
4
3
2
1
0
-1
f1 (ppm)

C1605181135.11.fid — C13_H1dec.UW CDCl3 /home/blacku/callisto blacku 47

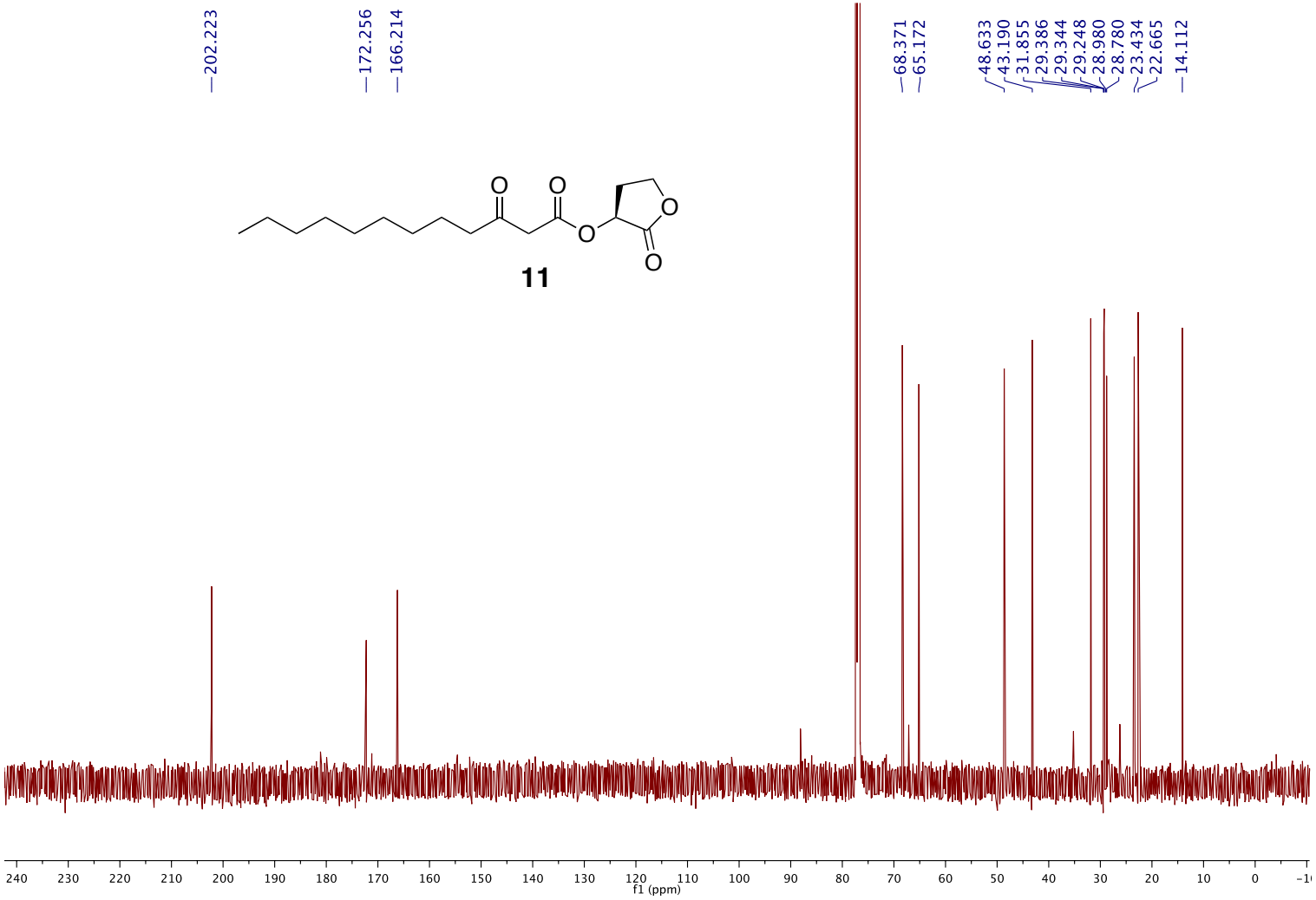

6.7 References

1. Fuqua, C., and Greenberg, E. P. (2002) Listening in on bacteria: acyl-homoserine lactone signalling., *Nature Rev. Mol. Cell Biol.3*, 685-695.

2. Kerr, K. G., and Snelling, A. M. (2009) *Pseudomonas aeruginosa*: a formidable and ever-present adversary, *J. Hosp. Infect. 73*, 338-344.

3. Mesaros, N., Nordmann, P., Plesiat, P., Roussel-Delvallez, M., Van Eldere, J., Glupczynski, Y., Van Laethem, Y., Jacobs, F., Lebecque, P., Malfroot, A., Tulkens, P. M., and Van Bambeke, F. (2007) *Pseudomonas aeruginosa*: Resistance and therapeutic options at the dawn of the 2d millenium, *Clin. Microbiol. Infect. 13*, 560-578.

4. Folkesson, A., Jelsbak, L., Yang, L., Johansen, H. K., Ciofu, O., Høiby, N., and Molin, S. (2012) Adaptation of *Pseudomonas aeruginosa* to the cystic fibrosis airway: an evolutionary perspective, *Nat. Rev. Microbiol. 10*, 841-851.

5. Schuster, M., and Greenberg, E. P. (2006) A network of networks: quorum-sensing gene regulation in *Pseudomonas aeruginosa*, *Int. J. Med. Microbiol. 296*, 73-81.

6. Ledgham, F., Ventre, I., Soscia, C., Foglino, M., Sturgis, J. N., and Lazdunski, A. (2003) Interactions of the quorum sensing regulator QscR: interaction with itself and the other regulators of *Pseudomonas aeruginosa* LasR and RhlR, *Mol. Microbiol. 48*, 199-210.

7. Williams, P., and Cámara, M. (2009) Quorum sensing and environmental adaptation in *Pseudomonas aeruginosa*: a tale of regulatory networks and multifunctional signal molecules, *Curr. Opin. Microbiol. 12*, 182-191.

8. Lequette, Y., Lee, J. H., Ledgham, F., Lazdunski, A., and Greenberg, E. P. (2006) A distinct QscR regulon in the *Pseudomonas aeruginosa* quorum-sensing circuit, *J. Bacteriol. 188*, 3365-3370.

9. Schuster, M., Schuster, M., Lostroh, C. P., Lostroh, C. P., Ogi, T., Ogi, T., Greenberg, E. P., and Greenberg, E. P. (2003) Identification, Timing, and Signal Specificity of *Pseudomonas aeruginosa* Quorum-Controlled Genes: a Transcriptome Analysis, *J. Bacteriol. 185*, 2066-2079.

10. Wagner, V. E., Bushnell, D., Passador, L., Brooks, A. I., and Iglewski, B. H. (2003) Microarray Analysis of *Pseudomonas aeruginosa* Quorum-Sensing Regulons : Effects of Growth Phase and Environment, *J. Bacteriol. 185*, 2080-2095.

11. Gambello, M. J., Kaye, S., and Iglewski, B. H. (1993) LasR of *Pseudomonas aeruginosa* Is a Transcriptional Activator of the Alkaline Protease Gene (apr) and an Enhancer of Exotoxin-A Expression, *Infect. Immun. 61*, 1180-1184.

12. Brint, J. M., and Ohman, D. E. (1995) Synthesis of multiple exoproducts in *Pseudomonas aeruginosa* is under the control of RhlR-RhlI, another set of regulators in strain PAO1 with homology to the autoinducer-responsive LuxR-LuxI family, *J. Bacteriol. 177*, 7155-7163.

13. Geske, G. D., O'Neill, J. C., Miller, D. M., Wezeman, R. J., Mattmann, M. E., Lin, Q., and Blackwell, H. E. (2008) Comparative analyses of N-acylated homoserine lactones reveal unique

structural features that dictate their ability to activate or inhibit quorum sensing, *ChemBioChem 9*, 389-400.

14. Mattmann, M. E., Shipway, P. M., Heth, N. J., and Blackwell, H. E. (2011) Potent and Selective Synthetic Modulators of a Quorum Sensing Repressor in *Pseudomonas aeruginosa* Identified from Second-Generation Libraries of *N*-Acylated L-Homoserine Lactones, *Chembiochem 12*, 942-949.

15. Geske, G. D., Wezeman, R. J., Siegel, A. P., and Blackwell, H. E. (2005) Small molecule inhibitors of bacterial quorum sensing and biofilm formation, *J. Am. Chem. Soc. 127*, 12762-12763.

16. Galloway, W. R. J. D., Hodgkinson, J. T., Bowden, S., Welch, M., and Spring, D. R. (2012) Applications of small molecule activators and inhibitors of quorum sensing in Gram-negative bacteria, *Trends Microbiol. 20*, 449-458.

17. Welsh, M. a., Eibergen, N. R., Moore, J. D., Blackwell, H. E., Welsh, M., Eibergen, N. R., Moore, J. D., and Blackwell, H. E. (2015) Small molecule disruption of quorum sensing cross-regulation in *Pseudomonas aeruginosa* causes major and unexpected alterations to virulence phenotypes, *J. Am. Chem. Soc. 137*, 1510-1519.

18. Eibergen, N. R., Moore, J. D., Mattmann, M. E., and Blackwell, H. E. (2015) Potent and Selective Modulation of the RhlR Quorum Sensing Receptor by Using Non-native Ligands : An Emerging Target for Virulence Control in *Pseudomonas aeruginosa*, *ChemBioChem 16*, 2348-2356.

19. Weng, L.-X., Yang, Y.-X., Zhang, Y.-Q., and Wang, L.-H. (2014) A new synthetic ligand that activates QscR and blocks antibiotic-tolerant biofilm formation in *Pseudomonas aeruginosa*, *Appl. Microbiol. Biotechnol. 98*, 2565-2572.

20. Zhang, R.-g., Pappas, K. M., Brace, J. L., Miller, P. C., Oulmassov, T., Molyneaux, J. M., Anderson, J. C., Bashkin, J. K., Winans, S. C., and Joachimiak, A. (2002) Structure of a bacterial quorum-sensing transcription factor complexed with pheromone and DNA, *Nature 417*, 971-974.

21. Reche, P. (2017) Sequence Identity And Similarity Tool, Secretaria General De Ciencia, Tecnologia E Innovacion of Spain. Available online at http://imed.med.ucm.es/Tools/sias.html.

22. Oinuma, K.-I., and Greenberg, E. P. (2011) Acyl-homoserine lactone binding to and stability of the orphan *Pseudomonas aeruginosa* quorum-sensing signal receptor QscR, *J. Bacteriol. 193*, 421-428.

23. Lee, J.-H., Lequette, Y., and Greenberg, E. P. (2006) Activity of purified QscR, a *Pseudomonas aeruginosa* orphan quorum-sensing transcription factor, *Mol. Microbiol. 59*, 602-609.

24. Lintz, M. J., Oinuma, K.-I., Wysoczynski, C. L., Greenberg, E. P., and Churchill, M. E. a. (2011) Crystal structure of QscR, a *Pseudomonas aeruginosa* quorum sensing signal receptor, *Proc. Natl. Acad. Sci. USA 108*, 15763-15768.

25. Bottomley, M. J., Muraglia, E., Bazzo, R., and Carfi, A. (2007) Molecular insights into quorum sensing in the human pathogen *Pseudomonas aeruginosa* from the structure of the virulence regulator LasR bound to its autoinducer, *J. Biol. Chem. 282*, 13592-13600.

26. Geske, G. D., O'Neill, J. C., Miller, D. M., Mattmann, M. E., and Blackwell, H. E. (2007) Modulation of bacterial quorum sensing with synthetic ligands: systematic evaluation of N-acylated homoserine lactones in multiple species and new insights into their mechanisms of action, *J. Am. Chem. Soc. 129*, 13613-13625.

27. Vannini, A., Volpari, C., Gargioli, C., Muraglia, E., Cortese, R., De Francesco, R., Neddermann, P., and Di Marco, S. (2002) The crystal structure of the quorum sensing protein TraR bound to its autoinducer and target DNA, *EMBO J. 21*, 4393-4401.

28. Boursier, M. E., Combs, J. B., and Blackwell, H. E. N-Acyl L-Homocysteine thiolactones are potent and stable synthetic modulators of the RhlR quorum sensing receptor in *Pseudomonas aeruginosa*, *In preparation*.

29. Glansdorp, F. G., Thomas, G. L., Lee, J. K., Dutton, J. M., Salmond, G. P. C., and Spring, D. R. (2004) Synthesis and stability of small molecule probes for *Pseudomonas aeruginosa* quorum sensing modulation, *Org. Biomol. Chem. 2*, 3329-3336.

30. O'Reilly, M. C., and Blackwell, H. E. (2016) Structure-Based Design and Biological Evaluation of Triphenyl Scaffold-Based Hybrid Compounds as Hydrolytically Stable Modulators of a LuxR-Type Quorum Sensing Receptor, *ACS Infect. Dis. 2*, 32-38.

31. Müh, U., Hare, B. J., Duerkop, B. a., Schuster, M., Hanzelka, B. L., Heim, R., Olson, E. R., and Greenberg, E. P. (2006) A structurally unrelated mimic of a *Pseudomonas aeruginosa* acyl-homoserine lactone quorum-sensing signal, *Proc. Natl. Acad. Sci. USA 103*, 16948-16952.

32. Müh, U., Schuster, M., Heim, R., Singh, A., Olson, E. R., and Greenberg, E. P. (2006) Novel *Pseudomonas aeruginosa* quorum-sensing inhibitors identified in an ultra-high-throughput screen, *Antimicrob. Agents Chemother. 50*, 3674-3679.

33. Moore, J. D., Rossi, F. M., Welsh, M. A., Nyffeler, K. E., and Blackwell, H. E. (2015) A Comparative Analysis of Synthetic Quorum Sensing Modulators in *Pseudomonas aeruginosa*: New Insights into Mechanism, Active Efflux Susceptibility, Phenotypic Response, and Next-Generation Ligand Design, *J. Am. Chem. Soc. 137*, 14626-14639.

34. Passador, L., Tucker, K. D., Guertin, K. R., Journet, M. P., Kende, a. S., Kende, A. S., and Iglewski, B. H. (1996) Functional analysis of the *Pseudomonas aeruginosa* autoinducer PAI, *J. Bacteriol. 178*, 5995-6000.

35. Smith, K. M., Bu, Y., and Suga, H. (2003) Induction and Inhibition of *Pseudomonas aeruginosa* Quorum Sensing by Synthetic Autoinducer Analogs, *Chem. Biol. 10*, 81-89.

36. McInnis, C. E., and Blackwell, H. E. (2011) Thiolactone modulators of quorum sensing revealed through library design and screening, *Bioorg. Med. Chem. 19*, 4820-4828.

37. McInnis, C. E., and Blackwell, H. E. (2011) Design, synthesis, and biological evaluation of abiotic, non-lactone modulators of LuxR-type quorum sensing, *Bioorg. Med. Chem. 19*, 4812-4819.

38. Mattmann, M. E., Geske, G. D., Worzalla, G. a., Chandler, J. R., Sappington, K. J., Greenberg, E. P., and Blackwell, H. E. (2008) Synthetic ligands that activate and inhibit a quorum-sensing regulator in *Pseudomonas aeruginosa*, *Bioorg. Med. Chem. Lett. 18*, 3072-3075.

39. Suga, H., and Bu, Y. (2004) Combinatorial libraries of autoinducer analogs, autoinducer agonists and antagonists, and methods of use thereof, WO 2004016213.

40. Horikawa, M., Tateda, K., Tuzuki, E., Ishii, Y., Ueda, C., Takabatake, T., Miyairi, S., Yamaguchi, K., and Ishiguro, M. (2006) Synthesis of *Pseudomonas* quorum-sensing autoinducer analogs and structural entities required for induction of apoptosis in macrophages, *Bioorg. Med. Chem. Lett. 16*, 2130-2133.

41. Castang, S., Chantegrel, B., Deshayes, C., Dolmazon, R., Gouet, P., Haser, R., Reverchon, S., Nasser, W., Hugouvieux-Cotte-Pattat, N., and Doutheau, A. (2004) *N*-Sulfonyl homoserine lactones as antagonists of bacterial quorum sensing, *Bioorg. Med. Chem. Lett. 14*, 5145-5149.

42. Jog, G. J., Igarashi, J., and Suga, H. (2006) Stereoisomers of P. aeruginosa autoinducer analog to probe the regulator binding site, *Chem. Biol. 13*, 123-128.

43. Hodgkinson, J. T., Galloway, W. R. J. D., Casoli, M., Keane, H., Su, X., Salmond, G. P. C., Welch, M., and Spring, D. R. (2011) Robust routes for the synthesis of N-acylated-l-homoserine lactone (AHL) quorum sensing molecules with high levels of enantiomeric purity, *Tetrahedron Lett. 52*, 3291-3294.

44. Schuster, M., Urbanowski, M. L., and Greenberg, E. P. (2004) Promoter specificity in *Pseudomonas aeruginosa* quorum sensing revealed by DNA binding of purified LasR., *Proc. Natl. Acad. Sci. USA 101*, 15833-15839.

45. Gerdt, Joseph P., McInnis, Christine E., Schell, Trevor L., Rossi, Francis M., and Blackwell, Helen E. (2014) Mutational Analysis of the Quorum-Sensing Receptor LasR Reveals Interactions that Govern Activation and Inhibition by Nonlactone Ligands, *Chem. Biol. 21*, 1361-1369.

46. Cordero, B., Gómez, V., Platero-Prats, A. E., Revés, M., Echeverría, J., Cremades, E., Barragán, F., and Alvarez, S. (2008) Covalent radii revisited, *Dalton Trans. 0*, 2832-2838.

47. Boursier, M. E., Moore, J. D., Heitman, K. N., Fungairino, S. P. S.-., Combs, J. B., Koenig, L. C., Shin, D., Brown, E. C., Nagarajan, R., and Blackwell, H. E. Structure-function analyses of the N-butyryl L-homoserine lactone quorum sensing signal define features critical to activity in the *Pseudomonas aeruginosa* RhlR receptor, *In preparation*.

48. Skowronek, P., and Gawronski, J. (1999) Absolute configuration of α -phthalimido carboxylic acid derivatives from circular dichroism spectra, *Tetrahedron: Asymmetry 10*, 4585-4590.

49. O'Reilly, M. C., and Blackwell, H. E. (2016) Structure-Based Design and Biological Evaluation of Triphenyl Scaffold-Based Hybrid Compounds as Hydrolytically Stable Modulators of a LuxR-Type Quorum Sensing Receptor, *ACS Infect. Dis. 2*, 32-38.

50. Murray, E., Crowley, R., Truman, A., Clarke, S., Cottam, J., Jadhav, G., Shea, P. O., Lindholm, C., Cockayne, A., Chhabra, R., Chan, W. C., Williams, P., Murray, E. J., Crowley, R. C., Clarke, S. R., Cottam, J. A., Jadhav, P., Steele, V. R., and Ram, S. (2014) Targeting

Staphylococcus aureus quorum sensing with non-peptidic small molecule inhibitors, *J. Med. Chem. 57*, 2813-2819.

CHAPTER 7:

Thesis Summary and Future Directions

7.1 Summary

Fully understanding and harnessing the complex QS system of *P. aeruginosa* truly requires diverse chemical probes and approaches. From the subtle perturbations in AHL chemical structure to working with the whole complex QS circuit in wild type *P. aeruginosa*, these studies have helped to expand the tools available to study this organism.

Through our rigorous work looking at SARs of the homoserine lactone head group in Chapters 2 and 7, we have gathered vital information about the way in which this moiety binds in each of the three LuxR-type receptors. We have begun to understand how best to make selective probes for each receptor while also increasing compound stability. These observations contributed to some of the most potent and stable known RhlR modulators, as detailed in Chapter 3, and will contribute to future library developments. With the mechanistic information obtained in Chapters 4 and 5, we acquired the ability to test LuxR-type receptor mechanism of action with non-native AHLs using a variety of techniques. We have a better understanding on how different classes of modulators regulate the target receptor. The key mechanism of action for many AHL partial agonists appears to center on protein dimerization. Finally, in Chapter 6 our work to develop a QS-response soft material allowed us to broaden the applicability of LCs to a population density-based signal. We successful introduced LCs to a complex mixture and still observed robust response.

This foundational work will continue forward in a variety of important ways.

7.2 Testing selective and stable AHLs in the wild type organism

The head group variations explored in this dissertation are ready for use in hybrid probe libraries. This would entail straightforward library generation using combinations of potent head groups and tail groups depending on the desired receptor target. Previous studies mixing potent head and tail groups have had limited success. However, hybrid leads generated in Chapter 3 suggest the incorporation of an agonist head group may be a promising way to start the library

generation process. Selective LasR head groups are intriguing for novel antagonists, whereas selective QscR head groups could yield potent agonists. Both directions of QS modulation may result in inhibition of different virulence factors in the circuit.

Compounds that use the alternative head groups will likely benefit from improved hydrolytic stability. Potent compounds found in the reporter screens should be tested in wild type *P. aeruginosa*. It is not clear whether the increased lifetime results in a more robust modulation of virulence phenotypes. However, because phenotypic assays typically last over 16 hours, we expect the new compounds to have an impact on QS during the entire time course.

7.3 Expanded use of FRET to monitor ligand binding

The successful FRET probe **MMF5** opens several avenues of research to explore AHL mode of action. First, this probe can be utilized with purified QscR in conditions that force a protein dimer to form. This could be chemically done through the introduction of a linker between two protein monomers. Alternatively, because QscR forms a dimer upon binding to DNA, the same in vitro FRET experiments could be performed with the inclusion of a DNA duplex of QscR's promoter region. In both situations the shape of a resulting dose response curve can be analyzed to look at binding cooperativity. If the binding of one ligand to the dimer causes an increased likelihood of a second ligand binding, the curve Hill slope will get steeper and indicate positive cooperativity. The inverse will occur and the Hill slope will be shallow if negative cooperativity occurs.

To remove the effects potentially caused by cell membrane adsorption and permeability issues, cell lysate can be used containing expressed QscR rather than whole cells. Cells prepared fresh or thawed from frozen stocks would be lysed, then subjected to a similar FRET assay as with the in vitro experiments using purified protein. This method would additionally allow for approximate lysate protein and QscR quantification through the use of standard protein quantification assays and SDS-PAGE analyses. Cell membranes may also be constraining QscR

to a dimer, and this technique allows for a direct comparison with cell-based FRET. With the proper optimization, this approach may allow for decreased labor between protein expression and the generation of binding data.

We foresee FRET being used in a variety of other LuxR-type receptors to look at ligand binding. Larger libraries of dansyl and cumarin-based AHLs can be easily generated and screened in a number of different bacterial systems. Upon discovery of a moderate agonist such as **MMF5**, proteins could be purified with the FRET probe, allowing for analysis without worrying about another displacement ligand.

7.4 QS responsive drug delivery

With the knowledge that LCs can selectively detect QS goods in *P. aeruginosa* cell culture, we can utilize the wide number of available LC systems to optimize detection conditions for varying AHL concentrations. Buffer or media composition plays a large role in the responsiveness of LCs. Moving away from poorly defined media such as LB and towards defined media with easily variable components would make for logical troubleshooting. Each media component could be assessed for its ability to increase or decrease LC sensitivity at varying concentrations.

LCs are primed for the release of both antibiotics and QS modulators. Once satisfactory optimizations have been performed for the desired amount of LC response and sensitivity, LCs can be loaded with the molecule of interest. The cargo is released when an orientation transition occurs. With increased sensitivity of LCs, low concentrations of AHLs can trigger the release of QS inhibitors or antibiotic before quorate is reached, increasing the likelihood of turning off virulence or killing cells.

APPENDIX I:

Mechanism of agonism and antagonism of the *Pseudomonas aeruginosa* quorum sensing regulator QscR with non-native ligands

Contributions: C. L. Wysoczynski-Horita, R. Hill, and K. Hansen of University of Colorado Denver performed biochemical experiments. M. E. Boursier performed reporter assays and assisted in writing. Helen E. Blackwell contributed writing. C. L. Wysoczynski-Horita and M. E. A. Churchill of University of Colorado Denver designed experiments, performed crystalography analysis, and prepared the manuscript.

*This chapter has been prepared as a manuscript intended for publication under the same title.

I.1 Abstract

Pseudomonas aeruginosa is an opportunistic pathogen that uses the process of quorum sensing (QS) to coordinate the expression of many virulence genes. During quorum sensing, *N*-acyl-homoserine lactone (AHL) signaling molecules regulate the activity of three LuxR-type transcription factors, LasR, RhlR, and QscR. To better understand *P. aeruginosa* QS signal reception, we examined the mechanism underlying the response of QscR to synthetic agonists and antagonists using biophysical and structural approaches. The structure of QscR bound to a synthetic agonist reveals a novel mode of ligand binding supporting a general mechanism for agonist activity. In turn, antagonists of QscR with partial agonist activity were found to destabilize and greatly impair QscR dimerization and DNA binding. These results highlight the diversity of LuxR-type receptor responses to small molecule agonists and antagonists and demonstrate the potential for chemical strategies for the selective targeting of individual quorum-sensing systems.

I.2 Introduction

Pseudomonas aeruginosa (P. a.) is an opportunistic human pathogen that uses a process of inter-cellular communication known as quorum sensing (QS) to promote virulence and biofilm formation.[1, 2] QS enables bacteria to sense their local bacterial population density through the synthesis, diffusion, and reception of small signaling molecules, which ultimately coordinates group behaviors.[3, 4] Since the discovery of the "Lux" quorum sensing system in *Vibrio fischeri*, dozens of species of Gram-negative bacteria have been found to utilize *N*-acyl L-homoserine lactones (AHLs) as their primary QS signal.[5] AHLs are neutral, lipid-like molecules consisting of a conserved L -homoserine lactone head group and an acyl-chain tail that can vary both in length and substituents.[6-8] AHLs are synthesized by LuxI-type AHL synthases and are recognized by intracellular LuxR-type AHL receptors that serve as transcription factors to regulate the activity of target genes once a threshold concentration of AHL, and thus a threshold cell density, is achieved.[9-13]

The *P. a.* QS circuitry is relatively complex and consists of a hierarchy of AHL-mediated signaling circuits that includes two major *lux*-like signaling pathways.[14] In the *rhl* system, the AHL synthase RhlI produces a C4-homoserine lactone (C4-HSL) that is recognized by the cognate AHL receptor RhlR, and in the *las* system the AHL synthase LasI produces 3-oxo-C12-HSL (3OC12-HSL) that is detected by the cognate AHL receptor LasR.[15] Both systems regulate genes that promote *P. a.* virulence.[1, 16, 17] The third AHL receptor, the quorum-sensing control receptor (QscR), is an orphan or LuxR "solo" receptor because it lacks a cognate AHL synthase.[18] Interestingly, QscR can respond to 3OC12-HSL produced via the *las* system to attenuate QS.[19-22] However, QscR also exhibits promiscuity in its response by sensing and being strongly activated (in many instances) by native AHL signals produced by other species.[22]

The development of synthetic small molecules designed to interfere with bacterial QS represents a potentially powerful approach to study fundamental aspects of QS mechanisms and modulate bacterial virulence phenotypes in bacterial pathogens, such as *P. a.*. Specifically,

targeting the LasR, RhlR and QscR AHL receptors could attenuate pathogenicity.[22-26] To this end, many groups,[1, 24, 25] including ours,[27-33] have developed libraries of synthetic small molecules toward these three *P. a*. receptors. These compounds, the bulk of which are AHL-derived, are capable of agonizing or antagonizing each of these receptors. Preliminary studies indicate they act by competing with the native AHL ligand for its binding site on the LuxR-type receptor. The ongoing optimization of these ligands (specifically, the antagonists), for both potency and receptor selectivity has slowed recently, due at least in part to challenges manipulating these receptors in vitro and characterizing the biochemical mechanisms by which the ligands act. Understanding the molecular interactions small molecules have with LuxR-type receptors that engender receptor antagonism (and agonism) would significantly aid ongoing research efforts in chemical probe design, as well as supplement our understanding of LuxR-type function in general.

To date, only four full-length structures of LuxR-type receptors have been reported: *P. a.* QscR,[34] *Chromobacterium violaceum* CviR,[35] *Agrobacterium tumefaciens* TraR,[36, 37] and *Escherichia coli* SdiA.[7, 38] These homodimeric AHL receptors have an N-terminal ligand-binding domain (LBD) that is connected through a flexible linker to the C-terminal DNA binding domain (DBD).[10, 11] Despite the relative paucity of structural data, the available structures reveal surprisingly different AHL binding pockets and symmetry.[11, 34] First, AHLs with short acyl chains appear exposed to solvent,[35, 37-39] but AHLs with long acyl chains are buried within the LBD away from the solvent.[34, 40] Second, structures with bound agonists generally form a criss-cross symmetric homodimer that poises the DBD for DNA binding, whereas TraR forms an asymmetric dimer when bound to DNA.[36, 37] Only the CviR structure captures a receptor bound to an antagonist, specifically a non-native AHL-analog (**CL**, Figure I.1A). Interestingly, this structure shows the CviR DBDs in an altered criss-cross configuration that would abrogate binding to the promoter region.[35] In view of these limited data, it is unclear whether mechanistic observations based on a single LuxR-type receptor–ligand interaction are broadly applicable in

this receptor class. Moreover, we lack any structural understanding of how a LuxR-type receptor can respond to multiple ligand-types, whether agonist or antagonist.

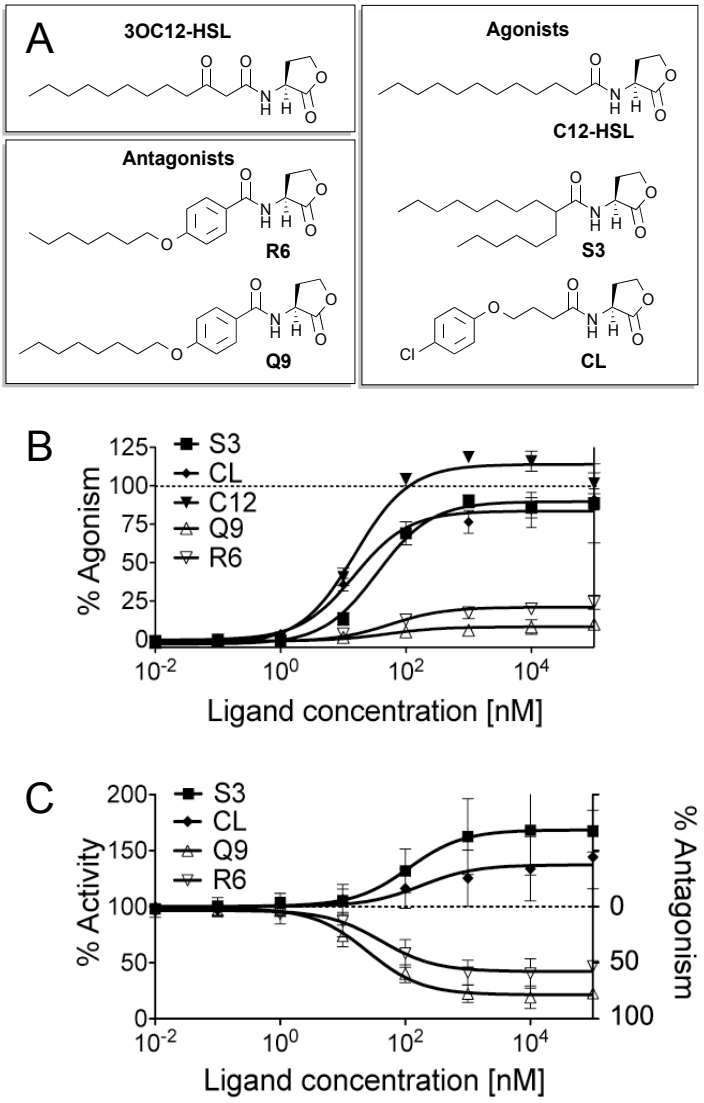

Figure I.1. Agonists and antagonists of QscR (A) Structures of native and non-native homoserine lactone (HSL) molecules used in this study. Atom names and numbers are shown. (B) Dose response curves for the activity synthetic compounds C12-HSL,**CL**, **R6**, **Q9**, and **S3** in *E. coli* using the QscR reporter. Agonist activity of the synthetic ligands was plotted assuming that 100% activity is equivalent to the activity of a natural agonist, 3-oxo-C12HSL (not shown). EC_{50} values calculated using GraphPad Prism (v. 6.0). Error bars are the s.e. of the means of triplicate samples. (C) Dose responses and antagonism IC_{50} values for AHLs **R6** and **Q9** in *E. coli* using the QscR reporter. Reporter activity was measured for varying concentrations of the synthetic ligands in the presence of a fixed concentration 15 nM of 3OC12-HSL. IC_{50} values, indicating the extent antagonism, were calculated using GraphPad Prism (v. 6.0). Error bars are the s.e. of the means of triplicate samples.

We sought to define the mechanisms by which a *P. a.* LuxR-type receptor can respond to either AHL agonists or antagonists. As LasR was not suitable for study because of its low solubility in vitro,[41-43] we chose QscR because full-length QscR is amenable to structural studies, and like LasR, it recognizes 3OC12-HSL.[34] Reporter-based assays were used to define a small set of synthetic AHL agonists and antagonists developed in our laboratories and elsewhere for investigation.[31, 44] The molecular mechanisms underlying the responses of QscR to these agonists and antagonists were examined using a variety of biochemical, biophysical and structural approaches. Agonists were found to stabilize QscR, increase dimerization and DNA binding, whereas antagonists were greatly impaired in these functions. Notably, one AHL agonist was found to recognize QscR using both "short-acyl chain" and "long-acyl chain" modes of binding. These results support a model for QscR response to agonists and antagonists that is distinct from the one operating in the response of LuxR-type receptors to short-chain AHLs.

I.3 Results

I.3.1 Activity of QscR in response to AHL analogs that serve as agonists and antagonists

Our laboratory has previously reported responses of QscR to AHL analogs in cell-based reporter assays.[28, 31] Based on these findings, AHLs **S3**, **Q9**, and **R6** (Figure I.1A) were selected for further study as they displayed a range of activities in comparison to 3OC12-HSL. In addition, a chloroaryl ligand reported by Bassler and co-workers, **CL** (Figure I.1A), was examined because it strongly antagonizes the LuxR-homolog CviR and is well understood from the [CviR:**CL**]$_2$ X-ray crystal structure.[35] The C12-HSL, the 3OC12-HSL analog simply lacking the 3-oxo group, was also included to examine a closely related mimetic and naturally occurring AHL.

To determine the relative potencies of these compounds, each was evaluated in an optimized cell based reporter assay for QscR agonism and antagonism. We utilized an *E. coli* reporter strain containing a QscR overexpression plasmid and a QscR-agonist activated β-galactosidase reporter gene (See experimental section).[22, 28] Plots of the percent agonism as a function of AHL

concentration allowed for the determination of the EC_{50} for each compound (Figure I.1B and Table I.1). The C12-HSL, **CL** and the branched-chain **S3** were found to be potent agonists of QscR activity, with EC_{50} values comparable to the native ligand OdDHL (15 nM). This activity profile for **CL** was interesting, as **CL** is an *antagonist* of CviR activity (see above). In turn, phenyl HSL derivatives **R6** and **Q9** were very weak QscR agonists, with EC_{50} values > 70 nM.

The antagonist activity of each compound was determined by examining the ability of the compound to compete with the naturally-occurring QscR ligand 3OC12-HSL at its EC_{50} value. As a function of concentration, the percent activities for **S3** and **CL** increased, as expected, due to their agonist activities. However, **Q9** and **R6** inhibited reporter activation by up to 80% with IC_{50} values in the mid-nanomolar range (Figure I.1C, Table I.1). The maximal inhibitory activity of the compounds is equal to the activation in the agonism assay, suggesting a "classical" partial agonist behavior. Notably, not only are compounds **Q9** and **R6** the most potent known inhibitors of QscR, they also are ten-fold more potent than the best inhibitors of LasR (using an analogous *E. coli* reporter) and do not display complex, "non-monotonic" partial agonist character.[45]

Table I.1 EC_{50} values for non-native compounds in QscR and LasR *E. coli* reporter strains.[a]

	IC_{50} [μM]		**EC_{50} [μM]**	
Compound	**QscR**	**LasR**	**QscR**	**LasR**
S3	-	-	0.036	1.7
CL[b]	-	0.49	0.016	33
Q9	0.026	0.76[c]	0.12	15
R6	0.042	>200	0.074	10

[a]Assays were performed using *E. coli* JLD271 (pJN105L/pSC11) or JLD271 (pJN105Q/pSC11-Q); see Experimental Section. For both assays, EC_{50} values were determined by testing AHLs over a range of concentrations (≤ 100μM). Assays were performed in triplicate, and 95% confidence intervals (CIs) were calculated from the SEM of n ≥ 3 trials. [b]LasR data collected by Moore *et. al.*[45] [c]CI is too wide to calculate. Full data set is shown in in Table I.7 and I.8, Supplemental Information.

I.3.2 The structure of QscR bound to S3 reveals a novel ligand binding mode

To date there are no structural details of a LuxR-type receptor that has been solved both in the presence of a small molecule antagonist or an agonist. Therefore, we made many attempts to co-

crystallize QscR with agonists C12-HSL, **S3**, and **CL** or antagonists **Q9** and **R6**, in order to investigate the structural basis underlying these activities. Following purification (Figure I.8A, Supplemental Information) full-length QscR together with agonist **S3** or C12-HSL (abbreviated QscR–**S3**, QscR–C12) were crystallized and the structures were determined using x-ray crystallography (Figure I.2A). The structures were solved at a resolution of 2.8 Å for QscR–**S3** and 2.5 Å for QscR–C12 using molecular replacement with our previously reported QscR–3OC12-HSL structure as the search model.[34] The refined QscR models (Table I.2) had continuous electron density in chain A from the N-terminal residue to the C-terminal residue Asn237 (Figure I.2). For the QscR–**S3** structure, chain B had regions of discontinuous electron density and B factors that were greatly elevated relative to chain A, which is consistent with the dearth of crystal packing contacts for chain B compared to chain A. There was clear electron density for the C12-HSL and **S3** ligands (Figure I.2B and C).

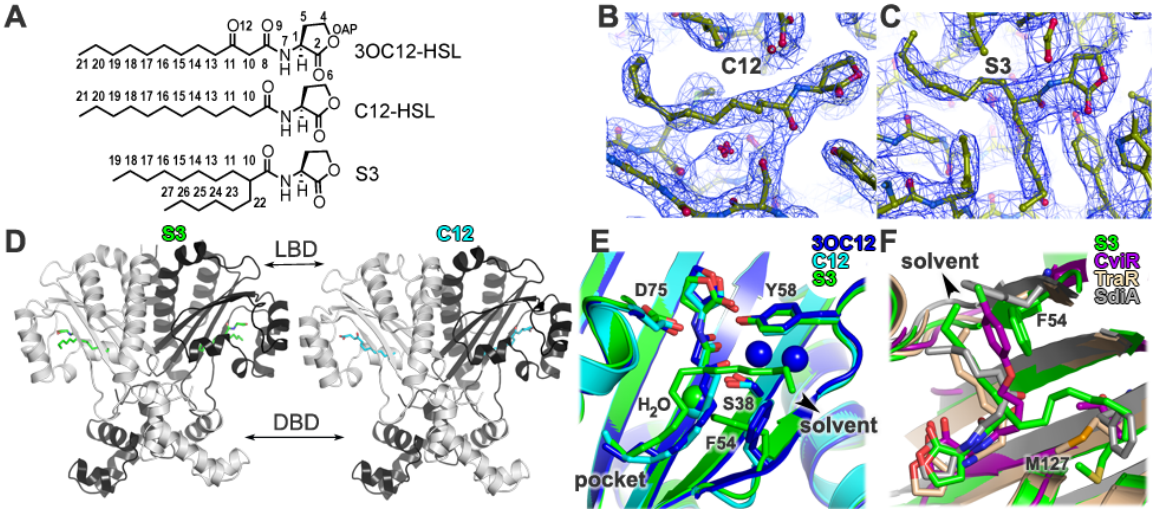

Figure I.2. Structural analyses of QscR-ligand complexes. (A) Chemical structures of 3OC12-HSL, C12-HSL, and **S3**. (B and C) Electron density of C12-HSL (B) or **S3** (C) in the QscR-complex crystal structures. Each 2mFo-DFc map was contoured at 1.4 σ. (D) The overall structure of the QscR–**S3** and QscR–C12 complexes. Chains A and B are colored in white or grey, respectively. **S3** is in green and C12 is in cyan. The LBD of Chain A is connected to the DBD through a flexible linker. The dimerized protein has a criss-cross symmetric architecture, where each domain has contacts with all of the others. (E) Overlay of QscR-ligand complexes. **S3** is in green, C12 in cyan and 3OC12 in blue. Spheres represent ordered solvent molecules within the structures. (F) Overlay of different AHL-receptor complexes. QscR–**S3** (green), CviR–**CL** (purple), TraR–3OC8-HSL (beige), and SdiA–3OC8-HSL are superimposed to illustrate the buried and solvent exposed region of the HSLs.

Table I.2. Statistics for crystallographic data collection and refinement

Data statistics	QscR-**S3**	QscR-C12
Spacegroup	$P3_121$	$P2_12_12_1$
Cell dimensions (Å)	a=94.12 b=94.12 c=105.68 α=90° β=90° γ=120°	a=57.59 b=91.91 c=94.00 α=90° β=90° γ=90°
Resolution range (Å)	47.06 - 2.80 (2.90 - 2.80)[a]	48.8 - 2.35 (2.48 - 2.35)[a]
Unique reflections	13,685 (1343)[a]	20,134 (2798)[a]
Redundancy	6.5 (6.3)[a]	4.0 (3.0)[a]
R_{sym}[b] (%)	9.0 (54.5)[a]	7.7 (55.9)[a]
Completeness (%)	99.3 (98.6)[a]	94.9 (91.6)[a]
Intensity (I/σ)	12.3 (2.8)[a]	11.8 (1.1)[a]
Wilson B factor (Å^2)	77.5	61.2
Refinement statistics		
Resolution Range (Å)	47.07-2.80 (3.02 - 2.80)[a]	48.8 - 2.50 (2.589 - 2.50)[a]
Unique reflections	14,344 (1379)	16,814 (1663)[a]
Rfree[c] (%)	26.6 (43.3)[a]	27.0 (36.5)[a]
Rworking (%)	21.2 (33.5)[a]	20.3 (30.3)[a]
Final Model		
Number of protein atoms	3816	3950
Number of ligand atoms	48	40
Number of solvent atoms	10	51
Average B factor (Å^2) (TLS groups)	94.6 (14)	34.1 (9)
R.m.s.d. bond lengths (Å)	0.002	0.007
R.m.s.d. bond angles (°)	0.42	0.87
Ramachandran Analysis	98% most favored; 1.7% allowed; 0.42% outlier	98% most favored; 1.7% allowed; 0.21% outlier

[a] High resolution shell
[b] $R_{sym} = \sum|I - \langle I \rangle|/\sum I$
[c] R_{free} calculated with an excluded set of 5%

Both QscR-ligand structures were virtually identical in overall architecture to QscR bound to the native agonist 3OC12-HSL (abbreviated QscR–3OC12). The subunits of QscR form a symmetrical criss-cross homodimer, where the LBD and DBD of one chain makes dimerization contacts with the adjacent chain LBD, poising the DBDs for DNA binding (Figure I.2D and Table I.9, Supplemental Information). The root mean square deviations (R.M.S.D.) of atomic positions for the individual domains of the three structures are 0.41 Å for the LBD and 0.18 Å for the DBD, indicating that the DBDs are more similar to each other than the LBDs. The R.M.S.D.

values for the single subunits and the full-length proteins are higher, which indicates that the structures have slightly different interdomain and intersubunit configurations (Table I.9, Supplemental Information). The R.M.S.D. of the Cα atoms for QscR-**S3** compared to QscR-3OC12 is 0.67Å, but for QscR–C12 compared to either QscR–**S3** or QscR–3OC12, the values are much higher, at 1.49 Å and 1.58 Å, respectively. The spacegroup and crystal packing of QscR–C12 is different from either QscR–**S3** or QscR–3OC12, which appears to slightly alter the rotation and translation of the LBDs relative to each other. Even considering the difference in crystal packing, the dimerization interfaces of the LBDs are well conserved in all of the QscR-ligand complexes. Contacts that had previously been validated using activity assays in *E. coli* with QscR–3OC12 were generally conserved in these structures.[34]

The substituents within the ligands 3OC12-HSL, **S3** and C12-HSL retain key agonist features. The C12-HSL acyl chain superimposes well with that of 3OC12-HSL. At atom 10 (Figure I.2A), **S3** branches into two aliphatic-chains of 6 and 8 carbons in length. The longer chain of **S3** is buried in the ligand-binding pocket, where it extends to the same position as both C12-HSL and 3OC12-HSL (Figure I.2E). Carbons C17-C19 of **S3** superimpose with C19-C21 of 3OC12-HSL and C12-HSL at the distal end of the pocket and interact with the same residues. This finding provides additional independent evidence that there is a region deep in the binding pocket, in close proximity to the LBD-A-DBD-B dimerization interface that is important for agonist activity.[34] We note that **S3** appears as an *S,S* diasteriomer in this crystal structure; as **S3** was prepared in a disteriomeric mixture, further compound purification and testing is required to confirm this structure as the preferred ligand in the QscR binding pocket.

C12-HSL is identical to 3OC12-HSL except that it lacks the carbonyl oxygen at the 3-position of the acyl chain (O12 in Figure I.2A). **S3** also lacks O12. The water molecules that form a hydrogen bond network within the 3OC12-HSL binding site near O12 are not seen in either the QscR–**S3** or QscR–C12 structures, but the water bridging Ser38, Ser129, and Met127 and the network of hydrogen bonds linked to O9 are conserved (Figure I.2E). Interestingly, for **S3** and

C12-HSL, which lack O12, the nearby atoms C8, O9, and C10 all superimpose well, surprisingly better than the overall lactone ring positions for all three ligands, and all three ligands appear to pivot about this point.

S3 bound to QscR mimics the features of AHLs with both long and short acyl chains found in the known LuxR-type receptor structures. One branch of **S3** is a 6-carbon, aliphatic chain extends out of the binding pocket into the solvent (Figure I.2 D and E), where it displaces the water molecules bound in QscR–3OC12 and Phe54 (Figure I.2F). Phe54 adopts an alternate rotamer that would sterically clash with the acyl chains of C12-HSL and 3OC12-HSL. However, Phe54 forms numerous van der Waals interactions with **S3** and also opens a channel to the solvent for the 6-carbon chain serving as a "gate keeper". Therefore, one branch of **S3** extends within the LBD, similarly to "long-acyl chain" AHLs bound to LasR and QscR.[34, 46] The other shorter chain mimics the "short-acyl chain" AHLs and analogs bound to CviR,[35] TraR,[36, 37] and SdiA[41] (Figure I.2F), which all exit the LBD toward the solvent. Thus, **S3** resembles both types of ligands due to its branched structure.

I.3.3 Relative to agonists, antagonists destabilize QscR

The structural analyses of LuxR-type receptors so far, including those described above for QscR, suggest the hypothesis that the mechanism of agonism and antagonism might be different between the receptors that recognize long-acyl chain AHLs (i.e., LasR and QscR) compared to receptors that respond to short-acyl chain AHLs (i.e., TraR, SdiA, and CviR). The mechanism of antagonism for CviR by **CL** is well understood and involves the stabilization of CviR in the antagonist bound form.[35] From studies in cells or in vitro comparing free QscR and LasR to agonist bound forms, the agonist bound form might be physically stabilized.[47, 48] These results suggest that there may be an alternative model for AHL receptor agonism and antagonism than that observed for CviR. Unfortunately, we have been unable to obtain crystals of QscR bound to the antagonists.

To understand the underlying basis for the antagonism of QscR, we instead compared the physiochemical stability of QscR with agonists or antagonists. Like some other LuxR-type receptors, such as TraR,[49] LasR,[50] and LuxR,[51]QscR is soluble and stable in cells with overexpression in the presence of agonists, but is largely insoluble upon expression with antagonists (Figure I.9, Supplemental Information). This observation suggests that QscR might be less stable in a complex with an antagonist than an agonist, and limited proteolytic digestion studies were used to examine this hypothesis (Figure I.3A and B, Figure I.10, Supplemental Information). An arginine in the linker between the LBD and DBD is susceptible to tryptic cleavage, and served as a useful handle for these experiments. Proteolytic digestion revealed that the QscR-agonist complexes had a nearly 2-fold greater half life ($t_{1/2}$) than the QscR-antagonist complexes (Figure I.3A and B, Table I.3, Figure I.10, Supplemental Information), supporting our hypothesis.

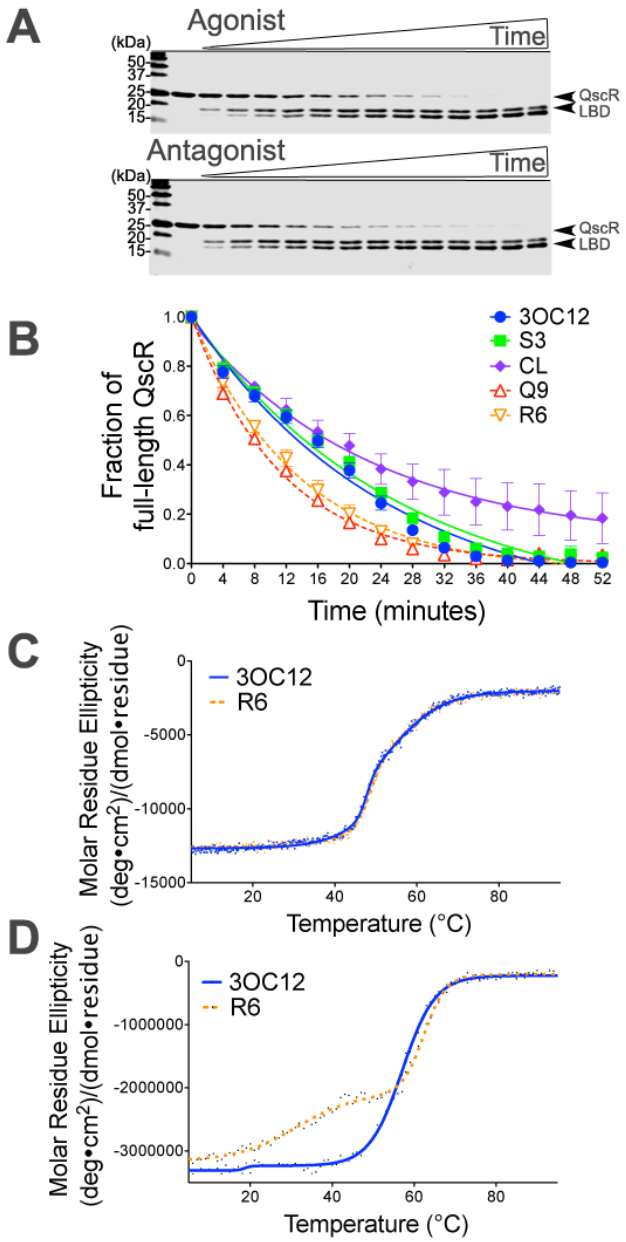

Figure I.3. Stability of QscR in the presence of agonists or antagonists (A) SDS-PAGE showing proteolytic digestion of QscR in the presence of trypsin for a representative agonist and antagonist. SDS-PAGE gels for each compound are shown in Figure I.10 (Supplemental Information). (B) Quantitation of the time-course of proteolysis for 3OC12-HSL, **S3**, **CL**, **Q9**, and **R6**. (C) Circular dichroism thermal denaturation plots of the QscR LBD in the presence of agonist 3OC12-HSL (blue) or antagonist **R6** (orange). D) Circular dichroism thermal denaturation plots of the QscR 3OC12-HSL (blue) or antagonist **R6** (orange).

Table I.3. Half lives of QscR-ligand complexes in the presence of Trypsin

Ligand	**3OC12-HSL**	**S3**	**CL**	**Q9**	**R6**
$t_{1/2}$ (min)	17.19	18.11	15.4	7.89	9.45

As another measure of the ability of ligands to stabilize QscR, we examined the thermal denaturation properties of one agonist complex, QscR-3OC12-HSL, and one antagonist complex, QscR-**R6**. As observed in the circular dichroism (CD) experiment, the denaturation curves were similar for that of the LBD alone, regardless of the ligand (Figure I.3C). However, for full-length QscR, a different pattern was observed. QscR-**R6** exhibited a pre-melting transition with the appearance of a second transition, whereas the denaturation curve for QscR-3OC12-HSL showed cooperative behavior consistent with the denaturation of one main species (Figure I.3D). These denaturation patterns support the model that the agonist stabilizes the formation of a cooperatively folded complex, which denatures as a single unit, whereas the domains or subunits appear to unfold separately for the antagonist complex.

I.3.4 Dimerization of QscR is altered by antagonist binding

Differences in the conformation of proteins can often be detected using nondenaturing electrophoretic mobility shift assays (EMSA). Using such EMSAs, we observed that QscR migrated differently when agonists or antagonists were present. QscR bound to the antagonists **Q9** or **R6** migrates as two species, whereas the agonists favor the formation of the more slowly migrating species (Figure I.4A). These EMSA results, together with both the increased exposure of the linker of QscR-antagonist complex to proteolysis and loss of cooperative unfolding in thermal denaturation experiments, suggested that the dimerization state of QscR might be different with bound agonist or antagonist.

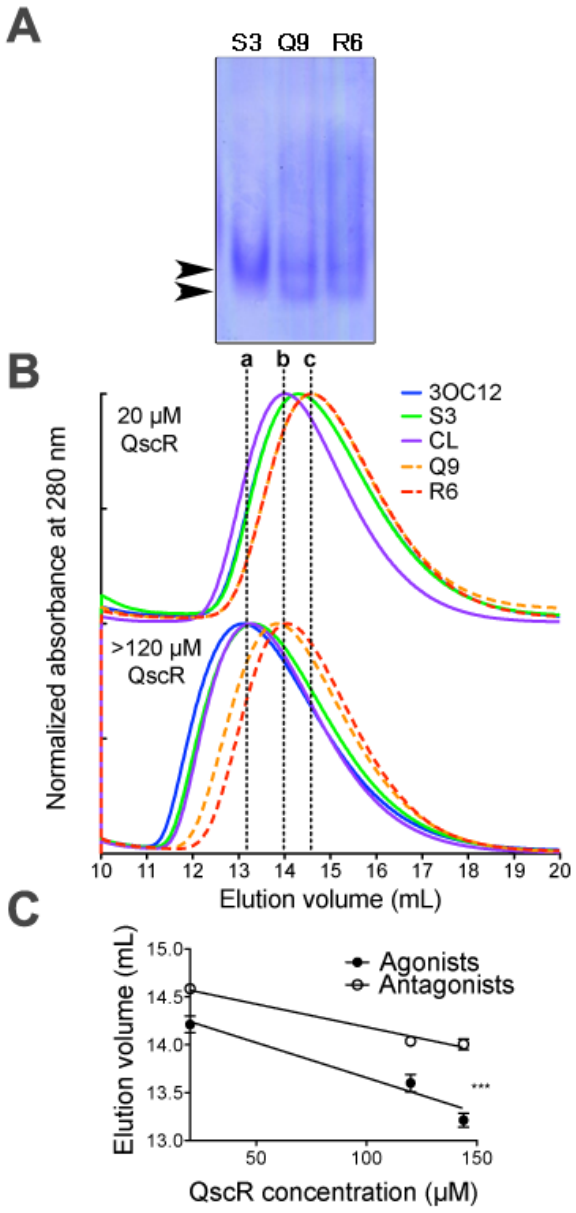

Figure I.4. Oligomerization of QscR bound to agonists or antagonists (A) Electrophoretic mobility shift assay assessing the mobility of QscR in the presence of the agonist 3OC12-HSL, agonist **S3**, or antagonist **Q9**. (B) Size-exclusion chromatography (SEC) of QscR at different concentrations with different compounds. The peaks of the traces were normalized to 1. Lines at 'a', 'b' and 'c' indicate the elution volumes observed for 'a' agonists at higher QscR concentrations, 'b' agonists at lower QscR concentration and antagonists at higher QscR concentrations, and 'c' antagonists at lower QscR concentration. (C) Graphical representation of all of the SEC elution volumes as a function of QscR concentration with agonists (closed circles) and antagonists (open squares). *** p-value <.001

In previously reported analytical size-exclusion chromatography experiments,[47] the elution volume of QscR decreased as the concentration of 3OC12-HSL increased from 1.4 μM – 160 μM, indicating the appearance of a larger complex, which was interpreted to be a QscR homodimer.

We used similar analytical size-exclusion chromatography experiments here to compare QscR with different concentrations of agonist or antagonist. The five ligands were tested with the following concentrations of QscR: 20 μM, 120 μM, 140.5 μM (and an additional concentration for the antagonists at 146.8 μM) (Figure I.4B). A plot of the elution volume as a function of complex concentration for the agonists compared to antagonists showed that QscR-agonist complexes consistently have a lower elution volume at all concentrations compared to the QscR-antagonist samples (Figure I.4C). These data suggest that agonist binding promotes a larger, dimeric form of QscR much more efficiently than antagonists.

Given that agonists compared to antagonists alter the QscR dimerization equilibrium and potentially the mode of dimerization, we examined the QscR-ligand complexes using protein crosslinking. Disuccinimidyl suberate (DSS) can crosslink lysines for which the Cα to Cα distance is up to approximately 21 Å. A representative SDS-PAGE showed that a QscR complex with an agonist 3OC12-HSL or **S3** in the presence of DSS forms a greater proportion of crosslinked dimers than the QscR–**Q9** antagonist complexes (Figure I.5 A and B). Crosslinked monomers were observed in all cases. To identify the positions of the crosslinks, we performed crosslinking mass spectrometry (XL-MS) analyses of the specific monomer and dimer complexes. Although only a few crosslinked peptides were observed (Figure I.5C), there were notable differences between the agonist and antagonist samples. Agonists promoted amino acid 63-223 intrasubunit crosslinks, whereas the 1-191 intrasubunit crosslink was observed only for the antagonist. The 1-1 and 208-208 intersubunit crosslinks were observed for the agonist complexes, but not for the antagonist complexes, and instead 121-223 was observed.

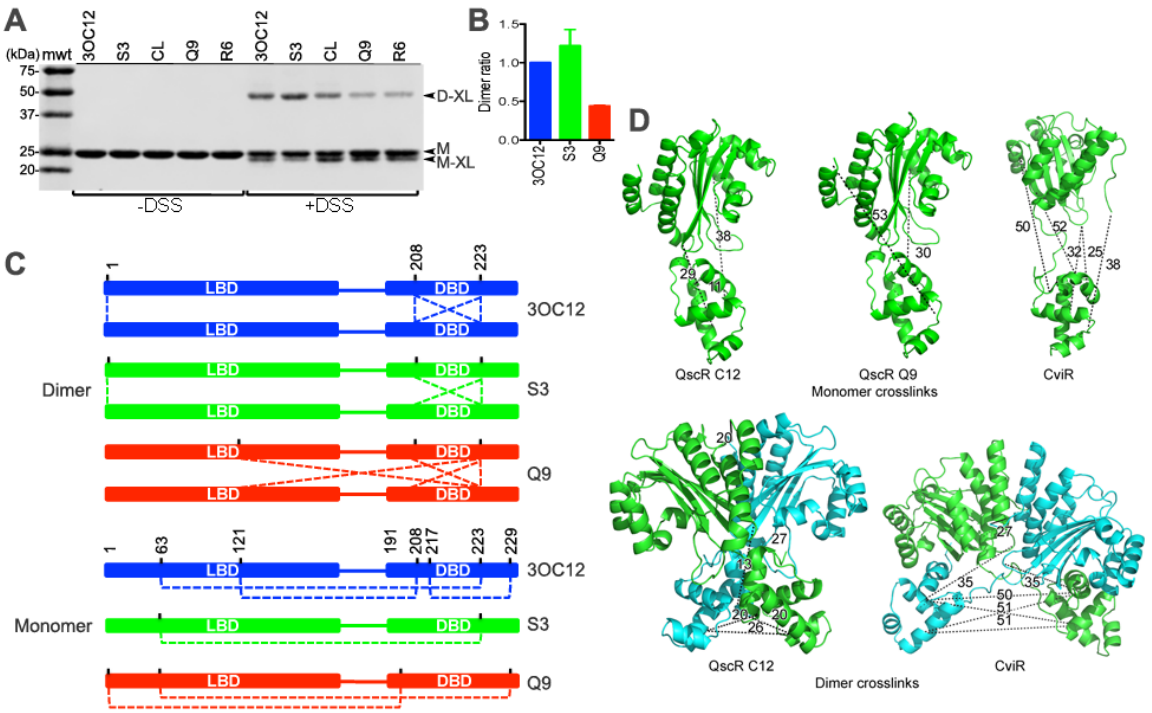

Figure I.5. QscR mass spectrometry crosslinking (XL-MS) in the presence of agonists or antagonists A) SDS-PAGE showing QscR complexes with either agonists or antagonists that have been treated without or with DSS. B) Quantitation of the ratio of crosslinked dimer to monomer from experiments represented in panel A. C) Crosslinked amino acids identified by XL-MS. The crosslinks for the monomer are shown below the dimer crosslinks in the panel, and colored blue for 3OC12, green for **S3** and red for **Q9**. D) Crosslinks observed in the monomers of QscR–C12 or QscR–**Q9** were mapped separately onto a QscR subunit showing the positions and distances in Å. The equivalent positions were mapped onto a CviR monomer. Lower panel: Crosslinks observed in the QscR dimers were mapped onto a QscR dimer to show positions and distances in Å. The equivalent crosslinks were mapped onto a CviR dimer.

To determine which AHL-receptor model(s) would satisfy the crosslinking constraints, the crosslinks were mapped onto the QscR-agonist and the reported CviR-antagonist structures (Figure I.5D and Table I.4).[35] The Cα to Cα distances between the crosslinked amino acid residues were used as a measure of similarity, where a distance of 21 Å is approximately a maximum distance for a DSS crosslink (Table I.4). Comparison of the models of the QscR monomer, QscR dimer, and CviR dimer revealed that the QscR-agonist crosslinks are completely consistent with the QscR dimer crystal structure, whereas one of the crosslinks for the antagonist (121-223) is not. The monomer "model" of QscR (chain A extracted from the crystal structure) does not match, which is not unexpected. In the same analyses applied to the equivalent residues

in the CviR structure, none of the crosslinks are consistent, except for one agonist crosslink between two residues that are close in space in the DBD. Therefore, the QscR dimer crosslinks are consistent with the QscR dimer crystal structure, and the CviR model does not appear to resemble any forms of QscR.

Table I.4. Crosslinks and inter-Ca distances

	QscR crosslink	QscR Inter Ca distance (Å)	CviR equivalent crosslink	CviR equivalent distance (Å)
	Monomer			
C12	63-223	38	85-245	52
C12	217-229	11	239-251	16
C12	121-208	29	147-230	32
Q9	1-191 (4-191)	53	7-213	38
Q9	63-229	30	85-251	50
	Dimer			
C12	1-1 (4-5)	20	7-7	27
C12	208-208	26	230-230	51
Both	223-223	13	245-245	50
Both	208-223	20	230-245	51
Q9	121-223	27*	147-245	35

I.3.5 DNA recognition by QscR is severely impaired in the presence of antagonists

The degree to which antagonists compared to agonists alter the DNA binding affinity of QscR is unknown. Therefore, we used EMSA to obtain the K_D values for the two types of complexes with DNA. A fluorescently labeled palindromic 31 base pair DNA duplex that containing the QscR binding site shifts up in the gel to give a well defined complex in the presence of the agonist ligands. For antagonists, in contrast, we observed a broad smeared band, which indicates that the complexes are dissociating in the gel, or that there are multiple forms of complexes. (Figure I.6A). The calculated K_D values from (Figure I.6B) for the QscR with agonists are nearly 2-orders of magnitude lower than for QscR with the antagonists (compare the average 1.2 nM to 77 nM, Table I.5). Moreover, the Hill coefficients differ (compare the average of 1.83 for agonists to 0.8 for antagonists). These results indicate that agonists promote high affinity cooperative DNA binding, in contrast to the antagonists that bind more weakly and do not

show cooperative DNA binding. These trends are analogous to those recently reported for LasR-DNA binding in the presence of agonist and antagonist ligands [48].

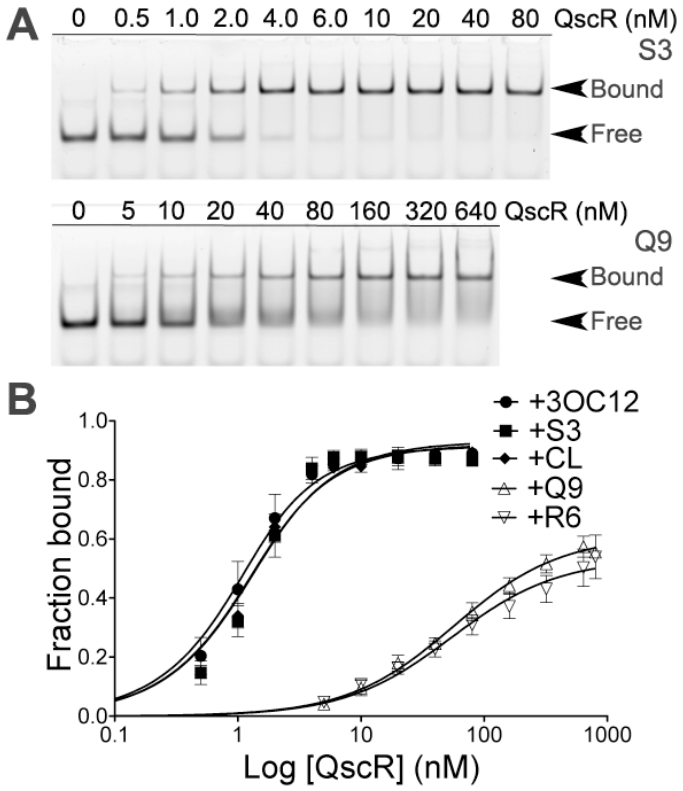

Figure I.6. DNA binding of QscR in the presence of agonists or antagonists (A) Representative electrophoretic mobility shift assays of DNA and QscR bound to **S3** and **Q9**, with concentrations of QscR and bound and free bands indicated. Representative EMSAs for OdDHL, **CL**, and **R6** are shown in Figure I.11 (Supplemental Information). B) Quantitative analyses of all EMSAs. Data were plotted and fit with the binding Eqn. 4, which accounts for ligand depletion. See Methods section for details.

Table I.5. DNA binding affinity of QscR with agonists and antagonists.

Compound	[a]K_D [nM]	[b]K_D [nM]	[b]Hill coefficient
3OC12-HSL	0.53 ± 0.23	1.0 ± 0.2	1.7 ± 0.4
S3	0.76 ± 0.29	1.3 ± 0.2	2.0 ± 0.4
CL	0.72 ± 0.21	1.2 ± 0.1	1.9 ± 0.3
Q9	56 ± 14	62 ± 27	0.9 ± 0.2
R6	54 ± 22	92 ± 30	0.7 ± 0.3

[a] Values calculated using Eqn 4. See Methods section.
[b] Values calculated using Eqn 5. See Methods section.

I.4 Discussion

The results presented here provide new insights into how both agonists and antagonists influence the structure and activity of QscR and support a new model for antagonism of AHL-mediated quorum sensing.

I.4.1 A mechanism for QscR antagonism

Currently there are several models for LuxR-type receptor responses to native AHLs.[10] TraR and LasR represent LuxR-type receptors for which agonists stabilize and dimerize otherwise unfolded protein (Figure I.7). Receptors such as LuxR are nonfunctional dimers that require AHL for DNA binding, whereas MrtR-type receptors are non-functional monomers that dimerize to bind DNA. In contrast, SdiA and others function as monomers in the absence or presence of agonists,[38, 52, 53] and dimerization is thought to be induced by DNA binding. The model for QscR activation resembles that of TraR and LasR, where agonists stabilize QscR to aggregation and proteolysis in the cell and bound AHL stabilizes the protein in vivo and in vitro.[47, 54, 55]

Less is known about AHL receptor antagonism. The model put forth for antagonism of CviR shows stabilization of dimeric CviR in a non-DNA binding form.[35] CviR together with the antagonist **CL** was less resistant to limited proteolysis than with an agonist.[35] Interestingly, it is the antagonist bound form of CviR that is more stable and is dimeric in solution than the agonist form (Figure I.7). In contrast, the biophysical studies reported here reveal that in vitro QscR is less stable with bound antagonists than agonists (Figure I.7). Further, **CL** behaves as a very strong *agonist* of QscR, in contrast to its antagonistic activity profile reported with CviR.[35]

AHL receptor dimerization on DNA is critical for transcriptional activation. In the presence of agonists QscR forms a relatively stable cooperatively folded dimer. In contrast, in the presence of antagonists, QscR is largely monomeric. Surprisingly, even DNA binding does not appear to induce stable dimeric QscR-antagonist complexes. This behavior of QscR presents a model for the antagonism of AHL receptors that is distinct from the model established for CviR (Figure I.7).

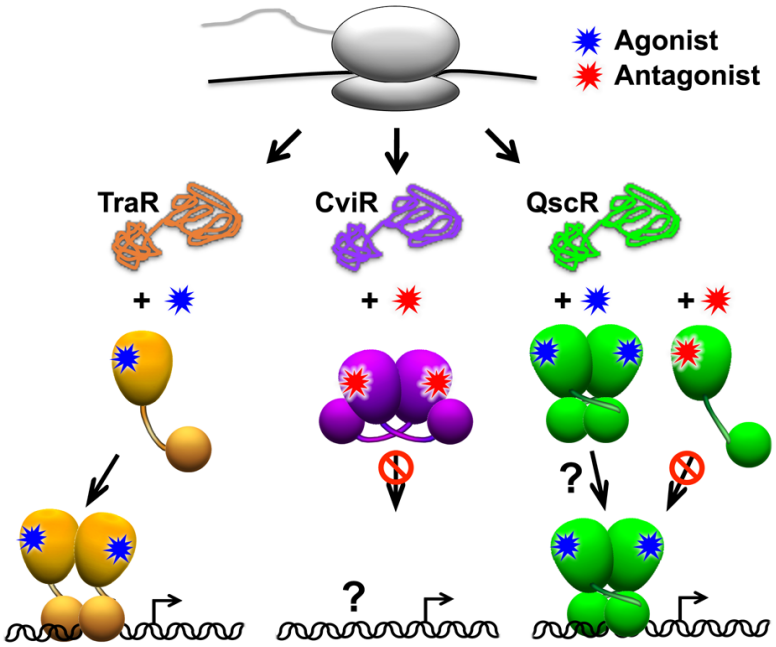

Figure I.7. Model for antagonism of QscR The well studied model systems QscR (green), CviR (purple) and TraR (beige) highlight different responses of AHL receptors toward agonists (blue) and antagonists (red).

I.4.2 A hot spot for agonists in QscR

In vivo, QscR responds with greatest activity to AHLs that have acyl chains that are between 10 and 14 carbons in length.[47] Consistent with this, our structural analyses of QscR bound to three different agonists (3OC12-HSL,[34] C12-HSL, and **S3**) highlight conserved contacts in the distal end of the AHL binding pocket. Structure-function studies of AHL libraries using reporter strains have also demonstrated that AHL agonists of QscR typically (but not always) possess aliphatic tails, and AHL antagonists usually have benzoyl type tails.[31] Despite the difference in the chemical nature of the "acyl chain substituent", the length of the substituents from the end to the 1-oxo-position of the HSL headgroup was similar, and compounds that were either too long or too short fail to activate QscR as potently.[31] **S3** has one branch of 8 carbons that, like C12-HSL and 3OC12-HSL, reaches the same position in the distal end of the QscR binding pocket. Interestingly, its agonistic activity was not abolished even when at the same time the **S3** C6 branch adopts a position much like an antagonist bound to CviR.[35]

In contrast to our expectations, based on the antagonism of CviR by **CL**,[35] we found that **CL** was a potent agonist of QscR with an EC_{50} value comparable to that of 3OC12-HSL. **CL** is bulkier at the distal end (away from the HSL) than any of the ligands studied here, and is well suited to the relatively large QscR binding pocket.[34] In fact, we previously found that C14-HSLs as well as biaryl and distal cyclohexane HSLs of similar length to **CL** have some agonistic activity in QscR.[31] Furthermore, the distance between the 1-oxo-position of the acyl-chain and the terminal atom of **CL** is nearly identical to that for C12-HSL, 3OC-12-HSL and **S3**. Therefore, we predict that **CL** would similarly bind in the acyl-chain pocket and stabilize the cooperatively folded structure.

There are now multiple lines of evidence that the distal region of the ligand-binding pocket is a critical feature of QscR agonism, and we now refer to it as the "agonist hot spot". We previously reported support for this model because a substitution of Gly 40 to Phe in QscR, near the distal end of the AHL pocket, resulted in increased response to 3OC6-HSL and a decreased response to 3OC12-HSL.[34] The Phe substitution is predicted to reduce the space in the pocket, which would allow AHLs with shorter acyl-chains to have better agonist activity. Like QscR, LasR has room to accommodate longer ligands,[40, 46] and these ligands superimpose in a hotspot in LasR created by different residues. In contrast, the SdiA,[38, 41] CviR, [35] and TraR [36, 37] structures show larger residues blocking this distal site, which indicates that agonists with short acyl chains may have a different mechanism of activation.

I.4.3 Implications for the design of new agonists or antagonists

For AHL receptors in general, it has been difficult to produce synthetic compounds with EC_{50} values that are lower than natural agonists, or with IC_{50} values that are lower than 100-1000x the EC_{50} of the natural agonists.[27-31] **S3** is one of the most potent synthetic QscR agonists reported to date (along with **CL**). **S3** is unusual because it is branched and exhibits two biologically relevant modes of binding. The long chain is buried in the LBD and is important for agonism. The short

chain adopts the mode of binding that has been observed for antagonists (CviR) and for agonists with short acyl chains (TraR and SdiA). This dual mode of binding of **S3** is possible because of a change in the rotamer of the key gatekeeper residue, Phe54, from a position that blocks the exit channel to one that opens it. The residues equivalent in TraR (Ala) and CviR (Val), are shorter and rather than closing the pocket, they appear to orient the exiting ligands. Interestingly, the structure of the equivalent Phe in SdiA is much like Phe54 QscR bound to C12-HSL and 3OC12-HSL.

The equivalent Phe in LasR adopts a completely different position in the reported structures of LasR, as the entire loop is oriented differently, perhaps as a result of crystal packing.[40] This structural difference from QscR can help explain the compound activity differences observed in cell-based reporter screening data for these two receptors. Indeed, **S3** shows much less activation of LasR (Table I.8, Supplemental Information), highlighting that the short chain mode of binding is likely less applicable for this receptor. **Q9** and **R6** are partial agonists with the most potent known IC50 values in the QscR cell based reporter, but in LasR these compounds have reduced potency values in both agonism and antagonism assays (Table I.8, Supplemental Information). Such activity further supports the differences between the exit channels in the two receptors; LasR cannot as easily accept bulk on the ligand alpha carbon. Interestingly, **CL** is extremely selective for QscR agonism. It activates QscR as potently as its "native" ligand 3OC12-HSL yet contains an aromatic ring. LasR, alternatively, is inhibited by **CL**.[45] This may be due to the ability of QscR to accommodate ligands that are longer and bulkier than 3OC12-HSL as compared to LasR.[28] Because compounds that selectively modulate specific LuxR-type *P. aeruginosa* receptors allow for more precise phenotype modulation, future QscR agonist development may benefit from added distal bulk that mimics the length and packing of a C12 ligand.

Although no crystal structures with any antagonists were obtained, our improved knowledge of the molecular mechanism of QscR agonism points to new design approaches to improve

antagonist activity. The distance between the 1-oxo-position and the distal end of the AHL binding pocket is rather strict. **R6** is approximately 25% longer than **S3**, and similar in length to C12-HSL and 3OC12-HSL, but it appears too bulky to fit in the restricted entrance to the binding pocket, and likely extends to the solvent. **Q9** exhibits lower partial agonist and higher antagonist activity than **R6**. However, **Q9** is even longer than **R6**, which also may favor exiting the binding pocket. One approach to the design of new antagonists would be to develop compounds with a hydrophobic moiety that cannot reach the agonist hotspot, but will contribute binding energy from other interactions. Additional interactions could come from a second branch that has hydrophobic character in the exit channel and hydrophilic character at the terminus to improve solubility and affinity, and concomitantly lower partial agonist activity. These types of compounds could be improved antagonists of QscR. Our results and model suggest that with further design modifications antagonists could be developed that have even less partial agonist activity, and notably, more potent IC_{50} values. More broadly, these design principles could be applied to other LuxR-type receptors that respond to AHLs with longer acyl chains, for the development of improved chemical probes and as strategies to further study QS as an anti-infective target.

I.5 Materials and Methods

I.5.1 Chemicals

Non-native AHLs were synthesized as described previously.[31] *N*-(3-oxododecanoyl) L-homoserine lactone (OdDHL) was purchased from Sigma–Aldrich. Chlorophenol red-β-D-galactopyranoside (CPRG) was purchased from Roche.

I.5.2 Strains and plasmids

Strains and plasmids used for this study are summarized in Table I.6. Media and reagents were obtained from commercial sources and were used according to manufacturer's instructions. Strains were grown in Luria broth (LB) at 37°C unless specified otherwise.

Table I.6. Bacterial strains and plasmids used in this study.

Strain or plasmid	Description	Reference/Source
Strain		
E. coli JLD271	K-12 ΔlacX74 sdiA271::Cam; Cl^R	*16*
E. coli BL21 DE3 pLysS	F^- *ompT hsdS*$_B$(r_B^- m_B^-) *gal dcm* (DE3) pLysS (Cam^R)	Invitrogen
Plasmids		
pET3a-qscR	QscR expression vector with T7 promoter; Ap^R	*47*
pJN105Q	arabinose-inducible QscR expression vector; Gm^R	*22*
pSC11-Q	PA1897'-lacZ transcriptional fusion; QscR reporter vector; Ap^R	*27*
pJN105L	arabinose-inducible LasR expression vector;Gm^R	*22*
pSC11	lasI'-lacZ transcriptional fusion; LasR reporter vector; Ap^R	*20*

I.5.3 Activity assays

Assays for QscR and LasR activity were performed as previously described utilizing the *E. coli* strain JLD271 harboring pJN105-type expression plasmids and pSC11-type reporter plasmids (pSC11Q/pJN105Q and pSC11/pJN105L for QscR and LasR, respectively). For antagonism assays, increasing concentrations of compound were screened against OdDHL at approximately its EC_{50} value in the QscR (15 nM) or LasR (2 nM) bacterial reporter strains. For both QscR and LasR agonism assays, increasing concentrations of compound were screened and compared to 100 μM 3OC12-HSL to define maximum activity. A modified Miller assay was performed using chlorophenol red-β-D-galactopyranoside (CPRG) as a β-galactosidase substrate. The amount of product was measured from the OD_{570} nm using a Synergy 2 plate reader. Enzymatic activity was calculated using the following equation (Eq. 1):

Eq. 1: Miller units = $1000*Abs_{570} / (OD_{600} * t * V)$.

Where t is the incubation time of substrate with lysate and V is the volume of culture. The IC_{50} and EC_{50} values were calculated with GraphPad Prism software (v. 6.0) using a variable slope sigmoidal curve fit defined by the following equation (Eq. 2):

Eq. 2: LogXb = LogEC50 + (1/HillSlope)*Log((2^(1/S))-1).

With a denominator of (1+10^((LogXb-X)*HillSlope))^S and numerator of Top-Bottom. The Y-axis shows the Bottom + (Numerator/Denominator).

I.5.4 Expression and purification of QscR

E. coli strain BL21 (DE3) pLysS (Invitrogen) containing pET3a-qscR[47] (gift from the Peter E. Greenberg, University of Washington) was precultured in LB broth with 100 μg/mL ampicillin and 34 μg/mL chloramphenicol at 37°C overnight. 1% of the pre-culture was added to 0.5 L LB containing 100 μg/mL ampicillin in each of 8 flasks. Cultures were grown at 37°C to an OD_{600} of 0.4-0.6, and the flasks were cooled on ice for 2 min. 3OC6-HSL was added to 50 μM and expression was induced using 0.5 mM IPTG (GoldBio). Cells were grown for 17 hr at 17°C, and harvested and stored at -80°C.

Buffers included lysis buffer (LYS), low salt buffer (LS), and LS with 1 M NaCl. *Lysis buffer*: 25 mM Tris, pH 7.8 at 4°C, 100 mM NaCl, 1 mM EDTA, 1 mM DTT, 10% glycerol, 0.01% Tween20, with a protease inhibitor cocktail tablet (Roche) and 100 μM of the desired compound (either 3OC12-HSL, agonist, or antagonist). *Low salt buffer*: 25 mM Tris, pH 7.8 at 4°C, 100 mM NaCl, 1 mM EDTA, 1 mM DTT, 10% glycerol, 0.01% Tween 20, 10 μM final concentration of the desired compound.

QscR was purified by resuspending cells in 100 mL of LYS buffer and lysing them using sonication and centrifugation at 17,000 RPM for 30 min at 4 °C. Ammonium sulfate (AS) fractionation of the cleared lysate was conducted at 45% AS saturation with stirring slowly for 30 min and incubation on ice for at least 4 hours. The precipitate was collected by centrifugation at

7,000 RPM for 10 min. It was resuspended in 30 mL of LYS buffer (with compound) and dialyzed against 2L of LS buffer. The sample was sterile filtered.

For chromatography, a tandem-connected GE HiTrap Q 5 mL column and GE Heparin 5 mL column was used. It was pre-equilibrated with LS buffer, loaded with the sample and washed to remove unbound proteins. The Q-column was disconnected, and QscR was eluted from the heparin column with a NaCl gradient from 0.1 M to 1.0 M. Fractions containing QscR were pooled and concentrated to 4 mL using a stirred-cell concentrator. Size exclusion chromatography (SEC) was performed (Superdex 75, GE Healthcare) in LS buffer, and pure QscR fractions were combined (Figure I.8A, Supplemental Information).

The QscR ligand binding domain (LBD) was obtained from full-length QscR (as above) but without protease inhibitors. 2 mg of trypsin was added to each 20 mL of lysate and incubated for 1.5 hr. The cleaved protein was purified by anion-exchange chromatography (HiTrap Q, GE Healthcare), and the LBD fractions were pooled and concentrated for further purification using SEC (Superdex 30, GE Healthcare; Figure I.8B, Supplemental Information). MALDI mass spectrometry was used to confirm the cleavage site in QscR at residue Arg167.

I.5.5 QscR solubility tests

Three 500 mL flasks with 100 mL LB and 100 μg/mL ampicillin were inoculated with 100 μL of a 6 mL overnight starter culture grown with 100 μg/mL ampicillin and 34 μg/mL chloramphenicol. The cells were grown at 37°C to an OD_{600} of 0.89. Either 3OC12-HSL, agonist or antagonist was added to each flask at a final concentration of at 50 μM and the flasks were cooled on ice for 2 min. Expression was induced with a final concentration of 0.5 mM IPTG (GoldBio), and the cells grown for 17 hr at 17°C. Cells were harvested and lysed in 25 mM sodium phosphate, pH 7.0, 1 mM DTT, 1 mM EDTA, 10% glycerol, 150 mM NaCl, 0.01% Tween20, with a protease inhibitor cocktail tablet (Roche). In addition, each compound was

added to a final concentration of 10 μM to the lysis buffer. The insoluble pellets were resuspended in 5 mL of lysis buffer. SDS-PAGE was used to evaluate 10 μL of each sample of the cleared lysate and resuspended pellet.

I.5.6 QscR-ligand structure determination and analyses

Each QscR–ligand complex was concentrated to approximately 3 mg/mL. Using vapor diffusion at 4 C° QscR–**S3** crystals were grown from added 0.2 M potassium citrate, 20 w/v PEG 3350 and 5% glycerol, and QscR–C12 from added 0.2 M sodium formate, 20 w/v PEG 3350. Diffraction data were collected at beamline I.4.2 (Advanced Light Source, Berkeley), and processed using d*trek.[56] The structures were solved at a resolution of 2.5 Å by molecular replacement using QscR as a model[34] with the PHASER module of the CCP4 or PHENIX software suite [57, 58]. The model was built using COOT[59] and refinement was conducted using PHENIX. Group TLS refinement was used in the refinement as there were large regions of chain B in QscR–**S3**, with much higher than average B-factors. Several sections of chain B are poorly defined due to this disorder.

The structures were analyzed for stereochemical and geometrical quality with the validation RCSB server.[60] The root mean squared deviation (R.M.S.D.) values were calculated using PyMol and COOT[59] and contacts were identified using CCP4. Figures were made using PyMol and Photoshop (Adobe).

I.5.7 Limited Proteolysis of QscR

QscR samples, purified with each desired compound, were diluted in LS buffer to a concentration of 17.98 μM and incubated with 250 μM of the compound for one hr at room temperature (RT). A 1 μM stock of trypsin was added at a 1:125 protein:protease ratio, and digestion performed at RT. Samples were drawn every four minutes and the reaction was

quenched with the addition of 2X SDS BME and boiling for 5 min. Reactions were resolved using SDS-PAGE. After Coomassie blue staining, the gels were imaged using the Li-Cor Odyssey imager at 700 nm, and quantified using ImageJ software. The rate and half-life ($t_{1/2}$) values were obtained using a one-phase decay curve-fitting model implemented in the GraphPad Prism program (Eq. 3):

Eq. 3: Y = (Y0 – Plateau)*exp(-K*X) + Plateau.

I.5.8 EMSA analysis of QscR with agonists and antagonists

QscR that was purified with compounds was concentrated to 0.55 mg/mL in sodium phosphate buffer. 100 μL aliquots were incubated at RT with either 100 μM 3OC12-HSL, 100 μM **S3**, or 100 μM **Q9** for one hr. Samples were loaded onto a 6% non-denaturing TBE polyacrylamide gel (37.5:1 acrylamide:bis-acrylamide ratio) and electrophoresed for 3 hr at 75 V at RT in 0.2 X TBE. Gels were stained using Coomassie blue.

I.5.9 Circular Dichroism

All of the CD spectra were recorded on a JASCO-J815 spectrophotometer with Peltier temperature control. Spectral scans were performed at 4°C and thermal denaturation data were collected at 222 nm using a temperature range of 4 to 95°C with a ramp rate of 1.5 °C/min. For the QscR-LBD complexes with each bound compound, samples of the QscR LBD that had been purified with 3OC6-HSL were first concentrated to 10 μM, and then dialyzed into 25 mM sodium phosphate buffer, pH 7.5 and 100 mM NaCl with 5 μM of the desired compound. The full-length QscR samples were prepared similarly. QscR–3OC6-HSL at 140.5 μM was incubated for 1 hr on ice with the desired compounds (3OC12-HSL, **S3**, **CL**, **Q9**, or **R6**) at a final concentration of 500 μM. Prior to acquisition of the spectra, the samples were diluted to 8 μM in 25 mM sodium phosphate, pH 7.5 and 100 mM NaCl.

I.5.10 Analytical size exclusion chromatography

QscR was purified with 3OC6-HSL and concentrated to either 20 μM or 140.5 μM. Samples were soaked with either 3OC12-HSL, **S3**, **CL**, **Q9**, or **R6** at a final concentration of 500 μM at 4°C for 2 hours. Samples were loaded onto an analytical Superdex 75 (10/300) column equilibrated in LS buffer at 4°C and the resulting traces normalized at the peak.

I.5.11 Crosslinking mass spectrometry of QscR-ligand complexes

Samples of 10 μM QscR, purified with 3OC6-HSL in buffer (50 mM sodium phosphate, pH 7.5, 100 mM NaCl, 1 mM EDTA, 0.5 mM TCEP, 0.01% Tween20, 10% glycerol), were soaked with 500 μM of each desired compound for 3 hr at 4°C. A 50/50 sample of ^{2}H-labeled and unlabeled DSS was added to a 10-fold excess. After 15 min at RT, the reactions were quenched using Tris, pH 7.4 at 50 mM. Samples were resolved using a 4-12% gradient Nupage™ gel in a Bis-Tris buffer and stained using Coomassie blue. Bands of approximately 50 kDa, 26 kDa, and 24 kDa were excised and processed as described by Hansen and coworkers.[61] Proteins were then digested overnight at RT with sequencing grade modified trypsin (Promega).

LC-MS/MS analyses were performed in the Proteomic Mass Spectrometry Facility at the U. Colorado-Anschutz Medical Campus. Each sample was analyzed in triplicate with technical duplicates. Nanoflow reversed-phase LC-MS/MS was performed using an Eksigent nanoLC-2D system (Eksigent) coupled to LTQ Orbitrap-Velos mass spectrometer (Thermo Fisher) as described previously.[62] Data acquisition was performed using Xcalibur™ (Version 2.1) software. Peak lists were generated from RAW files using PAVA (UCSF). Initial searches were performed on an in-house Mascot server (Version 2.3, Matrix Science), against both the SwissProt Database, and a custom database containing QscR, common lab contaminants, and randomized decoy sequences.

Crosslink searches were performed with Protein Prospector. Search conditions required trypsin specificity with up to 4 missed cleavages. Variable modifications included incorrect monoisotopic peak assignments, and the light (^{1}H) and heavy (^{2}H) full length and dead-end DSS mass additions. MS and MS/MS search tolerance was set to 10 and 25 ppm, respectively. Results were filtered according to parameters defined previously.[63] Crosslinks with a score difference above 0, and an expect value below 1 were considered, resulting in a false discovery rate of 0.48%.

I.5.12 QscR-DNA EMSA

Electrophoretic mobility shift assays (EMSA) were used to measure the affinity of QscR-ligand complexes for the PA1897 promoter region. A fluoresceine containing palindromic 31 base-pair DNA duplex [47] of sequence: 5' 6FAM-TGGACAACCTGCCCGATCGGGCAGGTTGTCC- 3' was purified using DEAE ion-exchange chromatography. QscR, purified in the presence of either 3OC12-HSL, **S3**, **CL**, **Q9**, or **R6**, was added to 1 nM DNA in increasing concentrations in LS buffer. After incubation for 1 hr at 4°C, the samples were electrophoresed for 45 min at 4°C using nondenaturing PAGE (as above). Gels were imaged using the Typhoon PhosphorImager (488 nm excitation, 526 BP filter) and quantified using ImageQuant software. Under ligand depletion conditions, binding curves were fit with Eq. 4:

Eq. 4: $Y=((B_{max})*(((DNA+x+K_D)-sqrt(((DNA+x+ K_D)^2)-(4*x*DNA)))/(2*DNA)))$,

where B_{max} is the maximum binding and x is the concentration of the DNA. To compare potential cooperativity, the binding curves were fit to a single-site cooperative binding isotherm (Eq. 5),

Eq. 5: $Y = ([P]^n / K_D) / (1 + [P]^n / K_D)$

where [P] is the total protein concentration, n is the Hill coefficient and Y is the fraction bound. The K_D values are the mean of at least three independent experiments.

I.6 Supplemental Information

Table I.7. Full activation and inhibition data for QscR with agonists and antagonists

Compound	IC_{50} [µM]	95% CI[a] [µM]	Inhibition (%)	EC_{50} [µM]	95% CI [µM]	Activation (%)
3OC12-AHL	-	-	-	0.015	0.012 - 0.018	100
C12-AHL	-	-	-	0.015	0.011 - 0.020	112
S3	-	-	-	0.036	0.021 - 0.060	88
CL	-	-	-	0.016	0.010 - 0.027	86
Q9	0.026	0.015 - 0.042	80	0.12	0.0037 - 3.6	11
R6	0.042	0.017 - 0.10	58	0.074	0.025 - 0.22	23

[a] CI = Confidence interval.

Table I.8. Activation and inhibition data for LasR with agonists and antagonists

Compound	IC_{50} [µM]	95 % CI [µM]	Inhibition (%)	EC_{50} [µM]	95 % CI [µM]	Activation (%)
S3	-	-	-	1.7	1.1 - 2.7	74
CL[45]	0.49	0.10 - 2.3	40	33	23 - 48	60
Q9	0.76	-[a]	17	15	1.8 - 120	37
R6	>200	-	13	10	6.1 - 17	65

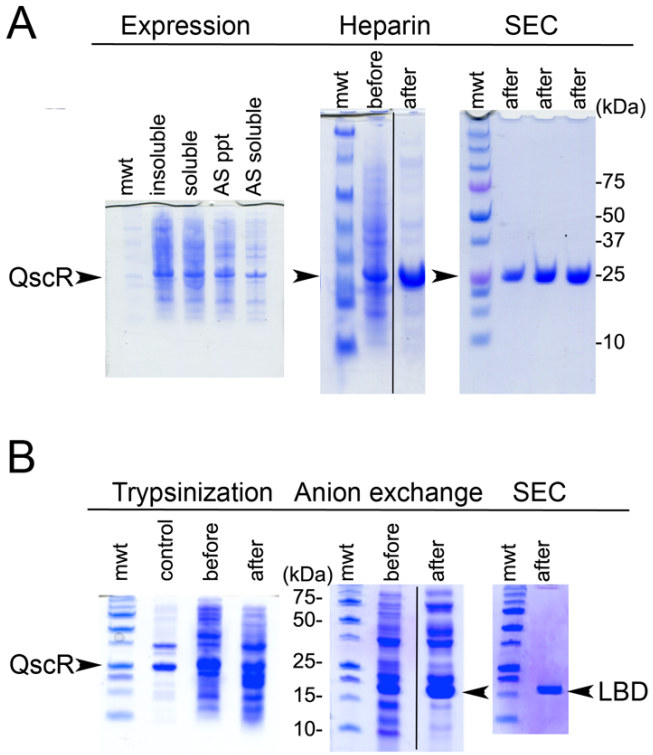

Figure I.8. Protein purification of full length QscR (A) and the ligand binding domain of QscR (B).

Table I.9: Structural comparison of QscR crystal structures and corresponding ligands.

Protein	**R.M.S.D. (Å)**			
Atoms	**3OC12-S3**	**3OC12-C12**	**S3-C12**	**3OC12-C12-S3**
LBD Cα	0.60	0.68	0.62	0.41
LBD backbone	0.62	0.68	0.62	0.41
LBD all	1.13	1.22	1.35	0.83
DBD Cα	0.28	0.32	0.34	0.18
DBD backbone	0.34	0.34	0.41	0.21
DBD all	0.65	0.87	0.84	0.46
1 chain Cα	1.05	0.75	0.84	
1 chain backbone	1.06	0.75	0.86	
1 chain all	1.43	1.24	1.43	
Ligand	**Pairwise distances (Å)**			**R.M.S.D. (Å)**
Atom	**3OC12-S3**	**3OC12-C12**	**S3-C12**	**3OC12-C12-S3**
C1	0.62	0.47	0.22	0.47
C2	0.29	0.47	0.34	0.37
O6	0.22	0.49	0.48	0.42
OAP	0.43	0.62	0.72	0.60
C4	0.89	0.58	0.82	0.77
C5	0.89	0.87	0.73	0.83
N7	0.81	0.62	0.20	0.60
C8	0.97	0.81	0.17	0.74
O9	0.87	0.82	0.20	0.70
C10	1.24	0.92	0.31	0.90
C11	1.88	0.93	2.44	1.86
C13	2.28	0.94	2.96	2.22

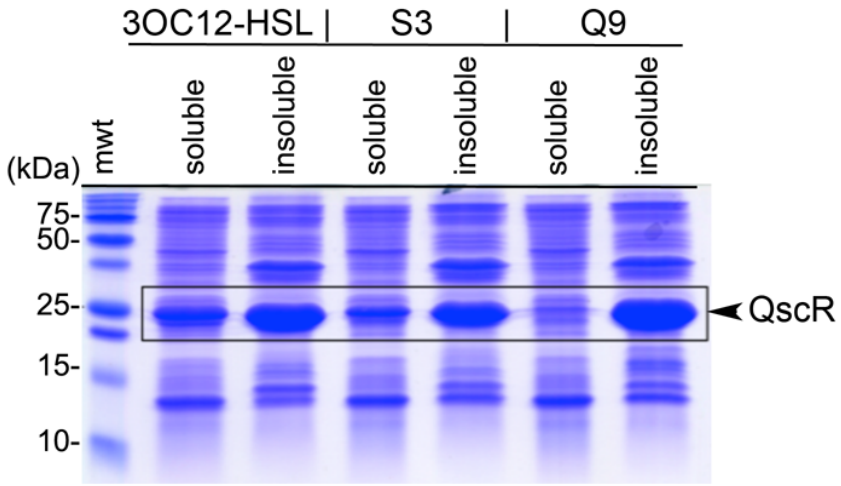

Figure I.9. QscR expressed with agonists 3OC12-HSL and **S3** or antagonist **Q9**.

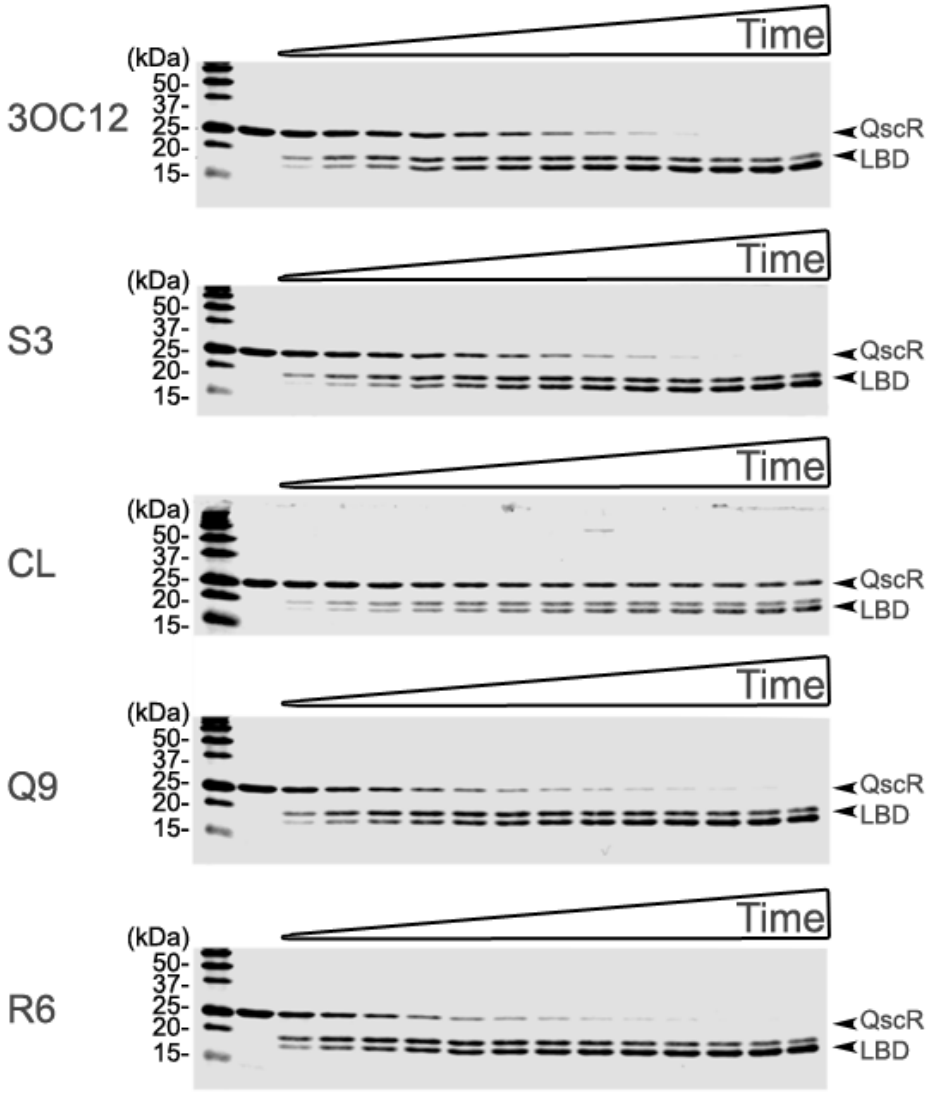

Figure I.10. SDS-PAGE showing proteolytic digestion of QscR in the presence of trypsin for all compounds tested.

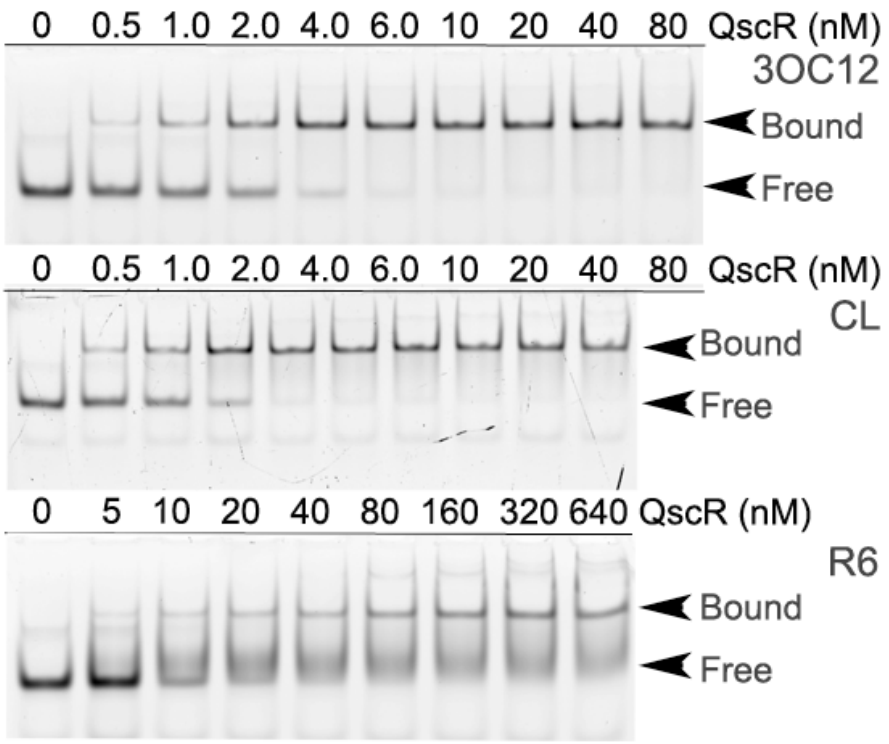

Figure I.11. Representative electrophoretic mobility shift assays of DNA and QscR bound to OdDHL, **CL**, and **R6** with concentrations of QscR and bound and free bands indicated.

I.7 References

1. Smith, R. S., and Iglewski, B. H. (2003) *P. aeruginosa* quorum-sensing systems and virulence, *Curr. Opin. Microbiol. 6*, 56-60.

2. Passador, L., and Iglewski, B. H. (1995) Quorum sensing and virulence gene regulation in *Pseudomonas aeruginosa*, In *Virulence mechanisms of bacterial pathogens.* (Roth, J. A., Ed.), pp 65-78, ASM Press, Washington.

3. Fuqua, W. C., Winans, S. C., and Greenberg, E. P. (1996) Census and consensus in bacterial ecosystems: The LuxR-LuxI family of quorum-sensing transcriptional regulators., *Ann. Rev. Microbiol. 50*, 727-751.

4. Miller, M. B., and Bassler, B. L. (2001) Quorum sensing in bacteria, *Annu. Rev. Microbiol. 55*, 165-199.

5. Whitehead, N. A., Barnard, A. M., Slater, H., Simpson, N. J., and Salmond, G. P. (2001) Quorum sensing in Gram-negative bacteria, *FEMS Microbiol. Rev. 25*, 365-404.

6. Eberhard, A., Burlingame, A. L., Eberhard, C., Kenyon, G. L., Nealson, K. H., and Oppenheimer, N. J. (1981) Structural identification of autoinducer of *Photobacterium fischeri*, *Biochem. 20*, 2444-2449.

7. Ruby, E. G. (1996) Lessons from a cooperative, bacterial-animal association: the Vibrio fischeri-Euprymna scolopes light organ symbiosis, *Annu. Rev. Microbiol. 50*, 591-624.

8. Eberl, L., Winson, M. K., Sternberg, C., Stewart, G. S., Christiansen, G., Chhabra, S. R., Bycroft, B., Williams, P., Molin, S., and Givskov, M. (1996) Involvement of *N*-acyl-L-hormoserine lactone autoinducers in controlling the multicellular behaviour of Serratia liquefaciens, *Mol. Microbiol. 20*, 127-136.

9. Schuster, M., Lostroh, C. P., Ogi, T., and Greenberg, E. P. (2003) Identification, timing, and signal specificity of *Pseudomonas aeruginosa* quorum-controlled genes: a transcriptome analysis, *J. Bacteriol. 185*, 2066-2079.

10. Stevens, A., Queneau, Y., Soulere, L., von Bodman, S., and Doutheau, A. (2011) Mechanisms and Synthetic Modulators of AHL-Deprendent Gene Regulation, *Chem. Rev. 111*, 4-27.

11. Churchill, M. E., and Chen, L. (2011) Structural Basis of Acyl-homoserine Lactone-Dependent Signaling, *Chem. Rev. 111*, 68-85.

12. Watson, W. T., Minogue, T. D., Val, D. L., Beck von Bodman, S., and Churchill, M. E. A. (2002) Structural Basis and Specificity of Acyl-homoserine lactone Signal Production in Bacterial Quorum Sensing, *Mol. Cell. 9*, 685-694.

13. Schuster, M., and Greenberg, E. P. (2008) LuxR-type Proteins in *Pseudomonas aeruginosa* Quorum Sensing: Distinct Mechanisms with Global Implications, In *Chemical Communication Among Bacteria.* (Winans, S. C., and Bassler, B. L., Eds.), pp 133-144, AMS Press.

14. Wagner, V. E., Li, L. L., Isabella, V. M., and Iglewski, B. H. (2007) Analysis of the hierarchy of quorum-sensing regulation in *Pseudomonas aeruginosa*, *Anal. Bioanal. Chem. 387*, 469-479.

15. Latifi, A., Foglino, M., Tanaka, K., Williams, P., and Lazdunski, A. (1996) A hierarchical quorum-sensing cascade in *Pseudomonas aeruginosa* links the transcriptional activators LasR and RhIR (VsmR) to expression of the stationary-phase sigma factor RpoS, *Mol. Microbiol. 21*, 1137-1146.

16. Lindsay, A., and Ahmer, B. M. (2005) Effect of sdiA on biosensors of N-acylhomoserine lactones, *J. Bacteriol. 187*, 5054-5058.

17. Seed, C. P., Passador, L., and Iglewski, B. H. (1995) Activation of the *Pseudomonas aeruginosa lasI* gene by LasR and the *Pseudomonas autoinducer* PAI: an autoinduction regulatory hierarchy, *J. Bacteriol. 177*, 654-659.

18. Chugani, S., and Greenberg, E. P. (2014) An evolving perspective on the *Pseudomonas aeruginosa* orphan quorum sensing regulator QscR, *Frontiers Cell. Infect. Microbiol. 4*, 152.

19. Lequette, Y., Lee, J. H., Ledgham, F., Lazdunski, A., and Greenberg, E. P. (2006) A distinct QscR regulon in the *Pseudomonas aeruginosa* quorum-sensing circuit, *J. Bacteriol. 188*, 3365-3370.

20. Chugani, S. A., Whiteley, M., Lee, K. M., D'Argenio, D., Manoll, C., and Greenberg, E. P. (2001) QscR, a modulator of quorum-sensing signal synthesis and virulence in *Pseudomonas aeruginosa*, *Proc. Natl. Acad. Sci. USA 98*, 2752-2757.

21. Fuqua, C. (2006) The QscR quorum-sensing regulon of *Pseudomonas aeruginosa*: an orphan claims its identity, *J. Bacteriol. 188*, 3169-3171.

22. Lee, J. H., Lequette, Y., and Greenberg, E. P. (2006) Activity of purified QscR, a *Pseudomonas aeruginosa* orphan quorum-sensing transcription factor, *Mol. Microbiol. 59*, 602-609.

23. Pearson, J. P., Feldman, M., Iglewski, B. H., and Prince, A. (2000) *Pseudomonas aeruginosa* cell-to-cell signaling is required for virulence in a model of acute pulmonary infection, *Infect. Immun. 68*, 4331-4334.

24. O'Loughlin, C. T., Miller, L. C., Siryaporn, A., Drescher, K., Semmelhack, M. F., and Bassler, B. L. (2013) A quorum-sensing inhibitor blocks *Pseudomonas aeruginosa* virulence and biofilm formation, *Proc. Natl. Acad. Sci. USA 110*, 17981-17986.

25. Weng, L.-X., Yang, Y.-X., Zhang, Y.-Q., and Wang, L.-H. (2014) A new synthetic ligand that activates QscR and blocks antibiotic-tolerant biofilm formation in *Pseudomonas aeruginosa*, *Appl. Microbiol. Biotechnol. 98*, 2565-2572.

26. Furiga, A., Lajoie, B., Hage, S. E., Baziard, G., and Roques, C. (2016) Impairment of *Pseudomonas aeruginosa* Biofilm Resistance to Antibiotics by Combining the Drugs with a New Quorum-Sensing Inhibitor, *Antimicrob. Agents Chemother. 60*, 1676-1686.

27. Eibergen, N. R., Moore, J. D., Mattmann, M. E., and Blackwell, H. E. (2015) Potent and Selective Modulation of the RhlR Quorum Sensing Receptor by Using Non-native Ligands : An

Emerging Target for Virulence Control in *Pseudomonas aeruginosa*, *ChemBioChem 16*, 2348-2356.

28. Mattmann, M. E., Geske, G. D., Worzalla, G. A., Chandler, J. R., Sappington, K. J., Greenberg, E. P., and Blackwell, H. E. (2008) Synthetic ligands that activate and inhibit a quorum-sensing regulator in *Pseudomonas aeruginosa*, *Bioorg. Med. Chem. Lett. 18*, 3072-3075.

29. Borlee, B. R., Geske, G. D., Blackwell, H. E., and Handelsman, J. (2010) Identification of synthetic inducers and inhibitors of the quorum-sensing regulator LasR in *Pseudomonas aeruginosa* by high-throughput screening, *Appl. Environ. Microbiol. 76*, 8255-8258.

30. Mattmann, M. E., and Blackwell, H. E. (2010) Small molecules that modulate quorum sensing and control virulence in *Pseudomonas aeruginosa*, *J. Org. Chem. 75*, 6737-6746.

31. Mattmann, M. E., Shipway, P. M., Heth, N. J., and Blackwell, H. E. (2011) Potent and selective synthetic modulators of a quorum sensing repressor in *Pseudomonas aeruginosa* identified from second-generation libraries of N-acylated L-homoserine lactones, *Chembiochem 12*, 942-949.

32. Geske, G. D., O'Neill, J. C., Miller, D. M., Mattmann, M. E., and Blackwell, H. E. (2007) Modulation of bacterial quorum sensing with synthetic ligands: systematic evaluation of N-acylated homoserine lactones in multiple species and new insights into their mechanisms of action, *J. Am. Chem. Soc. 129*, 13613-13625.

33. Geske, G. D., O'Neill, J. C., Miller, D. M., Wezeman, R. J., Mattmann, M. E., Lin, Q., and Blackwell, H. E. (2008) Comparative analyses of N-acylated homoserine lactones reveal unique structural features that dictate their ability to activate or inhibit quorum sensing, *ChemBioChem 9*, 389-400.

34. Lintz, M. J., Oinuma, K., Wysoczynski, C. L., Greenberg, E. P., and Churchill, M. E. (2011) Crystal structure of QscR, a *Pseudomonas aeruginosa* quorum sensing signal receptor, *Proc. Natl. Acad. Sci. USA 108*, 15763-15768.

35. Chen, G., Swem, L. R., Swem, D. L., Stauff, D. L., O'Loughlin, C. T., Jeffrey, P. D., Bassler, B. L., and Hughson, F. M. (2011) A strategy for antagonizing quorum sensing, *Mol Cell 42*, 199-209.

36. Zhang, R. G., Pappas, T., Brace, J. L., Miller, P. C., Oulmassov, T., Molyneaux, J. M., Anderson, J. C., Bashkin, J. K., Winans, S. C., and Joachimiak, A. (2002) Structure of a bacterial quorum-sensing transcription factor complexed with pheromone and DNA, *Nature 417*, 971-974.

37. Vannini, A., Volpari, C., Gargioli, C., Muraglia, E., Cortese, R., De Francesco, R., Neddermann, P., and Marco, S. D. (2002) The crystal structure of the quorum sensing protein TraR bound to its autoinducer and target DNA, *Embo J 21*, 4393-4401.

38. Nguyen, Y., Nguyen, N. X., Rogers, J. L., Liao, J., MacMillan, J. B., Jiang, Y., and Sperandio, V. (2015) Structural and mechanistic roles of novel chemical ligands on the SdiA quorum-sensing transcription regulator, *MBio 6*, e02429-14.

39. Zhang, R.-g., Pappas, K. M., Brace, J. L., Miller, P. C., Oulmassov, T., Molyneaux, J. M., Anderson, J. C., Bashkin, J. K., Winans, S. C., and Joachimiak, A. (2002) Structure of a bacterial quorum-sensing transcription factor complexed with pheromone and DNA, *Nature 417*, 971-974.

40. Zou, Y., and Nair, S. K. (2009) Molecular basis for the recognition of structurally distinct autoinducer mimics by the *Pseudomonas aeruginosa* LasR quorum-sensing signaling receptor, *Chem. Biol. 16*, 961-970.

41. Kim, T., Duong, T., Wu, C. A., Choi, J., Lan, N., Kang, S. W., Lokanath, N. K., Shin, D., Hwang, H. Y., and Kim, K. K. (2014) Structural insights into the molecular mechanism of *Escherichia coli* SdiA, a quorum-sensing receptor, *Acta Crystallogr. D Biol. Crystallogr. 70*, 694-707.

42. Wu, C., Lokanath, N. K., Kim, D. Y., Nguyen, L. D., and Kim, K. K. (2008) Crystallization and preliminary X-ray studies of SdiA from *Escherichia coli*, *Acta Crystallogr. Sect. F Struct. Biol. Cryst. Commun. 64*, 19-21.

43. Lerat, E., and Moran, N. A. (2004) The evolutionary history of quorum-sensing systems in bacteria, *Mol. Biol. Evol. 21*, 903-913.

44. Chen, G., Swem, L. R., Swem, D. L., Stauff, D. L., O'Loughlin, C. T., Jeffrey, P. D., Bassler, B. L., and Hughson, F. M. (2011) A Strategy for Antagonizing Quorum Sensing, *Mol. Cell 42*, 199-209.

45. Moore, J. D., Rossi, F. M., Welsh, M. A., Nyffeler, K. E., and Blackwell, H. E. (2015) A Comparative Analysis of Synthetic Quorum Sensing Modulators in *Pseudomonas aeruginosa*: New Insights into Mechanism, Active Efflux Susceptibility, Phenotypic Response, and Next-Generation Ligand Design, *J. Am. Chem. Soc. 137*, 14626-14639.

46. Bottomley, M. J., Muraglia, E., Bazzo, R., and Carfi, A. (2007) Molecular insights into quorum sensing in the human pathogen *Pseudomonas aeruginosa* from the structure of the virulence regulator LasR bound to its autoinducer, *J. Biol. Chem. 282*, 13592-13600.

47. Oinuma, K., and Greenberg, E. P. (2011) Acyl-homoserine lactone binding to and stability of the orphan *Pseudomonas aeruginosa* quorum-sensing signal receptor QscR, *J. Bacteriol. 193*, 421-428.

48. Suneby, E. G., Herndon, L. R., and Schneider, T. L. (2017) *Pseudomonas aeruginosa* LasR-DNA Binding Is Directly Inhibited by Quorum Sensing Antagonists, *ACS Infect. Dis. 3*, 183-189.

49. Zhu, J., and Winans, S. C. (1999) Autoinducer binding by the quorum-sensing regulator TraR increases affinity for target promoters in vitro and decreases TraR turnover rates in whole cells, *Proc. Natl. Acad. Sci. USA 96*, 4832-4837.

50. Schuster, M., Urbanowski, M. L., and Greenberg, E. P. (2004) Promoter specificity in *Pseudomonas aeruginosa* quorum sensing revealed by DNA binding of purified LasR, *Proc. Natl. Acad. Sci. USA 101*, 15833-15839.

51. Urbanowski, M. L., Lostroh, C. P., and Greenberg, E. P. (2004) Reversible acyl-homoserine lactone binding to purified *Vibrio fischeri* LuxR protein, *J. Bacteriol. 186*, 631-637.

52. Almeida, F. A., Pinto, U. M., and Vanetti, M. C. (2016) Novel insights from molecular docking of SdiA from *Salmonella Enteritidis* and *Escherichia coli* with quorum sensing and quorum quenching molecules, *Microb. Pathog. 99*, 178-190.

53. Yao, Y., Martinez-Yamout, M. a., Dickerson, T. J., Brogan, A. P., Wright, P. E., and Dyson, H. J. (2006) Structure of the Escherichia coli quorum sensing protein SdiA: activation of the folding switch by acyl homoserine lactones, *J. Mol. Bio. 355*, 262-273.

54. Corral Lugo, A., Daddaoua, A., Ortega, A., Morel, B., Diez Pena, A. I., Espinosa-Urgel, M., and Krell, T. (2017) Purification and characterization of *Pseudomonas aeruginosa* LasR expressed in acyl-homoserine lactone free Escherichia coli cultures, *Protein Expr. Purif. 130*, 107-114.

55. Zhu, J., and Winans, S. C. (2001) The quorum-sensing transcriptional regulator TraR requires its cognate signaling ligand for protein folding, protease resistance, and dimerization, *Proc. Nat. Acad. Sci. USA 98*, 1507-1512.

56. Pflugrath, J. W. (1999) The finer things in X-ray diffraction data collection, *Acta Crystallogr. D Biol. Crystallogr. 55 (Pt 10)*, 1718-1725.

57. Bailey, S. (1994) The CCP4 Suite - Programs for Protein Crystallography, *Acta Crystallogr. D Biol. Crystallogr. 50*, 760-763.

58. Adams, P. D., Afonine, P. V., Bunkoczi, G., Chen, V. B., Davis, I. W., Echols, N., Headd, J. J., Hung, L. W., Kapral, G. J., Grosse-Kunstleve, R. W., McCoy, A. J., Moriarty, N. W., Oeffner, R., Read, R. J., Richardson, D. C., Richardson, J. S., Terwilliger, T. C., and Zwart, P. H. (2010) PHENIX: a comprehensive Python-based system for macromolecular structure solution, *Acta Crystallogr. D Biol. Crystallogr. 66*, 213-221.

59. Emsley, P., and Cowtan, K. (2004) Coot: model-building tools for molecular graphics, *Acta Cryst. D60*, 2126-2132.

60. Rose, P. W., Prlic, A., Altunkaya, A., Bi, C., Bradley, A. R., Christie, C. H., Costanzo, L. D., Duarte, J. M., Dutta, S., Feng, Z., Green, R. K., Goodsell, D. S., Hudson, B., Kalro, T., Lowe, R., Peisach, E., Randle, C., Rose, A. S., Shao, C., Tao, Y. P., Valasatava, Y., Voigt, M., Westbrook, J. D., Woo, J., Yang, H., Young, J. Y., Zardecki, C., Berman, H. M., and Burley, S. K. (2017) The RCSB protein data bank: integrative view of protein, gene and 3D structural information, *Nucleic Acids Res. 45*, D271-D281.

61. Dzieciatkowska, M., Hill, R., and Hansen, K. C. (2014) GeLC-MS/MS Analysis of Complex Protein Mixtures, *Methods Mol. Biol. 1156*, 53-66.

62. Hill, R. C., Calle, E. a., Dzieciatkowska, M., Niklason, L. E., and Hansen, K. C. (2015) Quantification of Extracellular Matrix Proteins from a Rat Lung Scaffold to Provide a Molecular Readout for Tissue Engineering, *Mol. Cell. Proteomics 1*, 961-973.

63. Trnka, M., Baker, P., Robinson, P., Burlingame, A., and Chalkley, R. (2014) Matching cross-linked peptide spectra: only as good as the worse identification, *Mol. Cell. Proteomics 13*, 420-434.